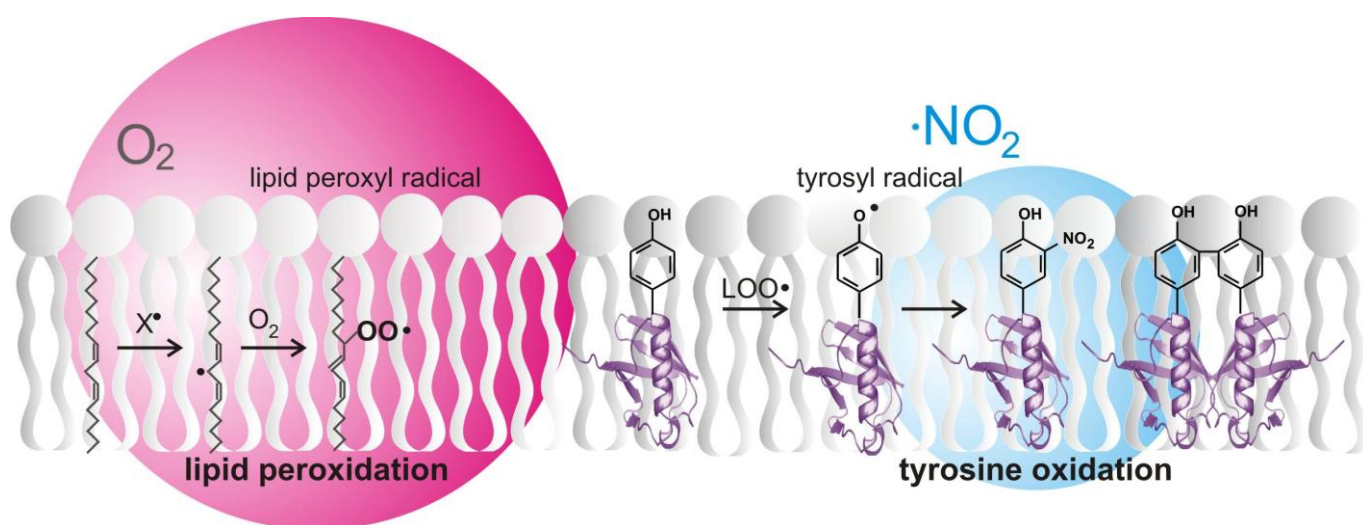


Dpto. de Bioquímica
Facultad de Medicina
Universidad de la República

Mecanismos Bioquímicos de la Nitración de Tirosinas en Membranas:

Estudios con Peroxinitrito y
Otros Sistemas Oxidantes

Lic. Silvina Bartesaghi Hierro
Director: Dr. Rafael Radi



Tesis de Doctorado en Química
Facultad de Química-PEDECIBA
Montevideo, Mayo 2010



PEDECIBA



CEINBIO

Centro de Investigaciones Biomédicas

a Anita y Lulú

Indice General

	Pagina
1. Resumen	1
2. Introducción	4
2.1 Nitración biológica como modificación oxidativa postraduccional.....	4
2.1.1 Antecedentes.....	4
2.1.2 Consecuencias biológicas.....	6
2.1.3 Aspectos cuantitativos.....	11
2.2 Especies oxidantes y nitrantes.....	13
2.2.1 Radical Superóxido.....	14
2.2.2 Peróxido de Hidrógeno.....	15
2.2.3 Radical hidroxilo.....	15
2.2.4 Oxido nítrico.....	16
2.2.5 Dióxido de nitrógeno.....	17
2.2.6 Peroxinitrito.....	18
2.2.7 Radical carbonato.....	19
2.2.8 Acido hipocloroso y cloruro de nitrilo.....	20
2.2.9 Integración de las rutas de ROS y RNS.....	21
2.3 Mecanismos de nitración de tirosinas.....	24
2.4 Determinantes fisicoquímicas de la nitración de tirosinas proteicas.....	27
2.4.1 Determinantes fisicoquímicas en entornos acuosos.....	28
2.4.2 Determinantes fisicoquímicas en entornos hidrofóbicos.....	29
2.5 Inhibición y reparación de la nitración de tirosinas: agentes anti-nitrantes endógenos y exógenos.....	31
2.5.1 Agentes endógenos.....	31
2.5.1.1 Enzimas antioxidantes.....	31
Peroxiredoxinas.....	31
Glutación peroxidasa.....	32
Hemoproteínas.....	33
2.5.1.2 Moléculas antioxidantes.....	33
Glutación.....	33
Acido Úrico.....	34
Acido lipoico.....	35
Reacciones de reparación.....	35
2.5.2 Agentes exógenos.....	36
2.5.2.1 Metalo Porfirinas.....	36
2.5.2.2 Nitroxidos.....	38
2.5.2.3 Ebselen.....	40
2.5.2.4 Péptidos de tirosina.....	40
2.6 Membranas biológicas y sistemas modelo.....	41
2.6.1 Estructura de las membranas biológicas.....	41
2.6.2 Sistemas modelo de membranas.....	45
Artículo: "Simulating Life's Envelopes".....	48
2.7 Permeabilidad y difusión de oxidantes en membranas.....	49
2.7.1 Permeabilidad de moléculas cargadas.....	49
2.7.2 Permeabilidad de moléculas neutras.....	51
2.7.3 Difusión y reparto en fases hidrofóbicas.....	52

2.8 Lipoperoxidación y otras modificaciones oxidativas en membranas.....	54
2.8.1 Etapas de la lipoperoxidación y formación de productos.....	54
2.8.2 El rol del α -tocoferol.....	57
2.8.3 Otros procesos oxidativos en membranas.....	59
3. Objetivos	61
4. Materiales y Métodos	62
4.1 Materiales.....	62
4.2 Métodos.....	63
4.2.1 Síntesis de BTBE y Productos Derivados.....	63
4.2.2 Síntesis y Purificación de Péptidos Transmembrana.....	63
4.2.3 Preparación de Liposomas e Incorporación de las Sondas.....	64
4.2.4 Síntesis y Cuantificación de Peroxinitrito.....	66
4.2.5 Sistemas Oxidantes.....	67
4.2.6 Cuantificación de 3-NT y 3-NO ₂ -BTBE por Espectrofotometría.....	67
4.2.7 Cromatografía Líquida de alta Performance (HPLC).....	68
4.2.8 Espectrometría de Masa (MS).....	69
4.2.9 Resonancia Paramagnética Electrónica (EPR).....	70
4.2.10 Productos de la Lipoperoxidación.....	71
4.2.11 Estudios Computacionales.....	72
4.2.12 Estimación de las distancias de difusión del peroxinitrito en suspensiones de liposomas.....	72
4.2.13 Análisis de los Resultados.....	73
5. Objetivo # 1. Estudio de los mecanismos de nitración de tirosinas en membranas mediada por peroxinitrito: utilización de la sonda hidrofóbica <i>N-t</i> -BOC- <i>tert</i> -butil ester L- tirosina incorporada a liposomas de fosfatidilcolina.....	74
5.1 Análisis del BTBE y sus productos de oxidación 3-nitro-BTBE and 3,3'- di-BTBE.....	74
5.2 Hidroxilación del BTBE mediada por peroxinitrito en liposomas de DLPC.....	77
5.3 Detección del radical fenoxilo derivado del BTBE por EPR.....	81
5.4 Oxidación del BTBE mediada por peroxinitrito: liposomas saturados e insaturados.....	83
5.5 Inhibición de la oxidación del BTBE por atrapadores de peroxinitrito y/o radicales derivados.....	85
5.6 Efecto del CO ₂ en la oxidación del BTBE.....	91
5.7 Efecto de complejos metálicos de transición sobre la nitración del BTBE mediada por peroxinitrito.....	93
5.8 Efecto del pH en la nitración, dimerización e hidroxilación del BTBE.....	95
5.9 Discusión.....	98
Publicación: "Mechanistic Studies of Peroxynitrite-Mediated Tyrosine Nitration in Membranes Using the hydrophobic Probe <i>N-t</i> -BOC-L-tyrosine <i>tert</i> -Butyl Ester"....	107

6. Objetivo # 2 Evaluación de la participación del proceso de lipoperoxidación en la nitración y dimerización de tirosinas en membranas.....	108
6.1 Participación de los radicales lipídicos en la oxidación del BTBE.....	108
6.2 Detección de los radicales lipídicos en la oxidación del BTBE por EPR.....	112
6.3 Lipoperoxidación y oxidación del BTBE mediadas por peroxinitrito: bolo vs infusión lenta.....	114
6.4 Efecto del grado de insaturación en la oxidación del BTBE mediada por peroxinitrito.....	117
6.5 Lipoperoxidación inducida por hemina y ABAP.....	118
6.6 Efecto del α -tocoferol en la oxidación del BTBE y en la lipoperoxidación.....	126
6.7 Consumo de oxígeno y determinación cinética de la reacción entre radicales LOO \cdot y BTBE.....	127
6.8 Discusión.....	134
Artículo: "Lipid Peroxyl Radicals Mediate Tyrosine Dimerization and Nitration in Membranes".....	141
Artículo: "Tyrosine <i>versus</i> Lipids".....	142
7. Objetivo # 3 Síntesis, caracterización y validación de péptidos transmembrana para el estudio de los mecanismos de nitración de tirosinas en membranas...	143
7.1 Síntesis de los péptidos.....	143
7.2 Purificación y caracterización de los péptidos.....	146
7.3 Formación de NO $_2$ -Y8 dependiente de peroxinitrito.....	149
7.4 Discusión.....	155
8. Conclusiones y Perspectivas	159
8.1 Conclusiones.....	159
8.2 Perspectivas.....	163
9. Referencias	164
10. Publicaciones	184
11. Anexos	192
11.1. Tabla de Abreviaturas.....	192
12. Agradecimientos	196

Indice de Tablas y Figuras

	Página
Tabla I. Efecto de la nitración en algunas proteínas seleccionadas.....	10
Figura 2.1 Formación y consecuencias de la nitración de tirosinas proteicas.....	11
Figura 2.2 Destinos del peroxinitrito.....	19
Figura 2.3 Formación de especies oxidantes y nitrantes a partir de especies reactivas del oxígeno (ROS) y nitrógeno (RNS), y sus puntos de interconexión.....	22
Tabla II. Modificaciones oxidativas representativas en biomoléculas.....	23
Figura 2.4 Mecanismo de formación de 3-NT y otros productos relacionados.....	26
Tabla III. Nitración y dimerización de proteínas asociadas a entornos hidrofóbicos.....	30
Figura 2.5 Metaloporfirinas como catalizadores de la descomposición del peroxinitrito.....	37
Figura 2.6 Mecanismo de reacción del Tempol.....	39
Figura 2.7 Estructura de la membrana biológica.....	42
Figura 2.8 Estructura de los fosfolípidos de membrana.....	43
Figura 2.9 Organización de los fosfolípidos en fases acuosas.....	44
Figura 2.10 Permeabilidad de especies oxidantes y nitrantes en membranas.....	52
Figura 2.11 Primeras etapas de la lipoperoxidación.....	55
Figura 2.12 Formación de productos durante la lipoperoxidación.....	57
Figura 2.13 Modificaciones oxidativas mediadas por radicales libres en Membranas.....	60
Figura 4.1. Formación del aducto entre el TBA y el MDA.....	72
Figura 5.1 Análisis del 3-nitro-BTBE y 3,3'-di-BTBE después de la adición peroxinitrito.....	76
Figura 5.2 Separación por HPLC y caracterización por MS del 3-hidroxi-BTBE.....	81

Figura 5.3. Detección del radical fenoxilo en liposomas saturados.....	82
Figura 5.4 Nitración y dimerización del BTBE mediada por peroxinitrito en liposomas con distinto grado de insaturación.....	84
Tabla IV: Efecto de distintos atrapadores en la oxidación del BTBE.....	86
Tabla V. Constantes de reacción de atrapadores con peroxinitrito y sus radicales derivados.....	87
Figura 5.5 Efecto de la desferrioxamina en la nitración y dimerización del BTBE.....	88
Tabla VI. Constantes de velocidad de las reacciones involucradas en la oxidación de tirosina/BTBE por peroxinitrito.....	89
Figura 5.6 Efecto del bicarbonato sobre la nitración y dimerización del BTBE mediada por peroxinitrito.....	92
Figura 5.7 Catálisis de la nitración del BTBE por hemina y Mn-tcpp.....	94
Tabla VII. Efecto de los complejos metálicos de transición en la nitración del BTBE.....	95
Figura 5.8A-B Oxidación del BTBE en función del pH.....	97
Figura 5.8C-D Simulación cinética química del efecto del pH sobre la oxidación de la tirosina y el BTBE.....	97
Figura 5.8E Efecto del pH en la nitración del BTBE catalizada por metales.....	98
Figura 5.9 Mecanismo propuesto de nitración para el BTBE incorporado a membranas.....	106
Figura 6.1 Efecto del oxígeno en la oxidación del BTBE mediada por el peroxinitrito.....	111
Figura 6.2 EPR-spin trapping de los radicales lipídicos y del radical fenoxilo derivado del BTBE.....	113

Figura 6.3 Oxidación del BTBE mediada por peroxinitrito: infusión lenta vs adición en bolo.....	116
Figura 6.4 Efecto del grado de insaturación en la oxidación del BTBE.....	118
Figura 6.5. Reacciones de los hidroperóxidos con hemina y formación de radicales lipídicos.....	119
Figura 6.6 Lipoperoxidación y oxidación del BTBE inducida por hemina.....	120
Figura 6.7 Oxidación del BTBE mediada por ABAP.....	121
Tabla VIII. Efecto del ABAP en la nitración y dimerización del BTBE.....	122
Figura 6.8A Separación por RP-HPLC de los productos de la oxidación del BTBE mediada por ABAP.....	123
Figura 6.8B Separación por RP-HPLC de los productos de oxidación de la tirosina mediada por ABAP.....	124
Tabla IX. Reacciones involucradas en la oxidación de tirosina y la lipoperoxidación.....	125
Figura 6.9 Efecto del α -tocoferol en la nitración del BTBE y la lipoperoxidación.....	127
Figura 6.10 Estudios de Oximetría.....	131
Figura 6.11 Formación de productos de la lipoperoxidación iniciada por hemina y ABAP.....	133
Figura 6.12 Mecanismo propuesto de reacción según el cual los radicales peroxilo son capaces de oxidar a la tirosina.....	139
Figura 7.1 Péptidos transmembrana y BTBE insertos en la bicapa.....	145
Figura 7.2 Purificación del péptido transmembrana por RP-HPLC.....	147

Figura 7.3 Caracterización de los péptidos transmembrana por ESI-MS.....	149
Figura 7.4 Caracterización del péptido NO ₂ -Y8 por RP-HPLC/MS.....	151
Figura 7.5 Formación de NO ₂ -Y8 en liposomas de DLPC.....	152
Figura 7.6 Comparación de los rendimientos de nitración en EYPC y DLPC.....	153
Figura 7.7 Efecto de oxígeno en la nitración de Y8.....	154
Figura 7.8 Estudios de dinámica molecular de péptidos transmembrana y su interacción con moléculas de agua.....	157
Figura 8.1 Productos de oxidación del BTBE por peroxinitrito y sus rendimientos relativos.....	160
Figura 8.2 Asociación de los procesos de oxidación de tirosinas y lipoperoxidación en membranas.....	161

1. Resumen

La nitración de tirosinas es una modificación oxidativa postraducciona que ocurre en proteínas por reacciones del peroxinitrito y otras especies nitrantes derivadas del óxido nítrico. Este proceso está asociado a condiciones de estrés nitrooxidativo en sistemas biológicos, y puede llevar a alteraciones en la estructura y función de proteínas. Hasta el presente, se han descrito mecanismos bioquímicos de nitración de tirosinas en sistemas acuosos, la mayoría de los cuales implican la participación de radicales libres, incluyendo el radical tirosilo. Sin embargo, un conjunto de proteínas nitradas en residuos de tirosina que han sido detectadas *in vivo*, están asociadas o incorporadas a biocompartimientos hidrofóbicos como biomembranas o lipoproteínas. En este sentido, los mecanismos bioquímicos y determinantes físico-químicas que participan en la nitración de tirosinas asociadas a ambientes hidrofóbicos pueden tener importantes diferencias con lo estudiado hasta el presente en sistemas acuosos, entre otros factores, porque en entornos hidrofóbicos existe una gran concentración de ácidos grasos insaturados que pueden competir por las especies nitrantes, y una exclusión de antioxidantes como el glutatión, que no se encuentran presentes en membranas y que por lo tanto no actúan inhibiendo la nitración como ocurre en fases acuosas; así como la relevancia de agentes nitrantes como el $\bullet\text{NO}$ y $\bullet\text{NO}_2$ que pueden fácilmente difundir hacia estos ambientes hidrofóbicos y concentrarse, favoreciendo las reacciones de nitración. Basado en estas consideraciones, en este trabajo de tesis hemos realizado un estudio exhaustivo de los mecanismos bioquímicos de nitración de tirosinas en sistemas modelo de membrana. Para ello, hemos utilizado sondas hidrofóbicas de tirosina en bicapas artificiales tales como, el análogo de bajo peso molecular BTBE (N-*t*-BOC *tert* butil ester L-tirosina) y péptidos hidrofóbicos de tirosina conteniendo 23 amino ácidos que fueron incorporados a liposomas de fosfatidilcolina. Los sistemas nitrantes y oxidantes utilizados en esta tesis fueron el peroxinitrito, un dador de radicales peroxilo, ABAP (2,2'-azobis (2) amidinopropano cloruro de hidrógeno) e hidroperóxidos en presencia de hemina en ausencia y presencia de nitrito (NO_2^-). Los resultados obtenidos indican

que la nitración de tirosinas en membranas ocurre por mecanismos radicalares, con la formación intermediaria del radical tirosilo; en el caso del BTBE además de la nitración para formar 3-nitroBTBE, las reacciones con peroxinitrito llevaron a la formación de cantidades menores de el dímero 3,3'-di-BTBE y del derivado hidroxilado 3-hidroxi-BTBE. Mientras que el rendimiento de nitración de BTBE en función de la concentración de peroxinitrito fue menor pero en el orden de lo observado en sistemas acuosos, el rendimiento de producto de dimerización fue mucho menor, en línea con una difusión limitada del radical tirosilo en la estructura organizada de la membrana. Por otra parte, la detección del derivado hidroxilado apoya el concepto de la homólisis de ONOOH a $\cdot\text{OH}$ y $\cdot\text{NO}_2$ en la superficie o en el interior de la bicapa. Se exploró el efecto de una serie de moléculas de relevancia biológica como atrapadores de radicales libres y metales de transición en los rendimientos de nitración, siendo el resultado más contrastante con lo ocurrido en fases acuosas, el efecto del CO_2 , el cual inhibió la nitración del BTBE incorporado a liposomas, lo que se explica por la incapacidad del radical carbonato ($\text{CO}_3\cdot^-$) de permear la membrana liposomal y oxidar por un electrón a la tirosina incorporada a la membrana. Un hallazgo particularmente importante de la tesis fue la observación que los procesos de nitración de BTBE ocurrían tanto en liposomas conteniendo fosfolípidos con ácidos grasos saturados (ej. DLPC, 1,2-dilauril-*sn*-glicero-3-fosfolina) como insaturados (ej. EYPC, fosfatidilcolina de yema huevo). Dada la alta abundancia de fosfolípidos y su reacción con radicales libres oxidantes para disparar procesos de lipoperoxidación, exploramos de que manera los radicales lipídicos podrían influir en el proceso de nitración. Los resultados indicaron que los radicales lipídicos peroxilo ($\text{LOO}\cdot$) son capaces de oxidar a la tirosina por un electrón para rendir radical tirosilo, y de esta manera alimentar el proceso de oxidación de tirosinas en membranas. En efecto, se logró la detección simultánea de los radicales tirosilo y lipídicos cuando se adicionó peroxinitrito a liposomas de PC conteniendo fosfolípidos insaturados y con BTBE incorporado. La constante de reacción determinada para la reacción entre radicales peroxilo lipídicos y la tirosina fue

$4.800 \text{ M}^{-1}\text{s}^{-1}$. La conexión entre el proceso de lipoperoxidación y la nitración de tirosina fue confirmada por una serie de experimentos, entre los cuales destacamos la inhibición concomitante de ambos procesos a bajas tensiones de oxígeno y por la incorporación a liposomas de alfa-tocoferol. Finalmente, pudimos sintetizar, purificar y utilizar en un conjunto exploratorio de experimentos a péptidos hidrofóbicos de 23 amino ácidos conteniendo tirosina en distinta posición de la estructura primaria y que se incorporan a través de la membrana liposomal. Hemos demostrado la capacidad del peroxinitrito de nitrar los residuos de tirosina de estos péptidos, confirmando los resultados principales obtenidos con BTBE. En suma, esta tesis ha aportado a las bases bioquímicas y mecánicas de la nitración de tirosina en proteínas asociadas a membranas.

2. Introducción

2.1 Nitración biológica como modificación oxidativa postraduccional

2.1.1 Antecedentes

El óxido nítrico ($\bullet\text{NO}$) es un mensajero intra e intercelular producido por las enzimas óxido nítrico sintasas (NOS), a partir de la oxidación aeróbica del amino ácido L-arginina. Fue originalmente conocido por sus funciones fisiológicas de señalización tanto a nivel del sistema circulatorio (como vasodilatador) como del sistema nervioso central (como neurotransmisor) (1, 2). Sin embargo, pronto se hizo evidente que el $\bullet\text{NO}$ también podría actuar como mediador citotóxico u efector patogénico en situaciones de sobreproducción de $\bullet\text{NO}$, tanto por inducción de la iNOS (isoforma inducible) en condiciones inflamatorias como por sobre-estimulación de las formas constitutivas eNOS y nNOS (isoformas endotelial y neuronal respectivamente) (3, 4).

Esta actividad citotóxica del $\bullet\text{NO}$, se debe fundamentalmente a la formación de especies intermediarias secundarias tales como el peroxinitrito¹ ($\text{ONOO}^-/\text{ONOOH}$) y el radical dióxido de nitrógeno ($\bullet\text{NO}_2$), los cuales tienen una reactividad y toxicidad mayores a las presentadas por el propio $\bullet\text{NO}$. La formación de especies reactivas del nitrógeno (RNS) requiere la presencia de oxidantes tales como el anión superóxido ($\text{O}_2^{\bullet-}$), metales de transición y peróxido de hidrógeno (H_2O_2) (3) y la sobreproducción de las mismas está relacionada con un número importante de patologías (5-10).

Una de las huellas moleculares de la reacción de RNS con biomoléculas es la nitración de tirosinas proteicas, una modificación postraduccional mediada por oxidantes derivados del $\bullet\text{NO}$, como el peroxinitrito y el $\bullet\text{NO}_2$, y constituye la sustitución de un átomo de hidrógeno por un grupo nitro ($-\text{NO}_2$, + 45 Da) en la posición 3 del anillo fenólico de la tirosina, para dar 3-nitrotirosina (3-NT). Trabajos pioneros enfocados en el estudio de la química de proteínas realizados por Sokolovsky y colaboradores en la década del 60 (11), demostraron que la nitración de tirosinas producida por agentes

¹ Los nombres recomendados por IUPAC para el peroxinitrito anion (ONOO^-) y el ácido peroxinitroso (ONOOH) ($\text{pK}_a = 6.8$) son oxoperoxonitrato (1-) y oxoperoxonitrato de hidrógeno, respectivamente. El término peroxinitrito se refiere a la suma de ambas especies.

nitranes como el tetranitrometano (TNM) resultaba en cambios dramáticos tanto en la estructura como en la función de las proteínas. Sin embargo, recién en la década de los 90 (12, 13), se pudo determinar la importancia biológica de la nitración de tirosinas proteicas, luego del reconocimiento de la formación de especies fuertemente oxidantes y nitrantes durante la oxidación biológica del $\bullet\text{NO}$, y la implicancia de sus radicales derivados en diversos procesos fisiopatológicos (12-16).

La formación de 3-NT fue demostrada por primera vez *in vivo* por Ohshima y colaboradores (17) que determinaron el aumento de niveles plasmáticos de 3-NT y su presencia en orina, luego de la administración a ratas de agentes nitrantes (TNM), lo cual llevo a definir a la 3-NT como un marcador de reacciones de nitración endógenas (17, 18).

Otra importante evidencia de que las reacciones de nitración eran factibles en sistemas biológicos fue reportada por Ischiropoulos en 1992 donde se demostró que el 4-hidroxifenilacetato, un análogo de la tirosina agregado exógenamente, era nitrado por las especies nitrantes producidas por macrófagos alveolares activados de rata, indicando que la formación de oxidantes en dichas células podría contribuir a la respuesta inflamatoria e inmune celular (13).

En un importante trabajo realizado por Beckman y colaboradores (19) se determinó la presencia de 3-NT en lesiones ateroscleróticas de cortes de arterias coronarias provenientes de autopsias de pacientes humanos con enfermedad coronaria, lo cual confirmó que oxidantes como el peroxinitrito provenientes del $\bullet\text{NO}$ son generados en la aterosclerosis humana y pueden ser responsables de la patogénesis.

A partir de entonces, la nitración de tirosinas proteicas producida por un número importante de intermediarios nitrantes de relevancia biológica fue establecida de manera sistemática tanto *in vitro* como *in vivo* (3, 20-25).

2.1.2 Consecuencias biológicas

La nitración de tirosinas proteicas es un proceso bioquímico relativamente selectivo y específico siendo en términos generales un proceso de bajo rendimiento, dado que son pocas las proteínas que se nitrán, y dentro de estas proteínas, no todas las tirosinas son capaces de nitrarse (26).

En efecto, los niveles reportados de 3-NT proteica en tejidos en condiciones inflamatorias, se encuentran en el rango de 10-100 pmol/mg de proteína, lo cual corresponde de 1-5 residuos de tirosina nitrados sobre un total de 10.000 tirosinas (100-500 $\mu\text{mol/mol}$) (3, 27).

El grado de modificación de tirosinas por nitración es comparable al de otras modificaciones oxidativas tales como la cloración (28, 29), bromación (30), e hidroxilación (31, 32) para dar los productos 3-cloro, 3-bromo y 3-hidroxitirosina respectivamente. Dichas modificaciones en proteínas pueden coexistir con la nitración de tirosina en relaciones variables, dependiendo del mecanismo de nitración que predomine. Otra modificación postraducciona (enzimática) relevante es la fosforilación de tirosina y, si bien no hay datos cuantitativos suficientes para hacer una comparación directa, es razonable plantear que ambos procesos pueden llegar a valores globales de rendimiento comparables (33).

El aumento de los niveles basales de 3-NT encontrados en condiciones normales, ha sido considerado una huella de daño nitrooxidativo *in vivo* tanto en modelos animales como en patologías humanas y se ha revelado como un fuerte biomarcador predictor de riesgo y progresión de enfermedad en condiciones, tales como los procesos inflamatorios agudos y crónicos, enfermedades cardiovasculares (34-36), neurodegenerativas (35, 37), cáncer y complicaciones de la diabetes, entre otros (3, 27, 38-40). Un trabajo reciente revisa exhaustivamente la relación del $\bullet\text{NO}$ y el peroxinitrito con diversos procesos fisiopatológicos (41).

Diversas patologías del sistema cardiovascular han sido asociadas con una producción aumentada de $\cdot\text{NO}$ y oxidantes derivados (35, 42), así como con una disminución de los mecanismos antioxidantes detoxificadores lo cual lleva a un estrés nitroxidativo (21). Una consecuencia importante de la presencia de estas especies oxidantes es la nitración de proteínas, ya sea mediada por peroxinitrito o por hemoperoxidasas (21). Se han detectado numerosas proteínas nitradas en los distintos compartimentos del sistema vascular, tanto en proteínas plasmáticas; (fibrinógeno (43, 44), plasmina (45), APO-A1 (46) y APO-B (47)), como de la pared vascular (ciclo-oxigenasa (48), prostaciclina sintasa (49) y Mn-SOD (50)) y miocardio (creatín quinasa fibrilar (51), α -actinina (52) y Ca^{2+} -retículo-sarcoplásmico ATPasa (SERCA) (53))

El rol de la 3-NT como factor emergente de enfermedad cardiovascular se ha demostrado en un trabajo que muestra una fuerte asociación entre los niveles de 3-NT y la enfermedad coronaria arterial (39). De una manera similar, se ha demostrado que la nitración de tirosinas proteicas juega un papel fundamental en el establecimiento y progresión de un número importante de enfermedades neurodegenerativas (35, 37, 54). La formación de 3-NT aparece como un evento temprano en la formación de las lesiones presentes en enfermedades como esclerosis lateral amiotrófica (ALS) (55) Parkinson (56-58) y Alzheimer (58-61). Diversas proteínas relacionadas con el proceso de neurodegeneración se encuentran nitradas y con su función o su conformación tridimensional alterada, como es el caso de la Mn-SOD y la subunidad liviana del neurofilamento en ALS, la α -sinucleína (62) y la tirosina hidroxilasa en enfermedad de Parkinson (63) y la proteína tau (τ) en enfermedad de Alzheimer (54, 58, 64).

Recientemente se demostró que los niveles de 3-NT en el líquido cefalorraquídeo se encuentran aumentados en pacientes con accidente cerebro vascular comparados con el grupo control, lo cual refuerza el concepto de que los oxidantes derivados del $\cdot\text{NO}$ como el peroxinitrito, juegan un importante papel en la patogénesis de un número

importante de enfermedades, lo cual puede utilizarse como estrategia farmacológica para el tratamiento de estas y otras enfermedades relacionadas (35).

La nitración de tirosinas proteicas puede afectar la función de las proteínas *in vitro* e *in vivo* ya sea a través de una pérdida o una ganancia de función. La adición de un grupo $-NO_2$ a una tirosina agrega un voluminoso grupo que si se ubica en un residuo crítico de tirosina puede afectar tanto la conformación tridimensional de la proteína como la función de la misma; generar impedimentos estéricos e incluso afectar las cascadas de fosforilación que involucran a una tirosina particular. Sin embargo, para que la pérdida de función adquiriera significancia biológica se requiere un importante grado de nitración de tirosinas críticas, lo cual, usualmente, es poco probable. Un notable y bien documentado ejemplo de alteración de la función proteica es la inactivación por nitración de la enzima superóxido dismutasa de manganeso (Mn-SOD) (3, 50, 65, 66), una enzima antioxidante mitocondrial crítica, modificada en condiciones inflamatorias. La nitración de la Mn-SOD ocurre sitio-específicamente en la tirosina 34, que se encuentra a 5 Å del sitio activo, donde el átomo de manganeso juega un papel clave en el proceso de la nitración (67-70). Otras proteínas en las cuales se ha reportado que la nitración puede causar una pérdida significativa de actividad *in vivo* tanto en modelos celulares como animales de enfermedad son la actina (anemia falciforme) (71), prostaciclina sintasa (disfunción vascular) (49, 72); tirosina hidroxilasa (en enfermedad de Parkinson) (56, 63, 73), y la prostaglandina endoperoxido sintasa-2 (PHS-2) (inflamación vascular) (74)

Alternativamente, y en un concepto más novedoso, la nitración de tirosinas puede llevar a la ganancia de una función previamente inexistente, y en cuyo caso una pequeña fracción de tirosinas modificadas, puede provocar un efecto biológico sustantivo. Un importante ejemplo de ganancia de función es el citocromo c que adquiere una fuerte actividad peroxidasa luego de la nitración de tirosinas (75-77), protein quinasa $C\epsilon$ (translocación e interacción con RACK2) (78) y glutatión S-transferasa (activación de la enzima) (79). De una manera similar, la nitración de

fibrinógeno puede acelerar los pasos de nucleación en la formación de fibras, y por lo tanto estimular la formación del coágulo sanguíneo (80) o la nitración de la proteína α -sinucleína puede dar lugar a la formación de agregados en los cuerpos de Lewy (81, 82). Otro ejemplo interesante es el observado en la proteína de shock térmico, hsp90, que es una chaperona capaz de cumplir múltiples funciones. Normalmente actúa inhibiendo las vías pro-apoptóticas, sin embargo este mecanismo de control se pierde cuando la hsp90 se nitra (NO_2 -hsp90). Es decir, que la nitración de la proteína, inhibe en parte la actividad de la misma, pero esta pérdida de actividad promueve la activación de vías apoptóticas, y es en ese sentido que el efecto final a nivel celular, corresponde a una ganancia de función pro-apoptótica (83). La Tabla I muestra el efecto de la nitración en algunas proteínas seleccionadas.

En suma, la nitración sitio-específica de tirosinas puede actuar como un mecanismo patogénico inactivando proteínas catalíticas, generando nuevas actividades tóxicas, o promoviendo ensamblajes aberrantes en proteínas estructurales en dichas enfermedades neurodegenerativas (58, 84).

Tabla I. Efecto de la nitración en algunas proteínas seleccionadas

Proteína	Función normal	Efecto de la nitración	Ref.
Citocromo c	Tranferencia de electrones	Actividad peroxidasa aumentada	(75, 76)
	Apoptosis	Disminución en la activación del apoptosoma, translocación al citosol y nucleo	(85) (86)
Fibrinógeno	Coagulación	Mayor agregación	(43)
Protein quinasa C ϵ	Quinasa serina treonina	Translocación y activación	(78)
Glutatión S-transferasa 1	Actividad glutatión peroxidasa	Actividad aumentada	(79)
α -sinucleína	Proteína pre-sináptica	Mayor agregación	(82)
neurofilamento L	Estructura axonal	Inhibe ensamblaje del NF	(87)
NGF	Factor neurotrófico	Apoptosis neuronal	(88)
Mn-SOD	Dismutación del superóxido	Inactivación	(24)
Prostaciclina Sintasa	Síntesis prostaciclina	Inactivación	(72)
Tirosina hidroxilasa	Síntesis de L-DOPA	Inactivación	(89)
PGH sintasa	Síntesis de PGH-2	Inactivación	(90, 91)
Glutamina Sintetasa	Condensación de glutamato y amonio	Inactivación	(92)
Ribonucléotico reductasa	Reducción de ribonucléotidos	Inactivación	(93)
Glutation reductasa	Reducción de GSSG	Inactivación	(94)
Citocromo P450	Metabolismo de xenobióticos	Inactivación	(95)
Ornitina decarboxilasa	Síntesis de putrescina	Inactivación	(96)
Protein quinasa C	Quinasa serina treonina	Inactivación	(97)
Complejo II	Transporte de electrones	Desacople de transporte	(98)
FGF-1	Factor de crecimiento	Inactivación	(99)

Modificada de (33).

Además de los cambios funcionales que puede provocar, la presencia de un grupo $-\text{NO}_2$ en el residuo de tirosina puede generar la producción de autoantígenos y disparar respuestas inmunitarias (3, 100, 101), y de hecho un método comúnmente utilizado para detectar proteínas nitradas en tejidos es mediante el uso de anticuerpos mono y policlonales anti-nitrotirosina (25, 102). En un trabajo realizado por Thomson y colaboradores (103) en pacientes con daño agudo pulmonar postraumático se aislaron inmunoglobulinas anti-3-NT, demostrando que el estrés nitroxidativo fue capaz de disparar una respuesta inmunitaria contra las proteínas nitradas durante el daño

pulmonar. La nitración puede también afectar cascadas de fosforilación (104, 105), y procesos de transducción de señales dependientes de tirosina quinasas, o promover la degradación de las proteínas por el proteosoma. Se ha propuesto la existencia de sistemas de reparación de las proteínas nitradas a través de una actividad “denitrasa” (106, 107), sin embargo esto es aún motivo de debate (108) (Figura 2.1).

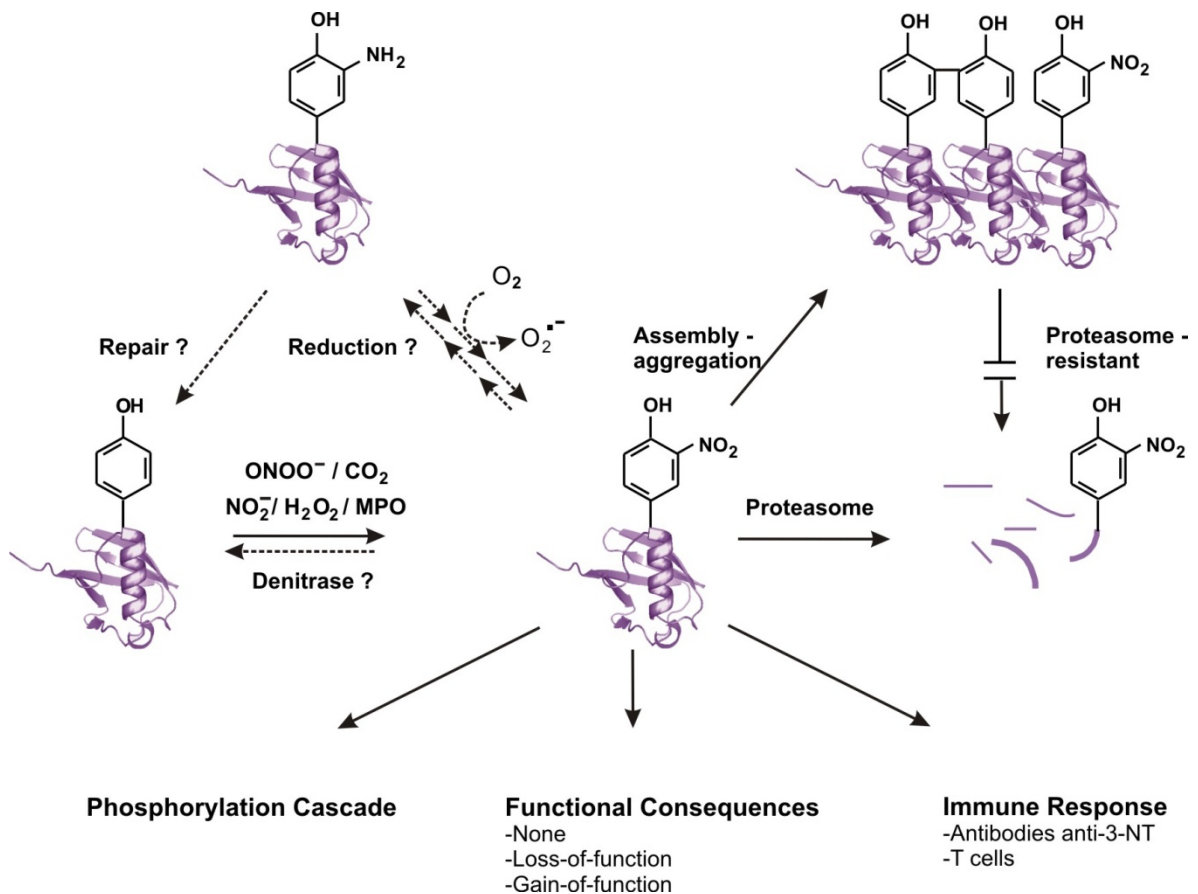


Figura 2.1 Formación y consecuencias de la nitración de tirosinas proteicas.
 Extraído de (33).

2.1.3 Aspectos cuantitativos

La cuantificación en muestras biológicas de 3-NT, implica un desafío experimental importante que ha requerido de profundas investigaciones. Se han desarrollado numerosas técnicas con el objetivo de poder determinar los niveles de 3-NT *in vivo*, así como los sitios de nitración. Estudios cuantitativos y proteómicos de los

niveles de 3-NT en proteínas muestran la presencia de niveles basales de nitración en condiciones normales que son aumentados dramáticamente en diversas patologías o modelos de enfermedad (21, 109). Existe un importante número de técnicas para la separación, detección y cuantificación de 3-NT en muestras biológicas, las cuales pueden agruparse en métodos basados o no en técnicas de espectrometría de masa (MS). Las técnicas independientes de espectrometría de masa incluyen las técnicas inmunológicas, basadas en las propiedades inmunogénicas de las proteínas nitradas (102); y técnicas de cromatografía líquida de alta performance (HPLC) acopladas a distintos sistemas de detección.

La detección inmunohistoquímica de 3-NT en tejidos fijados y células es una técnica altamente utilizada y de gran sensibilidad, incluso mayor que la obtenida por Western-Blot de homegenados de proteínas (110). Los métodos basados en anticuerpos son poco cuantitativos con excepción de el ensayo inmunoabsorbente ligado a enzimas (ELISA) (111, 112) desarrollado a partir de estándares de albúmina nitrada.

La hidrólisis total de proteínas es un método fundamental para la cuantificación de 3-NT, la cual puede ser ácida (113), alcalina (114) o proteolítica (115, 116). En relación a la proteólisis total en medio ácido es importante considerar la posibilidad de nitración por NO_2^- en medio ácido durante el procedimiento, lo cual debe ser descartado realizando controles apropiados.

Las técnicas de HPLC permiten la separación de la 3-NT de la tirosina libre dada su naturaleza más hidrofóbica. Acoplados a la separación por HPLC, pueden utilizarse diversos métodos de detección como UV-vis, fluorimétrica y electroquímica (109).

Los métodos basados en espectrometría de masa, ya sea asociados a cromatografía gaseosa (GC-MS) o líquida (LC-MS) se aplican para medir 3-NT, y pueden requerir o no de derivatización de la misma. Ambas técnicas aceptan la incorporación de isotópos marcados como estándares internos lo cual permite realizar medidas cuantitativas. El análisis global de la generación de 3-NT en proteínas de muestras humanas o modelos animales de enfermedad es un parámetro adecuado para

correlacionar el desarrollo de la enfermedad, farmacología o estrés nitroxidativo (22). Un estudio más profundo implicaría la identificación específica de la tirosina modificada dentro de cada proteína. En esta situación, la proteína se somete a hidrólisis proteolítica, por ejemplo con tripsina y se analizan los péptidos obtenidos por MALDI-TOF (75). La nitración en estos casos se confirma mediante electroforesis en dos dimensiones con anticuerpos anti-3-NT antes del análisis por MS.

Estudios proteómicos para identificar proteínas nitradas fueron aplicados por primera vez en un modelo de inflamación de ratas tratadas con lipopolisacárido (LPS) utilizando electroforesis en dos dimensiones y western blot con anticuerpos anti-3-NT para seleccionar las proteínas nitradas. Dichos autores fueron capaces de identificar 40 proteínas nitradas mediante análisis de MALDI-TOF de los péptidos obtenidos de la digestión con tripsina, sin embargo no pudieron mapear los sitios de nitración (117). Sacksteder y colaboradores detectaron proteínas nitradas endógenamente en cerebro de ratón utilizando análisis de LC-MS/MS en dos dimensiones. De las 7792 proteínas identificadas mapearon 29 proteínas que se encontraban nitradas en residuos de tirosina, las cuales preferentemente eran mitocondriales o del citoesqueleto (118). Posteriormente, el mismo grupo utilizando el método de enriquecimiento de 3-NT identificó los sitios de nitración de 102 proteínas en cerebro de ratón (119). Actualmente, se siguen desarrollando métodos para el enriquecimiento, detección y cuantificación de 3-NT en muestras biológicas (120).

2.2 Especies oxidantes y nitrantes

Durante el metabolismo aerobio normal se producen radicales libres como el $O_2^{\cdot-}$ y el $\cdot NO$ que cumplen funciones tanto de señalización como de defensa del organismo. El oxígeno es esencial para los organismos aeróbicos pero a su vez es fuente continua de especies oxidantes potencialmente tóxicas. Bajo condiciones fisiológicas, los organismos aeróbicos consumen casi la totalidad del oxígeno

molecular (O_2) en la cadena de transporte mitocondrial (121). Durante este proceso el oxígeno es reducido completamente a agua por cuatro electrones, sin la liberación de intermediarios del oxígeno parcialmente reducidos. Sin embargo, hay una fracción del O_2 (0.1-0.5%) que se reduce monovalentemente para dar $O_2^{\cdot-}$ y subsiguientemente H_2O_2 . Este último no es un radical libre (no tiene electrones desapareados), pero es un agente oxidante y da lugar al radical hidroxilo ($\cdot OH$) rápidamente (122).

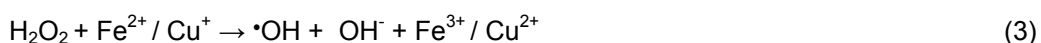
Además de la cadena de transporte de electrones mitocondrial, otras fuentes celulares y tisulares de $O_2^{\cdot-}$ son las enzimas xantino oxidasa (XO), NADPH oxidasas, la NOS desacoplada y el "redox cycling" de drogas. Diferentes perturbaciones en la homeostasis celular dan lugar a la sobreproducción de $O_2^{\cdot-}$ y H_2O_2 y otras especies estrechamente relacionadas como el $\cdot OH$ (123, 124). Un número importante de moléculas derivadas del $O_2^{\cdot-}$ y del $\cdot NO$ son altamente reactivas y pueden ser clasificadas de acuerdo al precursor del cual derivan en especies reactivas del oxígeno (ROS) y especies reactivas del nitrógeno (RNS), las cuales presentan propiedades físico-químicas características que deben ser consideradas al evaluar su reactividad y relevancia en sistemas biológicos. Las ROS incluyen al $O_2^{\cdot-}$, H_2O_2 , $\cdot OH$, radical carbonato ($CO_3^{\cdot-}$) y el ácido hipocloroso (HOCL).

Las RNS incluyen al $\cdot NO$, $\cdot NO_2$, N_2O_3 , N_2O_4 , HNO y al peroxinitrito.

2.2.1 Radical Superóxido

El radical superóxido ($O_2^{\cdot-}$) es una especie de corta vida media que deriva de la reducción monovalente del oxígeno molecular y puede actuar oxidando ($E^{0'} O_2^{\cdot-}/H_2O_2 = 0.94 V$) o reduciendo ($E^{0'} O_2 / O_2^{\cdot-} = -0.33 V$) a diferentes blancos celulares. A pH fisiológico se encuentra principalmente bajo la forma aniónica ya que tiene un pKa de 4,8. Debido a su naturaleza cargada, tiene una capacidad de difusión limitada a través de las membranas biológicas, y sus acciones están generalmente restringidas a su sitio de producción. En sistemas biológicos, la difusión del $O_2^{\cdot-}$ se encuentra limitada

proteínas, lípidos y ácidos nucleicos (DNA) mediante su adición para formar compuestos hidroxilados o por rápida abstracción de un electrón. Debido a su elevada reactividad (muchas reacciones son difusionales), la vida media del $\cdot\text{OH}$ es muy corta, por tanto ejerce su acción citotóxica sobre blancos muy cercanos al sitio de su producción. La generación de $\cdot\text{OH}$ tiene lugar a través de la reacción de Fenton (Ec. 3) e involucra la participación de centros metálicos de transición en estado reducido como el Fe^{2+} y el Cu^+ , que son regenerados en la reacción de Haber-Weiss (Ec. 4), o por la homólisis del peroxinitrito (ver más adelante).



2.2.4 Oxido nítrico

El óxido nítrico ($\cdot\text{NO}$) es un radical libre relativamente estable y poco reactivo ($E^{0'} \cdot\text{NO} / \text{NO}^- = 0.39 \text{ V}$) (133) capaz de cumplir funciones de señalización celular o actuar como mediador citotóxico a través de la formación de especies reactivas secundarias que presentan una reactividad mucho mayor que el propio $\cdot\text{NO}$ (134).

Las reacciones directas del $\cdot\text{NO}$ con biomoléculas involucran *i*) su función señalizadora a través de la reacción reversible con la enzima guanilato ciclasa, que da lugar a la síntesis de GMP cíclico, *ii*) la inhibición reversible de la respiración mitocondrial al unirse al complejo citocromo c oxidasa, *iii*) la reacción con el $\text{O}_2^{\cdot-}$ para formar peroxinitrito y *iv*) la acción antioxidante al reaccionar con radicales lipídicos cortando las cadenas de propagación. Existen también acciones indirectas del $\cdot\text{NO}$ que dependen de reacciones de oxidantes derivados del $\cdot\text{NO}$ (ver más adelante) y resultan en la modificación química permanente de biomoléculas tales como proteínas, ácidos nucleicos y lípidos (Tabla II). El $\cdot\text{NO}$ puede reaccionar con oxígeno dando lugar a la

formación de especies reactivas como el $\bullet\text{NO}_2$, un proceso que es más eficiente en entornos hidrofóbicos, así como nitrito (NO_2^-) y nitrato (NO_3^-).

Dada su naturaleza neutra e hidrofobicidad, es una molécula capaz de atravesar libremente y concentrarse en las membranas. A partir de $\bullet\text{NO}$, se pueden formar otras RNS tales como el N_2O_3 , que actúan principalmente mediando reacciones de nitrosación de tioles (Tabla II).

2.2.5 Dióxido de nitrógeno

El dióxido de nitrógeno ($\bullet\text{NO}_2$) puede producirse por la autooxidación del $\bullet\text{NO}$ (Ec. 5), la reacción del H_2O_2 con NO_2^- catalizada por metaloperoxidasas como la mieloperoxidasa (MPO) (135, 136) o por la homólisis del ácido peroxinitroso. El dióxido de nitrógeno da lugar a la formación de NO_2^- y NO_3^- (Ecs. 6 y 7), el cual puede a su vez actuar como fuente de $\bullet\text{NO}$ (137).

El $\bullet\text{NO}_2$ es un potente oxidante formado en sistemas biológicos ($E^0 \bullet\text{NO}_2/\text{NO}_2^- = 0.99 \text{ V}$) (138) capaz de concentrarse en membranas y reaccionar con biomoléculas, participando en reacciones de transferencia electrónica, recombinación con otros radicales, adición a dobles enlaces y abstracción de átomos de hidrógeno a compuestos insaturados, fenoles y tioles (135). Es especialmente importante en las reacciones de nitración de tirosinas proteicas y también participa en procesos de oxidación y nitración lipídica.



2.2.6 Peroxinitrito

El peroxinitrito es un agente fuertemente oxidante ($E^{0'} \text{ ONOOH/ NO}_2^- = 1,4 \text{ V}$) (139) formado *in vivo* por la reacción controlada por difusión entre el $\text{O}_2^{\bullet-}$ y el $\bullet\text{NO}$ ($k = 4\text{-}16 \times 10^9 \text{ M}^{-1}\text{s}^{-1}$) (127, 128, 140), debiéndose las diferencias a que las constantes reportadas fueron determinadas por técnicas distintas (Ec. 8).



El peroxinitrito anión (ONOO^-) está en equilibrio con el ácido peroxinitroso (ONOOH) ($\text{pK}_A = 6.8$), el cual luego de su homólisis da lugar a la formación de los radicales $\bullet\text{OH}$ y $\bullet\text{NO}_2$ en un rendimiento de 30%, y NO_3^- en un rendimiento del 70%. El peroxinitrito es una especie de corta vida media ($k_{\text{homólisis}} = 0.9 \text{ s}^{-1}$ a 37°C y $\text{pH } 7,4$ y $0,6 \text{ s}^{-1}$ a 25°C) (Ec. 9) que puede atravesar libremente las membranas en su forma protonada o a través de canales aniónicos en su forma desprotonada.



El peroxinitrito, puede reaccionar con diversas biomoléculas tales como anhídrido carbónico (CO_2) (141), metales de transición y tioles (3, 142). A través de estos procesos el peroxinitrito participa en reacciones de oxidación de tioles (reacción directa) o de nitración de tirosinas (reacción dependiente de sus radicales secundarios) (Figura 2.2).

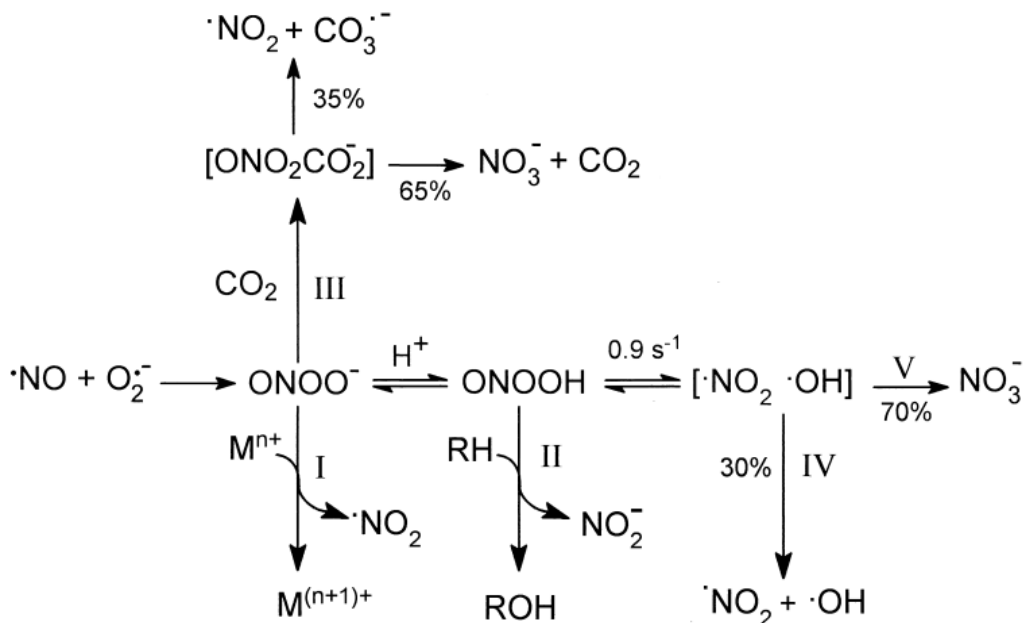


Figura 2.2 Destinos del peroxinitrito. El peroxinitrito puede reaccionar directamente con diversos blancos en oxidaciones mediadas por uno (metales de transición, I) o dos electrones (tioles, II); con el CO_2 , para formar el aducto nitrosoperoxocarboxilato (III) que se descompone para dar los radicales $\text{CO}_3^{\cdot-}$ y $\cdot\text{NO}_2$. El ácido peroxinitroso puede sufrir homólisis para rendir los radicales $\cdot\text{OH}$ y $\cdot\text{NO}_2$ con un rendimiento de 30 % (IV) o rearrreglar para dar NO_3^- con un rendimiento de 70%. (V) Extraído de (142).

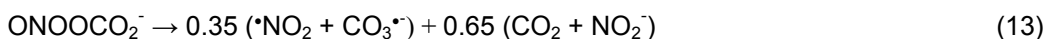
2.2.7 Radical carbonato

El radical carbonato ($\text{CO}_3^{\cdot-}$) puede formarse a partir de la homólisis del aducto nitrosoperoxocarboxilato (ONOOCO_2^-) donde también se forma $\cdot\text{NO}_2$; o del peroximonocarbonato (HCO_4^-) en presencia de reductores (Ecs. 10 y 11) (143, 144).



El HCO_4^- es una especie con una reactividad propia similar al ONOOCO_2^- , y en los últimos años ha sido motivo de debate en relación a cual es la especie precursora

en la formación del $\text{CO}_3^{\bullet-}$ durante la actividad peroxidática de la SOD. Algunos autores postularon la oxidación del CO_2 y del bicarbonato (HCO_3^-) (145, 146) mientras que Augusto y colaboradores han propuesto más recientemente la participación intermediaria del HCO_4^- (143, 144). En sistemas biológicos es muy relevante la reacción del peroxinitrito con CO_2 para dar ONOOCO_2^- , a partir del cual se forman estas dos especies fuertemente oxidantes (147) (Ec. 12).



El radical carbonato ($\text{CO}_3^{\bullet-}$) puede formarse por la oxidación por un electrón de los iones carbonato (CO_3^-) o HCO_3^- , siendo el radical $\cdot\text{OH}$ uno de los pocos oxidantes capaces de realizar esta oxidación, aunque de una manera poco eficiente (135).

El radical $\text{CO}_3^{\bullet-}$ tiene un $\text{pKa} < 0$ por lo que en sistemas biológicos siempre se encuentra en la forma aniónica (148). Es un oxidante fuerte ($E^0: \text{CO}_3^{\bullet-}/\text{HCO}_3^- = 1,78\text{V}$) capaz de oxidar una gran variedad de biomoléculas que incluyen alcoholes y aminos primarios, tioles y fenoles, amino ácidos como metionina y cisteína y tirosina (en este último promueve la oxidación por un electrón), complejos metálicos e iones inorgánicos entre otros (135). Dada su naturaleza cargada es incapaz de atravesar las membranas biológicas y por lo tanto sus acciones van a estar limitadas a sus sitios de formación.

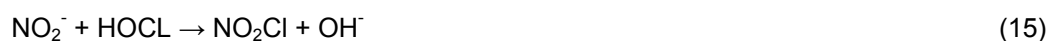
2.2.8 Acido hipocloroso y cloruro de nitrilo

Bajo condiciones inflamatorias, la MPO derivada de los neutrófilos cataliza la oxidación del cloruro (Cl^-) por H_2O_2 generando el oxidante hipoclorito (ClO^-), que se encuentra en equilibrio con el ácido hipocloroso (HOCl) ($\text{pKa} \sim 7.5$) (Ec. 14) El HOCl es capaz de reaccionar con diversas biomoléculas, particularmente con tioles (149-

151) y con grupos amino para formar cloraminas, que mantienen la capacidad oxidante del hipoclorito pero son menos reactivos (152).



El cloruro de nitrilo (NO_2Cl) se forma por la reacción del hipoclorito (HOCl), formado por la acción de la MPO con NO_2^- , una especie capaz de participar en reacciones de oxidación, nitración y cloración de tirosina (153) así como en la modificación de bases del DNA (154) (Ec. 15).



2.2.9 Integración de las rutas de ROS y RNS

La figura 2.3 muestra las principales rutas de formación y reacciones de las especies reactivas del oxígeno y el nitrógeno. Hay una ruta que parte del O_2 (ROS) y otra que parte del $\cdot\text{NO}$ (RNS), y también se muestran las interconexiones entre ambas rutas. Varias de estas especies oxidantes tienen sistemas enzimáticos de detoxificación.

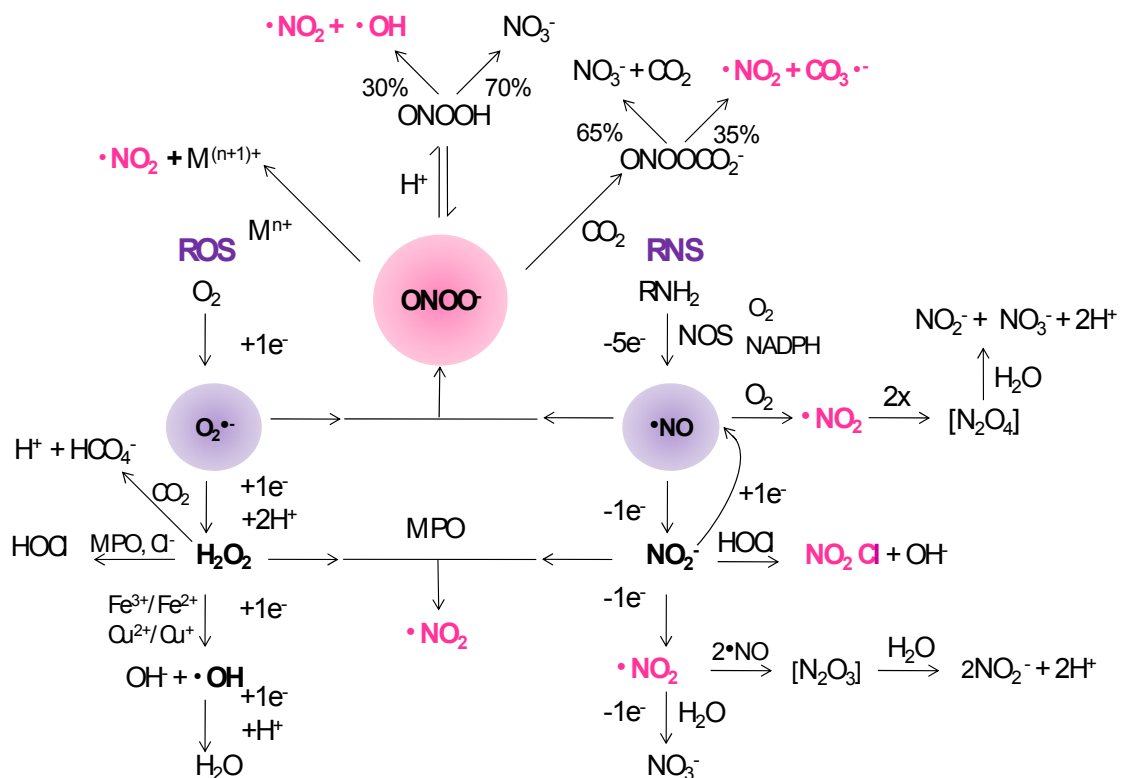
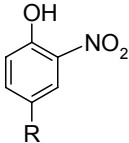
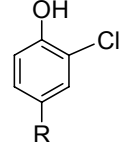
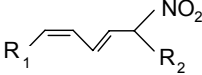
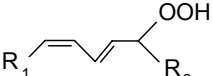
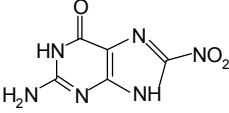


Figura 2.3 Formación de especies oxidantes y nitrantes a partir de especies reactivas del oxígeno (ROS) y nitrógeno (RNS), y sus puntos de interconexión.

En diversas condiciones fisiopatológicas, existen en sistemas biológicos, una formación excesiva de ROS y RNS las cuales pueden causar modificaciones y/o daño nitrooxidativo (21) a un número importante de biomoléculas. Estas modificaciones incluyen oxidación de amino ácidos proteicos tales como cisteína, metionina y triptófano (H_2O_2 , $HOCl$, $ONOO^-$, N_2O_4 , NO_2Cl) (155, 156); nitrosación de cisteína (N_2O_3 , HNO) (157-159); nitración de tirosinas ($\bullet NO_2$, peroxinitrito); cloración de tirosinas ($HOCl$); oxidación y nitración de lípidos ($\bullet OH$, $\bullet NO_2$, $ONOOH$) (160-162) y finalmente oxidación, nitración (sistema $MPO/H_2O_2/NO_2^-$ y radicales derivados del peroxinitrito) y reacciones de desaminación de bases del DNA (163-165), así como rupturas en la doble hebra del DNA (radicales derivados del peroxinitrito) (166-168) (Tabla II).

Tabla II. Modificaciones oxidativas representativas en biomoléculas

Modificación	Especie Reactiva	Principales Productos	Referencia
Nitración de tirosina	$\bullet\text{NO}_2$, ONOO^- NO_2Cl , HOCl	3-NO₂-Tyr 	(3) (153)
Cloración de tirosina	NO_2Cl , $\text{MPO}/\text{H}_2\text{O}_2/\text{Cl}^-$	3-Cl-Tyr 	(153)
Oxidación de amino ácidos:	H_2O_2 , $\bullet\text{OH}$ ONOO^- , N_2O_4 , NO_2Cl	Cys-S-S-Cys ^a , Cys-SO _n H ^b 3,3'-ditirosina 3-hidroxi-tirosina 3,4-dihidroxi-fenilalanina Metionina sulfóxido quirunenina, formiquirunenina	(155)
Cisteína Tirosina			
Metionina Tryptofano			
Nitrosación de cisteína	N_2O_3 , HNO , $\bullet\text{NO}$	Cys-SNO	(158)
Oxidación y nitración de lípidos	$\bullet\text{OH}$, $\text{ROO}\bullet$ $\bullet\text{NO}_2$, ONOO^- , HNO_2 , N_2O_3	Nitro-lípido  Hidroperóxido lipídico 	(160)
Modificación del DNA: Nitración / Oxidación	ONOO^- , $\bullet\text{NO}_2$, $\text{MPO}/\text{H}_2\text{O}_2/\text{NO}_2^-$ NO_2Cl , HClO N_2O_3 $\bullet\text{OH}$, ONOO^-	8-nitroguanosina 	(154) (164) (165) (168) (167)
Desaminación Ruptura de hebras			

^a disulfuro de cisteína

^b ácido sulfénico (n=1), sulfínico (n=2) y sulfónico (n=3)

2.3 Mecanismos de nitración de tirosinas

La nitración de tirosinas proteicas puede ocurrir biológicamente por una variedad de rutas, que generalmente involucran una química dependiente de radicales libres, como es el caso de la nitración mediada por peroxinitrito y hemoperoxidasas que requieren la formación de $\cdot\text{NO}_2$ y radical tirosilo ($\cdot\text{Tyr}$). La formación de 3-NT implica la ocurrencia de dos reacciones consecutivas: 1) La oxidación de la tirosina por un electrón para formar el radical $\cdot\text{Tyr}$ y 2) La reacción del $\cdot\text{NO}_2$ con el radical $\cdot\text{Tyr}$ en una reacción controlada por difusión para dar el producto final de la reacción (Figura 2.4, reacciones 1 y 2). Existen varios oxidantes capaces de promover la oxidación de la tirosina, que incluyen a los radicales derivados del peroxinitrito, $\cdot\text{OH}$, $\cdot\text{NO}_2$ y $\text{CO}_3^{\cdot-}$, el compuesto I y II de las hemoperoxidasas como la MPO y complejos oxo-metálicos de transición (3, 169). Uno de los objetivos de esta tesis, es estudiar si los radicales derivados del proceso de la lipoperoxidación como el radical peroxilo ($\text{LOO}\cdot$) es capaz de llevar a cabo la reacción de oxidación de la tirosina.

La oxidación de la tirosina por $\cdot\text{OH}$ a $\cdot\text{Tyr}$ ocurre rápidamente ($k = 1.3 \times 10^{10} \text{ M}^{-1} \text{ s}^{-1}$) pero con un rendimiento bajo (5%) (170), siendo el producto mayoritario un aducto $\text{Tyr-OH}\cdot$, que luego puede parcialmente rendir $\cdot\text{Tyr}$. Por otra parte la oxidación de tirosina por $\cdot\text{NO}_2$ es mucho más lenta ($k = 3.2 \times 10^5 \text{ M}^{-1} \text{ s}^{-1}$, pH 7.5) (171). El radical $\text{CO}_3^{\cdot-}$, es un buen oxidante para la tirosina ($k = 3 \times 10^7 \text{ M}^{-1} \text{ s}^{-1}$) (172) con un rendimiento de $\cdot\text{Tyr}$ importante, y los compuestos I y II de la MPO son capaces de oxidar a la tirosina por un electrón ($k = 2.93 \times 10^5 \text{ M}^{-1} \text{ s}^{-1}$ (173) y $k = 1.57 \times 10^4 \text{ M}^{-1} \text{ s}^{-1}$ (174) respectivamente). Complejos metálicos de transición de bajo peso molecular como las porfirinas de manganeso pueden dar lugar a la formación de un complejo oxo-metálico de alto estado de oxidación (O=Mn^{IV}) que puede a su vez actuar como oxidante de la tirosina ($k = 4.9 \times 10^3 \text{ M}^{-1} \text{ s}^{-1}$ para la porfirina MnTM-2-PyP) (175).

La segunda reacción que habitualmente lleva a la formación de 3-NT depende exclusivamente de la presencia de $\cdot\text{Tyr}$ y $\cdot\text{NO}_2$; dado que este último puede ser

formado durante la homólisis del ácido peroxinitroso, inicialmente se consideraba a la 3-NT como una huella molecular de la formación del mismo. Posteriormente se demostró la existencia de otro mecanismo alternativo de nitración de tirosinas en sistemas biológicos que implica la oxidación del NO_2^- en presencia de H_2O_2 catalizada por MPO y otras hemoperoxidasas (176). Por lo tanto, otras consideraciones experimentales deben tenerse en cuenta para definir si la formación de 3-NT ocurre por mecanismos dependientes o no de peroxinitrito (3).

En efecto, en el mecanismo dependiente de peroxidasas se requiere la presencia de H_2O_2 que es capaz de oxidar a la tirosina y al NO_2^- a $\cdot\text{Tyr}$ y $\cdot\text{NO}_2$ respectivamente, los cuales son necesarios para la formación de 3-NT en la segunda reacción. Tanto el Compuesto I como el Compuesto II de la hemoperoxidasas, son capaces de oxidar a la tirosina en la primera reacción aunque las constantes de velocidad indican que el CI oxida más eficientemente al NO_2^- que a la tirosina, y viceversa para el CII (174, 177).

La formación de 3-NT mediante el mecanismo radicalar ocurre a través de la presencia del radical $\cdot\text{Tyr}$ que puede a su vez combinarse con otras especies para dar productos alternativos. La recombinación de dos radicales $\cdot\text{Tyr}$ da lugar a la formación del dímero 3,3'-ditirosina (Figura 2.4, reacción 5) y alternativamente se puede dar la formación del producto de hidroxilación, 3,4-dihidroxifenilalanina tanto por el $\cdot\text{OH}$ como en presencia de hemoperoxidasas (Figura 2.4, reacción 6) (3).

En un ambiente altamente oxidante, se pueden formar otros productos de oxidación de la tirosina como la isoditirosina, tritirosina y pulcherosina (178).

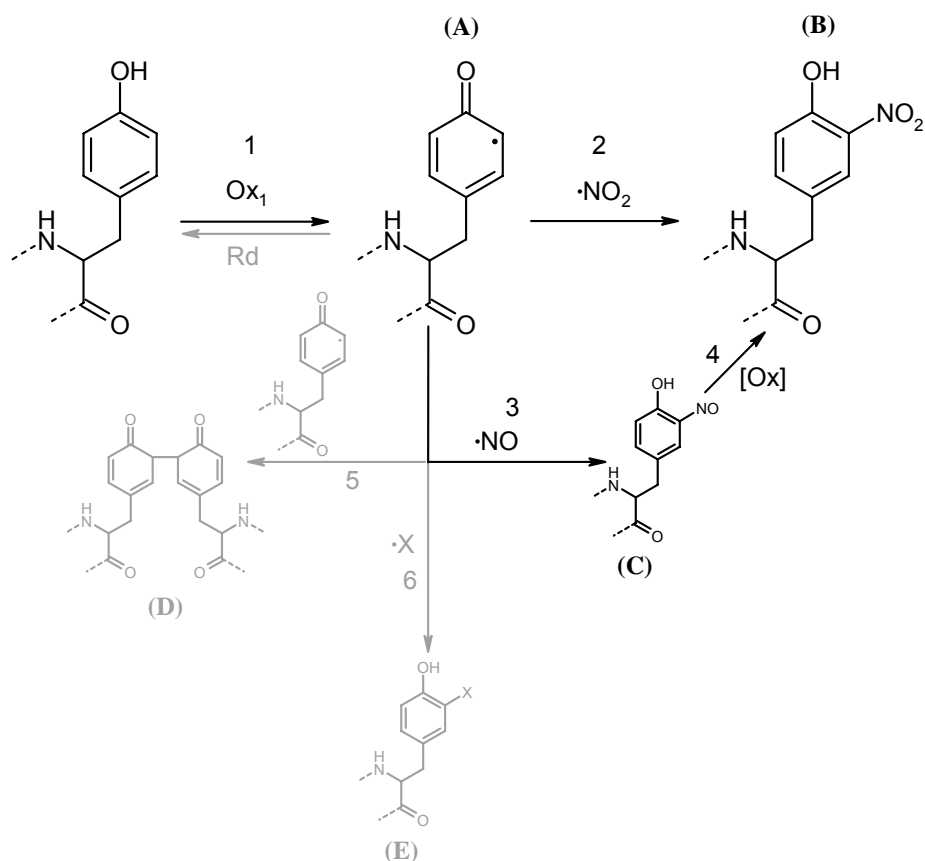
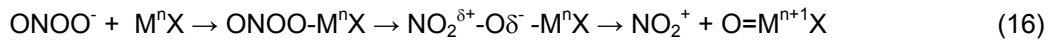


Figura 2.4 Mecanismo de formación de 3-NT y otros productos relacionados.

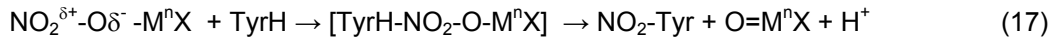
La tirosina puede ser oxidada por un electrón, para dar el radical $\cdot\text{Tyr}$ (A), que en reacción con el $\cdot\text{NO}_2$ da lugar a la formación de 3-NT (B). Alternativamente el $\cdot\text{Tyr}$ puede reaccionar con $\cdot\text{NO}$ para formar 3-nitrosotirosina (C) que evoluciona a 3-NT; recombinarse con otro $\cdot\text{Tyr}$ para formar el dímero 3,3'-ditirosina (D) o sufrir una reacción de adición para formar 3,4-dihidroxifenilalanina (E) Extraído de (169).

Un mecanismo alternativo para la formación de 3-NT es la reacción del radical $\cdot\text{Tyr}$ con $\cdot\text{NO}$ (Figura 2.3, reacción 3), para dar 3-nitrosotirosina la cual es oxidada por dos electrones en dos etapas para dar 3-NT a través de la formación intermedia del radical iminoxilo (3, 179, 180).

Finalmente, las reacciones del peroxinitrito con centros metálicos de transición pueden promover la nitración de tirosinas proteicas, en algunos casos esto podría ocurrir a través de un mecanismo no radicalar llamado nitración aromática electrofílica (3). En este mecanismo, el peroxinitrito forma un complejo con el metal de transición que actúa como un transportador polarizado de catión nitronio (NO_2^+), que luego libera el NO_2^+ por heterólisis (Ec. 16):



Luego el transportador o el propio NO_2^+ pueden oxidar a la tirosina por dos electrones para formar 3-NT a través de la formación de un intermediario (Ecs. 17-18):



La relevancia biológica de este mecanismo no está definida.

El NO_2Cl formado en la reacción catalizada por MPO del HOCl y NO_2^- (Figura 2), también podría nitrar a través de un mecanismo de nitración aromática electrofílica (153), aunque su relevancia en sistemas biológicos es muy poco probable (3, 181).

2.4 Determinantes fisicoquímicas de la nitración de tirosinas proteicas

La abundancia natural de la tirosina en las proteínas es de 3-4% de los amino ácidos totales, lo cual significa que una proteína contiene varios residuos de tirosina. Sin embargo los estudios de mapeo, muestran que solo se nitrán 1-2 de las tirosinas totales, y todavía no están claras las determinantes fisicoquímicas que regulan este proceso (108). Es claro que la nitración de tirosinas proteicas es un proceso relativamente selectivo y de bajo rendimiento, y que existen condiciones que favorecen de una manera u otra el proceso de nitración. En general, la nitración depende de varios factores como la estructura de la proteína, el mecanismo de nitración y el entorno en el cual se encuentra la misma, ya sea expuesta al solvente o sumergida en un ambiente más hidrofóbico.

2.4.1 Determinantes fisicoquímicas en entornos acuosos

En entornos acuosos, la nitración de tirosinas aumenta en presencia de CO₂, en la cercanía de metales de transición (182) o de sitios de unión para peroxidasas (183). En particular, algunos centros metálicos de transición favorecen sitio específicamente la nitración mediada por peroxinitrito, como es el caso de la nitración de la tirosina 34 de la SOD (66, 184), que lleva a su inactivación. Respecto a la estructura primaria, no se ha demostrado la ocurrencia de una secuencia consenso para que la nitración tenga lugar, aunque en un trabajo publicado por Eflering y colaboradores se sugiere que puede existir dicha secuencia (185). Numerosos trabajos postulan que la nitración se ve favorecida en presencia de residuos ácidos como aspartato y glutamato (20, 26, 108) o la ubicación de la tirosina en una estructura de loop (20, 26, 108, 118). Por el contrario, la nitración puede verse inhibida por la reacción de algunos amino ácidos con las especies nitrantes como el peroxinitrito (cisteína, metionina y triptófano) (186), o sus radicales derivados (histidina, fenilalina) y la cercanía de amino ácidos básicos (26), aunque estos resultados han sido recientemente desafiados (118). La cisteína también puede inhibir la nitración de tirosinas mediante la transferencia electrónica desde el residuo de tirosina al de cisteína a través del esqueleto proteico lo cual lleva a la reducción del radical tirosilo para dar tirosina y la formación concomitante de radical cisteínilo (187). Sin embargo, en estudios realizados *in vivo* en los cuales se aislaron las proteínas nitradas endógenamente de cerebro de ratón se encontró que la nitración se veía favorecida cuando se encontraban residuos de cisteína y metionina cercanos a la tirosina (118) y sorprendentemente, que la cercanía de amino ácidos cargados positivamente, también favorecían el proceso, mientras que dichas proteínas no son nitradas cuando estos amino ácidos están ausentes (118). Otros autores, demostraron recientemente en estudios *in vitro* que la presencia de metionina cercana al residuo de tirosina puede promover las reacciones de nitración a través de la transferencia de

electrones que favorecen la estabilización del radical tirosilo (188), en un mecanismo similar pero en sentido inverso al que tiene lugar entre cisteína y tirosina (187). Todavía no se conocen claramente los mecanismos por los cuales la nitración de tirosinas proteicas tiene lugar de forma selectiva en algunas proteínas y residuos de tirosina específicos (108).

2.4.2 Determinantes fisicoquímicas en entornos hidrofóbicos

Las determinantes fisicoquímicas de la nitración han sido previamente estudiadas fundamentalmente en entornos acuosos; sin embargo, estas pueden variar en entornos hidrofóbicos donde existe una gran concentración de ácidos grasos insaturados que pueden competir por las especies nitrantes, una exclusión de antioxidantes como el glutatión (que reacciona rápidamente con el $\bullet\text{NO}_2$ inhibiendo de esa manera la nitración), y la relevancia de agentes nitrantes como el $\bullet\text{NO}$ y $\bullet\text{NO}_2$ que pueden fácilmente difundir hacia estos ambientes hidrofóbicos y concentrarse, favoreciendo las reacciones de nitración (189, 190). Para comprender las determinantes fisicoquímicas que regulan el proceso de nitración en entornos hidrofóbicos (169, 191, 192), recientemente se han desarrollado análogos hidrofóbicos de la tirosina que pueden ser eficientemente incorporados a sistemas modelo formados por liposomas (192) y membranas, así como péptidos transmembrana con residuos de tirosina ubicados en distintas profundidades de la bicapa (191), sondas que serán utilizadas durante el desarrollo de esta tesis (169, 193).

Estudios realizados en nuestro laboratorio demuestran que los procesos de nitración en membranas tienen características particulares que pueden diferir de aquellas reportadas previamente para entornos polares, lo cual ha sido el objetivo de estudio de esta tesis (169). Estas consideraciones son de relevancia para comprender los procesos de nitración y dimerización de tirosinas en proteínas asociadas a biocompartimentos hidrofóbicos tales como biomembranas y lipoproteínas (Tabla III).

Tabla III. Nitración y dimerización de proteínas asociadas a entornos hidrofóbicos

Proteína	Ref
Nitración	
^a Proteínas de membrana de glóbulo rojo	(194)
Banda 3 glóbulo rojo	(195)
Ca-ATPasa de Retículo Sacoplásmico	(196)
Glutación S-transferasa microsomal	(79)
Apolipoproteína B	(197, 198)
Apolipoproteína A	(27, 199)
Complejo I mitocondrial	(200)
α -Sinucleína	(201)
Dimerización	
Proteínas de membrana de glóbulo rojo	(202)
α -Sinucleína	(201)
Membranas mitocondriales	(203)
Péptido β -amiloide	(204)
Apolipoproteína B	(205)
Apolipoproteína A	(206)

^a Nótese que muchas de las proteínas mencionadas sufren procesos de nitración y dimerización simultáneamente.

2.5 Inhibición y reparación de la nitración de tirosinas: agentes anti-nitrantes endógenos y exógenos

Existen en los sistemas biológicos mecanismos que pueden interferir con la formación de especies oxidantes ya sea a través de la acción de enzimas o de distintas moléculas presentes en las células. La inhibición de la nitración puede ocurrir por consumo de especies nitrantes ($\cdot\text{NO}_2$, $\text{CO}_3^{\cdot-}$, ONOO^-) o por reparación del radical $\cdot\text{Tyr}$, lo cual puede ocurrir a través de agentes endógenos u exógenos, siendo estos últimos potenciales fármacos en el tratamiento de diversos modelos de enfermedad o patologías humanas y cuyo desarrollo y progresión está asociada a la sobreproducción de especies oxidantes y/o nitrantes.

2.5.1 Agentes endógenos

2.5.1.1 Enzimas antioxidantes

Los sistemas biológicos cuentan con diversos mecanismos enzimáticos para la detoxificación de las ROS y RNS formadas durante el metabolismo normal o durante los eventos de estrés nitrooxidativo en los cuales existe una sobreproducción de especies oxidantes y nitrantes que pueden llevar a proceso de daño celular y/o tisular (207).

Peroxiredoxinas

Las peroxiredoxinas (Prx) son peroxidasas caracterizadas por tener una cisteína crítica y la ausencia de cofactores metálicos. Estas enzimas catalizan la reducción por dos electrones de H_2O_2 y otros peróxidos como el peroxinitrito u peróxidos orgánicos, usando un segundo sustrato, que generalmente es un reductor basado en tioles (207). Habitualmente, para la reacción de descomposición del peroxinitrito, en el primer paso de la catálisis el tiolato peroxidático reduce al ácido peroxinitroso por dos electrones para formar NO_2^- y ácido sulfénico (Ec. 19), el cual

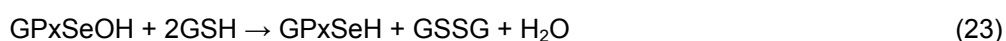
forma un disulfuro con un segundo grupo tiol (resolutivo) (Ec. 20), y el disulfuro es reciclado por la tioredoxina (TXN) en células de mamífero (Ec. 21).



Estas enzimas son muy eficientes y se encuentran a altas concentraciones en distintos compartimentos, estando fundamentalmente en el citosol, pero también se encuentran en mitocondrias y peroxisomas. La Pxr 2, por ejemplo, reacciona rápidamente con peroxinitrito ($k = 1,7 \times 10^7 \text{ M}^{-1} \text{ s}^{-1}$, pH 7,4 25°C) (208) y se encuentra a altas concentraciones en glóbulos rojos, con lo cual sería un sistema de gran relevancia de detoxificación fisiológica del peroxinitrito formado en el espacio intravascular.

Glutación peroxidasa

La enzima glutación peroxidasa (GPx) es una seleno-proteína que es capaz de reaccionar rápidamente con el peroxinitrito ($k = 8 \times 10^6 \text{ M}^{-1} \text{ s}^{-1}$, pH 7,4 25°C) (209), reduciendo el peroxinitrito a NO_2^- a expensas del glutación (Ecs. 19-20).



Hemoproteínas

Las hemoproteínas pueden reaccionar con el peroxinitrito de forma muy diversa llegando en algunos casos a reaccionar de manera muy rápida ($k > 10^6 \text{ M}^{-1} \text{ s}^{-1}$), como es el caso de la peroxidasa de rábano (HRP) y prostaglandín endoperoxido H-sintasa 1 que es oxidada por dos electrones para dar Compuesto I y NO_2^- , o la reacción mediada por la enzima MPO que, en una oxidación por un electrón da Compuesto II y $\cdot\text{NO}_2$, lo cual puede potencialmente catalizar reacciones de nitración. Algunas hemoperoxidasas como la oxihemoglobina catalizan la isomerización del peroxinitrito a NO_3^- , actuando de esta manera como atrapadores de peroxinitrito (210) (Ec. 24), mientras que otras hemoproteínas como la catalasa y el citocromo c reducido (Fe^{III}) no reaccionan con el peroxinitrito (207).



2.5.1.2 Moléculas antioxidantes

En la siguiente sección mencionaremos los ejemplos clásicos de moléculas endógenas antioxidantes, muchas de las cuales juegan un importante papel en la descomposición de especies nitrantes.

Glutación

El glutati6n (GSH), un tripéptido formado por los amino ácidos glutamato, glicina y cisteína, es el tiol intracelular más abundante y tiene un importante rol antioxidante ya que reacciona rápidamente con distintos radicales y peroxilos. Normalmente se encuentra bajo su forma reducida en una concentración de $\sim 5\text{mM}$ en el citosol celular. El GSH reacciona directamente con peroxinitrito con una constante de velocidad baja ($k = 1.350 \text{ M}^{-1}\text{s}^{-1}$ pH 7,4 y 37°C (14) y más rápidamente con $\cdot\text{NO}_2$ ($k \sim$

$2 \times 10^7 \text{ M}^{-1}\text{s}^{-1}$) (211). La acción antioxidante del GSH tiene lugar a través de tres mecanismos distintos: *i*) reacción directa del ácido peroxinitroso con la forma tiolato en una reacción mediada por dos electrones, que forma ácido sulfénico y posteriormente disulfuro (Ecs. 25-26); *ii*) reacción de los radicales derivados del peroxinitrito ($\cdot\text{OH}$, $\cdot\text{NO}_2$ y $\text{CO}_3^{\cdot-}$) que en reacción por un electrón forma radical tiílo ($\cdot\text{GS}$) (Ec. 27) y *iii*) reacción de reparación del radical tirosilo para rendir radical $\cdot\text{GS}$ (Ec. 28):



Habitualmente, la reacción inhibitoria del GSH sobre la nitración, es principalmente a través de su reacción con $\cdot\text{NO}_2$ (211).

Acido Úrico

El ácido úrico es un producto del metabolismo de las purinas, formado por acción de la enzima xantina oxidasa, que se encuentra ampliamente distribuido en concentraciones relativamente altas. En plasma, el ácido úrico está presente bajo la forma monoaniónica urato ($\text{pK}_a = 5,4$) y en concentración muy elevada en el orden de 200-500 μM . El ácido úrico contribuye en un 60% a la actividad antioxidante total del plasma en individuos sanos y es un atrapador de peroxinitrito, radicales derivados del mismo ($\cdot\text{NO}_2$ y $\cdot\text{OH}$) y radicales peroxilo. El urato reacciona con el ácido peroxinitroso ($k = 4,8 \times 10^2 \text{ M}^{-1}\text{s}^{-1}$) (212), y sus radicales derivados como el $\cdot\text{NO}_2$ ($k \sim 2 \times 10^7 \text{ M}^{-1}\text{s}^{-1}$) (211), lo cual puede explicar la eficiencia reportada de la inhibición por urato de

procesos mediados por peroxinitrito y su acción como potente agente anti-nitrante *in vitro* e *in vivo* (22).

Acido lipoico

El ácido lipoico (LA) es un disulfuro natural conocido inicialmente por su actividad como cofactor esencial de enzimas mitocondriales bioenergéticas, y se encuentra normalmente bajo su forma reducida, el ácido dihidrolipoico (DHLA). Es un micronutriente muy importante con propiedades farmacológicas diversas, y se ha utilizado para el tratamiento de polineuropatías asociadas a la diabetes mellitus (213) y enfermedades neurodegenerativas como enfermedad de Alzheimer (214), así como en la prevención de enfermedades cardiovasculares (215). Tiene distintas propiedades antioxidantes (216) basadas en su reacción directa con especies reactivas del $\cdot\text{NO}$, tales como peroxinitrito ($k = 1400 \text{ M}^{-1}\text{s}^{-1}$ pH 7,4 y 37°C) (217) o sus radicales derivados $\cdot\text{NO}_2$ ($k = 1.3 \times 10^6 \text{ M}^{-1}\text{s}^{-1}$) (218) y $\text{CO}_3^{\cdot-}$ ($k = 1.6 \times 10^9 \text{ M}^{-1}\text{s}^{-1}$) (218), HOCl y $\cdot\text{OH}$. Actúa también como quelante de metales de transición, aumenta los niveles citosólicos de GSH y ácido ascórbico, y participa a través de estos, en el reciclado de vitamina E. Las propiedades antioxidantes del LA pueden atribuirse en parte a su rápida reacción con los radicales $\text{CO}_3^{\cdot-}$ y $\cdot\text{NO}_2$ derivados del peroxinitrito, aunque la relevancia de estas reacciones *in vivo*, aún no está demostrada (218). Su aplicación como suplemento nutricional en complejos vitamínicos y tratamiento de distintas enfermedades ha sido exitosa y se siguen estudiando sus propiedades farmacológicas (219).

Reacciones de reparación

Como mencionamos previamente se puede afectar la formación de 3-NT ya sea por consumo de las especies nitrantes o por reducción del radical tirosilo. Tanto el ácido ascórbico como el GSH, dos moléculas biológicamente relevantes pueden llevar

a cabo esta reacción (Ec. 28). Dado que los estados estacionarios de $\cdot\text{Tyr}$ son bajos, este mecanismo es operativo solo a altas concentraciones de la molécula antioxidante.

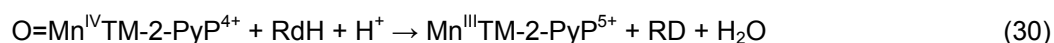
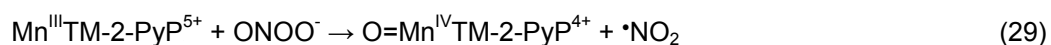
2.5.2 Agentes exógenos

Estas moléculas han sido utilizadas para el estudio de los mecanismos de nitración y debido a sus acciones anti-nitrantes se han ensayado en diversos modelos por su eventual acción farmacológica. Los atrapadores de peroxinitrito más eficientes pertenecen a dos grandes familias: selenoles y porfirinas metálicas (22, 207).

2.5.2.1 Metalo Porfirinas

Existen moléculas sintéticas que son capaces de reaccionar directamente con el peroxinitrito o con sus radicales derivados y por lo tanto pueden interferir con las reacciones de nitro-oxidación.

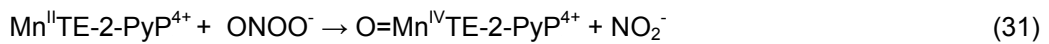
Las porfirinas de manganeso reaccionan rápidamente con el peroxinitrito y pueden reducirlo por uno o dos electrones. En el primer caso, la forma Mn^{III} participa de un ciclo catalítico que consiste en la formación de un complejo metálico que en sistemas biológicos es capaz de oxidar a un agente reductor (como el glutatión o el ácido ascórbico), como se muestra en las ecuaciones 29-30 para la porfirina $\text{Mn}^{\text{III}}\text{TM-2-PyP}$:



Las porfirinas de hierro también son capaces de catalizar la misma reacción, aunque con constantes de velocidad menores ($k < 10^7 \text{ M}^{-1} \text{ s}^{-1}$) (220). Las constantes de reacción dependen del tipo de porfirina y del pH ($k = 10^5 - 10^7 \text{ M}^{-1} \text{ s}^{-1}$), así como de la presencia de reductores, tales como el ascorbato, urato y glutatión ya que en ausencia

de los mismos, se forman dos especies fuertemente oxidantes como el complejo oxo-metálico ($O=Mn^{IV}TM-2-PyP^{4+}$) y el $\bullet NO_2$, que actuarían catalizando la nitración (221).

En el segundo caso, las porfirinas de manganeso en el estado redox $Mn^{(II)}$ pueden reducir al peroxinitrito por dos electrones, dando lugar a la formación de NO_2^- en lugar de $\bullet NO_2$, en una reacción rápida ($k > 10^7 M^{-1} s^{-1}$) (207, 222) (Ec. 31). La reducción de la porfirina en estado $Mn^{(III)}$ a $Mn^{(II)}$ requiere varios sustratos y puede ser catalizada por diferentes flavoenzimas presentes a nivel celular tales como la succinato deshidrogenasa y NADH deshidrogenasa a nivel mitocondrial y la xantina oxidasa (222) (Ec. 31):



Las porfirinas de hierro a su vez pueden catalizar la isomerización del peroxinitrito a NO_3^- , pero esta reacción solo sería relevante en ausencia de reductores tales como ascorbato y glutatión (223) (Figura 2.5).

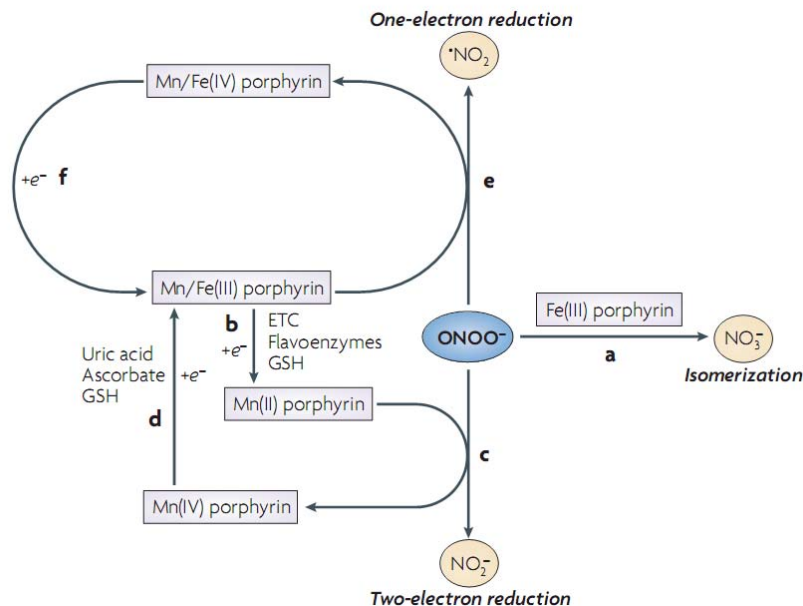


Figura 2.5 Metaloporfirinas como catalizadores de la descomposición del peroxinitrito. Extraído de (22).

2.5.2.2 Nitróxidos

Existe importante evidencia que la patogénesis de un gran número de enfermedades neurodegenerativas, cardiovasculares, pulmonares e inflamatorias involucran la acción de especies reactivas del oxígeno y pese a que se han realizado numerosos ensayos de intervención con antioxidantes como la vitamina C, E y β -caroteno estos no tuvieron el impacto esperado en la progresión de la enfermedad. De esta manera se ha trabajado en el desarrollo de nuevas moléculas que pudieran actuar como agentes terapéuticos en el tratamiento de dichas enfermedades (224) a través de su capacidad para reaccionar con especies reactivas derivadas del $\cdot\text{NO}$.

Los nitróxidos cíclicos son un grupo de radicales muy estables que son capaces de reaccionar con otros radicales libres y diversos blancos biológicos y de esa manera ejercer su actividad como antioxidantes, fundamentalmente alterando el estado redox de células y tejidos afectando su estado metabólico (224). Estas moléculas son capaces de reaccionar con radicales y diversos peróxidos; inhibir reacciones tipo Fenton y participar en reacciones de recombinación entre radicales (225). Los radicales libres formados por estos compuestos se encuentran estabilizados por el triple enlace entre el N y el O y por la presencia de grupos sustituyentes en la posición α de los anillos (normalmente grupos metilo). Los distintos tipos de nitróxidos difieren fundamentalmente en los grupos sustituyentes (R) que le confieren a la molécula propiedades fisicoquímicas diferentes (Figura 2.6A).

Los nitróxidos cíclicos pueden estar presentes en tres estados de oxidación (Figura 2.6A), que participan en distintos ciclos de oxido-reducción y tienen reactividades diferentes. Inicialmente fueron estudiados por su actividad SOD (226, 227), aunque actualmente se conoce su reacción con diversos radicales libres. Son capaces de inhibir las reacciones de lipoperoxidación ya sea por atrapamiento de los radicales iniciadores o por inhibición de las cadenas de propagación (228). También pueden ejercer su capacidad antioxidante a través de la inhibición de la formación de radicales

•OH por química de Fenton debido a su capacidad para oxidar metales de transición (229). Uno de los nitróxidos más conocidos, es el tempol (4-hidroxi-2,2,6,6-tetrametil-1-piperidina), que ha sido extensamente estudiado por su capacidad para reducir el daño oxidativo en distintos modelos celulares y animales (230). Se ha demostrado la reacción del tempol (o de sus formas catión oxoamonio e hidroxilamina con el peroxinitrito y sus radicales derivados ($\cdot\text{NO}_2$, $\text{CO}_3^{\cdot-}$) (224) lo cual demuestra que parte de su actividad antioxidante y antinitrante está basada en la detoxificación de especies reactivas del oxígeno. En este trabajo, el mecanismo propuesto de descomposición de especies nitrantes, involucra al peroxinitrito como especie responsable del retorno de la forma oxoamonio a la forma radical nitróxido, lo cual provoca un cambio en la química de nitración a nitrosación (Figura 2.6B) (224). En sistemas biológicos, el retorno podría ser realizado por reductores celulares como el GSH, lo que debe ser explorado.

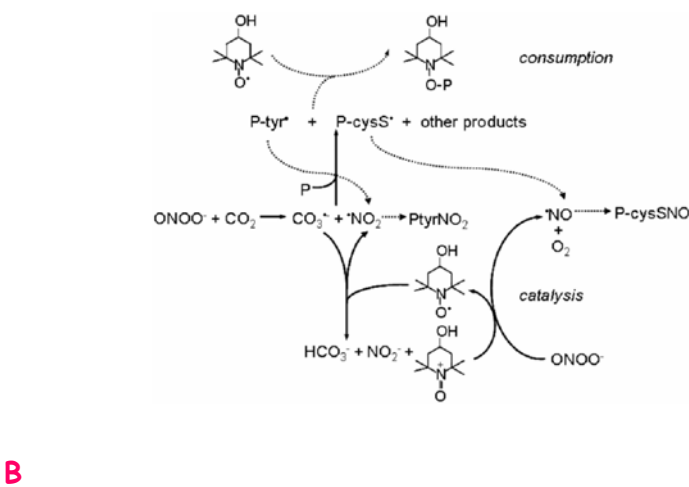
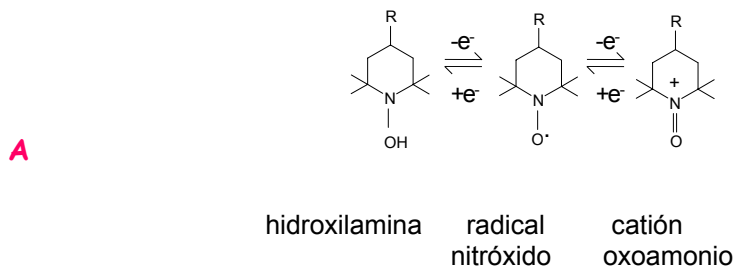


Figura 2.6 Mecanismo de reacción del Tempol. Extraído de (224).

El tempol ha sido ensayado en diversos modelos de enfermedad como la encefalomiелitis viral murina, donde se vio que el tratamiento con ésta molécula, inhibe fuertemente la nitración de tirosinas proteicas y revierte sensiblemente la neuroinflamación provocada por la infección mejorando la sobrevivencia de los ratones infectados. Estos estudios apoyan el desarrollo de estrategias terapéuticas basadas en nitróxidos y moléculas relacionadas para el tratamiento de enfermedades neuroinflamatorias como la esclerosis múltiple, lo cual tiene un gran impacto debido a la alta prevalencia de estas enfermedades y la falta de terapias efectivas para su tratamiento (231).

2.5.2.3 Ebselen

El ebselen es un seleno-compuesto que tiene una reactividad tipo glutatión peroxidasa capaz de reducir al peroxinitrito por dos electrones en una reacción rápida ($k = 2 \times 10^6 \text{ M}^{-1}\text{s}^{-1}$ pH 8, 25°C) (232), y siendo reducido a su forma original a expensas del glutatión. Ha sido utilizado en ensayos clínicos con prominentes resultados (233), e incluso en el tratamiento de enfermedades como el infarto cerebral donde se vio que la administración del mismo mejoraba sensiblemente la progresión de la enfermedad (234, 235).

2.5.2.4 Péptidos de tirosina

Se han utilizado tanto *in vivo* como *in vitro*, péptidos de tirosina para inhibir procesos nitroxidativos, mediante distintas estrategias para incorporar los péptidos a las células. En el primer caso se trata de tetrapéptidos que alternan amino ácidos básicos y aromáticos (dentro de los cuales se encuentra la tirosina), con una secuencia como la que se muestra a continuación: Dmt-D-Arg-Phe-Lys-NH₂ (236), los cuales se incorporan a las células a través de la interacción con las membranas. La otra estrategia es ingresar los péptidos a través de sustancias como el Charriot, o

liposomas que son incorporados a la célula (83). Es interesante destacar que cuando se sustituye en dichos péptidos el residuo de tirosina por fenilalanina, se pierde el efecto citoprotector. Si bien el mecanismo íntimo de acción anti-nitrante no está definido, se especula que altas concentraciones intracelulares de péptido sean capaces de atrapar especies nitrantes protegiendo a tirosinas críticas de modificaciones nitroxidativas. Alternativamente, los péptidos de tirosina podrían interferir interaccionando con el Compuesto I de las hemoperoxidasas, aunque aún restan por definirse los mecanismos de acción.

En suma, todos los compuestos mencionados anteriormente, proveen de una “prueba de concepto” y potencialmente representan herramientas farmacológicas para el tratamiento de enfermedades humanas cuya patogénesis está directamente relacionada con la formación de especies reactivas del nitrógeno y oxígeno; y por lo tanto, es importante profundizar los conocimientos en esta área para comprender como estas moléculas que interfieren con los procesos de nitración de tirosinas *in vitro*, pueden actuar como potenciales fármacos *in vivo*.

2.6 Membranas biológicas y sistemas modelo

2.6.1 Estructura de las membranas biológicas

Las membranas celulares son cruciales para la vida de la célula y su función es rodear la célula, definir sus límites, y mantener las diferencias esenciales entre el citosol y el medio ambiente extracelular. De la misma manera, dentro de las células eucariotas, las membranas del retículo endoplasmático, aparato de Golgi, mitocondrias, y otros organelos cumplen la función de mantener las diferencias características entre el contenido de cada organelo y el citosol. A pesar de sus diferentes funciones, y de la variabilidad en los porcentajes de sus componentes, todas las membranas biológicas tienen una estructura general común: un fluido bidimensional (“mosaico fluido”) (237) formado por una bicapa lipídica con proteínas

inmersas. Las membranas celulares son estructuras dinámicas y fluidas y la mayoría de sus moléculas son capaces de moverse en el plano de la bicapa, siendo el coeficiente de difusión para lípidos $D \sim 10 \mu\text{m}^2/\text{s}$ (238) y un valor significativamente menor el valor para las proteínas (239) (Figura 2.7).

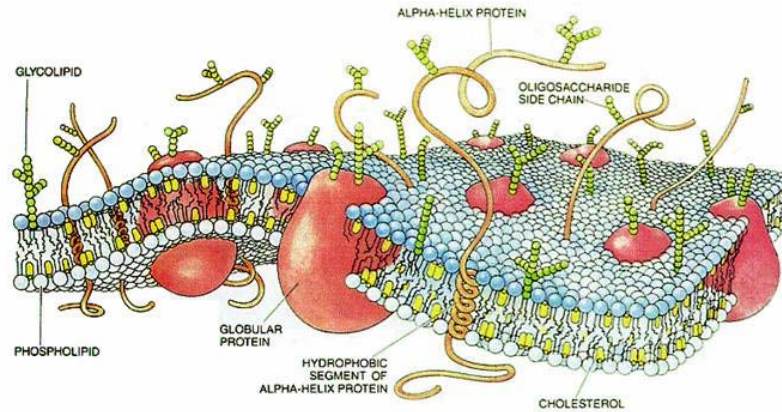


Figura 2.7 Estructura de la membrana biológica

Las moléculas de los lípidos se disponen como una doble capa continua de alrededor de 5-7 nm de espesor, la cual constituye la estructura básica de la membrana y sirve como una barrera impermeable al paso de la mayoría de moléculas solubles en agua. Los lípidos constituyen $\sim 50\%$ de la mayoría de las membranas animales, correspondiendo el otro 50 % a las proteínas. Las moléculas lipídicas constituyentes de las membranas son fundamentalmente fosfolípidos, moléculas anfipáticas que se caracterizan por presentar una cabeza polar, y una región hidrofóbica constituida por las colas hidrocarbonadas de 2 ácidos grasos (Figura 2.8). También se encuentran esfingolípidos, glicolípidos y esteroides fundamentalmente colesterol (en las membranas eucariotas), el cual cumple un importante rol en la regulación de la fluidez y la permeabilidad de la membrana ocupando los sitios libres existentes, y aumentando su rigidez y grado de ordenamiento (240). El contenido de colesterol en las membranas es variable pero normalmente constituye \sim el 23 % de los

lípidos presentes en la bicapa. En células procariontas, los carotenoides parecen cumplir una función similar a la del colesterol, regulando la fluidez de las membranas (241).

Los ácidos grasos pueden diferir en el largo pero normalmente contienen entre 14 y 24 carbonos. El ácido graso de una de las colas suele presentar solo enlaces simples entre sus átomos de carbono (saturado), mientras que el otro ácido graso presenta una o más insaturaciones, que generan un quiebre en la estructura.

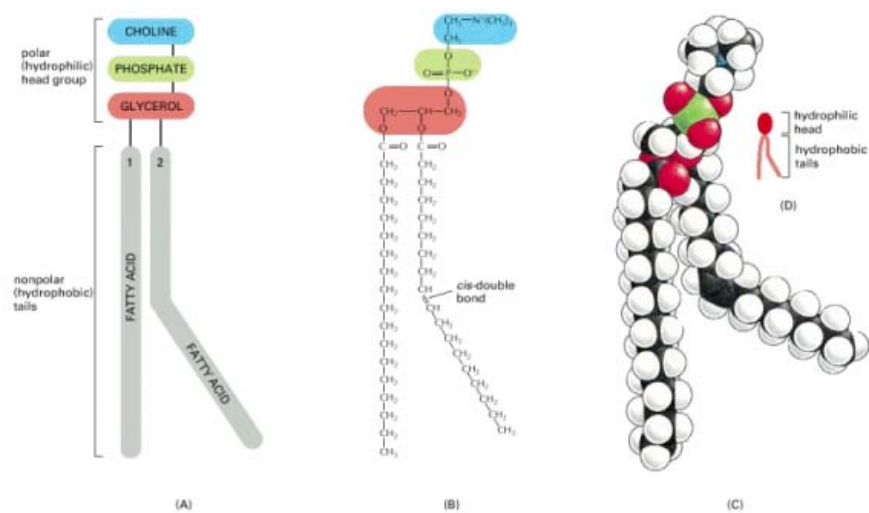


Figura 2.8 Estructura de los fosfolípidos de membrana

La naturaleza anfipática de los fosfolípidos hace que estas moléculas formen bicapas espontáneamente en ambientes acuosos (Figura 2.9). Las moléculas hidrofílicas se disuelven en agua porque contienen grupos polares (cargados o no) que pueden formar interacciones electroestáticas o puentes de hidrógeno con las moléculas de agua, por el contrario, las moléculas hidrofóbicas son insolubles en agua dado que todos o muchos de sus átomos son incapaces de interactuar con el agua. Por este motivo, los fosfolípidos se disponen de manera que las cabezas polares quedan expuestas al solvente, y sus colas hidrocarbonadas se empaquetan en el interior, escapando de la solución acuosa, formando micelas o bicapas (Figura 2.9).

Las micelas se forman habitualmente, por el empaquetamiento de moléculas lipídicas con una sola cola (ej. un ácido graso) y las cabezas polares expuestas hacia el solvente.

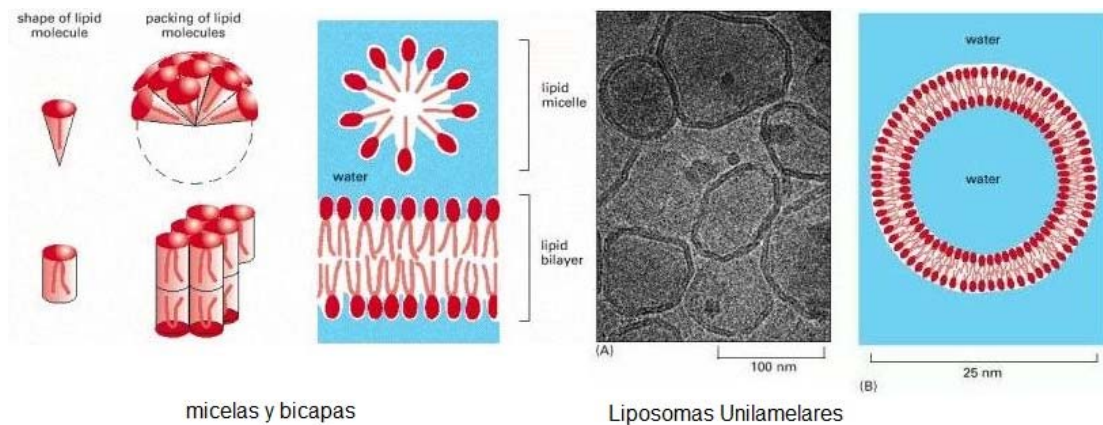


Figura 2.9 Organización de los fosfolípidos en fases acuosas

El otro componente fundamental de las membranas biológicas son las proteínas, cuya proporción varía dependiendo de la función celular, y son las responsables de las propiedades dinámicas de las membranas. Pueden ser proteínas integrales de membrana (intrínsecas) o periféricas (extrínsecas). Las primeras tienen regiones hidrofóbicas inmersas en la membrana y regiones hidrofílicas que se sitúan hacia el exterior de la misma. La nitración de tirosinas en estas proteínas puede tener, como vimos, determinantes fisicoquímicos particulares por encontrarse en un entorno hidrofóbico, alejado de la fase acuosa (Tabla III). Las proteínas inmersas en la bicapa lipídica median casi todas las demás funciones de la membrana, el transporte de moléculas específicas a través de ella, y la catálisis de reacciones asociadas. En la membrana plasmática, algunas proteínas sirven como vínculos estructurales que conectan distintos compartimentos, o actúan como receptores para la detección y la transducción de señales químicas en el entorno de la célula.

Las membranas también tienen glúcidos que se encuentran asociados mediante enlaces covalentes a lípidos (glicolípidos) y proteínas (glicoproteínas) y generalmente se encuentran en la cara externa de la membrana formando parte del glicocálix, donde cumplen una función importante en la interacción con el medio exterior (Figura 2.7).

Muchas propiedades fisicoquímicas de la membrana cambian con la profundidad de la misma, tales como la hidrofobicidad, difusión y concentración de moléculas como $\bullet\text{NO}$ y O_2 , penetración de iones y complejos metálicos, así como parámetros estructurales y dinámicos, tales como parámetros de ordenamiento y quiebre de las cadenas alquilo (240). Estas propiedades cambian en función del grado de saturación de las membranas, y se ven afectadas por el colesterol, péptidos unidos a membrana, proteínas integrales de membranas y otros componentes. Por este motivo el micro entorno en el cual se encuentra ubicado el blanco biológico en una membrana (ej. un residuo de tirosina proteica), puede cambiar drásticamente con la composición y la profundidad de la membrana, y esto tiene una relevancia muy importante en el marco de esta tesis, cuyo objetivo se centra en el estudio de los mecanismos de nitración en membranas y como se ven afectados dichos procesos con la profundidad de la bicapa, lo cual refuerza el concepto de que hay que tener en cuenta los factores micro ambientales para estudiar reacciones químicas que tienen lugar en una bicapa lipídica (240).

2.6.2 Sistemas modelo de membranas

Las membranas biológicas son sistemas muy complejos, debido a la presencia de miles de moléculas lipídicas formando una bicapa con proteínas inmersas ocupando una fracción importante de la misma, lo cual hace que el estudio por separado de los distintos componentes, y de los procesos biológicos asociados a membranas tenga un grado importante de dificultad. No es fácil aislar membranas

biológicas de células enteras, ya que las preparaciones de membranas plasmáticas suelen estar contaminadas con lípidos de membranas de otros organelos y cuya composición puede no ser exactamente igual a la de la membrana plásmatica, sin embargo existen protocolos adecuados para el aislamiento de membranas mitocondriales y microsomas. Muchos trabajos que estudian procesos asociados a las membranas biológicas, han sido realizados en glóbulos rojos, dado que es un sistema que carece de membranas internas (242-244), y esta ha sido una herramienta importante en los estudios de difusión y permeabilidad a través de las membranas biológicas. La otra alternativa es trabajar con sistemas modelo de membranas que se obtienen de fosfolípidos en fase acuosa que espontáneamente se agrupan formando micelas o liposomas (Figura 2.9).

Los liposomas son esferas formadas por bicapas de fosfolípidos que semejan a la estructura de la membrana plasmática, y que a diferencia de las micelas, tienen en su interior un volumen de solución acuosa (Figura 2.9). Los liposomas se pueden formar por sonicación o agitación vigorosa de suspensiones lipídicas en medios acuosos y pueden tener una (liposomas unilamelares) o varias capas de membrana (multilamelares), así como un tamaño definido. Los liposomas unilamelares se clasifican a su vez en función de su tamaño en pequeños (*small unilamellar vesicles*), intermedios (*intermediate-size unilamellar vesicles*) y grandes (*large unilamellar vesicles*), los cuales miden ~ 15, 100 y 1000 nm de diámetro respectivamente, mientras que los liposomas multilamelares normalmente están conformados por una población de vesículas con diámetros de ~ 100-1000 nm (245). Estos modelos son sistemas que permiten la realización de estudios en condiciones más controlados, apropiados para llevar a cabo estudios mecanísticos. El uso de sistemas modelos de membrana ha sido fundamental para el conocimiento de las propiedades físicas y químicas de las mismas, ya que en ellos se puede regular el porcentaje de ácidos grasos saturados e insaturados, así como la cantidad de colesterol. Sin embargo, estos modelos también han sido objeto de críticas por no representar exactamente las

propiedades de las membranas, fundamentalmente por la ausencia de las proteínas de membrana. En un artículo publicado recientemente en la revista de la American Chemical Society, *Chemical and Engineering News* (246) (ver más adelante), se discute la importancia del uso de estos modelos, resaltando su idoneidad para la mejor comprensión de muchos de los fenómenos físico-químicos asociados a membranas. Los experimentos en modelos permiten la elucidación del comportamiento físico de los lípidos y el colesterol (aún en ausencia de proteínas) y estos resultados se pueden aplicar a los sistemas biológicos más complejos. Una de las aplicaciones de sistemas modelos de membranas, es el uso de liposomas (como modelo de células artificiales), para la incorporación a células de drogas u otras moléculas, ya que el liposoma encapsula una solución acuosa en el interior de una bicapa lipídica, y de esa manera estas moléculas pueden incorporarse a otras células al fusionarse la membrana del liposoma con la membrana plasmática. En esta tesis, se trabajará con un sistema modelo de membranas (liposomas uni y multilamelares), con análogos hidrofóbicos de tirosina incorporados, que permitirán el estudio de los mecanismos de nitración en un sistema sumamente controlado y en el que podrán ensayarse un gran número de variables bioquímicas y fisicoquímicas. Sin embargo, no hay que perder de vista que se trata de un modelo y por tanto las conclusiones obtenidas deberán explorarse luego, en la medida de lo posible, en sistemas biológicos propiamente dichos.

SCIENCE & TECHNOLOGY

SIMULATING LIFE'S ENVELOPES

Models provide clues about **LIPID BEHAVIOR** in cell membranes, but they may have reached their limits

CELIA HENRY ARNAUD, C&EN WASHINGTON

THE PLASMA MEMBRANE, which surrounds biological cells, consists of hundreds—possibly even thousands—of different lipids that are arranged in a bilayer. Membrane proteins embedded in the bilayer occupy a large fraction of the membrane surface, and the cytoskeleton, a lattice-work of intracellular protein filaments, attaches to the inner side of the membrane. This complexity makes the plasma membrane and its constituent lipids difficult to study directly.

That's where model systems come in. These stripped-down constructions allow scientists to probe the behavior of lipid membranes under carefully controlled circumstances. Scientists have garnered a lot of insight about the membrane from model systems, but these idealized versions of membranes may be reaching the limits of what they can reveal about biology.

Cell biologists and biophysicists use lipid model systems to gain a physical and chemical understanding of the plasma membrane. Such models typically contain three components—an unsaturated lipid, a saturated lipid, and cholesterol. These three components stand in for the multitude of lipids found in the natural cell membrane. Even such simplified mixtures can answer questions about the behavior of the lipid portion of the membrane.

With model systems "you can get at fundamental physical-chemical questions," says Barbara A. Baird, a chemistry professor at Cornell University. Such questions include how the lipids organize themselves into multiple liquid phases, called domains, and under what conditions those phases form.

Of particular interest to re-

searchers studying membrane model systems is whether membranes can spontaneously form coexisting liquid phases in the absence of proteins. "You can understand how lipids work and then extrapolate and use that as a model of how they might work in a biological system," Baird says.

Model systems suggest membrane lipids are in a "very peculiar state," says Jay T. Groves, a chemistry professor at the University of California, Berkeley. The largely linear, oily molecules, each with a polar, hydrophilic end, seem to be near a critical point in their phase diagram—a combination of composition, pressure, and temperature at which two coexisting phases become identical.

The remarkable thing is that this behav-

ior occurs in lipid mixtures similar to those in cells. This suggests that cell membranes might hover around a critical point in the lipid phase diagram, where even small changes in conditions can trigger large changes in the membrane. "It's like the cell evolved itself a solvent that doesn't resist all the different things it would need to do," Groves says, referring to the way lipids serve as a versatile solvent conducive to signaling and other interactions on and among cells.

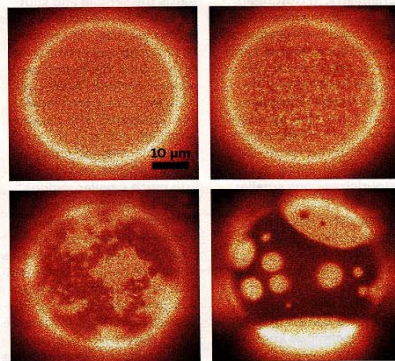
Model systems are valuable because "you can really affirm with no ambiguity whatsoever that lipids and cholesterol have these physical properties as a mixture," Groves says. "Those physical tendencies don't go away when you put this mixture into the membrane of a cell."

One of the key issues that can be addressed with model systems is lipid phase behavior. Using three-component systems, independent groups led by biophysicists Gerald Feigenson at Cornell and Sarah Keller at the University of Washington, Seattle, see lipid mixtures separate into coexisting phases. Seeing such phases in model systems is a first step toward answering the question of whether such domains exist in the intact cell membrane.

In a quest for biologically relevant model systems, Feigenson is moving toward more complicated four-component systems—three lipids plus a "judiciously chosen protein." He thinks such a mixture is the minimum for a model system to approximate a real system.

GIANT PLASMA membrane vesicles, or "blebs," offer an even closer approximation. Blebs, released by cells either naturally or by laboratory inducement, have compositions similar to cell membranes. They are more complicated than synthetic model systems but simpler than intact cell membranes, in part because they lack connection to an underlying cytoskeletal network. The group led by Baird and David Holowka at Cornell is studying the phase behavior of blebs. "I see this kind of work as a bridge between the well-defined model systems and the more complex biological systems," Baird says. Nevertheless, she notes, "it's pretty tricky business trying to relate it to a biological system and to a model system."

LIPIDS IN FLUX This three-component unilamellar vesicle starts with a uniform distribution of lipids (top left). Slightly above (top right) and below (bottom left) the critical temperature, the lipid composition and domain boundaries fluctuate. Far below the critical temperature (bottom right), phase-separated domains appear.



COURTESY OF LAUREL HANSEN, KIM SMITH & SARAH KELLER

WWW.CEN-ONLINE.ORG 31 FEBRUARY 9, 2009

SCIENCE & TECHNOLOGY

With model systems "you can get at fundamental physical chemical questions."

Mass spectrometric analysis shows that the lipid composition of blebs appears similar to the composition of the cell membrane, to the extent that the composition of the cell membrane is actually known, Baird says. Plasma membrane preparations from cells are often contaminated with lipids from the membranes surrounding internal organelles, which have different lipid compositions from the plasma membrane, she says. "The cleanest work on membranes was done on red blood cells because they don't have those internal membranes," Baird notes.

The work of Sarah L. Veatch, a postdoc in Baird's group, suggests that blebs exist

in a state near a critical point on a phase diagram (*ACS Chem. Biol.* 2008, 3, 287). At such points, the system goes through wide fluctuations and easily switches between a single phase and multiple phases. "This kind of fluctuating system can be harnessed to cause a rather dramatic change with the appropriate signal," such as a changing temperature, Baird says.

Veatch studied membrane behavior by fluorescence microscopy. At 20 °C, micrometer-sized domains form in the membranes. Extrapolating those findings to 37 °C suggests that nanometer-sized domains should form in biological membranes at physiological temperatures.

"The idea that Sarah Veatch can take blebs and see exactly the same behavior near critical points that we routinely see in purely synthetic vesicles is hugely exciting," Keller says. "It says that even our ridiculously simplified system just might really be biologically relevant."

One of the unanswered questions about cell membrane phase behavior involves the existence of so-called lipid rafts, which are minuscule, patchlike domains that are believed to be involved in protein clustering and cell signaling. These rafts are thought to consist of a more highly ordered cholesterol and sphingolipid-rich liquid phase (the "liquid ordered" phase) interspersed with a less ordered liquid phase (the "liquid disordered" phase). Although liquid-ordered phases have been seen in model systems, the evidence for their existence in natural cell membranes is hard to find. Un-

2.7 Permeabilidad y difusión de oxidantes en membranas

Una de las funciones de las membranas biológicas es delimitar y separar los distintos componentes de los organelos y sus funciones, y por lo tanto los sitios de acción de algunas especies oxidantes pueden estar restringidos por las membranas. Los mecanismos de nitración en membranas biológicas van a estar determinados en parte por la permeabilidad de las especies nitrantes a través de la bicapa, su difusión en medios hidrofóbicos y su reparto, propiedades que cambian notablemente respecto a la fase acuosa. Como regla general se puede decir que las moléculas neutras no electrolíticas pueden difundir libremente a través de la porción lipídica de la membrana, mientras que las especies cargadas necesitan formar su ácido conjugado o atravesarla a través de un canal iónico. Cuánto más pequeña e hidrofóbica es una molécula, mayor será su permeabilidad a través de las membranas (247).

2.7.1 Permeabilidad de moléculas cargadas

Las moléculas cargadas, no pueden atravesar las membranas lipídicas libremente y su reactividad va a estar limitada a su sitio de formación, como es el caso de los aniones $O_2^{\cdot-}$, $ONOO^-$ y radical $CO_3^{\cdot-}$. La difusión pasiva a través de las membranas de estas especies es energéticamente muy desfavorable y por lo tanto las membranas biológicas constituyen eficientes barreras para el paso de moléculas iónicas. Estas moléculas pueden atravesar las membranas mediante canales aniónicos como la banda 3 presente en glóbulos rojos. Estudios pioneros realizados por Fridovich y colaboradores a finales de la década del 70 demostraron, en experimentos realizados en membranas de eritrocitos, que el anión $O_2^{\cdot-}$ era capaz de atravesar las bicapas (244, 248). En dichos experimentos se encapsuló xantina oxidasa en el interior de glóbulos rojos lavados (fantasmas) y se determinó la capacidad del anión $O_2^{\cdot-}$ producido en el interior de las células de reducir al citocromo c agregado exógenamente. Estos trabajos demostraron por primera vez, que

efectivamente, el $O_2^{\cdot-}$ atravesaba la membrana reduciendo al citocromo c y que ese proceso era inhibido cuando se utilizaban inhibidores específicos de los canales iónicos. Dado que el superóxido tiene un pK_a de 4,8 a pH fisiológico va a estar mayoritariamente en su forma aniónica y por lo tanto la difusión de la especie protonada (HOO^{\cdot}) es casi inexistente.

Estudios posteriores realizados en la década del 90 con peroxinitrito en glóbulos rojos demostraron a su vez que el peroxinitrito era capaz de atravesar las membranas biológicas por dos mecanismos: la forma protonada por difusión simple y el anión $ONOO^-$ a través de los canales aniónicos (249, 250) presentes en estas células. Dado que el peroxinitrito tiene un pK_a de 6,8 a pH fisiológico se encuentran presentes tanto la especie aniónica como su forma protonada, y por lo tanto ambos mecanismos de transporte (difusión pasiva e intercambio aniónico) son biológicamente relevantes. Estos estudios fueron realizados en glóbulos rojos que tienen un número importante de copias del canal banda 3 ($\sim 10^7$ copias/cél). Sin embargo, en otros tipos de células existirían intercambiadores aniónicos similares que serían los responsables del transporte del anión peroxinitrito a través de la membrana (249).

Finalmente, el radical $CO_3^{\cdot-}$, es un oxidante más selectivo que el radical $\cdot OH$, pero más voluminoso y aniónico, por lo que al igual que otras moléculas cargadas es incapaz de atravesar las membranas libremente, y su difusión dependerá de su pasaje a través de canales aniónicos, aunque esto no se ha establecido específicamente. Debido a su pK_a (~ 0) (135) el radical $CO_3^{\cdot-}$ se encuentra siempre desprotonado en condiciones fisiológicas. Trabajos realizados en nuestro laboratorio en sistemas modelo de membranas (251) como en glóbulos rojos (243), así como en membranas de fosfolípidos (252) muestran que la permeabilidad del radical $CO_3^{\cdot-}$ a través de membranas es muy limitada (Figura 2.10).

2.7.2 Permeabilidad de moléculas neutras

A diferencia de lo que ocurre para las moléculas cargadas, las moléculas neutras tales como el H_2O , O_2 , $\cdot\text{OH}$ $\cdot\text{NO}$ y el $\cdot\text{NO}_2$ son capaces de atravesar libremente las bicapas y la permeabilidad dependerá fundamentalmente del tamaño y la hidrofobicidad de la molécula (247).

Para el caso del $\cdot\text{O}_2$ y del $\cdot\text{NO}$, la resistencia es casi nula, lo que hace que las membranas sean altamente permeables a estas moléculas. El $\cdot\text{NO}$ es sumamente permeable a membranas biológicas dada su naturaleza neutra, hidrofobicidad y pequeño tamaño (249) y el $\cdot\text{NO}_2$ tiene una permeabilidad similar a la observada para el ácido peroxinitroso (252). El H_2O_2 es una molécula hidrofílica cuya permeabilidad es similar a la del H_2O , y por lo tanto la membrana ofrece una resistencia media a su paso. Recientemente se ha demostrado que el H_2O_2 es capaz de utilizar canales acuosos de membrana (acuaporinas) que pueden aumentar notablemente su permeabilidad a través de membranas (247). El radical $\cdot\text{OH}$ puede formarse por lo homólisis del peroxinitrito o por la reducción catalizada por metales del H_2O_2 . Es una molécula polar no electrolítica que se espera tenga una permeabilidad similar a la del H_2O , sin embargo, debido a su alta reactividad, reaccionará muy cerca de su sitio de formación, sin llegar a difundir. Al enfrentarse a una membrana reaccionará rápidamente con los ácidos grasos más cercanos y con los grupos de las cabezas polares, por lo que es poco probable que el $\cdot\text{OH}$ puede atravesar efectivamente la bicapa (124). Sin embargo, este también podría formarse en el interior de la bicapa por homólisis del ácido peroxinitroso que haya permeado hacia el interior, siendo esta una posibilidad que será estudiada en el marco de esta tesis.

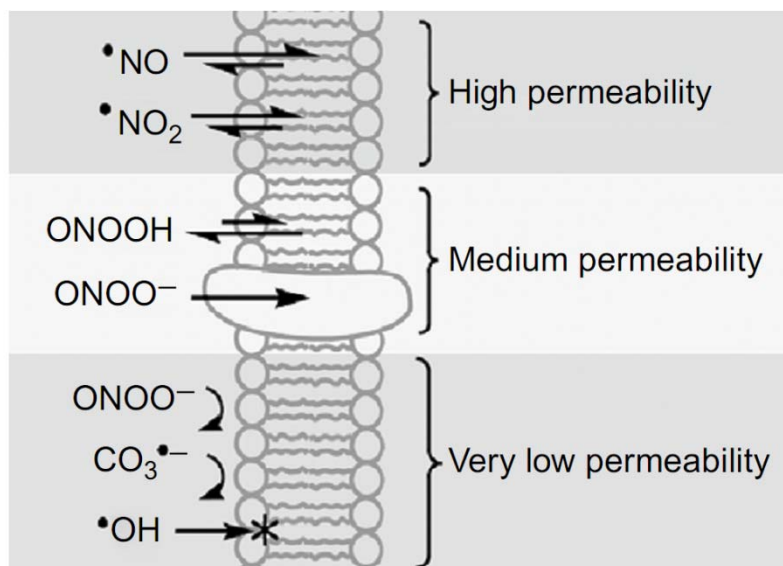


Figura 2.10 Permeabilidad de especies oxidantes y nitrantes en membranas.
 Extraído de (134).

2.7.3 Difusión y reparto en fases hidrofóbicas

Otro aspecto importante a tener en cuenta es el reparto de estas moléculas en las fases hidrofóbicas que puede hacer que algunas reacciones de nitración sean favorecidas en el interior de la bicapa. Un trabajo realizado por Kalyanaraman y colaboradores muestra que la nitración dependiente de peroxinitrito de análogos hidrofóbicos de tirosina y péptidos incorporados a membranas es mayor que la observada en fases acuosas para la tirosina libre, sugiriendo que el entorno hidrofóbico puede favorecer el proceso de nitración (192).

Se ha propuesto que el $\bullet\text{NO}$ juega un importante papel en la modulación de reacciones oxidativas en medios lipofílicos como membranas y lipoproteínas. Dos de los parámetros que regulan la reactividad en membranas del $\bullet\text{NO}$ son la difusión y el coeficiente de reparto. El $\bullet\text{NO}$ tiene un coeficiente de reparto de 3,6 en liposomas (DLPC y EYPC) respecto al agua, y de 3,0 en LDL (189, 190), y los valores de difusión se encuentran entre 3300-4500 $\mu\text{m}^2/\text{s}$ en buffer (249, 253) respecto a un valor de 1500 $\mu\text{m}^2/\text{s}$ en liposomas (134, 249).

El $\cdot\text{NO}_2$ tiene un coeficiente de reparto en membranas de 1,8 (190), lo cual indica que tanto el $\cdot\text{NO}$ como el $\cdot\text{NO}_2$ son capaces de concentrarse en entornos hidrofóbicos como membranas y lipoproteínas. Por otro lado, trabajos realizados por Moller y colaboradores, demostraron que la auto-oxidación del $\cdot\text{NO}$ para dar $\cdot\text{NO}_2$ ocurre a una velocidad 30 veces mayor en el interior de una membrana que en igual volumen de fase acuosa (190) (Figura 2.10).

Así como las reacciones de nitración en membranas pueden verse favorecidas por la concentración de algunas de las especies nitrantes, es importante tener en cuenta que la difusión de moléculas en entornos hidrofóbicos suele ser mucho menor que en fases acuosas, lo cual puede afectar el proceso. Una tirosina libre en fase acuosa tiene un coeficiente de difusión $D = 1000 \mu\text{m}^2/\text{s}$, (254) mientras que dicho valor disminuye a $\sim 5 \mu\text{m}^2/\text{s}$ (255) cuando la tirosina está en una membrana, y este valor sería aún menor en tirosinas presentes en péptidos o proteínas integrales de membrana. Esto tiene particular importancia en nuestro trabajo, ya que los rendimientos de dimerización de tirosina serán sensiblemente menores a los de nitración, debido a la baja difusión de estas moléculas respecto a una fase acuosa, lo cual llevaría a que la probabilidad de encuentro de dos radicales tirosilo en el interior de una bicapa sea muy baja (169).

En suma, la nitración de tirosinas en membranas estará determinada por la permeabilidad de las distintas especies nitrantes hacia el interior de la bicapa, siendo los aniones incapaces de atravesarla libremente y por lo tanto requerirán de canales iónicos; la difusión de las distintas especies en el interior de la misma, la cual será mucho más lenta respecto a la fase acuosa, y por último las propiedades de reparto, que determinarán su capacidad de concentrarse o no en una membrana o entorno lipoproteico (134).

2.8 Lipoperoxidación y otras modificaciones oxidativas en membranas

Las membranas biológicas contienen cantidades considerables de ácidos grasos insaturados y colesterol, que pueden sufrir oxidación, aunque también existen en membranas antioxidantes lipofílicos que estabilizan la estructura de la membrana y minimizan los procesos oxidativos. Los lípidos, al igual que los ácidos nucleicos, glúcidos y proteínas, pueden reaccionar con las ROS y RNS, en procesos que dan lugar a la formación de una gran variedad de productos (256).

2.8.1 Etapas de la lipoperoxidación y formación de productos

Los lípidos pueden ser oxidados a través de tres mecanismos: enzimáticos, no enzimáticos o a través de la reacción con radicales libres, siendo los productos, característicos de cada mecanismo. El proceso de lipoperoxidación en sistemas biológicos, se refiere al proceso de oxidación de lípidos, en el cual radicales libres tales como el $\cdot\text{OH}$ y el $\cdot\text{NO}_2$, oxidan moléculas lipídicas presentes en las membranas celulares a través de la abstracción de un electrón de los enlaces dobles de ácidos grasos, dando lugar a la formación de radicales lipídicos, lo cual resulta en daño celular. Este proceso ocurre a través de una reacción en cadena, y afecta fundamentalmente a los ácidos grasos poli-insaturados (PUFAs), ya que los grupos metileno ($-\text{CH}_2$) de los dobles enlaces, tienen hidrógenos especialmente susceptibles de sufrir la abstracción electrónica. Este proceso, consta de tres etapas: iniciación, propagación y terminación (257), (Figura 2.11).

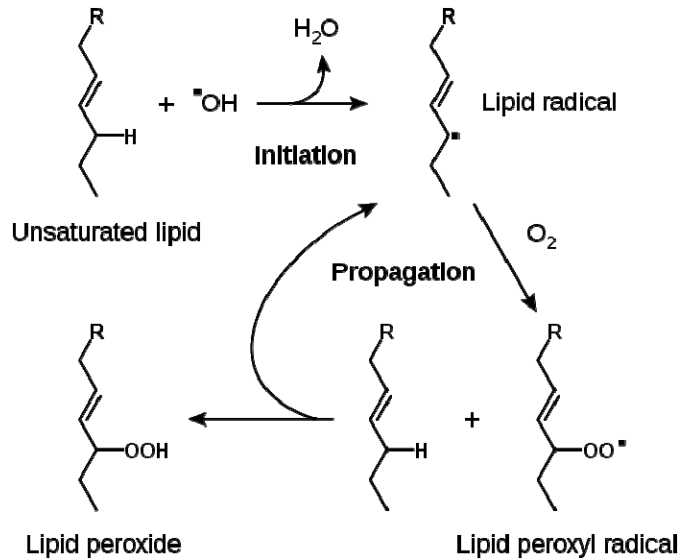


Figura 2.11 Primeras etapas de la lipoperoxidación

La iniciación es el proceso mediante el cual se produce un radical lipídico alquilo ($\text{L}\cdot$) mediante la reacción de una especie oxidante (radical iniciador) como el radical $\cdot\text{OH}$, con un ácido graso (LH) (Ec. 32):



El $\cdot\text{OH}$ puede reaccionar con ácidos grasos saturados ($k = 5 \times 10^8 \text{ M}^{-1}\text{s}^{-1}$) (258), e insaturados ($k = 5 \times 10^9 \text{ M}^{-1}\text{s}^{-1}$) (259) muy rápidamente para formar el radical $\text{L}\cdot$, cuando la reacción ocurre con un ácido graso saturado, el radical peroxilo formado no será capaz de propagar la reacción.

La propagación es un proceso que depende de la presencia de O_2 y consiste en la adición de una molécula de O_2 al radical $\text{L}\cdot$ para formar el radical peroxilo ($\text{LOO}\cdot$) (Ec. 33) y subsiguientemente radicales alquilo ($\text{LO}\cdot$), los cuales son especies fuertemente oxidantes capaces de causar daño a biomoléculas como proteínas.



El radical LOO^{\bullet} es capaz de oxidar a otro ácido graso y de esa manera propagar la reacción de lipoperoxidación, produciendo también un hidroperóxido lipídico ($LOOH$) (Ec. 34):



La terminación es el proceso mediante el cual reaccionan dos radicales libres para dar un producto no radicalar, cortando la propagación de la cadena. Esta reacción puede ocurrir entre dos radicales peroxilo (Ec. 35) o entre un radical lipídico (L^{\bullet} , LO^{\bullet} y LOO^{\bullet}) y el $\bullet NO$, que en estas condiciones, actúa como antioxidante en membranas, y da lugar a la formación de lípidos nitrados ($LOONO$) (160, 161).



También existen diversas moléculas antioxidantes presentes en las membranas capaces de terminar la propagación, tales como el α -tocoferol (vitamina E), carotenoides y el colesterol.

Durante la lipoperoxidación se forman una gran variedad de productos primarios y secundarios, tales como conjugados dienos, hidroperóxidos lipídicos ($LOOH$), alcanos (pentano y etano), así como los productos de escisión de ácidos grasos oxidados como el malondialdehído (MDA). Estos productos pueden ser cuantificados por distintas técnicas y muchos trabajos actuales están enfocados en el estudio de los efectos biológicos de estas moléculas producidas durante la lipoperoxidación (256, 257, 260) (Figura 2.12).

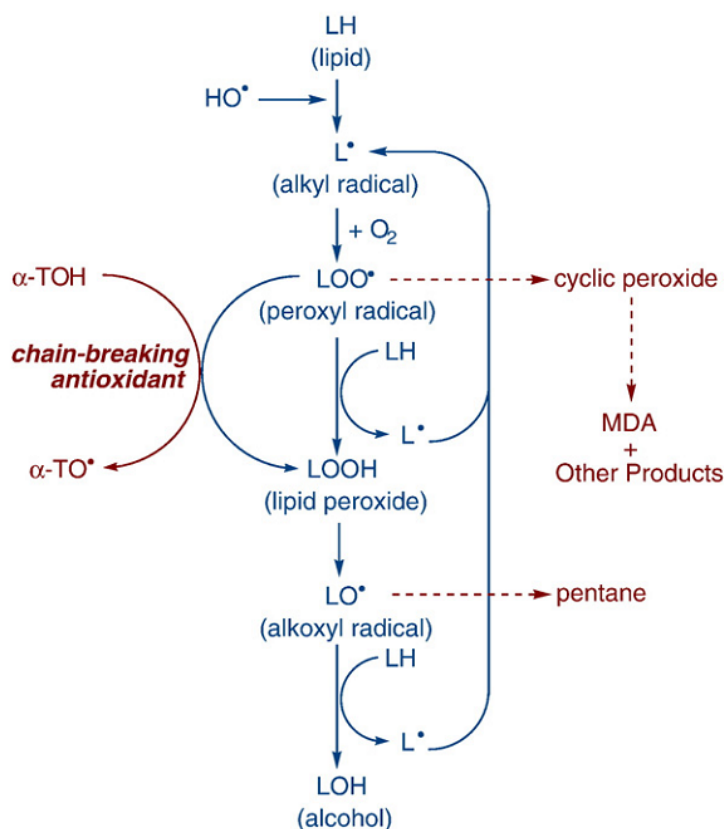


Figura 2.12 Formación de productos durante la lipoperoxidación. Extraído de (257).

2.8.2 El rol del α -tocoferol

Un compuesto lipofílico con importante capacidad antioxidante dentro de las membranas es el α -tocoferol (α -TOH). En efecto, esta molécula se ubica dentro de la bicapa lipídica, con el grupo -OH fenólico cercano a la interfase lípido-agua, y el resto de la molécula hacia el interior de la membrana. Se ha estimado que los niveles de tocoferol en una bicapa están en el orden de una molécula de α -TOH por cada 100-1000 moléculas de fosfolípidos (~10-100 μ M) (261) y esta concentración puede aumentar en condiciones de administración exógena del compuesto. La principal acción del α -TOH en membranas es actuar inhibiendo los procesos de lipoperoxidación actuando como un antioxidante que corta las cadenas de propagación; "chain-breaking antioxidant". Esta acción está realizada principalmente

por una rápida reacción del radical peroxilo del ácido graso (LOO^\bullet) con el α -TOH ($k = 5 \times 10^5 \text{ M}^{-1} \text{ s}^{-1}$; (262)), para rendir el correspondiente hidroperóxido lipídico y el radical α -tocoferoxilo (α -TO $^\bullet$) de acuerdo a la siguiente reacción:



Si bien desde el punto de vista químico esta no es una reacción de "terminación" propiamente dicha, ya que genera como radical secundario el α -TO $^\bullet$, desde el punto de vista biológico inhibe el proceso oxidativo dado que el α -TO $^\bullet$ es un radical relativamente estable, que puede a su vez en sistemas biológicos, ser rápidamente re-generado a α -TOH a través de una reacción con el ácido ascórbico en la zona de interfase lípido-agua (263). Es importante resaltar que en algunas condiciones experimentales se ha demostrado que el α -TO $^\bullet$, puede reiniciar procesos oxidativos (264); sin embargo, a niveles fisiológicos de α -TOH los destinos del α -TO $^\bullet$ son: *i*) reciclaje por ascorbato o *ii*) evolución a productos secundarios, tales como el producto de oxidación por un electron (α -tocoferil quinona), dímeros por combinación de dos moléculas de α -TO $^\bullet$ o formación de aductos de α -TO $^\bullet$ con radicales lipídicos (265). En trabajos publicados por Kalyanaraman (266, 267) y por nuestro grupo (268), se estudió la reactividad de α -TOH con peroxinitrito y sus radicales derivados; globalmente, las observaciones indican que los radicales derivados del peroxinitrito (ej. $\bullet\text{OH}$ y $\bullet\text{NO}_2$) oxidan por un electrón al α -TOH a α -TO $^\bullet$ que eventualmente puede rendir, por una segunda oxidación, el producto estable α -tocoferil quinona. Se espera, sin embargo, que en los procesos de lipoperoxidación mediados por peroxinitrito en membranas, el efecto mayoritario del α -TOH sea por reacción con LOO^\bullet , dado que la mayor concentración de ácidos grasos respecto a α -TOH, hace de los primeros el

blanco preferencial de los radicales derivados de peroxinitrito. Finalmente, es importante destacar que un análogo del α -TOH presente en menores concentraciones en membranas, el gamma-tocoferol (γ -TOH), también puede participar en los procesos de inhibición de la lipoperoxidación dependientes de peroxinitrito; en efecto, el γ -TOH puede atrapar directamente $\cdot\text{NO}_2$ y evolucionar a 5-nitro- γ -TOH, dado que el anillo fenólico contiene una posición no sustituida que puede adicionar $\cdot\text{NO}_2$ (266). Aunque inicialmente se planteó que el γ -TOH sería más importante que el α -TOH para inhibir procesos oxidativos en membranas, mediados por peroxinitrito y otras RNS (269), experimentos posteriores (266) demostraron que el α -TOH es suficiente y el compuesto preferencial para bloquear estos procesos.

2.8.3 Otros procesos oxidativos en membranas

Si bien el proceso predominante en membranas es el de lipoperoxidación, este se puede encontrar asociado a la nitración y oxidación de otras biomoléculas, como es el caso de la nitración de lípidos, que da lugar a la formación de nitrolípidos, una nueva clase de compuestos derivados de ácidos grasos que pueden tener acciones en señalización biológica (270-272). Además, se encuentran modificaciones en otros componentes de membrana y que incluyen *i*) oxidación, nitrosación y nitración de proteínas (Tabla II) y *ii*) oxidación de glúcidos, las cuales pueden modificar las propiedades físicas de las mismas (273, 274). Además, puede haber procesos de “cross-linking” proteína-proteína y lípido proteína (Figura. 2.13). Es importante resaltar, que los PUFAs que se encuentran en las membranas formando parte de los fosfolípidos y que son blanco del proceso de la lipoperoxidación, son a su vez moléculas capaces de propagar procesos oxidativos y participan en varias enfermedades neurodegenerativas y cardiovasculares (275), debido a su capacidad para formar radicales $\text{LOO}\cdot$. Cambios en la estructura de la membrana pueden influenciar la permeabilidad de la misma aumentando la entrada de calcio, lo cual

activa fosfolipasas que clivan los fosfolípidos rindiendo ácidos grasos libres. Estos ácidos grasos pueden activar enzimas como las lipo-oxigenasas y ciclo-oxigenasas, las cuales transforman los ácidos grasos poli-insaturados en LOOH. En determinadas condiciones el hierro presente en lipo-oxigenasas y en hemoproteínas (ej. grupo hemo de la hemoglobina) es liberado, atacando los LOOH formados y desatando una lipoperoxidación no enzimática. Los LOO• formados son mucho más oxidantes que los LOOH de los cuales provienen y pueden atacar distintas biomoléculas, incluyendo fosfolípidos y proteínas (275) (Figura 2.13).

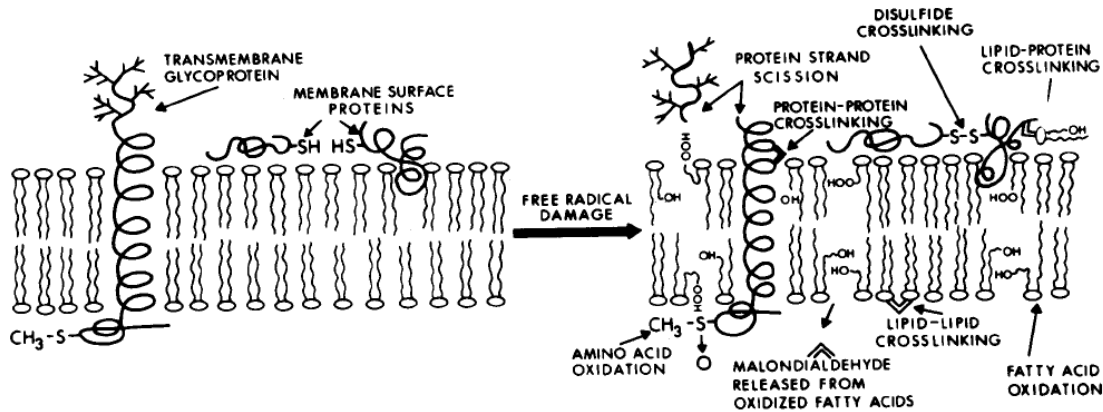


Figura 2.13 Modificaciones oxidativas mediadas por radicales libres en membranas. Extraído de (276).

En el marco de nuestra tesis, será particularmente importante definir la capacidad de los LOO• de oxidar residuos de tirosinas ubicados en el interior de la membrana.

3. Objetivos

Objetivo General:

Estudio de los mecanismos de nitración de tirosinas en membranas

Objetivo Específico # 1:

Estudio de los mecanismos de nitración de tirosinas en membranas mediada por peroxinitrito: utilización de la sonda hidrofóbica *N-t*-BOC-*tert*-butil ester L- tirosina incorporada a liposomas de fosfatidilcolina

Objetivo Específico # 2:

Evaluación de la participación del proceso de lipoperoxidación en la nitración y dimerización de tirosinas en membranas

Objetivo Específico # 3:

Síntesis, caracterización y validación de péptidos transmembrana para el estudio de los mecanismos de nitración de tirosinas en membranas

4. M & M

4.1 Materiales

Los siguientes compuestos químicos fueron adquiridos en Sigma: ácido dietilentriaminopentacético (DTPA), ácido etilendiaminotetracético (EDTA), dióxido de manganeso, bicarbonato de sodio, fosfato de sodio y potasio, L-tirosina, 3-nitrotirosina, *N*-acetil-tirosina, α -tocoferol, 2-metil-nitroso-propano (MNP), hemina, ácido úrico, 1,1,3,3 tetrametoxipropano, ácido lipoico, ácido *para*-hidroxifenilacético (pHPA), ácido deoxicólico, desferrioxamina mesilato y dimetilsulfóxido (DMSO). Los análogos hidrofóbicos utilizados en este trabajo: *N*-*t*-BOC *tert* butil ester L-tirosina (BTBE), 3-nitro-*N*-*t*-BOC *tert* butil ester L-tirosina (3-nitro-BTBE), 3,3'-di-*N*-*t*-BOC *tert* butil ester L-tirosina (3,3'-di-BTBE) y *N*-*t*-BOC *tert* butil ester fenilalanina (BPBE), así como los péptidos transmembrana fueron sintetizados en el Medical College of Wisconsin, USA. Los lípidos de fosfatidilcolina 1,2-dimiristoil-*sn*-glicero-3-fosfocolina (DMPC), 1,2-dilauril-*sn*-glicero-3-fosfocolina (DLPC), 1-palmitoil-2-linoleil-*sn*-glicero-3-fosfocolina (PLPC), fosfatidilcolina de yema de huevo y fosfatidilcolina de soja (EYPC y SBPC) fueron adquiridos en Avanti Polar Lípids (USA).

La 3,3'-ditirosina fue sintetizada mediante incubación de la L-tirosina (0.5 mM), peroxidasa de rábano (4.5 μ M) y H₂O₂ (500 μ M) en buffer fosfato 50 mM (pH 7.4) por 20 minutos a 25°C. La mezcla resultante fue centrifugada en un tubo Centricón (corte de 5000 Da) para remover la enzima y la concentración de 3,3'-di-tirosina fue determinada espectrofotométricamente a 315 nm (ϵ = 5700 M⁻¹cm⁻¹, pH 7.4 y 8380 M⁻¹cm⁻¹ a pH 9.9 (277)).

El azocompuesto ABAP (2,2'-azobis (2) amidinopropano cloruro de hidrógeno) fue adquirido en Wako Co (USA). Las metalo porfirinas Mn-tcpp (porfirina de Mn (III) meso-tetrakis (4-carboxilatofenilo) y Fe-tcpp (porfirina de Fe (III) meso-tetrakis (4-carboxilatofenilo) fueron adquiridas en Calbiochem. El H₂O₂ fue adquirido en Fluka. Los disolventes orgánicos para la síntesis de los compuestos orgánicos y

procedimientos de cromatografía líquida fueron de Baker o Mallinckrodt, de alta calidad.

La solución de hemina fue preparada en el momento en 0.1 M NaOH y mantenida a 4°C y en oscuridad hasta su uso. Los complejos con hierro-EDTA Fe^{III} y desferrioxamina-Fe^{III} fueron preparados mezclando volúmenes iguales de EDTA y desferrioxamina con cloruro férrico respectivamente en una relación 1,1:1. Las soluciones stock de Mn-tcpp y Fe-tcpp fueron 1,21 y 1,10 mM respectivamente, y fueron diluidas en NaOH 0.1 M.

Todos los reactivos utilizados fueron de alta pureza. Los gases utilizados, argón y nitrógeno fueron adquiridos en AGA (Uruguay). Todas las soluciones fueron preparadas con agua ultrapura desionizada para minimizar la contaminación trazas de metales.

4.2 Métodos

4.2.1 Síntesis de BTBE y Productos Derivados

El BTBE, 3-nitro-BTBE y 3,3'-di-BTBE fueron sintetizados en el Medical College of Wisconsin, USA como se describió previamente (192). El BPBE fue sintetizado utilizando el mismo procedimiento que para el BTBE, pero a partir de *t*-butilester L-fenilalanina disponible comercialmente (Sigma). Se prepararon soluciones metanólicas (1M) de cada uno de ellos, inmediatamente antes de su uso.

4.2.2 Síntesis y Purificación de Péptidos Transmembrana

Los péptidos transmembrana de 23 amino ácidos conteniendo un residuo de tirosina en la posición 4, 8 y 12 a partir del extremo amino terminal, fueron sintetizados por SB en el Medical College de Wisconsin, USA, mediante una síntesis en fase sólida como fue reportado previamente (191).

Los péptidos se sintetizaron con el extremo *N*-terminal acetilado y el *C*-terminal amidado, mediante el método de síntesis en fase sólida utilizando la resina *p*-amida metilbenzilhidrilamina (MBHA), utilizando *n*-(9-fluororenil) metoxicarbonilo (Fmoc), como grupos protectores. La resina MBHA (0,72 mmol / g, Novobiochem, La Jolla, California) se dejó overnight con *N*-metil piperidina (NMP) antes de iniciar la síntesis. El acoplamiento de los amino ácidos Fmoc se realizó utilizando volúmenes iguales de 1-hidroxibenzotriazol (HOBt) 0,5 M y di-isopropilcarbodi-imida (DIC) 0,5 M en NMP en un exceso molar de cinco veces en relación con el aminoácido. El grupo protector Fmoc se eliminó con 25% de piperidina en NMP, seguido por 3 lavados con NMP y diclorometano (DCM). Las cadenas laterales de los amino ácidos estaban protegidas de la siguiente manera: *t*-butilo (Tyr), y Boc (Lys). La acetilación del extremo *N*-terminal se realizó con el exceso de anhídrido acético en presencia de HOBt y DIC a temperatura ambiente durante 4 h. La desprotección y clivaje de la resina se llevaron a cabo usando una mezcla de ácido trifluoroacético (TFA), tri-isopropilsilano (TIS) y agua (90:5:5 v / v / v) durante 3 horas a temperatura ambiente. Los péptidos clivados fueron precipitados con éter dietílico frío y luego lavados 3 veces con éter dietílico y secados al vacío. Los péptidos crudos fueron purificados por RP-HPLC semi-preparativa en una columna C8 de 10 micras (1.0 x 25 cm, (Vydac, Hesperia, CA) utilizando un gradiente lineal de 10 a 80% de acetonitrilo en agua /0.1% TFA, durante 40 min. La pureza del péptido fue verificada por RP-HPLC analítica en una columna Vydac C18 (0.46 x 25 cm). La masa molecular de los péptidos sintetizados se validó mediante espectrometría de masa.

4.2.3 Preparación de Liposomas e Incorporación de las Sondas

La incorporación del BTBE y BPBE fue realizada como se describió inicialmente (192). Brevemente, se adicionó una solución metanólica de BTBE (0.35 mM) ó BPBE (0.35 mM) a una solución de lípidos de fosfatidilcolina en cloroformo

(0.35 mM). Bajo estas condiciones se incorpora más del 98 % del BTBE, como fue demostrado previamente (192). Se secó la mezcla bajo corriente de nitrógeno y se prepararon los liposomas uni y multilamelares por resuspensión en buffer fosfato 100 mM, 0.1 mM DTPA (pH 7.4), seguido de 10 ciclos de congelamiento-descongelamiento en nitrógeno líquido, o por resuspensión bajo agitación vigorosa en buffer fosfato, respectivamente. Los rendimientos de incorporación y formación de productos de oxidación del BTBE fueron similares en liposomas uni y multilamelares, y por lo tanto independientes de la morfología de la membrana, por lo que, dado que la preparación es más simple, la mayoría de los estudios fueron realizados en liposomas multilamelares. Es importante resaltar que se trabajó con un modelo de membranas lo cual, pese a no representar exactamente las condiciones de una membrana biológica, permitió realizar gran cantidad de experimentos, ensayando numerosas variables fisicoquímicas, en un sistema muy controlado y limpio, y estudiando el efecto de una variable por vez, lo cual sería muy difícil de realizar en sistemas de membranas celulares, cuya complejidad genera limitantes experimentales y muchas veces impide el análisis correcto de los resultados. En los experimentos con α -tocoferol, el mismo (en etanol), fue incorporado a la solución lipídica en cloroformo, previo a la evaporación bajo corriente de N_2 . Normalmente se trabajó con una concentración final de 30 mM liposomas y 0.3 mM de análogo hidrofóbico de tirosina, salvo en los casos que se indique de otra manera. Una vez preparados los liposomas (con la sonda incorporada), estos fueron expuestos a los distintos agentes oxidantes, y los productos de oxidación fueron extraídos con metanol, cloroformo y NaCl 5M en una proporción 1: 2.4: 0.4 v/v respectivamente, con eficiencias de recuperación mayores al 95% (192). Se centrifugaron las muestras por 10 minutos a 5000 rpm y se descartó el sobrenadante. Se secó la fracción remanente bajo corriente de N_2 y se guardaron las muestras hasta su uso. Inmediatamente antes de analizar las muestras por HPLC, se resuspendieron en 100 μ L de una mezcla KPi 15 mM (pH 3) (15 %): metanol (85 %). Los experimentos fueron siempre realizados a 25°C salvo cuando se trabajó con

DMPC (realizados a 37°C), para trabajar en cada caso por encima de la temperatura de transición de los distintos lípidos.

En los experimentos a bajas tensiones de oxígeno, se burbujearon los liposomas durante 30 minutos con Argón previo a la adición del oxidante.

El péptido transmembrana (Y8, 0.35 mM), fue incorporado a los liposomas de PC mediante el mismo procedimiento que el BTBE y tratado con peroxinitrito. Luego de preparadas las muestras, se adicionaron 600 µl de agua y se centrifugaron a 12000 rpm durante 2 hs, se removió el sobrenadante y se secaron bajo corriente de N₂. Previo a su análisis por HPLC, fueron resuspendidas en 50 µl de Metanol / TFA 2.5%. Alternativamente se realizó una extracción orgánica de las muestras como fue descrito para los liposomas con BTBE.

4.2.4 Síntesis y Cuantificación de Peroxinitrito

El peroxinitrito fue sintetizado en un reactor de flujo detenido a partir de nitrito de sodio (NaNO₂) y peróxido de hidrógeno (H₂O₂) como se describió previamente (15). El H₂O₂ remanente de la síntesis fue eliminado tratando a la solución stock de peroxinitrito con dióxido de manganeso granular y se guardó la solución alcalina hasta su uso a -20°C. La concentración de las soluciones se determinó diariamente, espectrofotométricamente midiendo la absorbancia a 302 nm ($\epsilon = 1670 \text{ M}^{-1}\text{cm}^{-1}$) (12, 16). La concentración de nitrito de las muestras fue estrictamente controlada y fue siempre menor al 20%, ya que concentraciones mayores pueden alterar los resultados obtenidos, ya que el nitrito puede reaccionar con $\cdot\text{OH}$ y otros oxidantes para rendir $\cdot\text{NO}_2$ y favorecer reacciones de nitración no deseadas. En los experimentos control, el peroxinitrito fue adicionado luego de su descomposición en buffer fosfato (100 mM) pH 7,4, para descartar el efecto de productos remanentes de su síntesis, nitrito y H₂O₂ (adición reversa de peroxinitrito).

4.2.5 Sistemas Oxidantes

El BTBE (u otras sondas) incorporado a liposomas fue oxidado mediante la adición de peroxinitrito, hemina, el dador de radicales peroxilo (ABAP) o reactivo de Fenton.

El peroxinitrito fue adicionado en forma de bolo bajo agitación vigorosa ($t_{1/2} = 2.5$ s a 25°C (14)) o mediante infusión continua utilizando un inyector automático (kd Scientific). Dado que la solución de peroxinitrito es alcalina el pH de las muestras fue estrictamente controlado luego de su tratamiento para asegurar que las variaciones no fueron significativas (< 0.1 unidades de pH).

La hemina fue adicionada directamente a los liposomas de fosfatidilcolina. Los liposomas insaturados (EYPC y SBPC) contienen niveles basales de hidroperóxidos preformados, que sirven como sustrato para la hemina.

El azocompuesto ABAP genera por termólisis radicales peroxilo (AOO^{\bullet}), por lo que las muestras fueron incubadas con ABAP a 37°C durante 2-3 hs para obtener una concentración final de (0-40 mM). El consumo de oxígeno dependiente de ABAP fue medido por oximetría de alta resolución (Oroboros 2K) rindiendo un flujo de radicales peroxilo de $0.3 \mu\text{M} / \text{min}$.

El reactivo de Fenton fue adicionado a los liposomas en presencia de H_2O_2 mediante una solución stock de sulfato ferroso (FeSO_4) (10 mM) en ácido sulfúrico (H_2SO_4) (2.5 mM) con una relación final de $\text{Fe}^{\text{II}} : \text{H}_2\text{O}_2 = 1$.

4.2.6 Cuantificación de 3-NT y 3-NO₂-BTBE por Espectrofotometría

En algunos experimentos con liposomas conteniendo ácidos grasos saturados (DLPC, DMPC), se cuantificó la formación de 3-nitro-BTBE por medición directa UV-Vis. Los liposomas fueron solubilizados con deoxicolato de sodio (1,2%) (278) y la solución se alcalinizó a pH 10 con 5 M NaOH. Se midió la formación de 3-nitro-BTBE a 424 nm pH 10 ($\epsilon = 4.000 \text{ M}^{-1} \text{ cm}^{-1}$). Del mismo modo, se midió la formación de 3-NT a

430 nm pH 10 ($\epsilon = 4.000 \text{ M}^{-1} \text{ cm}^{-1}$). Este método permite hacer rápidas determinaciones con resultados reproducibles y comparables a los obtenidos por HPLC pero solo puede ser usado con lípidos saturados, dado que con lípidos insaturados se obtienen otros productos que interfieren con la detección a 400 nm.

4.2.7 Cromatografía Líquida de alta Performance (HPLC)

El BTBE y sus productos de oxidación, 3-nitro-BTBE y 3,3'-di-BTBE se separaron por cromatografía líquida de alta performance de fase reversa (RP-HPLC) en un equipo Agilent 1200 equipado con sistema de detección UV-Vis y de fluorescencia utilizando una columna C18- Agilent Eclipse XDB-C18 de 5 micras (150 mm de longitud , 4.6 mm de diámetro). La fase móvil A consistió en 15 mM de KPi pH 3 y la fase móvil B consistió en metanol. Las condiciones cromatográficas fueron: flujo 1 ml / min, 75% de la fase móvil B durante 25 minutos, seguido de un aumento lineal de la fase móvil B a 100% durante 10 minutos. La detección UV-Vis se realizó a 280 nm para el BTBE ($\epsilon = 1200 \text{ M}^{-1} \text{ cm}^{-1}$) y a 280 y 360 nm para el 3-nitro-BTBE ($\epsilon = 1500 \text{ M}^{-1} \text{ cm}^{-1}$), que presenta una doble absorbancia característica. El 3,3'-di-BTBE fue detectado fluorimétricamente ($\lambda_{\text{exc}} = 294 \text{ nm}$, $\lambda_{\text{em}} = 401 \text{ nm}$). Se utilizaron BTBE, 3-nitro-BTBE y 3,3'-di-BTBE auténticos como estándares.

El producto de hidroxilación del BTBE (N-*t*-BOC 3,4-dihidroxi-L-fenilalanina) (3-OH-BTBE) fue separado con condiciones cromatográficas levemente diferentes. La fase móvil A consistió de agua y la fase móvil B fue metanol, realizándose un gradiente de 50-100% metanol en 35 minutos. Se realizó detección UV-vis a 280 nm y fluorimétrica ($\lambda_{\text{ex}} = 280 \text{ nm}$ y $\lambda_{\text{em}} = 306 \text{ nm}$).

La tirosina y sus productos de oxidación 3-NT y 3,3'-ditirosina se separaron por RP-HPLC, utilizando una columna C18 Partisil SAO-3 de 10 micras (250 mm de longitud, 4.6 mm de diámetro). La separación se realizó en forma isocrática en las siguientes condiciones cromatográficas: flujo 1 ml / min; 97% fase móvil A (KPi 15mM

pH 3) y el 3% fase móvil B (metanol) durante 30 minutos. La 3-NT se detectó por UV-Vis a 280 y 360 nm, y la 3,3'-ditirosina se midió por fluorescencia (λ_{ex} 280 nm y λ_{em} = 400 nm). Se utilizaron como estándares 3-NT y 3,3'-ditirosina auténticos. La nitración artificial del BTBE o tirosina durante el procedimiento cromatográfico debido a la presencia de nitrito en medio ácido fue descartada realizando controles adecuados de adición reversa de peroxinitrito.

Los péptidos transmembrana fueron purificados por RP-HPLC en el MCW bajo las siguientes condiciones cromatográficas: gradiente lineal de 40 % acetonitrilo / 0.1 % TFA en agua / 0.1 % TFA a 80 % acetonitrilo / 0.1 % TFA en agua durante 30 minutos. Se determinó una pureza > 95%.

Los productos de oxidación del péptido transmembrana luego de la adición de peroxinitrito, fueron separados por RP-HPLC, usando una columna C18-Agilent Eclipse XDB-C18 de 5 micras (150 mm de longitud, 4.6 mm de diámetro). Se utilizaron como fases móviles acetonitrilo y H₂O / 0.1% TFA, y el siguiente método de control: gradiente de 50-60 % acetonitrilo en 40 minutos, flujo 0.35 ml / min. Se realizó detección UV-Vis a 280 nm para el Y8, y a 280 y 360 nm para el derivado nitrado, NO₂-Y8.

4.2.8 Espectrometría de Masa (MS)

La formación de 3-OH-BTBE se analizó en un espectrómetro de masa Applied Biosystems, QTRAP triple cuadrupolo lineal (LIT) con trampa de iones equipado con una fuente de ionización de iones turbo spray (ESI). El espectrómetro de masa se operó en modo positivo y la configuración de ESI fue la siguiente: voltaje ionización 2500 V, temperatura 375°C; potencial de desagrupamiento 50 V, potencial de entrada 10 V, gas nebulizado 40 psi; gas accesorio 25 psi. Las muestras recogidas del HPLC se diluyeron en metanol (con 0.1% de ácido fórmico) y se inyectaron por infusión continua (10 μ L / min) con una concentración estimada de 10 nM. Se identificó el ion

molecular en $m/z = 353,2$ y el análisis de fragmentación del 3-hidroxi BTBE se llevó a cabo utilizando el LIT en el modo MS/MS usando la trampa de iones como detector. Los experimentos de fragmentación del ion molecular se llevaron a cabo utilizando diferentes energías de disociación que permitieron identificar los fragmentos del ion parental.

Los estudios de MS en péptidos fueron realizados en un espectrómetro Applied Biosystems, QTRAP triple cuadrupolo lineal (LIT) con trampa de iones equipado con una fuente de ionización de iones turbo spray (ESI). El espectrómetro de masa se operó en modo positivo. Se preparó una dilución de péptido en metanol (10 μ M) + 0.1 % ácido acético. Una vez purificados los péptidos y analizados por MS, estos fueron liofilizados y almacenados a -20°C hasta su uso.

4.2.9 Resonancia Paramagnética Electrónica (EPR)

Los experimentos de EPR se registraron a temperatura ambiente en un espectrómetro Bruker EMX operando a 9,8 GHz. Los parámetros del espectrómetro fueron los siguientes: ancho del barrido, 100 G; campo medio, 3505 G, constante de tiempo, 20,48 ms; tiempo de exploración, 42 s, modulación de amplitud, 1,0 G, modulación de la frecuencia, 100 kHz, ganancia del receptor, 1×10^6 ; potencia de microondas, 20 mW. Para la realización de los registros, las muestras fueron transferidas a un tubo capilar de 50 μ L. Dado que los radicales que se quieren detectar son especies muy inestables, se trabajó con la técnica de "spin trapping", para lo cual se usa una molécula atrapadora de spin, que forma un aducto con el radical de interés y este aducto es más estable y puede detectarse fácilmente. En este caso se trabajó con el atrapador 2-metil nitroso propano (MNP) (20 mM), que fue incubado con los liposomas (previo a la adición de peroxinitrito) durante 20 min. Dado que el MNP puede sufrir fotólisis y generar una señal diferente a la del radical fenoxilo, se realizó la incubación con las muestras cubiertas en papel de aluminio y se registraron las

señales en absoluta oscuridad de manera que la señal del MNP debido a la fotólisis del mismo no se observó durante las condiciones experimentales.

4.2.10 Productos de la Lipoperoxidación

El malondialdehído (MDA), uno de los subproductos de la lipoperoxidación, se midió espectrofotométricamente a través de la formación del aducto coloreado que se forma por su reacción con el ácido tiobarbitúrico (TBA) midiendo la absorbancia a 532 nm, ($\epsilon = 150.000 \text{ M}^{-1} \text{ cm}^{-1}$), como se describió previamente (16); el aducto está formado por 2 moléculas de TBA y una molécula de MDA (Figura 4.1). La lipoperoxidación genera una variedad de productos como aldehídos e hidroperóxidos lipídicos que aumentan a consecuencia del estrés oxidativo y pueden reaccionar con el TBA, aunque generalmente se utiliza este método como indicador general de la formación de MDA a 532 nm. Las curvas de calibración y evaluación de los contenidos MDA se realizaron con cantidades conocidas de MDA obtenidos a partir de la hidrólisis ácida del 1,1,3,3 tetrametoxipropano en 20% de ácido acético a pH 3,5. Para evitar la sobreoxidación de los lípidos durante el ensayo se añadió butilhidroxitolueno (BHT) 0,05% (w / v) al reactivo TBARS. La formación de hidroperóxidos lipídicos se evaluó por el ensayo de FOX (279). Brevemente, se añadieron 50 μL de liposomas a 950 μL de reactivo de FOX que consiste en xilenol orange (100 mM), Fe^{2+} (sulfato de amonio ferroso) (250 mM), H_2SO_4 (25 mM) y BHT (4mM) / metanol 90% (v / v). Las mezclas de reacción se incubaron 1 hora a temperatura ambiente y se midió la absorbancia a 560 nm. La concentración de hidroperóxidos lipídicos se estimó utilizando un coeficiente de extinción aparente de $43.000 \text{ M}^{-1} \text{ cm}^{-1}$ (279). El consumo de oxígeno durante los procesos de peroxidación lipídica fue medido por oximetría de alta resolución con un 2K Oxygraph (Oroboros Instruments, Austria).

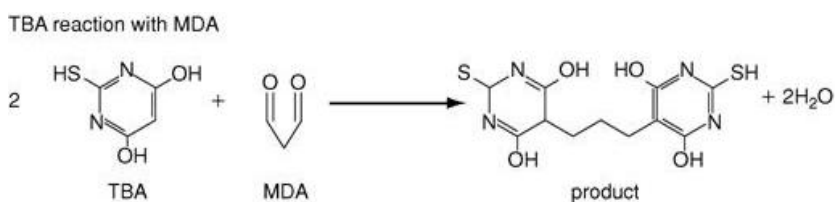


Figura 4.1. Formación del aducto entre el TBA y el MDA

4.2.11 Estudios Computacionales

Se realizaron simulaciones de cinética química asistidas por computadora con el software libre GEPASI 3.0 (www.gepasi.org) (280).

4.2.12 Estimación de las distancias de difusión del peroxinitrito en suspensiones de liposomas

Se estimó la distancia de difusión del peroxinitrito, asumiendo liposomas multilamelares de 5 capas concéntricas, con una concentración de 20 mg / ml, y un diámetro promedio externo de 1000 nm (245). De acuerdo a datos previos (252, 281), puede estimarse una concentración de vesículas de 0.20 nM, que corresponden a 3.65×10^{11} vesículas / ml. Basados en un modelo desarrollado en nuestro laboratorio (243), se puede calcular la distancia de difusión promedio del peroxinitrito en fase acuosa, antes de alcanzar una vesícula liposomal de la siguiente manera (Ec. 37):

$$\Delta x = r \cdot \sqrt{\frac{3}{4} \left(\sqrt[3]{\frac{4n\pi}{3}} \right)^2 - 1} \quad (37)$$

Donde n representa la relación entre volumen total de suspensión y volumen total de liposomas, y r representa el radio de la vesícula. De esta ecuación se obtiene una distancia Δx de 1.1 μm . El porcentaje de peroxinitrito adicionado que efectivamente puede alcanzar a un liposoma se puede determinar por la siguiente ecuación (Ec. 38):

$$\ln \left[\frac{[ONOO^-]_x}{[ONOO^-]_p} \right] = \frac{-\ln 2 \cdot \Delta x^2}{2 D_{ONOO^-} \cdot t_{1/2}} \quad (38)$$

donde $t_{1/2}$ representa la vida media del peroxinitrito en el medio extracelular, D_{ONOO^-} , es el coeficiente de difusión del peroxinitrito, considerado igual al del nitrato (NO_3^-), $1500 \mu m^2 s^{-1}$ (242, 254).

4.2.13 Análisis de los Resultados

Todos los experimentos reportados en esta tesis fueron repetidos un mínimo de tres veces. Los resultados son expresados como los valores promedios con sus desvíos estándares correspondientes. Los gráficos y los análisis matemáticos fueron realizados con el software OriginPro 8.0.

5. Resultados & Discusión

Obj. #1

5. Objetivo # 1. Estudio de los mecanismos de nitración de tirosinas en membranas mediada por peroxinitrito: utilización de la sonda hidrofóbica N-*t*-BOC-*tert*-butilester L-tirosina incorporada a liposomas de fosfatidilcolina.

El peroxinitrito es capaz de difundir a través de membranas y lipoproteínas e interactuar con ellas, promoviendo reacciones de oxidación y nitración en lípidos y proteínas. Sin embargo, todavía no se han realizado estudios mecanísticos profundos sobre la nitración de tirosinas en fases hidrofóbicas, y muchos de las suposiciones aceptadas para sistemas acuosos, pueden no ser válidas para entornos hidrofóbicos, debido a la diferente polaridad, las restricciones espaciales, y la difusión limitada tanto de moléculas blanco como de especies reactivas, entre otros factores. También se debe profundizar en el estudio del proceso de dimerización de tirosinas en membranas e hidroxilación, lo que no ha sido previamente estudiado. En el siguiente Objetivo Específico pretendemos profundizar en los mecanismos de oxidación de tirosinas en membranas, mediante el uso del análogo hidrofóbico de la tirosina, el BTBE, incorporado a liposomas de PC como sistema modelo de membranas, y peroxinitrito como agente oxidante y nitrante para estudiar las determinantes físico-químicas y bioquímicas que rigen el proceso de oxidación de tirosinas mediado por peroxinitrito.

5.1 Análisis del BTBE y sus productos de oxidación 3-nitro-BTBE and 3,3'-di- BTBE

Para estudiar los factores físico-químicos y bioquímicos que controlan la nitración de tirosinas en membranas, los liposomas de PC con BTBE incorporado fueron tratados con peroxinitrito. El BTBE, y sus productos de oxidación se cuantificaron por UV-Vis y / o fluorescencia luego de: *i*) la separación de los productos de oxidación por RP-HPLC del material obtenido en la extracción química orgánica o *ii*) la solubilización de los liposomas con ácido deoxicólico. La figura 5.1A muestra un cromatograma de HPLC típico obtenido de las muestras tratadas con peroxinitrito,

donde el BTBE, el 3-nitro-BTBE y el 3,3'-di-BTBE eluyen a los 7, 9 y 19 minutos, respectivamente. Por otra parte, el análisis espectrofotométrico de los liposomas luego de la solubilización con ácido deoxicólico (1.2 %), midiendo la absorbancia a 424 nm a pH 10, muestra la formación de 3-nitro-BTBE (Figura 5.1B). En liposomas de DLPC (30 mM) a pH 7,4 (Figura 5.1C), el peroxinitrito (0-2 mM) causó la formación de 3-nitro-BTBE en una forma dependiente de la concentración con rendimientos de ~ 3% (15 mM 3-nitro-BTBE con 500 μ M peroxinitrito), y estos resultados fueron similares a los obtenidos por HPLC (Figura 5.1C).

Es importante destacar que si bien, la medición espectrofotométrica directa de 3-nitro-BTBE luego de la solubilización con deoxicolato es un método muy práctico y reproducible para liposomas que contienen ácidos grasos saturados (DLPC, DMPC), este método no debe ser aplicado a liposomas con ácidos grasos insaturados (EYPC y SBPC), dado que el peroxinitrito conduce a la formación de otras especies como lípidos nitrados y oxidados, los cuales pueden absorber en la misma región del espectro y por lo tanto interferir con la detección de 3-nitro-BTBE (16).

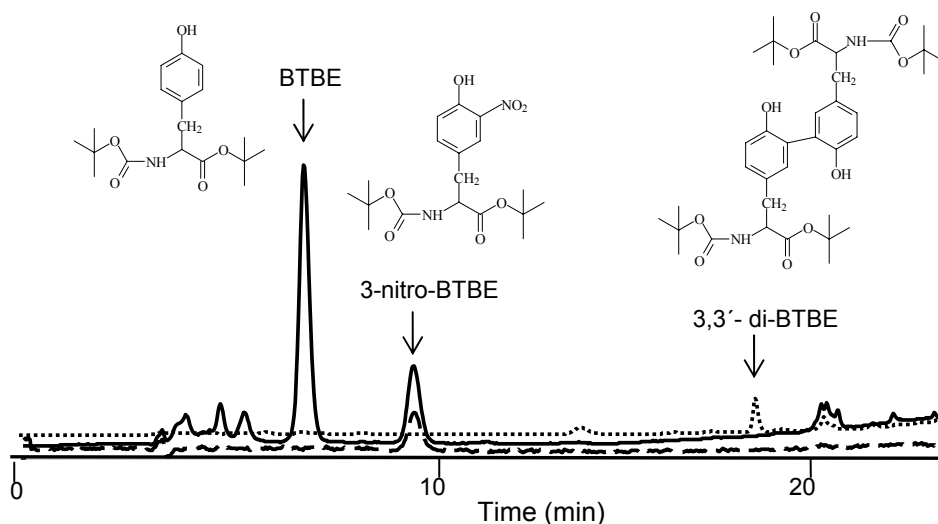


Figura 5.1A

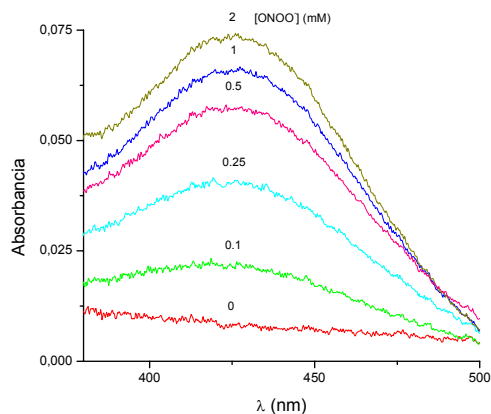


Figura 5.1B

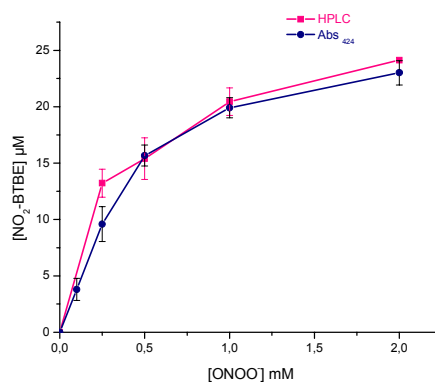


Figura 5.1C

Figura 5.1 Análisis del 3-nitro-BTBE y 3,3'-di-BTBE después de la adición peroxinitrito. El BTBE (0.3 mM) en liposomas de DLPC (30 mM) fue expuesto a peroxinitrito en buffer fosfato (100 mM), pH 7,4 / 0,1 mM de dtpa. **(A)** Los productos fueron separados luego de la extracción orgánica por RP-HPLC. El cromatograma de HPLC muestra la elución del BTBE, 3-nitro-BTBE y 3,3'-di-BTBE luego del tratamiento con ONOO^- (1 mM). Se indican las estructuras de los compuestos sobre los picos correspondientes. La detección se hizo por UV-Vis a 280 nm para BTBE (línea continua) y a 360 nm para 3-nitro-BTBE (línea discontinua). El 3,3'-di-BTBE se midió fluorimétricamente a 294 y 401 nm, λ de excitación y de emisión, respectivamente (línea punteada). **(B)** Los liposomas con BTBE incorporado fueron tratados con peroxinitrito y solubilizados con deoxicolato 1,2%, llevados a pH 10 con NaOH 5M y se registró el espectro UV-Vis del 3-nitro-BTBE en diferentes concentraciones de peroxinitrito. **(C)** Se realizó la cuantificación del 3-nitro-BTBE en función de la concentración de peroxinitrito, luego de la separación por HPLC (■) o de la solubilización con deoxicolato (●).

5.2 Hidroxilación del BTBE mediada por peroxinitrito en liposomas de DLPC

Trabajos previos, realizados por Zhang y colaboradores, mostraron la formación de 3-nitro-BTBE y 3,3'-di-BTBE, al tratar al BTBE incorporado a liposomas con peroxinitrito o el sistema MPO/H₂O₂/NO₂⁻; sin embargo la formación del derivado hidroxilado del BTBE en liposomas no había sido estudiada (192). Dado que es un compuesto más polar que el BTBE, las condiciones cromatográficas se ajustaron con el objetivo de detectar productos que eluyeran a tiempos menores de retención que el propio BTBE. Los experimentos se realizaron inicialmente a pH 6, ya que la hidroxilación como consecuencia de la homólisis del ONOOH, estaría favorecida en condiciones ácidas, y como control positivo de reacción de hidroxilación se utilizó un sistema de Fenton. Tanto en la condición con peroxinitrito, como con reactivo de Fenton, se detectó un nuevo pico, que eluyó a los 11 minutos (Figura 5.2A), el cual no pudo detectarse cuando los experimentos fueron realizados a pH 7,4 (no se muestra). El pico obtenido fue recolectado y analizado por MS (Figura 5.2B), y la masa molecular del ión resultante (m/z) fue de 353,2. El análisis ESI-MS en el modo positivo, normalmente genera iones protonados (M + H⁺), con lo cual para el derivado hidroxilado del BTBE se detectaría un ión con una relación m/z de 354,2, sin embargo se detectó el ion molecular tal y como ocurre con la *N*-acetil-tirosina y el α -tocoferol (datos no mostrados) (282, 283). La ausencia de un grupo capaz de protonarse, y el grupo fenólico oxidable del BTBE favorecen este tipo de ionización. El ión con relación m/z de 353.2 corresponde al catión radical molecular del derivado hidroxilado del BTBE, que por analogía con el sitio preferencial de hidroxilación para la tirosina y otros fenólicos, asignamos como 3-hidroxi-BTBE (32, 170). Es importante resaltar que el patron de fragmentación obtenido en la condición con peroxinitrito y Fenton fue el mismo. Entre los fragmentos se encontró un ión con una relación m/z de 335,3; que correspondería a la pérdida de una molécula de agua del ión parental. Asumiendo que el rendimiento cuántico de fluorescencia del 3-hidroxi-BTBE es similar al derivado

hidroxilado de la tirosina (3,4-dihidroxi-fenilalanina), se puede estimar que se formó 5 nM de producto hidroxilado a partir de 1 mM peroxinitrito a pH 6, lo cual indica que es un proceso de bajo rendimiento. En la Figura 5.2C, se puede observar la cuantificación comparativa de la formación de derivado hidroxilado en las diferentes condiciones estudiadas. La hidroxilación en presencia de Fe^{2+} sólo, se debe a su rápida oxidación en condiciones aerobias para dar $\text{O}_2^-/\text{H}_2\text{O}_2$, generándose en forma secundaria reactivo de Fenton. Sin embargo, el H_2O_2 sólo fue incapaz de hidroxilar al BTBE en ausencia de Fe^{2+} , lo cual indica que la generación de radical $\cdot\text{OH}$ requiere una reacción catalizada por Fe^{2+} . El reactivo de Fenton fue capaz de promover la hidroxilación del BTBE en una forma dependiente de la concentración de reactivo (*ej.* 0.3 mM y 0.6 mM), sin embargo la presencia de NO_2^- que reacciona rápidamente con $\cdot\text{OH}$ para dar $\cdot\text{NO}_2$ ($k = 6 \times 10^9 \text{ M}^{-1}\text{s}^{-1}$) inhibió completamente la formación de producto. El peroxinitrito (1 mM) también fue capaz de promover la hidroxilación del BTBE de una manera menos eficiente que con el reactivo de Fenton, y de vuelta la presencia de NO_2^- fue completamente inhibitoria.

Se pudo determinar la formación de los tres productos de oxidación del BTBE, 3-nitro-BTBE, 3,3'-di-BTBE y 3-hydroxi-BTBE (Figura 5.2A), y sus rendimientos relativos (Figura 8.1). Con el objetivo de determinar si la formación de estos productos tiene lugar a través de un mecanismo radicalar, se realizaron estudios de EPR.

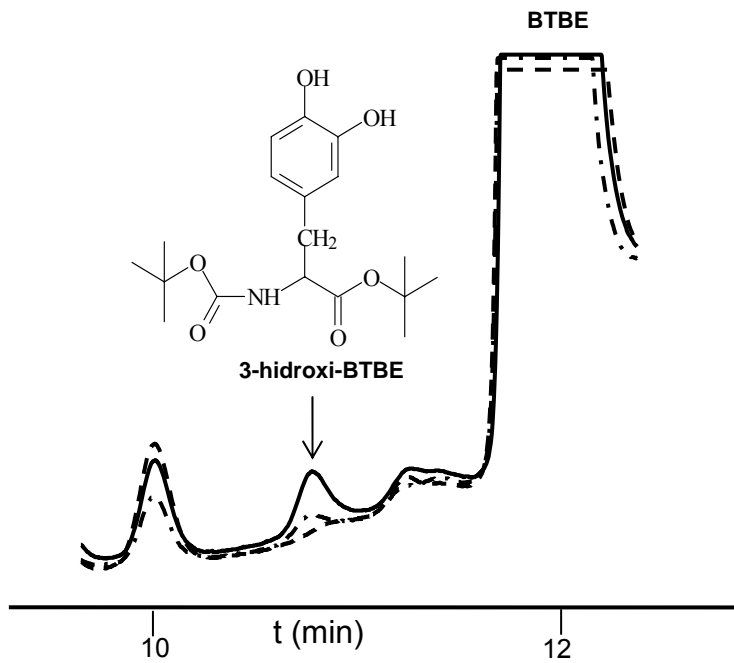


Figura 5.2A

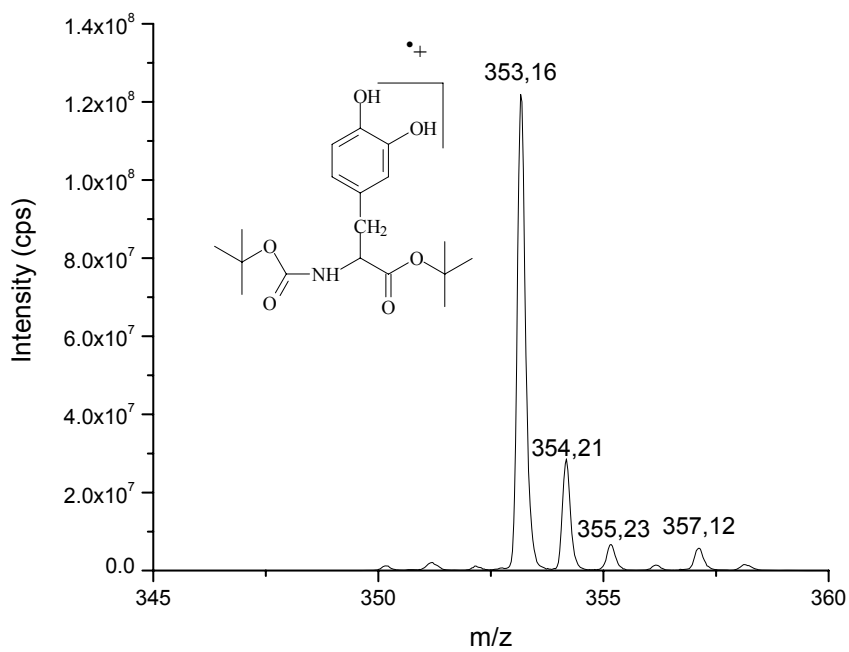


Figura 5.2B

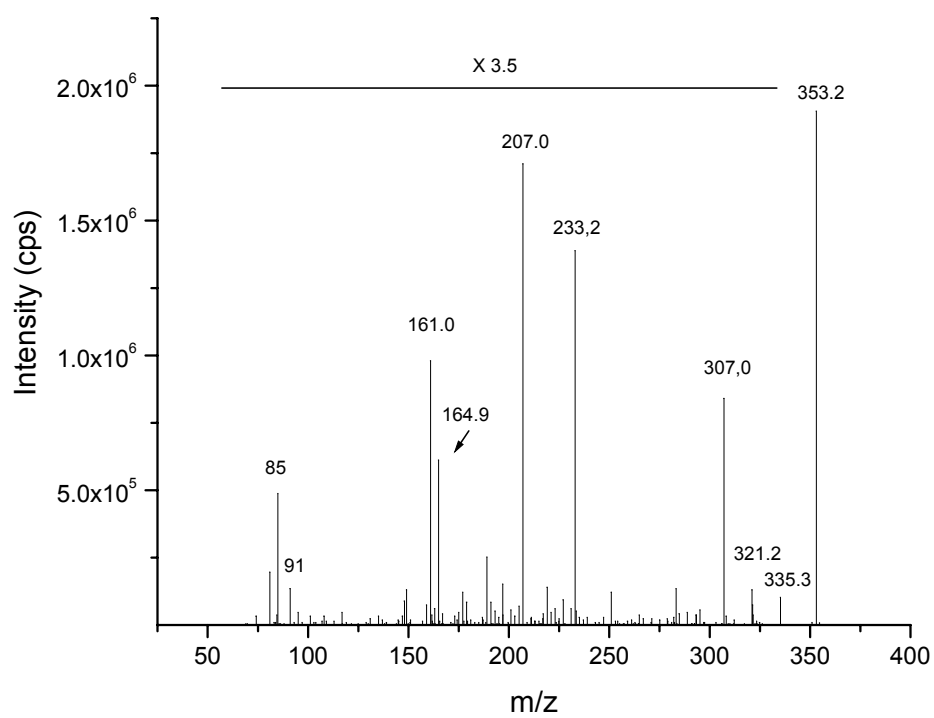


Figura 5.2C

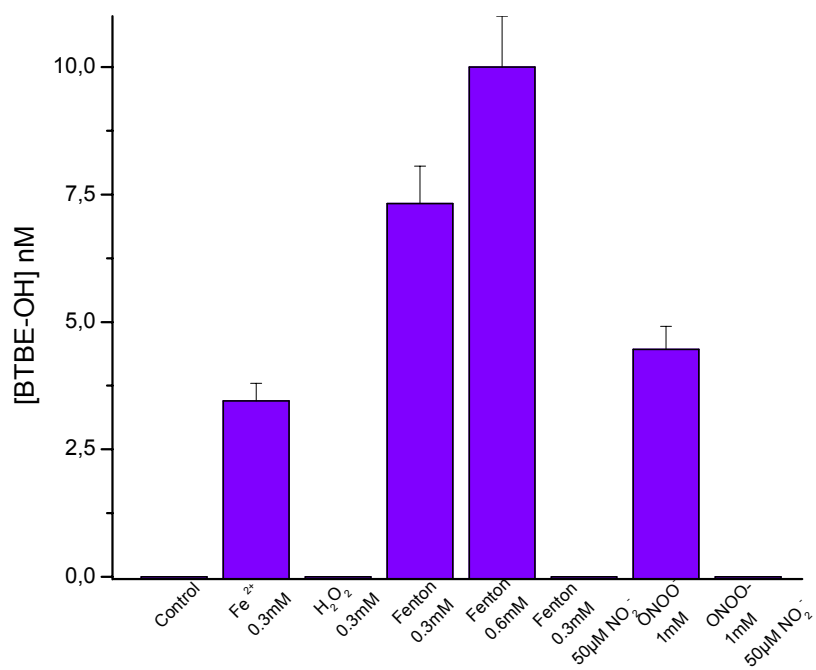


Figura 5.2D

Figura 5.2 Separación por HPLC y caracterización por MS del 3-hidroxi-BTBE. Los liposomas de DLPC (30 mM) (línea discontinua) con BTBE incorporado (0.3 mM) fueron expuestos a FeSO_4 (0.3 mM) + H_2O_2 (0.3 mM) (línea continua) o peroxinitrito (1 mM) (línea discontinua- puntos) en KPi (20 mM), pH 6 / 0.4 mM de dtpa. **(A)** La separación de los productos se realizó por RP-HPLC y se detectó un nuevo pico que eluyó a tiempos menores que el BTBE (12 min) y está presente en las condiciones con reactivo de Fenton y peroxinitrito. **Caracterización del pico eluído a los 11 min por ES-MS.** **(B)** El análisis por scan de masa de alta resolución muestra la formación del ion molecular con una m/z de 353,2 y su distribución isotópica. Se muestra la estructura propuesta para el 3-hidroxi-BTBE. **(C) Análisis MS/MS** (usando la LIT como detector) del ion m/z 353,2 muestra el patrón de fragmentación de la 3-hidroxi-BTBE. **(D) Cuantificación de la formación de 3-hidroxi-BTBE por un sistema de Fenton o peroxinitrito y el efecto del nitrito.** Las reacciones se llevaron a cabo a pH 6 y las condiciones se indican en el gráfico. Los valores de 3-hidroxi-BTBE se estimaron suponiendo un rendimiento cuántico de fluorescencia similar al de la 3,4-di-hidroxi-fenilalanina (derivado hidroxilado de la tirosina).

5.3 Detección del radical fenoxilo derivado del BTBE por EPR

Se utilizó la técnica de EPR spin-trapping para estudiar la formación del radical fenoxilo derivado del BTBE durante la nitración mediada por los radicales derivados del peroxinitrito, utilizando el aducto de spin MNP, como se describió previamente (191). La adición de peroxinitrito a liposomas de DLPC con BTBE pre-incorporado resultó en una señal de 3 líneas parcialmente inmovilizada (Figura 5.3, línea a) similar a la que se obtiene con el radical tirosilo. No se observó la formación del radical cuando los liposomas fueron tratados con peroxinitrito descompuesto (Figura 5.3, línea b), o en ausencia de BTBE (Figura 5.3, línea c). Cuando los liposomas fueron disueltos en etanol, se obtiene una clara señal de tres líneas, dada la mayor movilidad del aducto de spin. (Figura 5.3, línea d). La fotólisis del MNP también puede dar lugar a una señal de 3 líneas pero con un a_N diferente (Figura 5.3, línea e). Debido a la baja relación señal ruido, no se pudo resolver el espectro del aducto de spin para resolver los parámetros de desdoblamiento hiperfino, sin embargo los datos son completamente consistentes con la oxidación (mediada por los radicales derivados del peroxinitrito) por un electrón del BTBE para dar la formación del radical fenoxilo derivado del BTBE en el interior de la membrana, lo cual demostraría que la nitración de tirosinas en membranas tiene lugar a través de un mecanismo que involucra la

formación intermediaria del radical tirosilo, tal y como ocurre para las tirosinas en fases acuosas.

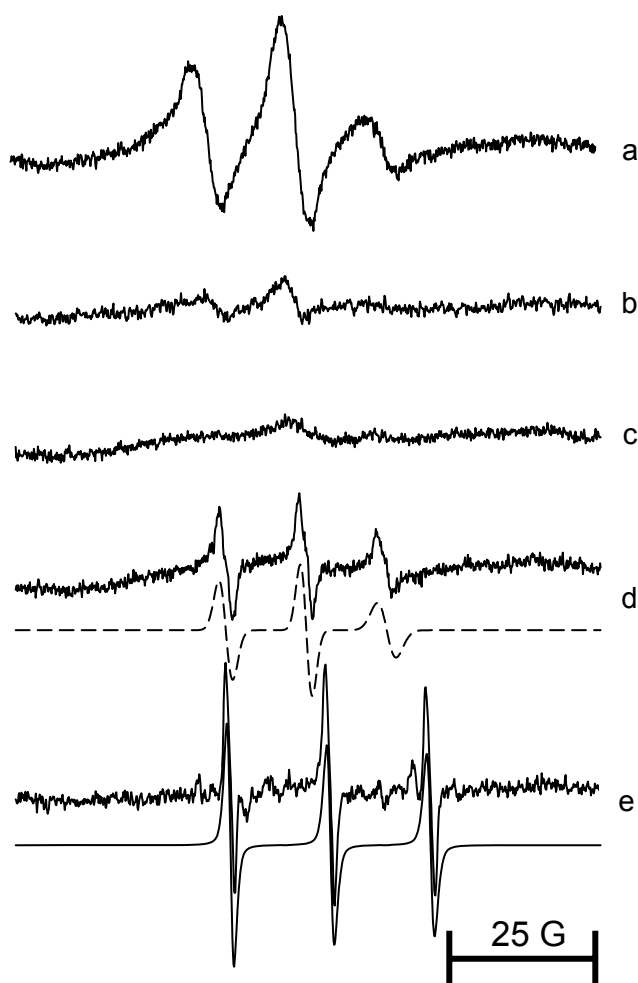


Figura 5.3. Detección del radical fenoxilo en liposomas saturados. Los liposomas de DLPC (45 mM) con BTBE (2.25 mM) pre-incorporado en buffer fosfato (100 mM), pH 7,4 / 0,1 mM de dtpa fueron incubados durante 20 minutos con el spin trap MNP (20 mM) y las muestras fueron posteriormente transferidas a una celda capilar de 100 μ L para las mediciones de EPR **(a)** muestras tratadas con peroxinitrito (5 mM); **(b)** adición reversa del peroxinitrito; **(c)** adición de peroxinitrito a liposomas sin BTBE; **(d)** adición de peroxinitrito en presencia de MNP a liposomas con BTBE, disueltos en etanol y su correspondiente simulación y **(e)** señal obtenida de la fotólisis del MNP y su correspondiente simulación. Los datos corresponden al promedio de 100 scans.

5.4 Oxidación del BTBE mediada por peroxinitrito: liposomas saturados e insaturados

Los radicales $\cdot\text{OH}$ y $\cdot\text{NO}_2$ reaccionan rápidamente con los ácidos grasos insaturados, por lo que estudiamos los rendimientos de nitración y dimerización del BTBE en liposomas de PC con cantidades variables de ácidos grasos insaturados, para determinar si estos son capaces de competir por las especies nitrantes e inhibir el proceso de nitración. La adición de peroxinitrito (0-2 mM) causó un aumento en los rendimientos de nitración y dimerización del BTBE pre-incorporado en forma dosis dependiente tanto en liposomas saturados de DLPC y DMPC, como insaturados de EYPC y SBPC (Figura 5.4A). Los rendimientos de nitración fueron muy similares en DLPC y DMPC, pero, sin embargo, fueron mayores en los liposomas de EYPC, a pesar del alto porcentaje de ácidos grasos insaturados (~ 24%) presentes en estos fosfolípidos. El peroxinitrito, además de promover la nitración en todos los tipos de liposomas, también causó la oxidación del BTBE para rendir el dímero correspondiente, 3,3'-di-BTBE, siendo los rendimientos máximos de dimerización a 250 μM de peroxinitrito, y sensiblemente mayores para EYPC que para DLPC (~ 0.11% y 0.02%, respectivamente; Figura. 5.4B). El perfil de la dosis respuesta de dimerización del BTBE fue similar al obtenido previamente para tirosina libre, que presentó rendimientos máximos a 200 μM peroxinitrito (~ 0.24%) (192). En todos los casos, los rendimientos de nitración fueron significativamente mayores que los de dimerización a pH 7.4, fortaleciendo la idea de que la nitración es la modificación oxidativa mediada por peroxinitrito predominante en membranas, a pH fisiológico (192).

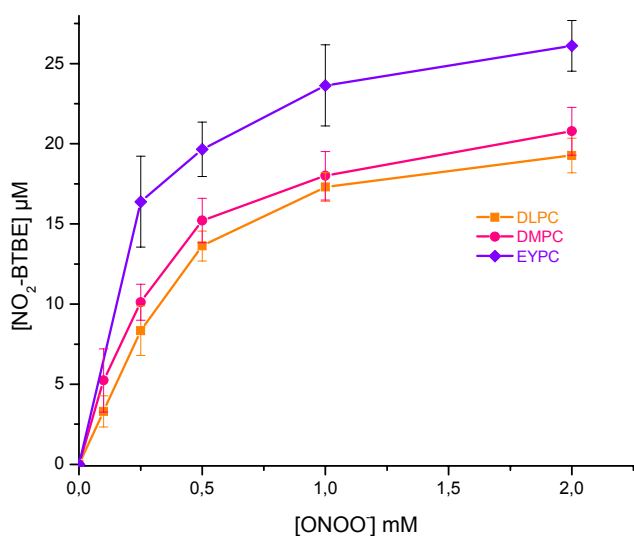


Figura 5.4A

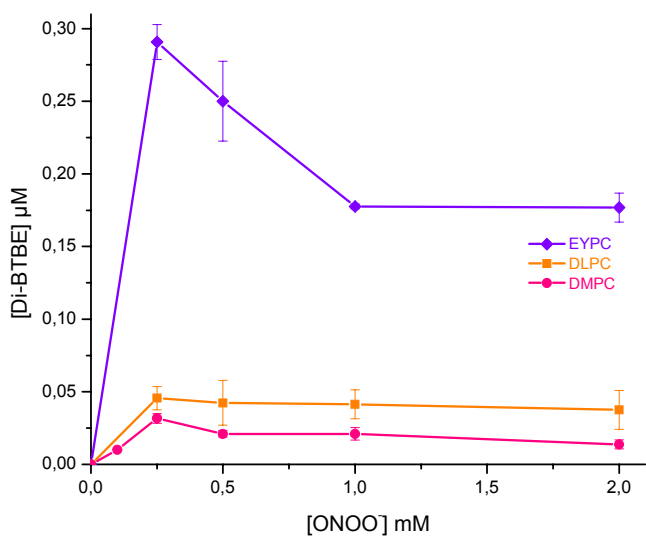


Figura 5.4B

Figura 5.4 Nitricación y dimerización del BTBE mediada por peroxinitrito en liposomas con distinto grado de insaturación. El BTBE (0.3 mM), incorporado a liposomas de DLPC (■), DMPC (●) y EYPC (◆) (30 mM) fue tratado con distintas concentraciones de peroxinitrito en buffer KPi (100 mM), pH 7,4 / 0,1 mM dtpa; la temperatura de incubación fue 21°C para todos los liposomas, excepto para DMPC que fue 37°C. **(A)** 3-nitro-BTBE y **(B)** 3,3'-di-BTBE fueron determinados luego de la separación por RP-HPLC.

5.5 Inhibición de la oxidación del BTBE por atrapadores de peroxinitrito y/o radicales derivados

Con el objetivo de profundizar en el estudio de los mecanismos de nitración mediados por peroxinitrito en membranas, estudiamos el efecto de varios atrapadores seleccionados, que reaccionan con constantes de velocidad conocidas con el peroxinitrito o con sus radicales derivados $\cdot\text{OH}$ y $\cdot\text{NO}_2$ (Tablas V y VI). Es importante resaltar que, salvo el ácido lipoico (LA), que tiene un carácter hidrofóbico y puede reaccionar en la fase lipídica o en la interfase lípido/agua, el resto de los atrapadores ensayados son polares y por lo tanto reaccionarán principalmente en la fase acuosa (218). La nitración y dimerización del BTBE fueron inhibidas por glutatión, ácido lipoico, pHPA, tirosina, dimetilsulfóxido (DMSO), manitol y ácido úrico (Tabla IV), en una forma que fue compatible con sus distintas reactividades con el peroxinitrito o sus radicales derivados (Tabla V). El quelante de metales, DTPA no tuvo efecto en la nitración del BTBE, sin embargo, la desferrioxamina (DF) inhibió fuertemente la formación de 3-nitro-BTBE y 3,3'-di-BTBE, en una forma dosis dependiente (Figuras. 5.5A e inset), en un grado que es compatible con sus reacciones con $\cdot\text{OH}$ y $\cdot\text{NO}_2$ (284), lo cual fue recapitulado en simulaciones asistidas por computadora (Figura 5.5B), para lo cual se utilizaron las constantes de reacción de la Tabla VI, que involucran las reacciones del peroxinitrito y sus radicales derivados con la tirosina, así como las reacciones con la DF. Finalmente, la presencia de NO_2^- también inhibió la nitración del BTBE lo que resalta el papel de los radicales $\cdot\text{OH}$, en la formación de 3-nitro-BTBE, a pesar de la importante formación de $\cdot\text{NO}_2$ que tiene lugar en esta condición.

Tabla IV: Efecto de distintos atrapadores en la oxidación del BTBE

Condición ^a	NO ₂ -BTBE (μM)	Di-BTBE (μM)
ONOO ⁻ (0.5 mM)	9.06 ± 0.78	0.017 ± 0.002
+ GSH (0.1 mM)	5.1 ± 1.0	ND
+ GSH (1.0 mM)	1.65 ± 0.26	ND
+ LA (0.1 mM)	1.32 ± 0.01	0.011 ± 0.002
+ pHPA (0.3 mM)	5.60 ± 0.77	0.012 ± 0.002
+ Tirosina (1 mM)	4.10 ± 0.66	ND
+ DMSO (10 mM)	6.59 ± 0.60	0.006 ± 0.001
+ Manitol (50 mM)	2.15 ± 0.87	0
+ Acido Urico (0.3 mM)	0	0
+ dtpa (0.1 mM)	9.8 ± 1.1	0.007 ± 0.001
+ DF (0.1 mM)	0.71 ± 0.15	0
+ Nitrito (50 mM)	5.6 ± 1.1	ND
+ HCO ₃ ⁻ (25 mM)	2.32 ± 0	0.008 ± 0
Adición Reversa de ONOO ⁻	0	0

Los liposomas de DLPC (30 mM) con BTBE (0.3 mM) pre-incorporado fueron expuestos a peroxinitrito (0.5 mM) en presencia de las concentraciones indicadas de los distintos atrapadores, y la formación de 3-nitro-BTBE y 3,3'-di-BTBE fue analizada luego de la separación por RP-HPLC. En los casos donde solo se reporta la formación de 3-nitro-BTBE, las determinaciones fueron realizadas por medidas espectrofotométricas directas luego de la solubilización con deoxicolato (1.2%). La adición reversa de peroxinitrito representa una condición control con peroxinitrito descompuesto en buffer. (ND: no determinado). ^a Las constantes de velocidad individuales de los atrapadores estudiados con el peroxinitrito o con sus radicales derivados se muestran en la Tabla V.

Tabla V. Constantes de reacción de atrapadores con peroxinitrito y sus radicales derivados

Compuesto	Peroxinitrito		$\cdot\text{NO}_2$		$\text{CO}_3^{\cdot-}$		$\cdot\text{OH}$	
	k_2 ($\text{M}^{-1}\text{s}^{-1}$)	Ref.	k_2 ($\text{M}^{-1}\text{s}^{-1}$)	Ref.	k_2 ($\text{M}^{-1}\text{s}^{-1}$)	Ref.	k_2 ($\text{M}^{-1}\text{s}^{-1}$)	Ref.
DF	0	(284)	7.6×10^6	(284)	1.7×10^9	(284)	1.3×10^{10}	(285)
GSH	650	(14)	2×10^7	(211)	5.3×10^6	(286)	2.3×10^{10}	(287)
LA	800	(217)	1.3×10^6	(218)	1.6×10^9	(218)	4.3×10^{10}	(288)
dtpa	0 ^a		ND		1.7×10^7 ^c	(289)	5.3×10^9	(289)
Acido Urico	155 ^b	(290)	1.8×10^7	(211)	1.7×10^9	(218)	7.2×10^9	(291)
DMSO	2.6 ^d		ND		ND		6.5×10^9 ^e	(292)
Manitol	0	(293)	ND		ND		2.1×10^9	(294)
Tirosina	0	(295)	3.2×10^5	(171)	4.5×10^7	(286)	1.3×10^{10}	(170)

Los valores fueron reportados a pH 7.4 y 25°C a no ser que se indique lo contrario

ND: No determinado

^a A concentraciones $\leq 100 \mu\text{M}$, el dtpa no aumenta la velocidad de descomposición del peroxinitrito

^b 37°C

^c pH = 11

^d pH 6.8 y 23°C

^e pH 4-5

^f Mismos valores que los asumidos para HPA

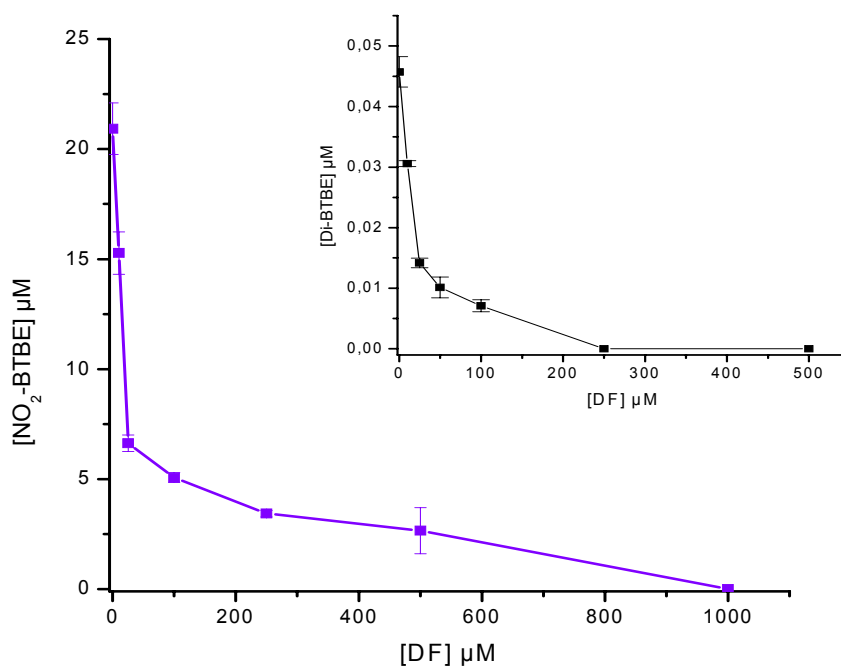


Figura 5.5A Efecto de la desferrioxamina en la nitración y dimerización del BTBE. Los liposomas de DLPC (30 mM) con BTBE (0.3 mM) pre-incorporado fueron expuestos a distintas concentraciones de desferrioxamina (0-1mM) y tratados con peroxinitrito (0.5 mM). Se cuantificó la formación de 3-nitro-BTBE por UV-vis, luego de la separación por RP-HPLC de los productos de extracción orgánica de las suspensiones de liposomas. Inset: El 3,3'-di-BTBE fue medido fluorimétricamente luego de la separación por RP-HPLC.

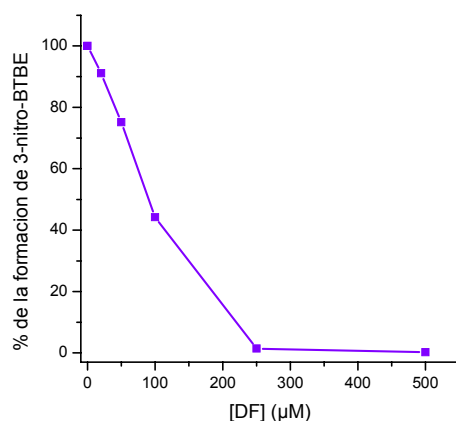


Figura 5.5B Simulación cinética química del efecto de la desferrioxamina sobre la nitración del BTBE. Se realizaron simulaciones químicas asistidas por computadora, considerando las mismas concentraciones iniciales de BTBE, peroxinitrito, nitrito, dtpa y KPi que se utilizaron en las condiciones experimentales. Para las simulaciones se utilizaron las reacciones 1-40 de la Tabla VI.

Tabla VI. Constantes de velocidad de las reacciones involucradas en la oxidación de tirosina/BTBE por peroxinitrito

Reaction	k	Referencia
1) ONOOH \rightarrow NO ₃ ⁻	0.9 s ⁻¹	(296) ¹
2) ONOOH \rightarrow ·NO ₂ + ·OH	0.35 s ⁻¹	(296)
3) Tyr + ·OH \rightarrow Tyr ⁻ + OH ⁻	6.5 x 10 ⁸ M ⁻¹ s ⁻¹	(170) ¹
4) Tyr + ·OH \rightarrow ·OH-Tyr	1.24 x 10 ¹⁰ M ⁻¹ ·s ⁻¹	(170) ²
5) Tyr ⁻ + ·OH \rightarrow Tyr + OH ⁻	6.5 x 10 ⁸ M ⁻¹ ·s ⁻¹	(170) ²
6) Tyr ⁻ + ·OH \rightarrow ·OH-Tyr	1.24 x 10 ¹⁰ M ⁻¹ ·s ⁻¹	(170) ²
7) ·OH-Tyr + HPO ₄ ²⁻ \rightarrow Tyr + H ₂ O + HPO ₄ ²⁻	5.8 x 10 ⁷ M ⁻¹ ·s ⁻¹	(297)
8) ·OH-Tyr + O ₂ \rightarrow OH-Tyr-OO ⁻	2 x 10 ⁹ M ⁻¹ ·s ⁻¹	(297)
9) OH-Tyr-OO ⁻ \rightarrow OH-Tyr + O ₂ ⁻	1.3 x 10 ⁵ s ⁻¹	(297)
10) Tyr ⁻ + ·NO ₂ \rightarrow Tyr + NO ₂ ⁻	2.9 x 10 ⁷ M ⁻¹ ·s ⁻¹	(298)
11) 2 Tyr ⁻ \rightarrow Di-Tyr	2.25 x 10 ⁸ M ⁻¹ ·s ⁻¹	(299) ³
12) Tyr + ·NO ₂ \rightarrow NO ₂ -Tyr	1.35 x 10 ⁹ M ⁻¹ ·s ⁻¹	(171, 300) ⁴
13) Tyr + ·NO ₂ \rightarrow Products	1.65 x 10 ⁹ M ⁻¹ ·s ⁻¹	(171, 300) ⁴
14) 2 ·NO ₂ \rightleftharpoons N ₂ O ₄	k _f = 4.5 x 10 ⁸ M ⁻¹ ·s ⁻¹ , k _r = 6900 s ⁻¹	(301, 302)
15) N ₂ O ₄ \rightarrow NO ₂ ⁻ + NO ₃ ⁻ + 2 H ⁺	1000 s ⁻¹	(301, 302)
16) ·NO ₂ + ·OH \rightarrow NO ₃ ⁻ + H ₂ O	4.5 x 10 ⁹ M ⁻¹ ·s ⁻¹	(303)
17) NO ₂ ⁻ + ·OH \rightarrow ·NO ₂ + H ₂ O	6 x 10 ⁹ M ⁻¹ ·s ⁻¹	(303)
18) ·OH + ONOO ⁻ \rightarrow OH ⁻ + NO ₂ + O ₂	4.8 x 10 ⁹ M ⁻¹ ·s ⁻¹	(304)
19) ONOOH \rightleftharpoons H ⁺ + ONOO ⁻	k _f = 15800 s ⁻¹ , k _r = 1 x 10 ¹¹ M ⁻¹ ·s ⁻¹	(15)
20) Tyr \rightleftharpoons H ⁺ + Tyr ⁻	k _f = 10 s ⁻¹ , k _r = 1 x 10 ¹¹ M ⁻¹ ·s ⁻¹	5
21) H ₂ PO ₄ ⁻ \rightleftharpoons H ⁺ + HPO ₄ ²⁻	k _f = 15800 s ⁻¹ , k _r = 1 x 10 ¹¹ M ⁻¹ ·s ⁻¹	5
22) ONOO ⁻ \rightleftharpoons O ₂ ⁻ + ·NO	k _f = 0.02 s ⁻¹ , k _r = 6.7 x 10 ⁹ M ⁻¹ ·s ⁻¹	(126, 305)
23) ·NO + ·NO ₂ \rightleftharpoons N ₂ O ₃	k _f = 1.1 x 10 ⁹ M ⁻¹ ·s ⁻¹ , k _r = 8.4 x 10 ⁴ s ⁻¹	(302)
24) N ₂ O ₃ \rightarrow NO ₂ ⁻ + NO ₃ ⁻ + 2 H ⁺	80000 s ⁻¹	(306, 307) ⁶
25) N ₂ O ₃ + ONOO ⁻ \rightarrow 2 ·NO ₂ + NO ₂ ⁻	1 x 10 ⁷ M ⁻¹ ·s ⁻¹	(307)
26) O ₂ ⁻ + ·NO ₂ \rightleftharpoons O ₂ NOO ⁻	k _f = 4.5 x 10 ⁹ M ⁻¹ ·s ⁻¹ , k _r = 1.35 s ⁻¹	(308)
27) O ₂ NOO ⁻ \rightarrow O ₂ + NO ₂ ⁻	1.05 s ⁻¹	(308)
28) O ₂ NOOH \rightleftharpoons O ₂ NOO ⁻ + H ⁺	k _f = 1.3 x 10 ⁵ s ⁻¹ , k _r = 1 x 10 ¹¹ M ⁻¹ ·s ⁻¹	(309)
29) Tyr ⁻ + O ₂ ⁻ \rightarrow Products	1.5 x 10 ⁹ M ⁻¹ ·s ⁻¹	(299)
30) ·OH + HPO ₄ ²⁻ \rightarrow Products	1.5 x 10 ⁵ M ⁻¹ ·s ⁻¹	(310)
31) ·OH + H ₂ PO ₄ ⁻ \rightarrow Products	2 x 10 ⁴ M ⁻¹ ·s ⁻¹	(310)
32) 2 O ₂ ⁻ + 2 H ⁺ \rightarrow H ₂ O ₂ + O ₂	2 x 10 ⁵ M ⁻¹ ·s ⁻¹	(311)
33) 2 ·NO + O ₂ \rightarrow 2 ·NO ₂	2.9 x 10 ⁶ M ⁻² ·s ⁻¹	(140)
34) Tyr ⁻ + ·NO \rightleftharpoons TyrONO	k _f = 1 x 10 ⁹ M ⁻¹ ·s ⁻¹ , k _r = 1 x 10 ³ s ⁻¹	(300, 312)
35) TyrONO \rightarrow Products	0.18 s ⁻¹	(300)
36) ·OH + Lipids \rightarrow Products	6.4 x 10 ⁸ M ⁻¹ ·s ⁻¹	(258)
37) ·OH + dtpa \rightarrow Products	5.3 x 10 ⁹ M ⁻¹ ·s ⁻¹	(289)
38) ·OH + DF \rightarrow DF ⁻ + OH ⁻	1.3 x 10 ¹⁰ M ⁻¹ ·s ⁻¹	(285)
39) ·NO ₂ + DF \rightarrow DF ⁻ + NO ₂ ⁻	7.6 x 10 ⁶ M ⁻¹ ·s ⁻¹	(284)
40) Tyr ⁻ + DF \rightarrow DF ⁻ + Tyr	6.3 x 10 ⁶ M ⁻¹ ·s ⁻¹	(284)

¹ Las constantes de reacción para las reacciones 1 y 2 fueron calculadas a partir de la constante de homólisis del peroxinitrito independiente de pH a 25°C (1.25 s^{-1}), teniendo en cuenta que durante la homólisis catalizada por protón, se forman $\cdot\text{NO}_2$ y $\cdot\text{OH}$ en rendimientos de 30%.

² La constante global para la reacción entre tirosina y $\cdot\text{OH}$ es $1,3 \times 10^{10} \text{ M}^{-1}\text{s}^{-1}$. Esta reacción lleva a la formación de aductos Tyr-OH \cdot en rendimientos de 95% (predominantemente en la posición 3) y radical $\cdot\text{Tyr}$ en el 5% restante (170).

³ La constante de velocidad para la reacción de entre 2 radicales $\cdot\text{BTBE}$ para dar 3,3'-di BTBE es 100 veces menor que la observada para tirosina libre ($k = 2.25 \times 10^6 \text{ M}^{-1}\text{s}^{-1}$) debido a la baja difusión del BTBE en la membrana.

⁴ Las constantes de velocidad para las reacciones 12 y 13 fueron calculadas a partir de la constante reportada de segundo orden para la recombinación entre $\cdot\text{Tyr}$ y $\cdot\text{NO}_2$ ($k = 3 \times 10^9 \text{ M}^{-1}\text{s}^{-1}$) (171), resultando en la formación del aducto que lleva a la formación de 3-NT en rendimientos de 45% (300).

⁵ Los valores K_f para las reacciones 19-21 y 28 fueron calculados a partir de los valores de pKa reportados de los ácidos correspondientes, y asumiendo una protonación controlada por difusión de sus bases conjugadas.

⁶ Las constantes de velocidad para la reacción 24 fue calculada como: $k_{24} = 2 \times 10^3 \text{ s}^{-1} + 8 \times 10^5 \text{ M}^{-1}\text{s}^{-1} [\text{fosfato}](\text{M})$ (306, 307).

5.6 Efecto del CO₂ en la oxidación del BTBE

Es importante destacar, que en sistemas acuosos el par bicarbonato/anhídrido carbónico (HCO₃⁻/CO₂) es capaz de promover un aumento en los rendimientos de nitración, ya que el radical CO₃^{•-} formado, es capaz de promover la oxidación por un electrón de la tirosina para dar radical tirosilo de forma muy eficiente. Sin embargo, hasta el momento no se había estudiado el efecto del CO₂ en compartimentos hidrofóbicos. Cuando se trataron los liposomas con peroxinitrito en presencia de 25 mM HCO₃⁻, (1.3 mM CO₂), se inhibió la nitración del BTBE (Tabla IV). La presencia de HCO₃⁻, inhibió la nitración y la dimerización del BTBE en una forma dosis dependiente (Figuras 5.6A y 5.6B). En presencia de CO₂, el peroxinitrito forma radical CO₃^{•-} el cual es incapaz de atravesar las membranas debido a su naturaleza cargada, lo cual indicaría que la inhibición observada puede deberse a la falta de permeabilidad del CO₃^{•-} hacia el interior de la membrana.

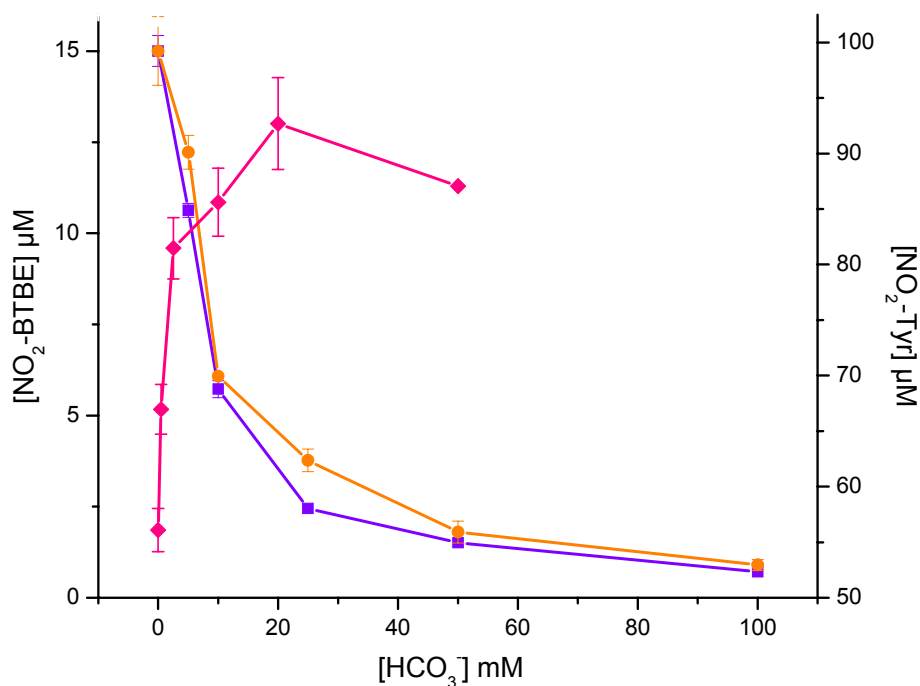


Figura 5.6A

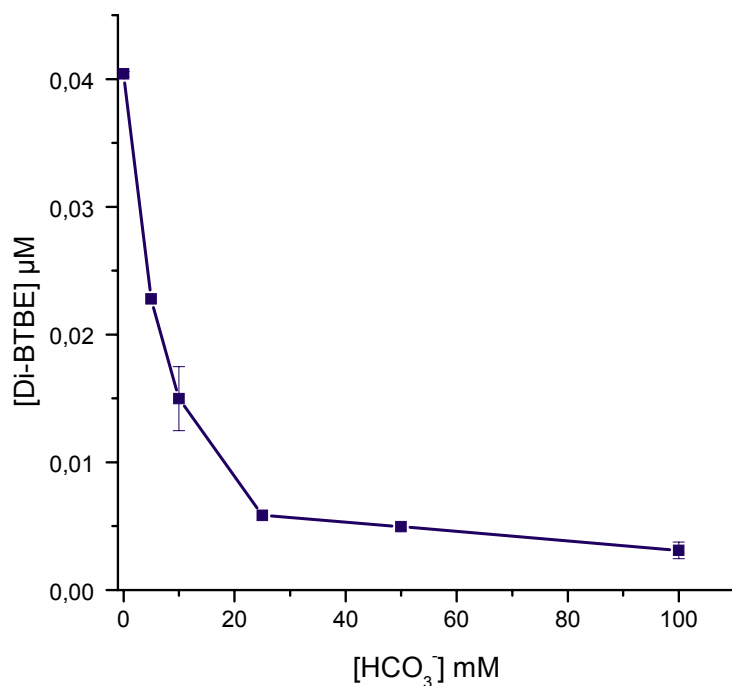


Figura 5.6B

Figura 5.6 Efecto del bicarbonato sobre la nitración y dimerización del BTBE mediada por peroxinitrito. Los liposomas de DLPC (30 mM) con BTBE preincorporado (0.3 mM) fueron tratados con peroxinitrito (0.5 mM) en presencia de distintas concentraciones de bicarbonato (0- 100 mM) en KPi (100 mM) pH 7,4 / 0,1 mM dtpa. Los productos de nitración (A) y dimerización (B) fueron analizados por UV-Vis y fluorescencia respectivamente, luego de la separación por RP-HPLC (■) o de la solubilización con 1,2% de deoxicolato (●). La formación de 3-nitrotirosina fue medida directamente por espectrofotometría (◆).

5.7 Efecto de complejos metálicos de transición sobre la nitración del BTBE mediada por peroxinitrito

Algunos complejos metálicos de transición son capaces de aumentar la nitración mediada por peroxinitrito de compuestos fenólicos en medios acuosos a través de un mecanismo de catálisis redox (3, 67). Con el fin de determinar el rol de los metales en membranas, se estudió el efecto de diferentes complejos metálicos en la nitración y dimerización del BTBE en liposomas con ácidos grasos saturados (DLPC) e insaturados (EYPC). Los rendimientos de nitración en liposomas de DLPC aumentaron significativamente en presencia de hemina, Fe-EDTA y las metalo porfirinas de manganeso y hierro, Mn-tcpp y Fe-tcpp, mientras que la ferrioxamina (complejo desferrioxamina-hierro) no tuvo ningún efecto sobre la nitración. En liposomas de EYPC, la nitración aumentó en presencia de hemina y Mn-tcpp, mientras que el Fe-edta y Fe-tcpp no tuvieron efecto (Tabla VII). De los resultados obtenidos, surge que en sistemas simples que contienen fosfolípidos saturados (DLPC), los complejos metálicos de transición actuaron catalizando la nitración. De hecho, en liposomas de DPLC la hemina y Mn-tcpp promovieron un aumento de la nitración y dimerización (no se muestra) del BTBE en una forma dependiente de la concentración. En particular, la hemina resultó ser un potente catalizador de la nitración, provocando un aumento ~ 5 veces en los rendimientos (15% a pH 7.4) a 25 μ M hemina (Figura 5.7).

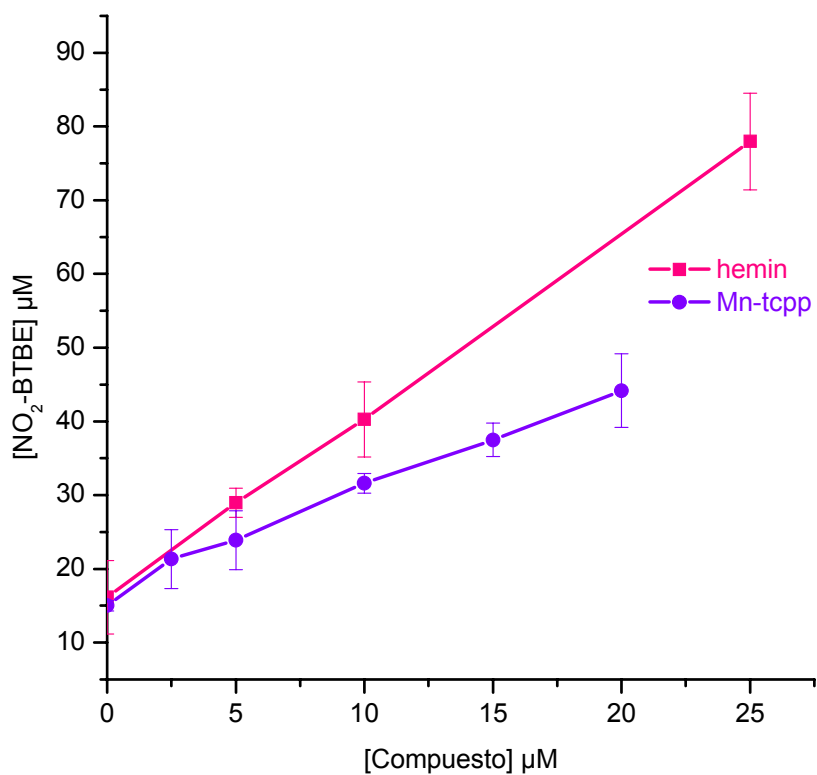


Figura 5.7 Catálisis de la nitración del BTBE por hemina y Mn-tcpp. Los liposomas de DLPC (30 mM) con BTBE pre-incorporado (0.3 mM) fueron tratados con peroxinitrito (0.5 mM) en la presencia de distintas concentraciones de hemina (■) y Mn-tcpp (●) a pH 7,4, y el contenido de 3-nitro-BTBE fue analizado luego de la separación por RP-HPLC.

Tabla VII. Efecto de los complejos metálicos de transición en la nitración del BTBE

Condición	NO ₂ -BTBE (μM)	
	DLPC	EYPC
ONOO ⁻ (0.5 mM)	14.1 ± 1.9	18.0 ± 2.8
+ Fe-edta (0.1 mM)	22.5 ± 2.2	7.5 ± 1.7
+ Fe-DF (0.1 mM)	15.2 ± 1.1	ND
+ Hemina (25 μM)	78.0 ± 5.5	97.1 ± 4.4
+ Mn-tccp (20 μM)	41.2 ± 1.2	20.6 ± 2.0
+ Fe-tccp (50 μM)	31.5 ± 5.0	5.71 ± 0.05
Adición reversa de ONOO ⁻	0	0

Los liposomas de DLPC y EYPC (30 mM) con BTBE incorporado (0.3 mM) fueron incubados con las concentraciones indicadas de los diferentes complejos metálicos y tratados con peroxinitrito (0.5 mM). La formación de 3-nitro-BTBE fue analizada luego de la separación por RP-HPLC.

5.8 Efecto del pH en la nitración, dimerización e hidroxilación del BTBE

Se estudió el efecto del pH en la nitración, dimerización e hidroxilación del BTBE, para determinar en qué medida su incorporación en un ambiente hidrofóbico afecta a la dependencia observada en la tirosina libre. Los cambios en el pH alterarán la concentración de protones en la fase acuosa e indirectamente estos pueden influir la química del BTBE incorporado en los liposomas. Se estudió la formación de 3-nitro-BTBE en función del pH, observándose una curva en forma de campana con un rendimiento máximo a un pH de 7.5 (Figura 5.8A) y comparable a la curva observada

para la 3-NT libre. La formación de 3,3'-di-BTBE fue muy baja a pH <8, pero aumentó significativamente a pH alcalino (Figura 5.8B). Como se indicó anteriormente, el 3-hidroxi-BTBE se detectó a un pH de 6, pero no a pH 7.4. Los perfiles de nitración, dimerización e hidroxilación para tirosina y BTBE (Figuras 5.8C y D) fueron recapitulados mediante simulaciones asistidas por computadora, considerando un mecanismo radicalar de oxidación de la tirosina mediada por peroxinitrito (3, 300, 313) y un rendimiento de dimerización relativamente bajo (reacción entre dos radicales fenoxilos derivados del BTBE). Por otro lado, los perfiles de nitración del BTBE en función del pH presentaron un comportamiento completamente diferente en presencia de hemina y Mn-tcpp, resultando un aumento continuo de 3-nitro-BTBE a pH alcalino (Figura 5.8E), alcanzando rendimientos nitración de 17 y 20%, respectivamente, a pH 9.

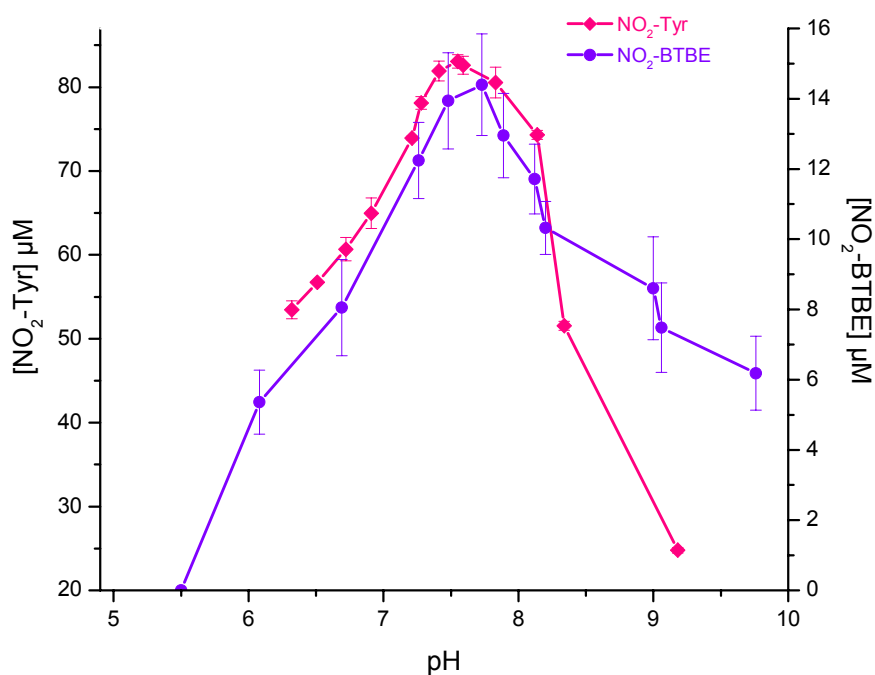


Figura 5.8A

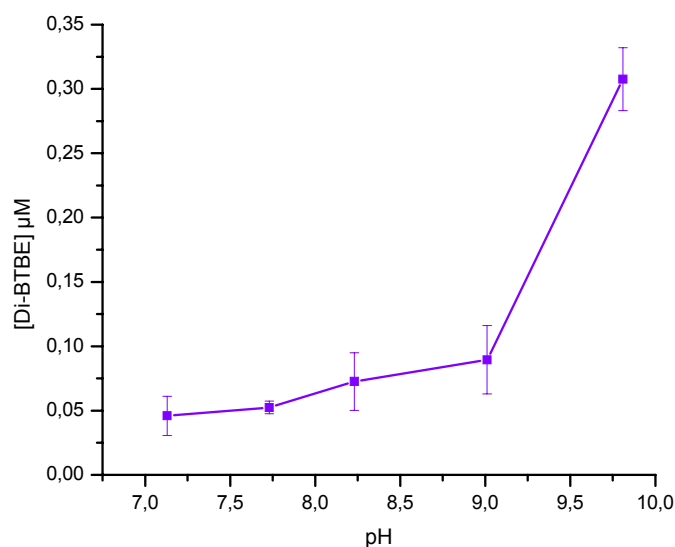


Figura 5.8B

Figura 5.8A-B Oxidación del BTBE en función del pH. Los liposomas de DLPC (30 mM) con BTBE pre-incorporado fueron preparados luego de la resuspensión de lípidos en KPi (100 mM) / 0,1 mM dtpa a los diferentes pH estudiados. Luego, estos liposomas con BTBE (0.3 mM), o tirosina libre (0.3 mM) fueron tratados con peroxinitrito (0.5 mM) a los distintos pH. **(A)** 3-nitro-BTBE (●) y **(B)** 3,3'-di-BTBE (■) fueron analizados luego de la separación por RP-HPLC, mientras que la 3-nitrotirosina (◆) fue medida directamente por espectrofotometría.

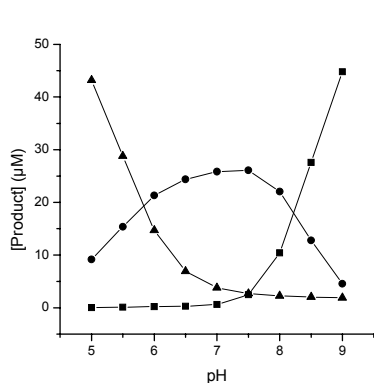


Figura 5.8C

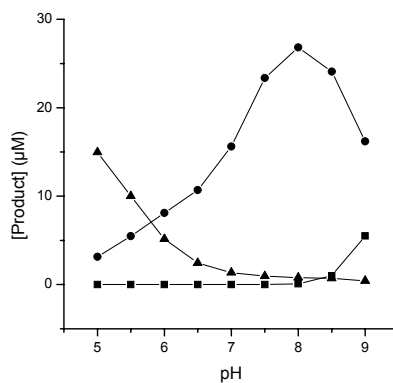


Figura 5.8D

Figura 5.8C-D Simulación cinética química del efecto del pH sobre la oxidación de la tirosina y el BTBE. Se estudió el efecto del pH en la formación dependiente de peroxinitrito de 3-NT (●), 3,4-dihidroxifenilalinalina (▲) y 3,3'-ditirosina (■) **(C)**, y 3-nitro-BTBE (●), 3-hidroxi-BTBE (▲) y 3,3'-di-BTBE (■) **(D)**, por simulaciones asistidas por computadora. Las concentraciones iniciales de BTBE, peroxynitrito y buffer KPi, fueron de 0.3 mM, 0.5 mM y 100 mM, respectivamente. Las concentraciones de nitrito y dtpa fueron de 0.15 y 0.1 mM, respectivamente. Para las simulaciones se utilizaron las reacciones 1-37 de la Tabla VI.

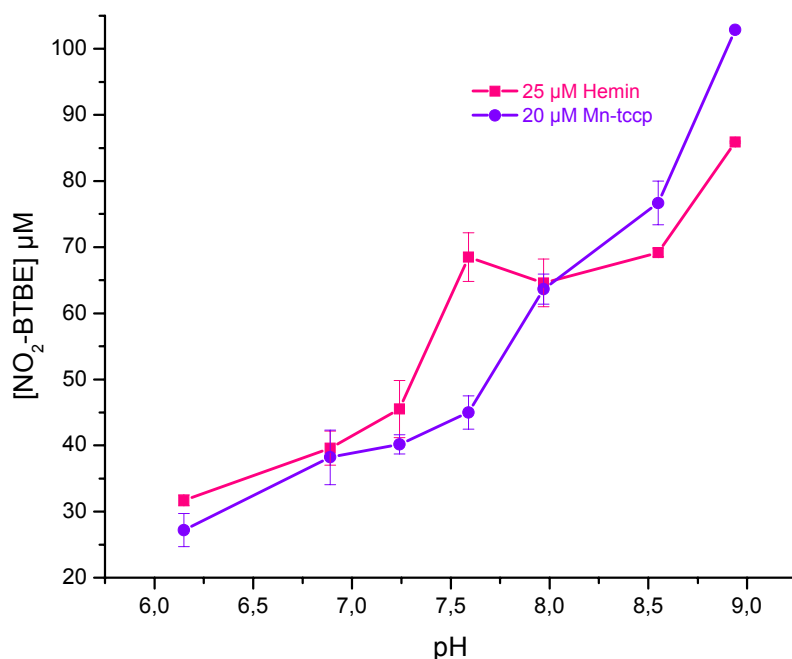


Figura 5.8E Efecto del pH en la nitración del BTBE catalizada por metales. Los liposomas de DLPC (30 mM) con BTBE pre-incorporado (0.3 mM) fueron preparados como en la figura 5.8A y tratados con peroxinitrito (0.5 mM) en presencia de hemina (25 μM) y Mn-tccp (20 μM) a los distintos pH.

5.9 Discusión

En este Objetivo Específico hemos utilizado la sonda hidrofóbica de tirosina, el BTBE, para establecer los mecanismos de nitración de tirosina dependientes de peroxinitrito en membranas y explorar factores que controlan el nivel de nitración, así como otras modificaciones oxidativas tales como la dimerización y la hidroxilación de tirosina. Aquí se confirmó que el peroxinitrito fue capaz de inducir la formación de 3-nitro-BTBE y 3,3'-di-BTBE en liposomas de DLPC (Figura 5.1); más aún, un derivado hidroxilado de BTBE, asignado como el 3-hidroxi-BTBE, fue detectado por primera vez (Figura 5.2). A pH 7.4, la nitración fue el proceso predominante con un rendimiento de 3% respecto al peroxinitrito adicionado, en liposomas de DPLC (frente a 6-8% en

tirosina libre) en comparación a la dimerización (0.02% de rendimiento) e hidroxilación (0% de rendimiento).

Además de ser formado en liposomas que contienen ácidos grasos saturados (DLPC y DMPC), el 3-nitro-BTBE también fue medido en liposomas con ácidos grasos insaturados como EYPC (Figura 5.4A) y SBPC (datos no mostrados), que contienen cantidades sustanciales de ácidos grasos poli-insaturados que son fácilmente oxidables por especies derivadas del peroxinitrito (16, 161). Por otra parte, los rendimientos de dimerización a pesar de ser relativamente bajos, fueron más altos en liposomas de EYPC que en liposomas de DLPC (Figura 5.4B), lo que sugiere que los procesos secundarios, como la lipoperoxidación pueden participar en reacciones de oxidación del BTBE cuando están presentes ácidos grasos poli-insaturados (ver más abajo y Objetivo Específico #2 de la tesis). La tirosina en solución acuosa no reacciona directamente con el peroxinitrito (295), y por tanto la formación de 3-NT depende de las reacciones de los radicales derivados del peroxinitrito ($\cdot\text{OH}$, $\cdot\text{NO}_2$, $\text{CO}_3\cdot^-$) (3). En el caso de la nitración del BTBE, los datos también apoyan a un mecanismo mediado por radicales libres iniciado por la homólisis de ONOOH ya sea en las proximidades o dentro de la membrana. En primer lugar, la hidroxilación del BTBE (Figura 5.2) se explica por una reacción de adición de $\cdot\text{OH}$ al BTBE en la cercanía del sitio de homólisis ya que el $\cdot\text{OH}$ reacciona con las moléculas blanco a pocos diámetros moleculares de su lugar de formación; el $\cdot\text{OH}$, formado a partir de ONOOH en la fase acuosa, sobre la superficie de los liposomas, es capaz de penetrar las vesículas de PC y reaccionar con las porciones aromáticas de la sonda incorporada en el interior de membrana, como se ha demostrado en estudios de radiólisis del agua (258). Es importante resaltar que, el $\cdot\text{OH}$ podría también formarse en el interior de los liposomas dado que el ONOOH es capaz de atravesar la bicapa lipídica (242, 250), y ya ha sido establecido que la homólisis de ONOOH ocurre en solventes apróticos (192). En segundo lugar, las inhibiciones de la nitración y dimerización (Tabla V) podrían explicarse en buena parte, sobre la base de la cinética de competencia simple con

atrapadores de radicales libres. En tercer lugar, la detección del radical fenoxilo derivado del BTBE y el perfil de pH de la nitración son plenamente consistentes con un mecanismo de reacción radicalar que lleva a las modificaciones oxidativas observadas en el BTBE. Es importante destacar que en este trabajo, los procesos de nitración, dimerización, e hidroxilación de la tirosina (tirosina en fase acuosa y análogo hidrofóbico) dependientes de la homólisis de peroxinitrito en función del pH se racionalizaron con un modelo cinético donde participan reacciones de radicales libres (Figuras 5.8C y D). Tanto los perfiles de pH como los rendimientos de oxidación obtenidos *in silico* concuerdan bien con los datos experimentales obtenidos *in vitro* para tirosina y BTBE. En el caso de BTBE, las constantes de reacción de velocidad reales con los radicales primarios (es decir, $\cdot\text{OH}$ y $\cdot\text{NO}_2$), no se conocen y se supone que son iguales a las de tirosina, sin embargo, para la reacción de dimerización (es decir, la combinación de dos radicales fenoxilos derivados del BTBE para formar 3,3'-di-BTBE, el valor de la constante de velocidad se redujo a 100 veces ($k = 2.25 \times 10^6 \text{ M}^{-1}\text{s}^{-1}$) con respecto a la correspondiente de los radicales tirosilo ($k = 2.25 \times 10^8 \text{ M}^{-1}\text{s}^{-1}$) debido a la restricción en el movimiento lateral de moléculas en la organizada estructura de la bicapa, lo que resulta en un bajo rendimiento de dimerización con respecto al de nitración (Figuras 5.4 y 5.8). De hecho, mientras que el valor de coeficiente de difusión (D) para aminoácidos como la tirosina en la fase acuosa es del orden de $800\text{-}1000 \mu\text{m}^2 \text{ s}^{-1}$ (254), se estima que D para el BTBE en liposomas de PC puede ser $\sim 5 \mu\text{m}^2 \text{ s}^{-1}$, como puede extrapolarse a partir de datos de fluorescencia obtenidos con sondas aromáticas hidrofóbicas de pireno (255), infiriendo una disminución de 100 a 200 veces en la difusión del radical tirosilo en el interior de la membrana. La dimerización intermolecular de tirosinas integrada a péptidos y proteínas, será aún menos probable ya que los valores de D son $\sim 10^3\text{-}10^4$ veces menores que en solución (239, 255) y de acuerdo con datos recientes que indican la ausencia de dimerización de tirosina en péptidos transmembrana expuestos a peroxinitrito (191). Por otra parte, el $\cdot\text{NO}$ y el $\cdot\text{NO}_2$ se concentran 4-5-veces en

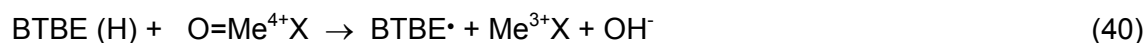
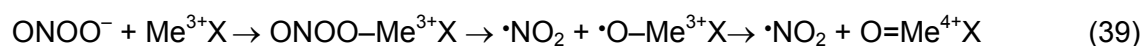
ambientes hidrofóbicos, siendo el valor aparente de D (D'_{NO}) = $1500 \mu\text{m}^2 \text{s}^{-1}$), el cual es muy cercano al obtenido en fase acuosa de $4500 \mu\text{m}^2\text{s}^{-1}$ (189).

El modelo cinético propuesto en esta investigación también predice que el grupo hidroxilo fenólico de BTBE incorporado a liposomas juega un papel, como en el caso de la tirosina, en la dependencia del pH ($\text{pKa} \sim 10$) y que no hay necesidad de implicar a otros grupos disociables presentes en las moléculas de PC, como el grupo fosfato y la colina de la cabeza polar del fosfolípido. Así, los datos cinéticos sostienen que el BTBE incorporado a liposomas acomoda sus grupo hidroxilo hacia la interfase lípido/agua, de acuerdo con los datos estructurales (192), que indican que la concentración más alta de BTBE está presente cerca de la esqueleto del glicerol de los fosfolípidos. Contrariamente a lo observado para la tirosina (Figura 5.6), la presencia de bicarbonato disminuyó la nitración y dimerización del BTBE (Figura 5.6). En los sistemas heterogéneos la presencia de bicarbonato puede limitar las acciones oxidantes del peroxinitrito (172, 243, 313) por mecanismos que involucran la reacción rápida del ONOO^- con el CO_2 en la fase acuosa. En condiciones con 25 mM de bicarbonato a pH 7.4 (1.3 mM de CO_2) y 25°C , la vida media de peroxinitrito se reduce de 2.7s a 24 ms (172, 243), lo cual corresponde a una distancia de difusión media en solución homogénea de $\sim 8,5 \mu\text{m}$. Sin embargo, como se indica en la sección de Materiales y Métodos, en la ecuación 33, a la concentración de vesículas de nuestros experimentos (es decir, 3.65×10^{11} vesículas / mL), la distancia media de difusión del peroxinitrito a un liposoma (Δx) es de sólo el $1.1 \mu\text{m}$. Así, de acuerdo a la ecuación 34 en presencia de 1.3 mM de CO_2 menos de 2% de peroxinitrito adicionado reacciona con el CO_2 antes de encontrar una vesícula liposomal. Incluso en la condición de mayor concentración de CO_2 estudiada (5.4 mM de CO_2 en equilibrio con 100 mM de HCO_3^- , Figura 5.6) menos del 5% de la difusión del peroxinitrito será inhibida por el CO_2 externo. Por lo tanto, el peroxinitrito agregado tuvo acceso a las vesículas en suspensión en todas las condiciones experimentales, y la inhibición de las oxidaciones

BTBE por el CO_2 no puede ser consecuencia de una difusión limitada debido a la disminución de la vida media de peroxinitrito (172, 243). El ONOOH, es capaz de atravesar la membrana liposomal, pero no el anión peroxinitrito (242, 250, 252); sin embargo, el ácido ONOOH no reacciona directamente con las moléculas de PC o con el BTBE, y por lo tanto su consumo en el interior la membrana dependerá sólo de la homólisis a $\cdot\text{OH}$ y $\cdot\text{NO}_2$, lo cual será un proceso relativamente lento y en este escenario, se establece un *cuasi-equilibrio* entre el peroxinitrito en el medio acuoso y la fase lipídica (252) (Figura 5.9). En presencia de CO_2 , sólo la fracción de peroxinitrito anión presente en la fase acuosa reaccionará fácilmente para producir ONOOCO_2^- y subsiguientemente radicales $\text{CO}_3^{\cdot-}$ y $\cdot\text{NO}_2$. El $\text{CO}_3^{\cdot-}$ posee una carga negativa ($\text{pKa} < 0$) (148) y es incapaz de permear hacia el interior de la bicapa lipídica (148) para promover la oxidación de un electrón de BTBE, como ha sido bien establecido en estudios de la reacción de membranas de PC con otros radicales anionicos tales como $\text{Br}_2^{\cdot-}$ y $\text{Cl}_2^{\cdot-}$ (258). A medida que el peroxinitrito "extraliposomal" se consume, ocurre una retro-difusión de ONOOH a la solución, el cual luego de desprotonarse reacciona con el CO_2 , con un efecto global de una disminución en los rendimientos de la oxidación BTBE. Globalmente, los datos apoyan que el bicarbonato facilitará la nitración de residuos de tirosina expuestos al solvente, mientras que inhibirá la nitración de residuos de tirosina ubicados en los dominios transmembrana o asociados a los entornos de las lipoproteínas.

Una observación interesante de este trabajo fue que complejos metálicos de transición fueron capaces de aumentar significativamente la nitración del BTBE dependiente de peroxinitrito (Tabla VII y Figura 5.7). En particular, la hemina y la metalo porfirina, Mn-tcpp fueron fuertes catalizadores de la nitración. La hemina es extremadamente tóxica cuando es liberada de su anclaje natural, la molécula de globina, como se observa en una variedad de condiciones fisiopatológicas y en los glóbulos rojos envejecidos (314). Al ser una molécula hidrofóbica, la hemina tiene afinidad por las membranas celulares, intercalándose entre los fosfolípidos de la

bicapa, donde puede participar en reacciones de oxidación y nitración (315, 316). El Mn-tcpp (también conocido como Mn-tbap) y otras porfirinas de manganeso, han sido ampliamente utilizadas como compuestos miméticos de la enzima SOD y por su actividad peroxinitrito reductasa. Mientras que la nitración de tirosina catalizada por Mn-tcpp es inhibida en fases acuosas por agentes reductores solubles tales como el glutatión, el ascorbato y el ácido úrico (por su rápida reacción con $O=Mn^{4+}$ formado por la oxidación por un electrón del Mn^{3+} , mediada por peroxinitrito) (Figura 2.4), estos reductores no pueden atravesar las membranas, y por lo tanto las acciones prooxidantes en ambientes hidrofóbicos del $O=Mn^{4+}$ -tcpp y $O=Fe^{4+}$ -hemina pueden ser más pronunciadas (250) y explicar parte de su toxicidad. Con hemina y Mn-tccp, los rendimientos de la nitración se incrementaron considerablemente (Figura 5.7), lo que indica que los complejos metálicos se encontraban en las proximidades de BTBE y sostienen un mecanismo de reacción en que el metal de transición ($Me^{3+}X$, Ec. 35) sirve como un ácido de Lewis para facilitar la formación de un complejo transitorio con peroxinitrito ($ONOO-Me^{3+}X$); en este complejo el enlace O-O se debilita y sufre homólisis a $\cdot NO_2$ y una forma del intermediario oxo-metal con un estado de oxidación alto (3) lo que promueve eficientemente la oxidación por un electrón de BTBE a su correspondiente radical fenoxilo ($\cdot BTBE$) (Ecs. 39 - 41):



El mecanismo de reacción planteado en las ecuaciones anteriores (Ecs. 39-41) se ve reforzado por la dependencia del pH de los rendimientos de nitración en

presencia de complejos de metales de transición (Figura 5.8E), que es completamente diferente a lo observado en su ausencia (Figura 5.8A), totalmente coherente con la mayor estabilidad de los complejos oxo-metálicos a pH alcalino (317), y en consonancia con datos anteriores (315, 316).

Se determinó que la nitración y dimerización del BTBE, tanto en la ausencia (Figura 5.4) como en presencia (Figura 5.7) de los complejos de metales de transición ocurre en liposomas con ácidos grasos saturados (DLPC y DMPC) y poli-insaturados (EYPC y SBPC). Los ácidos grasos poli-insaturados son buenos blancos de oxidantes fuertes, tales como el $\cdot\text{OH}$ y complejos oxo-metálicos. Por otra parte, tanto en liposomas de EYPC como SBPC (30 mM) la concentración de ácidos grasos poli-insaturados (7,3 y 17 mM, respectivamente) (245) es mucho mayor que la de BTBE (0,3 mM) y por lo tanto, esto compiten por la reacción con los radicales derivados del peroxinitrito que participan en la lipoperoxidación (16) y la nitración de tirosina (161). Por lo tanto, teniendo en cuenta un mecanismo cinético de competencia simple, se debería esperar una profunda inhibición en las oxidaciones del BTBE en liposomas de EYPC y SBPC, salvo que la oxidación del BTBE esté asociada al proceso de oxidación de los lípidos, lo cual será objeto de estudio en el Objetivo #2 de la presente tesis.

El BTBE es relativamente fácil de sintetizar, estable y puede ser fácilmente utilizado como una sonda para realizar una amplia gama de estudios sobre la nitración de tirosina en ambientes hidrofóbicos. El BTBE incorporado en liposomas representa un sistema modelo para estudiar una variedad de factores que pueden controlar procesos de nitración en biomembranas, y que incluyen la influencia de atrapadores de radicales libres y catalizadores de la nitración. En ese sentido, además del método que consiste en la separación de los productos derivados de BTBE con la técnica de HPLC más demandante para el experimentador (Figura 5.1A), se puso a punto el protocolo presentado en esta tesis, que consiste en la solubilización de liposomas conteniendo ácidos grasos saturados por deoxicolato seguido por espectrofotometría directa para la determinación de 3-nitro-BTBE (Figura 5.1B), el cual resultó ser muy

simple y reproducible (Figuras 5.1C). Como una alternativa para el BTBE, pueden ser utilizados péptidos transmembrana conteniendo tirosinas a distintas profundidades e incorporados a liposomas (169, 191), lo cual será evaluado en el Objetivo #3 de la presente tesis.

En resumen, en este Objetivo Específico, se mostró que el BTBE fue una sonda útil para definir mecanismos de nitración dependientes de peroxinitrito en una membrana modelo y se pudo obtener información importante acerca de los factores biológicamente relevantes tales como el efecto del CO₂ y la hemina, que modulan la nitración y otros procesos de oxidación de tirosinas en entornos hidrofóbicos. Además, debido a la difusión mínima del •OH, la detección de la 3-hidroxi-BTBE confirmó la homólisis “sitio específica” del ONOOH a •OH y •NO₂ en la cercanía o incluso dentro de la bicapa lipídica, lo cual es coherente con los mayores rendimientos de nitración en péptidos transmembrana conteniendo residuos de tirosina localizados más profundamente en la bicapa (191). Los estudios que utilizan BTBE incorporado en liposomas, membranas celulares y lipoproteínas servirán para profundizar los estudios de mecanismos de nitración y conocer otros factores que controlan la nitración de proteínas por mecanismos peroxinitrito-dependientes e independientes (por ejemplo, a través hemina y metaloproteínas en presencia de NO₂⁻ y H₂O₂). La figura 5.9 resume los distintos aspectos mecanísticos abarcados durante este objetivo experimental.

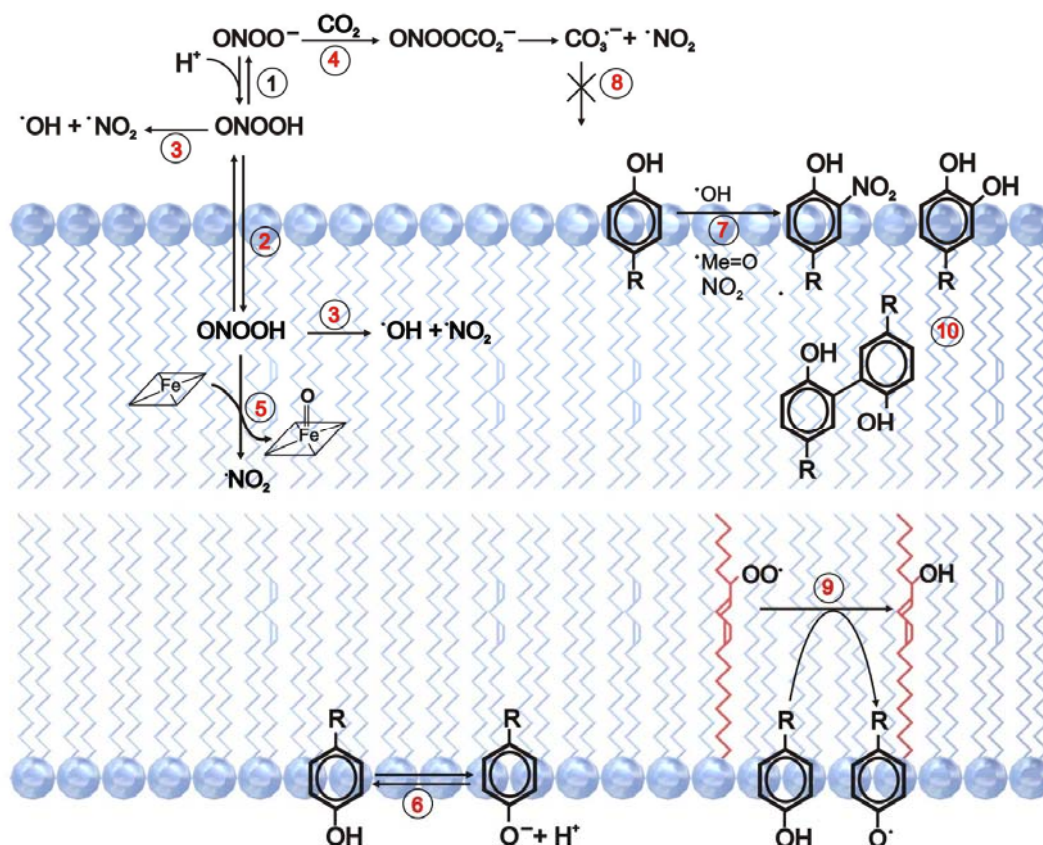


Figura 5.9 Mecanismo propuesto de nitración para el BTBE incorporado a membranas. El ONOO^- adicionado en la fase acuosa está en equilibrio con el ONOOH (1), el cual puede rápidamente atravesar la membrana (2), y sufrir homólisis tanto en la fase acuosa como en la fase lipídica (3), o reaccionar con CO_2 en la fase acuosa (4) para dar lugar a la formación de los radicales $\cdot\text{NO}_2$ y $\text{CO}_3\cdot^-$. En la fase lipídica, el ONOOH podría reaccionar directamente con la hemina para rendir el complejo oxo-metálico $\text{O}=\text{Fe}^{4+}$ y $\cdot\text{NO}_2$ (5). El BTBE se incorpora a la membrana con el grupo fenólico cercano a la interfase lípido-agua (6), y puede sufrir oxidación por un electrón para rendir el radical fenoxilo derivado del BTBE que a su vez puede reaccionar con $\cdot\text{NO}_2$ para dar el derivado nitrado (7). El radical $\text{CO}_3\cdot^-$ formado en la fase acuosa es incapaz de atravesar las membranas e ingresar al compartimento donde se encuentra ubicado el BTBE (8). En presencia de ácidos grasos insaturados, los radicales primarios reaccionarán con ellos preferencialmente e iniciarán lipoperoxidación, y los radicales peroxilo y alcoxilo (9) formados durante la lipoperoxidación pueden promover la oxidación del BTBE y llevar a la formación de productos de nitración y dimerización. El proceso indicado en (9) será específicamente estudiado en el Objetivo Específico #2.

6. Resultados y Discusión

Obj. #2

6. Objetivo # 2 Evaluación de la participación del proceso de lipoperoxidación en la nitración y dimerización de tirosinas en membranas.

Los radicales lipídicos (alcoxilo y peroxilo) formados durante la lipoperoxidación son especies capaces de oxidar blancos biológicos (RH), incluyendo cadenas laterales de proteínas (275). Dados los potenciales de reducción, ($E^{\circ}_{LO\cdot / LOH} = 1.76$ V, para alcoxilo y $E^{\circ}_{LOO\cdot / LOOH} = 1.02$ V para el radical peroxilo), es termodinámicamente posible que dichos radicales oxiden a la tirosina para formar radical fenoxilo, ($E^{\circ}_{Tyr\cdot / Tyr_H} = 0.88$ V), sin embargo los radicales alquilo son incapaces de llevar a cabo dicha reacción ($E^{\circ}_{L\cdot / LH} = 0.6$ V). En este Objetivo Especifico nos planteamos estudiar si los radicales lipídicos son capaces de oxidar a la tirosina para dar lugar a la formación de radical tirosilo, y alimentar de esa manera el proceso de nitración en compartimentos hidrofóbicos. Para testear esta hipótesis, estudiamos la nitración y dimerización del análogo hidrofóbico de la tirosina, BTBE en liposomas con distinto grado de insaturación promovida por distintos agentes oxidantes, peroxinitrito, hemina y el dador de radicales peroxilo, ABAP, y la relación que tienen dichos procesos con la lipoperoxidación.

6.1 Participación de los radicales lipídicos en la oxidación del BTBE

Con el objetivo de analizar la relación de los procesos de nitración y lipoperoxidación, estudiamos la oxidación del BTBE en sistemas formados por liposomas con distinto grado de insaturación: DLPC (contiene solamente ácidos grasos saturados) y EYPC y SBPC (que tienen 24 y 57% de insaturación) respectivamente. Al tratar los liposomas de DLPC (con BTBE incorporado) con peroxinitrito (1 mM), se detectó la formación de 3-nitro-BTBE y 3,3'-di-BTBE con rendimientos de hasta el 2.5% y 0.01% respecto a la concentración inicial de peroxinitrito, respectivamente (Figuras 6.1A y B), de acuerdo con resultados previos (192, 251). Cuando se trabajó con liposomas de EYPC y SBPC, que tienen un

importante porcentaje de ácidos grasos insaturados, también se detectaron niveles significativos de ambos productos de oxidación (Figuras 6.1A y B). Estos resultados indican que la oxidación del BTBE ocurre aún en presencia de altas concentraciones de ácidos grasos insaturados (~ 15 y 34 mM para EYPC y SBPC respectivamente), mucho mayores que las del propio BTBE (0.3 mM). Para evaluar la participación de los radicales derivados de la lipoperoxidación en la oxidación del BTBE, los experimentos también se llevaron a cabo a bajas tensiones de oxígeno (Figura 6.1), lo cual debería dar lugar a una inhibición en la formación LOO^\bullet , dado que es un proceso que implica la participación del oxígeno (Ec. 29) tanto en liposomas saturados (258) como insaturados. De hecho, a bajas tensiones de oxígeno, los rendimientos de nitración y dimerización del BTBE fueron sustancialmente menores, en ambos tipos de liposomas (Figura 6.1A y B). Por el contrario, cuando se expuso tirosina (0.3 mM) a peroxinitrito (1 mM) en buffer fosfato (100 mM, pH 7.3, 0.1 mM dtpa), la ausencia de oxígeno no tuvo efecto sobre los rendimientos de nitración y dimerización (~ 6 % and 0.25 % respectivamente) en fase acuosa (datos no mostrados), indicando que la formación de LOO^\bullet es un evento clave en la oxidación del BTBE.

Paralelamente, se evaluó la lipoperoxidación en las muestras mediante la cuantificación de malondialdehído (MDA), un importante producto de la degradación de lípidos durante el proceso de la lipoperoxidación. El peroxinitrito provocó la formación de MDA en liposomas de EYPC y SBPC con BTBE incorporado (Figura 6.1C), de acuerdo con nuestras observaciones previas (251). Cabe resaltar que los niveles de MDA fueron sensiblemente menores a bajas tensiones de oxígeno, revelando la inhibición de la formación de radicales peroxilo durante la peroxidación lipídica. Como es de esperar, no se detectó la formación de MDA en liposomas saturados de DLPC. Por lo tanto, en liposomas con ácidos grasos insaturados, como EYPC y SBPC, la oxidación del BTBE, y la lipoperoxidación ocurren simultáneamente siendo ambos procesos inhibidos a bajas tensiones de oxígeno.

Los niveles de LOOH fueron significativamente mayores que los de productos de oxidación del BTBE, lo cual soporta que lipoperoxidación es el proceso oxidativo mayoritario dentro de la membrana.

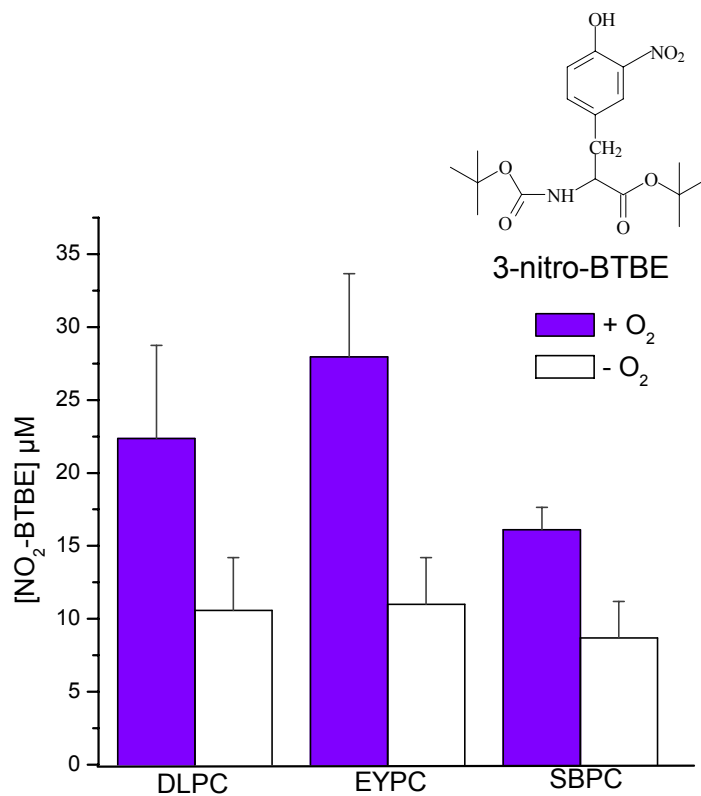


Figura 6.1A

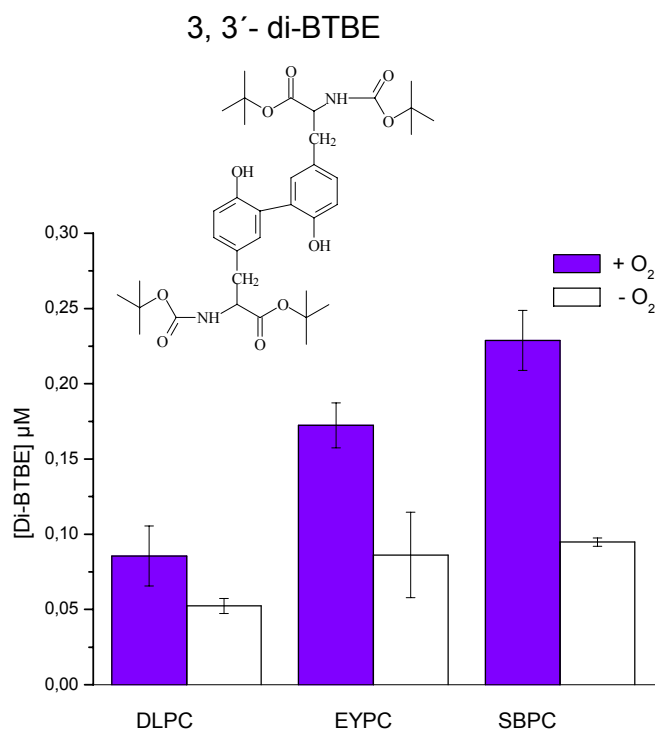


Figura 6.1B

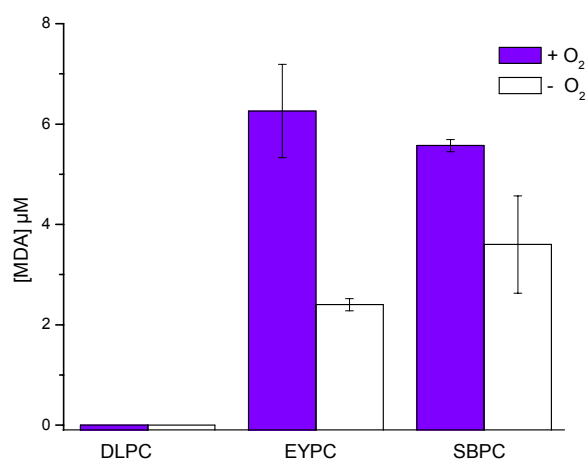
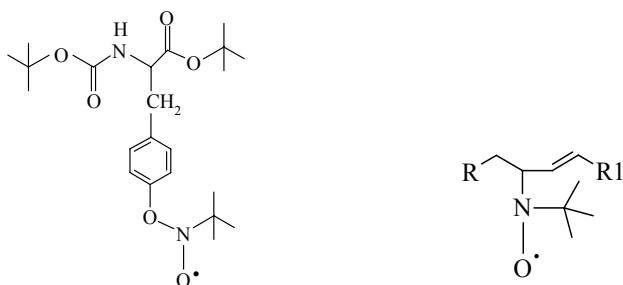
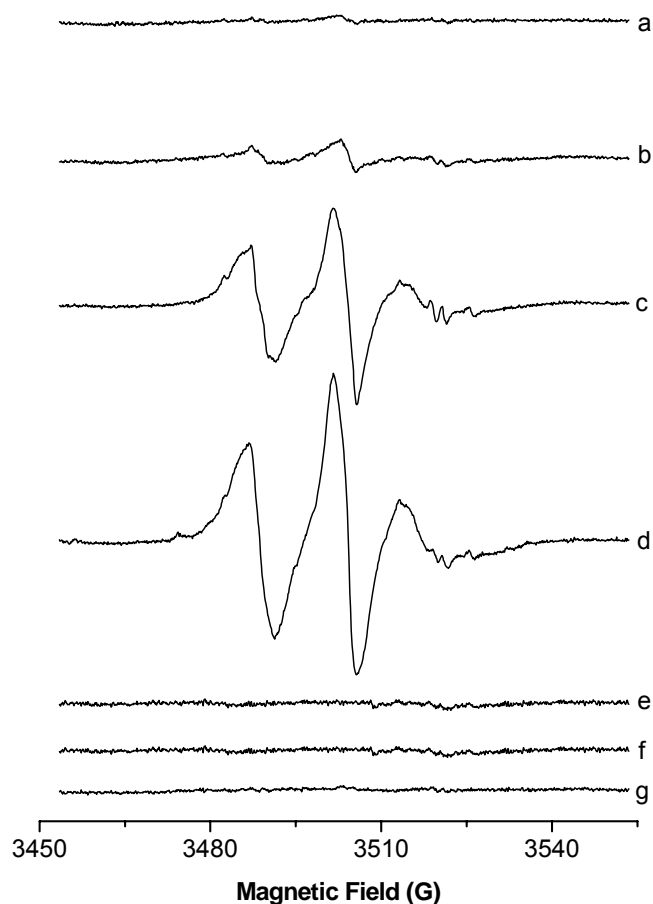


Figura 6.1C

Figura 6.1 Efecto del oxígeno en la oxidación del BTBE mediada por peroxinitrito. El BTBE (0.3 mM) fue incorporado a los distintos liposomas de DLPC, EYPC y SBPC (30 mM) que fueron expuestos a peroxinitrito (1 mM) en la presencia de oxígeno (200 μM) o a bajas tensiones de oxígeno (~ 5 μM). Se analizaron las muestras para (A) 3-nitro-BTBE, (B) 3,3'-di-BTBE y (C) MDA. Los niveles basales de MDA en EYPC, SBPC y DLPC fueron 4.88 ± 1.09 ; 4.97 ± 0.72 and 0, respectivamente. Las estructuras del 3-nitro-BTBE y el 3,3'-di-BTBE se muestran en los respectivos paneles.

6.2 Detección de los radicales lipídicos en la oxidación del BTBE por EPR

Se realizaron estudios de EPR-spin trapping para la detección de los radicales lipídicos y fenoxilo derivados del BTBE, formados durante la exposición a peroxinitrito en presencia de MNP, como se describió previamente (193, 251). No se detectó ninguna señal al exponer a los liposomas de DLPC a peroxinitrito en ausencia de BTBE (Figura 6.2 línea a). Por otro lado cuando, se trataron con peroxinitrito liposomas de DLPC con BTBE incorporado, se obtuvo una señal anisotrópica de 3 líneas, confirmando la formación de un radical fenoxilo parcialmente inmovilizado en el interior de la membrana (Figura 6.2 línea b), de acuerdo con trabajos previos (193, 251). Cuando los liposomas de DLPC tratados con peroxinitrito, se disolvieron con etanol (con BTBE incorporado), se obtuvo una señal de 3 líneas más clara y bien resuelta, que a pesar de la baja relación señal / ruido, permitió la determinación de una constante de desdoblamiento hiperfino de $a_N \sim 13.8$ G, lo cual es consistente con la formación de un aducto entre el MNP y el producto de oxidación por un electrón del BTBE (318). En liposomas de EYPC, el peroxinitrito causó la formación de un aducto, en ausencia de BTBE, lo cual es compatible con la formación de un aducto MNP-radical alquilo (aducto centrado en un carbono) con una constante de desdoblamiento hiperfino estimada de $a_N \sim 15$ G (Figura 6.2 línea c). Cuando el BTBE fue incorporado a los liposomas de EYPC, la señal obtenida fue mucho mayor (Figura 6.2 línea d), sugiriendo la coexistencia de radicales lipídicos y radicales fenoxilo derivados del BTBE, y confirmando la asociación temporal entre los procesos de lipoperoxidación y oxidación del BTBE. No se detectó señal, cuando se trató los liposomas de DLPC y EYPC con peroxinitrito descompuesto (Figura 6.2 líneas e y f), o si el MNP fue adicionado luego del peroxinitrito (Figura 6.2 línea g). Las estructuras de los respectivos aductos (MNP-radical fenoxilo, y MNP-radical alquilo) se muestran debajo de las señales.

A**B** MNP- radical fenoxilo

MNP-radical alquilo

Figura 6.2 EPR-spin trapping de los radicales lipídicos y del radical fenoxilo derivado del BTBE. Liposomas de DLPC o EYPC (45 mM) con BTBE (2.5 mM) pre-incorporado en buffer fosfato (100 mM) pH 7,4 / 0,1 mM dpta, fueron incubados durante 20 minutos con el spin-trap MNP (20 mM) y expuestos a peroxinitrito (5 mM). Las muestras fueron posteriormente transferidas a una celda capilar de 50 μ l para los registros de EPR. **(A)** (a) Liposomas de DLPC + peroxinitrito; (b) liposomas de DLPC con BTBE + peroxinitrito; (c) liposomas de EYPC + peroxinitrito; (d) liposomas EYPC con BTBE + peroxinitrito, (e) igual que en b, pero con adición reversa de peroxinitrito (f) igual que en d con adición reversa de peroxinitrito; (g) peroxinitrito solamente. **(B)** Las estructuras de los aductos MNP-radical fenoxilo y MNP-radical alquilo se muestran y se corresponden con las señales obtenidas en las líneas b y c del panel A, respectivamente.

6.3 Lipoperoxidación y oxidación del BTBE mediadas por peroxinitrito: bolo vs infusión lenta.

El peroxinitrito tiene una corta vida media en buffer fosfato (100 mM, pH 7,4 y 25° C) ($t_{1/2}$ 2.5 s), debido a la homólisis catalizada por protón para dar $\cdot\text{OH}$ and $\cdot\text{NO}_2$ con un rendimiento del 30 % (14). Por lo tanto, la adición de peroxinitrito mediante un único bolo, a una mezcla de reacción, puede resultar en una alta concentración inicial de radicales, que pueden provocar procesos oxidativos importantes en moléculas blanco, aunque no necesariamente reflejan la magnitud de dichos procesos, en condiciones biológicamente relevantes, donde el peroxinitrito se forma en un flujo continuo (300, 319). Esta consideración es relevante para procesos como la lipoperoxidación, que dependen de reacciones de propagación, las cuales pueden terminar prematuramente si se tiene un flujo muy grande de radicales iniciales. En este sentido, los experimentos fueron realizados para estudiar la lipoperoxidación y la oxidación del BTBE, adicionando el peroxinitrito como un único bolo o a través de una infusión continua durante 30 minutos (1 μM / min). La adición de peroxinitrito al BTBE incorporado a liposomas de EYPC, resultó en una formación de MDA dependiente de la concentración (Figura 6.3A), siendo los rendimientos de formación de MDA, 2-3 veces mayores cuando el peroxinitrito se adicionó mediante una infusión lenta. De modo similar, los rendimientos de nitración y dimerización del BTBE (Figura 6.3B, C y D), en ambos tipos de liposomas (DLPC y EYPC), fueron hasta 3 veces mayores en la adición por infusión lenta de peroxinitrito. Adicionalmente, la oxidación del BTBE, y la formación de MDA (Figura 6.3E) en liposomas de EYPC, fueron significativamente menores, cuando el peroxinitrito en infusión lenta se adicionó en condiciones de baja tensión de oxígeno, todo lo cual indicaría una asociación entre el proceso de oxidación del BTBE y la lipoperoxidación.

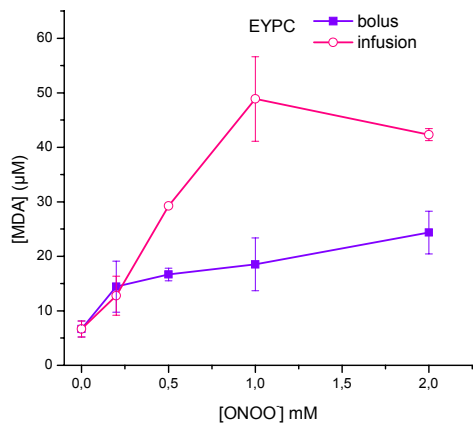


Figura 6.3A

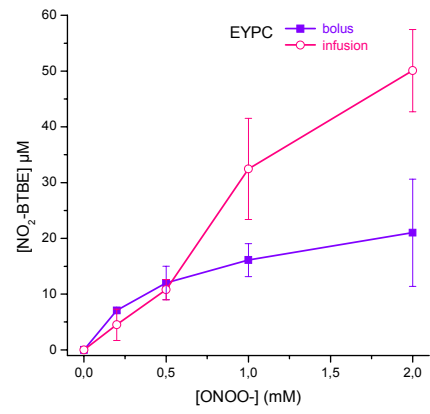


Figura 6.3B

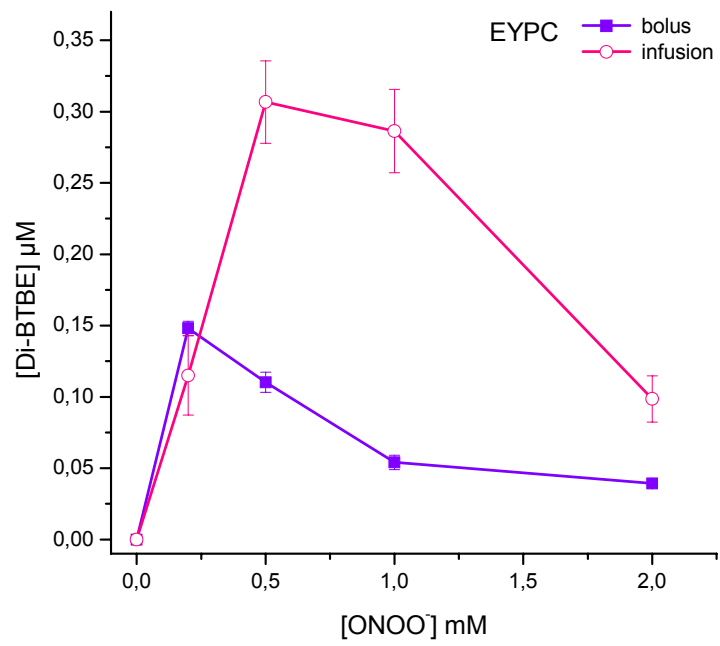


Figura 6.3C

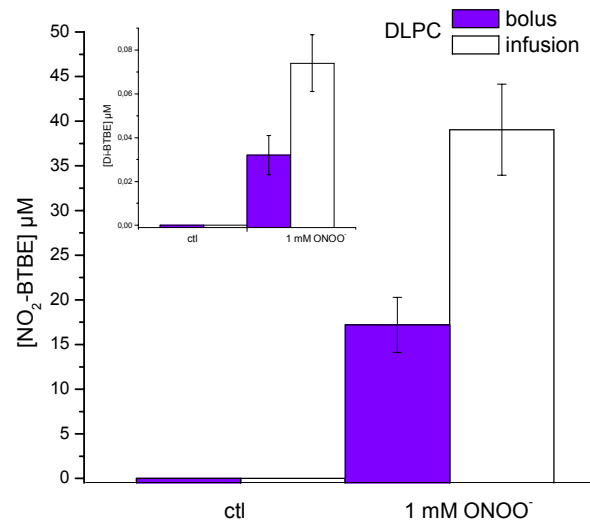


Figura 6.3D

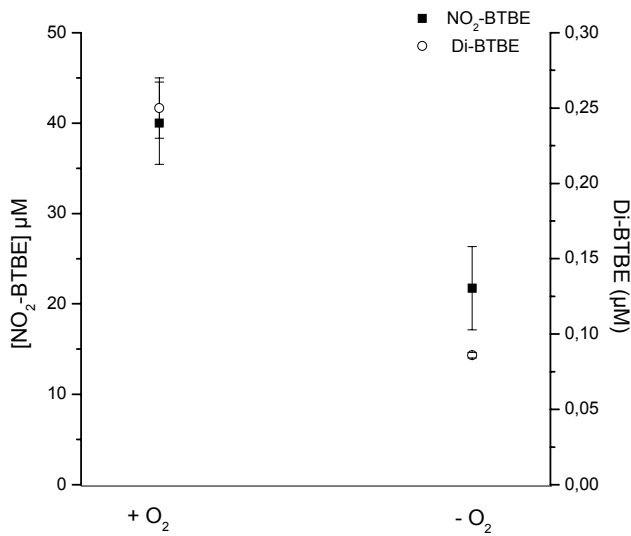


Figura 6.3E

Figura 6.3 Oxidación del BTBE mediada por peroxinitrito: infusión lenta vs adición en bolo. Liposomas de DLPC y EYPC (30 mM) con BTBE (0.3 mM) pre-incorporado fueron tratados con peroxinitrito ya sea mediante una infusión continua (○) o por un bolo único (■), de manera de alcanzar una concentración final de 0.2-2 mM. Se analizaron las muestras para 3-nitro-BTBE, 3,3'-di-BTBE y MDA. EYPC: (A) MDA, (B) 3-nitro-BTBE, (C) 3,3'-di-BTBE. DLPC: (D) 3-nitro-BTBE y 3,3'-di-BTBE (inset). (E) Liposomas con BTBE (0.3 mM) fueron expuestos a una infusión de peroxinitrito (1 mM) en presencia y ausencia de O₂, y se determinó la formación de 3-nitro-BTBE y 3,3'-di-BTBE como previamente.

6.4 Efecto del grado de insaturación en la oxidación del BTBE mediada por peroxinitrito.

Se estudió la oxidación del BTBE en función del porcentaje de ácidos grasos insaturados presentes en los fosfolípidos, utilizando mezclas con proporciones variables de DLPC y PLPC. Los rendimientos de nitración y dimerización fueron significativos en todo el rango de insaturación (0-100%), observándose una tendencia al aumento en los rendimientos de oxidación del BTBE, cuando el contenido de PLPC fue cercano al 40%, y una disminución en valores cercanos al 100% de PLPC. Estos resultados muestran, que a pesar del porcentaje variable de ácidos grasos insaturados en las mezclas de liposomas (~ 0-30 mM ácido linolénico), la oxidación del BTBE ocurrió de manera consistente en todo el rango de insaturación estudiado. Estos datos sostienen que no sería aplicable un modelo de competencia simple, donde los ácidos grasos insaturados compiten con el BTBE por los radicales derivados del peroxinitrito, y que las reacciones secundarias de radicales lipídicos con el BTBE pueden también contribuir a las reacciones de nitración y dimerización (Figura 6.4).

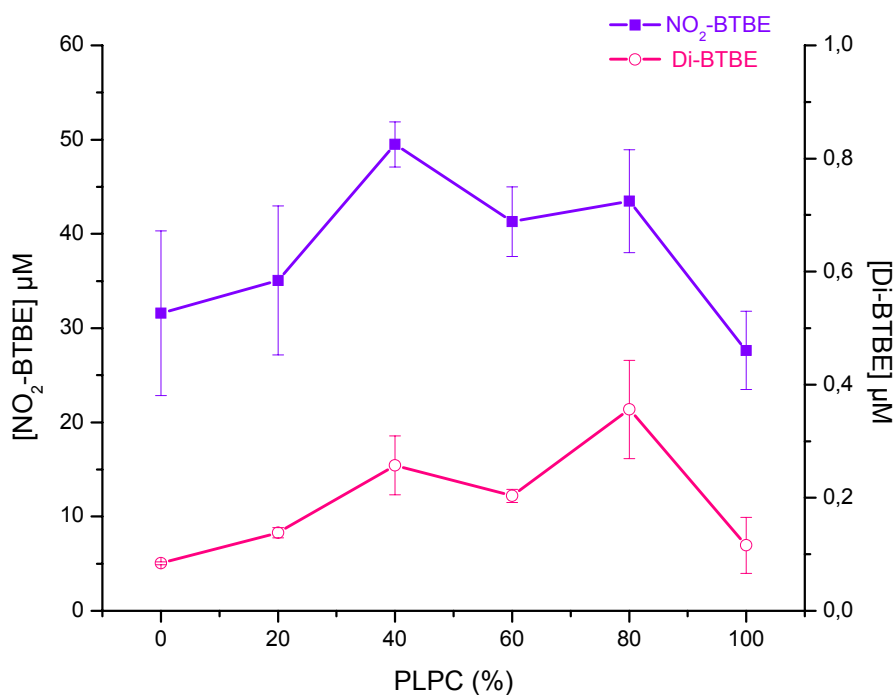


Figura 6.4 Efecto del grado de insaturación en la oxidación del BTBE. Se estudió la nitración (■) y dimerización (○) del BTBE en función de la composición de ácidos grasos insaturados, usando liposomas con mezclas de DLPC y PLPC (0-100 % PLPC), con BTBE (0.3 mM) pre-incorporado y tratados con peroxinitrito (1 mM).

6.5 Lipoperoxidación inducida por hemina y ABAP

Para demostrar que la lipoperoxidación y la oxidación del BTBE están relacionadas, se expusieron liposomas con BTBE incorporado a dos sistemas de oxidación distintos: hemina y ABAP, los cuales dan lugar a la formación de radicales LOO• en liposomas que contienen ácidos grasos insaturados. La hemina libre interactúa fácilmente con membranas (320) e inicia la lipoperoxidación en liposomas insaturados por reacción con los hidroperóxidos lipídicos preformados que están siempre presentes en distinta proporción en liposomas insaturados (el contenido de hidroperóxidos en preparaciones bien conservadas representan en nuestras muestras de 30 mM liposomas, una concentración de ~ 45-80 mM, es decir entre 0.075-0.13% del total de ácidos grasos insaturados, determinado por el ensayo de FOX). La

Hemina-(Fe³⁺) promueve la oxidación por un electrón de LOOH rindiendo LOO• y hemina en el estado redox Fe²⁺ (Figura 6.5). A su vez, la hemina reducida puede generar LO• por reducción de LOOH. Reacciones secundarias pueden a su vez generar cantidades variables de O₂^{•-}, H₂O₂ y compuestos oxo hemo-Fe⁴⁺=O, que pueden amplificar el proceso de oxidación mediado por hemina (320).

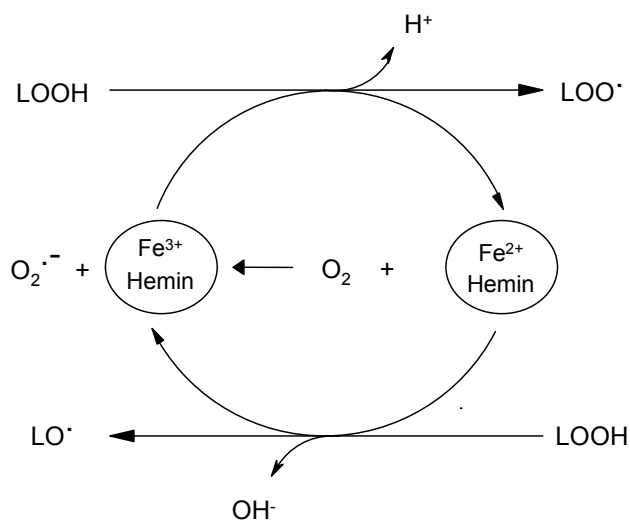


Figura 6.5. Reacciones de los hidropéroxidos con hemina y formación de radicales lipídicos.

En liposomas de EYPC, la hemina provocó la formación de 3,3'-di-BTBE y MDA en una forma dosis dependiente (Figura 6.6A y B). Por el contrario, en liposomas de DLPC (saturados), en los cuales la hemina no es capaz de promover lipoperoxidación, no se detectó la formación de of 3,3'-di-BTBE. Estos datos, implican la participación de los radicales LOO• formados durante la reacción de la hemina con los hidropéroxidos lipídicos en la dimerización del BTBE (Figura 6.5).

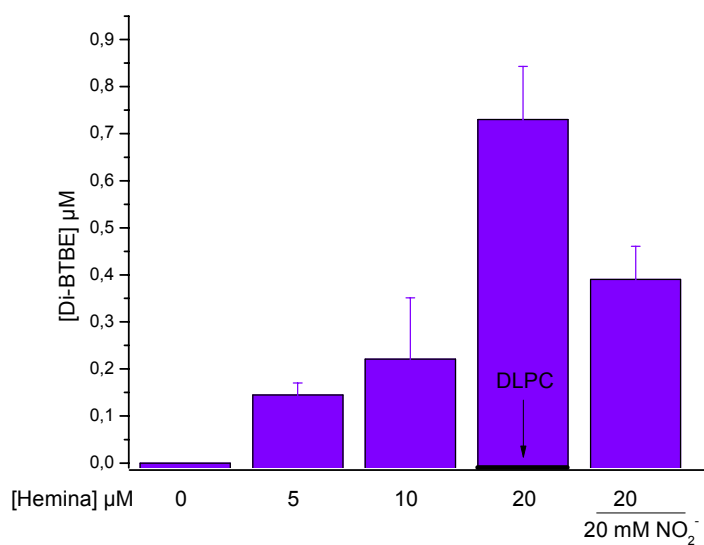


Figura 6.6A

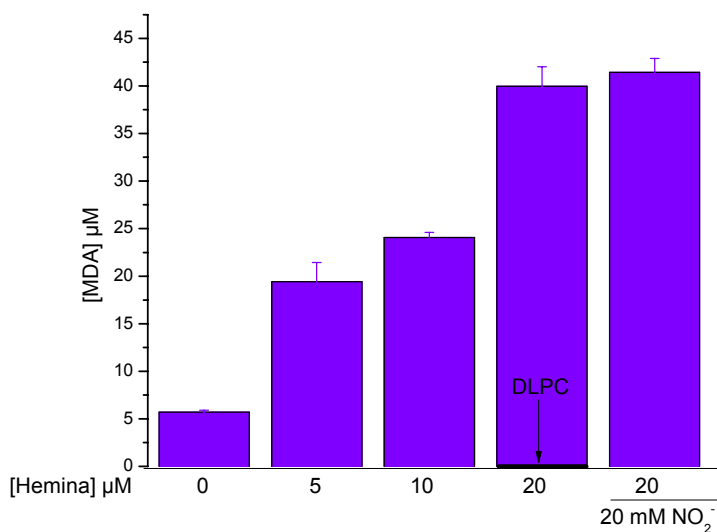
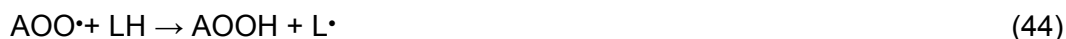


Figura 6.6B

Figura 6.6 Lipoperoxidación y oxidación del BTBE inducida por hemina. Liposomas de DLPC y EYPC (30 mM) con BTBE (0.3 mM) fueron expuestos a hemina (0-20 μM) en KPi (100 mM) pH 7,3 / 0,1 mM dtpa, y se determinó la formación de **(A)** 3,3'-di-BTBE, y **(B)** MDA. Las flechas indican los valores correspondientes a los liposomas de DLPC, que fue cero para todas las condiciones.

Posteriormente, realizamos experimentos utilizando el dador de peroxilos orgánicos, ABAP, que genera un flujo de radicales peroxilo por termólisis:



El ABAP inicia el proceso de lipoperoxidación en liposomas con ácidos grasos insaturados como EYPC, por la reacción de los radicales peroxilo derivados del ABAP ($AOO\cdot$) con un ácido graso insaturado para dar un radical alquilo ($L\cdot$), que luego de la adición de oxígeno, forma radicales $LOO\cdot$ (Ecs. 42-44). La adición de ABAP a liposomas de DLPC y EYPC con BTBE pre-incorporado, resultó en la formación de 3,3'-di-BTBE en ambos tipos de liposomas (Figura 6.7A y 6.8A), pero solo en los liposomas de EYPC pudo detectarse la formación de MDA.

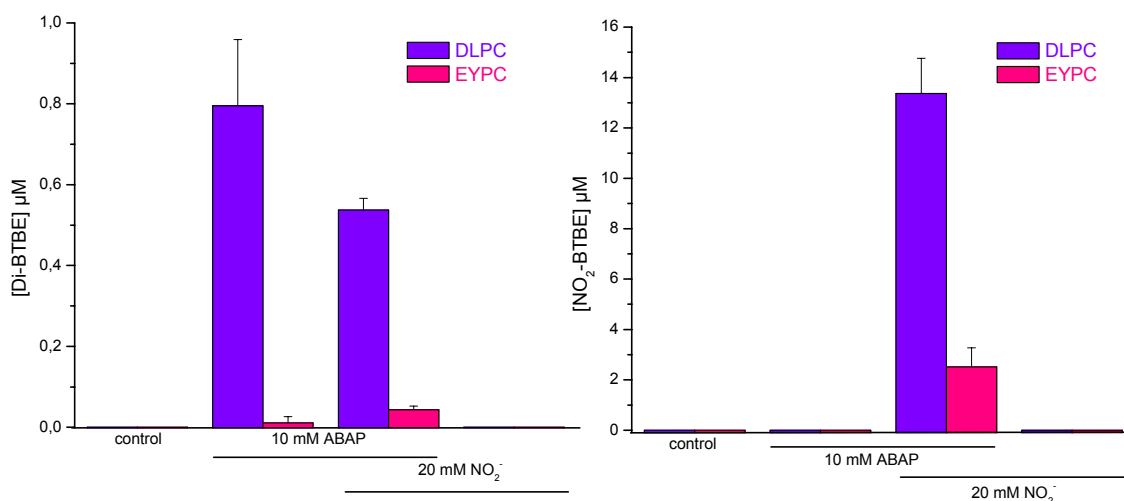


Figura 6.7 Oxidación del BTBE mediada por ABAP. Los liposomas de DLPC y EYPC (30 mM) con BTBE incorporado (0.3 mM) fueron incubados con ABAP (10 mM, flujo 0,3 μM /min) durante 2hs a 37°C en presencia y ausencia de NO₂⁻ (20 mM) y las muestras analizadas para 3-nitro-BTBE y 3,3'-di-BTBE luego de la separación por RP-HPLC. Se realizó el mismo experimento a bajas tensiones de oxígeno (~ 5 μM). La Tabla VIII resume los datos obtenidos en las distintas condiciones.

Tabla VIII. Efecto del ABAP en la nitración y dimerización del BTBE

Condición	EYPC		DLPC	
	NO ₂ -BTBE (μ M)	Di-BTBE (μ M)	NO ₂ -BTBE (μ M)	Di-BTBE (μ M)
Control	0	0	0	0
ABAP	0	0.011 \pm 0.001	0	0.79 \pm 0.164
ABAP + NO ₂ ⁻	2.5 \pm 0.76	0.043 \pm 0.008	16.15 \pm 1.39	0.537 \pm 0.029
ABAP - O ₂	0	0	0	0.32 \pm 0.065
ABAP + NO ₂ ⁻ - O ₂	1.46 \pm 0.8	ND*	9.43 \pm 2	ND
NO ₂ ⁻	0	0	0	0

*ND: No determinada

Tanto los radicales peroxilo derivados del ABAP (en DLPC), como los radicales LOO[•] formados durante la lipoperoxidación (en EYPC), son capaces de reaccionar con el BTBE para rendir el radical fenoxilo derivado del BTBE, y subsecuentemente formar 3,3'-di-BTBE. Es interesante resaltar, que cuando las muestras fueron expuestas a ABAP en presencia de NO₂⁻, se pudo detectar la formación de 3,3'-di-BTBE y 3-nitro-BTBE, demostrando que los radicales peroxilo derivados del ABAP, también son capaces de oxidar al NO₂⁻ para rendir [•]NO₂ (321) (Tablas VIII y IX, Figuras 6.7A y B). Bajas tensiones de oxígeno, disminuyeron los rendimientos de oxidación del BTBE inducido por ABAP + NO₂⁻, en ambos tipos de liposomas, confirmando el rol de los radicales LOO[•] en este proceso. En experimentos control realizados únicamente en presencia de NO₂⁻, no pudo observarse la formación de productos (Tabla VIII). La figura 6.8A muestra los cromatogramas obtenidos de las condiciones mencionadas anteriormente, donde se puede ver la formación de 3,3'-di-BTBE y 3-nitro-BTBE cuando las muestras están en presencia de NO₂⁻.

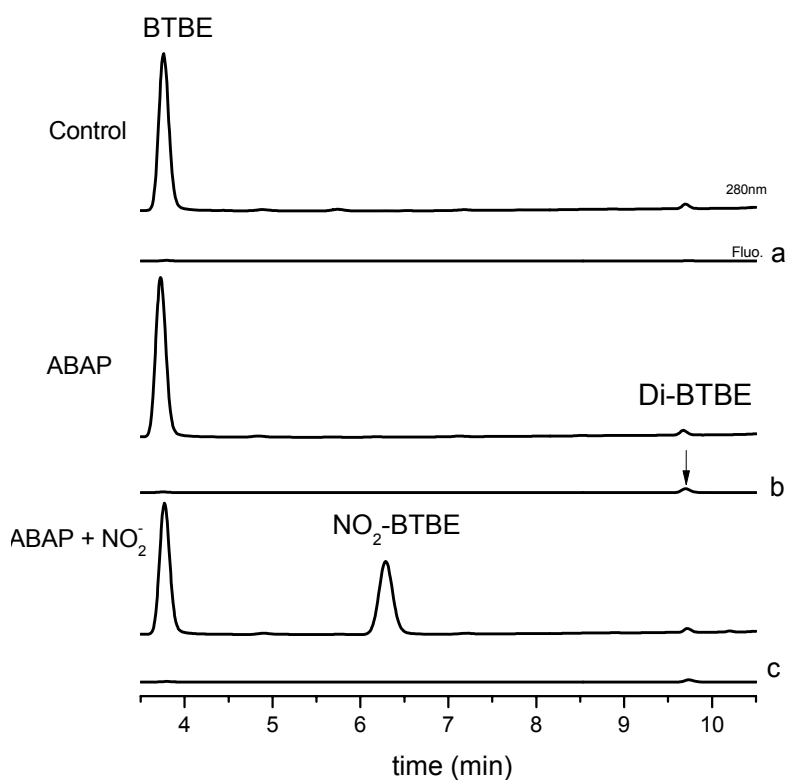


Figura 6.8A Separación por RP-HPLC de los productos de la oxidación del BTBE mediada por ABAP. Los liposomas de DLPC y EYPC (30 mM) con BTBE incorporado (0.3 mM) fueron incubados con ABAP (10 mM, flujo 0,3 μ M /min) durante 2hs a 37°C en presencia y ausencia de NO_2^- (20 mM) y las muestras analizadas para 3-nitro-BTBE y 3,3'-di-BTBE luego de la separación por RP-HPLC.

Para determinar específicamente la reacción entre los radicales peroxilo y la tirosina, estudiamos el efecto del ABAP en la oxidación de tirosina libre en fase acuosa (Figura 6.8B). La exposición de tirosina a radicales peroxilos derivados del ABAP, resultó en la formación de 3,3-ditirosina (Figura 6.8B, línea b). Cuando la incubación fue realizada en presencia de NO_2^- , pudo detectarse la formación de ambos productos, 3,3-ditirosina y 3-NT (Figura 6.8B, línea c). Los rendimientos de nitración y dimerización fueron menores para la tirosina en fase acuosa que para el BTBE incorporado en liposomas, lo cual puede sugerir que la oxidación de la tirosina por radicales peroxilo puede ocurrir más fácilmente en entornos no polares. Este resultado muestra de manera contundente que la tirosina (además del BTBE) puede ser oxidada

por radicales peroxilo, lo cual genera una fuerte evidencia sobre la participación del proceso de la lipoperoxidación en la nitración de tirosinas asociadas a compartimentos hidrofóbicos.

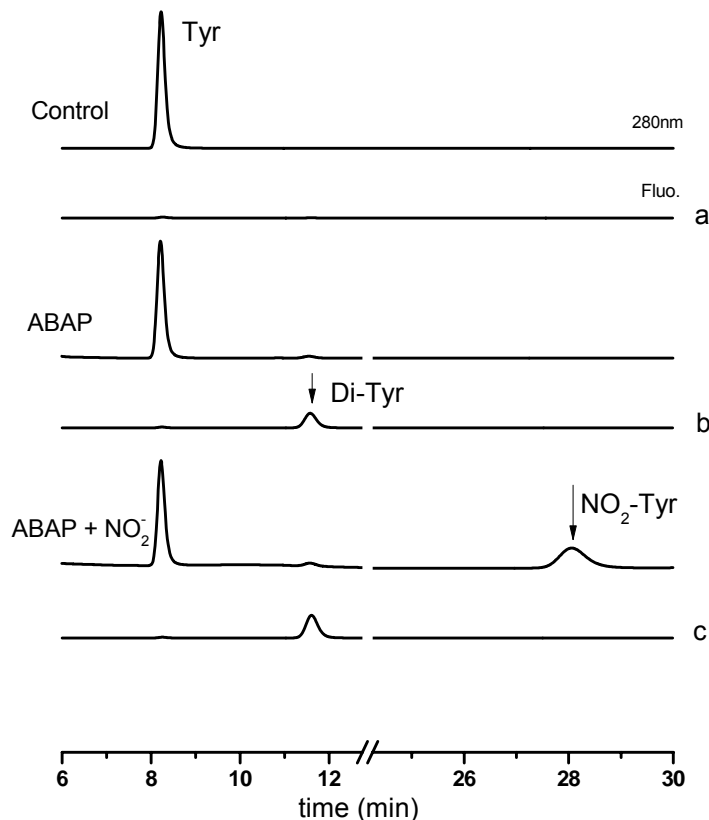


Figura 6.8B Separación por RP-HPLC de los productos de oxidación de la tirosina mediada por ABAP. Tirosina libre en fase acuosa (0.3 mM) en KPi (100 mM) pH 7,3 / 0,1 mM dtpa, fue incubada con ABAP (10 mM) durante 2h a 37°C y se analizó la formación de 3-NT y 3,3'-ditirosina luego de la separación por RP-HPLC.

La Tabla IX resume las constantes de velocidad de las reacciones que involucran por un lado, la oxidación de tirosina para dar lugar a la formación de productos tales como 3-NT y 3,3'-ditirosina, y por otros las reacciones involucradas en el proceso de lipoperoxidación, y la acción del α -tocoferol. Esta serie de ecuaciones fueron utilizadas en las simulaciones químicas que recapitulaban los datos experimentales y apoyaron la vinculación entre el proceso de nitración de la tirosina/BTBE, y el de la lipoperoxidación.

Tabla IX. Reacciones involucradas en la oxidación de tirosina y la lipoperoxidación.

Reacción	$k(M^{-1}s^{-1})$	Ref.
${}^aL + \bullet OH \rightarrow L\bullet + OH^-$	1×10^{10}	(259)
$L + \bullet NO_2 \rightarrow L\bullet + NO_2^-$	2×10^5	(171)
$Tyr + \bullet OH \rightarrow \bullet Tyr + OH^-$	1.24×10^{10}	(170)
$Tyr + \bullet OH \rightarrow \bullet TyrOH^b + OH^-$	6.5×10^8	(170)
$Tyr + \bullet NO_2 \rightarrow \bullet Tyr + NO_2^-$	3.2×10^5	(171)
$\bullet Tyr + \bullet NO_2 \rightarrow 3\text{-nitro-Tyr}$	3×10^9	(171)
$2 \bullet Tyr \rightarrow 3\text{-}3'\text{-diTyr}$	2.25×10^8	(299)
	${}^c2.25 \times 10^6$	(251)
$L\bullet + O_2 \rightarrow LOO\bullet$	3×10^8	(322)
$LOO\bullet + L \rightarrow LOOH + \bullet L$	37	(323)
$2 LOO\bullet \rightarrow LOOH + O_2$	10^7	(322)
$LOO\bullet + L\bullet \rightarrow LOOL$	5×10^7	(322)
$2 L\bullet \rightarrow LL$	5×10^8	(322)
$LOO\bullet + NO_2^- \rightarrow LOOH + \bullet NO_2$	4.5×10^6	(321) ^d
$LOO\bullet + Tyr \rightarrow LOOH + \bullet Tyr$	4.8×10^3	Esta tesis
${}^e\alpha\text{-TOH} + LOO\bullet \rightarrow \alpha\text{-TO}\bullet + LOOH$	5×10^5	(324)
$\alpha\text{-TOH} + \bullet NO_2 \rightarrow \alpha\text{-TO}\bullet + NO_2^-$	1×10^5	(324)
$\alpha\text{-TOH} + \bullet OH \rightarrow \alpha\text{-TO}\bullet + OH^-$	3.8×10^9	(262)

Las reacciones que involucran lípidos se refieren a aquellos que contienen ácidos grasos insaturados a no ser que se indique lo contrario.

^a Los lípidos que contienen ácidos grasos saturados también son oxidados por $\bullet OH$ (258).

^b Este radical se deshidrata rápidamente y evoluciona a radical tirosilo bajo las condiciones experimentales utilizadas.

^c La dimerización de tirosina en membranas ocurre a una velocidad al menos 100 veces menor que en fases acuosas.

^d Esta constante de reacción fue reportada para el la reducción del radical acetoperoxilo por nitrito.

^e Se indican los mecanismos de descomposición de radicales por el $\alpha\text{-TOH}$.

6.6 Efecto del α -tocoferol en la oxidación del BTBE y en la lipoperoxidación

El α -tocoferol es un conocido antioxidante, capaz de cortar las cadenas de propagación, al reaccionar con radicales LOO^\bullet con una constante de velocidad $k = 5 \times 10^5 \text{ M}^{-1}\text{s}^{-1}$ (262) para rendir hidroperóxidos y el radical estable α -tocoferoxilo ($\alpha\text{-TO}^\bullet$) (Ec. 31). La incorporación de α -tocoferol a liposomas de EYPC, inhibió la nitración del BTBE mediada por peroxinitrito (Figura 6.9A), la dimerización (no se muestra) y la lipoperoxidación en una forma dosis dependiente (Figura 6.9B). Es interesante notar que el α -tocoferol, también inhibió la oxidación del BTBE en liposomas de DLPC, incapaces de sufrir lipoperoxidación. El efecto del α -tocoferol se explica por la reacción entre α -tocoferol y LOO^\bullet . En el caso de los liposomas de DLPC, la reacción del α -tocoferol con $\bullet\text{NO}_2$ ($k = 1 \times 10^5 \text{ M}^{-1}\text{s}^{-1}$) (324) se torna relevante para explicar el efecto del α -tocoferol en sistemas con ácidos grasos saturados.

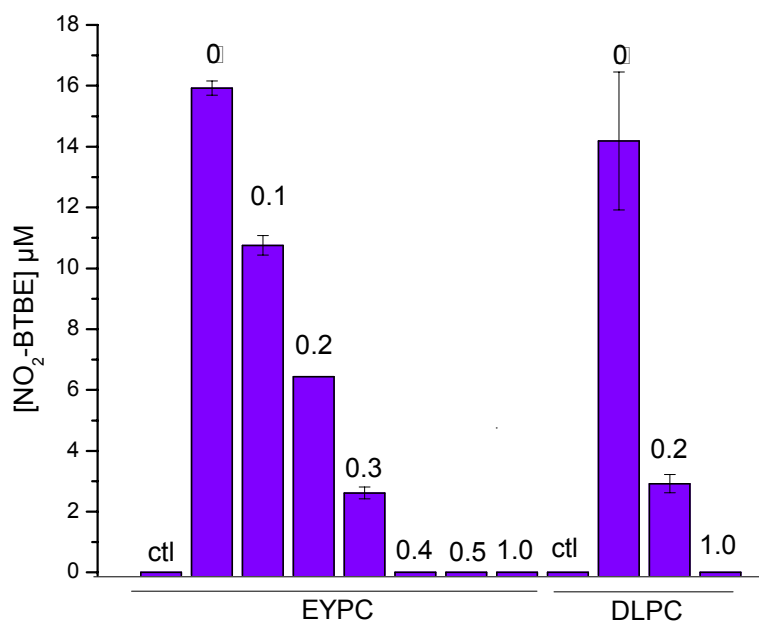


Figura 6.9A

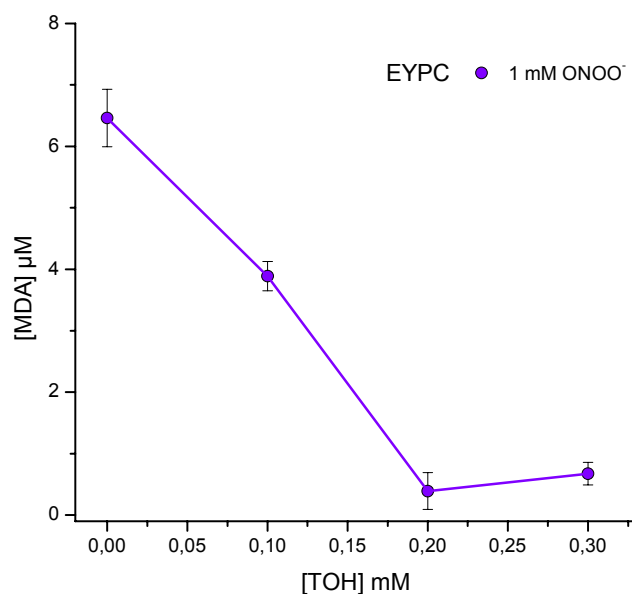


Figura 6.9B

Figura 6.9 Efecto del α -tocoferol en la nitración del BTBE y la lipoperoxidación. Liposomas de EYPC y DLPC (30 mM) con las cantidades indicadas de α -tocoferol pre-incorporadas (0.1 -1 mM) además del BTBE (0.3 mM), fueron tratados con peroxinitrito (1 mM). Se analizó la formación de (A) 3-nitro-BTBE y (B) MDA.

6.7 Consumo de oxígeno y determinación cinética de la reacción entre radicales $LOO\cdot$ y BTBE

Se realizaron experimentos para medir el consumo de oxígeno asociado a la lipoperoxidación iniciada por hemina y ABAP y la potencial acción antioxidante del BTBE para cortar cadenas de propagación. Si los radicales lipídicos efectivamente reaccionan de manera significativa con el BTBE, el análogo hidrofóbico de la tirosina debería inhibir el consumo de oxígeno. En liposomas de EYPC (pero no de DPLC) (en ausencia de BTBE) se muestra una disminución en la concentración de oxígeno basal. Se observa un consumo de oxígeno luego de la adición de ABAP o hemina (Figura 6.10A), de acuerdo con las fases de iniciación y propagación de la lipoperoxidación.

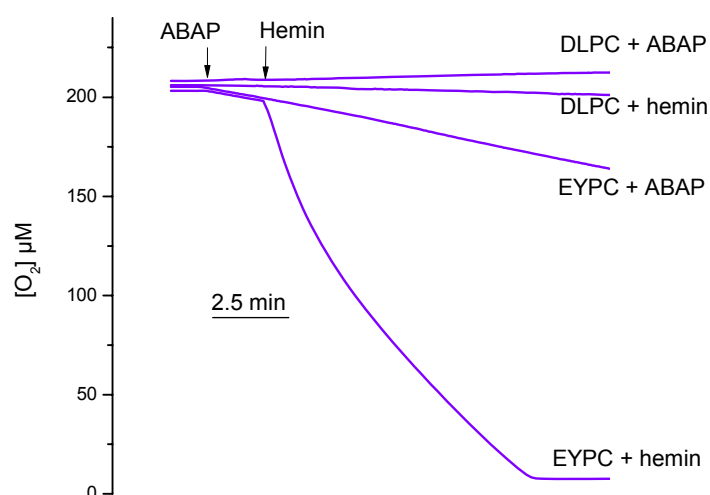


Figura 6.10A

Por el contrario, en liposomas de DLPC, no se observó consumo de oxígeno luego de la adición de ABAP o hemina (Figura 6.10A). La incorporación de α -tocoferol a liposomas de EYPC resultó en una disminución significativa en la tasa de consumo de oxígeno inducida por los oxidantes hemina y ABAP (Figura 6.10B). El grado de inhibición en el consumo de oxígeno por α -tocoferol fue compatible con las constantes de velocidad de LOO \cdot con cadenas alquílicas adyacentes ($k = 36 \text{ M}^{-1}\text{s}^{-1}$) (323) y con α -tocoferol ($k = 5 \times 10^5 \text{ M}^{-1}\text{s}^{-1}$) (262), como se mencionó previamente. La acción inhibitoria del α -tocoferol también se observó cuando este fue añadido exógenamente durante el curso temporal de los estudios de consumo de oxígeno, pero en este caso, su efecto fue menos potente que cuando fue pre-incorporado a los liposomas, debido a la más baja penetración a la estructura del liposoma preformado en el marco de tiempo del experimento. La incorporación del BTBE a los liposomas de EYPC dio lugar a una inhibición en el consumo de oxígeno dosis-dependiente, durante la oxidación inducida por hemina y ABAP, lo cual es consistente con una reacción entre el BTBE y los radicales lipídicos derivados de la lipoperoxidación (Figura 6.10B).

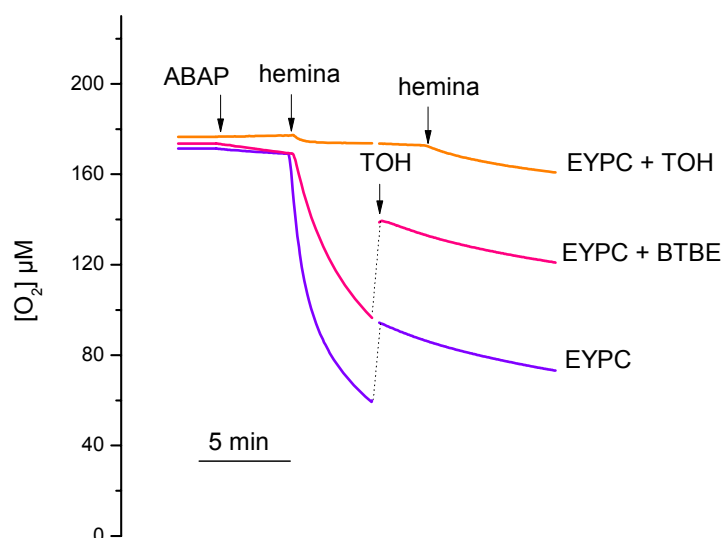


Figura 6.10B

Para descartar efectos sutiles en la estructura de las membranas liposomales debido a la incorporación del BTBE, los experimentos se realizaron con un análogo hidrofóbico de la fenilalanina (BTPE) pre-incorporado a los liposomas (Figura 6.10C). En estas condiciones, el consumo de oxígeno fue idéntico al observado para la condición control de EYPC (sin BTBE), lo cual está de acuerdo con una participación directa del grupo fenol (-OH) del BTBE en la reacción que conduce a la inhibición del consumo de oxígeno dependiente de la lipoperoxidación, dado que este grupo no está presente en el derivado hidrofóbico de la fenilalanina (Figura 6.10C).

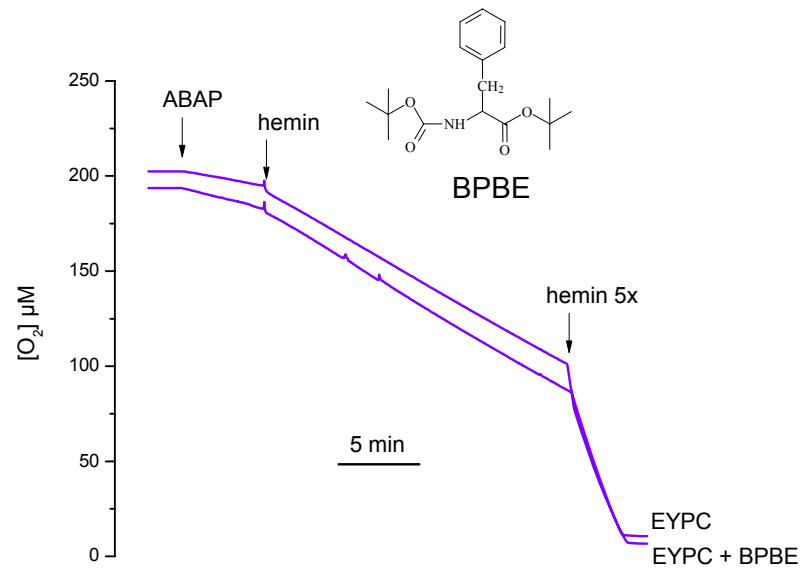


Figura 6.10C

Se analizaron los distintos valores de inhibición del consumo de oxígeno obtenidos con concentraciones crecientes de BTBE pre-incorporado a liposomas de EYPC, con el fin de obtener una constante de reacción estimada de segundo orden entre los radicales $LOO\cdot$ y el BTBE. Un gráfico que relaciona la fracción de inhibición del consumo de oxígeno en función de la concentración del BTBE muestra una competencia directa del BTBE por los radicales peroxilo derivados de la lipoperoxidación (Figura 6.10D).

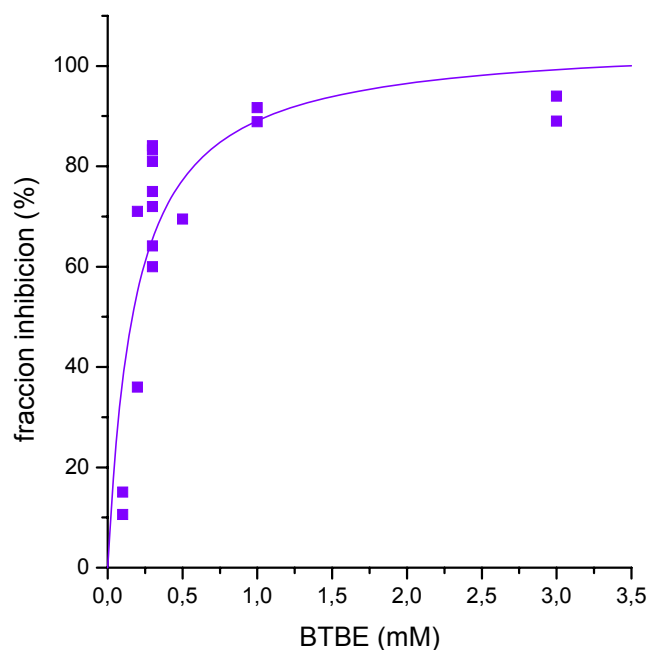


Figura 6.10D

Figura 6.10 Estudios de Oximetría. Se realizaron estudios de oximetría para determinar la lipoperoxidación inducida por ABAP (10 mM) y hemina (1 μ M) en NaPi 100 mM (pH 7,3) / 0,1 mM dtpa. **(A)** Liposomas de EYPC y DLPC (6.25 mM). **(B)** Liposomas de EYPC conteniendo BTBE (0.3 mM) o α -tocoferol (0.3 mM). La flecha indica la adición exógena de α -tocoferol (0.25 mM). **(C)** BPBE (0.3 mM) incorporado a liposomas de EYPC. **(D)** Liposomas de EYPC con distintas concentraciones de BTBE (0.1-3 mM) fueron expuestos a ABAP (10 mM) y hemina (1 μ M) y se determinó la inhibición en el consumo de oxígeno en función de la concentración de BTBE. La estructura del BPBE se muestra en el panel correspondiente.

Se calculó para cada concentración de BTBE el porcentaje de inhibición y se graficaron en función de la concentración del BTBE. Estos datos, nos permiten estimar una constante de reacción de segundo orden aparente $k = 4.8 \times 10^3 \text{ M}^{-1}\text{s}^{-1}$ para la siguiente reacción (Ec. 45):



Este valor de constante, es comparable con el obtenido independientemente a partir de los experimentos con α -tocoferol. De los datos obtenidos en las Figuras 6.10B y C, uno puede concluir que se obtiene una inhibición de 87 %, con 5 μ M α -tocoferol, y 1 mM BTBE. Considerando un factor estequiométrico de $n = 2$ para el α -tocoferol (325), se puede plantear la siguiente ecuación:

$$2 \times k_{toc} [\alpha\text{-tocoferol}] = k_{BTBE} [\text{BTBE}] \quad (46)$$

De manera que: $2 \times k_{toc} [\alpha\text{-tocoferol}] / [\text{BTBE}] = k_{BTBE} = 5 \times 10^3 \text{ M}^{-1}\text{s}^{-1}$, valor muy similar al obtenido experimentalmente. Por otro lado, los rendimientos de hidroperóxidos y MDA disminuyeron en presencia de BTBE (Figuras 6.11A, B y C), lo cual estaría de acuerdo con una reacción entre el BTBE y los radicales LOO^\bullet y con los datos de oximetría.

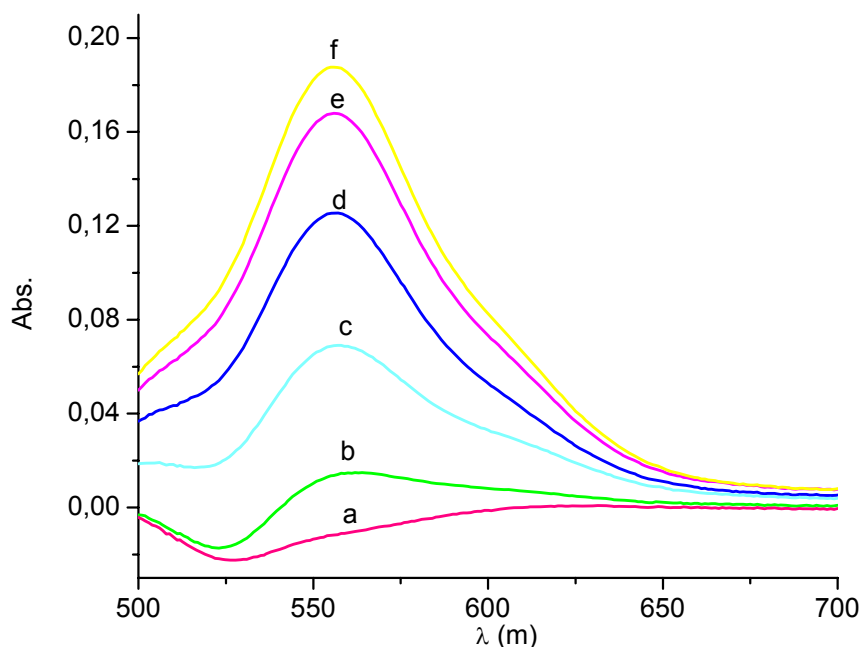


Figura 6.11A

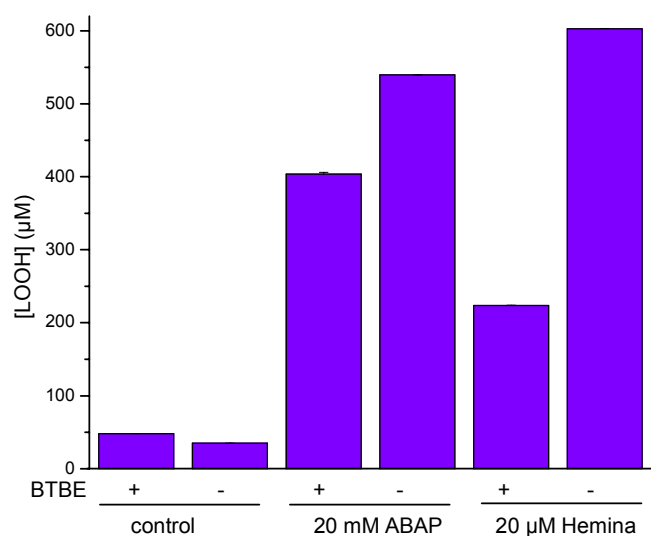


Figura 6.11B

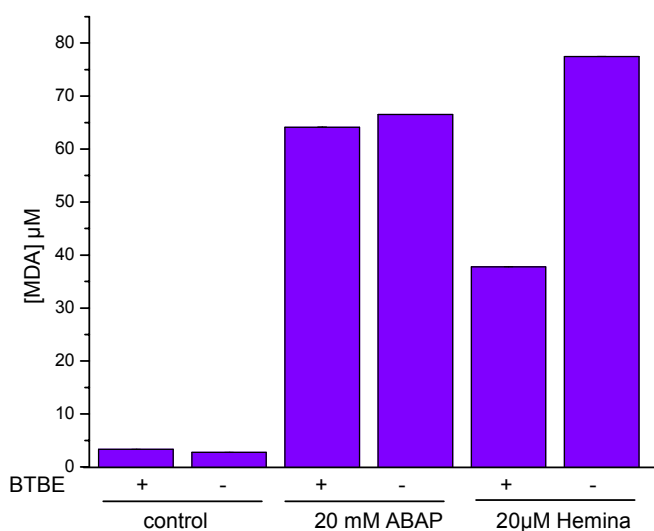


Figura 6.11C

Figura 6.11 Formación de productos de la lipoperoxidación iniciada por hemina y ABAP. Liposomas de EYPC en ausencia y presencia de BTBE (0.3 mM), fueron expuestos a hemina (30 min) y ABAP (2.5hs) y se determinó el contenido de hidroperóxidos lipídicos por el ensayo de FOX. **(A)** Espectros UV-Vis de las muestras: (a) – BTBE; (b) + BTBE; (c) + BTBE + hemina; (d) + BTBE + ABAP; (e) – BTBE + ABAP; (f) – BTBE + hemina, con las concentraciones indicadas **(B)** Determinación de los hidroperóxidos lipídicos de las muestras analizadas en A. **(C)** Formación de MDA en las mismas muestras que en A.

6.8 Discusión

Los radicales $\cdot\text{OH}$, $\text{CO}_3\cdot^-$, $\cdot\text{NO}_2$; los compuestos I y II de las hemoperoxidasas y los centros metálicos de transición con alto estado de oxidación (3), son oxidantes biológicamente relevantes, capaces de oxidar a la tirosina por un electrón en fases acuosas. Sin embargo, no se había estudiado en profundidad que tipo de oxidantes participan en la oxidación de tirosinas asociadas a entornos hidrofóbicos tales como membranas o lipoproteínas, y en ese sentido se debe considerar que: por un lado, algunos de los oxidantes pueden tener dificultad para permear hacia la fase lipídica (ej. oxidantes aniónicos) y por otro, los ácidos grasos insaturados presentes en altas concentraciones en dichos compartimentos y con importante reactividad, pueden constituir el blanco preferencial para el ataque oxidativo inicial, inhibiendo de esa manera las reacciones de oxidación de las tirosinas presentes en membrana. Por este motivo, los mecanismos por los cuales los residuos de tirosina sufren reacciones de oxidación (nitración, dimerización e hidroxilación) en compartimentos hidrofóbicos pueden tener características diferentes a las descritas previamente para fases acuosas.

En este Objetivo Específico, hemos estudiado mediante un sistema modelo de membranas formado por liposomas de PC con un análogo hidrofóbico de la tirosina pre-incorporado, si los radicales derivados de la lipoperoxidación, son capaces de mediar el proceso de oxidación de la tirosina, para dar lugar a la formación de radical tirosilo que posteriormente puede formar 3-NT y 3,3'-ditirosina.

La lipoperoxidación fue iniciada por tres sistemas de oxidación independientes: peroxinitrito, hemina y ABAP. El peroxinitrito promueve la lipoperoxidación y nitración de tirosina en compartimentos hidrofóbicos luego de la homólisis del ácido peroxinitroso (ONOOH) para dar $\cdot\text{OH}$ y $\cdot\text{NO}_2$ en el interior o en las proximidades de la membrana lipídica (16, 22, 251). En liposomas insaturados de EYPC, la relación de concentración ácidos grasos insaturados / BTBE (50 / 1) y las constantes de velocidad

participantes (Tabla IX), determinan que el ataque inicial de los radicales derivados del peroxinitrito se produce sobre los ácidos grasos, generando radicales alquilo (pentadienilo) que evolucionan a radicales LOO•, que son las especies que propagan el proceso. Alternativamente, se generaron radicales lipídicos por la reacción de la hemina con hidroperóxidos preformados para rendir LOO• (326), o por ABAP, cuyos radicales peroxilos difunden hacia los liposomas y reaccionan con las cadenas alquilo de los ácidos grasos insaturados iniciando la lipoperoxidación. Los radicales LOO•, reaccionan rápidamente con compuestos fenólicos, que pueden ejercer actividades antioxidantes *in vitro* e *in vivo*. Por ejemplo, los radicales peroxilo del linoleato reaccionan con compuestos tales como el α -tocoferol, curcumina y quercetina con constantes de velocidad que se encuentran en el rango de $k \sim 10^6$ - 10^7 M⁻¹s⁻¹ (327-330). En el caso de la tirosina, que es otro compuesto fenólico, la reacción con radicales LOO• es termodinámicamente posible, sin embargo, la tirosina no es un buen dador de electrones, y por lo tanto la reacción puede estar cinéticamente desfavorecida. Es interesante notar que los ambientes hidrofóbicos pueden aumentar la reactividad de compuestos fenólicos tales como la tirosina, por los radicales LOO•. En ese sentido, se realizaron análisis con el objetivo de demostrar la reacción entre los radicales LOO• y el análogo hidrofóbico de la tirosina, BTBE.

Los radicales LO• también se forman durante el proceso de la lipoperoxidación, a través de la oxidación por un electrón de los LOOH (331), o por ruptura de intermediarios tetróxidos formados durante la reacción de 2 radicales LOO•. Estas especies son potentes oxidantes incluso más que los radicales LOO• pero una vez formados normalmente rearreglan para formar radicales epoxialilicos, que a su vez luego de reaccionar con O₂ forman radicales peroxilo (332), y por este motivo no se ha considerado al radical LO•, como posible oxidante de la tirosina, ya que una vez formado rápidamente evolucionará hacia otras especies.

La evidencia que hemos reunido para apoyar la participación de los radicales $\text{LOO}\cdot$ en los procesos de oxidación de la tirosina promovidos por los tres sistemas de oxidación ensayados se pueden resumir de la siguiente manera: a) la oxidación de tirosina (BTBE) ocurre en forma significativa en liposomas de PC que contienen ácidos grasos insaturados; b) la oxidación de la tirosina en liposomas (BTBE), pero no en fases acuosas, se redujo cuando las muestras se encontraban a bajas concentraciones de oxígeno; c) se pudieron detectar simultáneamente los radicales lipídicos y radicales tirosilo; d) el α -tocoferol inhibió fuertemente la oxidación de tirosina; e) el BTBE (pero no el BPBE) inhibió parcialmente el proceso de la lipoperoxidación; f) los cambios en los niveles de oxidación de la tirosina y los productos de la peroxidación siguieron una tendencia paralela y g) los datos están de acuerdo con un proceso conjunto que incluye los mecanismos radicalares de la lipoperoxidación y la oxidación de la tirosina, vinculados por una “reacción de conexión”, representada por la oxidación de la tirosina por un electrón mediada por $\text{LOO}\cdot$ (Ec.29 y Tabla IX). En lo que respecta a la reactividad de los radicales peroxilo con la tirosina, los datos mostraron que los radicales peroxilo derivados del ABAP son capaces de oxidar tanto al BTBE en liposomas de DLPC (saturados), como a la tirosina libre (Tabla VII y Fig. 6.8A y B), pero los rendimientos de reacción fueron mucho mayores para el BTBE, lo cual es compatible con el concepto de que la reacción de los compuestos fenólicos con los radicales oxidantes se ve influida por un efecto cinético del solvente (333, 334). De hecho, diferentes compuestos fenólicos (por ejemplo, la quercetina y epicatequina) reaccionan con radicales peroxilo a velocidades similares que las observadas para el α -tocoferol en solventes no polares, pero no en solventes polares capaces de formar puentes de hidrógeno. En solventes que son fuertes aceptores de enlaces de hidrógeno, las constantes de velocidad de los radicales peroxilo con compuestos fenólicos son mucho menores, e incluso dichas constantes pueden llegar a ser indetectables (335). Los solventes polares pueden por un lado interferir con la estabilización intramolecular (puentes de hidrógeno) del radical

fenoxilo, y por otro generar un impedimento estérico para la aproximación del radical peroxilo a los complejos solvente-fenol, lo que reduce la constante de velocidad de la abstracción del átomo de hidrógeno. Estas consideraciones adquieren importancia en las fases heterogéneas de bicapas lipídicas, donde la localización de los grupos fenólicos influirá en su eficacia para reaccionar con radicales. En el caso de radicales $\text{LOO}\cdot$ generados en EYPC, se estimó una constante de velocidad de segundo orden con BTBE, obtenida mediante estudios de consumo de oxígeno, usando dos enfoques diferentes, considerando "blancos primarios" independientes; es decir, ácidos grasos insaturados ($k_{\text{LH}} \sim 10\text{-}50 \text{ M}^{-1}\text{s}^{-1}$ y α -tocoferol ($k_{\alpha\text{TOH}} = 1 \times 10^5$, (262)) (Fig. 6.10). El valor de constante de reacción entre el radical peroxilo y el BTBE fue $k_{\text{BTBE}} = 4.8 \times 10^3 \text{ M}^{-1}\text{s}^{-1}$, el cual es compatible con las propiedades redox de la tirosina. Se han reportado las reacciones de radicales orgánicos peroxilo halogenados (conocidos por ser más reactivos que los radicales peroxilo lípidos) con tirosina a pH alcalino, donde la mayor parte de la tirosina está en la forma desprotonada ($\text{pK}_{\text{Tyr-OH}} \sim 10$), con constantes de velocidad elevadas, cercanas a $10^8 \text{ M}^{-1}\text{s}^{-1}$ (336). La oxidación de la forma protonada del fenol por radicales peroxilo (como se esperaba a un pH neutro o dentro de una estructura hidrofóbica) es significativamente menos favorable, lo cual está de acuerdo con el valor relativamente bajo k_{BTBE} en el rango de $10^3 \text{ M}^{-1}\text{s}^{-1}$ obtenidos.

Los rendimientos relativos de la dimerización de la tirosina y la oxidación se ven afectados por la estructura de biomembranas (192, 251, 337), y hemos estimado un coeficiente de difusión (D) para el BTBE en liposomas de PC $\sim 5 \mu\text{m}^2 \text{ s}^{-1}$ (251). Por lo tanto, el valor de la constante de velocidad se reduce de 100-200 veces ($k \sim 1.2 \times 10^6 \text{ M}^{-1}\text{s}^{-1}$) con respecto al valor correspondiente a los radicales tirosilo ($k = 2,25 \times 10^8 \text{ M}^{-1}\text{s}^{-1}$). Por otra parte, el $\cdot\text{NO}_2$ es capaz de concentrarse en entornos hidrofóbicos (190), y el valor D ($D_{\cdot\text{NO}_2}$) es de $\sim 1500 \mu\text{m}^2\text{s}^{-1}$, muy próximo al obtenido en fase acuosa de $4500 \mu\text{m}^2\text{s}^{-1}$ (189), por lo tanto la nitración está cinéticamente impedida en

membranas, de acuerdo con las mayores relaciones 3-nitro-BTBE / 3,3'-diBTBE obtenidas durante la exposición a peroxinitrito del BTBE incorporado a membranas.

Nuestros datos también indican que el α -tocoferol es capaz de modular la oxidación de tirosinas en membranas a través de la inhibición de la lipoperoxidación. En este sentido, es importante considerar que el grado de inhibición es una función de los niveles de α -tocoferol que, en condiciones biológicamente relevantes (~ 1 molécula de α -tocoferol por cada 100-1000 moléculas de fosfolípidos de membrana; (261)) puede no ser suficiente para evitar plenamente los eventos de oxidación de tirosina en biomembranas (337, 338) o en sistemas de membranas modelo (este trabajo, ver Fig. 6.9A de 0-0.3 mM α -tocoferol en 30 mM DLPC). Por lo tanto, podemos predecir que un aumento en los niveles de α -tocoferol en células / tejidos debería resultar en una atenuación de la oxidación de las tirosinas proteicas tanto en membranas como en lipoproteínas. Además de los productos formados durante la lipoperoxidación, tienen lugar reacciones secundarias con los radicales lipídicos intermediarios, cuando se encuentran presentes peroxinitrito y / o $\cdot\text{NO}_2$, que llevan a la formación de lípidos nitrados (161) (Ec. 47).



Además, puede tener lugar una reacción de terminación entre $\cdot\text{LOO}$ y $\cdot\text{Tyr}$ para producir aductos con estructura del tipo Diels-Alder (339)(Ec. 48):



Los fosfolípidos de membrana tienen un bajo valor D ($D_{\text{PL}} \sim 0.5\text{-}1 \mu\text{m}^2 \text{s}^{-1}$, (239)), pero

debido a su abundancia la formación de aductos tirosilo-fosfolípidos es un proceso probable y deberá ser abordado en trabajos futuros.

En resumen, los datos presentados en este documento confirman que los radicales LOO• formados durante el proceso de la lipoperoxidación, participan en los procesos de oxidación de tirosina en biocompartimentos hidrofóbicos y proporcionan una nueva visión mecanística para la comprensión de la nitración de proteínas en lipoproteínas y membranas (Fig. 6.12). En particular, los niveles celulares y tisulares de oxígeno representan un factor no reconocido previamente que puede afectar seriamente los rendimientos de la oxidación de tirosina mediante la intermediación de los radicales peroxilo

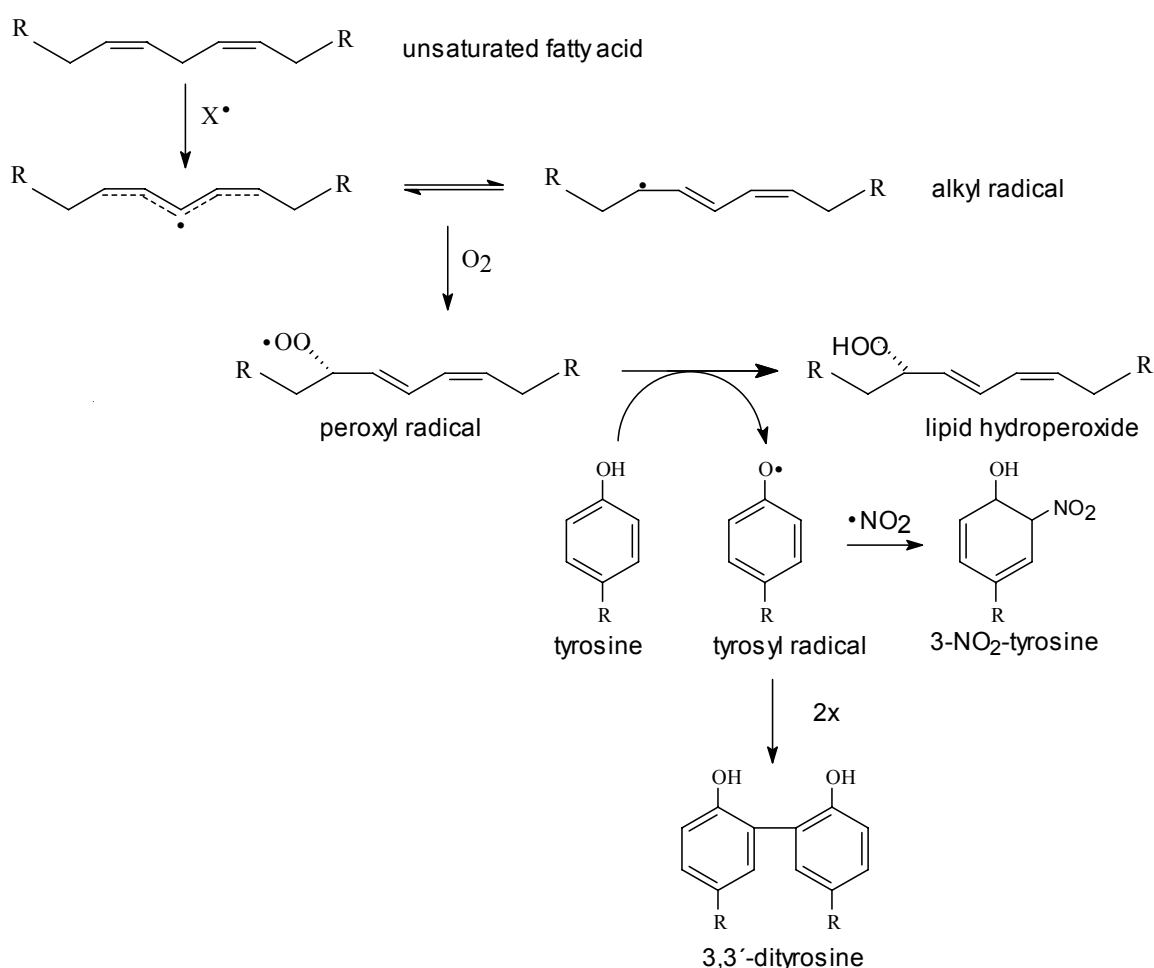


Figura 6.12 Mecanismo propuesto de reacción según el cual los radicales peroxilo son capaces de oxidar a la tirosina.

Los resultados también determinaron que la nitración del análogo hidrofóbico de la tirosina, BTBE, fue inhibida por la presencia de CO₂, contrariamente a lo observado para tirosinas en fases acuosas, probablemente debido a la imposibilidad que tiene el radical carbonato formado en la reacción con peroxinitrito de entrar hacia el interior de las membranas (251). De la misma manera se demostró que la nitración era favorecida en presencia de complejos metálicos de transición como porfirinas de hierro y manganeso y que los ácidos grasos insaturados de las membranas pueden promover las reacciones de nitración a través de la reacción del radical peroxilo formado durante la lipoperoxidación y la tirosina, dando lugar a la formación del radical tirosilo. En este trabajo se demuestra por primera vez la fuerte asociación que existe entre los procesos de nitración de tirosinas asociadas a compartimentos hidrofóbicos y las reacciones de lipoperoxidación de los lípidos de membrana (340), que se conectan a través de la formación de radicales LOO•, los cuales son capaces de oxidar a la tirosina y alimentar el proceso de oxidación de tirosinas, a través de la formación del intermediario radical tirosilo.

7. Resultados y Discusión

Obj. #3

7. Objetivo # 3 Síntesis, caracterización y validación de péptidos transmembrana para el estudio de los mecanismos de nitración de tirosinas en membranas.

En este Objetivo Específico, nos proponemos sintetizar, caracterizar y validar péptidos de tirosina, con capacidad de incorporarse en membranas, y con el residuo de tirosina en distintas posiciones respecto al extremo amino terminal, concretamente en la posición 4, 8 y 12 (Y4, Y8 e Y12); con el fin de aplicar los conocimientos adquiridos en los Objetivos Específicos #1 y #2 en un sistema modelo de mayor similitud con proteínas. Estos péptidos nos permiten seguir profundizando en los mecanismos de nitración de tirosinas en membranas, con estudios más comparables a lo que ocurriría en, por ejemplo, un “loop” de una proteína transmembrana, y por lo tanto, de mayor relevancia biológica. Para ello generamos esta herramienta, e incorporamos los péptidos a un sistema modelo de membranas, formado por liposomas de PC, y evaluamos la nitración de estos péptidos por peroxinitrito. Se completó la síntesis y purificación de los diferentes péptidos en forma exitosa. Los experimentos llevados a cabo hasta el momento han sido realizados con el péptido Y8 para trabajar inicialmente con la condición más intermedia, en cuanto a la profundidad de tirosina dentro de la bicapa. Futuros experimentos incluirán a toda la serie de péptidos sintetizados de manera de poder realizar estudios comparativos.

7.1 Síntesis de los péptidos

Los péptidos transmembrana de 23 amino ácidos conteniendo tirosina en diferentes posiciones (Y4, Y8 e Y12) fueron sintetizados tal cual lo indicado en Materiales y Métodos. La secuencia de los péptidos sintetizados es la siguiente:

Péptido	Secuencia	PM
Y4	Ac-NH-KKAYALALALALALALALAKK-CONH ₂	2350
Y8	Ac-NH-KKALALAYALALALALALALAKK-CONH ₂	2350
Y12	Ac-NH-KKALALALALAYALALALALAKK-CONH ₂	2350

Como se observa en las secuencias, los péptidos tienen 23 amino ácidos y contienen el amino ácido básico lisina (K) en los extremos amino y carboxilo terminal, seguidos de una alternancia de amino ácidos alifáticos alanina-leucina (A-L), y el amino ácido tirosina (Y) ubicado en la posición 4, 8 o 12 respecto al extremo amino terminal (péptidos Y4, Y8 e Y12). Esta secuencia primaria aporta amino ácidos hidrófilos en sus extremos para la interacción en la interfase lípido-agua que permiten su anclaje en los extremos de la bicapa (lisinas), y amino ácidos de menor solubilidad en agua en la zona central, para facilitar su inserción y estabilidad dentro de la bicapa fosfolipídica (alaninas y leucinas). Se espera que el péptido interaccionando con la membrana, adquiera una estructura secundaria de α -hélice, la cual se estabilizará por puentes de hidrógeno (Fig. 7.1).

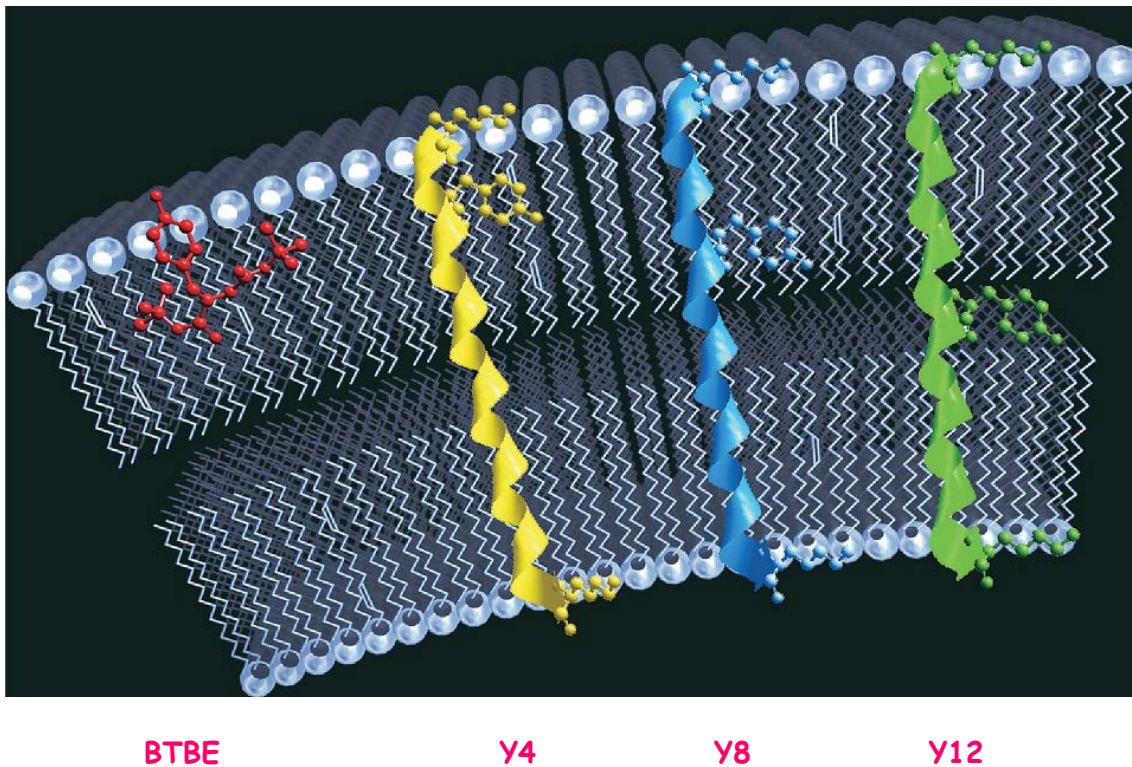


Figura 7.1 Péptidos transmembrana y BTBE insertos en la bicapa. El BTBE se ancla en la bicapa a través de su porción *tert*-butilo, mientras que el anillo aromático queda inmerso en la misma, con el grupo OH cercano a la interfase lipido-agua. Los péptidos tienen el residuo de tirosina ubicado a distintas profundidades: Y4 con la tirosina muy superficial cercana a la interfase, Y8 e Y12 con el residuo de tirosina ubicado en la profundidad de la bicapa. Extraído de (169).

Alternativamente, se realizó un procedimiento de síntesis similar al anterior pero agregando un residuo más de lisina en el extremo carboxi-terminal de los tres péptidos (Y'4, Y'8 e Y'12), con la secuencia que se muestra a continuación, teniendo en este caso, un péptido de 24 amino ácidos, con el objetivo de aumentar la solubilidad de los mismos y poder hacer estudios comparativos. Estos estudios nos permitirán más adelante sintetizar péptidos con más cantidad de lisinas e incorporar tirosinas en este extremo (incluido en la fase acuosa), de manera de comparar la nitración de residuos de tirosinas ubicados en el interior de la membrana, con residuos de tirosina presentes en la región del péptido que queda expuesta al solvente, como

ocurre en proteínas que tienen una región integral de membrana y una porción periférica.

Péptido	Secuencia	PM
Y´4	Ac-NH-KKAYALALALALALALALAKKK-CONH ₂	2478
Y´8	Ac-NH-KKALALAYALALALALALALAKKK-CONH ₂	2478
Y´12	Ac-NH-KKALALALALAYALALALALAKKK-CONH ₂	2478

7.2 Purificación y caracterización de los péptidos

Se sintetizaron cada uno de los péptidos como se describió previamente, y el producto crudo resultante de la síntesis fue sometido a RP-HPLC, siendo la fracción mayoritaria en cada caso, recolectada, y sometida a análisis de MS para confirmar su identidad. Se muestran los cromatogramas obtenidos de la purificación de los péptidos Y4, Y8 e Y12 respectivamente (Figura 7.2 A, B y C). Los datos de MS confirmaron la presencia de 2 iones mayoritarios con relaciones m/z de 588 y 784 para los péptidos de 23 amino ácidos (cuya masa es 2350 Da), que corresponden a las especies con dos y tres cargas respectivamente (Figura 7.3A). Cuando se hizo la reconstrucción de masa a partir de estos datos se obtuvo un ión de m/z = 2352 (Figura 7.3B). La figura muestra el análisis del péptido Y8 que será utilizado en los futuros experimentos, pero los resultados fueron idénticos para los péptidos Y4 e Y12.

De manera similar los péptidos Y´4, Y´8 e Y´12 fueron purificados y analizados por MS, obteniéndose en este caso un ión mayoritario de relación m/z = 2479 (no se muestra), lo cual está de acuerdo con la masa calculada de 2478 + H⁺. Una vez confirmada la identidad de los péptidos, estos fueron liofilizados y almacenados a -20°C hasta su uso.

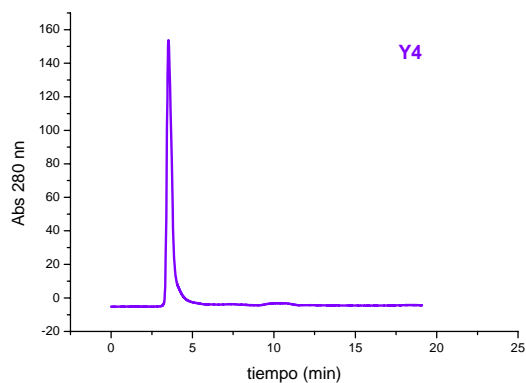


Figura 7.2A

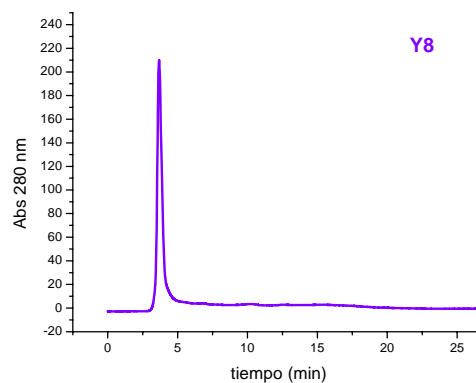


Figura 7.2B

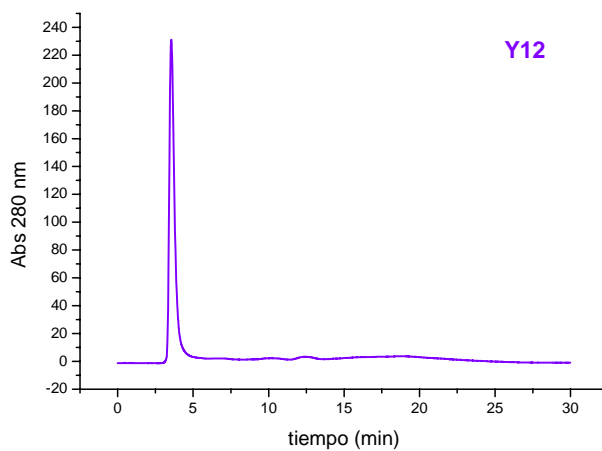


Figura 7.2C

Figura 7.2 Purificación del péptido transmembrana por RP-HPLC. Luego de la síntesis, los péptidos fueron sometidos a RP-HPLC y la fracción mayoritaria fue recolectada. Dicha fracción se analizó por MS y se volvió a someter a HPLC para comprobar su pureza. **(A)** Y4, **(B)** Y8 y **(C)** Y12. Las condiciones cromatográficas de purificación fueron: gradiente lineal de 40 % acetonitrilo - 0.1 % TFA en agua / 0.1 % TFA a 80 % acetonitrilo - 0.1 % TFA en agua / 0.1 % TFA durante 30 minutos. Se determinó una pureza > 95%.

Los experimentos preliminares mostrados en este Objetivo Específico fueron realizados con el péptido Y8 de 23 amino ácidos, con lo que futuros experimentos incluirán a los otros tipos de péptidos presentados anteriormente.

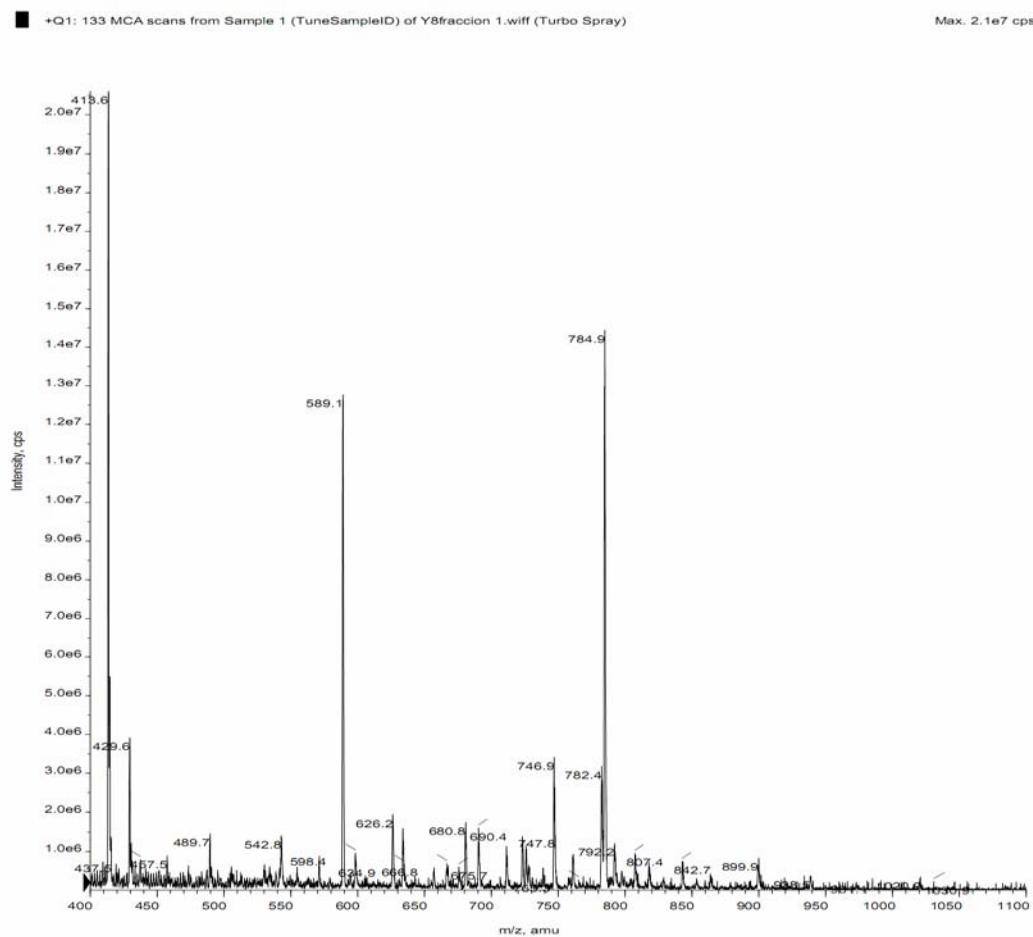


Figura 7.3A

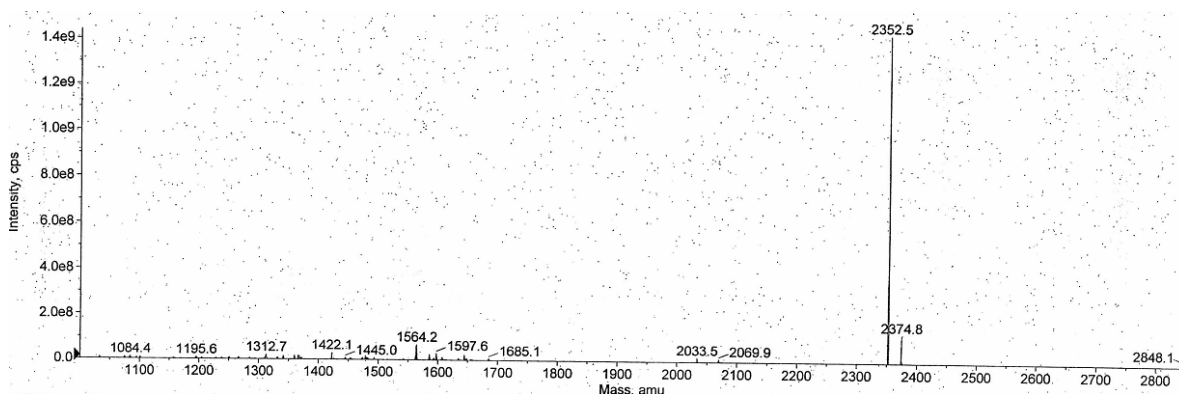


Figura 7.3B

Figura 7.3 Caracterización de los péptidos transmembrana por ESI-MS. El péptido Y8 (10 μ M) en metanol / ácido acético (0.1 %) de 23 aminoácidos fue sometido a análisis de ESI-MS en modo positivo. **(A)** Scan de masa en Q1 **(B)** Reconstrucción de masa. Se calcularon las masas de la siguiente manera: 128,2 Da para K, 71,1 Da para A, 113,1 Da para L y 163,2 Da para Y. El grupo amida provoca un aumento adicional de 16 Da, lo cual da una masa molecular de 2350 Da para los péptidos de 23 amino ácidos.

7.3 Formación de NO_2 -Y8 dependiente de peroxinitrito.

A los efectos de validar la utilidad del péptido de tirosina para estudiar procesos de nitración en membranas, en primer lugar, se desarrolló un método de RP-HPLC para separar el péptido de su producto de nitración, ya que lo reportado previamente fue realizado en un equipo de HPLC capilar (191), para lo cual se hicieron varias pruebas hasta lograr las condiciones óptimas de análisis en el equipamiento disponible actualmente. Inicialmente, el péptido Y8 disuelto en metanol (sin liposomas) fue expuesto a peroxinitrito e inyectado en la columna de HPLC directamente. Este estudio preliminar, mostró la presencia de un segundo pico en el cromatograma de HPLC con un tiempo de retención mayor al del péptido nativo y en el que utilizando el

detector UV-Vis se observó una doble absorbancia (280/360), compatible con la nitración del residuo tirosina en Y8 (Figura 7.4A).

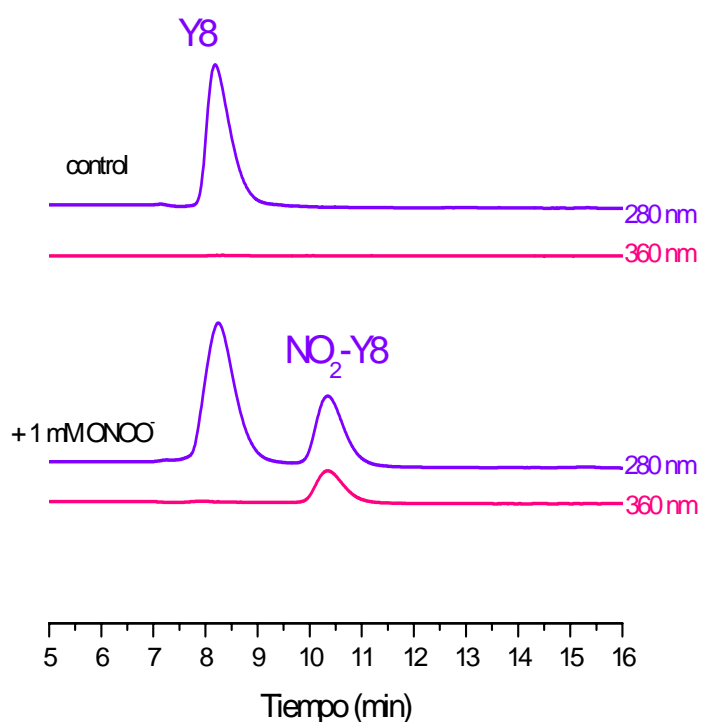


Figura 7.4A

Este pico fue recolectado y su identidad confirmada por MS, al encontrarse un ión con un aumento neto de masa de 45 Da, sobre la masa de 2350 Da correspondiente al péptido Y8, e indicativo de la presencia de un grupo nitro (-NO₂) en la molécula. La figura 7.4B muestra el análisis de scan de MS en Q1, en el cual se puede observar la presencia de 2 iones mayoritarios con relación $m/z = 799$ y 600 que corresponden a los iones di y tricargados + un grupo -NO₂ respectivamente. La reconstrucción de masa para estos datos da un ión de 2396 de acuerdo a la masa esperada ($2350 + 45 + H^+$) (no se muestra). Los datos fueron corroborados usando un standard de nitro-Y8 provisto por el MCW y que fue preparado por exposición a tetranitrometano.

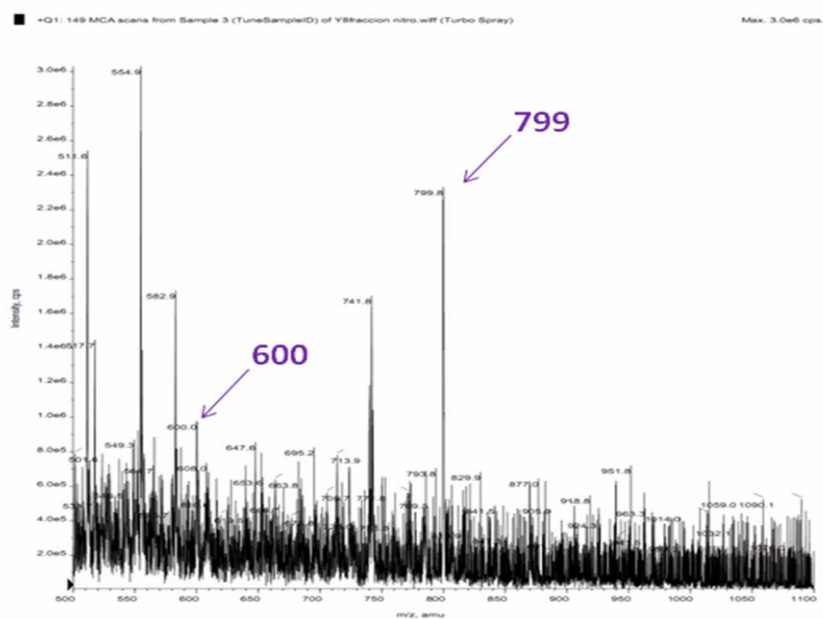


Figura 7.4B

Figura 7.4 Caracterización del péptido NO₂-Y8 por RP-HPLC/MS. El péptido Y8 en metanol fue tratado con peroxinitrito (1mM) y los productos resultantes de la reacción fueron (A) separados por RP-HPLC con detección UV-Vis a 280 y 360 nm. (B) Los picos fueron recolectados y sometidos a análisis de ESI-MS en modo positivo. Se muestra la caracterización por MS del NO₂-Y8.

En los siguientes experimentos, los péptidos purificados fueron incorporados a liposomas multilamerales de PC tal cual se describió previamente (191), obteniéndose un rendimiento de incorporación mayor al 95%. Los liposomas de DLPC y EYPC conteniendo el péptido Y8 fueron expuestos a peroxinitrito en diferentes condiciones experimentales; en primer lugar, para liposomas de DLPC se observó la formación de nitro-Y8 al tratarlos con peroxinitrito (Figura 7.5). El rendimiento de nitración para 1 mM peroxinitrito fue menor al observado con BTBE, en el orden de 0,4 % en relación a la concentración de peroxinitrito adicionado.

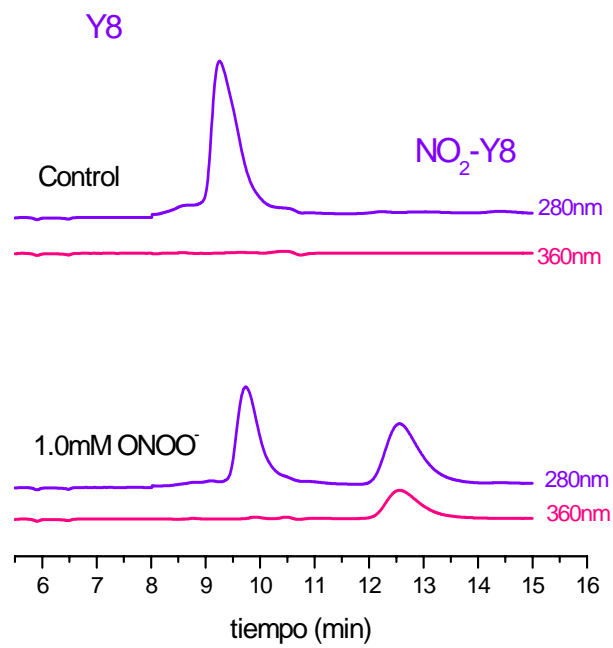


Figura 7.5 Formación de NO₂-Y8 en liposomas de DLPC. Liposomas de DLPC (30 mM) con Y8 pre-incorporado (0.3 mM) fueron tratados con peroxinitrito (1 mM) en KPi (100 mM) pH 7,3 / 0,1 mM dtpa y sometidos a RP-HPLC con detección UV-Vis a 280 y 360 nm.

En segundo lugar, se compararon rendimientos de nitración en liposomas conteniendo fosfolípidos con ácidos grasos saturados e insaturados (ej. DLPC y EYPC), habiéndose observado nitración significativa en ambos tipos de liposomas (Figura 7.6).

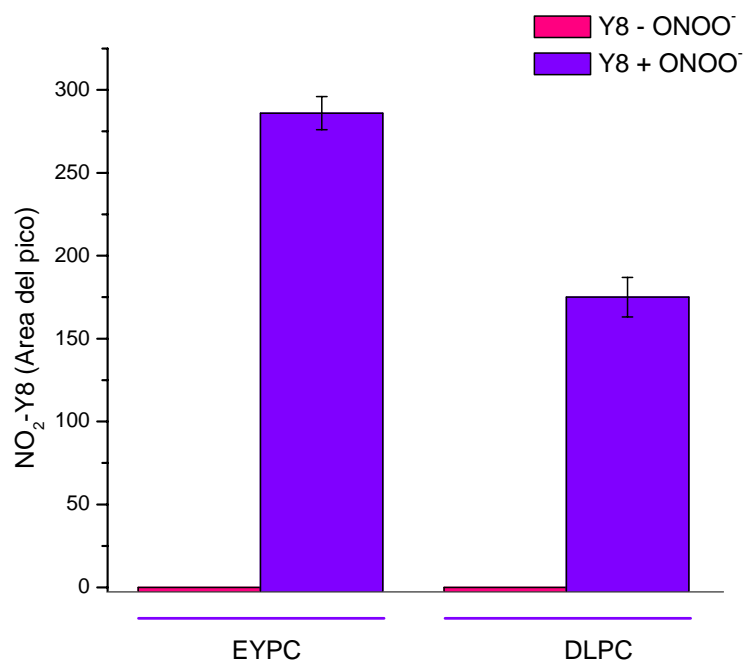


Figura 7.6 Comparación de los rendimientos de nitración en EYPC y DLPC. Liposomas de DLPC y EYPC (30 mM) con Y8 pre-incorporado (0.3 mM) fueron tratados con peroxinitrito (0.5 mM) en KPi (100 mM) pH 7,4 / 0,1 mM dtpa. Los productos Y8 y NO₂-Y8 fueron separados por RP-HPLC midiendo la absorbancia a 280 y 360 nm.

En tercer lugar, se realizaron experimentos con liposomas de DLPC y EYPC en condiciones de baja tensión de oxígeno con el objetivo de determinar si los procesos de lipoperoxidación se asocian a la nitración de tirosina, tal cual lo observado para el BTBE en el Objetivo Específico #2. Estos resultados preliminares muestran un rendimiento de nitración levemente inferior cuando los liposomas son burbujeados con Argón, lo cual estaría de acuerdo con los datos obtenidos en el Objetivo Específico # 2

(Figura 7.7) e implicarían la participación de los radicales lipídicos formados durante la lipoperoxidación en las reacciones de nitración en el interior de la bicapa.

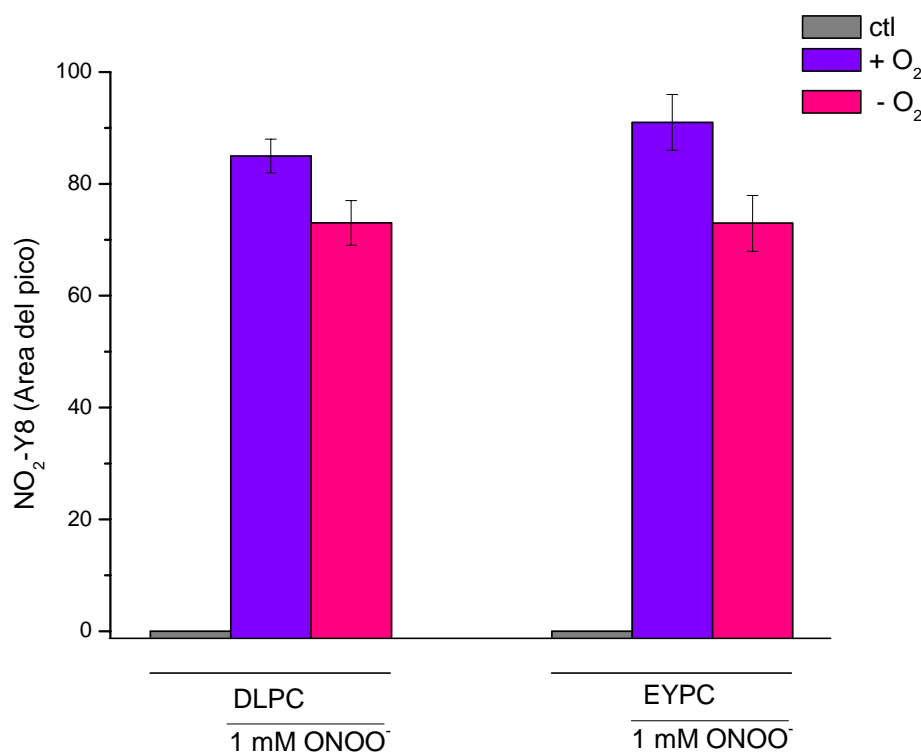


Figura 7.7 Efecto de oxígeno en la nitración de Y8. Liposomas de DLPC y EYPC (30 mM) con Y8 pre-incorporado (0.3 mM) fueron expuestos a peroxinitrito (1 mM) en presencia o a bajas tensiones de oxígeno (burbujeados durante 30 minutos con argón). Las muestras fueron analizadas por RP-HPLC con detección UV-Vis a 280 y 360 nm.

Es importante resaltar que no se detectó la formación de dímeros de tirosina en ninguna de las condiciones testeadas, lo que está en línea con un reporte previo (191), y es consistente con la baja probabilidad de colisión de dos radicales tirosilo dentro de la membrana, debido a su bajo coeficiente de difusión estimado ($D < 1 \mu\text{m s}^{-1}$; (254)).

7.4 Discusión

Globalmente, los resultados demostraron nuestra capacidad para sintetizar péptidos con residuos de tirosina ubicados a distintas alturas y purificarlos con altos rendimientos, además de incorporarlos en forma eficiente a sistemas modelo de membranas, para estudiar el proceso de nitración de tirosinas en compartimentos hidrofóbicos. En este Objetivo Específico, pudimos detectar la formación del derivado nitrado del péptido tratado con peroxinitrito ($\text{NO}_2\text{-Y8}$) con rendimientos significativos (0,4 % respecto al peroxinitrito adicionado), y que no pudo detectarse, como era esperado, la formación de productos de dimerización, y de acuerdo con trabajos anteriores (191). Además, la presencia de nitro-tirosina en forma significativa en liposomas insaturados de EYPC y el efecto inhibitorio de la disminución de la tensión de oxígeno, están en absoluta concordancia con lo observado en el Objetivo Específico #2 acerca de la conexión entre los procesos de lipoperoxidación y nitración de tirosinas en entornos hidrofóbicos, la cual ocurre a través de la formación del radical tirosilo mediada por radicales peroxilo lipídicos; por lo tanto los resultados obtenidos en el Objetivo # 3 en péptidos conteniendo tirosina reproducen nuestros resultados con BTBE de los Objetivos #1 y #2 de esta tesis. De esta manera podemos concluir que dichos péptidos fueron sintetizados, purificados y validados para su uso como sondas hidrofóbicas en el estudio de mecanismos de nitración de tirosinas en membranas y que los estudios preliminares obtenidos recapitulan los experimentos realizados con el BTBE.

Si bien nuestros resultados son preliminares, en relación al rol de la lipoperoxidación en procesos de nitración de residuos de tirosina en péptidos, un trabajo previo realizado por Zhang y colaboradores, (191) mostró que la nitración de Y8 mediada por peroxinitrito-derivado de SIN-1, en liposomas con relaciones variables de PLPC/DLPC (0-100 %), disminuye a medida que el grado de insaturación de los liposomas aumenta, lo que a primera vista puede aparecer como discordante. Sin

embargo, un análisis detallado de los resultados y su confrontación contra datos generados por nosotros por simulaciones cinéticas, claramente muestran que el grado de inhibición experimental observado es significativamente menor al esperado teóricamente en una competencia simple donde los radicales derivados de peroxinitrito (es decir $\cdot\text{OH}$ y $\cdot\text{NO}_2$) reaccionarán contra el ácido graso ó la tirosina. Por ejemplo, en un valor de 40% de insaturación y considerando las constantes de reacción reportadas para la oxidación de tirosina y ácidos grasos por $\cdot\text{NO}_2$ y $\cdot\text{OH}$, se esperaría una inhibición $> 90\%$, mientras que solo se observa un 40 % de inhibición. Esta observación apoya la existencia de reacciones secundarias de radicales derivados de lípidos con la tirosina, lo que deberá ser confirmado con experimentos diseñados específicamente con peroxinitrito auténtico a tal fin.

Trabajos anteriores demostraron que el BTBE se incorpora eficientemente en membranas, distribuyéndose a lo largo de toda la bicapa, pero estando su mayor concentración en la zona del esqueleto de glicerol del fosfolípido con el grupo OH fenólico en la zona de la interfase con agua (192), lo cual le confiere a este grupo capacidad para disociarse al correspondiente fenolato ($pK_a \sim 10$). Sin embargo, cuando el residuo de tirosina se encuentra inmerso en la profundidad de la bicapa la capacidad de interacción con agua se pierde progresivamente lo que a su vez puede tener importante influencia en la química de nitración. En efecto, estudios preliminares de spin-labeling aportaron acerca de la ubicación precisa de las tirosinas en los péptidos Y4, Y8 e Y12 en la profundidad de la membrana (191). Estudios de dinámica molecular que estamos realizando en colaboración con el equipo del Dr. Darío Estrín (Facultad de Ciencias Exactas, Universidad de Buenos Aires) se han enfocado a caracterizar la relación entre la posición de los residuos de tirosina en los péptidos transmembrana dentro de la bicapa y su interacción con el agua circundante. Estos estudios muestran que las moléculas de agua se ubican interaccionando con las cabezas polares de los fosfolípidos en un número de ~ 50 moléculas de agua por cada molécula de fosfolípido, y que la cantidad de moléculas de agua en el interior de la

bicapa disminuye a medida que aumenta la profundidad, estando prácticamente excluída en el centro de la bicapa (~ 20-25 Å de la superficie) (Figura 7.8A).

Se realizaron análisis similares incorporando a la bicapa los péptidos Y4, Y8 e Y12, y se pudo determinar que, mientras el residuo Y4, a través de su grupo OH fenólico interacciona con moléculas de agua en la región de la interfase (similar a lo que ocurría con una parte mayoritaria del BTBE), los residuos Y8 (no se muestra) e Y12 están mayoritariamente exentos de agua, ubicados en la región interna de la bicapa (Figuras 7.8B y C y D).

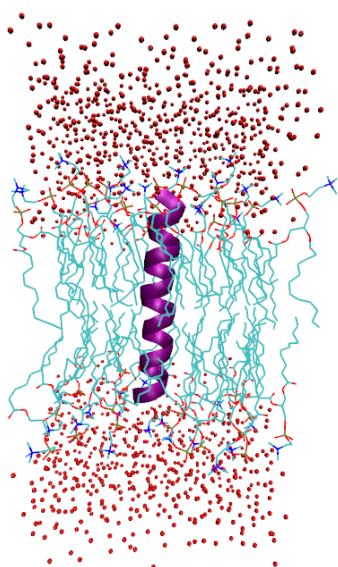


Figura 7.8A

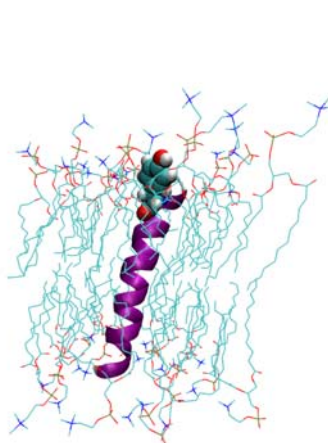


Figura 7.8B

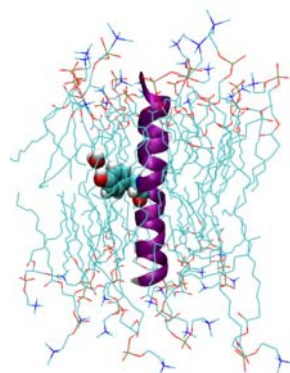


Figura 7.8C

Figura 7.8 Estudios de dinámica molecular de péptidos transmembrana y su interacción con moléculas de agua. (A) Distribución relativa de las moléculas de agua en el exterior, superficie e interior de una bicapa y su relación con una secuencia polipeptídica transmembrana. Ubicación relativa del residuo de tirosina en posición (B) 4 (Y4) y (C) 12 (Y12) de una secuencia polipeptídica transmembrana. Nótese que mientras Y4 aproxima el grupo OH fenólico a la interfase lípido/agua, el grupo -OH del péptido Y12 se encuentra en el centro de la bicapa, lo que impide su interacción con el agua. El péptido Y8 se encuentra en una situación intermedia entre Y4 e Y12.

Los datos de dinámica molecular indican que mientras que el péptido Y4 podría estar parcialmente disociado a nivel del grupo -OH (pKa ~ 10), dada su cercanía con

la interfase lípido / agua; en el caso de los péptidos Y8 e Y12, la ionización del grupo -OH es prácticamente inexistente debido a la ausencia de moléculas de agua en esa región de la membrana. Restan por estudiar los efectos de estos fenómenos sobre la reactividad de las tirosinas con los oxidantes, dado que, mientras la pérdida de la ionización disminuye la reactividad con $\cdot\text{NO}_2$ (porque este reacciona más rápidamente con la forma fenolato de la tirosina), por otro lado, la exclusión de agua, favorecería la reacción con los radicales peroxilo, entre otros varios aspectos a considerar.

La confirmación de estos resultados iniciales, abren la posibilidad de realizar en forma más exhaustiva, estudios similares a los realizados en los Objetivos Específicos #1 y #2, explorando asuntos como el rendimiento relativo de nitración de tirosina mediada por peroxinitrito en residuos ubicados a diferentes profundidades (ej. Y4, Y8, Y12), el rol del grado de insaturación lipídica, la relación espacial dentro de la membrana de los residuos peroxilo lipídicos y la tirosina, y los efectos moduladores en la nitración de cambios en la secuencia primaria del péptido (ej. incorporación de residuos de cisteína). También pretendemos realizar estudios de hidroxilación de tirosina en péptidos que contengan residuos a diferentes profundidades en la membrana de manera de ayudar a definir la ocurrencia de la homólisis del ONOOH y poder definir la relevancia de este proceso en la fase hidrofóbica respecto a lo que tiene lugar en la fase acuosa (207, 251).

En suma, si bien la síntesis de péptidos transmembrana conteniendo tirosinas es una tarea más compleja y costosa que la correspondiente a BTBE, la química de reacción con especies oxidantes y nitrantes seguramente reflejen mejor lo que puede ocurrir con proteínas de la membrana (187, 192) y deberán ser usadas más extensivamente en el futuro. Una limitante es que, a diferencia del BTBE, resulta poco probable que se incorporen en las membranas biológicas. Por lo tanto, los péptidos transmembrana aparecen como valiosas sondas complementarias al BTBE para el estudio de los mecanismos de nitración de tirosinas en membranas.

8. Conclusiones & Perspectivas

8.1 Conclusiones

Los resultados obtenidos durante el desarrollo de los Objetivos Específicos de esta tesis, nos han permitido llegar a una serie de conclusiones respecto a los mecanismos bioquímicos de la nitración de tirosinas en membranas y que podemos resumir de la siguiente manera:

- ✓ Tanto el BTBE con los péptidos transmembrana con residuos de tirosina en diferentes posiciones (Y4, Y8 e Y12), fueron exitosamente utilizados como sondas, para comprender los mecanismos de nitración y oxidación de tirosinas en membranas, a través de su incorporación a liposomas de PC.
- ✓ Los mecanismos de nitración por peroxinitrito en membranas dependen de procesos radicalares, que requieren la formación intermedia de radical tirosilo, tal y como ocurre en sistemas acuosos.
- ✓ La nitración de tirosinas en membranas es un proceso significativamente más favorecido que la dimerización debido, entre otros factores, a la difusión facilitada del $\cdot\text{NO}_2$ en la bicapa, y su mayor concentración respecto a la fase acuosa, en contraste con la baja difusión del radical tirosilo en la estructura organizada de la bicapa.
- ✓ La identificación del derivado hidroxilado de la tirosina (3-hidroxi-BTBE) es consistente con la homólisis del ácido peroxinitroso (ONOOH) en la superficie y/o dentro de la bicapa.
- ✓ Las reacciones de nitración en membranas son inhibidas por compuestos que atrapan peroxinitrito o sus radicales derivados, mientras que son estimuladas por centros metálicos de transición (ej. hemina) que catalizan reacciones de nitración dentro de la bicapa.

- ✓ A diferencia de lo que ocurre para tirosinas en fases acuosas, el CO_2 , inhibe la nitración y dimerización del BTBE, debido a la baja permeabilidad del radical carbonato hacia el interior de la membrana.

La figura 8.1 muestra la oxidación del BTBE en membranas mediada por peroxinitrito, y los productos resultantes, los cuales fueron caracterizados en el Objetivo Específico #1, así como sus rendimientos relativos, donde se destaca la formación de 3- NO_2 -BTBE como producto mayoritario en el interior de la membrana, así como la formación intermedia del radical fenoxilo derivado del BTBE.

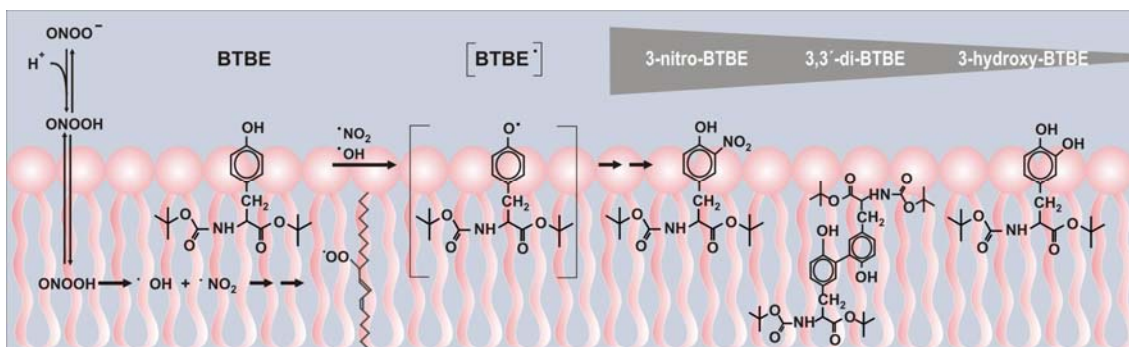


Figura 8.1 Productos de oxidación del BTBE por peroxinitrito y sus rendimientos relativos. Extraído de (193).

Respecto al Objetivo Específico #2 podemos destacar las siguientes conclusiones:

- ✓ La nitración de tirosinas en membranas es un proceso que se encuentra íntimamente relacionado con el proceso de lipoperoxidación.
- ✓ En efecto, una nueva reacción de oxidación de tirosina a radical tirosilo ha sido identificada en sistemas de membrana, la cual depende de la formación de radicales peroxilo de ácidos grasos insaturados.
- ✓ La constante de velocidad entre los radicales peroxilo, derivados de la lipoperoxidación y la tirosina fue determinada como $k = 4.800 \text{ M}^{-1}\text{s}^{-1}$, la cual es

suficiente para competir con las reacciones de propagación de la lipoperoxidación (Ver artículo Tyrosine vs Lipids).

- ✓ La identificación de esta reacción establece una **conexión** entre los procesos de lipoperoxidación y nitración/oxidación de tirosinas en sistemas biológicos.
- ✓ Dada su vinculación con la formación de radicales peroxilo lipídicos, los procesos de nitración de tirosina en membranas son estimulados en la presencia de oxígeno molecular e inhibidos por antioxidantes lipofílicos cortadores de cadenas tal como el α -tocoferol.

La figura 8.2 muestra la asociación existente entre las reacciones de nitración en membranas y la lipoperoxidación demostrada en el Objetivo Específico #2, así como la molécula responsable de llevar a cabo la reacción de conexión, el radical peroxilo, capaz de oxidar a la tirosina para rendir radical tirosilo, especie intermedia en la formación de productos de nitración y dimerización.

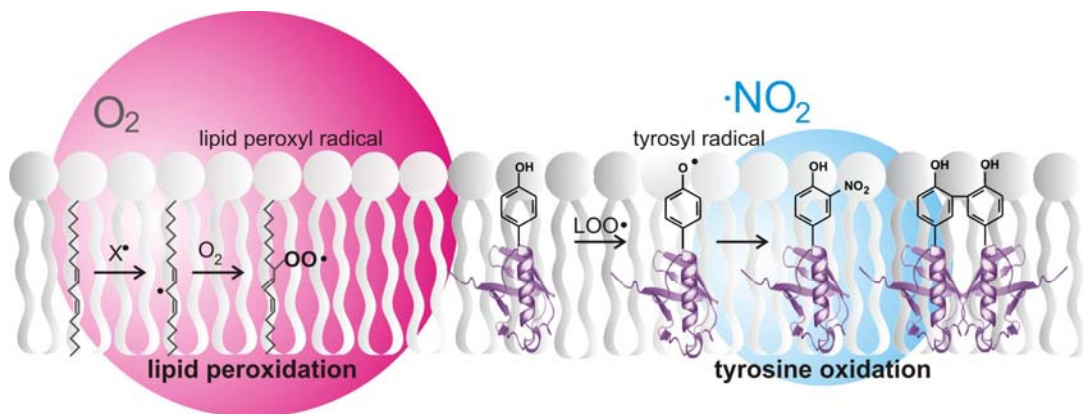


Figura 8.2 Asociación de los procesos de oxidación de tirosinas y lipoperoxidación en membranas. Extraído de (340).

- ✓ Podemos agregar que estudios realizados en células y en tejidos animales en condiciones de estrés oxidativo, apoyan el concepto de la nitración de tirosinas en membranas por procesos radicalares dependientes de la lipoperoxidación, así como la asociación espacial de ambos procesos determinada por análisis inmunohistoquímicos en dichos modelos

Respecto al Objetivo Específico #3 podemos realizar las siguientes consideraciones:

- ✓ Fuimos capaces de sintetizar, purificar y validar los péptidos transmembrana con los residuos de tirosina en distintas posiciones.
- ✓ El tratamiento de dichos péptidos con peroxinitrito permitió la detección del producto nitrado (NO₂-Y8) mientras que no se pudo detectar la formación de dímero de tirosina.
- ✓ Los rendimientos de nitración fueron significativos en liposomas con ácidos grasos saturados (DLPC) e insaturados (EYPC), siendo mayores en estos últimos, sugiriendo que la lipoperoxidación, al igual que lo ocurre con el BTBE, está alimentando el proceso de nitración.
- ✓ Los experimentos preliminares realizados a bajas tensiones de oxígeno muestran que los rendimientos de nitración son menores que cuando nos encontramos frente a tensiones de oxígeno normales, lo cual apoya la participación de la lipoperoxidación en la nitración de los residuos de tirosina de los péptidos.
- ✓ Finalmente podemos concluir que el trabajo presentado en esta tesis, ha permitido el uso y validación de sondas hidrofóbicas de tirosina, aportando información mecanística fundamental para la comprensión de los procesos de nitración y oxidación de tirosinas presentes en biocompartimentos hidrofóbicos, lo cual es de relevancia para comprender los procesos de oxidación y nitración de tirosinas en lipoproteínas y membranas biológicas.

8.2 Perspectivas

Los estudios realizados durante el transcurso de esta tesis serán profundizados abarcando otros aspectos relacionados con lo estudiado hasta el momento, y que pueden resumirse de la siguiente manera:

- ✓ Análisis con otros agentes oxidantes y nitrantes en liposomas con BTBE preincorporado (Ej. MPO/H₂O₂/NO₂⁻), y péptidos transmembrana.
- ✓ Profundización en los estudios preliminares realizados con péptidos, acerca de la relación entre la lipoperoxidación y la nitración de tirosina, en liposomas con diferentes grados de insaturación y péptidos transmembrana con tirosinas ubicadas a diferentes profundidades de la membrana.
- ✓ Estudiar la modulación de la nitración de tirosina de péptidos transmembrana conteniendo residuos de cisteína; rol de la transferencia electrónica intramolecular en los rendimientos de nitración.
- ✓ Evaluación del posible efecto modulador del daño nitro-oxidativo en sistemas celulares de análogos hidrofóbicos de tirosina que se concentran en distintos compartimientos celulares (Ej. mito-BTBE).
- ✓ Estudio de las bases mecánicas de los efectos citoprotectores de péptidos conteniendo tirosinas que penetran a células.
- ✓ Establecimiento de la relación fenomenológica y mecánica entre los procesos de lipoperoxidación y nitración proteica en modelos animales de enfermedad.

9. Referencias

1. Ignarro, L. J. (1990) Biosynthesis and metabolism of endothelium-derived nitric oxide, *Annu Rev Pharmacol Toxicol* 30, 535-560.
2. Moncada, S., and Higgs, E. A. (2006) Nitric oxide and the vascular endothelium, *Handb Exp Pharmacol*, 213-254.
3. Radi, R. (2004) Nitric oxide, oxidants, and protein tyrosine nitration, *Proc Natl Acad Sci U S A* 101, 4003-4008.
4. Kanwar, J. R., Kanwar, R. K., Burrow, H., and Baratchi, S. (2009) Recent advances on the roles of NO in cancer and chronic inflammatory disorders, *Curr Med Chem* 16, 2373-2394.
5. Allen, C. L., and Bayraktutan, U. (2009) Oxidative stress and its role in the pathogenesis of ischaemic stroke, *Int J Stroke* 4, 461-470.
6. Bolanos, J. P., Moro, M. A., Lizasoain, I., and Almeida, A. (2009) Mitochondria and reactive oxygen and nitrogen species in neurological disorders and stroke: Therapeutic implications, *Adv Drug Deliv Rev* 61, 1299-1315.
7. Gkaliagkousi, E., Douma, S., Zamboulis, C., and Ferro, A. (2009) Nitric oxide dysfunction in vascular endothelium and platelets: role in essential hypertension, *J Hypertens* 27, 2310-2320.
8. Hollenberg, S. M., and Cinel, I. (2009) Bench-to-bedside review: nitric oxide in critical illness--update 2008, *Crit Care* 13, 218.
9. Leopold, J. A., and Loscalzo, J. (2009) Oxidative risk for atherothrombotic cardiovascular disease, *Free Radic Biol Med* 47, 1673-1706.
10. Perez-Matute, P., Zulet, M. A., and Martinez, J. A. (2009) Reactive species and diabetes: counteracting oxidative stress to improve health, *Curr Opin Pharmacol* 9, 771-779.
11. Sokolovsky, M., Riordan, J. F., and Vallee, B. L. (1966) Tetranitromethane. A reagent for the nitration of tyrosyl residues in proteins, *Biochemistry* 5, 3582-3589.
12. Beckman, J. S., Beckman, T. W., Chen, J., Marshall, P. A., and Freeman, B. A. (1990) Apparent hydroxyl radical production by peroxynitrite: implications for endothelial injury from nitric oxide and superoxide, *Proc Natl Acad Sci U S A* 87, 1620-1624.
13. Ischiropoulos, H., Zhu, L., and Beckman, J. S. (1992) Peroxynitrite formation from macrophage-derived nitric oxide, *Arch Biochem Biophys* 298, 446-451.
14. Koppenol, W. H., Moreno, J. J., Pryor, W. A., Ischiropoulos, H., and Beckman, J. S. (1992) Peroxynitrite, a cloaked oxidant formed by nitric oxide and superoxide, *Chem Res Toxicol* 5, 834-842.
15. Radi, R., Beckman, J. S., Bush, K. M., and Freeman, B. A. (1991) Peroxynitrite oxidation of sulfhydryls. The cytotoxic potential of superoxide and nitric oxide, *J Biol Chem* 266, 4244-4250.
16. Radi, R., Beckman, J. S., Bush, K. M., and Freeman, B. A. (1991) Peroxynitrite-induced membrane lipid peroxidation: the cytotoxic potential of superoxide and nitric oxide, *Arch Biochem Biophys* 288, 481-487.
17. Ohshima, H., Friesen, M., Brouet, I., and Bartsch, H. (1990) Nitrotyrosine as a new marker for endogenous nitrosation and nitration of proteins, *Food Chem Toxicol* 28, 647-652.
18. Ohshima, H., Brouet, I., Friesen, M., and Bartsch, H. (1991) Nitrotyrosine as a new marker for endogenous nitrosation and nitration, *IARC Sci Publ*, 443-448.
19. Beckman, J. S., Ye, Y. Z., Anderson, P. G., Chen, J., Accavitti, M. A., Tarpey, M. M., and White, C. R. (1994) Extensive nitration of protein tyrosines in human atherosclerosis detected by immunohistochemistry, *Biol Chem Hoppe Seyler* 375, 81-88.
20. Ischiropoulos, H. (2003) Biological Selectivity and Functional Aspects of Protein Tyrosine Nitration, *Biochem. Biophys. Res. Commun.* 305, 776-783.
21. Peluffo, G., and Radi, R. (2007) Biochemistry of protein tyrosine nitration in cardiovascular pathology, *Cardiovasc Res* 75, 291-302.

22. Szabo, C., Ischiropoulos, H., and Radi, R. (2007) Peroxynitrite: biochemistry, pathophysiology and development of therapeutics, *Nat Rev Drug Discov* 6, 662-680.
23. Turko, I. V., Li, L., Aulak, K. S., Stuehr, D. J., Chang, J. Y., and Murad, F. (2003) Protein tyrosine nitration in the mitochondria from diabetic mouse heart. Implications to dysfunctional mitochondria in diabetes, *J Biol Chem* 278, 33972-33977.
24. MacMillan-Crow, L. A. C., J.P.; Kerby, J.D.; Beckman, J. S.; Thompson, J.A. (1996) Nitration and inactivation of manganese superoxide dismutase in chronic rejection of human renal allografts., *Proc Natl Acad Sci U S A* 93, 11853-11858.
25. Brito, C., Naviliat, M., Tiscornia, A. C., Vuillier, F., Gualco, G., Dighiero, G., Radi, R., and Cayota, A. M. (1999) Peroxynitrite inhibits T lymphocyte activation and proliferation by promoting impairment of tyrosine phosphorylation and peroxynitrite- driven apoptotic death, *J Immunol* 162, 3356-3366.
26. Souza, J. M., Daikhin, E., Yudkoff, M., Raman, C. S., and Ischiropoulos, H. (1999) Factors determining the selectivity of protein tyrosine nitration, *Arch Biochem Biophys* 371, 169-178.
27. Zheng, L., Settle, M., Brubaker, G., Schmitt, D., Hazen, S. L., Smith, J. D., and Kinter, M. (2005) Localization of nitration and chlorination sites on apolipoprotein A-I catalyzed by myeloperoxidase in human atheroma and associated oxidative impairment in ABCA1-dependent cholesterol efflux from macrophages, *J Biol Chem* 280, 38-47.
28. Hazen, S. L., and Heinecke, J. W. (1997) 3-Chlorotyrosine, a specific marker of myeloperoxidase-catalyzed oxidation, is markedly elevated in low density lipoprotein isolated from human atherosclerotic intima, *J Clin Invest* 99, 2075-2081.
29. Whiteman, M., and Spencer, J. P. (2008) Loss of 3-chlorotyrosine by inflammatory oxidants: implications for the use of 3-chlorotyrosine as a biomarker in vivo, *Biochem Biophys Res Commun* 371, 50-53.
30. Senthilmohan, R., and Kettle, A. J. (2006) Bromination and chlorination reactions of myeloperoxidase at physiological concentrations of bromide and chloride, *Arch Biochem Biophys* 445, 235-244.
31. Linares, E., Giorgio, S., Mortara, R. A., Santos, C. X., Yamada, A. T., and Augusto, O. (2001) Role of peroxynitrite in macrophage microbicidal mechanisms in vivo revealed by protein nitration and hydroxylation, *Free Radic Biol Med* 30, 1234-1242.
32. Santos, C. X., Bonini, M. G., and Augusto, O. (2000) Role of the carbonate radical anion in tyrosine nitration and hydroxylation by peroxynitrite, *Arch Biochem Biophys* 377, 146-152.
33. Souza, J. M., Peluffo, G., and Radi, R. (2008) Protein tyrosine nitration-functional alteration or just a biomarker?, *Free Radic Biol Med* 45, 357-366.
34. Turko, I. V., and Murad, F. (2002) Protein nitration in cardiovascular diseases, *Pharmacol Rev* 54, 619-634.
35. Isobe, C., Abe, T., and Terayama, Y. (2009) Remarkable increase in 3-nitrotyrosine in the cerebrospinal fluid in patients with lacunar stroke, *Brain Res* 1305, 132-136.
36. Liu, B., Tewari, A. K., Zhang, L., Green-Church, K. B., Zweier, J. L., Chen, Y. R., and He, G. (2009) Proteomic analysis of protein tyrosine nitration after ischemia reperfusion injury: mitochondria as the major target, *Biochim Biophys Acta* 1794, 476-485.
37. Butterfield, D. A., Reed, T. T., Perluigi, M., De Marco, C., Coccia, R., Keller, J. N., Markesbery, W. R., and Sultana, R. (2007) Elevated levels of 3-nitrotyrosine in brain from subjects with amnesic mild cognitive impairment: implications for the role of nitration in the progression of Alzheimer's disease, *Brain Res* 1148, 243-248.

38. Ceriello, A. (2002) Nitrotyrosine: new findings as a marker of postprandial oxidative stress, *Int J Clin Pract Suppl*, 51-58.
39. Shishehbor, M. H., Aviles, R. J., Brennan, M. L., Fu, X., Goormastic, M., Pearce, G. L., Gokce, N., Keaney, J. F., Jr., Penn, M. S., Sprecher, D. L., Vita, J. A., and Hazen, S. L. (2003) Association of nitrotyrosine levels with cardiovascular disease and modulation by statin therapy, *Jama* 289, 1675-1680.
40. Zhang, R., Brennan, M. L., Fu, X., Aviles, R. J., Pearce, G. L., Penn, M. S., Topol, E. J., Sprecher, D. L., and Hazen, S. L. (2001) Association between myeloperoxidase levels and risk of coronary artery disease, *Jama* 286, 2136-2142.
41. Pacher, P., Beckman, J. S., and Liaudet, L. (2007) Nitric oxide and peroxynitrite in health and disease, *Physiol Rev* 87, 315-424.
42. Lefer, D. J., and Granger, D. N. (2000) Oxidative stress and cardiac disease, *Am J Med* 109, 315-323.
43. Parastatidis, I., Thomson, L., Burke, A., Chernysh, I., Nagaswami, C., Visser, J., Stamer, S., Liebler, D. C., Koliakos, G., Heijnen, H. F., Fitzgerald, G. A., Weisel, J. W., and Ischiropoulos, H. (2008) Fibrinogen beta-chain tyrosine nitration is a prothrombotic risk factor, *J Biol Chem* 283, 33846-33853.
44. Rudnicka, A. R., Mt-Isa, S., and Meade, T. W. (2006) Associations of plasma fibrinogen and factor VII clotting activity with coronary heart disease and stroke: prospective cohort study from the screening phase of the Thrombosis Prevention Trial, *J Thromb Haemost* 4, 2405-2410.
45. Nowak, P., Kolodziejczyk, J., and Wachowicz, B. (2004) Peroxynitrite and fibrinolytic system: the effect of peroxynitrite on plasmin activity, *Mol Cell Biochem* 267, 141-146.
46. Shao, B., Tang, C., Heinecke, J. W., and Oram, J. F. (2010) Oxidation of apolipoprotein A-I by myeloperoxidase impairs the initial interactions with ABCA1 required for signaling and cholesterol export, *J Lipid Res*.
47. Hamilton, R. T., Asatryan, L., Nilsen, J. T., Isas, J. M., Gallaher, T. K., Sawamura, T., and Hsiai, T. K. (2008) LDL protein nitration: implication for LDL protein unfolding, *Arch Biochem Biophys* 479, 1-14.
48. Deeb, R. S., Cheung, C., Nuriel, T., Lamon, B. D., Upmacis, R. K., Gross, S. S., and Hajjar, D. P. (2010) Physical evidence for substrate binding in preventing cyclooxygenase inactivation under nitrative stress, *J Am Chem Soc* 132, 3914-3922.
49. He, C., Choi, H. C., and Xie, Z. (2010) Enhanced Tyrosine Nitration of Prostacyclin Synthase Is Associated with Increased Inflammation in Atherosclerotic Carotid Arteries from Type 2 Diabetic Patients, *Am J Pathol*.
50. Redondo-Horcajo, M., Romero, N., Martinez-Acedo, P., Martinez-Ruiz, A., Quijano, C., Lourenco, C. F., Movilla, N., Enriquez, J. A., Rodriguez-Pascual, F., Rial, E., Radi, R., Vazquez, J., and Lamas, S. (2010) Cyclosporine A-induced nitration of tyrosine 34 MnSOD in endothelial cells: role of mitochondrial superoxide, *Cardiovasc Res*.
51. Kanski, J., and Schoneich, C. (2005) Protein nitration in biological aging: proteomic and tandem mass spectrometric characterization of nitrated sites, *Methods Enzymol* 396, 160-171.
52. Cardoso, M. H., Morganti, R. P., Lilla, S., Murad, F., De Nucci, G., Antunes, E., and Marcondes, S. (2010) The role of superoxide anion in the inhibitory effect of SIN-1 in thrombin-activated human platelet adhesion, *Eur J Pharmacol* 627, 229-234.
53. Xu, S., Ying, J., Jiang, B., Guo, W., Adachi, T., Sharov, V., Lazar, H., Menzoian, J., Knyushko, T. V., Bigelow, D. J., Schoneich, C., and Cohen, R. A. (2006) Detection of Sequence-Specific Tyrosine Nitration of Manganese SOD and SERCA in Cardiovascular Disease and Aging, *AJP-Heart* 290, 2220-2227.

54. Reynolds, M. R., Berry, R. W., and Binder, L. I. (2007) Nitration in neurodegeneration: deciphering the "Hows" "nYs", *Biochemistry* **46**, 7325-7336.
55. Cassina, P., Cassina, A., Pehar, M., Castellanos, R., Gandelman, M., de Leon, A., Robinson, K. M., Mason, R. P., Beckman, J. S., Barbeito, L., and Radi, R. (2008) Mitochondrial dysfunction in SOD1G93A-bearing astrocytes promotes motor neuron degeneration: prevention by mitochondrial-targeted antioxidants, *J Neurosci* **28**, 4115-4122.
56. Giasson, B. I., Ischiropoulos, H., Lee, V. M., and Trojanowski, J. Q. (2002) The relationship between oxidative/nitrative stress and pathological inclusions in Alzheimer's and Parkinson's diseases, *Free Radic Biol Med* **32**, 1264-1275.
57. Good, P. F., Hsu, A., Werner, P., Perl, D. P., and Olanow, C. W. (1998) Protein nitration in Parkinson's disease, *J Neuropathol Exp Neurol* **57**, 338-342.
58. Martinez, A., Portero-Otin, M., Pamplona, R., and Ferrer, I. (2009) Protein Targets of Oxidative Damage in Human Neurodegenerative Diseases with Abnormal Protein Aggregates, *Brain Pathol.*
59. Reynolds, M. R., Berry, R. W., and Binder, L. I. (2005) Site-specific nitration differentially influences tau assembly in vitro, *Biochemistry* **44**, 13997-14009.
60. Reynolds, M. R., Berry, R. W., and Binder, L. I. (2005) Site-specific nitration and oxidative dityrosine bridging of the tau protein by peroxynitrite: implications for Alzheimer's disease, *Biochemistry* **44**, 1690-1700.
61. Reynolds, M. R., Lukas, T. J., Berry, R. W., and Binder, L. I. (2006) Peroxynitrite-mediated tau modifications stabilize preformed filaments and destabilize microtubules through distinct mechanisms, *Biochemistry* **45**, 4314-4326.
62. Danielson, S. R., Held, J. M., Schilling, B., Oo, M., Gibson, B. W., and Andersen, J. K. (2009) Preferentially increased nitration of alpha-synuclein at tyrosine-39 in a cellular oxidative model of Parkinson's disease, *Anal Chem* **81**, 7823-7828.
63. Larsen, T. R., Soderling, A. S., Caidahl, K., Roepstorff, P., and Gramsbergen, J. B. (2008) Nitration of soluble proteins in organotypic culture models of Parkinson's disease, *Neurochem Int* **52**, 487-494.
64. Reyes, J. F., Reynolds, M. R., Horowitz, P. M., Fu, Y., Guillozet-Bongaarts, A. L., Berry, R., and Binder, L. I. (2008) A possible link between astrocyte activation and tau nitration in Alzheimer's disease, *Neurobiol Dis* **31**, 198-208.
65. MacMillan-Crow, L. A., Crow, J. P., Kerby, J. D., Beckman, J. S., and Thompson, J. A. (1996) Nitration and inactivation of manganese superoxide dismutase in chronic rejection of human renal allografts, *Proc Natl Acad Sci U S A* **93**, 11853-11858.
66. Quijano, C., Hernandez-Saavedra, D., Castro, L., McCord, J. M., Freeman, B. A., and Radi, R. (2001) Reaction of peroxynitrite with Mn-superoxide dismutase. Role of the metal center in decomposition kinetics and nitration, *J Biol Chem* **276**, 11631-11638.
67. Beckman, J. S., Ischiropoulos, H., Zhu, L., van der Woerd, M., Smith, C., Chen, J., Harrison, J., Martin, J. C., and Tsai, M. (1992) Kinetics of superoxide dismutase- and iron-catalyzed nitration of phenolics by peroxynitrite, *Arch Biochem Biophys* **298**, 438-445.
68. Quijano, C., Romero, N., and Radi, R. (2005) Tyrosine nitration by superoxide and nitric oxide fluxes in biological systems: modeling the impact of superoxide dismutase and nitric oxide diffusion, *Free Radic Biol Med* **39**, 728-741.
69. Quint, P., Reutzler, R., Mikulski, R., McKenna, R., and Silverman, D. N. (2006) Crystal structure of nitrated human manganese superoxide dismutase: mechanism of inactivation, *Free Radic Biol Med* **40**, 453-458.
70. Yamakura, F., Taka, H., Fujimura, T., and Murayama, K. (1998) Inactivation of Human Manganese-superoxide Dismutase by Peroxynitrite is caused by

- Exclusive Nitration of Tyrosine 34 to 3-Nitrotyrosine, *J Biol Chem* 273, 14085-14089.
71. Aslan, M., Ryan, T. M., Townes, T. M., Coward, L., Kirk, M. C., Barnes, S., Alexander, C. B., Rosenfeld, S. S., and Freeman, B. A. (2003) Nitric oxide-dependent generation of reactive species in sickle cell disease. Actin tyrosine induces defective cytoskeletal polymerization, *J Biol Chem* 278, 4194-4204.
 72. Zou, M., Martin, C., and Ullrich, V. (1997) Tyrosine nitration as a mechanism of selective inactivation of prostacyclin synthase by peroxynitrite, *Biol Chem* 378, 707-713.
 73. Ischiropoulos, H., and Beckman, J. S. (2003) Oxidative stress and nitration in neurodegeneration: cause, effect, or association?, *J Clin Invest* 111, 163-169.
 74. Schildknecht, S., Heinz, K., Daiber, A., Hamacher, J., Kavakli, C., Ullrich, V., and Bachschmid, M. (2006) Autocatalytic tyrosine nitration of prostaglandin endoperoxide synthase-2 in LPS-stimulated RAW 264.7 macrophages, *Biochem Biophys Res Commun* 340, 318-325.
 75. Batthyany, C., Souza, J. M., Duran, R., Cassina, A., Cervenansky, C., and Radi, R. (2005) Time course and site(s) of cytochrome c tyrosine nitration by peroxynitrite, *Biochemistry* 44, 8038-8046.
 76. Cassina, A. M., Hodara, R., Souza, J. M., Thomson, L., Castro, L., Ischiropoulos, H., Freeman, B. A., and Radi, R. (2000) Cytochrome c nitration by peroxynitrite, *J Biol Chem* 275, 21409-21415.
 77. Abriata, L. A., Cassina, A., Tortora, V., Marin, M., Souza, J. M., Castro, L., Vila, A. J., and Radi, R. (2009) Nitration of solvent-exposed tyrosine 74 on cytochrome c triggers heme iron-methionine 80 bond disruption. Nuclear magnetic resonance and optical spectroscopy studies, *J Biol Chem* 284, 17-26.
 78. Balafanova, Z., Bolli, R., Zhang, J., Zheng, Y., Pass, J. M., Bhatnagar, A., Tang, X. L., Wang, O., Cardwell, E., and Ping, P. (2002) Nitric oxide (NO) induces nitration of protein kinase Cepsilon (PKCepsilon), facilitating PKCepsilon translocation via enhanced PKCepsilon-RACK2 interactions: a novel mechanism of no-triggered activation of PKCepsilon, *J Biol Chem* 277, 15021-15027.
 79. Ji, Y., Neverova, I., Van Eyk, J. E., and Bennet, B. M. (2006) Nitration of tyrosine 92 mediates the activation of rat microsomal glutathione-S-transferase by peroxynitrite, *J Biol Chem* 281, 1986-1991.
 80. Vadseth, C., Souza, J. M., Thomson, L., Seagraves, A., Nagaswami, C., Scheiner, T., Torbet, J., Vilaire, G., Bennett, J. S., Murciano, J. C., Muzykantov, V., Penn, M. S., Hazen, S. L., Weisel, J. W., and Ischiropoulos, H. (2004) Prothrombotic state induced by post-translational modification of fibrinogen by reactive nitrogen species, *J Biol Chem* 279, 8820-8826.
 81. Giasson, B. I., Duda, J. E., Murray, I. V., Chen, Q., Souza, J. M., Hurtig, H. I., Ischiropoulos, H., Trojanowski, J. Q., and Lee, V. M. (2000) Oxidative damage linked to neurodegeneration by selective alpha-synuclein nitration in synucleinopathy lesions, *Science* 290, 985-989.
 82. Hodara, R., Norris, E. H., Giasson, B. I., Mishizen-Eberz, A. J., Lynch, D. R., Lee, V. M., and Ischiropoulos, H. (2004) Functional consequences of alpha-synuclein tyrosine nitration: diminished binding to lipid vesicles and increased fibril formation, *J Biol Chem* 279, 47746-47753.
 83. Ye, Y., Quijano, C., Robinson, K. M., Ricart, K. C., Strayer, A. L., Sahawneh, M. A., Shacka, J. J., Kirk, M., Barnes, S., Accavitti-Loper, M. A., Radi, R., Beckman, J. S., and Estevez, A. G. (2007) Prevention of peroxynitrite-induced apoptosis of motor neurons and PC12 cells by tyrosine-containing peptides, *J Biol Chem* 282, 6324-6337.
 84. Seet, R. C., Lee, C. Y., Lim, E. C., Tan, J. J., Quek, A. M., Chong, W. L., Looi, W. F., Huang, S. H., Wang, H., Chan, Y. H., and Halliwell, B. (2010) Oxidative

- damage in Parkinson disease: Measurement using accurate biomarkers, *Free Radic Biol Med* 48, 560-566.
85. Souza, J. M., Castro, L., Cassina, A. M., Batthyany, C., and Radi, R. (2008) Nitrocytochrome c: synthesis, purification, and functional studies, *Methods Enzymol* 441, 197-215.
 86. Godoy, L. C., Munoz-Pinedo, C., Castro, L., Cardaci, S., Schonhoff, C. M., King, M., Tortora, V., Marin, M., Miao, Q., Jiang, J. F., Kapralov, A., Jemmerson, R., Silkstone, G. G., Patel, J. N., Evans, J. E., Wilson, M. T., Green, D. R., Kagan, V. E., Radi, R., and Mannick, J. B. (2009) Disruption of the M80-Fe ligation stimulates the translocation of cytochrome c to the cytoplasm and nucleus in nonapoptotic cells, *Proc Natl Acad Sci U S A* 106, 2653-2658.
 87. Crow, J. P., Ye, Y. Z., Strong, M., Kirk, M., Barnes, S., and Beckman, J. S. (1997) Superoxide dismutase catalyzes nitration of tyrosines by peroxynitrite in the rod and head domains of neurofilament-L, *J Neurochem* 69, 1945-1953.
 88. Pehar, M., Vargas, M. R., Robinson, K. M., Cassina, P., England, P., Beckman, J. S., Alzari, P. M., and Barbeito, L. (2006) Peroxynitrite transforms nerve growth factor into an apoptotic factor for motor neurons, *Free Radic Biol Med* 41, 1632-1644.
 89. Blanchard-Fillion, B., Souza, J. M., Friel, T., Jiang, G. C., Vrana, K., Sharov, V., Barron, L., Schoneich, C., Quijano, C., Alvarez, B., Radi, R., Przedborski, S., Fernando, G. S., Horwitz, J., and Ischiropoulos, H. (2001) Nitration and inactivation of tyrosine hydroxylase by peroxynitrite, *J Biol Chem* 276, 46017-46023.
 90. Goodwin, D. C., Gunther, M. R., Hsi, L. C., Crews, B. C., Eling, T. E., Mason, R. P., and Marnett, L. J. (1998) Nitric oxide trapping of tyrosyl radicals generated during prostaglandin endoperoxide synthase turnover. Detection of the radical derivative of tyrosine 385, *J Biol Chem* 273, 8903-8909.
 91. Trostchansky, A., O'Donnell, V. B., Goodwin, D. C., Landino, L. M., Marnett, L. J., Radi, R., and Rubbo, H. (2007) Interactions between nitric oxide and peroxynitrite during prostaglandin endoperoxide H synthase-1 catalysis: a free radical mechanism of inactivation, *Free Radic Biol Med* 42, 1029-1038.
 92. Berlett, B. S., Friguet, B., Yim, M. B., Chock, P. B., and Stadtman, E. R. (1996) Peroxynitrite-mediated nitration of tyrosine residues in Escherichia coli glutamine synthetase mimics adenylation: relevance to signal transduction, *Proc Natl Acad Sci U S A* 93, 1776-1780.
 93. Guittet, O., Ducastel, B., Salem, J. S., Henry, Y., Rubin, H., Lemaire, G., and Lepoivre, M. (1998) Differential sensitivity of the tyrosyl radical of mouse ribonucleotide reductase to nitric oxide and peroxynitrite, *J Biol Chem* 273, 22136-22144.
 94. Savvides, S. N., Scheiwein, M., Bohme, C. C., Arteel, G. E., Karplus, P. A., Becker, K., and Schirmer, R. H. (2002) Crystal structure of the antioxidant enzyme glutathione reductase inactivated by peroxynitrite, *J Biol Chem* 277, 2779-2784.
 95. Roberts, E. S., Lin, H., Crowley, J. R., Vuletich, J. L., Osawa, Y., and Hollenberg, P. F. (1998) Peroxynitrite-mediated nitration of tyrosine and inactivation of the catalytic activity of cytochrome P450 2B1, *Chem Res Toxicol* 11, 1067-1074.
 96. Seidel, E. R., Ragan, V., and Liu, L. (2001) Peroxynitrite inhibits the activity of ornithine decarboxylase, *Life Sci* 68, 1477-1483.
 97. Knapp, L. T., Kanterewicz, B. I., Hayes, E. L., and Klann, E. (2001) Peroxynitrite-induced tyrosine nitration and inhibition of protein kinase C, *Biochem Biophys Res Commun* 286, 764-770.

98. Zhang, L., Chen, C. L., Kang, P. T., Garg, V., Hu, K., Green-Church, K. B., and Chen, Y. R. (2010) Peroxynitrite-mediated oxidative modifications of complex II: relevance in myocardial infarction, *Biochemistry* 49, 2529-2539.
99. Bagnasco, P., MacMillan-Crow, L. A., Greendorfer, J. S., Young, C. J., Andrews, L., and Thompson, J. A. (2003) Peroxynitrite modulates acidic fibroblast growth factor (FGF-1) activity, *Arch Biochem Biophys* 419, 178-189.
100. Herzog, J., Maekawa, Y., Cirrito, T. P., Illian, B. S., and Unanue, E. R. (2005) Activated antigen-presenting cells select and present chemically modified peptides recognized by unique CD4 T cells, *Proc Natl Acad Sci U S A* 102, 7928-7933.
101. Whiteman, M., Spencer, J. P. E., Zhu, Y. Z., Armstrong, J. S., and Schantz, J. T. (2006) Peroxynitrite-modified collagen-II induces p38/Erk and NF-kB-dependent synthesis of prostaglandin E2 and nitric oxide in chondrogenically differentiated mesenchymal progenitor cells, *OsteoArthritis and Cartilage* 14, 460-470.
102. Ye, Y. Z., Strong, M., Huang, Z. Q., and Beckman, J. S. (1996) Antibodies that recognize nitrotyrosine, *Methods Enzymol* 269, 201-209.
103. Thomson, L., Christie, J., Vadseth, C., Lancken, P. N., Fu, X., Hazen, S. L., and Ischiropoulos, H. (2007) Identification of immunoglobulins that recognize 3-nitrotyrosine in patients with acute lung injury after major trauma, *Am J Respir Cell Mol Biol* 36, 152-157.
104. Kong, S. K., Yim, M. B., Stadtman, E. R., and Chock, P. B. (1996) Peroxynitrite disables the tyrosine phosphorylation regulatory mechanism: Lymphocyte-specific tyrosine kinase fails to phosphorylate nitrated cdc2(6-20)NH2 peptide, *Proc Natl Acad Sci U S A* 93, 3377-3382.
105. Tien, M., Berlett, B. S., Levine, R. L., Chock, P. B., and Stadtman, E. R. (1999) Peroxynitrite-mediated modification of proteins at physiological carbon dioxide concentration: pH dependence of carbonyl formation, tyrosine nitration, and methionine oxidation, *Proc Natl Acad Sci U S A* 96, 7809-7814.
106. Irie, Y., Saeki, M., Kamisaki, Y., Martin, E., and Murad, F. (2003) Histone H1.2 is a substrate for denitrase, an activity that reduces nitrotyrosine immunoreactivity in proteins, *Proc Natl Acad Sci U S A* 100, 5634-5639.
107. Kamisaki, Y., Wada, K., Bian, K., Balabanli, B., Davis, K., Martin, E., Behbod, F., Lee, Y. C., and Murad, F. (1998) An activity in rat tissues that modifies nitrotyrosine-containing proteins, *Proc Natl Acad Sci U S A* 95, 11584-11589.
108. Abello, N., Kerstjens, H. A., Postma, D. S., and Bischoff, R. (2009) Protein tyrosine nitration: selectivity, physicochemical and biological consequences, denitration, and proteomics methods for the identification of tyrosine-nitrated proteins, *J Proteome Res* 8, 3222-3238.
109. Souza, J. M., Bartesaghi, S., Peluffo, G., and Radi, R. (2010) Nitrotyrosine: Quantitative analysis, mapping in proteins and biological significance, in *Biomarkers for Antioxidant Defense and Oxidative Damage: Principles and Practical Applications*.
110. Viera, L., Ye, Y. Z., Estevez, A. G., and Beckman, J. S. (1999) Immunohistochemical methods to detect nitrotyrosine, *Methods Enzymol* 301, 373-381.
111. ter Steege, J. C., Koster-Kamphuis, L., van Straaten, E. A., Forget, P. P., and Buurman, W. A. (1998) Nitrotyrosine in plasma of celiac disease patients as detected by a new sandwich ELISA, *Free Radic Biol Med* 25, 953-963.
112. Khan, J., Brennand, D. M., Bradley, N., Gao, B., Bruckdorfer, R., and Jacobs, M. (1998) 3-Nitrotyrosine in the proteins of human plasma determined by an ELISA method, *Biochem J* 332 (Pt 3), 807-808.
113. Fountoulakis, M., and Lahm, H. W. (1998) Hydrolysis and amino acid composition of proteins, *J Chromatogr A* 826, 109-134.

114. Frost, M. T., Halliwell, B., and Moore, K. P. (2000) Analysis of free and protein-bound nitrotyrosine in human plasma by a gas chromatography/mass spectrometry method that avoids nitration artifacts, *Biochem J* 345 Pt 3, 453-458.
115. Hensley, K., Maidt, M. L., Yu, Z., Sang, H., Markesbery, W. R., and Floyd, R. A. (1998) Electrochemical analysis of protein nitrotyrosine and dityrosine in the Alzheimer brain indicates region-specific accumulation, *J Neurosci* 18, 8126-8132.
116. Shigenaga, M. K., Lee, H. H., Blount, B. C., Christen, S., Shigeno, E. T., Yip, H., and Ames, B. N. (1997) Inflammation and NO(X)-induced nitration: assay for 3-nitrotyrosine by HPLC with electrochemical detection, *Proc Natl Acad Sci U S A* 94, 3211-3216.
117. Aulak, K. S., Miyagi, M., Yan, L., West, K. A., Massillon, D., Crabb, J. W., and Stuehr, D. J. (2001) Proteomic method identifies proteins nitrated in vivo during inflammatory challenge, *Proc Natl Acad Sci U S A* 98, 12056-12061.
118. Sacksteder, C. A., Qian, W. J., Knyushko, T. V., Wang, H., Chin, M. H., Lacan, G., Melega, W. P., Camp, D. G., 2nd, Smith, R. D., Smith, D. J., Squier, T. C., and Bigelow, D. J. (2006) Endogenously nitrated proteins in mouse brain: links to neurodegenerative disease, *Biochemistry* 45, 8009-8022.
119. Zhang, Q., Qian, W. J., Knyushko, T. V., Clauss, T. R., Purvine, S. O., Moore, R. J., Sacksteder, C. A., Chin, M. H., Smith, D. J., Camp, D. G., 2nd, Bigelow, D. J., and Smith, R. D. (2007) A method for selective enrichment and analysis of nitrotyrosine-containing peptides in complex proteome samples, *J Proteome Res* 6, 2257-2268.
120. Abello, N., Barroso, B., Kerstjens, H. A., Postma, D. S., and Bischoff, R. (2010) Chemical labeling and enrichment of nitrotyrosine-containing peptides, *Talanta* 80, 1503-1512.
121. Chance, B., Sies, H., and Boveris, A. (1979) Hydroperoxide metabolism in mammalian organs, *Physiol Rev* 59, 527-605.
122. Radi, R. (1993) Biological antioxidant defenses, *Toxicol Ind Health* 9, 53-62.
123. Freeman, B. A., and Crapo, J. D. (1981) Hyperoxia increases oxygen radical production in rat lungs and lung mitochondria, *J Biol Chem* 256, 10986-10992.
124. Gutteridge, J. M., and Halliwell, B. (2000) Free radicals and antioxidants in the year 2000. A historical look to the future, *Ann N Y Acad Sci* 899, 136-147.
125. Liochev, S. I., and Fridovich, I. (2007) The effects of superoxide dismutase on H₂O₂ formation, *Free Radic Biol Med* 42, 1465-1469.
126. Goldstein, S., and Czapski, G. (1995) The reaction of NO. with O₂.- and HO₂.: a pulse radiolysis study, *Free Radic Biol Med* 19, 505-510.
127. Kissner, R., Nauser, T., Bugnon, P., Lye, P. G., and Koppenol, W. H. (1997) Formation and properties of peroxyxynitrite as studied by laser flash photolysis, high-pressure stopped-flow technique, and pulse radiolysis, *Chem Res Toxicol* 10, 1285-1292.
128. Padmaja, S., and Huie, R. E. (1993) The reaction of nitric oxide with organic peroxy radicals, *Biochem Biophys Res Commun* 195, 539-544.
129. Fridovich, I. (1997) Superoxide anion radical (O₂.-), superoxide dismutases, and related matters, *J Biol Chem* 272, 18515-18517.
130. Winterbourn, C. C., and Metodiewa, D. (1999) Reactivity of biologically important thiol compounds with superoxide and hydrogen peroxide, *Free Radic Biol Med* 27, 322-328.
131. Rhee, S. G. (2006) Cell signaling. H₂O₂, a necessary evil for cell signaling, *Science* 312, 1882-1883.
132. Buettner, G. R. (1993) The pecking order of free radicals and antioxidants: lipid peroxidation, alpha-tocopherol, and ascorbate, *Arch Biochem Biophys* 300, 535-543.

133. Koppenol, W. H. (1998) The basic chemistry of nitrogen monoxide and peroxyxynitrite, *Free Radic Biol Med* 25, 385-391.
134. Trostchansky, A., Moller, M., Bartesaghi, S., Botti, H., Denicola, A., Radi, R., and Rubbo, H. (2010) Nitric Oxide Redox Biochemistry in Lipid Environments, in *Nitric Oxide Biology and Pathobiology* (Ignarro, J. L., Ed.) Second ed., pp 27-60, Academic Press, San Diego.
135. Augusto, O., Bonini, M. G., Amanso, A. M., Linares, E., Santos, C. C., and De Menezes, S. L. (2002) Nitrogen dioxide and carbonate radical anion: two emerging radicals in biology, *Free Radic Biol Med* 32, 841-859.
136. Kirsch, M., Korth, H. G., Sustmann, R., and de Groot, H. (2002) The pathobiochemistry of nitrogen dioxide, *Biol Chem* 383, 389-399.
137. Jansson, E. A., Huang, L., Malkey, R., Govoni, M., Nihlen, C., Olsson, A., Stensdotter, M., Petersson, J., Holm, L., Weitzberg, E., and Lundberg, J. O. (2008) A mammalian functional nitrate reductase that regulates nitrite and nitric oxide homeostasis, *Nat Chem Biol* 4, 411-417.
138. Stanbury, D. M. (1989) Reduction potentials involving inorganic free radicals in aqueous solutions., *Advances in Inorganic Chemistry* 33, 69-138.
139. Radi, R., Denicola, A., Alvarez, B., Ferrer-Sueta, G., and Rubbo, H. (2000) The biological chemistry of peroxyxynitrite, in *Nitric Oxide Biology and Pathobiology* (Ignarro, J. L., Ed.) First ed., pp 57-82, Academic Press, San Diego.
140. Goldstein, S., and Czapski, G. (1995) Kinetics of nitric oxide autoxidation in aqueous solution in the absence and presence of various reductants. The nature of the oxidizing intermediates, *J Am Chem Soc* 117, 12078-12084.
141. Radi, R., Cosgrove, T. P., Beckman, J. S., and Freeman, B. A. (1993) Peroxyxynitrite-induced luminol chemiluminescence, *Biochem J* 290, 51-57.
142. Radi, R., Peluffo, G., Alvarez, M. N., Naviliat, M., and Cayota, A. (2001) Unraveling peroxyxynitrite formation in biological systems, *Free Radic Biol Med* 30, 463-488.
143. Trindade, D. F., Cerchiaro, G., and Augusto, O. (2006) A role for peroxyxymonocarbonate in the stimulation of biathiol peroxidation by the bicarbonate/carbon dioxide pair, *Chem Res Toxicol* 19, 1475-1482.
144. Medinas, D. B., Toledo, J. C., Jr., Cerchiaro, G., do-Amaral, A. T., de-Rezende, L., Malvezzi, A., and Augusto, O. (2009) Peroxyxymonocarbonate and carbonate radical displace the hydroxyl-like oxidant in the Sod1 peroxidase activity under physiological conditions, *Chem Res Toxicol* 22, 639-648.
145. Zhang, H., Joseph, J., Felix, C., and Kalyanaraman, B. (2000) Bicarbonate enhances the hydroxylation, nitration, and peroxidation reactions catalyzed by copper, zinc superoxide dismutase. Intermediacy of carbonate anion radical, *J Biol Chem* 275, 14038-14045.
146. Liochev, S. I., and Fridovich, I. (2002) Copper, zinc superoxide dismutase and H₂O₂. Effects of bicarbonate on inactivation and oxidations of NADPH and urate, and on consumption of H₂O₂, *J Biol Chem* 277, 34674-34678.
147. Bonini, M. G., Radi, R., Ferrer-Sueta, G., Ferreira, A. M., and Augusto, O. (1999) Direct EPR detection of the carbonate radical anion produced from peroxyxynitrite and carbon dioxide, *J Biol Chem* 274, 10802-10806.
148. Czapski, G. (1999) Acidity of the Carbonate Radical, *J Phys Chem A* 103, 3447-3450.
149. Folkes, L. K., Candeias, L. P., and Wardman, P. (1995) Kinetics and mechanisms of hypochlorous acid reactions, *Arch Biochem Biophys* 323, 120-126.
150. Prutz, W. A. (1996) Hypochlorous acid interactions with thiols, nucleotides, DNA, and other biological substrates, *Arch Biochem Biophys* 332, 110-120.
151. Winterbourn, C. C., Garcia, R. C., and Segal, A. W. (1985) Production of the superoxide adduct of myeloperoxidase (compound III) by stimulated human

- neutrophils and its reactivity with hydrogen peroxide and chloride, *Biochem J* 228, 583-592.
152. Peskin, A. V., and Winterbourn, C. C. (2003) Histamine chloramine reactivity with thiol compounds, ascorbate, and methionine and with intracellular glutathione, *Free Radic Biol Med* 35, 1252-1260.
 153. Eiserich, J. P., Cross, C. E., Jones, A. D., Halliwell, B., and van der Vliet, A. (1996) Formation of nitrating and chlorinating species by reaction of nitrite with hypochlorous acid. A novel mechanism for nitric oxide-mediated protein modification, *J Biol Chem* 271, 19199-19208.
 154. Whiteman, M., Spencer, J. P., Jenner, A., and Halliwell, B. (1999) Hypochlorous acid-induced DNA base modification: potentiation by nitrite: biomarkers of DNA damage by reactive oxygen species, *Biochem Biophys Res Commun* 257, 572-576.
 155. Fedorova, M., Kuleva, N., and Hoffmann, R. (2010) Identification of Cysteine, Methionine and Tryptophan Residues of Actin Oxidized In vivo during Oxidative Stress, *J Proteome Res*.
 156. Pryor, W. A., Jin, X., and Squadrito, G. L. (1994) One- and two-electron oxidations of methionine by peroxyxynitrite, *Proc Natl Acad Sci U S A* 91, 11173-11177.
 157. Allen, B. W., Stamler, J. S., and Piantadosi, C. A. (2009) Hemoglobin, nitric oxide and molecular mechanisms of hypoxic vasodilation, *Trends Mol Med* 15, 452-460.
 158. Lancaster, J. R., Jr. (2008) Protein cysteine thiol nitrosation: maker or marker of reactive nitrogen species-induced nonerythroid cellular signaling?, *Nitric Oxide* 19, 68-72.
 159. Landino, L. M. (2008) Protein thiol modification by peroxyxynitrite anion and nitric oxide donors, *Methods Enzymol* 440, 95-109.
 160. O'Donnell, V. B., Eiserich, J. P., Chumley, P. H., Jablonsky, M. J., Krishna, N. R., Kirk, M., Barnes, S., Darley-Usmar, V. M., and Freeman, B. A. (1999) Nitration of unsaturated fatty acids by nitric oxide-derived reactive nitrogen species peroxyxynitrite, nitrous acid, nitrogen dioxide, and nitronium ion, *Chem Res Toxicol* 12, 83-92.
 161. Rubbo, H., Radi, R., Trujillo, M., Telleri, R., Kalyanaraman, B., Barnes, S., Kirk, M., and Freeman, B. A. (1994) Nitric oxide regulation of superoxide and peroxyxynitrite-dependent lipid peroxidation. Formation of novel nitrogen-containing oxidized lipid derivatives, *J Biol Chem* 269, 26066-26075.
 162. Rubbo, H., and Radi, R. (2008) Protein and lipid nitration: role in redox signaling and injury, *Biochim Biophys Acta* 1780, 1318-1324.
 163. Akaike, T., Okamoto, S., Sawa, T., Yoshitake, J., Tamura, F., Ichimori, K., Miyazaki, K., Sasamoto, K., and Maeda, H. (2003) 8-nitroguanosine formation in viral pneumonia and its implication for pathogenesis, *Proc Natl Acad Sci U S A* 100, 685-690.
 164. Byun, J., Henderson, J. P., Mueller, D. M., and Heinecke, J. W. (1999) 8-Nitro-2'-deoxyguanosine, a specific marker of oxidation by reactive nitrogen species, is generated by the myeloperoxidase-hydrogen peroxide-nitrite system of activated human phagocytes, *Biochemistry* 38, 2590-2600.
 165. Caulfield, J. L., Wishnok, J. S., and Tannenbaum, S. R. (1998) Nitric oxide-induced deamination of cytosine and guanine in deoxynucleosides and oligonucleotides, *J Biol Chem* 273, 12689-12695.
 166. Chen, W., Jia, Z., Zhu, H., Zhou, K., Li, Y., and Misra, H. P. (2010) Ethyl pyruvate inhibits peroxyxynitrite-induced DNA damage and hydroxyl radical generation: implications for neuroprotection, *Neurochem Res* 35, 336-342.
 167. Kennedy, L. J., Moore, K., Jr., Caulfield, J. L., Tannenbaum, S. R., and Dedon, P. C. (1997) Quantitation of 8-oxoguanine and strand breaks produced by four oxidizing agents, *Chem Res Toxicol* 10, 386-392.

168. Suquet, C., Warren, J. J., Seth, N., and Hurst, J. K. (2010) Comparative study of HOCl-inflicted damage to bacterial DNA ex vivo and within cells, *Arch Biochem Biophys* 493, 135-142.
169. Bartesaghi, S., Ferrer-Sueta, G., Peluffo, G., Valez, V., Zhang, H., Kalyanaraman, B., and Radi, R. (2007) Protein tyrosine nitration in hydrophilic and hydrophobic environments, *Amino Acids* 32, 501-515.
170. Solar, S., Solar, W., and Getoff, N. (1984) Reactivity of OH with tyrosine in aqueous solution studied by pulse radiolysis, *J Phys Chem* 88, 2091-2095.
171. Prutz, W. A., Monig, H., Butler, J., and Land, E. J. (1985) Reactions of nitrogen dioxide in aqueous model systems: oxidation of tyrosine units in peptides and proteins, *Arch Biochem Biophys* 243, 125-134.
172. Denicola, A., Freeman, B. A., Trujillo, M., and Radi, R. (1996) Peroxynitrite reaction with carbon dioxide/bicarbonate: kinetics and influence on peroxynitrite-mediated oxidations, *Arch Biochem Biophys* 333, 49-58.
173. Tien, M. (1999) Myeloperoxidase-catalyzed oxidation of tyrosine, *Arch Biochem Biophys* 367, 61-66.
174. Marquez, L. A., and Dunford, H. B. (1995) Kinetics of oxidation of tyrosine and dityrosine by myeloperoxidase compounds I and II. Implications for lipoprotein peroxidation studies, *J Biol Chem* 270, 30434-30440.
175. Ferrer-Sueta, G., Vitturi, D., Batinic-Haberle, I., Fridovich, I., Goldstein, S., Czapski, G., and Radi, R. (2003) Reactions of manganese porphyrins with peroxynitrite and carbonate radical anion, *J Biol Chem* 278, 27432-27438.
176. van der Vliet, A., Eiserich, J. P., Halliwell, B., and Cross, C. E. (1997) Formation of reactive nitrogen species during peroxidase-catalyzed oxidation of nitrite. A potential additional mechanism of nitric oxide-dependent toxicity, *J Biol Chem* 272, 7617-7625.
177. Burner, U., Furtmuller, P. G., Kettle, A. J., Koppenol, W. H., and Obinger, C. (2000) Mechanism of reaction of myeloperoxidase with nitrite, *J Biol Chem* 275, 20597-20601.
178. Jacob, J. S., Cistola, D. P., Hsu, F. F., Muzaffar, S., Mueller, D. M., Hazen, S. L., and Heinecke, J. W. (1996) Human phagocytes employ the myeloperoxidase-hydrogen peroxide system to synthesize dityrosine, trityrosine, pulcherosine, and isodityrosine by a tyrosyl radical-dependent pathway, *J Biol Chem* 271, 19950-19956.
179. Gunther, M. R., Hsi, L. C., Curtis, J. F., Gierse, J. K., Marnett, L. J., Eling, T. E., and Mason, R. P. (1997) Nitric oxide trapping of the tyrosyl radical of prostaglandin H synthase-2 leads to tyrosine iminoxyl radical and nitrotyrosine formation, *J Biol Chem* 272, 17086-17090.
180. Sanakis, Y., Goussias, C., Mason, R. P., and Petrouleas, V. (1997) NO interacts with the tyrosine radical Y(D) of photosystem II to form an iminoxyl radical, *Biochemistry* 36, 1411-1417.
181. Whiteman, M., Siau, J. L., and Halliwell, B. (2003) Lack of tyrosine nitration by hypochlorous acid in the presence of physiological concentrations of nitrite. Implications for the role of nitryl chloride in tyrosine nitration in vivo, *J Biol Chem* 278, 8380-8384.
182. Daiber, A., Bachschmid, M., Beckman, J. S., Munzel, T., and Ullrich, V. (2004) The impact of metal catalysis on protein tyrosine nitration by peroxynitrite, *Biochem Biophys Res Commun* 317, 873-881.
183. Shao, B., Bergt, C., Fu, X., Green, P., Voss, J. C., Oda, M. N., Oram, J. F., and Heinecke, J. W. (2005) Tyrosine 192 in apolipoprotein A-I is the major site of nitration and chlorination by myeloperoxidase, but only chlorination markedly impairs ABCA1-dependent cholesterol transport, *J Biol Chem* 280, 5983-5993.
184. Schmidt, P., Youhnovski, N., Daiber, A., Balan, A., Arsic, M., Bachschmid, M., Przybylski, M., and Ullrich, V. (2003) Specific nitration at tyrosine 430 revealed

- by high resolution mass spectrometry as basis for redox regulation of bovine prostacyclin synthase, *J Biol Chem* 278, 12813-12819.
185. Elfering, S. L., Haynes, V. L., Traaseth, N. J., Ettl, A., and Giulivi, C. (2004) Aspects, mechanism, and biological relevance of mitochondrial protein nitration sustained by mitochondrial nitric oxide synthase, *Am J Physiol Heart Circ Physiol* 286, H22-29.
 186. Alvarez, B., and Radi, R. (2003) Peroxynitrite reactivity with amino acids and proteins, *Amino Acids* 25, 295-311.
 187. Zhang, H., Xu, Y., Joseph, J., and Kalyanaram, B. (2005) Intramolecular electron transfer between tyrosyl radical and cysteine residue inhibits tyrosine nitration and induces thiyl radical formation in model peptides with MPO, H₂O₂ and NO₂⁻: EPR spin trapping studies, *J Biol Chem* 280, 40684-40698.
 188. Zhang, H., Zielonka, J., Sikora, A., Joseph, J., Xu, Y., and Kalyanaram, B. (2009) The effect of neighboring methionine residue on tyrosine nitration and oxidation in peptides treated with MPO, H₂O₂, and NO₂⁽⁻⁾ or peroxynitrite and bicarbonate: role of intramolecular electron transfer mechanism?, *Arch Biochem Biophys* 484, 134-145.
 189. Moller, M., Botti, H., Batthyany, C., Rubbo, H., Radi, R., and Denicola, A. (2005) Direct measurement of nitric oxide and oxygen partitioning into liposomes and low density lipoprotein, *J Biol Chem* 280, 8850-8854.
 190. Moller, M. N., Li, Q., Vitturi, D. A., Robinson, J. M., Lancaster, J. R., Jr., and Denicola, A. (2007) Membrane "lens" effect: focusing the formation of reactive nitrogen oxides from the *NO/O₂ reaction, *Chem Res Toxicol* 20, 709-714.
 191. Zhang, H., Bhargava, K., Keszler, A., Feix, J., Hogg, N., Joseph, J., and Kalyanaram, B. (2003) Transmembrane nitration of hydrophobic tyrosyl peptides. Localization, characterization, mechanism of nitration, and biological implications, *J Biol Chem* 278, 8969-8978.
 192. Zhang, H., Joseph, J., Feix, J., Hogg, N., and Kalyanaram, B. (2001) Nitration and oxidation of a hydrophobic tyrosine probe by peroxynitrite in membranes: comparison with nitration and oxidation of tyrosine by peroxynitrite in aqueous solution, *Biochemistry* 40, 7675-7686.
 193. Bartesaghi, S., Peluffo, G., Zhang, H., Joseph, J., Kalyanaram, B., and Radi, R. (2008) Tyrosine nitration, dimerization, and hydroxylation by peroxynitrite in membranes as studied by the hydrophobic probe N-t-BOC-l-tyrosine tert-butyl ester, *Methods Enzymol* 441, 217-236.
 194. Velsor, L. W., Ballinger, C. A., Patel, J., and Postlethwait, E. M. (2003) Influence of epithelial lining fluid lipids on NO₂-induced membrane oxidation and nitration, *Free Radic Biol Med* 34, 720-733.
 195. Mallozzi, C., Di Stasi, A. M., and Minetti, M. (1997) Peroxynitrite modulates tyrosine-dependent signal transduction pathway of human erythrocyte band 3, *Faseb J* 11, 1281-1290.
 196. Viner, R. I., Ferrington, D. A., Williams, T. D., Bigelow, D. J., and Schoneich, C. (1999) Protein modification during biological aging: selective tyrosine nitration of the SERCA2a isoform of sarcoplasmic reticulum Ca²⁺-ATPase in skeletal muscle., *Biochem J* 340, 657-669.
 197. Hazen, S. L., Zhang, R., Shen, Z., Wu, W., Podrez, E. A., MacPherson, J. C., Schmitt, D., Mitra, S. N., Mukhopadhyay, C., Chen, Y. R., Cohen, P. A., Hoff, H. F., and Abu-Soud, H. M. (1999) Formation of Nitric Oxide-Derived Oxidants by Myeloperoxidase in Monocytes: Pathways for Monocyte-Mediated Protein Nitration and Lipid Peroxidation In Vivo, *Circ Res* 85, 950-958.
 198. Hsiai, T. K., Hwang, J., Barr, M. L., Correa, A., Hamilton, R., Alavi, M., Rouhanizadeh, M., Cadenas, E., and Hazen, S. L. (2007) Hemodynamics influences vascular peroxynitrite formation: Implication for low-density lipoprotein apo-B-100 nitration, *Free Radic Biol Med* 42, 519-529.

199. Zheng, L., Nukuna, B., Brennan, M. L., Sun, M., Goormastic, M., Settle, M., Schmitt, D., Fu, X., Thomson, L., Fox, P. L., Ischiropoulos, H., Smith, J. D., Kinter, M., and Hazen, S. L. (2004) Apolipoprotein A-I is a Selective Target for Myeloperoxidase-Catalyzed Oxidation and Functional Impairment in Subjects with Cardiovascular Disease., *J Clin Invest* 114, 529-541.
200. Murray, J., Taylor, S. W., Zhang, B., Ghosh, S. S., and Capaldi, R. A. (2003) Oxidative damage to mitochondrial complex I due to peroxynitrite: identification of reactive tyrosines by mass spectrometry, *J Biol Chem* 278, 37223-37230.
201. Zhou, W., Milder, J. B., and Freed, C. R. (2008) Transgenic mice overexpressing tyrosine-to-cysteine mutant human alpha-synuclein: a progressive neurodegenerative model of diffuse Lewy body disease, *J Biol Chem* 283, 9863-9870.
202. Robaszekiewicz, A., Bartosz, G., and Soszynski, M. (2008) N-chloroamino acids cause oxidative protein modifications in the erythrocyte membrane, *Mech Ageing Dev* 129, 572-579.
203. Kaplan, P., Tatarkova, Z., Racay, P., Lehotsky, J., Pavlikova, M., and Dobrota, D. (2007) Oxidative modifications of cardiac mitochondria and inhibition of cytochrome c oxidase activity by 4-hydroxynonenal, *Redox Rep* 12, 211-218.
204. Smith, D. P., Ciccotosto, G. D., Tew, D. J., Fodero-Tavoletti, M. T., Johanssen, T., Masters, C. L., Barnham, K. J., and Cappai, R. (2007) Concentration dependent Cu²⁺ induced aggregation and dityrosine formation of the Alzheimer's disease amyloid-beta peptide, *Biochemistry* 46, 2881-2891.
205. O'Connel, A. M., Gieseg, S. P., and Stanley, K. K. (1994) Hypochlorite oxidation causes cross-linking of LP (A), *Biochim Biophys Acta* 1225, 180-186.
206. Ziouzenkova, O., Asatryan, L., Akmal, M., Tetta, C., Wratten, M. L., Loseto-Wich, G., Jurgens, G., Heinecke, J., and Sevanian, A. (1999) Oxidative cross-linking of ApoB100 and hemoglobin results in low density lipoprotein modification in blood. Relevance to atherogenesis caused by hemodialysis, *J Biol Chem* 274, 18916-18924.
207. Ferrer-Sueta, G., and Radi, R. (2009) Chemical biology of peroxynitrite: kinetics, diffusion, and radicals, *ACS Chem Biol* 4, 161-177.
208. Manta, B., Hugo, M., Ortiz, C., Ferrer-Sueta, G., Trujillo, M., and Denicola, A. (2009) The peroxidase and peroxynitrite reductase activity of human erythrocyte peroxiredoxin 2, *Arch Biochem Biophys* 484, 146-154.
209. Briviba, K., Kissner, R., Koppenol, W. H., and Sies, H. (1998) Kinetic study of the reaction of glutathione peroxidase with peroxynitrite, *Chem Res Toxicol* 11, 1398-1401.
210. Romero, N., Radi, R., Linares, E., Augusto, O., Detweiler, C. D., Mason, R. P., and Denicola, A. (2003) Reaction of human hemoglobin with peroxynitrite. Isomerization to nitrate and secondary formation of protein radicals, *J Biol Chem* 278, 44049-44057.
211. Ford, E., Hughes, M. N., and Wardman, P. (2002) Kinetics of the reactions of nitrogen dioxide with glutathione, cysteine, and uric acid at physiological pH, *Free Radic Biol Med* 32, 1314-1323.
212. Santos, C. X., Anjos, E. I., and Augusto, O. (1999) Uric acid oxidation by peroxynitrite: multiple reactions, free radical formation, and amplification of lipid oxidation, *Arch Biochem Biophys* 372, 285-294.
213. Singh, U., and Jialal, I. (2008) Alpha-lipoic acid supplementation and diabetes, *Nutr Rev* 66, 646-657.
214. Maczurek, A., Hager, K., Kenklies, M., Sharman, M., Martins, R., Engel, J., Carlson, D. A., and Munch, G. (2008) Lipoic acid as an anti-inflammatory and neuroprotective treatment for Alzheimer's disease, *Adv Drug Deliv Rev* 60, 1463-1470.
215. Ghibu, S., Richard, C., Vergely, C., Zeller, M., Cottin, Y., and Rochette, L. (2009) Antioxidant properties of an endogenous thiol: Alpha-lipoic acid, useful in

- the prevention of cardiovascular diseases, *J Cardiovasc Pharmacol* 54, 391-398.
216. Packer, L., Witt, E. H., and Tritschler, H. J. (1995) alpha-Lipoic acid as a biological antioxidant, *Free Radic Biol Med* 19, 227-250.
 217. Trujillo, M., and Radi, R. (2002) Peroxynitrite reaction with the reduced and the oxidized forms of lipoic acid: new insights into the reaction of peroxynitrite with thiols, *Arch Biochem Biophys* 397, 91-98.
 218. Trujillo, M., Folkes, L., Bartesaghi, S., Kalyanaraman, B., Wardman, P., and Radi, R. (2005) Peroxynitrite-derived carbonate and nitrogen dioxide radicals readily react with lipoic and dihydrolipoic acid, *Free Radic Biol Med* 39, 279-288.
 219. Shay, K. P., Moreau, R. F., Smith, E. J., Smith, A. R., and Hagen, T. M. (2009) Alpha-lipoic acid as a dietary supplement: molecular mechanisms and therapeutic potential, *Biochim Biophys Acta* 1790, 1149-1160.
 220. Lee, J., Hunt, J. A., and Groves, J. T. (1998) Mechanism of iron porphyrin reactions with peroxynitrite, *J Am Chem Soc* 120, 7493-7501.
 221. Ferrer-Sueta, G., Ruiz-Ramirez, L., and Radi, R. (1997) Ternary copper complexes and manganese (III) tetrakis(4-benzoic acid) porphyrin catalyze peroxynitrite-dependent nitration of aromatics, *Chem Res Toxicol* 10, 1338-1344.
 222. Ferrer-Sueta, G., Hannibal, L., Batinic-Haberle, I., and Radi, R. (2006) Reduction of manganese porphyrins by flavoenzymes and submitochondrial particles: a catalytic cycle for the reduction of peroxynitrite, *Free Radic Biol Med* 41, 503-512.
 223. Stern, M. K., Jensen, M. J., and Kramer, K. (1996) Peroxynitrite decomposition catalysts, *J Am Chem Soc* 118, 8375-8736.
 224. Augusto, O., Trindade, D. F., Linares, E., and Vaz, S. M. (2008) Cyclic nitroxides inhibit the toxicity of nitric oxide-derived oxidants: mechanisms and implications, *Anais de Academia Brasileira de Ciências* 80, 179-189.
 225. Soule, B. P., Hyodo, F., Matsumoto, K., Simone, N. L., Cook, J. A., Krishna, M. C., and Mitchell, J. B. (2007) The chemistry and biology of nitroxide compounds, *Free Radic Biol Med* 42, 1632-1650.
 226. Krishna, M. C., Grahame, D. A., Samuni, A., Mitchell, J. B., and Russo, A. (1992) Oxoammonium cation intermediate in the nitroxide-catalyzed dismutation of superoxide, *Proc Natl Acad Sci U S A* 89, 5537-5541.
 227. Samuni, A., Krishna, C. M., Riesz, P., Finkelstein, E., and Russo, A. (1988) A novel metal-free low molecular weight superoxide dismutase mimic, *J Biol Chem* 263, 17921-17924.
 228. Miura, Y., Utsumi, H., and Hamada, A. (1993) Antioxidant activity of nitroxide radicals in lipid peroxidation of rat liver microsomes, *Arch Biochem Biophys* 300, 148-156.
 229. Mitchell, J. B., Samuni, A., Krishna, M. C., DeGraff, W. G., Ahn, M. S., Samuni, U., and Russo, A. (1990) Biologically active metal-independent superoxide dismutase mimics, *Biochemistry* 29, 2802-2807.
 230. Vaz, S. M., and Augusto, O. (2008) Inhibition of myeloperoxidase-mediated protein nitration by tempol: Kinetics, mechanism, and implications, *Proc Natl Acad Sci U S A* 105, 8191-8196.
 231. Tshako, M. H., Augusto, O., Linares, E., Chadi, G., Giorgio, S., and Pereira, C. A. (2010) Tempol ameliorates murine viral encephalomyelitis by preserving the blood-brain barrier, reducing viral load, and lessening inflammation, *Free Radic Biol Med* 48, 704-712.
 232. Masumoto, H., Kissner, R., Koppenol, W. H., and Sies, H. (1996) Kinetic study of the reaction of ebselen with peroxynitrite, *FEBS Lett* 398, 179-182.

233. Takase, T., Ohta, T., Ogawa, R., Tsuji, M., Tamura, Y., Kazuki, S., and Miyamoto, T. (1999) Effect of ebselen on contractile responses in perfused rabbit basilar artery, *Neurosurgery* 44, 370-377; discussion 377-378.
234. Ogawa, A., Yoshimoto, T., Kikuchi, H., Sano, K., Saito, I., Yamaguchi, T., and Yasuhara, H. (1999) Ebselen in acute middle cerebral artery occlusion: a placebo-controlled, double-blind clinical trial, *Cerebrovasc Dis* 9, 112-118.
235. Yamaguchi, T., Sano, K., Takakura, K., Saito, I., Shinohara, Y., Asano, T., and Yasuhara, H. (1998) Ebselen in acute ischemic stroke: a placebo-controlled, double-blind clinical trial. Ebselen Study Group, *Stroke* 29, 12-17.
236. Zhao, K., Luo, G., Zhao, G. M., Schiller, P. W., and Szeto, H. H. (2003) Transcellular transport of a highly polar 3+ net charge opioid tetrapeptide, *J Pharmacol Exp Ther* 304, 425-432.
237. Singer, S. J., and Nicholson, G. L. (1972) The fluid mosaic model of the structure of cell membranes, *Science* 175, 720-731.
238. Pali, T., and Horvath, L. I. (1989) Lipid lateral diffusion measurements in model membranes, *Acta Physiol Hung* 74, 311-314.
239. Sackmann, E., Trauble, H., Galla, H., and Overath, P. (1973) Lateral Diffusion, Protein Mobility and Phase Transitions in Escherichia coli Membranes. A Spin Label Study, *Biochemistry* 12, 5360-5369.
240. Subczynski, W. K., Widomska, J., and Feix, J. B. (2009) Physical properties of lipid bilayers from EPR spin labeling and their influence on chemical reactions in a membrane environment, *Free Radic Biol Med* 46, 707-718.
241. Subczynski, W. K., and Wisniewska, A. (2000) Physical properties of lipid bilayer membranes: relevance to membrane biological functions, *Acta Biochim Pol* 47, 613-625.
242. Denicola, A., Souza, J. M., and Radi, R. (1998) Diffusion of peroxynitrite across erythrocyte membranes, *Proc Natl Acad Sci U S A* 95, 3566-3571.
243. Romero, N., Denicola, A., Souza, J. M., and Radi, R. (1999) Diffusion of peroxynitrite in the presence of carbon dioxide, *Arch Biochem Biophys* 368, 23-30.
244. Lynch, R. E., and Fridovich, I. (1978) Permeation of the erythrocyte stroma by superoxide radical, *J Biol Chem* 253, 4697-4699.
245. New, R. R. C. (1989) *Liposomes a Practical Approach*, Oxford, New York.
246. Henry Arnaud, C. (2009) Cell Membranes: Using models to probe lipids behaviour, in *Chemical and Engineering News*, pp 31-33, American Chemical Society.
247. Moller, M. N., Lancaster, J. R., Jr., and Denicola, A. (2008) The interaction of reactive oxygen and nitrogen species with membranes, in *Free radical effects on membranes* (Matalon, S., Ed.), pp 23-43, Academic Press Inc.
248. Lynch, R. E., and Fridovich, I. (1978) Effects of superoxide on the erythrocyte membrane, *J Biol Chem* 253, 1838-1845.
249. Denicola, A., Souza, J. M., Radi, R., and Lissi, E. (1996) Nitric oxide diffusion in membranes determined by fluorescence quenching, *Arch Biochem Biophys* 328, 208-212.
250. Marla, S. S., Lee, J. and Groves, JT. (1997) Peroxynitrite rapidly permeates phospholipid membranes, *Proc Natl Acad Sci U S A* 94, 14243-14248.
251. Bartesaghi, S., Valez, V., Trujillo, M., Peluffo, G., Romero, N., Zhang, H., Kalyanaraman, B., and Radi, R. (2006) Mechanistic Studies of Peroxynitrite-Mediated Tyrosine Nitration in Membranes Using the Hydrophobic Probe *N-t*-BOC-L-tyrosine *tert*-Butyl Ester, *Biochemistry* 45, 6813-6825.
252. Khairutdinov, R. F., Coddington, J. W., and Hurst, J. K. (2000) Permeation of phospholipid membranes by peroxynitrite, *Biochemistry* 39, 14238-14249.
253. Malinski, T., Taha, Z., Grunfeld, S., Patton, S., Kapturczak, M., and Tombouljan, P. (1993) Diffusion of nitric oxide in the aorta wall monitored in situ by porphyrinic microsensors, *Biochem Biophys Res Commun* 193, 1076-1082.

254. Lide, D. R. (1990) *Handbook of Chemistry and Physics*, 71st ed ed., Boca Raton, FL.
255. Vanderkooi, J. M., and Callis, J. B. (1974) Pyrene. A probe of lateral diffusion in the hydrophobic region of membranes, *Biochemistry* 13, 4000-4006.
256. Niki, E., Yoshida, Y., Saito, Y., and Noguchi, N. (2005) Lipid peroxidation: mechanisms, inhibition, and biological effects, *Biochem Biophys Res Commun* 338, 668-676.
257. Sachdev, S., and Davies, K. J. (2008) Production, detection, and adaptive responses to free radicals in exercise, *Free Radic Biol Med* 44, 215-223.
258. Barber, D. J. W., and Thomas, J. K. (1978) Reactions of radicals with lecithin bilayers, *Radiation Research* 74, 51-65.
259. Buxton, G. V., Greenstock, G. L., Helman, W. P., and Ross, A. B. (1988) *J. Phys Chem Ref Data* 17, 513-886.
260. Porter, N. A. (1984) Chemistry of lipid peroxidation, *Methods Enzymol* 105, 273-282.
261. Atkinson, J., Epanand, R. F., and Epanand, R. M. (2008) Tocopherols and tocotrienols in membranes: a critical review, *Free Radic Biol Med* 44, 739-764.
262. Niki, E., Saito, T., Kawakami, A., and Kamiya, Y. (1984) Inhibition of oxidation of methyl linoleate in solution by vitamin E and vitamin C, *J Biol Chem* 259, 4177-4182.
263. Niki, E., Tsuchiya, R., Tanimura, R., and Kamiya, Y. (1982) Regeneration of Vitamin E from a-chromanoxo radical by glutathione and vitamin C., *Chem Lett*, 789-792.
264. Thomas, S. R., and Stocker, R. (2000) Molecular action of vitamin E in lipoprotein oxidation: implications for atherosclerosis, *Free Radic Biol Med* 28, 1795-1805.
265. Yamauchi, R. (2007) Addition products of alpha-tocopherol with lipid-derived free radicals, *Vitam Horm* 76, 309-327.
266. Goss, S. P., Hogg, N., and Kalyanaraman, B. (1999) The effect of alpha-tocopherol on the nitration of gamma-tocopherol by peroxy nitrite, *Arch Biochem Biophys* 363, 333-340.
267. Hogg, N., Joseph, J., and Kalyanaraman, B. (1994) The oxidation of alpha-tocopherol and trolox by peroxy nitrite, *Arch Biochem Biophys* 314, 153-158.
268. Botti, H., Batthyany, C., Trostchansky, A., Radi, R., Freeman, B. A., and Rubbo, H. (2004) Peroxynitrite-mediated alpha-tocopherol oxidation in low-density lipoprotein: a mechanistic approach, *Free Radic Biol Med* 36, 152-162.
269. Christen, S., Woodall, A. A., Shigenaga, M. K., Southwell-Keely, P. T., Duncan, M. W., and Ames, B. N. (1997) gamma-tocopherol traps mutagenic electrophiles such as NO(X) and complements alpha-tocopherol: physiological implications, *Proc Natl Acad Sci U S A* 94, 3217-3222.
270. Schopfer, F. J., Lin, Y., Baker, P. R., Cui, T., Garcia-Barrio, M., Zhang, J., Chen, K., Chen, Y. E., and Freeman, B. A. (2005) Nitrooleic acid: an endogenous peroxisome proliferator-activated receptor gamma ligand, *Proc Natl Acad Sci U S A* 102, 2340-2345.
271. Trostchansky, A., and Rubbo, H. (2007) Lipid nitration and formation of lipid-protein adducts: biological insights, *Amino Acids* 32, 517-522.
272. Trostchansky, A., Souza, J. M., Ferreira, A., Ferrari, M., Blanco, F., Trujillo, M., Castro, D., Cerecetto, H., Baker, P. R., O'Donnell, V. B., and Rubbo, H. (2007) Synthesis, isomer characterization, and anti-inflammatory properties of nitroarachidonate, *Biochemistry* 46, 4645-4653.
273. Wang, X., Wu, Z., Song, G., Wang, H., Long, M., and Cai, S. (1999) Effects of oxidative damage of membrane protein thiol groups on erythrocyte membrane viscoelasticities, *Clin Hemorheol Microcirc* 21, 137-146.

274. Browne, P., Shalev, O., and Hebbel, R. P. (1998) The molecular pathobiology of cell membrane iron: the sickle red cell as a model, *Free Radic Biol Med* 24, 1040-1048.
275. Spitteller, G. (2006) Peroxyl radicals: inductors of neurodegenerative and other inflammatory diseases. Their origin and how they transform cholesterol, phospholipids, plasmalogens, polyunsaturated fatty acids, sugars, and proteins into deleterious products, *Free Radic Biol Med* 41, 362-387.
276. Freeman, B. A., and Crapo, J. D. (1982) Biology of disease: free radicals and tissue injury, *Lab Invest* 47, 412-426.
277. Malencik, D. A., Sprouse, J. F., Swanson, C. A., and Anderson, S. R. (1996) Dityrosine: preparation, isolation, and analysis, *Anal Biochem* 242, 202-213.
278. Buege, J. A., and Aust, S. D. (1978) Microsomal lipid peroxidation, *Methods Enzymol* 52, 302-310.
279. Jiang, Z. Y., Woollard, A. C., and Wolff, S. P. (1991) Lipid hydroperoxide measurement by oxidation of Fe²⁺ in the presence of xylenol orange. Comparison with the TBA assay and an iodometric method, *Lipids* 26, 853-856.
280. Mendes, P. (1997) Biochemistry by numbers: simulation of biochemical pathways with Gepasi 3, *Trends Biochem Sci* 22, 361-363.
281. Huang, C., and Mason, J. T. (1978) Geometric packing constraints in egg phosphatidylcholine vesicles, *Proc Natl Acad Sci U S A* 75, 308-310.
282. Lauridsen, C., Leonard, S. W., Griffin, D. A., Liebler, D. C., McClure, T. D., and Traber, M. G. (2001) Quantitative Analysis by Liquid Chromatography-Tandem Mass Spectrometry of Deuterium-Labeled and Unlabeled Vitamin E in Biological Samples, *Analytical Biochemistry* 289, 89-95.
283. Mottier, P., Gremaud, E., Guy, P. A., and Turesky, R. (2002) Comparison of Gas Chromatography-Mass Spectrometry and Liquid Chromatography-Tandem Mass Spectrometry Methods to Quantify alpha-Tocopherol and alpha-Tocopherolquinone Levels in Human Plasma, *Analytical Biochemistry* 301, 128-135.
284. Bartesaghi, S., Trujillo, M., Denicola, A., Folkes, L., Wardman, P., and Radi, R. (2004) Reactions of desferrioxamine with peroxynitrite-derived carbonate and nitrogen dioxide radicals, *Free Radic Biol Med* 36, 471-483.
285. Hoe, S., Rowley, D. A., and Halliwell, B. (1982) Reactions of ferrioxamine and desferrioxamine with the hydroxyl radical, *Chem Biol Interact* 41, 75-81.
286. Chen, S. N., and Hoffman, M. Z. (1973) Rate constants for the reaction of carbonate radical with compounds of biochemical interest in neutral aqueous solution., *Radiat Res* 56, 40-47.
287. Misik, V., Mak, I. T., Stafford, R. E., and Weglicki, W. B. (1993) Reactions of captopril and epicaltopril with transition metal ions and hydroxyl radicals: an EPR spectroscopy study, *Free Radic Biol Med* 15, 611-619.
288. Scott, B. C., Aruoma, O. I., Evans, P. J., O'Neill, C., Van der Vliet, A., Cross, C. E., Tritschler, H., and Halliwell, B. (1994) Lipoic and dihydrolipoic acids as antioxidants. A critical evaluation, *Free Radic Res* 20, 119-133.
289. Cabelli, D. E., Rush, J. D., Thomas, M. J., and Bielski, B. H. J. (1989) *J Phys Chem* 93, 3579-3586.
290. Squadrito, G. L., Cueto, R., Splenser, A. E., Valavanidis, A., Zhang, H., Uppu, R. M., and Pryor, W. A. (2000) Reaction of uric acid with peroxynitrite and implications for the mechanism of neuroprotection by uric acid, *Arch Biochem Biophys* 376, 333-337.
291. Masuda, T., Shirohara, H., and Kondo, M. (1975) *J Radiat Res* 16, 153-161.
292. 3.0., N. S. R. D. V.
293. Alvarez, B., and Radi, R. (2001) Peroxynitrite decay in the presence of hydrogen peroxide, mannitol and ethanol: a reappraisal, *Free Radic Res* 34, 467-475.

294. Goldstein, S., and Czapski, G. (1984) Mannitol as an OH. scavenger in aqueous solutions and in biological systems, *Int J Radiat Biol Relat Stud Phys Chem Med* 46, 725-729.
295. Alvarez, B., Ferrer-Sueta, G., Freeman, B. A., and Radi, R. (1999) Kinetics of peroxyxynitrite reaction with amino acids and human serum albumin, *J Biol Chem* 274, 842-848.
296. Radi, R., Ferrer-Sueta, G., and Rubbo, H. (2000) *Nitric Oxide*, San Diego.
297. Mvula, E., Schuchmann, M. N., and von Sonntag, C. (2001) Reactions of phenol-OH-adduct radicals. Phenoxy radical formation by water elimination vs. oxidation by dioxygen., *J Chem Soc Perkin Trans. 2*, 264-268.
298. Alfassi, Z. B. (1987) Selective oxidation of tyrosine. Oxidation by NO₂ and ClO₂ at basic pH, *Radiat Phys Chem* 29, 405-406.
299. Jin, F., Leicht, J., and von Sonntag, C. (1993) The superoxide radical reacts with tyrosine-derived phenoxy radicals by addition rather than by electron transfer., *J. Chem. Soc. Perkin Trans. 2*, 1583-1588.
300. Goldstein, S., Czapski, G., Lind, J., and Merenyi, G. (2000) Tyrosine nitration by simultaneous generation of (.)NO and O-(2) under physiological conditions. How the radicals do the job, *J Biol Chem* 275, 3031-3036.
301. Von Graetz, M., Henglein, A., Lilie, J., and Beck, G. (1969) Pulsradiolytische Untersuchung einiger elementar prozesse der oxydation undreduktion des nitritions, *Ber. Bunsenges Phys Chem* 73, 646-653.
302. Mallard, W. G., Ross, A. B., and Helman, W. (1998) NIST Standard References Database 40, Version 3.
303. Logager, T., and Sehested, K. (1993) Formation and decay of peroxyxynitrous acid: A pulse radiolysis study, *J Phys Chem* 97, 6664-6669.
304. Goldstein, S., Saha, A., Lyman, S., and Czapski, G. (1998) Oxidation of peroxyxynitrite by Inorganic Radicals: A pulse radiolysis study, *J Am Chem Soc* 120, 5549-5554.
305. Merenyi, G., Lind, J., Goldstein, S., and Czapski, G. (1998) Peroxyxynitrous acid homolyzes into *OH and *NO₂ radicals, *Chem Res Toxicol* 11, 712-713.
306. Caulfield, J. L., Singh, S. P., Wishnok, J. S., Deen, W. M., and Tannenbaum, S. R. (1996) Bicarbonate inhibits N-nitrosation in oxygenated nitric oxide solutions, *J Biol Chem* 271, 25859-25863.
307. Goldstein, S., Czapski, G., Lind, J., and Merenyi, G. (1999) Effect of *NO on the decomposition of peroxyxynitrite: reaction of N₂O₃ with ONOO, *Chem Res Toxicol* 12, 132-136.
308. Goldstein, S., Czapski, G., Lind, J., and Merenyi, G. (1998) Mechanism of decomposition of peroxyxynitric ion (O₂NOO⁻): Evidence for the formation of O₂- and .NO₂ radicals, *Inorg Chem* 1998, 3943-3947.
309. Olson, L. P., Bartberger, M. D., and Houk, K. N. (2003) Peroxyxynitrate and peroxyxynitrite: a complete basis set investigation of similarities and differences between these NO_x species, *J Am Chem Soc* 125, 3999-4006.
310. Maruthamuthu, P., and Neta, P. (1978) Phosphate radicals. Spectra, acid base equilibria, and reactions with inorganic compounds, *J Phys Chem* 82, 710-713.
311. Fridovich, I. (1989) Superoxide dismutases. An adaptation to a paramagnetic gas, *J Biol Chem* 264, 7761-7764.
312. Eiserich, J. P., Butler, J., van der Vliet, A., Cross, C. E., and Halliwell, B. (1995) Nitric oxide rapidly scavenges tyrosine and tryptophan radicals, *Biochem J* 310 (Pt 3), 745-749.
313. Lyman, S. V., Jiang, Q., and Hurst, J. K. (1996) Mechanism of carbon dioxide-catalyzed oxidation of tyrosine by peroxyxynitrite, *Biochemistry* 35, 7855-7861.
314. Sullivan, S. G., Baysal, E. and Stern, A. (1992) Inhibition of hemin-induced hemolysis by desferrioxamine: binding of hemin to red cell membranes and the effects of alteration of membrane sulfhydryl groups, *Biochim Biophys Acta* 1104, 38:44.

315. Bian, K., Gao, Z., Weisbrodt, N., and Murad, F. (2003) The nature of heme/iron-induced protein tyrosine nitration, *Proc Natl Acad Sci U S A* 100, 5712-5717.
316. Thomas, D. D., Espey, M. G., Vitek, M. P., Miranda, K. M., and Wink, D. A. (2002) Protein nitration is mediated by heme and free metals through Fenton-type chemistry: an alternative to the NO/O₂- reaction, *Proc Natl Acad Sci U S A* 99, 12691-12696.
317. Ferrer-Sueta, G., Batinic-Haberle, I., Spasojevic, I., Fridovich, I., and Radi, R. (1999) Catalytic scavenging of peroxyxynitrite by isomeric Mn(III) N-methylpyridylporphyrins in the presence of reductants, *Chem Res Toxicol* 12, 442-449.
318. Mossoba, M., Makino, K., and Riesz, P. (1982) Photoionization of aromatic amino acids in aqueous solutions. A spin-trapping and electron spin resonance study, *J Phys Chem* 86, 3478-3483.
319. Rubbo, H., Denicola, A., and Radi, R. (1994) Peroxyxynitrite inactivates thiol-containing enzymes of *Trypanosoma cruzi* energetic metabolism and inhibits cell respiration, *Arch Biochem Biophys* 308, 96-102.
320. Kalyanaraman, B., Mottley, C., and Mason, R. P. (1983) A direct electron spin resonance and spin-trapping investigation of peroxy free radical formation by hematin/hydroperoxide systems, *J Biol Chem* 258, 3855-3858.
321. El-Agamey, A. (2009) Laser flash photolysis of new water-soluble peroxy radical precursor, *Journal of Photochemistry and Photobiology A: Chemistry* 203, 13-17.
322. Babbs, C. F., and Steiner, M. G. (1990) Simulation of free radical reactions in biology and medicine: a new two-compartment kinetic model of intracellular lipid peroxidation, *Free Radic Biol Med* 8, 471-485.
323. Gebicki, J. M., and Bielski, B. H. J. (1981) *J Am Chem Soc* 103, 7020-7025.
324. Davies, M. J., Forni, L. G., and Willson, R. L. (1988) Vitamin E analogue Trolox C. E.s.r. and pulse-radiolysis studies of free-radical reactions, *Biochem J* 255, 513-522.
325. Wayner, D. D., Burton, G. W., Ingold, K. U., and Locke, S. (1985) Quantitative measurement of the total, peroxy radical-trapping antioxidant capability of human blood plasma by controlled peroxidation. The important contribution made by plasma proteins, *FEBS Lett* 187, 33-37.
326. Rubbo, H., Radi, R., Anselmi, D., Kirk, M., Barnes, S., Butler, J., Eiserich, J. P., and Freeman, B. A. (2000) Nitric oxide reaction with lipid peroxy radicals spares alpha-tocopherol during lipid peroxidation. Greater oxidant protection from the pair nitric oxide/alpha-tocopherol than alpha-tocopherol/ascorbate, *J Biol Chem* 275, 10812-10818.
327. Pedrielli, P., Pedulli, G. F., and Skibsted, L. H. (2001) Antioxidant mechanism of flavonoids. Solvent effect on rate constant for chain-breaking reaction of quercetin and epicatechin in autoxidation of methyl linoleate, *J Agric Food Chem* 49, 3034-3040.
328. Priyadarsini, K. I. (1997) Free radical reactions of curcumin in membrane models, *Free Radic Biol Med* 23, 838-843.
329. Priyadarsini, K. I., Guha, S. N., and Rao, M. N. (1998) Physico-chemical properties and antioxidant activities of methoxy phenols, *Free Radic Biol Med* 24, 933-941.
330. Erben-Russ, M., Bors, W., and Saran, M. (1987) Reactions of linoleic acid peroxy radicals with phenolic antioxidants: a pulse radiolysis study, *Int J Radiat Biol Relat Stud Phys Chem Med* 52, 393-412.
331. Lee, S. H., Oe, T., and Blair, I. A. (2001) Vitamin C-induced decomposition of lipid hydroperoxides to endogenous genotoxins, *Science* 292, 2083-2086.
332. Wilcox, A. L., and Marnett, L. J. (1993) Polyunsaturated fatty acid alkoxy radicals exist as carbon-centered epoxyallylic radicals: a key step in hydroperoxide-amplified lipid peroxidation, *Chem Res Toxicol* 6, 413-416.

333. Amorati, R., Catarzi, F., Menichetti, S., Pedulli, G. F., and Viglianisi, C. (2008) Effect of ortho-SR groups on O-H bond strength and H-atom donating ability of phenols: a possible role for the Tyr-Cys link in galactose oxidase active site?, *J Am Chem Soc* *130*, 237-244.
334. Foti, M., and Ruberto, G. (2001) Kinetic solvent effects on phenolic antioxidants determined by spectrophotometric measurements, *J Agric Food Chem* *49*, 342-348.
335. Valgimigli, L., Banks, J. T., Luszyk, J., and Ingold, K. U. (1999) Solvent Effects on the Antioxidant Activity of Vitamin E(1), *J Org Chem* *64*, 3381-3383.
336. Kapoor, S. K., and Gopinathan, C. (1992) Reactions of halogenated organic peroxy radicals with various purine derivatives, tyrosine and thymine: a pulse radiolysis study, *International of Chemical Kinetics* *24*, 1035-1042.
337. Romero, N., Peluffo, G., Bartesaghi, S., Zhang, H., Joseph, J., Kalyanaraman, B., and Radi, R. (2007) Incorporation of the hydrophobic probe N-t-BOC-L-tyrosine tert-butyl ester (BTBE) to red blood cell membranes to study peroxynitrite-dependent reactions, *Chem Res Toxicol* (*in press*).
338. Stadler, K., Bonini, M. G., Dallas, S., Jiang, J., Radi, R., Mason, R. P., and Kadiiska, M. B. (2008) Involvement of inducible nitric oxide synthase in hydroxyl radical-mediated lipid peroxidation in streptozotocin-induced diabetes, *Free Radic Biol Med* *45*, 866-874.
339. Masuda, T., Bando, H., Maekawa, T., Takeda, Y., and Yamaguchi, H. (2000) A Novel Radical Terminated Compound Produced in the Antioxidation Process of Curcumin Against Oxidation of a Fatty Acid Ester, *Tetrahedron Lett* *41*, 2157-2160.
340. Bartesaghi, S., Wenzel, J., Trujillo, M., Lopez, M., Joseph, J., Kalyanaraman, B., and Radi, R. (2010) Lipid Peroxyl Radicals Mediate Tyrosine Dimerization and Nitration in Membranes, *Chem Res Toxicol*.

10. Publicaciones

Publicaciones relacionadas con la tesis

1. **Incorporation of the hydrophobic probe N-t-BOC-L-tyrosine tert butyl ester to red blood cell membranes to study peroxy-nitrite-dependent reactions.** Romero, N.; Peluffo, G.; **Bartesaghi, S.**; Zhang, H.; Joseph, J.; Kalyanaraman, B.; and Radi, R. *Chemical Research in Toxicology*, **20** (11):1638-1648 (2007)
2. **Peroxy-nitrite-derived carbonate and nitrogen dioxide radicals readily react with lipoic and dihydrolipoic acid.** Trujillo, M.; Folkes, L.; **Bartesaghi, S.**; Kalyanaraman, B.; Wardman, P.; and Radi, R. *Free Rad Biol Med* **39**, 279-288 (2005)

Presentaciones en congresos

Asistencia y presentación de póster en Free Radicals and Antioxidants in Chile: **"Tyrosine oxidation and nitration inhibition in membranes by alpha-tocopherol"**. **S. Bartesaghi**; J. Wenzel; M. Trujillo, M. López. J. Joseph, B. Kalyanaraman and R. Radi

Asistencia y presentación de póster en Society for Free Radical Biology and Medicine 15th Annual Meeting: **"Lipid Peroxyl Radicals Mediate Tyrosine Dimerization and Nitration in Membranes"**. **Bartesaghi, S.**; Trujillo, M.; López, M.; Joseph, J.; Balaraman K.; and Radi R. Indianapolis, USA (Nov. 2008).

Asistencia y presentación de póster al Tercer Workshop de Química Bioinorgánica: **"Transferencia electrónica y reactividad de grupos hemo y no hemo"**. **Bartesaghi, S.**; Trujillo, M.; Kalyanaraman, B.; and Radi, R. Facultad de Ciencias Exactas y Naturales, Universidad de Buenos Aires, Buenos Aires, Argentina (13-14 Mar 2008).

Asistencia y presentación de poster en Society for Free Radical Biology and Medicine 14th Annual Meeting: **"Relationship between tyrosine nitration and lipid radical dependent processes"**. **Bartesaghi, S.**; Trujillo, M.; Peluffo, G.; Joseph, J.; Zhang, H.; Kalyanaraman, B.; Radi, R. Washington DC, USA (14-18 Nov 2007).

Asistencia y presentación oral (seleccionada) en Free Radicals in Montevideo 2007: V Meeting of SFRBM - South American Group and V International Conference on Peroxynitrite and Reactive Nitrogen Species: **"Relationship between tyrosine nitration and lipid radical-dependent processes"**. Montevideo, Uruguay (Sept 2-6 2007).

Asistencia y presentación oral (seleccionada) Society for Free Radical Biology and Medicine 13th Annual Meeting: **"Tyrosine nitration in hydrophobic environments requires lipid radical-dependent processes"**. Denver, CO. USA (Nov 2006).

Asistencia y presentación oral (seleccionada) en Oxygen Radicals Gordon Research Conference: **"Mechanistic studies of peroxy-nitrite mediated tyrosine nitration in membranes using the hydrophobic probe N-t-BOC-L-tyrosine tert butyl ester: BTBE"**. Ventura, CA, USA (Feb 2006).

Asistencia y presentación oral (seleccionada) en *IV South American Group for Free*

Radical Research, Águas de Lindóia: “**N-t-BOC-l-tyrosine tert butyl ester (BTBE) incorporated into phosphatidylcholine liposomes for mechanistic studies of nitration in hydrophobic environments**”. Bartesaghi, S.; Valez, V.; Trujillo, M.; Peluffo, G.; Romero, N.; Zhang, H.; Kalyanaraman, B.; and Radi, R. San Pablo, Brasil (Jun 2005)

Asistencia y presentación de póster en *IV South American Group for Free Radical Research*, Águas de Lindóia: “**Peroxynitrite-derived carbonate and nitrogen dioxide radicals readily react with lipoic and dihydrolipoic acid**”. Trujillo, M.; Bartesaghi, S.; Folkes, L.; Kalyanaraman, B.; Wardman, P.; and Radi, R. San Pablo, Brasil (Jun 2005).

Asistencia y presentación de poster en 11th Annual Meeting of Society for Free Radical Biology and Medicine: “**N-t-BOC-l-tyrosine tert butyl ester (BTBE) as a hydrophobic probe to study peroxynitrite biochemistry in biomembranes and lipoproteins**”. Bartesaghi, S.; Romero, N.; Batthyány, C.; Trujillo, M.; Zhang, H.; Joseph, J.; Kalyanaraman, B.; and Radi, R. St. Thomas USVI (Nov 2004).

Pasantías en el Extranjero

Estadía en la Universidad de Buenos Aires, Facultad de Ciencias Exactas. Adquisición de conocimientos de simulación computacional sobre los mecanismos de oxidación de tirosina y cisteína en fases hidrofóbicas (Marzo 2010).

Pasantía en la Universidad de Coimbra. **Detección de Oxido Nítrico in vivo en hipocampo de rata** (Nov 2009).

Presentación del Seminario: “Mechanisms and Biological Consequences of Tyrosine nitration”

Visita al Medical College de Wisconsin. Presentación de Seminario: “**Lipid peroxy radicals mediate tyrosine nitration and dimerization in membranes**” (Nov. 2008).

Pasantía en el Medical College de Wisconsin, Dr. Balaraman Kalyanaraman: Síntesis de Péptidos de tirosina y cisteína. Técnicas de EPR (Nov. 2007).

Pasantía en el Medical College de Wisconsin, Dr. Balaraman Kalyanaraman: Síntesis, Purificación y Caracterización de Péptidos Transmembrana (Nov. 2006).

Lipid Peroxyl Radicals Mediate Tyrosine Dimerization and Nitration in Membranes

Silvina Bartesaghi,^{†,‡,§} Jorge Wenzel,^{‡,§} Madia Trujillo,^{‡,§} Marcos López,^{||} Joy Joseph,^{||} Balaraman Kalyanaraman,^{||} and Rafael Radi^{*,‡,§}

Departamento de Histología y Embriología, Departamento de Bioquímica, and Center for Free Radical and Biomedical Research, Facultad de Medicina, Universidad de la República, Avda. General Flores 2125, 11800 Montevideo, Uruguay, and Department of Biophysics and Free Radical Research Center, Medical College of Wisconsin, 8701 Watertown Plank Road, Milwaukee, Wisconsin 53226

Received December 16, 2009

Protein tyrosine dimerization and nitration by biologically relevant oxidants usually depend on the intermediate formation of tyrosyl radical ([•]Tyr). In the case of tyrosine oxidation in proteins associated with hydrophobic biocompartments, the participation of unsaturated fatty acids in the process must be considered since they typically constitute preferential targets for the initial oxidative attack. Thus, we postulate that lipid-derived radicals mediate the one-electron oxidation of tyrosine to [•]Tyr, which can afterward react with another [•]Tyr or with nitrogen dioxide ([•]NO₂) to yield 3,3'-dityrosine or 3-nitrotyrosine within the hydrophobic structure, respectively. To test this hypothesis, we have studied tyrosine oxidation in saturated and unsaturated fatty acid-containing phosphatidylcholine (PC) liposomes with an incorporated hydrophobic tyrosine analogue BTBE (*N-t*-BOC L-tyrosine *tert*-butyl ester) and its relationship with lipid peroxidation promoted by three oxidation systems, namely, peroxyxynitrite, hemin, and 2,2'-azobis (2-amidinopropane) hydrochloride. In all cases, significant tyrosine (BTBE) oxidation was seen in unsaturated PC liposomes, in a way that was largely decreased at low oxygen concentrations. Tyrosine oxidation levels paralleled those of lipid peroxidation (i.e., malondialdehyde and lipid hydroperoxides), lipid-derived radicals and BTBE phenoxyl radicals were simultaneously detected by electron spin resonance spin trapping, supporting an association between the two processes. Indeed, α -tocopherol, a known reactant with lipid peroxyl radicals (LOO[•]), inhibited both tyrosine oxidation and lipid peroxidation induced by all three oxidation systems. Moreover, oxidant-stimulated liposomal oxygen consumption was dose dependently inhibited by BTBE but not by its phenylalanine analogue, BPBE (*N-t*-BOC L-phenylalanine *tert*-butyl ester), providing direct evidence for the reaction between LOO[•] and the phenol moiety in BTBE, with an estimated second-order rate constant of $4.8 \times 10^3 \text{ M}^{-1} \text{ s}^{-1}$. In summary, the data presented herein demonstrate that LOO[•] mediates tyrosine oxidation processes in hydrophobic biocompartments and provide a new mechanistic insight to understand protein oxidation and nitration in lipoproteins and biomembranes.

Introduction

Tyrosine dimerization and nitration to 3,3'-dityrosine and 3-nitrotyrosine (3-nitro-Tyr),¹ respectively, represent biologically relevant oxidative post-translational modifications in proteins generated by the reactions with reactive oxygen and nitrogen

intermediates both in vitro and in vivo. These tyrosine oxidation processes depend on the intermediate formation of tyrosyl radical ([•]Tyr), a transient species formed by the one-electron oxidation of tyrosine. For instance, 3,3'-dityrosine formation results from the termination reaction between two [•]Tyr radicals with the formation of a new C–C bond; 3,3'-dityrosine participates in protein cross-linking (*I*) and also serves as a marker for oxidatively damaged proteins. Indeed, elevated levels of 3,3'-dityrosine can be found as a product of aging, inflammation, exposure to UV and γ -radiation, and other oxidative stress conditions (2–4). Tyrosine nitration in biological systems is also a free radical process (5) produced by nitric oxide ([•]NO)-derived oxidants such as peroxyxynitrite² and nitrogen dioxide radical ([•]NO₂) (5); typically, the final step in nitration involves the diffusion-controlled reaction of [•]Tyr with [•]NO₂. The product of this reaction, 3-nitro-Tyr, is a footprint of nitro-oxidative damage in vivo, being revealed as a strong biomarker and predictor of disease progression in conditions such as inflammation, cardiovascular disease, and neurodegeneration (6–9).

² IUPAC-recommended names for peroxyxynitrite anion (ONOO⁻) and peroxyxynitrous acid (ONOOH) ($\text{p}K_{\text{a}} = 6.8$) are oxoperoxonitrate (1-) and hydrogen oxoperoxonitrate, respectively. The term peroxyxynitrite is used to refer to the sum of ONOO⁻ and ONOOH.

* To whom correspondence should be addressed. Tel: +598-2-9249561. Fax: +598-2-9249563. E-mail: rradi@fmed.edu.uy.

[†] Departamento de Histología y Embriología, Facultad de Medicina, Universidad de la República.

[‡] Departamento de Bioquímica, Facultad de Medicina, Universidad de la República.

[§] Center for Free Radical and Biomedical Research, Facultad de Medicina, Universidad de la República.

^{||} Medical College of Wisconsin.

¹ Abbreviations: BTBE, *N-t*-BOC L-tyrosine *tert* butyl ester; BPBE, *N-t*-BOC L-phenylalanine *tert* butyl ester; DLPC, 1,2-dilauroyl-*sn*-glycero-3-phosphocholine; PLPC, 1-palmitoyl-2-linoleoyl-*sn*-glycero-3-phosphocholine; EYPC, egg chicken yolk L- α -phosphatidylcholine; SBPC, soybean-L- α -phosphatidylcholine; dtpa, diethylenetriaminepentaacetic acid; [•]NO, nitric oxide; O₂^{•-}, superoxide; 3-nitro-Tyr, 3-nitrotyrosine; [•]Tyr, tyrosyl radical; PC, phosphatidylcholine; RP-HPLC, reverse-phase high-performance liquid chromatography; ABAP, 2,2'-azobis (2-amidinopropane) hydrochloride; MDA, malondialdehyde; FOX, ferrous oxide-xylenol orange assay; LOO[•], lipid peroxyl radical; LO[•], lipid alkoxyl radical; TBARS, thiobarbituric acid reactive species; ESR, electron spin resonance; BHT, butylated hydroxytoluene; MNP, 2-methyl nitrosopropane; BOC, butoxypropylcarbonate.

Protein tyrosine nitration could result in dramatic changes in protein structure and can affect biological activity either by a loss [e.g., Mn-SOD (10–12)] or by a gain of function [e.g., nerve growth factor (13) and cytochrome *c* (14, 15); recently reviewed in ref 16].

As 3,3'-dityrosine and 3-nitro-Tyr formation require the intermediacy of [•]Tyr, both tyrosine oxidation products can be formed simultaneously in oxidizing environments where [•]NO and reactive oxygen intermediate radicals (e.g., superoxide radical, O₂^{•-}, hydrogen peroxide, H₂O₂) coexist. Specifically, this chemistry can be performed by peroxynitrite, a powerful oxidant and cytotoxic species formed in vivo by the diffusion-controlled reaction between [•]NO and O₂^{•-} (5, 17–19). Peroxynitrite does not directly react with tyrosine (20) but promotes tyrosine dimerization and nitration due to the reactions of peroxynitrite-derived species such as hydroxyl radical ([•]OH), carbonate radical (CO₃^{•-}), [•]NO₂ and the high oxidation state of redox-active metal centers [Me⁽ⁿ⁺¹⁾⁺=O, where Me is Fe, Cu, or Mn] (recently reviewed in ref 21) that can oxidize tyrosine to yield [•]Tyr, which then combines with another [•]Tyr or [•]NO₂ to yield 3,3'-dityrosine or 3-nitro-Tyr, respectively (22). For free tyrosine or tyrosine analogues in aqueous solution, the 3,3'-dityrosine/3-nitro-Tyr ratio after peroxynitrite exposure typically range in values of 1/20–1/25; however, this ratio may change if peroxynitrite is added as a single bolus or by slow infusion, depends on the tyrosine and peroxynitrite concentration, and may become smaller in proteins, reflecting the relative ease of the nitration reaction with respect to the dimerization reaction, due to diffusional and steric limitations. In addition, other tyrosine oxidation products from peroxynitrite can be formed, including the hydroxylated derivative 3,4-dihydroxyphenylalanine (DOPA) (23). Of note, 3-nitro-Tyr was initially considered a specific marker of peroxynitrite; however, there is now agreement that tyrosine nitration can also occur biologically by peroxynitrite-independent mechanisms, which include hydrogen peroxide (H₂O₂)-dependent nitrite oxidation catalyzed by heme (24) and hemoperoxidases [e.g., myeloperoxidase (25) and eosinophil peroxidase (26); reviewed in ref 5], pathways that also lead to the formation of 3,3'-dityrosine.

Protein tyrosine dimerization and nitration sites and yields depend on the protein structure, oxidation mechanism, and the environment where the protein tyrosine residues are located (22, 27). In this last regard, most of the mechanistic studies of oxidation for free and protein tyrosines have been performed in aqueous solution (10, 11, 28). However, many protein tyrosine residues shown to be dimerized and nitrated either in vitro and in vivo are associated with nonpolar compartments, such as red cell membrane proteins (29–31), mitochondrial membrane proteins (32–34), sarcoplasmic reticulum Ca²⁺ ATPase, microsomal glutathione S-transferase (35), and apolipoproteins A and B (3, 25, 36). Within these proteins, in some cases, oxidized tyrosines have been shown in cytosolic or extracellular domains [e.g., Tyr 192 and apoA-I (36)] but in other cases in domains closely related to lipids [e.g., Tyr 39 in α -synuclein (37)]. Also, reversible interactions of phospholipids with proteins can modulate tyrosine oxidation yields and sites, as observed for the cases of apoA-I (36), α -synuclein (38), and matrix metalloproteinase MMP-13 during wound repair (39).

Physicochemical factors controlling tyrosine oxidation in hydrophobic biocompartments such as biomembranes and lipoproteins differ from those in aqueous solution. For example, hydrophobic phases contain a high concentration of unsaturated fatty acids and exclude key antioxidant molecules that are potent inhibitors of tyrosine oxidation in aqueous phases such as

glutathione (22). In addition, there is a differential distribution of oxidizing species in the lipid vs aqueous phase: While [•]NO₂ can readily diffuse, concentrate, and react in the hydrophobic compartment (40), CO₃^{•-} and heme proteins have limited action due to the restricted permeation and steric restrictions, respectively. Another important aspect to consider is the restricted lateral diffusion of [•]Tyr in the organized structure of membranes, which limits the dimerization process and results in smaller 3,3'-dityrosine/3-nitro-Tyr ratios than those observed in aqueous phases (~1/100–1/400) (41).

The need to further investigate tyrosine oxidation mechanisms in hydrophobic environments has led to the development of probes such as hydrophobic tyrosine analogues (41, 42) and tyrosine-containing transmembrane peptides (42). In this regard, *N*-*t*-BOC L-tyrosine *tert*-butyl ester (BTBE) is a stable tyrosine analogue that we have previously used to study peroxynitrite and MPO-mediated tyrosine oxidation in lipid phases including liposomes and biomembranes (41–43). BTBE can be efficiently incorporated (>98%) into phosphatidylcholine (PC) liposomes, and the formation of BTBE-derived phenoxyl radicals and oxidation products (i.e., 3-nitro-BTBE, 3,3'-di-BTBE, and 3-hydroxy-BTBE) has been evaluated (41–43). Previous observations (41, 43) and kinetic considerations prompted us to investigate in depth how the unsaturated fatty acids present in high concentrations in membranes and other hydrophobic compartments may influence peroxynitrite-mediated tyrosine oxidation mechanisms and yields. Indeed, peroxynitrite is a known inductor of lipid peroxidation via free radical reactions (44) initiated after the homolysis of ONOOH to [•]OH and [•]NO₂ (21); unsaturated fatty acids readily react with [•]OH ($k = 1 \times 10^{10} \text{ M}^{-1} \text{ s}^{-1}$) (45) and to a lesser extent with [•]NO₂ ($k = 2 \times 10^5 \text{ M}^{-1} \text{ s}^{-1}$ for linoleate at pH 9.4) (46, 47), both of which promote hydrogen abstraction from a *bis*-allylic hydrogen to initiate a chain reaction. Therefore, at a first glance, an increased level of unsaturation in PC liposomes could result in a decrease of tyrosine oxidation yields. However, peroxynitrite-dependent BTBE nitration and dimerization yields were still high in PC liposomes containing a large polyunsaturated fatty acid content (41). These data indicate that a simple competition kinetic model does not apply and suggest that lipid-derived radicals mediate tyrosine oxidation within the membrane. Indeed, lipid peroxidation is an oxygen-dependent process that results in the formation of peroxy (LOO[•]) (eqs 1–3) and, secondarily, alkoxy radicals (LO[•]) (48–50).



These lipid-derived radicals are reactive species that can in turn oxidize biological targets (RH) including protein side chains (51). According to the one-electron redox potential of alkoxy ($E^{\circ}_{\text{LO}^{\bullet}/\text{LOH}} = 1.76 \text{ V}$) and peroxy radicals ($E^{\circ}_{\text{LOO}^{\bullet}/\text{LOOH}} = 1.02 \text{ V}$), it is thermodynamically possible for both species to oxidize tyrosine to the phenoxyl radical ($E^{\circ}_{\text{Tyr}^{\bullet}/\text{TyrH}} = 0.88 \text{ V}$), while the alkyl radicals ($E^{\circ}_{\text{L}^{\bullet}/\text{LH}} = 0.6 \text{ V}$) are not able to perform that oxidation. Herein, we postulate that LOO[•] is capable of oxidizing tyrosine to [•]Tyr, therefore, fueling the tyrosine oxidation pathway in hydrophobic biocompartments. To test this hypothesis, we have studied BTBE dimerization and nitration in PC liposomes of different unsaturation degrees promoted by three different oxidation systems, namely, peroxynitrite, hemin, and the peroxy

radical donor 2,2'-azobis (2-amidinopropane) hydrochloride (ABAP), and their relationship with the lipid peroxidation process.

Experimental Procedures

Chemicals. Diethylentriaminepentaacetic acid (dtpa), manganese dioxide, sodium bicarbonate, mono- and dibasic potassium phosphate, L-tyrosine, 3-nitro-Tyr, α -tocopherol, 2-methyl nitrosopropane (MNP), 1,1,3,3-tetramethoxypropane, and hemin were purchased from Sigma. BTBE, 3-nitro-*N*-*t*-BOC L-tyrosine *tert*-butyl ester (3-nitro-BTBE) and 3,3'-di-*N*-*t*-BOC L-tyrosine *tert*-butyl ester (3,3'-di-BTBE) were prepared and handled as previously (42). *N*-*t*-BOC L-phenylalanine *tert*-butyl ester (BPBE) was synthesized for the first time using an identical procedure as the one previously described for BTBE but starting from commercially available (Sigma) L-phenylalanine-*t*-butylester (42). Stock BTBE solutions (1 M) were prepared in methanol immediately before use. 3,3'-Dityrosine was synthesized by incubating 0.5 mM L-tyrosine, 0.2 mg/mL (4.5 μ M) horseradish peroxidase, and 500 μ M H₂O₂ in 50 mM phosphate buffer (pH 7.4) for 20 min at 25 °C. The resulting mixture was centrifuged through a Centricon tube (molecular mass cutoff 5000 Da) to remove the enzyme, and the concentration of 3,3'-dityrosine was obtained and determined spectrophotometrically at 315 nm using an extinction coefficient of 5700 M⁻¹ cm⁻¹ (pH 7.4) and 8380 M⁻¹ cm⁻¹ (pH 9.9) (52). 1,2-Dilauroyl-*sn*-glycero-3-phosphocholine (DLPC), 1-palmitoyl-2-linoleoyl-*sn*-glycero-3-phosphocholine (PLPC), and egg yolk and soybean PC [egg chicken yolk L- α -phosphatidylcholine (EYPC) and soybean-L- α -phosphatidylcholine (SBPC)] were from Avanti Polar Lipids. Organic solvents for the synthesis of standards and chromatography were from Baker or Mallinckrodt. All other compounds were reagent grade.

A stock hemin solution was freshly prepared in 0.1 N NaOH and kept in the dark at 4 °C until use. ABAP was purchased from Wako Chemicals USA. A fresh stock solution (100 mM) was prepared in water, and incubations were performed at 37 °C for the indicated times. Argon and nitrogen gases were purchased from AGA Chemical Co. (Uruguay). All solutions were prepared with highly pure deionized nanopure water to minimize trace metal contamination.

Peroxyntirite Synthesis and Quantitation. Peroxyntirite was synthesized in a quenched-flow reactor from sodium nitrite (NaNO₂) and hydrogen peroxide (H₂O₂) under acidic conditions as described previously (53). The H₂O₂ remaining from the synthesis was eliminated by treating the stock solutions of peroxyntirite with granular manganese dioxide, and the alkaline peroxyntirite stock solution was kept at -20 °C until use. Peroxyntirite concentrations were determined spectrophotometrically at 302 nm ($\epsilon = 1670$ M⁻¹ cm⁻¹) (44, 54). The nitrite concentration in the preparations was typically lower than 20% with respect to peroxyntirite. The control of nitrite levels was critical for obtaining reproducible data as, if present in excess, it can react with \cdot OH and other oxidants and yield \cdot NO₂ (41). In control experiments, peroxyntirite was allowed to decompose to nitrate in 100 mM phosphate buffer, pH 7.4, before use, that is, "reverse order addition" of peroxyntirite.

BTBE Incorporation into Liposomes and Oxidizing Systems. BTBE incorporation into liposomes was carried out as in refs 41 and 42 with minor modifications. Briefly, a methanolic solution of BTBE (0.35 mM) was added to 35 mM PC lipids dissolved in chloroform. Under these conditions, more than 98% BTBE was incorporated (42). The mixture was then dried under a stream of nitrogen gas. Previous studies from our group (41, 42) already indicated that BTBE incorporation yields and formation of oxidation products from peroxyntirite were comparable in unilamellar and multilamellar liposomes and therefore not dependent on the membrane morphology. Therefore, because of the more simple preparation procedure, reported experiments were carried out mainly with multilamellar liposomes. Multilamellar liposomes were formed by thoroughly mixing the dried lipid with 100 mM sodium phosphate buffer (pH 7.4) plus 0.1 mM dtpa. For experiments with

α -tocopherol-containing liposomes, α -tocopherol (in ethanol) was added at the desired concentration to the lipid solution in chloroform with or without BTBE, and liposomes were prepared thereafter as indicated above. Liposomes (30 mM PC and 0.3 mM BTBE) were exposed to peroxyntirite, hemin, or ABAP under different conditions throughout the work. BTBE and BTBE-derived products (e.g., 3-nitro-BTBE and 3,3'-di-BTBE) were extracted with chloroform, methanol, and 5 M NaCl as reported previously [1:2:4:0.4, sample: methanol:chloroform:NaCl v/v with recovery efficiencies for all compounds >95% (42)]. Samples were then dried and stored at -20 °C. Immediately before HPLC separation, samples were resuspended in 100 μ L of a mixture containing 85% methanol and 15% KPi (15 mM), pH 3. Experiments with liposomes were performed at 25 °C, a temperature above the transition phase temperatures of the different liposomes and at 37 °C when ABAP was used as an oxidant.

Oxidation Systems. BTBE-containing PC liposomes were oxidized by the addition of either peroxyntirite, hemin, or the organic peroxy radical donor ABAP. Peroxyntirite was added as a single bolus under vigorous vortexing [$t_{1/2} = 2.5$ s at 25 °C (55)] or by slow infusion using a motor-driven syringe system (K₄ Scientific) under continuous stirring. Because of the addition of alkaline peroxyntirite solutions, the final pH was also checked at the end of the incubation to ensure that there were no significant variations (<0.1 pH units). Hemin was added directly to the PC liposomes; EYPC and SBPC liposomes always contain a basal level of preformed lipid hydroperoxides that serve as the redox substrate for hemin. Alternatively, *tert*-butyl hydroperoxide was used as a hemin reactant in DLPC liposomes. Finally, in the case of ABAP, samples were incubated at 37 °C for 2–3 h to achieve a final ABAP concentration of 0–40 mM. ABAP-dependent oxygen consumption was measured using a high-resolution oxymeter (Oroboros 2K) yielding a flux of 0.3 μ M/min of peroxy radical. Experiments under low oxygen tension (ca. 5 μ M) were carried out by extensively purging samples under argon for 30 min.

Lipid Peroxidation Analysis. Malondialdehyde (MDA), a byproduct of lipid peroxidation, was measured as a thiobarbituric acid reactive substance at 532 nm ($\epsilon = 150000$ M⁻¹ cm⁻¹), as previously described (44). Calibration curves and assessment of MDA content were performed with known amounts of MDA obtained from the acid hydrolysis of 1,1,3,3-tetramethoxypropane in 20% acetic acid, pH 3.5. To prevent further peroxidation of lipids during assay procedures, 0.05% (w/v) of butylated hydroxytoluene (BHT) was added to the thiobarbituric acid reactive species (TBARS) reagent. Lipid hydroperoxide formation was evaluated by the ferrous oxide-xylenol orange (FOX) assay (56). Briefly, 50 μ L of the liposome sample was added to 950 μ L of FOX reagent consisting of 100 mM xylenol orange, 250 mM Fe²⁺ (ferrous ammonium sulfate), 25 mM H₂SO₄, and 4 mM BHT in 90% (v/v) methanol. Reaction mixtures were incubated for 1 h at room temperature, and the absorbance was measured at 560 nm. The concentration of lipid hydroperoxides was estimated with the apparent extinction coefficient of 43000 M⁻¹ cm⁻¹ (56). Oxygen consumption during lipid peroxidation processes was measured by high-resolution oxymetry using an Oxygraph 2K (Oroboros Instruments, Austria).

HPLC Analysis. BTBE, 3-nitro-BTBE, and 3,3'-di-BTBE were separated on a Agilent 1200 system equipped with UV-vis and fluorescence detectors by reverse-phase HPLC using a Agilent Eclipse XDB-C18 5 μ m column (150 mm length, 4.6 mm i.d.). Mobile phase A consisted of 15 mM phosphate buffer, pH 3, and mobile phase B consisted of methanol. Chromatographic conditions were as follows: flow, 1 mL/min; 75% mobile phase B for 25 min, followed by a linear increase to 100% mobile phase B for 10 min. UV-vis settings for BTBE were 280 nm and $\epsilon = 1200$ M⁻¹ cm⁻¹ and for 3-nitro-BTBE were 360 nm and $\epsilon = 1500$ M⁻¹ cm⁻¹. 3,3'-di-BTBE was detected fluorimetrically at $\lambda_{ex} = 294$ nm and $\lambda_{em} = 401$ nm. Authentic 3-nitro-BTBE and 3,3'-di-BTBE were used as standards.

3-Nitro-Tyr and 3,3'-dityrosine were separated by reverse-phase high-performance liquid chromatography (RP-HPLC), using a

Partisil ODS-3 10 μm (250 mm length, 4.6 mm i.d.) C18 column as previously reported with minor modifications (41). Briefly, separation of tyrosine oxidation products was performed by isocratic RP-HPLC. Chromatographic conditions were as follows: flow, 1 mL/min; 97% mobile phase A (KPi, 15 mM, pH 3) and 3% mobile phase B (methanol) for 30 min. 3-Nitro-Tyr was measured by UV detection (280 and 360 nm), and 3,3'-dityrosine was measured fluorometrically ($\lambda_{\text{ex}} = 280 \text{ nm}$ and $\lambda_{\text{em}} = 400 \text{ nm}$). Authentic 3,3'-dityrosine and 3-nitro-Tyr were used as standards. Artfactual BTBE or tyrosine nitration during the chromatographic separation procedure due to nitrite-dependent nitration at acidic pH were ruled out by appropriate controls using predecomposed peroxyntirite.

ESR Spin Trapping Measurements. ESR spectra were recorded at room temperature on a Bruker EMX spectrometer operating at 9.8 GHz. Typical spectrometer parameters were as follows: sweep width, 100 G; center field, 3505 G; time constant, 20.48 ms; scan time, 42 s; modulation amplitude, 1.0 G; modulation frequency, 100 kHz; receiver gain, 1×10^6 ; and microwave power, 20 mW. Samples were subsequently transferred to a 50 μL capillary tube for ESR measurements.

MNP (20 mM) was used as a spin trap; its photolysis may occur during the experiments and leads to the formation of a three line signal corresponding to the di-*tert*-butyl nitroxide radical, but it has a different a_N of 17.1 G. To minimize this, all liposomes preparations and solutions were covered with aluminum foil, and spectra were recorded in the dark; therefore, the signal due to photolysis was not seen under our experimental conditions.

General Experimental Conditions. Experiments were typically carried out in the presence of BTBE (0.3 mM) in PC liposomes (30 mM) in 100 mM sodium phosphate plus 0.1 mM dtpa (pH 7.4) and 25 $^\circ\text{C}$ unless otherwise stated.

Data Analysis. All experiments reported herein were repeated a minimum of three times. Results are expressed as mean values with the corresponding standard deviations. Graphics and data analysis were performed using Origin 8.0.

Results

Participation of Lipid-Derived Radicals on BTBE Oxidation. When BTBE-containing DLPC liposomes were treated with peroxyntirite (1 mM), 3-nitro-BTBE and 3,3'-di-BTBE were formed in yields of up to 2.5 and 0.01% with respect to initial peroxyntirite concentration, respectively (Figure 1A,B), in agreement with previous results (41, 57). Significant levels of both BTBE oxidation products were also formed in EYPC (Figure 1) and SBPC, which contain a significant proportion of unsaturated fatty acids, ~ 24 and 57%, respectively. Thus, in spite of the fact that for EYPC and SBPC (30 mM) unsaturated fatty acids correspond to ~ 15 and 34 mM, respectively, a much larger concentration than that of BTBE (0.3 mM), the BTBE oxidation process was still operative.

To assess the participation of lipid-derived radicals in BTBE oxidation, experiments were also performed under low oxygen tensions (Figure 1), which should result in an inhibition of LOO^\bullet formation (eq 2) in both saturated³ (58) and unsaturated fatty acids. Indeed, under these conditions, BTBE nitration and dimerization yields were substantially decreased in either saturated and unsaturated fatty acid-containing liposomes (Figure 1A,B). In parallel, we evaluated lipid peroxidation in the samples by quantitating MDA, a well-known breakdown product of peroxidized lipids. Peroxyntirite caused MDA formation in BTBE-containing EYPC and SBPC liposomes (Figure 1C), in

³ Saturated fatty acids (e.g., lauric acid in DLPC) will also react with $\cdot\text{OH}$ at fast rates [$k \sim 5 \times 10^8 \text{ M}^{-1} \text{ s}^{-1}$ (58)] to yield the alkyl radical. This can evolve to lauric acid peroxy radical that, however, will not be capable of propagating a lipid peroxidation chain reaction in DLPC liposomes due to the lack of unsaturated fatty acids. Still, the peroxy radical could be potentially reactive with other targets such as BTBE (vide infra).

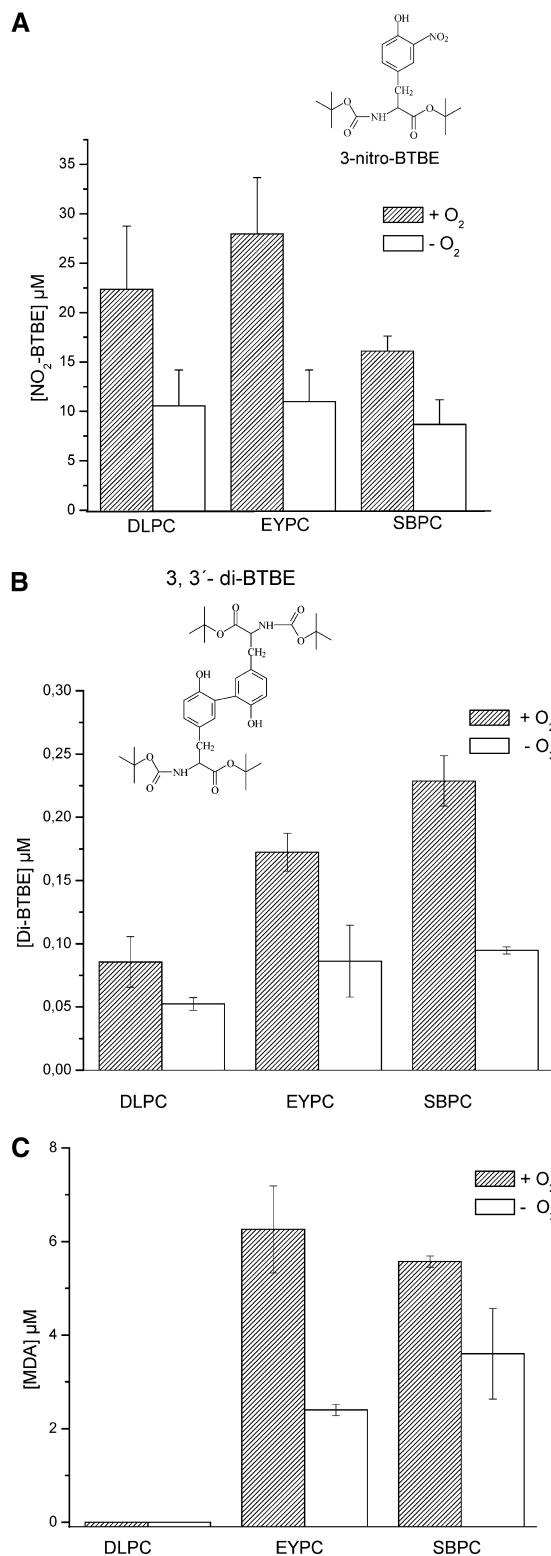


Figure 1. Effect of oxygen on peroxyntirite-dependent BTBE oxidation and lipid peroxidation. BTBE (0.3 mM) was incorporated into the different liposomes DLPC, EYPC, and SBPC (30 mM) and exposed to peroxyntirite (1 mM) in the presence of oxygen (200 μM) or under low oxygen tensions ($\sim 5 \mu\text{M}$). Samples were analyzed for (A) 3-nitro-BTBE, (B) 3,3'-di-BTBE, and (C) MDA contents. The data on MDA show its increase over basal levels upon addition of peroxyntirite. Basal levels in EYPC, SBPC and DLPC were 4.5, 5 and 0 μM , respectively. Structures of 3-nitro-BTBE and 3,3'-di-BTBE are indicated in the corresponding panels.

agreement with our previous observations (41); importantly, MDA levels were reduced under low oxygen concentration, revealing the inhibition of the lipid peroxidation process. As

expected, no MDA was detected in DLPC samples. Thus, in unsaturated fatty acid-containing liposomes (EYPC and SBPC), BTBE oxidation and lipid peroxidation occurred simultaneously and were both inhibited at low oxygen levels. Lipid hydroperoxide levels were significantly higher (over 1 order of magnitude) than those obtained for BTBE oxidation products, in agreement with the idea that lipid peroxidation is the main process within the membrane. On the other hand, when tyrosine (0.3 mM) was exposed to peroxynitrite (1 mM) in 100 mM phosphate buffer (pH 7.3) and 0.1 mM DTPA, oxygen did not influence tyrosine nitration and dimerization yields (~ 6 and 0.25%) with respect to peroxynitrite in the aqueous phase (not shown). Overall, the data point to the formation of LOO^{\bullet} as key intermediates in the BTBE oxidation process.

Electron spin resonance (ESR) spin trapping was used to detect the lipid-derived and BTBE phenoxyl radicals formed during peroxynitrite exposures using MNP as described previously (41, 59). In DLPC liposomes, no ESR signal was obtained in the absence of BTBE when exposed to peroxynitrite (Figure 2, line a). On the other hand, BTBE-containing DLPC liposomes treated with peroxynitrite resulted in an anisotropic three line signal, confirming the formation of a partially immobilized phenoxyl radical in the interior of the membrane (Figure 2, line b) and in agreement with our previous work (41, 60). When peroxynitrite-treated BTBE containing DLPC liposomes was dissolved in ethanol (60), a sharper and clear three line signal was obtained, which, despite the low signal-to-noise ratio, allowed the determination of a hyperfine constant of 13.8 G; this is consistent with a MNP adduct with the one-electron oxidation of BTBE (61). In EYPC liposomes, peroxynitrite caused the formation of a MNP adduct in the absence of BTBE, compatible with the formation of MNP-lipid alkyl (carbon-centered adduct) radical adducts (Figure 2, line c) with an estimated hyperfine splitting constant $a_N \sim 15$ G (59). When BTBE was incorporated into liposomes, the signal was even larger (Figure 2, line d), supporting the coexistence of lipid-derived and BTBE phenoxyl radicals and confirming the temporal association between the lipid peroxidation and the BTBE oxidation processes. No ESR spectrum was obtained in DLPC or EYPC liposomes when treated with decomposed peroxynitrite (Figure 2, lines e and f) or if MNP was added after peroxynitrite (Figure 2, line g) or if peroxynitrite was added to MNP only (without liposomes, not shown).

Slow Infusion vs Bolus Addition of Peroxynitrite in Lipid Peroxidation and BTBE Oxidation. Peroxynitrite has a short half-life in 100 mM phosphate buffer, pH 7.4, and 25 °C ($t_{1/2} = 2.5$ s) due to the proton-catalyzed homolysis to $\cdot\text{OH}$ and $\cdot\text{NO}_2$ in 30% yields (55). Thus, the addition of peroxynitrite to reaction mixtures as a single bolus may result in a high initial concentration of radicals, and the extent of oxidation processes in target molecules do not necessarily reflect the expected outcome in more biologically relevant conditions where peroxynitrite is formed as a continuous flow (62, 63). This consideration becomes particularly important in lipid peroxidation processes that depend on propagation reactions where an initial large flux of radicals will prematurely terminate the process. Thus, experiments were performed to study lipid peroxidation and BTBE oxidation yields with peroxynitrite addition as a single bolus or by slow infusion for up to 30 min (1 $\mu\text{M}/\text{min}$). Peroxynitrite addition to BTBE-containing EYPC liposomes resulted in dose-dependent formation of MDA (Figure 3A); MDA yields were increased 2–3-fold when peroxynitrite was added as a slow infusion. Similarly, BTBE nitration and dimerization (Figure 3B–D) yields in both EYPC and DLPC

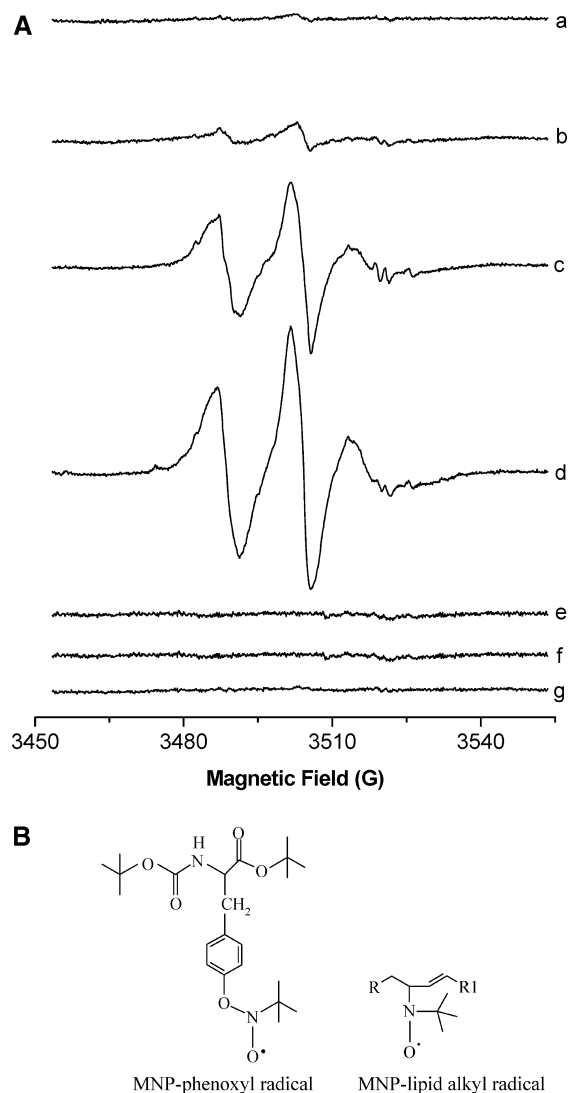


Figure 2. ESR spin trapping of BTBE phenoxyl and LOO^{\bullet} . (A) Reaction mixtures consisting of BTBE (2.5 mM) incorporated into 45 mM DLPC liposomes in 100 mM phosphate buffer (pH 7.4) containing dtpa (0.1 mM) were treated with 20 mM MNP spin trap and rapidly mixed with 5 mM peroxynitrite. Samples were subsequently transferred to a 50 μL capillary tube for EPR measurements. (a) DLPC liposomes plus peroxynitrite, (b) BTBE-containing DLPC liposomes plus peroxynitrite, (c) EYPC liposomes plus peroxynitrite, (d) BTBE-containing EYPC liposomes plus peroxynitrite, (e) same as b with reverse order addition of peroxynitrite, (f) same as d with reverse order addition of peroxynitrite, and (g) peroxynitrite only. (B) The structures of the MNP-phenoxyl and MNP-lipid alkyl radical adducts are shown and correspond to the signals obtained in lines b and c of panel A, respectively. Both spin adducts are present in line d.

by peroxynitrite infusion were up to 3-fold higher than with bolus addition. Moreover, BTBE oxidation (Figure 3E) and MDA formation (not shown) yields in EYPC were significantly reduced under low oxygen tensions when peroxynitrite was added as a slow infusion. The data further support an association between the lipid peroxidation and the BTBE oxidation processes.

Effect of Phospholipid Unsaturation Degree in Peroxynitrite-Mediated BTBE Oxidation. BTBE oxidation was studied as a function of fatty acid unsaturation by using liposomes containing variable mixtures of DLPC and PLPC. Nitration and dimerization yields were significant through all the phospholipid unsaturation range (0–100%). A tendency toward increased BTBE oxidation yields was observed at around 40% PLPC content, while a slight decrease was observed at 100% PLPC. Thus, in spite of a largely variable content of unsaturated fatty acids in the liposomal mixtures (from 0 to 30 mM linolenic

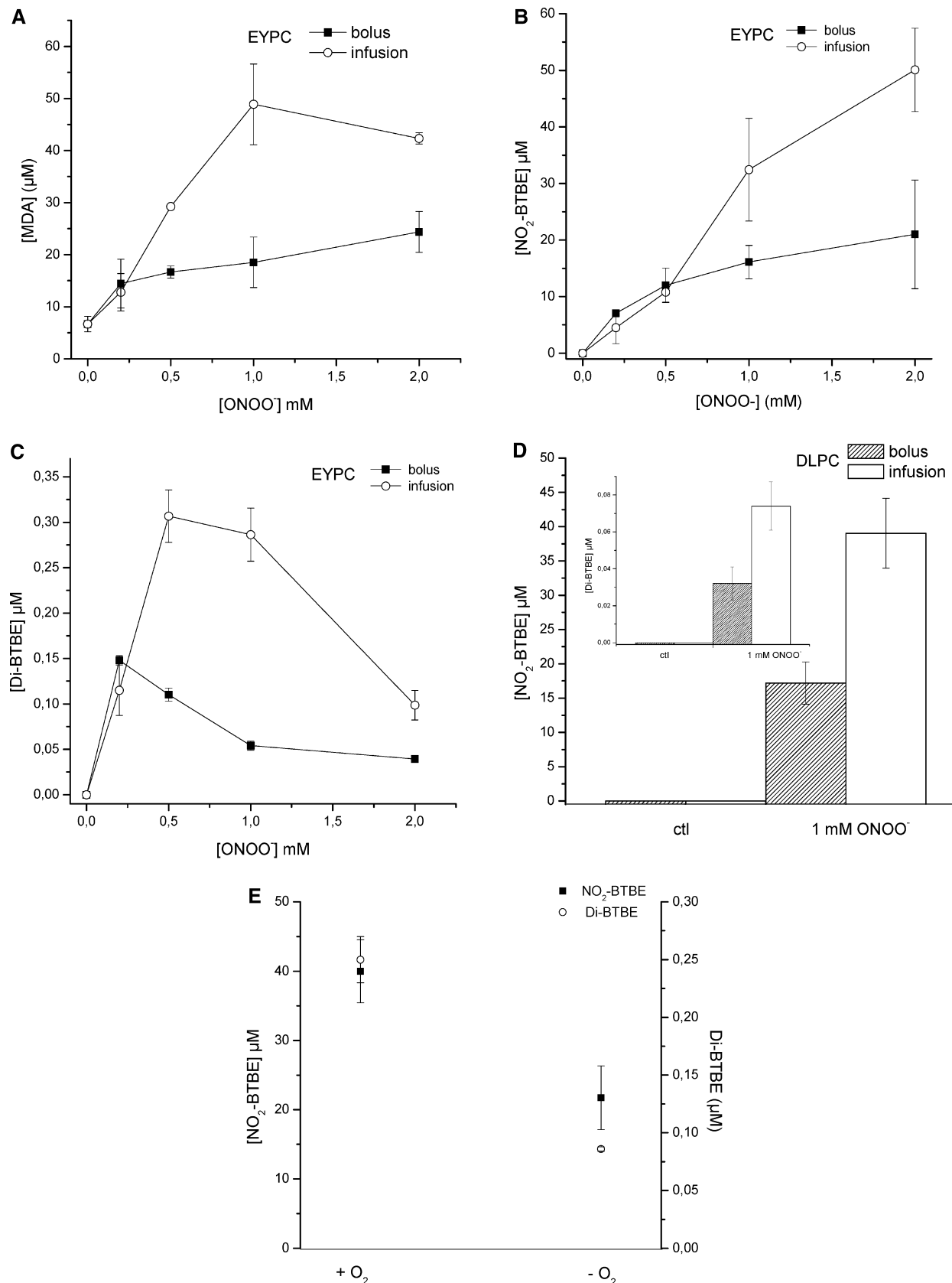


Figure 3. Peroxynitrite-mediated oxidations: slow infusion versus bolus addition. BTBE (0.3 mM) was incorporated into EYPC and DLPC liposomes (30 mM) and exposed to peroxynitrite either as a single bolus (■) or by slow infusion (○) to achieve final concentrations of 0.2–2 mM. Samples were analyzed for 3-nitro-BTBE, 3,3'-di-BTBE, and MDA contents. EYPC: (A) MDA, (B) 3-nitro-BTBE, and (C) 3,3'-di-BTBE. DLPC: (D) 3-nitro-BTBE and 3,3'-di-BTBE (inset). (E) BTBE- (0.3 mM) containing liposomes were exposed to slow infusion of peroxynitrite (1 mM) in the presence and absence of oxygen, and 3-nitro-BTBE and 3,3'-di-BTBE were measured as previously.

acid), BTBE oxidation was consistently present. Thus, the data support that a simple kinetic competition model, where unsaturated fatty acids simply outcompete BTBE for peroxynitrite-

derived radicals, does not apply and that secondary reactions of lipid-derived radicals with BTBE must contribute to nitration and dimerization reactions (Figure 4).

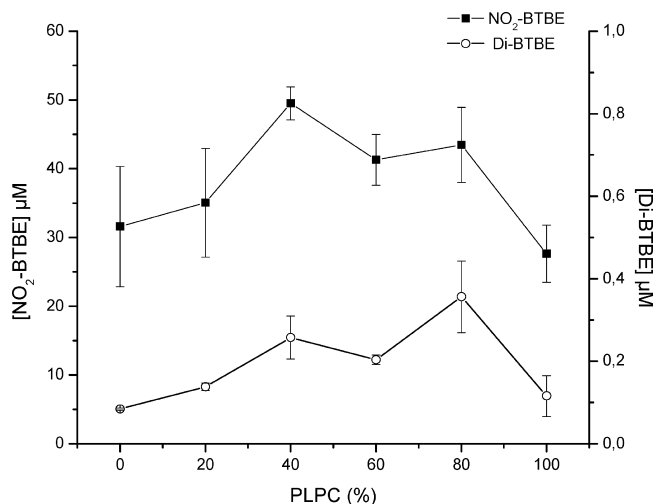
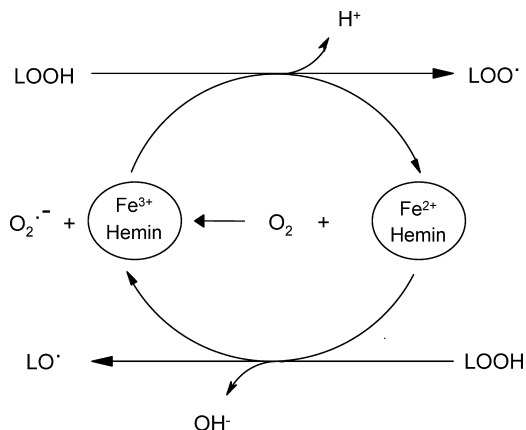


Figure 4. Lipid unsaturation degree and BTBE oxidation. BTBE nitration (■) and dimerization (○) were studied as a function of fatty acid unsaturation by using mixtures of DLPC and PLPC (0–100% PLPC) liposomes containing 0.3 mM BTBE and treated with peroxynitrite (1 mM).

Scheme 1. Lipid Hydroperoxide Reactions with Hemin and Lipid-Derived Radicals Formation^a



^a Lipid hydroperoxide (LOOH) can react with hemin either in Fe³⁺ or Fe²⁺ redox states to yield LOO[•] or LO[•], respectively. Secondly, hemin in the reduced state (Fe²⁺) can yield O₂^{•-} that can further participate in redox reactions.

Hemin and ABAP-Induced Lipid Peroxidation. To further demonstrate that lipid peroxidation processes are related with BTBE oxidation, we exposed BTBE-containing liposomes to two other oxidation systems, namely, hemin and ABAP, both of which lead to the formation of LOO[•] in unsaturated fatty acid-containing liposomes. Free hemin readily interacts with membranes (64) and initiates lipid peroxidation in unsaturated liposomes by reaction with LOOH always present in variable extents in EYPC and SBPC (typical hydroperoxide contents in well-stored preparations represent in our 30 mM liposome samples ~45–80 μM, 0.075–0.13%, total unsaturated fatty acid as determined by the FOX assay). Hemin (Fe³⁺) promotes the one-electron oxidation of LOOH to yield LOO[•] and hemin in the Fe²⁺ redox state (Scheme 1). In turn, the reduced hemin can generate LO[•] by reduction of LOOH.

Secondary reactions in the system generate variable amounts of O₂^{•-}, H₂O₂, and heme-Fe⁴⁺=O that can amplify the process (64). In EYPC liposomes, hemin induced 3,3'-di-BTBE and MDA formation in a dose-dependent manner (Figure 5). On the other hand, in DLPC liposomes (saturated), where hemin can not cause lipid peroxidation, no formation of 3,3'-di-BTBE

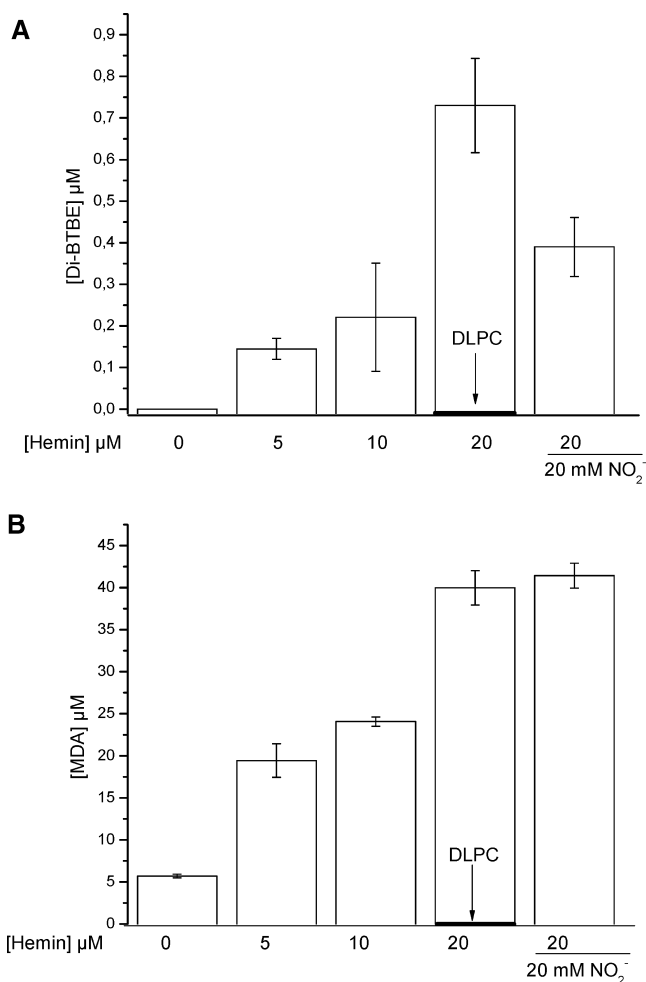


Figure 5. Hemin-induced lipid peroxidation and BTBE oxidation. BTBE- (0.3 mM) containing DLPC and EYPC liposomes (30 mM) were exposed to hemin (5–20 μM) in 100 mM sodium phosphate, pH 7.3, plus 0.1 mM DTPA. Samples were analyzed for (A) 3,3'-di-BTBE and (B) MDA contents. The arrow indicates the values corresponding to DLPC liposomes that were zero for both measurements under all reaction conditions.

was detected. Thus, the data imply the participation of LOO[•] radicals formed from the reaction of hemin with lipid hydroperoxides (Scheme 1) in the BTBE dimerization process.

Second, we performed experiments using the organic peroxy radical donor, ABAP, which generates a flux of peroxy radicals by thermolysis.



ABAP initiates lipid peroxidation in unsaturated fatty acid-containing liposomes such as EYPC, by the reaction of the ABAP-derived peroxy radicals (AOO[•]) with an unsaturated alkyl chain to yield the alkyl radical (L[•]), which then (eqs 4–6), after oxygen addition, forms LOO[•]. The addition of ABAP to BTBE-containing liposomes resulted in the formation of 3,3'-di-BTBE in both DLPC and EYPC liposomes (Table 1 and Figure 6A), but MDA formation was observed in EYPC liposomes only. Thus, either ABAP-derived (in the DLPC experiment) or lipid-derived (in the EYPC one) peroxy radicals react with BTBE to yield BTBE-derived phenoxyl radical and

Table 1. ABAP-Mediated BTBE Oxidation^a

condition	EYPC		DLPC	
	NO ₂ -BTBE (μM)	di-BTBE (μM)	NO ₂ -BTBE (μM)	di-BTBE (μM)
control	0	0	0	0
ABAP	0	0.011 ± 0.001	0	0.79 ± 0.164
ABAP + NO ₂ ⁻	2.5 ± 0.76	0.043 ± 0.008	16.15 ± 1.39	0.537 ± 0.029
ABAP - O ₂	0	0	0	0.32 ± 0.065
ABAP + NO ₂ ⁻ - O ₂	1.46 ± 0.8	ND ^b	9.43 ± 2	ND
NO ₂ ⁻	0	0	0	0

^a BTBE (0.3 mM) was incorporated into DLPC and EYPC liposomes (30 mM), and the mixture was incubated for 2 h at 37 °C with ABAP (10 mM, 0.3 μM/min flux of peroxy radicals) in the presence and absence of nitrite (NO₂⁻) (20 mM), and 3-nitro-BTBE and 3,3'-di-BTBE contents were measured. The same experiment was performed in the presence of low oxygen tensions (~5 μM). ^b ND, not determined.

subsequently 3,3'-di-BTBE. Interestingly, samples treated with ABAP plus nitrite resulted in the formation of both 3,3'-di-BTBE and 3-NO₂-BTBE, supporting that ABAP-derived peroxy radicals can also oxidize nitrite to [•]NO₂ (Tables 1 and 2) (65). Low oxygen levels decreased BTBE oxidation yields induced by ABAP plus nitrite, in both DLPC and EYPC liposomes, confirming the role of LOO[•] in the process. Control experiments with nitrite only showed no formation of BTBE oxidation products (Table 1).

To specifically address the reaction of organic peroxy radicals with tyrosine, we studied the effect of ABAP on free tyrosine oxidation in aqueous phase (Figure 6B). Tyrosine exposure to ABAP-derived peroxy radicals resulted in the formation of 3,3'-dityrosine (Figure 6B, line b); when nitrite was added to the incubation mixture, both tyrosine oxidation products, 3-nitro-Tyr and 3,3'-dityrosine, were formed (Figure 6B, line c). Tyrosine nitration and dimerization yields were lower with free tyrosine in aqueous solution than those observed for BTBE in liposomes, which suggest that tyrosine oxidation by peroxy radicals more easily occurs in nonpolar environments.

Effect of α-Tocopherol on BTBE Oxidation and Lipid Peroxidation. α-Tocopherol is a well-known lipophilic chain-breaking antioxidant that reacts with LOO[•] with a rate constant of 5 × 10⁵ M⁻¹ s⁻¹ (66) to yield lipid hydroperoxides and the stable α-tocopheroxyl radical (eq 7):



α-Tocopherol incorporated into EYPC liposomes inhibited peroxy nitrite-mediated BTBE nitration (Figure 7A), dimerization (not shown), and lipid peroxidation (Figure 7B) in a dose-dependent manner. Interestingly, α-tocopherol also inhibited BTBE oxidation in DLPC liposomes, where no lipid peroxidation occurs. The effect of α-tocopherol is explained by the reaction between α-tocopherol with LOO[•]. In the case of DLPC, the reaction of α-tocopherol with [•]NO₂ [*k* = 1 × 10⁵ M⁻¹ s⁻¹ (67)] also becomes relevant to explain the inhibition of BTBE oxidation.

Oxygen Consumption Studies and Kinetic Determination of LOO[•] Reaction with BTBE. Experiments were performed to measure the oxygen consumption associated with lipid peroxidation initiated by hemin and ABAP and the potential chain-breaking reaction of BTBE. If LOO[•] react to a significant extent with BTBE, then, the hydrophobic tyrosine analogue should inhibit oxygen consumption. In EYPC (but not in DLPC) liposomes (in the absence of BTBE), a basal decrease in oxygen concentration is shown. Oxygen consumption is observed upon the addition of either ABAP or hemin (Figure 8A), in agreement with the initiation and propagation phases of lipid peroxidation. In contrast, no further oxygen consumption was observed in DLPC liposomes after ABAP or hemin addition (Figure 8A). The incorporation of α-tocopherol to EYPC

liposomes resulted in a significant decrease in oxidant-induced oxygen consumption rates (Figure 8B). The extent of inhibition in oxygen consumption by α-tocopherol is compatible with the previously reported rate constants of LOO[•] with adjacent alkyl chains (*k* = 36 M⁻¹ s⁻¹) (68) and with α-tocopherol (*k* = 5 × 10⁵ M⁻¹ s⁻¹) (66). The inhibitory action of α-tocopherol was also observed if added exogenously during the time course of the oxygen consumption studies but was less potent than when preincorporated, due to the suboptimal penetration in the preformed liposome structure within the time frame of the experiment. Remarkably, the incorporation of BTBE to the EYPC liposomes resulted in a dose-dependent inhibition of both hemin- and ABAP-induced oxygen consumption rates, which is consistent with the reaction of BTBE with lipid-derived radicals (Figure 8B). To discard subtle structural effects in the liposomal membranes due to BTBE incorporation, experiments were performed using a phenylalanine hydrophobic analogue (BTPE) preincorporated to the liposomes (Figure 8C). In this case, oxygen consumption rates were identical to the one observed in control EYPC (without BTBE), which is in agreement with a direct participation of the phenolic-OH moiety in the BTBE in reaction leading to inhibition of lipid peroxidation-dependent oxygen consumption, which is not present in the phenylalanine derivative (Figure 8C).

The dose-dependent inhibition of oxygen consumption by increasing concentrations of preincorporated BTBE in EYPC liposomes was further analyzed to obtain an estimated second-order rate constant for the reaction of LOO[•] with BTBE. A plot that relates the inhibition fraction in oxygen consumption as a function of BTBE concentration is in agreement with a direct competition of BTBE for the LOO[•] (Figure 8D). These data allow the estimation of an apparent second-order rate constant of 4.8 × 10³ M⁻¹ s⁻¹ for the following reaction:



This rate constant value compares well with an independent determination considering the α-tocopherol studies. From data in Figure 8B,C, one concludes that 87% inhibition is obtained with 5 μM α-tocopherol or 1 mM BTBE. Considering the stoichiometric factor *n* = 2 for α-tocopherol (69), thus, 2 × *k*_{toc} [α-tocopherol] = *k*_{BTBE} [BTBE], so 2 × *k*_{toc} [α-tocopherol]/[BTBE] = *k*_{BTBE} = 5 × 10³ M⁻¹ s⁻¹. In addition, both MDA and hydroperoxide yields were decreased in the presence of BTBE, in agreement with a reaction between BTBE and LOO[•] (Figure 8E,F) and with the oxygen consumption data.

Discussion

Previously identified and biologically relevant one-electron oxidants for tyrosine in aqueous environments include [•]OH, CO₃^{•-}, and [•]NO₂, compounds I and II of hemeperoxidases, and

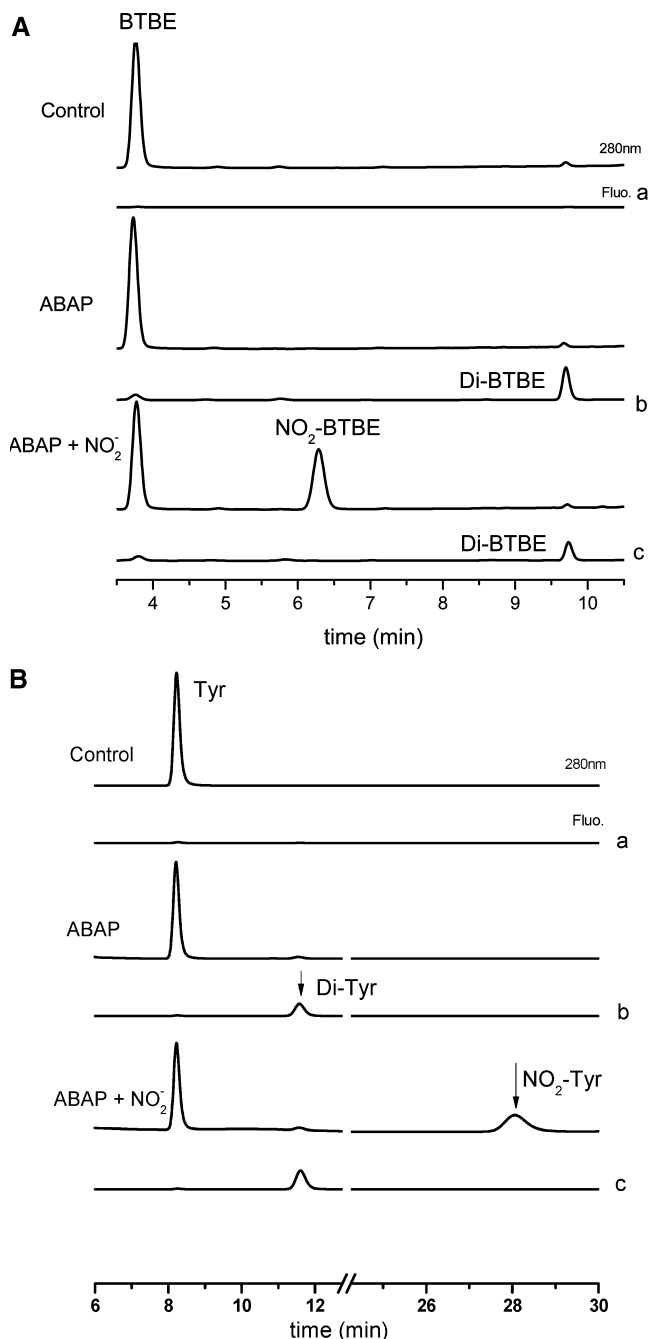


Figure 6. ABAP-induced BTBE and tyrosine oxidation. (A) (a) BTBE (0.3 mM) containing DLPC liposomes in 100 mM sodium phosphate (pH 7.3) plus 0.1 mM DTPA were exposed to (b) ABAP (20 mM) in the absence and (c) presence of nitrite (40 mM), and 3-nitro-BTBE and 3,3'-di-BTBE were measured. (B) (a) Tyrosine (0.3 mM) in 100 mM sodium phosphate (pH 7.3) plus 0.1 mM DTPA was exposed to (b) ABAP (20 mM) in the absence and (c) presence of nitrite (40 mM), and 3-nitro-Tyr and 3,3'-dityrosine were measured.

high oxidation states of transition metal centers (5). However, in the case of tyrosine oxidation in proteins associated with hydrophobic biocompartments such as membranes or lipoproteins, (a) some of the oxidants may not easily reach or permeate the lipid phase, and (b) unsaturated fatty acids, due to their reactivity and large concentration, constitute preferential targets for the initial oxidative attack. Thus, mechanisms by which tyrosine residues become dimerized and nitrated in hydrophobic biocompartments seem to have unique characteristics from those previously described in hydrophilic phases. In this work, we have explored, using a validated model system of PC liposomes containing a hydrophobic tyrosine analogue (BTBE), whether

lipid-derived radicals generated during lipid peroxidation processes can mediate tyrosine oxidation to $^{\bullet}\text{Tyr}$, the first step in the path to 3,3'-dityrosine or 3-nitro-Tyr.

Lipid peroxidation was initiated by three independent oxidation systems, namely, peroxy-nitrite, hemin, and ABAP. Peroxy-nitrite promotes lipid peroxidation and tyrosine nitration in hydrophobic compartments secondary to homolysis of peroxy-nitrous acid (ONOOH) to $^{\bullet}\text{OH}$ and $^{\bullet}\text{NO}_2$ inside or at close proximity of the lipid phase (41, 44, 70). In EYPC, for instance, the large concentration ratio of unsaturated fatty acid/BTBE (50/1) and the participating rate constants (see Table 2) determine that the initial attack of peroxy-nitrite-derived radicals occurs at the fatty acid moieties; this initial reaction yields the alkyl (pentadienyl) radical that upon oxygen addition evolves to LOO^{\bullet} , which propagates the process (44). Alternatively, lipid-derived radicals were generated by the reaction of hemin with pre-existing lipid hydroperoxides to directly yield LOO^{\bullet} or by ABAP whose peroxy radical derivative diffuses to the liposomes and reacts with unsaturated alkyl chains to initiate lipid peroxidation as well (71). LOO^{\bullet} are known to react at fast rates with some phenolic compounds, including α -tocopherol and other dietary compounds that may exert antioxidant actions in vitro and in vivo. For example, linoleate peroxy radicals react with phenolic antioxidant compounds such as α -tocopherol, curcumin, and quercetin with rate constants in the range $\sim 10^6$ – $10^7 \text{ M}^{-1} \text{ s}^{-1}$ (72–75). In the case of tyrosine, another phenolic compound, the reaction with LOO^{\bullet} is thermodynamically possible; however, tyrosine is not a particularly good hydrogen donor; therefore, the reaction may be kinetically hindered. Interestingly, hydrophobic phases may increase the reactivity of phenolic compounds such as tyrosine for LOO^{\bullet} (see below). Thus, extensive studies were performed herein to unambiguously show the existence of the LOO^{\bullet} reaction with the hydrophobic tyrosine analogue BTBE.⁴

The evidence that we have gathered herein to support the participation of LOO^{\bullet} in the tyrosine oxidation processes promoted by the three different tested oxidation systems can be summarized as follows: (a) Tyrosine (BTBE) oxidation was seen in significant extents in unsaturated fatty acid-containing PC liposomes, (b) tyrosine oxidation in liposomes (but not in aqueous phase) was decreased under low oxygen concentrations, (c) lipid-derived and $^{\bullet}\text{Tyr}$ were simultaneously detected, (d) α -tocopherol strongly inhibited tyrosine oxidation, (e) BTBE (but not BPTTE) partially inhibited lipid peroxidation processes, (f) changes in the levels of tyrosine oxidation and lipid peroxidation products followed a parallel trend, and (g) the data are in agreement with an overall process involving the free radical mechanisms of lipid peroxidation and tyrosine oxidation plus a "connecting reaction" represented by one-electron oxidation of tyrosine by LOO^{\bullet} (eq 7) (see also Table 2).

With regard to the reactivity of peroxy radicals with tyrosine, the data showed that ABAP-derived peroxy radicals were already capable of oxidizing both BTBE in DLPC (saturated) liposomes as well as free tyrosine (Table 1 and Figure 6), but reaction yields were much larger for BTBE, compatible with the concept that the reaction of phenolic compounds with oxidizing radicals is influenced by a kinetic solvent effect (76, 77). Indeed, different phenolic compounds (e.g., quercetin

⁴ Alkoxy radicals (LO^{\bullet}) are also formed in lipid peroxidation processes via one-electron reduction of lipid hydroperoxides (48) or breakdown of tetroxide intermediates formed by the coupling of lipid two peroxy radicals; alkoxy radicals are far more potent oxidizing species than LOO^{\bullet} but mainly rearrange to epoxyallylic radicals (50), which in turn, after coupling to O_2 , become a secondary peroxy radical.

Table 2. Main Reactions Involved in Tyrosine Oxidation in Hydrophobic Environments and the Connection to Lipid Peroxidation^a

reaction	k ($M^{-1} s^{-1}$)	reference
$L^b + \cdot OH \rightarrow L\cdot + OH^-$	1×10^{10}	45
$L + \cdot NO_2 \rightarrow L\cdot + NO_2^-$	2×10^5	46
$Tyr + \cdot OH \rightarrow \cdot Tyr + OH^-$	1.24×10^{10}	90
$Tyr + \cdot OH \rightarrow \cdot TyrOH^c + OH^-$	6.5×10^8	90
$Tyr + \cdot NO_2 \rightarrow \cdot Tyr + NO_2^-$	3.2×10^5	46
$\cdot Tyr + \cdot NO_2 \rightarrow 3\text{-nitro-Tyr}$	3×10^9	46
$2\cdot Tyr \rightarrow 3,3'\text{-di-Tyr}$	2.25×10^8	91
	2.25×10^{6d}	41
$L\cdot + O_2 \rightarrow LOO\cdot$	3×10^8	92
$LOO\cdot + L \rightarrow LOOH + \cdot L$	37	68
$2LOO\cdot \rightarrow LOOH + O_2$	10^7	92
$LOO\cdot + L\cdot \rightarrow LOOL$	5×10^7	92
$2L\cdot \rightarrow LL$	5×10^8	92
$LOO\cdot + NO_2^- \rightarrow LOOH + \cdot NO_2$	4.5×10^6	65 ^e
$LOO\cdot + Tyr \rightarrow LOOH + \cdot Tyr$	4.8×10^3	this work
$\alpha\text{-tocopherol}^f + LOO\cdot \rightarrow \alpha\text{-tocopheryl}\cdot + LOOH$	5×10^5	67
$\alpha\text{-tocopherol} + \cdot NO_2 \rightarrow \alpha\text{-tocopheryl}\cdot + NO_2^-$	1×10^5	67
$\alpha\text{-tocopherol} + \cdot OH \rightarrow \alpha\text{-tocopheryl}\cdot + OH^-$	3.8×10^9	66

^a Reactions involving lipids refer to those containing unsaturated fatty acid unless otherwise indicated. ^b Lipids composed of saturated fatty acid are also oxidized by hydroxyl radicals at similar rates (58). ^c This radical rapidly dehydrates and evolves to $\cdot Tyr$ under the experimental conditions employed herein. ^d Value for tyrosine dimerization in membranes, expected to occur at least 100 times slower than in the aqueous phase. ^e This rate constant has been reported for acetylperoxyl radical reduction by nitrite. ^f The radical scavenging mechanisms of α -tocopherol are indicated.

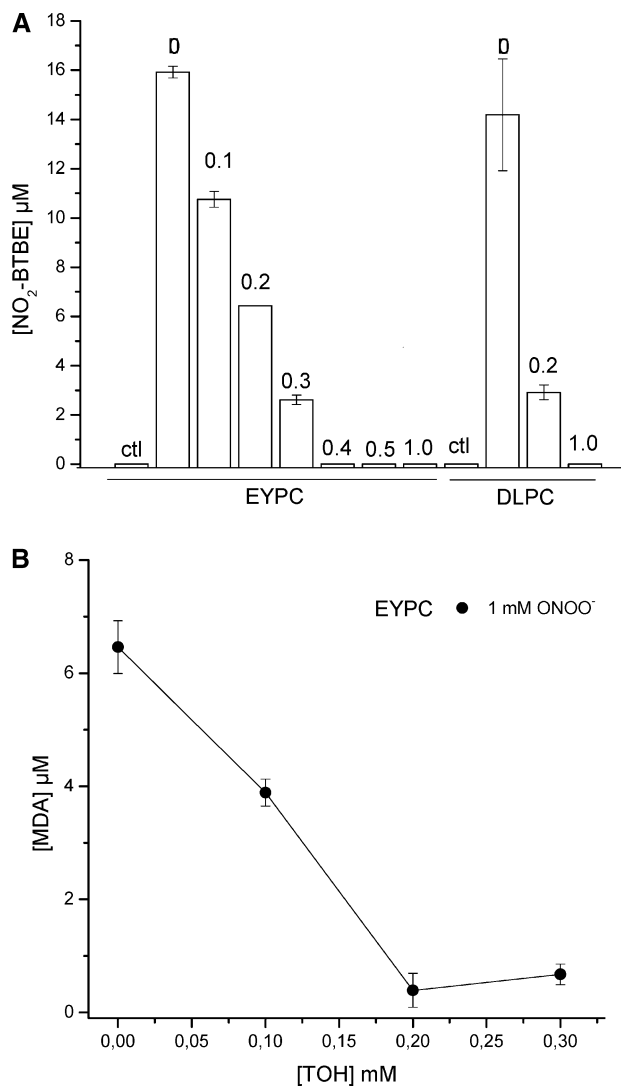


Figure 7. Effect of α -tocopherol on lipid peroxidation and BTBE oxidation. The indicated concentrations of α -tocopherol (0.1–1 mM) were preincorporated to different EYPC and DLPC preparations (30 mM) and treated with peroxynitrite (1 mM); samples were analyzed for (A) 3-nitro-BTBE and (B) MDA contents.

and epicatechin) react with peroxy radicals at similar rates than α -tocopherol in nonpolar solvents but not in hydrogen-bonding solvents. In solvents that are strong hydrogen bond acceptors, the rate constants of peroxy radicals with phenolic compounds dramatically decline and may even become undetectable⁵ (78). Polar solvents (a) interfere with the intramolecular stabilization (H-bonding) of the phenoxyl radical and (b) generate steric hindrance for the approach of the peroxy radical to the solvent-complexed phenol, which reduces the rate constant of H-atom abstraction. Such considerations become important in heterogeneous phases of lipid bilayers, where the localization of the phenolic groups will influence their effectiveness to trap peroxy radicals. In the case of LOO[•] generated in EYPC, an estimated second-order rate constant for the reaction with BTBE was obtained by oxygen consumption studies, using two different approaches considering independent “primary targets”, namely, unsaturated fatty acids ($k_{LH} \sim 10\text{--}50 \text{ M}^{-1} \text{ s}^{-1}$) and α -tocopherol [$k_{\alpha\text{-toc}} = 5 \times 10^5 \text{ M}^{-1} \text{ s}^{-1}$ (66)] (Figure 8). The estimated k_{BTBE} of $4.8 \times 10^3 \text{ M}^{-1} \text{ s}^{-1}$ is compatible with the redox properties

⁵ For instance, a decrease by a factor of 36 in the k value has been observed for the reaction of α -tocopherol with cumylperoxy radicals when changing from hexane to *tert*-butyl alcohol (78).

of tyrosine and the lack of an “induction period” in oxygen consumption studies when lipid peroxidation was initiated in BTBE-containing liposomes; this moderate rate constant (1/200 of that of α -tocopherol) is still larger than that of LOO[•] with LH [e.g., the reaction of linoleic acid peroxy radical with linoleic acid, $k = 36 \text{ M}^{-1} \text{ s}^{-1}$ in 70% EtOH (68)]. The reactions of halogenated organic peroxy radicals (known to be more reactive than LOO[•]) with tyrosine have been reported at alkaline pH, where most of the tyrosine is in the phenolate form ($pK_{\text{Tyr-OH}} \sim 10$), with values approaching $10^8 \text{ M}^{-1} \text{ s}^{-1}$ (79). Oxidation of the protonated form of the phenol by peroxy radicals (as expected at neutral pH or when inside a hydrophobic structure) is significantly less favorable, in full agreement with the k_{BTBE} value in the range of $10^3 \text{ M}^{-1} \text{ s}^{-1}$ obtained.

In a previous work (57), the nitration of a transmembrane peptide containing tyrosine in position eight from the C terminus (ca. Y-8 at a depth of $\sim 20 \text{ \AA}$ from the surface) induced by the peroxynitrite donor 3-morpholinopyridone hydrochloride (SIN-1) was progressively inhibited with increasing unsaturation degree of the DLPC:PLPC mixtures. A closer look to the data indicates that the extent of inhibition was significantly less than that predicted by a simple competition of Y-8 with unsaturated fatty acids [e.g., at 40% liposome unsaturation and considering the reported rate constant values for hydroxyl radical and nitrogen dioxide-dependent fatty acid and tyrosine oxidation (Table 2), over 90% inhibition of tyrosine oxidation would be expected, but only 40% inhibition was actually observed].

The relative yields of tyrosine dimerization and oxidation are largely affected by the biomembrane structure (41–43, 80), and we have estimated a diffusion coefficient (D) for BTBE in PC liposomes as ca. $5 \mu\text{m}^2 \text{ s}^{-1}$ (41). Thus, the rate constant value is lowered 100–200-fold ($k \sim 1\text{--}2 \times 10^6 \text{ M}^{-1} \text{ s}^{-1}$) with respect to the corresponding one of Tyr ($k = 2.25 \times 10^8 \text{ M}^{-1} \text{ s}^{-1}$). Intermolecular tyrosine dimerization will be even less likely in integral peptides and proteins as D values become $>10^3\text{--}10^4$ times smaller than in solution depending on protein size (e.g., $D \sim 0.1\text{--}0.5 \mu\text{m}^2 \text{ s}^{-1}$) (81, 82) and in line with the lack of tyrosine dimerization on transmembrane peptides treated with peroxynitrite (57). On the other hand, [•]NO₂ concentrates to some extent in hydrophobic environments (83), and the D value (D [•]NO₂) is $\sim 1500 \mu\text{m}^2 \text{ s}^{-1}$, very close to that of the aqueous phase of $4500 \mu\text{m}^2 \text{ s}^{-1}$ (84); thus, nitration in membranes is not kinetically impeded, a concept that is in perfect agreement with the large 3-nitro-BTBE/3,3'-diBTBE ratios found during peroxynitrite exposures.

Significant evidence supports that lipid peroxidation and tyrosine oxidation processes are associated with oxidative stress-related processes and pathophysiology (31, 43, 85, 86); for instance, membrane protein tyrosine (and BTBE) oxidation and nitration were evidenced in red blood cells exposed to peroxynitrite, in a process that was inhibited under low oxygen tensions (43). In a related way, accumulation of protein 3-nitro-Tyr and 4-hydroxynonenal protein adducts has been simultaneously detected in liver and kidney in a model of type I diabetes where peroxynitrite has been identified as a key mediator of lipid peroxidation (86). Future work should address whether both processes in vivo are mechanistically linked as suggested by our in vitro model studies. Our data also indicate that α -tocopherol can potentially modulate tyrosine oxidation yields in membranes by inhibiting lipid peroxidation. In this regard, it is important to consider that the extent of inhibition is a function of α -tocopherol levels that under biologically relevant

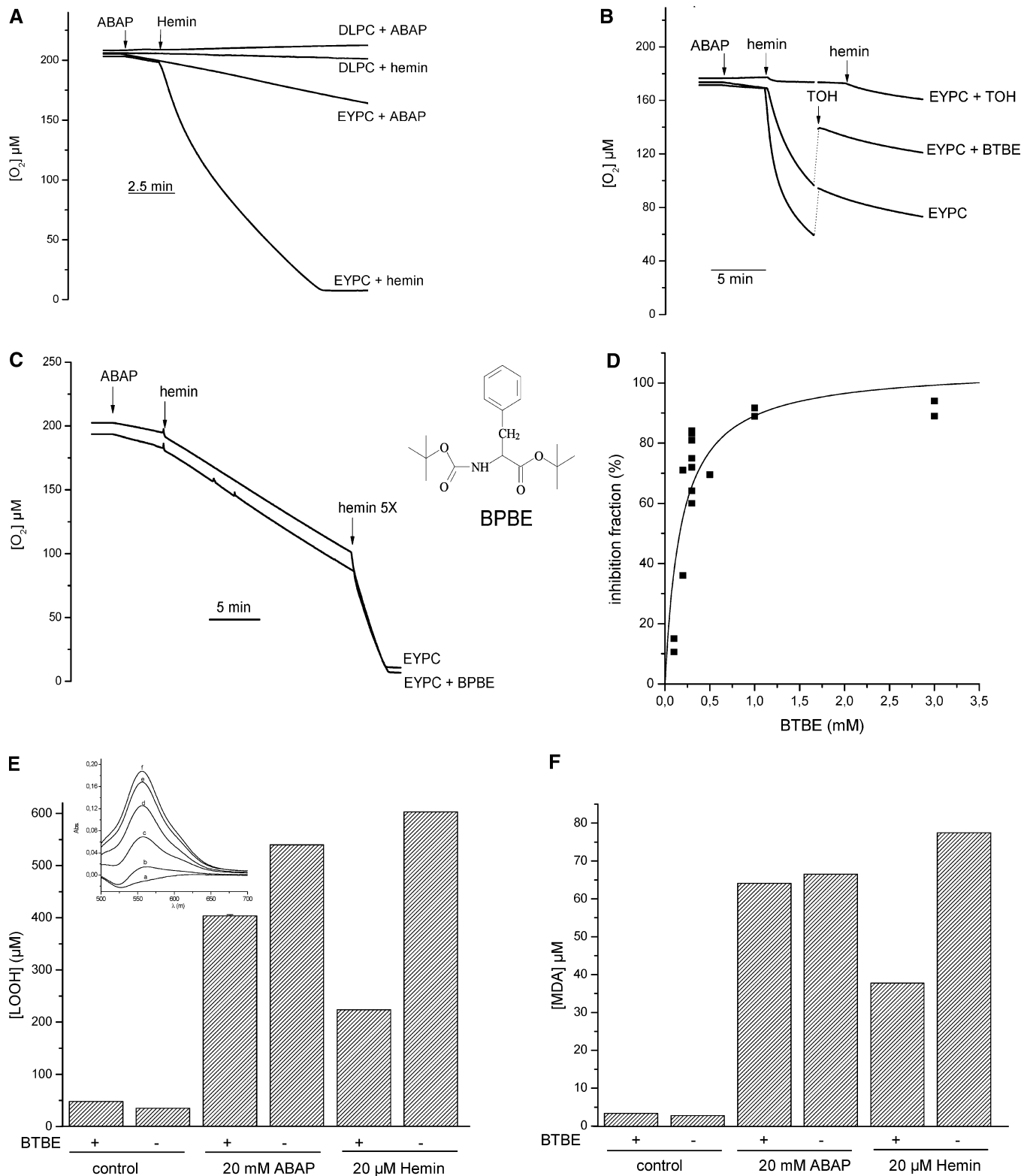


Figure 8. Oxygen consumption studies. Oxygen consumption was measured in a 2K Oxygraph to assess ABAP- (10 mM) and hemin- (1 μ M) induced lipid peroxidation in 100 mM sodium phosphate (pH 7.3) plus 0.1 mM DTPA. (A) EYPC and DLPC liposomes (6.25 mM). (B) BTBE (0.3 mM) or α -tocopherol (0.3 mM) containing EYPC liposomes. The arrow indicates the exogenous addition of 0.25 mM α -tocopherol; the transient increase in oxygen levels observed in this record is due to oxygen dissolved in the volume of reagent added (C) BPBE (0.3 mM) and control EYPC liposomes. (D) EYPC liposomes in the absence and presence of different concentrations of BTBE (0.1–3 mM) were exposed to ABAP (10 mM) and hemin (1 μ M), and oxygen consumption inhibition was evaluated as a function of BTBE concentration. (E) EYPC liposomes with or without BTBE (0.3 mM) were exposed to hemin (30 min) and ABAP (2.5 h), and the lipid hydroperoxide content was measured. Inset: UV-vis spectra of the same samples shown in E: (a) –BTBE, (b) +BTBE, (c) +BTBE + hemin, (d) +BTBE + ABAP, (e) –BTBE + ABAP, and (f) –BTBE + hemin. (F) The same samples as panel E in which the MDA content was measured. The structure of BPBE is indicated in the corresponding panel.

conditions [ca. 1 molecule of α -tocopherol per 100–1000 molecules of membrane phospholipid (87)] may not be sufficient

to fully prevent tyrosine oxidation events in either biomembranes (43, 86) or model membranes (this work, see Figure 7A at 0–0.3

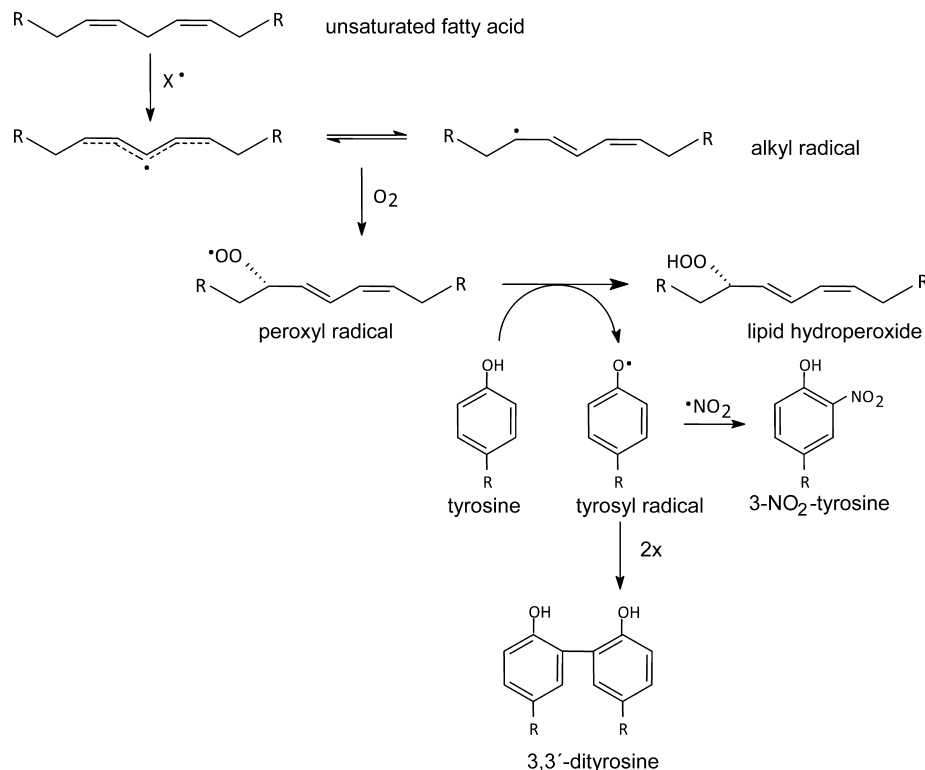


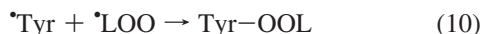
Figure 9. Proposed reaction mechanism by which LOO[•] participate in tyrosine oxidation.

mM α -tocopherol for 30 mM DLPC). Thus, we predict that an increase of cell/tissue levels of α -tocopherol should result in attenuation of protein tyrosine oxidation in both biomembranes and lipoproteins.

In addition to lipid peroxidation products, other side reactions take place on lipid radical intermediates when peroxynitrite and/or [•]NO₂ are present, leading to the formation of small amounts of nitrated lipids (88) (eq 9)



Additionally, a termination reaction between [•]LOO and [•]Tyr may occur yielding Diels–Alder-type structures (89) (eq 10):



Membrane phospholipids have a low *D* value (*D*_{PL} ca. 0.5–1 $\mu\text{m}^2 \text{s}^{-1}$ (81)), but because of their abundance, the formation of tyrosyl–phospholipid adducts is at least probable and deserves investigation in further studies.

In summary, the data presented herein support that [•]LOO participates in tyrosine oxidation processes in hydrophobic biocompartments and provides a new mechanistic insight to understand protein nitration in lipoproteins and biomembranes (Figure 9). Notably, cell and tissue oxygen levels become a previously unrecognized factor that will critically influence tyrosine oxidation yields via the intermediacy of LOO[•].

Acknowledgment. This work was supported by grants from the Howard Hughes Medical Institute and International Centre for Genetic Engineering and Biotechnology to R.R., National Institutes of Health to B.K. and R.R. (2 R01HL063119-05), and Agencia Nacional de Investigación e Innovación (ANII)/Fondo Clemente Estable to S.B. (FCE_362). S.B. was partially

supported by a fellowship of ANII. R.R. is a Howard Hughes International Research Scholar.

References

- (1) Bodaness, R. S., Leclair, M., and Zigler, J. S., Jr. (1984) An analysis of the H₂O₂-mediated crosslinking of lens crystallins catalyzed by the heme-undecapeptide from cytochrome c. *Arch. Biochem. Biophys.* 231, 461–469.
- (2) Giulivi, C., Traaseth, N. J., and Davies, K. J. (2003) Tyrosine oxidation products: analysis and biological relevance. *Amino Acids* 25, 227–232.
- (3) Heinecke, J. W. (2002) Tyrosyl radical production by myeloperoxidase: A phagocyte pathway for lipid peroxidation and dityrosine cross-linking of proteins. *Toxicology* 177, 11–22.
- (4) Hsiai, T. K., Hwang, J., Barr, M. L., Correa, A., Hamilton, R., Alavi, M., Rouhanizadeh, M., Cadenas, E., and Hazen, S. L. (2007) Hemodynamics influences vascular peroxynitrite formation: Implication for low-density lipoprotein apo-B-100 nitration. *Free Radical Biol. Med.* 42, 519–529.
- (5) Radi, R. (2004) Nitric oxide, oxidants, and protein tyrosine nitration. *Proc. Natl. Acad. Sci. U.S.A.* 101, 4003–4008.
- (6) Ischiropoulos, H. (2003) Biological selectivity and functional aspects of protein tyrosine nitration. *Biochem. Biophys. Res. Commun.* 305, 776–783.
- (7) Peluffo, G., and Radi, R. (2007) Biochemistry of protein tyrosine nitration in cardiovascular pathology. *Cardiovasc. Res.* 75, 291–302.
- (8) Reynolds, M. R., Berry, R. W., and Binder, L. I. (2007) Nitration in neurodegeneration: Deciphering the “Hows” “nYs”. *Biochemistry* 46, 7325–7336.
- (9) Shishebor, M. H., Aviles, R. J., Brennan, M. L., Fu, X., Goormastic, M., Pearce, G. L., Gokce, N., Keaney, J. F., Jr., Penn, M. S., Sprecher, D. L., Vita, J. A., and Hazen, S. L. (2003) Association of nitrotyrosine levels with cardiovascular disease and modulation by statin therapy. *J. Am. Med. Assoc.* 289, 1675–1680.
- (10) Beckman, J. S., Ischiropoulos, H., Zhu, L., van der Woerd, M., Smith, C., Chen, J., Harrison, J., Martin, J. C., and Tsai, M. (1992) Kinetics of superoxide dismutase- and iron-catalyzed nitration of phenolics by peroxynitrite. *Arch. Biochem. Biophys.* 298, 438–445.
- (11) Quijano, C., Hernandez-Saavedra, D., Castro, L., McCord, J. M., Freeman, B. A., and Radi, R. (2001) Reaction of peroxynitrite with Mn-superoxide dismutase. Role of the metal center in decomposition kinetics and nitration. *J. Biol. Chem.* 276, 11631–11638.

- (12) Quint, P., Reutzel, R., Mikulski, R., McKenna, R., and Silverman, D. N. (2006) Crystal structure of nitrated human manganese superoxide dismutase: Mechanism of inactivation. *Free Radical Biol. Med.* **40**, 453–458.
- (13) Pehar, M., Vargas, M. R., Robinson, K. M., Cassina, P., Diaz-Amarilla, P. J., Hagen, T. M., Radi, R., Barbeito, L., and Beckman, J. S. (2007) Mitochondrial superoxide production and nuclear factor erythroid 2-related factor 2 activation in p75 neurotrophin receptor-induced motor neuron apoptosis. *J. Neurosci.* **27**, 7777–7785.
- (14) Bathyany, C., Souza, J. M., Duran, R., Cassina, A., Cervenansky, C., and Radi, R. (2005) Time course and site(s) of cytochrome c tyrosine nitration by peroxynitrite. *Biochemistry* **44**, 8038–8046.
- (15) Cassina, A. M., Hodara, R., Souza, J. M., Thomson, L., Castro, L., Ischiropoulos, H., Freeman, B. A., and Radi, R. (2000) Cytochrome c nitration by peroxynitrite. *J. Biol. Chem.* **275**, 21409–21415.
- (16) Souza, J. M., Peluffo, G., and Radi, R. (2008) Protein tyrosine nitration—Functional alteration or just a biomarker? *Free Radical Biol. Med.* **45**, 357–366.
- (17) Estevez, A. G., Crow, J. P., Sampson, J. B., Reiter, C., Zhuang, Y., Richardson, G. J., Tarpey, M. M., Barbeito, L., and Beckman, J. S. (1999) Induction of nitric oxide-dependent apoptosis in motor neurons by zinc-deficient superoxide dismutase. *Science* **286**, 2498–2500.
- (18) Ischiropoulos, H., and Beckman, J. S. (2003) Oxidative stress and nitration in neurodegeneration: cause, effect, or association? *J. Clin. Invest.* **111**, 163–169.
- (19) Radi, R., Peluffo, G., Alvarez, M. N., Naviliat, M., and Cayota, A. (2001) Unraveling peroxynitrite formation in biological systems. *Free Radical Biol. Med.* **30**, 463–488.
- (20) Alvarez, B., Ferrer-Sueta, G., Freeman, B. A., and Radi, R. (1999) Kinetics of peroxynitrite reaction with amino acids and human serum albumin. *J. Biol. Chem.* **274**, 842–848.
- (21) Ferrer-Sueta, G., and Radi, R. (2009) Chemical biology of peroxynitrite: kinetics, diffusion, and radicals. *ACS Chem. Biol.* **4**, 161–177.
- (22) Bartasaghi, S., Ferrer-Sueta, G., Peluffo, G., Valez, V., Zhang, H., Kalyanaraman, B., and Radi, R. (2007) Protein tyrosine nitration in hydrophilic and hydrophobic environments. *Amino Acids* **32**, 501–515.
- (23) Santos, C. X., Bonini, M. G., and Augusto, O. (2000) Role of the carbonate radical anion in tyrosine nitration and hydroxylation by peroxynitrite. *Arch. Biochem. Biophys.* **377**, 146–152.
- (24) Bian, K., Gao, Z., Weisbrodt, N., and Murad, F. (2003) The nature of heme/iron-induced protein tyrosine nitration. *Proc. Natl. Acad. Sci. U.S.A.* **100**, 5712–5717.
- (25) Hazen, S. L., Zhang, R., Shen, Z., Wu, W., Podrez, E. A., MacPherson, J. C., Schmitt, D., Mitra, S. N., Mukhopadhyay, C., Chen, Y., Cohen, P. A., Hoff, H. F., and Abu-Soud, H. M. (1999) Formation of nitric oxide-derived oxidants by myeloperoxidase in monocytes: Pathways for monocyte-mediated protein nitration and lipid peroxidation In vivo. *Circ. Res.* **85**, 950–958.
- (26) Wu, W., Chen, Y., and Hazen, S. L. (1999) Eosinophil peroxidase nitrates protein tyrosyl residues. Implications for oxidative damage by nitrating intermediates in eosinophilic inflammatory disorders. *J. Biol. Chem.* **274**, 25933–25944.
- (27) Souza, J. M., Daikhin, E., Yudkoff, M., Raman, C. S., and Ischiropoulos, H. (1999) Factors determining the selectivity of protein tyrosine nitration. *Arch. Biochem. Biophys.* **371**, 169–178.
- (28) Abriata, L. A., Cassina, A., Tortora, V., Marin, M., Souza, J. M., Castro, L., Vila, A. J., and Radi, R. (2009) Nitration of solvent-exposed tyrosine 74 on cytochrome c triggers heme iron-methionine 80 bond disruption. Nuclear magnetic resonance and optical spectroscopy studies. *J. Biol. Chem.* **284**, 17–26.
- (29) Mallozzi, C., Di Stasi, A. M., and Minetti, M. (1997) Peroxynitrite modulates tyrosine-dependent signal transduction pathway of human erythrocyte band 3. *FASEB J.* **11**, 1281–1290.
- (30) Robaszekiewicz, A., Bartosz, G., and Soszynski, M. (2008) N-chloroamino acids cause oxidative protein modifications in the erythrocyte membrane. *Mech. Ageing Dev.* **129**, 572–579.
- (31) Velsor, L. W., Ballinger, C. A., Patel, J., and Postlethwait, E. M. (2003) Influence of epithelial lining fluid lipids on NO(2)-induced membrane oxidation and nitration. *Free Radical Biol. Med.* **34**, 720–733.
- (32) Kaplan, P., Tatarikova, Z., Racay, P., Lehotsky, J., Pavlikova, M., and Dobrota, D. (2007) Oxidative modifications of cardiac mitochondria and inhibition of cytochrome c oxidase activity by 4-hydroxynonenal. *Redox Rep.* **12**, 211–218.
- (33) Murray, J., Taylor, S. W., Zhang, B., Ghosh, S. S., and Capaldi, R. A. (2003) Oxidative damage to mitochondrial complex I due to peroxynitrite: Identification of reactive tyrosines by mass spectrometry. *J. Biol. Chem.* **278**, 37223–37230.
- (34) Poderoso, J. J. (2009) The formation of peroxynitrite in the applied physiology of mitochondrial nitric oxide. *Arch. Biochem. Biophys.* **484**, 214–220.
- (35) Xu, S., Ying, J., Jiang, B., Guo, W., Adachi, T., Sharov, V., Lazar, H., Menzoiian, J., Knyushko, T. V., Bigelow, D. J., Schoneich, C., and Cohen, R. A. (2006) Detection of sequence-specific tyrosine nitration of manganese SOD and SERCA in cardiovascular disease and aging. *AJP-Heart* **290**, 2220–2227.
- (36) Shao, B., Bergt, C., Fu, X., Green, P., Voss, J. C., Oda, M. N., Oram, J. F., and Heinecke, J. W. (2005) Tyrosine 192 in apolipoprotein A-I is the major site of nitration and chlorination by myeloperoxidase, but only chlorination markedly impairs ABCA1-dependent cholesterol transport. *J. Biol. Chem.* **280**, 5983–5993.
- (37) Zhou, W., Milder, J. B., and Freed, C. R. (2008) Transgenic mice overexpressing tyrosine-to-cysteine mutant human alpha-synuclein: a progressive neurodegenerative model of diffuse Lewy body disease. *J. Biol. Chem.* **283**, 9863–9870.
- (38) Vadseth, C., Souza, J. M., Thomson, L., Seagraves, A., Nagaswami, C., Scheiner, T., Torbet, J., Vilaire, G., Bennett, J. S., Murciano, J. C., Muzykantov, V., Penn, M. S., Hazen, S. L., Weisel, J. W., and Ischiropoulos, H. (2004) Pro-thrombotic state induced by post-translational modification of fibrinogen by reactive nitrogen species. *J. Biol. Chem.* **279**, 8820–8826.
- (39) Lizarbe, T. R., Garcia-Rama, C., Tarin, C., Saura, M., Calvo, E., Lopez, J. A., Lopez-Otin, C., Folgueras, A. R., Lamas, S., and Zaragoza, C. (2008) Nitric oxide elicits functional MMP-13 protein-tyrosine nitration during wound repair. *FASEB J.* **22**, 3207–3215.
- (40) Moller, M. N., Li, Q., Lancaster, J. R., Jr., and Denicola, A. (2007) Acceleration of nitric oxide autoxidation and nitrosation by membranes. *IUBMB Life* **59**, 243–248.
- (41) Bartasaghi, S., Valez, V., Trujillo, M., Peluffo, G., Romero, N., Zhang, H., Kalyanaraman, B., and Radi, R. (2006) Mechanistic studies of peroxynitrite-mediated tyrosine nitration in membranes using the hydrophobic probe *N*-*t*-BOC-L-tyrosine *tert*-butyl ester. *Biochemistry* **45**, 6813–6825.
- (42) Zhang, H., Joseph, J., Feix, J., Hogg, N., and Kalyanaraman, B. (2001) Nitration and oxidation of a hydrophobic tyrosine probe by peroxynitrite in membranes: Comparison with nitration and oxidation of tyrosine by peroxynitrite in aqueous solution. *Biochemistry* **40**, 7675–7686.
- (43) Romero, N., Peluffo, G., Bartasaghi, S., Zhang, H., Joseph, J., Kalyanaraman, B., and Radi, R. (2007) Incorporation of the hydrophobic probe *N*-*t*-BOC-L-tyrosine *tert*-butyl ester to red blood cell membranes to study peroxynitrite-dependent reactions. *Chem. Res. Toxicol.* **20**, 1638–1648.
- (44) Radi, R., Beckman, J. S., Bush, K. M., and Freeman, B. A. (1991) Peroxynitrite-induced membrane lipid peroxidation: The cytotoxic potential of superoxide and nitric oxide. *Arch. Biochem. Biophys.* **288**, 481–487.
- (45) Buxton, G. V., Greenstock, C. L., Helman, W. P., and Ross, A. B. (1988) Critical review of rate constants for reactions of hydrated electrons, hydrogen atoms and hydroxyl radicals ($\text{OH}^\bullet/\text{O}^\bullet$) in aqueous solution. *J. Phys. Chem. Ref. Data* **17**, 513.
- (46) Prutz, W. A., Monig, H., Butler, J., and Land, E. J. (1985) Reactions of nitrogen dioxide in aqueous model systems: Oxidation of tyrosine units in peptides and proteins. *Arch. Biochem. Biophys.* **243**, 125–134.
- (47) Pryor, W. A., and Lightsey, J. W. (1981) Mechanisms of nitrogen dioxide reactions: initiation of lipid peroxidation and the production of nitrous acid. *Science* **214**, 435–437.
- (48) Lee, S. H., Oe, T., and Blair, I. A. (2001) Vitamin C-induced decomposition of lipid hydroperoxides to endogenous genotoxins. *Science* **292**, 2083–2086.
- (49) Niki, E., Yoshida, Y., Saito, Y., and Noguchi, N. (2005) Lipid peroxidation: mechanisms, inhibition, and biological effects. *Biochem. Biophys. Res. Commun.* **338**, 668–676.
- (50) Wilcox, A. L., and Marnett, L. J. (1993) Polyunsaturated fatty acid alkoxyl radicals exist as carbon-centered epoxyallylic radicals: A key step in hydroperoxide-amplified lipid peroxidation. *Chem. Res. Toxicol.* **6**, 413–416.
- (51) Spittler, G. (2006) Peroxyl radicals: inductors of neurodegenerative and other inflammatory diseases. Their origin and how they transform cholesterol, phospholipids, plasmalogens, polyunsaturated fatty acids, sugars, and proteins into deleterious products. *Free Radical Biol. Med.* **41**, 362–387.
- (52) Malencik, D. A., Sprouse, J. F., Swanson, C. A., and Anderson, S. R. (1996) Dityrosine: preparation, isolation, and analysis. *Anal. Biochem.* **242**, 202–213.
- (53) Radi, R., Beckman, J. S., Bush, K. M., and Freeman, B. A. (1991) Peroxynitrite oxidation of sulfhydryls. The cytotoxic potential of superoxide and nitric oxide. *J. Biol. Chem.* **266**, 4244–4250.
- (54) Beckman, J. S., Beckman, T. W., Chen, J., Marshall, P. A., and Freeman, B. A. (1990) Apparent hydroxyl radical production by peroxynitrite: Implications for endothelial injury from nitric oxide and superoxide. *Proc. Natl. Acad. Sci. U.S.A.* **87**, 1620–1624.
- (55) Koppenol, W. H., Moreno, J. J., Pryor, W. A., Ischiropoulos, H., and Beckman, J. S. (1992) Peroxynitrite, a cloaked oxidant formed by nitric oxide and superoxide. *Chem. Res. Toxicol.* **5**, 834–842.

- (56) Jiang, Z. Y., Woollard, A. C., and Wolff, S. P. (1991) Lipid hydroperoxide measurement by oxidation of Fe²⁺ in the presence of xylenol orange. Comparison with the TBA assay and an iodometric method. *Lipids* 26, 853–856.
- (57) Zhang, H., Bhargava, K., Keszler, A., Feix, J., Hogg, N., Joseph, J., and Kalyanaraman, B. (2003) Transmembrane nitration of hydrophobic tyrosyl peptides. Localization, characterization, mechanism of nitration, and biological implications. *J. Biol. Chem.* 278, 8969–8978.
- (58) Barber, D. J. W., and Thomas, J. K. (1978) Reactions of radicals with lecithin bilayers. *Radiat. Res.* 74, 51–65.
- (59) Feix, J. B., and Kalyanaraman, B. (1989) Spin trapping of lipid-derived radicals in liposomes. *Biochim. Biophys. Acta* 992, 230–235.
- (60) Bartesaghi, S., Peluffo, G., Zhang, H., Joseph, J., Kalyanaraman, B., and Radi, R. (2008) Tyrosine nitration, dimerization, and hydroxylation by peroxynitrite in membranes as studied by the hydrophobic probe *N*-*t*-BOC-L-tyrosine *tert*-butyl ester. *Methods Enzymol.* 441, 217–236.
- (61) Mossoba, M., Makino, K., and Riesz, P. (1982) Photoionization of aromatic amino acids in aqueous solutions. A spin-trapping and electron spin resonance study. *J. Phys. Chem.* 86, 3478–3483.
- (62) Goldstein, S., Czapski, G., Lind, J., and Merenyi, G. (2000) Tyrosine nitration by simultaneous generation of (•)NO and O(•) under physiological conditions. How the radicals do the job. *J. Biol. Chem.* 275, 3031–3036.
- (63) Rubbo, H., Denicola, A., and Radi, R. (1994) Peroxynitrite inactivates thiol-containing enzymes of *Trypanosoma cruzi* energetic metabolism and inhibits cell respiration. *Arch. Biochem. Biophys.* 308, 96–102.
- (64) Kalyanaraman, B., Mottley, C., and Mason, R. P. (1983) A direct electron spin resonance and spin-trapping investigation of peroxy free radical formation by hematin/hydroperoxide systems. *J. Biol. Chem.* 258, 3855–3858.
- (65) El-Agamey, A. (2009) Laser flash photolysis of new water-soluble peroxy radical precursor. *J. Photochem. Photobiol. A: Chem.* 203, 13–17.
- (66) Niki, E., Saito, T., Kawakami, A., and Kamiya, Y. (1984) Inhibition of oxidation of methyl linoleate in solution by vitamin E and vitamin C. *J. Biol. Chem.* 259, 4177–4182.
- (67) Davies, M. J., Forni, L. G., and Willson, R. L. (1988) Vitamin E analogue Trolox C. E.s.r. and pulse-radiolysis studies of free-radical reactions. *Biochem. J.* 255, 513–522.
- (68) Gebicki, J. M., and Bielski, B. H. J. (1981) *J. Am. Chem. Soc.* 103, 7020–7025.
- (69) Wayner, D. D., Burton, G. W., Ingold, K. U., and Locke, S. (1985) Quantitative measurement of the total, peroxy radical-trapping antioxidant capability of human blood plasma by controlled peroxidation. The important contribution made by plasma proteins. *FEBS Lett.* 187, 33–37.
- (70) Szabo, C., Ischiropoulos, H., and Radi, R. (2007) Peroxynitrite: biochemistry, pathophysiology and development of therapeutics. *Nat. Rev. Drug Discovery* 6, 662–680.
- (71) Rubbo, H., Radi, R., Anselmi, D., Kirk, M., Barnes, S., Butler, J., Eiserich, J. P., and Freeman, B. A. (2000) Nitric oxide reaction with lipid peroxy radicals spares alpha-tocopherol during lipid peroxidation. Greater oxidant protection from the pair nitric oxide/alpha-tocopherol than alpha-tocopherol/ascorbate. *J. Biol. Chem.* 275, 10812–10818.
- (72) Erben-Russ, M., Bors, W., and Saran, M. (1987) Reactions of linoleic acid peroxy radicals with phenolic antioxidants: A pulse radiolysis study. *Int. J. Radiat. Biol. Relat. Stud. Phys. Chem. Med.* 52, 393–412.
- (73) Pedrielli, P., Pedulli, G. F., and Skibsted, L. H. (2001) Antioxidant mechanism of flavonoids. Solvent effect on rate constant for chain-breaking reaction of quercetin and epicatechin in autoxidation of methyl linoleate. *J. Agric. Food Chem.* 49, 3034–3040.
- (74) Priyadarsini, K. I. (1997) Free radical reactions of curcumin in membrane models. *Free Radical Biol. Med.* 23, 838–843.
- (75) Priyadarsini, K. I., Guha, S. N., and Rao, M. N. (1998) Physicochemical properties and antioxidant activities of methoxy phenols. *Free Radical Biol. Med.* 24, 933–941.
- (76) Amorati, R., Catarzi, F., Menichetti, S., Pedulli, G. F., and Viglianisi, C. (2008) Effect of ortho-SR groups on O-H bond strength and H-atom donating ability of phenols: A possible role for the Tyr-Cys link in galactose oxidase active site? *J. Am. Chem. Soc.* 130, 237–244.
- (77) Foti, M., and Ruberto, G. (2001) Kinetic solvent effects on phenolic antioxidants determined by spectrophotometric measurements. *J. Agric. Food Chem.* 49, 342–348.
- (78) Valgimigli, L., Banks, J. T., Luszyk, J., and Ingold, K. U. (1999) Solvent effects on the antioxidant activity of vitamin E(1). *J. Org. Chem.* 64, 3381–3383.
- (79) Kapoor, S. K., and Gopinathan, C. (1992) Reactions of halogenated organic peroxy radicals with various purine derivatives, tyrosine and thymine: A pulse radiolysis study. *Int. Chem. Kinet.* 24, 1035–1042.
- (80) Lide, D. R. (1990) *Handbook of Chemistry and Physics*, 71st ed., CRC Press, Boca Raton, FL.
- (81) Sackmann, E., Trauble, H., Galla, H., and Overath, P. (1973) Lateral diffusion, protein mobility and phase transitions in *Escherichia coli* membranes. A spin label study. *Biochemistry* 12, 5360–5369.
- (82) Vanderkooij, J., Fischkoff, S., Chance, B., and Cooper, R. A. (1974) Fluorescent probe analysis of the lipid architecture of natural and experimental cholesterol-rich membranes. *Biochemistry* 13, 1589–1595.
- (83) Moller, M. N., Li, Q., Vitturi, D. A., Robinson, J. M., Lancaster, J. R., Jr., and Denicola, A. (2007) Membrane “lens” effect: Focusing the formation of reactive nitrogen oxides from the *NO/O₂ reaction. *Chem. Res. Toxicol.* 20, 709–714.
- (84) Moller, M., Botti, H., Batthyany, C., Rubbo, H., Radi, R., and Denicola, A. (2005) Direct measurement of nitric oxide and oxygen partitioning into liposomes and low density lipoprotein. *J. Biol. Chem.* 280, 8850–8854.
- (85) Hamilton, R. T., Asatryan, L., Nilsen, J. T., Isas, J. M., Gallaher, T. K., Sawamura, T., and Hsiai, T. K. (2008) LDL protein nitration: implication for LDL protein unfolding. *Arch. Biochem. Biophys.* 479, 1–14.
- (86) Stadler, K., Bonini, M. G., Dallas, S., Jiang, J., Radi, R., Mason, R. P., and Kadiiska, M. B. (2008) Involvement of inducible nitric oxide synthase in hydroxyl radical-mediated lipid peroxidation in streptozotocin-induced diabetes. *Free Radical Biol. Med.* 45, 866–874.
- (87) Atkinson, J., Epand, R. F., and Epand, R. M. (2008) Tocopherols and tocotrienols in membranes: A critical review. *Free Radical Biol. Med.* 44, 739–764.
- (88) Rubbo, H., Radi, R., Trujillo, M., Telleri, R., Kalyanaraman, B., Barnes, S., Kirk, M., and Freeman, B. A. (1994) Nitric oxide regulation of superoxide and peroxynitrite-dependent lipid peroxidation. Formation of novel nitrogen-containing oxidized lipid derivatives. *J. Biol. Chem.* 269, 26066–26075.
- (89) Masuda, T., Bando, H., Maekawa, T., Takeda, Y., and Yamaguchi, H. (2000) A novel radical terminated compound produced in the antioxidation process of curcumin against oxidation of a fatty acid ester. *Tetrahedron Lett.* 41, 2157–2160.
- (90) Solar, S., Solar, W., and Getoff, N. (1984) Reactivity of OH with tyrosine in aqueous solution studied by pulse radiolysis. *J. Phys. Chem.* 88, 2091–2095.
- (91) Jin, F., Leitich, J., and Sonntag, C. v. (1993) *J. Chem. Soc., Perkin Trans. 2* 1583–1588.
- (92) Babbs, C. F., and Steiner, M. G. (1990) Simulation of free radical reactions in biology and medicine: A new two-compartment kinetic model of intracellular lipid peroxidation. *Free Radical Biol. Med.* 8, 471–485.

TX900446R

In this issue

Tyrosine versus Lipids

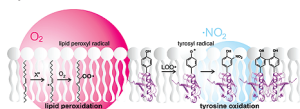
The tyrosine residues of proteins are vulnerable to one electron oxidation during periods of oxidative stress. The resulting tyrosyl radical (\bullet Tyr) can undergo further reactions, including dimerization, yielding 3,3'-di-tyrosine, and addition with species such as \bullet NO₂, which yields 3-nitro-tyrosine (3-NT). 3-NT is an established biomarker for conditions of oxidative and nitrosative stress, such as inflammation, cardiovascular disease, and neurodegeneration.

Most studies of \bullet Tyr formation and reactivity have been carried out in aqueous solution, ignoring the fact that many vulnerable protein tyrosine residues are localized within the hydrophobic regions of cellular membranes. Membrane polyunsaturated fatty acids (PUFAs) are highly susceptible to free radical oxidations that would be expected to influence Tyr oxidation. Now Bartesaghi et al. (p 821) explore \bullet Tyr chemistry in a lipid environment using *N*- γ -BOC L-tyrosine *tert*-butyl ester (BTBE), a hydrophobic Tyr analogue, incorporated into phospholipid liposomes.

Using peroxynitrite as oxidant, Bartesaghi et al. found that BTBE oxidation to 3,3'-di-BTBE or to 3-nitro-BTBE occurred regardless of the PUFA content of the liposomes. Lipid peroxidation also occurred in PUFA-containing liposomes as indicated by the generation of lipid peroxides and malondialdehyde (MDA). Electron spin resonance studies confirmed the presence of both tyrosyl and lipid-derived radicals. Lipid and BTBE oxidation were both

inhibited by low (O₂) or the addition of α -tocopherol.

These results indicate that PUFAs do not prevent Tyr oxidation by acting as free radical scavengers and suggest that lipid peroxy radicals (LOO \bullet), formed during PUFA oxidation in the presence of O₂, actually promote \bullet Tyr formation. This hypothesis was supported by the finding that hemin and 2,2'-azobis-(2-amidino-propane) hydrochloride (ABAP), both of which generate peroxy radicals, promoted BTBE oxidation in liposomes.



Bartesaghi et al. showed that BTBE suppresses O₂ consumption in ABAP- or hemin-treated PUFA-containing liposomes, indicating that BTBE competes with PUFAs for reaction with LOO \bullet . They used these data to calculate the rate constant for the reaction of BTBE with LOO \bullet , showing that this reaction is faster than the reaction of LOO \bullet with another PUFA. The results clearly demonstrate that Tyr oxidation can take place in a lipid environment as an oxygen-dependent pathway that connects lipid peroxidation to processes that lead to oxidative protein modifications.

The Trouble With Chlorine

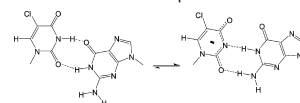
During the inflammatory response, leukocytes produce reactive species, including O₂⁻, H₂O₂, and HOCl that are directed toward killing the invading pathogen. However, these species also nonspecifically react with host cell components, leading to toxic damage. The

most likely product of the reaction of HOCl with nucleic acids in vivo is 5-chlorouracil (CIU). Since cells in culture metabolize 5-chloro-2'-deoxyuridine (CldU) and incorporate it into DNA, Kim et al. (p 740) explored the DNA polymerase-directed coding properties of CIU and its susceptibility to repair by the human selective monofunctional uracil-DNA glycosylase-1 (hSMUG1).

Mass spectrometry experiments confirmed that human K-562 cells incorporate CldU from culture medium into DNA. Following two cell doublings in the presence of 10 μ M CldU, the ratio of CIU to T in K-562 DNA was 0.89:1. These cells showed little evidence of toxicity, suggesting that CIU substitutes for T in vivo.

Using human DNA polymerase β , avian myeloblastosis virus reverse transcriptase, and *E. coli* Klenow fragment (exo-) as model human, viral, and prokaryotic polymerases, respectively, Kim et al. explored the ability of each enzyme to incorporate dATP versus dGTP across from CIU in a

synthetic template primer oligonucleotide. They found that, for all three polymerases, the k_{cat}/K_m for incorporation of dATP was approximately 4 orders of magnitude greater than that for dGTP, indicating that CIU is primarily recognized as T. However, increasing the pH of the incubation medium from 6.5 to 8.5 increased the tendency of the polymerases to misincorporate dGTP. Kim et al. explained this finding on the basis of the electron-withdrawing properties of Cl in CIU, which increase the acidity of the N1 and N3 protons. Ionization at these positions with increasing pH allows CIU to form a stable base pair with G that has similar geometry to a normal Watson-Crick pair.



Studies using a well-characterized CIU-containing oligonucleotide duplex as substrate revealed that CIU is subject to hydrolysis by hSMUG1 when paired with G, but not when paired with A. Since pairing of CIU with

Special Features

Many human disorders of toxicologic origin result from a complex interplay among genetic, chemical, and physiological factors. Dissecting the contributions of each of these factors can be a daunting task. Editorial Advisory Board member Andrew Smith (Smith and Elder, p 712) now reports on such an effort. Using porphyria cutanea tarda as a model, Smith and Elder demonstrate how a genetically determined enzyme deficiency combines with exposures to external toxicants to result in this disease of skin photosensitivity. Do not miss this fascinating story!

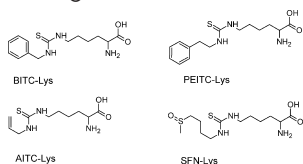
A is highly favored, these results suggest that CIU lesions are likely to persist *in vivo*. However, Kim et al. note that the repair of a CIU-G base pair by hSMUG1 will lead to the removal of the CIU and its replacement with C, resulting in a T to C transition. Together, these results provide an important foundation for understanding the implications of halogenated DNA damage *in vivo*.

Did You Eat Your Broccoli?

Diets rich in cruciferous vegetables are associated with a reduced risk of cancer. This benefit has been attributed to the vegetables' high levels of isothiocyanate glucosinolates (IGs). IGs are hydrolyzed by gut microflora to free isothiocyanates (ITCs), which have been shown to inhibit drug metabolizing enzymes, induce cell cycle arrest and apoptosis, and promote oxidative stress. How these activities contribute to ITCs' antitumor effects remains uncertain, but there is clearly a need for biomarkers of IG and ITC consumption so that their correlation with cancer prevention can be reliably assessed. Now Kumar and Sabbioni (p 756) have addressed this need.

The primary route of ITC metabolism is thiol conjugation with glutathione, producing *N*-acetylcysteine conjugates as the major urinary metabolites. These mercapturic acids have been used as biomarkers of ITC consumption, but they are unstable and reflect intake from only the past 24 h. To devise a better assay, Kumar and Sabbioni exploited the fact that ITC-thiol conjugates are revers-

ible, releasing free ITCs which are then available to react with proteins. Over time, protein conjugates become the major *in vivo* reservoir of ITCs, suggesting that these conjugates could serve as a biomarker of long-term ITC ingestion.



To test this hypothesis, Kumar and Sabbioni synthesized lysine conjugates of benzyl isothiocyanate (BITC), phenylethyl isothiocyanate (PEITC), allyl isothiocyanate (AITC), and D,L-sulforaphane (SFN). They also synthesized stable isotope-labeled conjugates using (¹³C₆¹⁵N₂)-lysine and the cysteine, valine, and aspartic acid conjugates of BITC. These compounds provided standards for the most likely products of the reaction of vegetable-derived ITCs with albumin (Alb) and hemoglobin (Hb).

With these tools in hand, Kumar and Sabbioni identified BITC-Lys in a Pronase E digest of Alb that had been reacted *in vitro* with BITC. Incubation of all four ITCs with Alb revealed a relative reactivity of BITC > PEITC > AITC > SFN, with the lysine conjugate identified as the major product for all.

Analysis of Alb from mice fed the acetyl-cysteine conjugate of PEITC revealed PEITC-Lys adducts. Similarly, BITC-Lys and PEITC-Lys were found in the Alb and Hb of a human volunteer following consumption of water cress plus garden cress, and SFN-Lys was detected following the consumption of broccoli. These species co-

incided with the main ITCs in the consumed vegetables. The Alb conjugates decreased in the blood with a half-life of approximately 21 days, similar to that of Alb.

The results support the use of ITC-lysine conjugates in Alb or Hb to monitor long-term ITC consumption. These reliable biomarkers will be valuable tools to fully assess the anticancer activity of dietary ITCs.

Lethal Touch

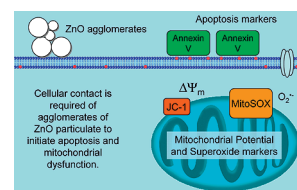
As nanomaterials appear in a growing number of consumer products, concerns about their toxicity intensifies. Oxides of Zn, Ti, and Si are commonly found in foods and cosmetics, so their gastrointestinal toxicity is of particular relevance. Consequently, Moos et al. (p 733) have explored the mechanisms of toxicity of ZnO nanoparticles in human colon-derived RKO cells.

Moos et al. investigated a commercial preparation of ZnO nanoparticles (nZnO) and a second preparation (mZnO), defined by their mesh cut size. Although mZnO contained particles from <100 nM to >1 μM, the ratio of surface area of nZnO to mZnO was 7.5:1, confirming a substantial difference in average particle size. Both preparations formed 500–2000 nm aggregates in the cell culture medium.

When applied directly to cells, nZnO (LC₅₀ = 15 μg/cm²) was approximately twice as toxic as mZnO (LC₅₀ = 29 μg/cm²), indicating some effect of particle size or geometry on toxicity. Toxicity occurred at particle exposures that might be expected from accidental ingestion of ZnO-contain-

ing sunscreen. When cells were separated from the particles by a dialysis membrane or a Transwell membrane, no toxicity was observed, indicating that direct contact between the cells and particles was required. Staining cells with propidium iodide and annexin V following treatment with toxic concentrations of nZnO or mZnO suggested that cell death was primarily the result of apoptosis. Further studies using the fluorescent dye JC-1 indicated a loss of mitochondrial membrane potential, and mitoSOX red staining revealed increased levels of O₂⁻ production in the toxic cells.

Similar concentrations of Zn²⁺ appeared in the culture medium of cells incubated in direct contact with particles or separated from particles in the Transwell apparatus. This observation, coupled with the failure to elicit toxic responses in the presence of comparable concentrations of Zn²⁺ alone, indicated that particle-induced toxicity was not the result of solubilization to yield the free metal ion.



Together, the data suggest a strong role for direct cell contact in mediating nZnO and mZnO toxicity. It remains to be seen whether particle uptake is also required, but these studies provide important clues to the mechanisms of toxicity of these common materials.

TX100055Q

**Nitrotyrosine: Quantitative analysis, mapping in proteins
and biological significance**

By José M. Souza^{1,2}, Silvina Bartesaghi^{1,2,3}, Gonzalo
Peluffo^{1,2} and Rafael Radi^{1,2,*}.

¹Departamento de Bioquímica, ²Center for Free Radical and
Biomedical Research and ³Departamento de Histología y
Embriología, Facultad de Medicina, Universidad de la
República.

* To whom correspondence should be addressed: Dr. Rafael
Radi, Departamento de Bioquímica, Facultad de Medicina,
Universidad de la República, General Flores 2125, 11800,
Montevideo, Uruguay, e-mail: rradi@fmed.edu.uy.

Telephone (5982) 9249561

FAX (5982)9249563.

Running title: Nitrotyrosine measurements

Nitric Oxide Redox Biochemistry in Lipid Environments

Andrés Trostchansky^{1,2}, Matías N. Möller^{2,4}, Silvina Bartesaghi¹⁻³, Horacio Botti^{2,5}, Ana Denicola^{2,4}, Rafael Radi^{1,2} and Homero Rubbo^{1,2}

¹Departamento de Bioquímica, Facultad de Medicina

²Center for Free Radical and Biomedical Research

³Departamento de Histología y Embriología, Facultad de Medicina

⁴Laboratorio de Fisiología Biológica, Facultad de Ciencias, Universidad de la República

⁵Unidad de Cristalografía de Proteínas, Instituto Pasteur de Montevideo, Uruguay

SUMMARY

Protein as well as lipid oxidation and nitration represent key signaling and injury processes during nitro-oxidative conditions. In this chapter, we emphasize the chemistry and physical interactions of nitric oxide and reactive nitrogen species within lipid environments, i.e. cell membranes and lipoproteins. The key reactions of reactive nitrogen species in lipid milieu are discussed, including nitric oxide autoxidation, peroxyxynitrite homolysis, tyrosine nitration and lipid-protein adduct formation in biologically relevant systems. Mechanisms of nitrotyrosine and nitro-fatty acid formation in membranes and cells are also discussed along with their key biological and redox signaling actions.

Keywords: nitric oxide, peroxyxynitrite, reactive nitrogen species, nitration, LDL, nitro-fatty acids, nitrotyrosine, inflammation

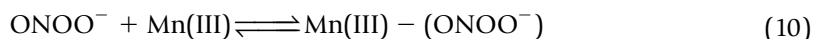
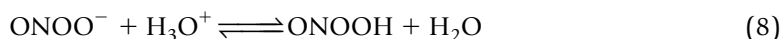
CHEMISTRY OF NITRIC OXIDE AND REACTIVE NITROGEN SPECIES

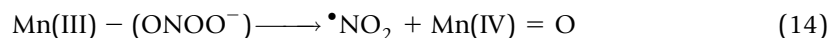
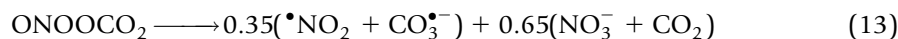
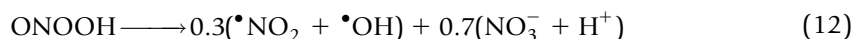
Nitric oxide (nitrogen monoxide, $\cdot\text{NO}$) is produced by the aerobic oxidation of *L*-arginine catalyzed by nitric oxide synthases (Alderton et al., 2001). It is found as a gas in its standard state and has a low solubility in water (1.95 mM atm^{-1} at 25°C) (Shaw and Vosper, 1977; Zacharia and Deen, 2005). It has a bond length of 115.1 pm and a bond order of 2.5 due to the presence of an unpaired electron in an antibonding π^* molecular orbital (Radi, 1996). This radical reacts exclusively with other paramagnetic species, such as other radicals or metal centers (Radi, 1996). The rates of reaction are usually fast, approaching the diffusion

limit for some radicals, while reactions with metal centers and metal-bound oxygen occur more slowly (for oxyhemoglobin, Eq. (2), $k = 8.9 \times 10^7 \text{ M}^{-1} \text{ s}^{-1}$) (Czapski and Goldstein, 1995; Herold et al., 2001; Nauser and Koppenol, 2002; Padmaja and Huie, 1993). It can also react with dioxygen (O_2 ; $\bullet\text{NO}$ autoxidation) in an overall third-order reaction ($k = 1.5\text{--}3 \times 10^6 \text{ M}^{-2} \text{ s}^{-1}$) (Awad and Stanbury, 1993; Ford et al., 1993; Goldstein and Czapski, 1995) to yield nitrogen dioxide ($\bullet\text{NO}_2$). Supposed elementary steps are described in Eqs. (3)–(5) (Goldstein and Czapski, 1995). Nitrous anhydride (N_2O_3) is an additional intermediate in $\bullet\text{NO}$ autoxidation (Eq. 6), while nitrite (NO_2^-) is the major final product in water (Eq. 7).

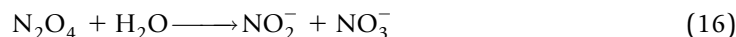


The reaction of $\bullet\text{NO}$ with the superoxide anion ($\text{O}_2^{\bullet-}$; Eq. 1) is extremely fast and approaches the diffusion limit ($k = 4.3\text{--}20 \times 10^9 \text{ M}^{-1} \text{ s}^{-1}$) (Czapski and Goldstein, 1995; Nauser and Koppenol, 2002). The product of this reaction is peroxynitrite anion (ONOO^-), which can yield a variety of potent oxidants (Radi et al., 2000). The chemistry of peroxynitrite is complex and was analyzed by us in detail in the first edition of this book (Radi et al., 2000). Briefly, peroxynitrite anion is a rather stable molecule at alkaline pH but can react with Lewis acids, i.e. H_3O^+ or CO_2 , and electrophilic transition metal centers (Eqs. 8–10) leading to kinetically distinguishable direct and indirect pathways of target molecule oxidation. At $\text{pH} < 9$ peroxynitrite anion is in rapid equilibrium with peroxynitrous acid ($\text{pK}_a = 6.8$, Eq. 8). The latter reacts selectively with nucleophiles, more rapidly with thiols, through overall second-order 'direct' reactions (Eq. 11). Distinctly, the addition of peroxynitrite anion to Lewis acids destabilizes the peroxy (O-O) bond allowing 'indirect' homolytic pathways to take place (Eqs. 12–14), which are zero order in target molecule at high target concentrations. Indirect oxidations elicited by peroxynitrite in the presence of H_3O^+ , CO_2 and electrophilic transition metal centers are of a radical nature, and typically involve $\bullet\text{NO}_2$, hydroxyl radical ($\bullet\text{OH}$), carbonate radical ($\text{CO}_3^{\bullet-}$) or metal-bound oxygen radicals ($\text{M} = \text{O}^\bullet$) which are formed, with characteristic yields, as proximal oxidants (Eqs. 12–14).





Nitrogen dioxide is not only a product of the homolysis of peroxyxynitrite derivatives but also a product of •NO autoxidation and NO_2^- oxidation by metalloperoxidases (Augusto et al., 2002). It has a dipole moment of 0.289 D (Heitz et al., 1991) and low solubility in water (10–14 mM atm⁻¹ at 20 °C) (Cheung et al., 2000). The N–O bond length is 119.7 pm, with a bond angle of 134.3 °. The unpaired electron is delocalized through the three atoms, but the higher spin density is located at the nitrogen (Augusto et al., 2002). Nitrogen dioxide is a potent oxidizing molecule ($E^\circ = 1.04 \text{ V}$) (Stanbury, 1989) which can react with a variety of targets at moderately high rates (Augusto et al., 2002; Huie, 1994). Nitrogen dioxide can dimerize to form N_2O_4 (Eq. 15, in water at 20 °C, $K = 6\text{--}6.5 \times 10^4 \text{ M}^{-1}$) which is rapidly hydrolyzed to NO_2^- and nitrate (NO_3^- ; Eq. 16, $k = 1 \times 10^3 \text{ s}^{-1}$) (Augusto et al., 2002; Cheung et al., 2000). Since $K \cong 6.2 \times 10^4 \text{ M}^{-1}$, most of the oxidative potency of •NO₂ at low concentrations can be ascribed to •NO₂ itself.



Nitrogen dioxide is involved in the formation of NO_2^- and a reaction with target molecules which can then undergo further reaction to yield oxidation, nitrosation, dimerization and nitration products (Augusto et al., 2002).

The hydroxyl radical is an extremely reactive short-lived radical. It can oxidize practically any molecule at near diffusion-controlled rates. In cells, the high abundance of targets and the high reactivity of •OH restricts its radius of reaction to three to four molecular diameters from the site of its formation (Hutchinson, 1957). The carbonate radical is a bulky and charged molecule with a very low pK_a ($\text{pK}_a = 0$; Augusto et al., 2002) which cannot penetrate into lipid membranes and reduces lipid oxidation by peroxyxynitrite (Botti et al., 2004a; Khairutdinov et al., 2000; Romero et al., 1999). However, $\text{CO}_3^{\bullet-}$ aids in membrane or lipoprotein surface protein oxidation and nitration by peroxyxynitrite (Botti et al., 2005; Romero et al., 2007).

PHYSICAL INTERACTIONS OF NITRIC OXIDE AND REACTIVE NITROGEN SPECIES WITH LIPID MEMBRANES AND LIPOPROTEINS

The main function of lipid membranes is to separate and regulate the content of the cell interior. For many substances, lipid membranes function as an effective barrier preventing free transport in and out of the cell. The permeability of a membrane (P_m) to the different molecules depends on the solubility of the molecule in the membrane (K_p) and the diffusivity of

the molecule across the membrane (D_m). According to the simple diffusion–solubility theory, the relation between these parameters is (Diamond and Katz, 1974; Lieb and Stein, 1986):

$$P_m = \frac{K_p D_m}{\delta_m} \quad (17)$$

where δ_m is the thickness of the membrane and D_m is more precisely the self-diffusion coefficient of the molecule in the lipid portion of the membrane in the normal direction to the bilayer. This widely accepted model assumes isotropic diffusion of the molecule in the membrane, a condition met by most lipid bilayers above the main transition temperature with a non-oversaturating cholesterol content (Fischkoff and Vanderkooi, 1975; Kusumi and Hyde, 1982; Subczynski et al., 1996), and also negligible interfacial resistance to solute movement (Zwolinski et al., 1949).

Both physical and chemical processes involving lipid environments will depend on the ability of $\bullet\text{NO}$ or reactive nitrogen species (RNS) to penetrate the membrane. Knowing P_m , K_p or D_m helps in obtaining a detailed mechanistic picture of these processes.

Solubility

K_p is the partition coefficient for the molecule between the membrane and the aqueous phase (Eq. 18), i.e. the equilibrium constant that relates the concentrations of the molecule inside and outside the membrane.

$$K_p = \frac{[\text{NO}]_m}{[\text{NO}]_{\text{aq}}} \quad (18)$$

Early experiments showed that $\bullet\text{NO}$ solubility in organic solvents was, on average, eight times higher than in water (Malinski et al., 1993; Shaw and Vosper, 1977), suggesting that the solubility of $\bullet\text{NO}$ in membranes should also be high. More recently, it was shown that $\bullet\text{NO}$ is actually 3.6–4.4 times more soluble in membranes and 3.4 times more soluble in low density lipoprotein (LDL) than in water (Möller et al., 2005; Möller et al., 2008; Möller et al., 2007b). The higher concentration of $\bullet\text{NO}$ inside the membrane leads to an increase in reaction rates relative to the aqueous phase (the effective concentration is higher), which is best exemplified by the acceleration of $\bullet\text{NO}$ autoxidation by membranes ('lens effect', see below) (Liu et al., 1998b; Möller et al., 2007a; Möller et al., 2007b).

Data on $\bullet\text{NO}_2$ solubility in organic solvents are scarce due to its high reactivity. One report indicates that $\bullet\text{NO}_2$ is 1.5–1.9 times more soluble in organic solvents than in water (Mendiara and Perissinotti, 2003), suggesting that solubility in the membrane should be slightly higher or nearly the same as in water. Therefore, no significant acceleration of $\bullet\text{NO}_2$ reactions in the membrane due to a local concentration effect would be expected.

Determination of peroxyxynitrous acid solubility in organic solvents is difficult due to its high reactivity and short lifetime. Considering its high polarity and the low reported permeability coefficient across lipid bilayers (Khairutdinov et al., 2000; Marla et al., 1997; Möller et al., 2008) a low solubility would be expected, with $K_p^{\text{ONOOH}} < K_p^{\text{H}_2\text{O}} \cong 0.0005$.

It should be emphasized that a high solubility in a lipid environment does not mean that $\bullet\text{NO}$ or RNS will be 'stored' in lipids and live longer, since diffusion in and out of the lipid phase is very fast (Denicola et al., 1996; Subczynski et al., 1996).

Diffusion

The diffusion coefficient of $\bullet\text{NO}$ across the membrane (D_m) indicates how fast the molecule can travel due to random movements. Being uncharged, net transport of $\bullet\text{NO}$ will occur if differences in $\bullet\text{NO}$ chemical potential exist through space. In membranes and lipoproteins,

diffusion is usually slower than in aqueous solution due to the higher microviscosity, so that diffusion-controlled reactions will occur at a lower rate in lipid media. The experimental determination of the diffusion coefficient depends on •NO interaction with fluorescent or spin probes inserted in the membrane. The parameter readily available from these experiments is the apparent diffusion (D'_m), the product $K_p D_m$, because the change in local concentration of the molecule also affects the frequency of collisions.

Studying the quenching of fluorescence of pyrene derivatives located at different depths in the membrane by •NO, [Denicola et al. \(1996\)](#) found that D'_m for •NO at the interface and at the center of an egg yolk phosphatidylcholine membrane was $1.7 \times 10^{-5} \text{ cm}^2 \text{ s}^{-1}$ and $1.5 \times 10^{-5} \text{ cm}^2 \text{ s}^{-1}$, respectively. In erythrocyte membranes (ghosts) it was found that apparent diffusion was 2.6 times higher in the center of the bilayer than in the interface ($D'_m = 1.3 \times 10^{-5} \text{ cm}^2 \text{ s}^{-1}$ and $D'_m = 0.5 \times 10^{-5} \text{ cm}^2 \text{ s}^{-1}$, respectively) ([Denicola et al., 1996](#)). Using a similar approach, it was found that at 37°C D'_m in the center of dipalmitoyl- and dimiristoylphosphatidylcholine membranes was 0.7 and $1.1 \times 10^{-5} \text{ cm}^2 \text{ s}^{-1}$, respectively, and it decreased 25% in the presence of 30% cholesterol ([Miersch et al., 2008](#)). These apparent diffusion coefficients for •NO in membranes are only two to three times lower than the diffusion coefficient for •NO in water, $D_w = 2.2\text{--}4.5 \times 10^{-5} \text{ cm}^2 \text{ s}^{-1}$ ([Denicola et al., 1996](#); [Zacharia and Deen, 2005](#)), indicating that membranes are not important barriers to •NO diffusion.

Taking the average value for the apparent diffusion coefficient in membranes ($\sim 1 \times 10^{-5} \text{ cm}^2 \text{ s}^{-1}$) and using Eq. (19) relating the average displacement $\langle \bar{x} \rangle$ to D and time in three dimensions, we can estimate that •NO could travel 50–200 μm from its biological source (biological half-life for •NO = 0.5–5 s), a distance comparable to 5–20 times the mean diameter of a cell.

$$\langle \bar{x} \rangle = \sqrt{6Dt} \quad (19)$$

THE CASE OF LDL

The oxidation of LDL is related to the pathogenesis of atherosclerosis in ways that are still not fully understood. Nitric oxide is a potent inhibitor of LDL oxidation and may be an important antioxidant for LDL *in vivo* (see below). The main antioxidant in LDL, α -tocopherol (α -TOH), is mostly restricted to the outer phospholipid monolayer while the cholesteryl-ester rich core is devoid of this antioxidant. Fluorescence quenching experiments showed that •NO could easily get into the LDL core. The apparent diffusion of •NO in LDL's core was similar to that in the surface phospholipid monolayer ([Table 1](#)) and similar or just a half that in water ([Denicola et al., 2002](#)). Therefore, •NO would find little resistance to entering LDL's core and stopping its oxidation. Interestingly, oxidized LDL showed a higher apparent diffusion in both regions ([Table 1](#)), indicating that lipid peroxidation products lead to a looser lipoprotein structure, allowing for easier •NO penetration.

REAL DIFFUSION

Real diffusion, calculated for •NO based on the independently determined apparent diffusion coefficients and K_p in membranes and LDL, yielded interesting results on the mechanism of •NO diffusion in lipid milieu. It was found that $D_m = 3.9 \times 10^{-6} \text{ cm}^2 \text{ s}^{-1}$ in LDL and $D_m = 3.1 \times 10^{-6} \text{ cm}^2 \text{ s}^{-1}$ in egg yolk phosphatidylcholine membranes; just 6–12 times less than D_m in water ([Möller et al., 2005](#)). An intriguing matter was that microviscosity (η) in a lipid membrane is ~ 100 times higher than in water, and considering the Einstein-Stokes relation (Eq. 20) a much lower D_m was expected ($D \propto 1/\eta$):

$$D = \frac{k_B T}{6\pi r \eta} \quad (20)$$

Table 1 Apparent diffusion of $\bullet\text{NO}$ in native and oxidized LDL (Denicola et al., 2002)

	D'_{surface} ($10^{-5}\text{cm}^2\text{s}^{-1}$)	D'_{core} ($10^{-5}\text{cm}^2\text{s}^{-1}$)
Native LDL	2.3	1.7
Oxidized LDL	4.9	3.0

However, this difference can be reconciled after realizing that membranes and lipoproteins do not behave as *stokesian* media for small molecules (Fischkoff and Vanderkooi, 1975; Möller et al., 2005) and thus the diffusion is less sensitive to changes in local η . Considering small molecules like $\bullet\text{NO}$ in this kind of media, $D \propto 1/\eta^a$, where $a < 1$. Taking this into consideration, the influence of cholesterol in decreasing $\bullet\text{NO}$ apparent diffusion should be explained by a decrease in $\bullet\text{NO}$ solubility rather than significant changes in the real diffusion coefficient.

Permeability

P_m is the velocity at which the molecule crosses the membrane (it has units of distance over time, i.e. cm s^{-1}) and indicates how easy it is for the molecule to move across the membrane (in a direction normal to the membrane surface). Membrane permeability to $\bullet\text{NO}$ is so high that direct measurements are nearly impossible to perform, since almost inevitably the water layer surrounding the membrane offers a higher resistance to $\bullet\text{NO}$ transport than the membrane itself (Liu et al., 1998a, 2002). However, permeability data can be obtained from the apparent diffusion ($K_p D_m$) which can easily be converted to permeability using adequate assumptions and Eq. (17) or related expressions (Subczynski et al., 1996). As already mentioned, the apparent diffusion in phospholipid and erythrocyte membranes was only two to three times lower than in water (Denicola et al., 1996; Miersch et al., 2008). Using spin probes, it was calculated that permeability coefficients for $\bullet\text{NO}$ were 63 and 77 cm s^{-1} in phospholipid membranes with and without cholesterol, respectively; 30% greater than the permeability through an equally thick layer of water (Subczynski et al., 1996). Therefore, most biological membranes represent low barriers to $\bullet\text{NO}$ transport (Fig. 1), yet it may be significant. It has been observed that increasing the cholesterol content in the plasma membrane of fibroblasts leads to a lower activation of soluble guanylyl cyclase and a lower phosphorylation of the vasodilator-stimulated phosphoprotein by externally added $\bullet\text{NO}$, suggesting that altered membrane composition can modify cell responses to $\bullet\text{NO}$, possibly through changes in $\bullet\text{NO}$ permeability (Miersch et al., 2008).

Peroxynitrite crosses cell membranes via different routes (Fig. 1). Peroxynitrite anion can penetrate cells through anion exchangers, while peroxynitrous acid can cross through the lipid part by simple diffusion (Denicola et al., 1998). Due to its ionic nature, the permeability of pure lipid membranes to peroxynitrite anion is extremely low. On the other hand, peroxynitrous acid is able to cross pure lipid membranes at rates similar to that of water molecules ($P_m = 4\text{--}13 \times 10^{-4}\text{cm s}^{-1}$; Khairutdinov et al., 2000; Marla et al., 1997; Möller et al., 2008). It is $10^4\text{--}10^5$ times less permeant than $\bullet\text{NO}$, so it can be said that membranes offer a moderate barrier to peroxynitrous acid transport (Fig. 1) (Möller et al., 2008). This limitation may be of great relevance in light of the mechanisms of microbial adaptation to stress involving changes in membrane properties (lipid unsaturation, acyl chain length, etc.) (Branco et al., 2004).

Data on $\bullet\text{NO}_2$ permeability obtained from indirect experiments using peroxynitrite as a source of this radical indicate that its permeability is similar to or higher than that of peroxynitrous acid (Khairutdinov et al., 2000). Recently available data on $\bullet\text{NO}_2$ solubility in organic solvents indicate that $\bullet\text{NO}_2$ should be similarly or slightly more soluble in membranes than

in water, and therefore should have a permeability slightly lower than •NO (Mendiara and Perissinotti, 2003).

In summary, lipid membranes are very permeable to •NO and possibly to •NO₂, but less permeable to peroxynitrous acid (Fig. 1).

ERYTHROCYTE MEMBRANE PERMEABILITY TO NITRIC OXIDE

Many attempts have been made to determine the permeability of the erythrocyte membrane to •NO (Gorczyński et al., 2007; Liao et al., 1999; Liu et al., 2002; Liu et al., 2007). This parameter is of key importance in order to understand •NO bioactivity and metabolism in the vasculature. A more general model for non-electrolyte permeation is needed to explain •NO permeability across complex anisotropic media like the red blood cell membrane. Zwolinski et al. (1949) proposed a general equation for permeation through bilayer systems, integrating interfacial barriers (Eq. 21).

$$\frac{1}{P_b} = \frac{\delta}{K_p D_m} + \frac{2\lambda}{D_{sm}} \quad (21)$$

where P_b is the permeability constant of the lipid bilayer, δ and λ are the widths of the hydrocarbon core and of each interfacial region, respectively, and D_{sm} is the apparent diffusion coefficient across the interfacial region (which is due to phospholipid headgroup and hydration regions; and for the case of erythrocytes, it may reasonably include membrane-associated proteins and their effect upon phospholipid dynamics). Each term on the right represents in series resistances to diffusive transport due to the hydrophobic core (R_{hc}) and the interfacial zone (R_{sm}). Data of ours and other groups on the erythrocyte membrane can be used to calculate P_m according to this equation. Taking: $\lambda = 1.5$ nm, $\delta = 3$ nm (Hristova and White, 1998; Wiener and White, 1992), $K_p D_m = 1.3 \times 10^{-5} \text{ cm}^2 \text{ s}^{-1}$ (Denicola et al., 1996) and $D_{sm} = 5 \times 10^{-6} \text{ cm}^2 \text{ s}^{-1}$ (Denicola et al., 1996), we get $P_b \approx 12.0 \text{ cm s}^{-1}$. If we now include •NO transport through the glycocalix of the erythrocyte membrane with an apparent diffusion coefficient D_g , similar to that of •NO in water (D_w (37°C) = $3.4 \times 10^{-5} \text{ cm}^2 \text{ s}^{-1}$ (Liu et al., 2007)), we obtain an expression for the permeability of the erythrocyte membrane (Eq. 22):

$$\frac{1}{P_{em}} = \frac{\delta}{K_p D_m} + \frac{2\lambda}{D_{sm}} + \frac{\Lambda}{D_g} \quad (22)$$

where $\Lambda \cong 50$ nm (Sackmann, 1995). Using Eq. (22) we obtain $P_{em} = 4.3 \text{ cm s}^{-1}$. The contribution of the stagnant water layer or unstirred layer (UL) can also be calculated (Eq. 23):

$$\frac{1}{P_{app}} = \frac{\delta}{K_p D_m} + \frac{2\lambda}{D_{sm}} + \frac{\Lambda}{D_g} + \frac{UL}{D_w} \quad (23)$$

Most of the variability between reported values of the permeability constant of •NO through the erythrocyte boundaries can be ascribed to different sizes of the unilamellar liposomes (UL). In the work by Liu et al. (2007) electrochemical determinations of steady-state concentrations of •NO combined with mathematical modeling were used to determine $P_{em} = 4.5 \text{ cm s}^{-1}$, taking care of UL effects with UL values ranging from 2 from 4 μm and $D_w = 3.4 \times 10^{-5} \text{ cm}^2 \text{ s}^{-1}$ (37°C). Their results can thus be directly compared with our calculations of P_{em} . The reported values of permeability by Liao et al. (1999) that are almost two orders of magnitude lower than our calculated value for P_{em} could be explained considering

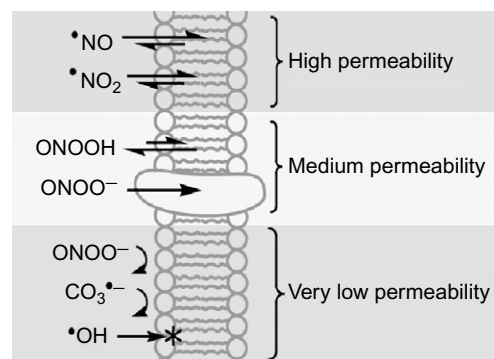


FIGURE 1

Permeability of a biological lipid membrane to •NO and derived reactive species. The permeability is related to the ability of the species to penetrate and react in the lipid environment. Peroxynitrite anion can cross lipid membranes such as red blood cell membranes through anion exchangers, but permeability through the lipid part is very low.

that the last term in Eq. 23 was not considered or evaluated separately. Actually, that low permeability constant is in reasonable agreement with calculated values of P_{app} considering $UL = 4 \mu\text{m}$ ($P_{app} = 0.08 \text{ cm s}^{-1}$).

To summarize, current knowledge supports the permeability of the erythrocyte membrane to $\bullet\text{NO}$ being comparable to that of a water layer of the same thickness (5.6 nm) (4.5 vs 6.1 cm s^{-1}). The resistance is distributed as follows: $R_{hc} < R_{sm} < R_g \ll R_{UL}$. Extracellular resistance is the main factor explaining diminished $\bullet\text{NO}$ inactivation by red blood cells compared to free oxyhemoglobin, as previously shown (Chen et al., 2006; Liu et al., 1998a, 2002). It is important to note that the value of $P_{em} = 4.3 \text{ cm s}^{-1}$ we calculate is independent of the oxygenation state of intra-erythrocytic hemoglobin, leaving unexplained the reported variations of P_{em} with $p\text{O}_2$ (Gorczynski et al., 2007).

REACTIONS OF REACTIVE NITROGEN SPECIES IN LIPID MILIEU

In lipid environments, where there is low polarity, high packing and high viscosity, the reactions of $\bullet\text{NO}$ and RNS will be distinct from those in the aqueous phase. Two kinds of effects may be expected, depending on the type of reaction. If the reaction is diffusion limited, the rate of reaction inside the lipid phase will be modified by $K_p D_m$ relative to D_w . If the reaction is activation controlled, the rate will be mainly affected by K_p . Table 2 shows a selected list of reactions involving RNS that are relevant within membranes. The reactions are classified on a kinetic basis as diffusion- or activation-controlled processes. Below we discuss in detail the cases of a) $\bullet\text{NO}$ autoxidation, b) peroxyxynitrous acid homolysis, c) $\bullet\text{NO}$ -mediated lipid oxidation inhibition, d) protein tyrosine nitration, and e) formation of covalent lipo-protein products.

Acceleration of nitric oxide autoxidation by membranes

Nitric oxide autoxidation is a complex third-order reaction, the elementary reactions of which have not been unambiguously identified, but a possible mechanism is described in Eqs. (3)–(5) (Goldstein and Czapski, 1995). This reaction is activation controlled, and membranes and lipoproteins have a dramatic effect on the rate of autoxidation (Liu et al., 1998b; Möller et al., 2007a,b). Liu et al. (1998b) found that the rate of $\bullet\text{NO}$ disappearance increased considerably after adding phospholipid or hepatocyte membranes. In a heterogeneous system containing lipids and water, the observed rate of $\bullet\text{NO}$ autoxidation will be a

Table 2 Diffusion- and activation-controlled reactions of $\bullet\text{NO}$ and RNS	
Diffusion controlled	Activation controlled
$r'_m = r_w K_p D_m / D_w$	$r'_m = r_w K_p$
$\bullet\text{NO} + \text{R}\bullet \rightarrow \text{RNO}$	$2 \bullet\text{NO} + \text{O}_2 \rightarrow 2 \bullet\text{NO}_2$
$\bullet\text{NO} + \text{LOO}\bullet \rightarrow \text{LOONO}$	$\text{ONOOH} \rightarrow \bullet\text{NO}_2 + \bullet\text{OH}$
$\bullet\text{NO}_2 + \text{LOO}\bullet \rightarrow \text{LOONO}_2$	$\bullet\text{NO}_2 + \text{LH} \rightarrow \text{L}\bullet / \text{NO}_2\text{-L}\bullet$
$\bullet\text{OH} + \text{LH} \rightarrow \text{L}\bullet + \text{H}_2\text{O}$	$\bullet\text{NO}_2 + \text{Tyr} \rightarrow \text{Tyr}\bullet + \text{HNO}_2$
$\bullet\text{NO} + \bullet\text{OOH} \rightarrow \text{ONOOH}$	$\text{CO}_3^{\bullet-} + \text{Tyr} \rightarrow \text{Tyr}\bullet + \text{HCO}_3^-$
$\bullet\text{NO}_2 + \text{Tyr}\bullet \rightarrow \text{NO}_2\text{-Tyr}$	
$\bullet\text{OH} + \text{Tyr} \rightarrow \text{Tyr}\bullet / \text{OH-Tyr}\bullet$	

Influence of changes in solubility (K_p) and diffusion (D) on the observed rate of reaction in lipid media (r'_m) relative to the reaction in water (r_w).

composite of the rate in water (Eq. 24; Goldstein and Czapski, 1995) and in the membrane, which can be expressed as Eq. 25:

$$\frac{-d[\text{NO}]}{dt} = 4k[\text{NO}]^2[\text{O}_2] \quad (24)$$

$$\frac{-d[\text{NO}]}{dt} = (1 + a(V_m/V_T))4k[\text{NO}]^2[\text{O}_2] \quad (25)$$

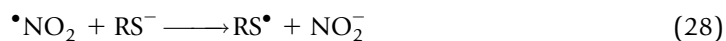
where V_m/V_T is the fractional volume occupied by the lipid and a the acceleration factor. The latter may be influenced by the higher concentration of both •NO and O_2 in the membrane and changes in the intrinsic rate constant (k'/k):

$$a = K_p^{\text{O}_2} (K_p^{\text{NO}})^2 k/k' \quad (26)$$

According to Liu et al. (1998b), the reaction occurred 300 times faster inside the membrane than in water (the so-called 'lens effect'). This acceleration was attributed mostly to the higher local concentration of both •NO and O_2 in the membrane, and was consistent with $K_p^{\text{O}_2} = 3$ and theoretical $K_p^{\text{NO}} = 9$. The role of the hydrophobic phase in this acceleration was elegantly demonstrated using micelles of detergents with neutrally, negatively and positively charged headgroups and critical micellar concentration. Only after the critical micellar concentration was achieved did acceleration occur (Liu et al., 1998b). In a recent mechanistic study, a , $K_p^{\text{O}_2}$ and K_p^{NO} were independently determined in phospholipid membranes and LDL, and theoretical versus experimental a values were compared (Möller et al., 2007b). The solubility for O_2 and •NO in membranes was found to be similar ($K_p^{\text{O}_2} = K_p^{\text{NO}} \sim 3$), and expected values for a calculated as $K_p^{\text{O}_2}(K_p^{\text{NO}})^2$ were very close to those determined directly ($a \sim 30$), but an order of magnitude lower than the acceleration observed previously (Liu et al., 1998b). In this work, $a = 24$, which was consistent with experimentally determined $K_p^{\text{O}_2} = 2.6$ and $K_p^{\text{NO}} = 3.0$ in LDL (Möller et al., 2007b). No change in the intrinsic rate constant was expected, since this is very similar in carbon tetrachloride and water ($k_{(\text{CCl}_4)} = 2.8 \times 10^6 \text{ M}^{-2} \text{ s}^{-1}$, $k_{(\text{water})} = 1.5\text{--}3 \times 10^6 \text{ M}^{-2} \text{ s}^{-1}$; Awad and Stanbury, 1993; Ford et al., 1993; Goldstein and Czapski, 1995; Nottingham and Sutter, 1986).

This 'lens effect' is especially relevant to thiol and amine nitrosation. Thiol nitrosation has been reported to be involved in physiological and pathological processes, including inhibition of platelet degranulation and aggregation after S-nitrosation of N-ethylmaleimide-sensitive factor (Morrell et al., 2005) and promotion of apoptosis through glyceraldehyde-3-phosphate dehydrogenase S-nitrosation (Hara et al., 2005), and to have a possible role in promoting sporadic Parkinson disease (Yao et al., 2004) and in delaying amyotrophic lateral sclerosis (Schonhoff et al., 2006). Amine nitrosation by •NO-derived species has been associated mainly with carcinogenesis after DNA base nitrosation, deamination, oxidation and nitration (Dedon and Tannenbaum, 2004). Although nitrosation is undoubtedly an important modification, the biological mechanisms of nitrosation have remained obscure. The classical source of nitrosating species is •NO autoxidation via formation of N_2O_3 (Hogg, 2002), as it reacts rapidly with thiolates and amines acting as an electrophilic reagent (Eq. 27). Alternatively, nitrosation can occur through one electron oxidation of the thiol by •NO₂, and then •NO addition to the thiyl radical (Eqs. 28 and 29; Espey et al., 2002; Goldstein and Czapski, 1996; Jourdeuil et al., 2003). The autoxidation of •NO in the aqueous phase is considered to be too slow to be biologically relevant, but membranes may constitute an important site of formation of nitrosating species.





As evidenced by stopped-flow and triiodide reductive chemiluminescence, the formation of oxidizing species and *S*-nitrosothiols from $\bullet\text{NO}$ and O_2 was also accelerated about 30 times in lipid phases (Möller et al., 2007b). Accordingly, thiol nitrosation was the predominant modification in native LDL exposed to $\bullet\text{NO}$ under aerobic conditions (Möller et al., 2007b).

Considering an acceleration factor of 30, and that lipid membranes account for 3% of total cell volume, it is estimated that 50% of $\bullet\text{NO}$ autoxidation will occur in the small volume of cell membranes (Möller et al., 2007b). Biomolecules in or close to the membrane will be exposed to a 30-fold higher flux of nitrosating species derived from $\bullet\text{NO}$ autoxidation. It should be taken into account that nitrosation will also be greatly influenced by the reactivity and availability of targets, and thus very reactive and abundant biomolecules, even distant from the membrane, may blur the expected higher amount of nitrosated biomolecules near the membrane.

Peroxynitrite homolysis within the membrane

Peroxynitrite serves as a pathogenic mediator in a variety of disease states (Estevez et al., 1999; Ischiropoulos, 2003; Peluffo and Radi, 2007; Radi, 2004; Szabo et al., 2007). Peroxynitrite can undergo proton-catalyzed homolysis (Beckman et al., 1990; Radi et al., 1991b) to $\bullet\text{NO}_2$ and $\bullet\text{OH}$ in $\sim 30\%$ yields, with an observed first-order rate constant of $\sim 1 \text{ s}^{-1}$ at pH 7.4 and 37°C and a pH-independent rate constant of peroxynitrous acid homolysis in aqueous media of $k_{\text{H}}^{\text{a}} = 4.5 \text{ s}^{-1}$ at 37°C (Augusto et al., 1994; Beckman et al., 1990; Merenyi et al., 1999). Early work on lipid peroxidation (Radi et al., 1991a) and nitration (Rubbo et al., 1994) suggested the existence of peroxynitrite homolysis within the membrane, as both $\bullet\text{OH}$ and $\bullet\text{NO}_2$ can abstract an electron from unsaturated fatty acids to initiate lipid radical-dependent processes. In this regard, the relative lack of direct peroxynitrite targets in hydrophobic compartments (Botti et al., 2004b, 2005) makes homolysis a more likely decay mechanism. As an activation controlled-process, it is expected that the rate of peroxynitrous acid homolysis will be influenced by K_{p} but not by the diffusion coefficient of peroxynitrous acid in lipid environments. Indirect evidence supports that k_{H} in aqueous media (k_{H}^{a}) is similar to k_{H} in hydrophobic phases (k_{H}^{h} ; Botti et al., 2004a) and therefore the apparent first-order constant of homolysis in hydrophobic environments $k_{\text{H}}^{\text{H}}_{\text{app}}$ can be estimated by Eq. 30:

$$k_{\text{H}}^{\text{H}}_{\text{app}} = K_{\text{p}}k_{\text{H}}^{\text{h}} \sim K_{\text{p}}k_{\text{H}}^{\text{a}} \leq 0.0005 \times 4.5 \text{ s}^{-1} = 2.25 \times 10^{-3} \text{ s}^{-1} \quad (30)$$

where the K_{p} of water is taken as an upper limit estimation of the partition coefficient of peroxynitrous acid. Due to the predominance of direct reactions with biological targets such as CO_2 , highly reactive protein thiols, glutathione (GSH) and bound metals (Szabo et al., 2007), peroxynitrite homolysis is a quantitatively minor process of biological hydrophilic phases. Accordingly, peroxynitrite diffusion towards membranes could also be limited by hydrophilic targets, most notably CO_2 ($k_2 = 4.6 \times 10^4 \text{ M}^{-1} \text{ s}^{-1}$ at 37°C and pH 7.4) (Denicola et al., 1998; Botti, 2004a). Further studies and recent work show that the homolysis of peroxynitrite within or in close proximity to the bilayer may be of high relevance. These studies have been performed using α -TOH in LDL, as well as a hydrophobic tyrosine analog, *N*-*t*-BOC *L*-tyrosine *tert* butyl ester (BTBE), incorporated into phosphatidylcholine liposomes, as probes for oxidative processes within lipid environments. The yield of oxidation of unsaturated lipids in LDL (as evaluated by the two-electron oxidation of α -TOH to α -tocopheryl quinone) in the absence of hydrophilic targets was 20–25% with respect to

peroxynitrite but decreased to 1–2% in the presence of physiologic concentrations of CO_2 (Botti et al., 2004a, 2005), indicating that in the presence of targets for peroxynitrite (CO_2) and •NO_2 ($\text{CO}_3^{\bullet-}$), homolysis in aqueous compartments may not be quantitatively relevant for free radical-dependent lipid oxidation. Moreover, if both aqueous •NO_2 and •OH were able to initiate lipid oxidation in the absence of CO_2 , the expected yield of oxidation would have been $\sim 60\%$, suggesting that most of the •OH formed in the aqueous phase cannot reach the unsaturated lipids of LDL.

The initial observation by HPLC/MS-based methods of the presence of a hydroxylated-derivative of BTBE (3-hydroxy-BTBE) is indicative of the addition reaction of •OH at the phenolic ring (Bartasaghi et al., 2006; Radi, 2004); additionally, the one-electron oxidation product of the tyrosine analog formed by either •NO_2 or •OH , leading to the formation of the corresponding phenoxyl radical, was shown by EPR-spin trapping. The fate of the phenoxyl radical may differ depending on the presence or absence of •NO_2 , i.e. forming 3-nitrotyrosine or radical-radical reactions between two tyrosyl radicals yielding 3,3'-dityrosine. Thus, the products from the homolysis of peroxynitrous acid within hydrophobic biocompartments could initiate free radical processes both in fatty acids and protein residues (e.g. tyrosine) resulting in both oxidation and nitration reactions (Fig. 2).

Diffusion control over NO antioxidant reactions in membranes and lipoproteins

Although •NO -derived metabolites may exert oxidative modifications in LDL through peroxynitrite, •NO_2 and/or the NO_2^- -myeloperoxidase system (Hsiai et al., 2007; Leeuwenburgh et al., 1997a; Seccia et al., 1997; Zheng et al., 2005), •NO itself inhibits lipid oxidation-dependent processes. Nitric oxide causes a prolongation of the lag time and inhibition of the rate of lipid oxidation during the propagation phase of LDL oxidation through its chain breaking activity (Rubbo and O'Donnell, 2005; Rubbo et al., 1995; Rubbo et al., 2002b). Moreover, fragmentation of apolipoprotein B-100 by oxidants, loss of amino groups and protein–lipid fluorescent adduct formation are prevented by physiologically relevant fluxes of •NO (Trostchansky et al., 2001). This is due to the diffusion-limited reaction between •NO and lipid radicals generated during LDL oxidation, preventing the formation of both lipid hydroperoxides and aldehydes (Botti et al., 2005; Rubbo et al., 1998; Rubbo et al., 2002a; Rubbo et al., 1995; Rubbo and Radi, 2001; Trostchansky et al., 2001).

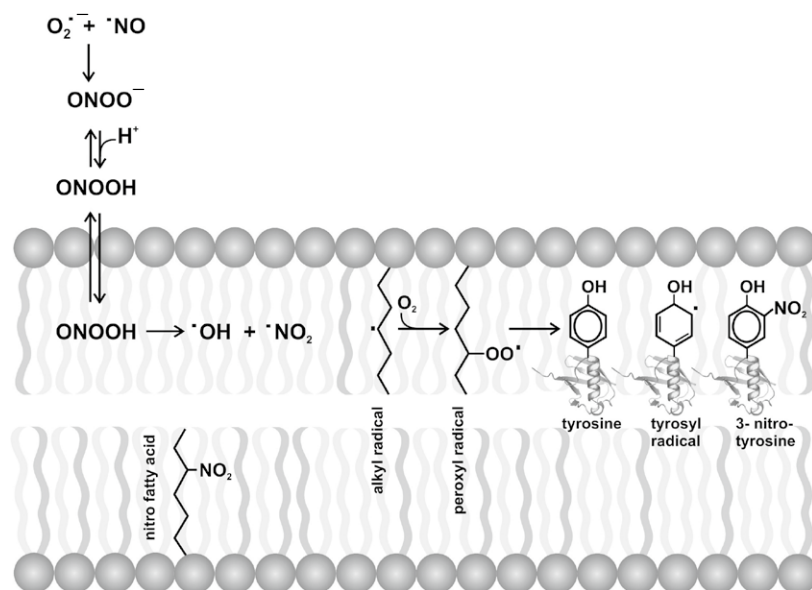


FIGURE 2

Mechanisms of peroxynitrite-mediated lipid oxidation and tyrosine nitration in biomembranes. Peroxynitrous acid is a neutral biomolecule that can permeate across hydrophobic biocompartments where it homolyzes to •OH and •NO_2 radicals; these radicals can initiate lipid oxidation processes in the membrane. While LOO^{\bullet} will typically propagate lipid oxidation damage, they could also react with membrane-associated proteins leading to the formation of tyrosyl radicals. Then 3-NT is formed due to its fast reaction with •NO_2 . Peroxynitrite-derived radicals in the membrane could also lead to the nitration of unsaturated fatty acids as well as intra- or intermolecular protein 3,3'-dityrosine cross links and lipid–protein adduct formation.

The reactivity of $\bullet\text{NO}$ inside lipid-containing structures is linked to its diffusion and solubility. The rate constant in homogeneous media for the reaction of $\bullet\text{NO}$ with alkylperoxyl radicals is known to be near the diffusion limit (Goldstein et al., 2004; Padmaja and Huie, 1993). The rate constant in lipid environments, e.g. LDL, for the reaction of $\bullet\text{NO}$ with lipid peroxyl radicals ($\text{LOO}\bullet$; k_{T}^{NO}) can be estimated from previous works (Botti et al., 2004a; Möller et al., 2007b). This is possible because $\bullet\text{NO}$ and $\alpha\text{-TOH}$ directly compete for $\text{LOO}\bullet$ (Botti et al., 2004a), which is the lipid peroxidation chain-carrying radical. Given $k_{\text{inh}}^{\alpha\text{-TOH}} = 5.9 \times 10^5 \text{ M}^{-1} \text{ s}^{-1}$ (Culbertson et al., 2002), and considering $\bullet\text{NO}$ autoxidation (Eq. 23) (Möller et al., 2007b), the published data on $\alpha\text{-TOH}$ sparing by controlled $\bullet\text{NO}$ fluxes (Botti et al., 2004a; Rubbo et al., 2000) can be explained by computer-assisted simulations only if an apparent rate constant of reaction of $\bullet\text{NO}$ with $\text{LOO}\bullet$ of $0.9\text{--}2.0 \times 10^9 \text{ M}^{-1} \text{ s}^{-1}$ is used. The apparent rate constant (k_{T}^{h}) could be additionally estimated from the rate constant in water (k_{T}^{w}) using Eq. (31). Considering $D'_{\text{m}} = 2 \times 10^{-5} \text{ cm}^2 \text{ s}^{-1}$, $D_{\text{w}} = 4.5 \times 10^{-5} \text{ cm}^2 \text{ s}^{-1}$ (Denicola et al., 2002) and $k_{\text{T}}^{\text{w}} = 1\text{--}3 \times 10^9 \text{ M}^{-1} \text{ s}^{-1}$ (Goldstein et al., 2004; Padmaja and Huie, 1993), a theoretical $k_{\text{T}}^{\text{h}} = 0.4\text{--}1.3 \times 10^9 \text{ M}^{-1} \text{ s}^{-1}$ is obtained which is in agreement with the values estimated from kinetic simulations of the $\alpha\text{-TOH}$ sparing ability of $\bullet\text{NO}$ in LDL. The real rate constant for the $\text{LOO}\bullet$ and $\bullet\text{NO}$ termination reaction can be calculated using $K_{\text{p}} = 3$ (Eq. 32), $k_{\text{T}}^{\text{h}} = 1.3\text{--}4.3 \times 10^8 \text{ M}^{-1} \text{ s}^{-1}$; this is 7–10 times slower than in water, an effect purely attributed to the higher η of the lipid media and the resulting slower diffusion (Eq. 32).

$$k_{\text{T}}^{\text{h}} = k_{\text{T}}^{\text{w}} \frac{K_{\text{p}} D_{\text{m}}}{D_{\text{w}}} = k_{\text{T}}^{\text{w}} \frac{D'_{\text{m}}}{D_{\text{w}}} \quad (31)$$

$$k_{\text{T}}^{\text{h}} = k_{\text{T}}^{\text{w}} \frac{D_{\text{m}}}{D_{\text{w}}} = k_{\text{T}}^{\text{w}} \frac{D'_{\text{m}}}{K_{\text{p}} D_{\text{w}}} \quad (32)$$

Many biological effects of $\bullet\text{NO}$ are critically related to the rate of $\bullet\text{NO}$ formation, which determines the extent of antioxidant versus pro-oxidant actions (Botti et al., 2005; Möller et al., 2007b; Rubbo and Radi, 2001; Rubbo et al., 1995, 1998, 2002a). It is known that under physiological conditions in the vessel wall, the steady-state concentration of $\bullet\text{NO}$ (250–500 nM; reviewed in Buerk, 2001) exceeds that of $\text{O}_2^{\bullet-}$, resulting in a high $\bullet\text{NO}/\text{O}_2^{\bullet-}$ ratio (Wever et al., 1998). However, enhanced $\text{O}_2^{\bullet-}$ production by vascular cells has been observed under different pathogenic stimuli that may shift the proportion of $\bullet\text{NO}$ yielding peroxynitrite, thus decreasing $\bullet\text{NO}$ bioactivity and its antioxidant properties.

Tyrosine nitration in membranes

The nitration of protein tyrosine residues constitutes the substitution of hydrogen by a nitro group ($-\text{NO}_2$) in position 3 of the phenolic ring, and represents a post-translational modification produced by $\bullet\text{NO}$ -derived oxidants such as peroxynitrite (Bartesaghi et al., 2007; Radi, 2004; Souza et al., 2008), 3-nitrotyrosine (3-NT) being the product of this reaction. Many tyrosine residues shown to be nitrated *in vitro* and *in vivo* are in proteins associated to non-polar compartments such as red cell membrane proteins, band-3 protein (Mallozzi et al., 1997), sarcoplasmic reticulum Ca^{2+} ATPase (Viner et al., 1999; Xu et al., 2006), microsomal glutathione S-transferase (Ji et al., 2006), apolipoproteins (Hazen et al., 1999; Shao et al., 2005) and mitochondrial proteins such as complex I (Murray et al., 2003).

Although some nitrated tyrosine residues in membrane-associated proteins have been shown in cytosolic or extracellular domains, others are located in domains closely related to lipid bilayer (Bartesaghi et al., 2007). Biological membranes are rich in proteins which are intimately associated to lipids; therefore, the redox processes taking place within membranes

may start either in proteins or lipids and be rapidly propagated to the adjacent biomolecules. As an illustrative example, it is worth noting that protein tyrosyl radicals in prostaglandin endoperoxide H synthase can enzymatically initiate lipid oxidation, i.e. oxidize arachidonic acid (AA, 20:4) to prostaglandins through the abstraction of a hydrogen atom by a tyrosine phenoxyl radical (Goodwin et al., 1998), and similar general oxidation mechanisms could take place non-enzymatically (Bartesaghi et al., 2007). To add more complexity, concomitant lipid and protein oxidation processes in biomembranes can facilitate formation of a variety of termination products such as lipid-protein adducts (see below).

The location and extent of 3-NT formation has been shown to depend on the protein structure, the nitration mechanism (i.e. peroxyxynitrite or heme peroxidase dependent; Radi, 2004) and the environment where the redox reactions are taking place (i.e. hydrophilic or hydrophobic) (for recent reviews see Bartesaghi et al., 2007; Souza et al., 2008). In this context, physicochemical factors controlling tyrosine nitration in hydrophobic environments may differ from those in aqueous solutions (Bartesaghi et al., 2007). Indeed, tyrosine nitration in proteins associated to hydrophobic biocompartments has particular features since key antioxidant molecules that are normally present in the aqueous phase, such as GSH, are excluded. In addition, some of the key peroxyxynitrite-derived one-electron oxidants in aqueous phases, e.g. $\text{CO}_3^{\bullet-}$ do not permeate across lipid milieu and thus have limited access to 'hydrophobic' tyrosines (Bartesaghi et al., 2006; Zhang et al., 2001). On the other hand, •NO₂ may diffuse towards the hydrophobic compartment facilitating the nitration pathway. Moreover, transition metal centers can catalyze nitration reactions in lipid phases, having a key role in the modifications generated by RNS (Bartesaghi et al., 2006).

Within the membranes, unsaturated fatty acids represent the preferential targets for free radical attack. Peroxyxynitrous acid derived •OH and •NO₂ initiate lipid oxidation processes, which are propagated by the action of LOO•; alternatively, LOO• could react with an amino acid residue of a membrane-associated protein to promote protein oxidation. We have recently shown that tyrosine can be readily oxidized by alkoxyl (RO•) and peroxy (ROO•) radicals to form the tyrosyl radical which can subsequently react with •NO₂ to yield 3-NT (Fig. 2) (Bartesaghi et al., 2007). This process can be modulated by the membrane- and lipoprotein-associated α-TOH due to its chain-breaking reaction with LOO• (Rubbo et al., 2000).

Two different types of probes have been developed in order to study the mechanisms of tyrosine nitration in membranes. As explained above, BTBE is a hydrophobic tyrosine analog that has been efficiently incorporated into model membranes (Bartesaghi et al., 2006; Zhang et al., 2001), red blood cells (Romero et al., 2007) and lipoproteins (Bartesaghi and Radi, unpublished data). This compound has been instrumental in assessing tyrosine nitration and dimerization yields in membranes as well as their modulation by lipid composition and environmental factors such as CO₂, transition metals and pH (Bartesaghi et al., 2006). While the yield of tyrosine nitration in saturated 1,2-dimyristoyl-*sn*-glycerol-3-phosphocholine liposomes is similar to that observed in the hydrophilic phase (ca. 3% with respect to peroxyxynitrite added), tyrosine dimerization in hydrophobic milieu is significantly decreased due to the very limited diffusion of tyrosyl radicals within the membrane (Bartesaghi et al., 2007). Two other relevant observations are: (i) CO₂ inhibits peroxyxynitrite-mediated nitration in hydrophobic milieu, and (ii) membrane-associated transition metal centers can be potent nitration catalysts, e.g. heme which can be released during hemoglobin degradation.

As a second probe, membrane-spanning peptides containing 23 amino acids with a single tyrosine residue at positions 4, 8 and 12 (Y-4, Y-8, Y-12, respectively) have been synthesized and incorporated successfully into phosphatidylcholine liposomes (Zhang et al., 2003). These peptides closely resemble the structure of a protein transmembrane domain, and thus are very useful for studying the relevance for nitration yields of the intramembrane location of tyrosine residues, the role of neighboring amino acids (i.e. cysteine and methionine), as well as the lipid composition of the membrane. The data obtained suggest that the degree of

nitration is dependent on the depth of the tyrosine residue within the bilayer (peroxynitrite-mediated nitration was higher in deeply located tyrosines (Y-12 peptide) while the myeloperoxidase/ NO_2^- /hydrogen peroxide-dependent nitration was only efficient for superficially located tyrosines (Y-4 peptide) (Zhang et al., 2003). Data obtained with the available hydrophobic tyrosyl probes (Bartesaghi et al., 2006; Zhang et al., 2003; Zhang et al., 2001) suggest that some assumptions valid for the aqueous phase (e.g. enhanced nitration by CO_2 , efficiency of the myeloperoxidase system) are not readily applicable or not applicable at all in lipid phases. The differences in polarity and structure of the environment which influence protein conformation, limit acid–base chemistry and cause spatial restrictions and diffusional constraints can explain the observed results. Moreover, the distribution of reactants and target molecules, free radical scavengers and nitration catalysts among other factors, is also affected. Additionally, data obtained with BTBE indicated that lipid-derived radicals arising from RNS are critical intermediates in protein tyrosine nitration in hydrophobic biocompartments. In summary, while BTBE is suitable for studying general mechanisms of tyrosine nitration and oxidation in lipid milieu, tyrosine-containing transmembrane peptides are more useful for understanding the diffusion and reactions of nitrating intermediates at the membrane, revealing the influence of the amino acid sequence through competing and intramolecular transfer reactions (Zhang et al., 2008).

Nitration of LDL *in vitro* and *in vivo*

It is well recognized that oxidative and/or enzyme-mediated modifications of LDL are necessary for the acquisition of the pro-inflammatory properties present during the initiation and progression of atherosclerosis (Asatryan et al., 2005; Damasceno et al., 2006; Hamilton et al., 2008). Moreover, post-translational modifications of apoB-100 are elevated in atherosclerotic lesion. In particular, measurements of 3-NT in LDL isolated from human atherosclerotic lesions show that there is a striking 90-fold increase compared with circulating LDL (Hamilton et al., 2008; Hsiai et al., 2007; Leeuwenburgh et al., 1997b).

Shear stress acting on endothelial cells at arterial bifurcations or branching points regulates both NADPH oxidase, a major source of endothelial $\text{O}_2^{\bullet-}$, and endothelial NO synthase (NOS1) activities (De Keulenaer et al., 1998; Ziegler et al., 1998). In this way, shear stress influences the formation of peroxynitrite due to the imbalance between $\text{O}_2^{\bullet-}$ and $\bullet\text{NO}$ production in the vasculature, thus inducing LDL tyrosine nitration (Hsiai et al., 2007). Detection of 3-NT in fatty streaks of coronary arteries in close association with foam cells, vascular endothelium, and in the neointima of atherosclerotic lesions indicates $\bullet\text{NO}$ -derived oxidant-dependent reactions during both early and chronic stages of atherosclerosis (Schartl et al., 2001). Oxidation of LDL by peroxynitrite results in extensive tyrosine nitration and accumulation of lipid peroxides, which produces changes in apoB-100 folding (Hamilton et al., 2008). The pattern of LDL nitration *in vivo* is similar to that observed for peroxynitrite-oxidized LDL. Moreover, apoB-100 nitration at the LDL receptor binding site prevents its normal uptake (Hamilton et al., 2008) in accordance with the interaction of peroxynitrite-treated LDL with CD36 (Guy et al., 2001).

As an additional mechanism for LDL nitration, myeloperoxidase-generated RNS has been proposed as a physiologically plausible pathway for converting LDL into an atherogenic form (Podrez et al., 1999). These observations raise the possibility that during oxidative stress processes within the vascular wall, $\bullet\text{NO}$ may promote atherogenesis in contrast to its well established direct anti-atherogenic effects.

Formation of lipid–protein adducts by RNS

It is well reported in the literature that peroxynitrite can initiate lipid oxidation and nitration leading to the formation of diverse reactive fatty acid-derived oxidized products. These products may have harmful as well as signaling effects due to their capacity to covalently modify amino acidic protein residues by either Schiff's base formation or Michael addition reactions

(Batthyany et al., 2006; Trostchansky et al., 2001; Trostchansky et al., 2006; Uchida, 2000). The relevance of the formation of lipid–protein adducts in different biological models will be discussed below.

MODULATION OF α -SYN OXIDATION AND NITRATION BY PHOSPHOLIPID MEMBRANES

α -Synuclein (α -syn) is a soluble thermo-stable protein having 140 amino acid residues, which is characterized by acidic stretches toward the C-terminal and six repetitive amino acid sequences of the prototype KTKEGV. α -Synuclein does not assume a stable globular structure as typical globular proteins; instead it has a disordered conformation or random coil structure (Weinreb et al., 1996). However, in association with small unilamellar vesicles (20–25 nm diameter) rich in acidic phospholipid, i.e. phosphatidylserine and phosphatidic acid (Davidson et al., 1998; Jo et al., 2000), the helical structure of the protein is stabilized (Davidson et al., 1998). The degenerated repeats, reminiscent of those in A₂ apolipoproteins (Davidson et al., 1998; Perrin et al., 2000; Segrest et al., 1992) and projected in a helical wheel having a hydrophilic and a hydrophobic face, are involved in the interaction with lipids.

The formation of lipid–protein adducts is a consequence of the oxidative breakdown of polyunsaturated lipids yielding lipid hydroperoxides (LOOH) and aldehydes that may react with lysines or histidines in the protein milieu through mechanisms that yield different end products: Schiff's bases or Michael addition reactions (Fruebis et al., 1992; Itakura et al., 2000; Requena et al., 1997; Steinbrecher, 1987; Tsai et al., 1998). Although aldehydes could react with lysines to form Schiff's bases adducts, the major reactions occur through Michael addition reactions forming hemiacetal adducts with histidines (Requena et al., 1997). 4-Hydroxynonenal (4-HNE) has been implicated as a key mediator in the onset and progression of several cardiovascular as well as neurodegenerative diseases (Uchida, 2000). In fact, wild-type α -syn is a major component of Lewy bodies in sporadic Parkinson's disease and α -syn modified by 4-HNE may play a major pathogenic role. In this context, we have recently demonstrated the formation of 4-HNE–protein adducts in a α -syn/liposome model (Trostchansky et al., 2006). α -Syn bears a resemblance to the A₂ apolipoprotein family through the 11-residue periodicity showing amphipathic α -helices that participate in a variety of lipid and protein interactions, including its binding to membranes (Davidson et al., 1998; Perrin et al., 2000; Segrest et al., 1992). This cluster is characterized by the presence of lysine and histidine residues in the nonpolar/polar interface, stabilizing lipid–protein interactions (Davidson et al., 1998; Perrin et al., 2000). We have demonstrated that acidic phospholipids modulate peroxynitrite-mediated α -syn oxidation, nitration and stable oligomer formation, particularly in the presence of high concentrations of unsaturated fatty acids. Under these experimental conditions, lipid oxidation-derived products can react with α -syn leading to the formation of fluorescent lipid–protein adducts. Mass spectrometry analysis demonstrated that 4-HNE could modify α -syn at His50 within the lipid-binding domain of the protein amino acid sequence. From this, we postulate that α -syn nitration and oxidation by peroxynitrite can be modulated by the lipid environment, which may promote the formation of α -syn–lipid adducts as a novel post-translational α -syn modification (Trostchansky et al., 2006).

PROTEIN MODIFICATION BY OXIDIZED FATTY ACIDS IN LDL

The LDL particle consists of an apolar core of cholesteryl esters and triglycerides, surrounded by a monolayer of phospholipids, unesterified cholesterol and one molecule of apolipoprotein B-100 (4536 amino acids) showing many oxidizable residues including histidine, lysine, cysteine and tyrosine (Esterbauer et al., 1992; Kenar et al., 1996; Orlova et al., 1999). Both the lipid and the protein components of LDL could be potentially oxidized and nitrated by peroxynitrite. Whichever mechanisms will ultimately prove to be involved in the initiation of oxidative processes in the LDL particle, it seems clear that the processes following initiation include protein oxidation, loss of antioxidants and lipid oxidation propagation reactions (Fig. 3).

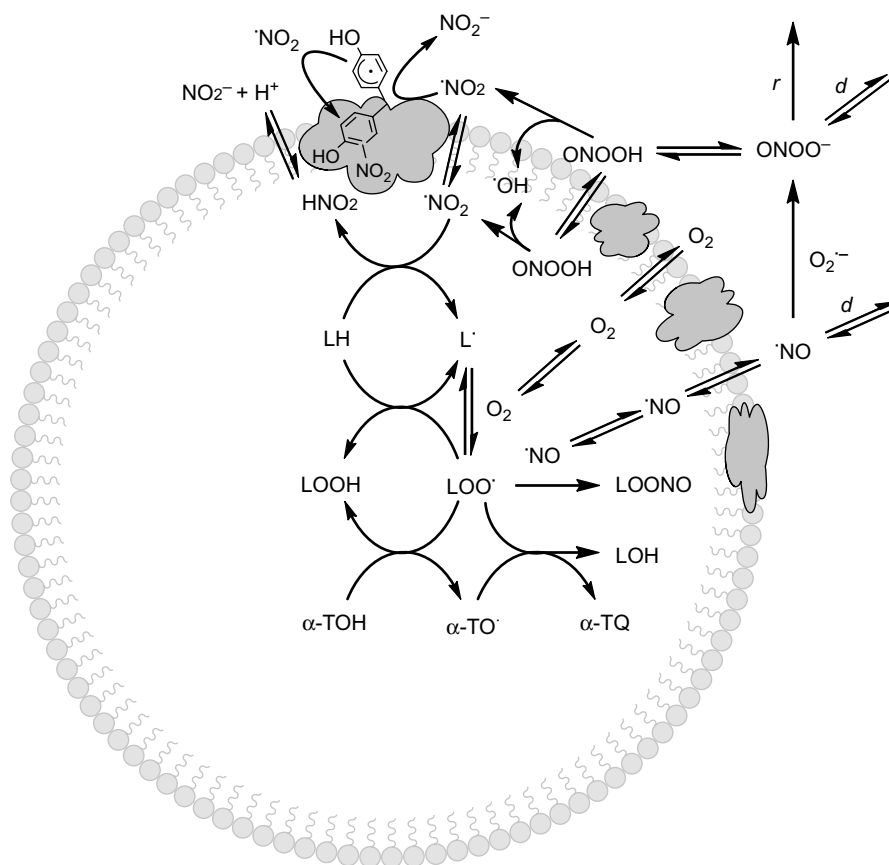
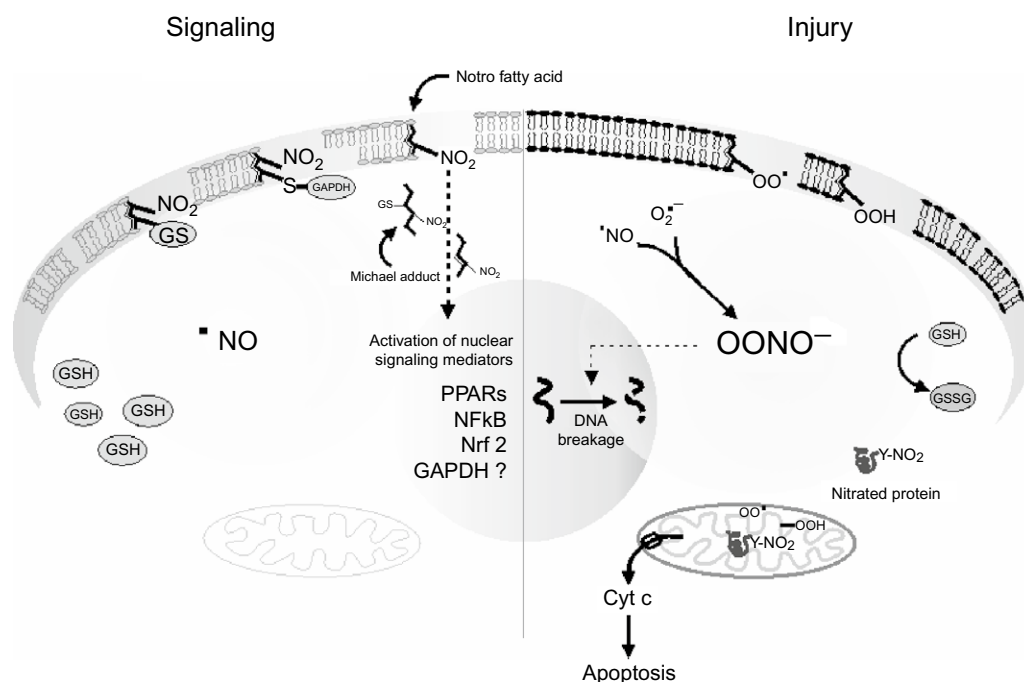


FIGURE 3

Reaction–diffusion processes involving reactive nitrogen species and lipo-protein structures. While $\cdot\text{NO}_2$ behaves as an efficient lipid peroxidation initiator, $\cdot\text{NO}$ is involved in termination reactions with $\text{LOO}\cdot$. Peroxynitrite-derived $\cdot\text{OH}$ may react near the particle's surface. RH is a hydrophilic reductant; LH is an unsaturated fatty acid, $\alpha\text{-TOH}$ is α -tocopherol; $\alpha\text{-TO}\cdot$ is α -tocopheroxyl radical; $\alpha\text{-TQ}$ is α -tocopheroxyl quinone. The *r* and *d* characters are used to indicate reaction and diffusion processes, respectively. For simplicity, oxidation and nitration reactions within the protein structure are not shown.

One of the major changes that occurs during LDL oxidation is the formation of lipid–protein adducts making the LDL particle more electronegative (Fruebis et al., 1992; Itakura et al., 2000; Requena et al., 1997; Steinbrecher, 1987; Tsai et al., 1998). The conversion of native LDL to a more negatively charged form and the concomitant formation of lipid–protein adducts was primarily associated with the modification of lysine residues in apo B-100 (Fruebis et al., 1992; Itabe et al., 2000; Itakura et al., 2000; Requena et al., 1997; Steinbrecher, 1987). Other mechanisms for adduct formation in LDL include reactions between head amino groups of phospholipids and lipid oxidation products (Boullier et al., 2000; Itabe et al., 2000). Lipid–protein adducts represent ligands for macrophage scavenger receptors that contribute to foam cell formation and the subsequent development of atherosclerotic lesions (Boullier et al., 2000; Horkko et al., 1999; Steinbrecher et al., 1989). The relevance of formation of these adducts *in vivo* has been supported by specific antibodies that recognize antigenic epitopes in human atherosclerotic lesions (Horkko et al., 1999; Kato and Osawa, 1998; Kim et al., 1997).

A few years ago, we reported the formation of lipid–protein adducts in LDL oxidized by controlled low fluxes of peroxynitrite (Trostchansky et al., 2001). In different model systems, including our observation in peroxynitrite-mediated LDL oxidation, the presence of covalent modifications in proteins by lipid oxidation products were determined due to their characteristic excitation and emission maxima at 350–365 nm and 420 nm, respectively (Fruebis et al., 1992; Itakura et al., 2000; Requena et al., 1997; Tsai et al., 1998). The widening of the

**FIGURE 4**

Role of nitric oxide and reactive nitrogen species in signaling and injury. Nitric oxide may exert signaling activities due to the formation of nitro-fatty acids which in turn form Michael adducts with glutathione and transcription factors (left side). Under nitrooxidative conditions, •NO exhibits a prooxidant effect due to the formation of peroxynitrite, consumption of glutathione, and oxidation and nitration of lipids and proteins (right side). Reproduced from Rubbo and Radi (2008).

emission maximum with time suggests that both lipid hydroperoxide and its decomposition products (i.e. aldehydes) generate fluorescent adducts during peroxynitrite-dependent LDL oxidation (Trostchansky et al., 2001). This is also supported by the fact that time courses of fluorescence in peroxynitrite-treated LDL correlated well with the increase in TBARS (thio-barbituric acid reactive substances), CLOOH (cholesteryl linoleate hydroperoxide) and REM (relative electrophoretic mobility), as well as a progressive decrease in the number of reactive lysine ϵ -amino groups (Requena et al., 1997; Steinbrecher et al., 1987). A fast depletion of lysine residues was previously observed after treatment of LDL with peroxynitrite (Boren et al., 1998). Importantly, there is no direct reaction between peroxynitrite and lysine but rather lysine is oxidized by secondary radicals arising from peroxynitrite proton-catalyzed decomposition or from lipid radicals (Alvarez et al., 1999).

OTHER LIPID-PROTEIN ADDUCTS IN BIOLOGY

Nitric oxide-derived reactive species both oxidize and nitrate unsaturated fatty acids yielding an array of hydroxyl, hydroperoxy, nitro and nitrohydroxy derivatives (see below). In particular, lipid oxidation and/or nitration transform fatty acids into potent electrophiles capable of covalently modify proteins (Alexander et al., 2006; Baker et al., 2007; Batthyany et al., 2006). The addition of a nitro group ($-\text{NO}_2$) to a double bond at the carbon chain of the unsaturated fatty acids (for example from the reaction with peroxynitrite; Baker et al., 2005) leads to the formation of nitroalkenes exhibiting potent electrophilic properties: the alkenyl nitro configuration of nitroalkenes indicates potential electrophilic reactivity of the β -carbon adjacent to the nitro-bonded carbon. This would promote reactivity with nucleophiles (i.e. Cys or His residues) via Michael addition reactions yielding a new carbon-carbon or carbon-heteroatom bond framework (Alexander et al., 2006; Baker et al., 2007; Batthyany et al., 2006). In biological milieu, this reaction occurs as a conjugate addition of nucleophilic centers to the electrophilic carbon β - to the nitro-bonded carbon in the nitroalkene (Batthyany et al., 2006) (Fig. 4).

Mass spectrometry (MS) analysis showed the formation of GSH nitroalkylation *in vitro* and *in vivo* (Alexander et al., 2006; Batthyany et al., 2006). Collision-induced dissociation of nitroalkylated GSH and structural analysis by MS/MS/MS confirmed that nitroalkenes are bonded to nucleophilic Cys residues (Batthyany et al., 2006). Moreover, these authors also

observed the formation of nitroalkylated proteins (glyceraldehyde-3-phosphate dehydrogenase, GAPDH) *in vitro* and *in vivo*. MS analysis showed that not only were Cys residues adducted by nitroalkenes; His residues were also nitroalkylated by electrophilic attack (Batthyany et al., 2006). In contrast to other lipid-derived electrophiles, nitroalkylation of Cys and His is reversible (Alexander et al., 2006; Batthyany et al., 2006; Schopfer et al., 2009). Nitroalkenes react with thiols with second-order rates equivalent to, or significantly greater than, those for other lipid-derived electrophiles having an inverse relationship with thiol pKa values (Baker et al., 2007). More recently, Schopfer et al. (2009) described the reversible reaction of nitroalkenes with the thiol of β -mercaptoethanol as a useful tool for detection and quantification of nitroalkylated proteins *in vitro* and *in vivo*.

Modulation of LDL oxidation by α -tocopherol-NO donors

Taking the lesson from \bullet NO as an antioxidant, it is important to develop antioxidants for lipid environments that can react at diffusion-controlled rates with the propagating radical (Lopez et al., 2005; Parinandi et al., 2007; Wallace et al., 2002). Therefore, synthesis should have three main objectives: (a) increase the intrinsic reactivity of the molecule with the chain-carrying species, (b) enhance the partition/solubility of the compound in lipid environments, and (c) decrease the size of the antioxidant in order to increase the real diffusion in highly viscous media such as membranes and lipoproteins.

The design of hybrid molecules by combining the lipid moiety of α -TOH with \bullet NO-releasing moieties capable of being incorporated into LDL may be a promising approach for treating atherosclerosis (Lopez et al., 2005). Furoxans represent an important class of \bullet NO donors (Wang et al., 2002). It is known that furoxans are able to release \bullet NO at physiological pH, in the presence of thiol cofactors (Feelisch et al., 1992; Medana et al., 1994). On the basis of these observations, we have developed a therapeutic concept of combining, in the same molecule, LDL incorporation capacity and \bullet NO-releasing properties to cause site-specific inhibition of lipid peroxidation. These α -TOH/furoxan hybrid compounds released \bullet NO and were effectively incorporated into LDL having endogenous antioxidant and vasorelaxation properties (Lopez et al., 2005).

LIPID NITRATION AND ITS ROLE IN INFLAMMATION

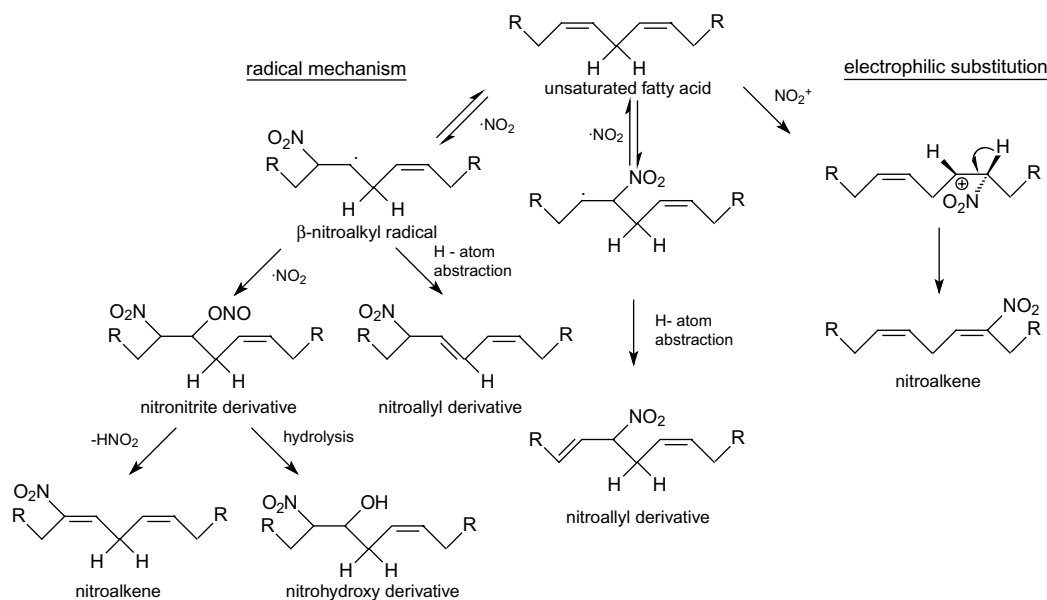
Free as well as esterified fatty acids are important components of lipoproteins and membranes that can be modified by oxidative and nitrative damage. Nitric oxide as well as \bullet NO-derived species react with unsaturated fatty acids yielding a variety of oxidized and nitrated products (Rubbo et al., 1994). At the same time, plasmatic proteins as well as the protein moiety of lipoproteins can be nitrated by RNS (Alvarez et al., 1999; Amirmansour et al., 1999; Hamilton et al., 2008; Hsiai et al., 2007; Leeuwenburgh et al., 1997b). These modifications represent important events during chronic inflammatory diseases such as atherosclerosis (Podrez et al., 1999). Thus, it is important to understand the mechanisms and effects that nitration of either lipids or proteins have on inflammation.

Mechanisms of formation of nitro-fatty acids

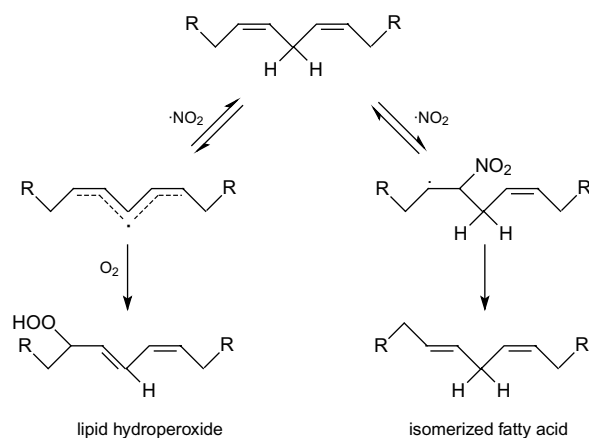
In the last 15 years, the nitration of unsaturated fatty acids by RNS has been extensively studied (Baker et al., 2004; Balazy et al., 2001; Lim et al., 2002; Lima et al., 2002; Trostchansky et al., 2007b). However, the exact mechanism of nitration *in vivo*, radical versus electrophilic addition, remains unknown (Fig. 5).

A relevant nitrating agent, \bullet NO₂, derives from \bullet NO autoxidation (Radi et al., 2000), peroxynitrite homolysis (Radi et al., 2000), metalloperoxidase nitrite oxidation (Podrez et al., 1999) or acidification of NO₂⁻ at low pH (e.g. pH < 4) to nitrous acid (HNO₂) (Napolitano et al., 2000). Nitrogen dioxide can react with unsaturated lipids and lipid radicals leading to *cis-trans* isomerized, oxidized and/or nitro-allylic, nitroalkene, dinitro or nitro-hydroxy lipid

low oxygen tension: lipid nitration



high oxygen tension: lipid oxidation

**FIGURE 5**

Mechanisms of nitro-fatty acids formation. Nitrogen dioxide can mediate oxidation and nitration of unsaturated fatty acids under anaerobic or aerobic conditions: $\cdot\text{NO}_2$ reacts with unsaturated fatty acids through a radical pathway yielding a β -nitroalkyl radical that, at low oxygen tensions, combines with other $\cdot\text{NO}_2$ molecules to form nitro/nitrite intermediates. Nitroalkenes or nitrohydroxy derivatives can be formed due to the loss of HNO_2 or hydrolysis, respectively. In addition, electrophilic substitution at the double bond by NO_2^+ yields nitroalkenes. At greater oxygen tensions, the formed oxidants react with unsaturated fatty acids enhancing lipid oxidation processes yielding hydroperoxides or isomerized lipid derivatives. Reproduced from Trostchansky and Rubbo (2008).

derivatives (Fig. 5). Accordingly, Napolitano et al. (2000) reported acid-induced nitration of oleic and linoleic acid by NO_2^- . They propose that $\cdot\text{NO}_2$, produced from HNO_2 decomposition, adds to the double bond yielding a β -nitroalkyl radical that, in turn, reacts with another $\cdot\text{NO}_2$ generating nitro/nitrite intermediates. Nitroalkenes are formed from these intermediates due to the loss of HNO_2 while its hydrolysis yields nitroalcohols. These processes should be possible *in vivo* since NO_2^- is present in saliva and physiological fluids at levels up to $210\ \mu\text{M}$ (Pannala et al., 2003). Thus, NO_2^- will be exposed to low pH in the gastric compartment as well as in phagocytic lysosomes or in tissues after post-ischemic reperfusion.

Peroxynitrite-derived radicals react with unsaturated fatty acids leading to the formation of different nitrated products representing a mixture of stereo- or positional isomers (O'Donnell et al., 1999a). These products would arise from peroxynitrous acid-derived $\cdot\text{NO}_2$ reaction with a carbon-centered radical or a lipid peroxyl radical, potentially via a caged radical rearrangement of unstable alkyl peroxynitrite intermediates (LOONO) (Rubbo et al., 1994). Some nitrogen-containing lipid intermediates appear to be highly unstable and may decompose to reinitiate radical processes. In fact, LOONO has at least two potential fates: (a) internal rearrangement to give the more stable LONO₂ and (b) homolytic cleavage to

LO^\bullet and $\bullet\text{NO}_2$ with rearrangement of LO^\bullet to an epoxyallylic acid radical $\text{L}(\text{O})^\bullet$ followed by recombination of $\text{L}(\text{O})^\bullet$ with $\bullet\text{NO}_2$ (O'Donnell et al., 1999a). However, in aqueous milieu LOONO simply hydrolyzes to generate LOOH and NO_2^- (O'Donnell et al., 1999b). Nitration of unsaturated fatty acids by peroxynitrite will be favored at low oxygen tensions (Napolitano et al., 2004; O'Donnell et al., 1999a). By ^1H NMR analysis, an approximate formation ratio of 1:1 for the nitroalkenes:allylic nitro derivatives was estimated suggesting the presence of two different routes for nitration of fatty acids, the nitroalkenes and allylic nitro derivatives being the stable end products of competing nitration pathways (Napolitano et al., 2000). Another mechanism for nitroalkene formation may be the addition of NO_2^+ by electrophilic substitution at the double bond (O'Donnell et al., 1999a; O'Donnell and Freeman, 2001).

In the case of arachidonic acid (AA), a precursor of potent signaling molecules (i.e. prostaglandins, thromboxanes, isoprostanes), nitration may divert the normal cyclooxygenase-dependent metabolic pathway. A complex mixture of products has been identified when $\bullet\text{NO}_2$ reacts with AA including cis-trans isomerization derivatives and nitrohydroxyarachidonate ($\text{AA}(\text{OH})\text{NO}_2$) (Balazy et al., 2001). Peroxynitrite is also able to isomerize AA to trans-AA, a process of significance in pathologies associated with an increase in RNS production (Balazy and Poff, 2004). The isomerization is likely to involve the reversible binding of $\bullet\text{NO}_2$ and formation of a nitroarachidonyl radical followed by elimination of $\bullet\text{NO}_2$ and generation of a trans bond. Hydrophobic membranes may facilitate reactions where $\bullet\text{NO}$, $\bullet\text{NO}_2$, arachidonyl (AA^\bullet) and arachidonyl peroxy (AAOO^\bullet) radicals are likely to be simultaneously present, i.e. in cell membranes under oxidative/nitrative stress conditions. The half-life of AAOO^\bullet (0.1–0.2 s) is sufficiently long for the reaction with $\bullet\text{NO}_2$ to occur, leading to arachidonyl peroxynitrites (AAOONO)/nitrates that could rearrange into nitroarachidonate (AANO_2), $\text{AA}(\text{OH})\text{NO}_2$ and nitroepoxyarachidonate (Balazy and Poff, 2004).

Formation of anti-inflammatory nitrolipids during macrophage activation

We have recently demonstrated the correlation of $\bullet\text{NO}$ production and nitrated lipids formation in a cell model of inflammation (Ferreira et al., 2009). Macrophages are key cells in the onset of inflammatory responses, playing a role in the first line of defense against invading pathogens. They possess a repertoire of receptors whose binding to ligands activates signaling pathways linked to the production of inflammatory mediators (i.e. cytokines and biolipids) and highly reactive oxygen and nitrogen species (Dobrovolskaia and Vogel, 2002; Kaisho and Akira, 2006). In particular, $\bullet\text{NO}$ is one of the most important free radicals synthesized during macrophage activation by the inducible nitric oxide synthase (NOS2) (Thoma-Uszynski et al., 2001; Werling et al., 2004). Our results show that during activation of macrophages by an inflammatory stimulus, cholesteryl linoleate becomes nitrated at the fatty acid moiety in a process that correlates with NOS2 expression.

Nitro-fatty acids exhibit many important biological and physiological properties. Nitroalkenes such as nitrolinoleic acid (LNO_2), nitrooleic acid (OANO_2) and AANO_2 decay faster in phosphate buffer than in organic solvent due to solvolysis in aqueous solutions, a process accompanied by the release of $\bullet\text{NO}$ (Baker et al., 2005; Gorczynski et al., 2007; Lima et al., 2005; Schopfer et al., 2005a; Trostchansky et al., 2007b). The releasing of $\bullet\text{NO}$ was related with the vasorelaxing properties of nitroalkenes, i.e. AANO_2 and $\text{AA}(\text{OH})\text{NO}_2$ induced vasorelaxation in an endothelium-independent manner by a mechanism that involved soluble guanylate cyclase (Balazy et al., 2001; Trostchansky et al., 2007b). Nitro-fatty acids stability in hydrophobic environments was evaluated for LNO_2 where $\bullet\text{NO}$ release was inhibited when the nitroalkene was inserted in phosphatidylcholine/cholesterol liposomes. These data reveal that LNO_2 will be stable in hydrophobic environments and that cell and lipoproteins can serve as an endogenous reserve for LNO_2 and $\bullet\text{NO}$ cell signaling capabilities (Schopfer et al., 2005a).

Free as well as esterified nitrated lipids exert anti-inflammatory actions through peroxisome proliferator activated receptor γ (PPAR γ)-dependent and -independent mechanisms

(Baker et al., 2005; Coles et al., 2002; Schopfer et al., 2005b; Trostchansky et al., 2007b; Wright et al., 2006). PPAR γ is a nuclear hormone receptor that binds lipophilic ligands. Downstream effects of PPAR γ activation include modulation of metabolic and cellular differentiation genes and regulation of inflammatory responses (Marx, 2002; Marx et al., 2004; Marx et al., 2002). In the vasculature, PPAR γ is expressed in monocytes, macrophages, smooth muscle cells and endothelium and plays a central role in regulating the expression of genes related to lipid trafficking, cell proliferation and inflammatory signaling (Marx et al., 2004). Freeman's group has demonstrated that nitroalkenes are the most potent PPAR γ ligands, able to activate PPAR γ at biologically relevant concentrations as low as 100 nM (Baker et al., 2005; Li et al., 2008; Schopfer et al., 2005b). They also demonstrated that PPAR γ activation occurs through a nitroalkylation reaction with critical Cys (Li et al., 2008). Nitroalkenes mediate cell differentiation in adipocytes, CD36 expression in macrophages and inflammatory-related signaling events in endothelium (e.g. inhibition of vascular cell adhesion molecule-1 expression and function).

Activation of phagocytic leukocytes, including neutrophils, is a central feature of inflammatory diseases. Neutrophil function *in vivo* can be regulated through •NO- and eicosanoid-dependent mechanisms (Coles et al., 2002), where nitrated fatty acids could influence neutrophil activation. In fact, LNO₂ inhibits *N*-formyl-Met-Leu-Phe- and phorbol 12-myristate 13-acetate-mediated activation of human neutrophils. Superoxide generation, degranulation, and CD11b expression were also inhibited by LNO₂, at concentrations of 0.1–1 μ M. These actions occurred in concert with attenuated increases in intracellular Ca⁺² and increased intracellular camp (Coles et al., 2002). Recruitment of leukocytes to the arterial wall is an important event in atherogenesis (Bilato and Crow, 1996; Potter et al., 1998; Tayeh and Scicli, 1998). This is mediated via leukocyte integrin receptors, including CD11b. Inhibition of *N*-formyl-Met-Leu-Phe-induced CD11b expression by LNO₂ indicates that nitrated fatty acids also modulate leukocyte responses associated with the development of vascular disease (Coles et al., 2002).

Recent studies have shown that heme oxygenase 1 (HO-1) plays a central role in vascular inflammatory signaling reactions and mediates a protective response in inflammatory diseases. HO-1 is the rate-limiting step in the degradation of heme, yielding biliverdin, iron and carbon monoxide (CO), that displays anti-inflammatory, vasodilatory and immune modulatory functions (Abraham and Kappas, 2005). Wright et al. (2006) reported that LNO₂ mediates the induction of HO-1 by PPAR γ - independent and both •NO-dependent and -independent mechanisms. Considering the vascular protective effects of HO-1 expression, LNO₂ induction of HO-1 represents a key novel cell signaling action of inflammatory-derived nitroalkenes.

It has been well established that AA signaling cascades and •NO pathways are intrinsically related (Salvemini et al., 1995). Therefore, we evaluated the ability of AANO₂ to exert anti-inflammatory actions during macrophage activation by lipopolysaccharide/interferon- γ (Trostchansky et al., 2007b). Micromolar levels of AANO₂ caused a reduction of •NO generation when cells were activated, exhibiting a transcriptional effect rather than acting on NOS2 synthesis/activity (Trostchansky et al., 2007b). Down-regulation of NOS2 by AANO₂ under an inflammatory stimulus should contribute to the physiological shut down of the inflammatory response in macrophages.

Potential pitfalls for nitrated lipids detection and quantitation *in vivo*

Lipid nitration represents a growing area in the interface of lipid oxidation and RNS metabolism which has increased in importance over the last 10 years (Freeman et al., 2008; Rubbo and O'Donnell, 2005; Rubbo and Radi, 2008). However, in order to clarify the formation, detection, quantitation and biological roles of nitrated fatty acids *in vivo* there are some potential pitfalls that should be critically addressed. As discussed above, there are many structural possibilities for nitro-fatty acids (i.e. allyl and vinyl nitro-fatty acids, nitrohydroxy derivatives that have been detected in cardiac tissue, human blood and urine) (Baker et al., 2005; Balazy

et al., 2001; Ferreira et al., 2009; Jain et al., 2008; Lima et al., 2003), but most of the studies on the physicochemical and biological characterization as well as *in vivo* detection have been performed using nitroalkenes as standards. Indeed, different potential positional isomers of nitro-fatty acids – and not only nitroalkenes or nitrohydroxy-fatty acids – should be present in biological samples, whose biological properties remain to be studied (Napolitano et al., 2000; Napolitano et al., 2004). Even with the available nitroalkene standards, there are additional problems regarding quantitation in biological samples. For example, Lima et al. (2002) found an increase of LNO₂ in human plasma of hypercholesterolemic patients. However, the total concentration of LNO₂ was not determined since they analyzed the ratio of the analyte to the internal standard which was a mixture of isomers, lacking specific standards for most of the positional isomers of all polyunsaturated fatty acids. At the time, Freeman and colleagues made the effort to synthesize and characterize 10- and 12-LNO₂ (Baker et al., 2004), while the 9- and 13-LNO₂ isomers were not synthesized, but failed to determine which isomers should preferentially be formed *in vivo*. In the case of AA, there are also many potential AANO₂ isomers that would be expected to be formed *in vivo*. This is an open question and it should be noted that in addition to the isomers synthesized and characterized by our group (Trostchansky et al., 2007a), prostaglandin endoperoxide H synthase should represent a key source of AANO₂: during cyclooxygenase catalysis, stereospecific AA-derived radicals (AA[•], AAOO[•]) are formed, being potential sources of AANO₂ due to its reaction with [•]NO and [•]NO₂. This has physiological importance since stereospecific formation of AANO₂ may have the potential to modulate the normal metabolic fate of AA (Trostchansky et al., 2007a). Fatty acids are biologically present in free and esterified forms, but the release and stability of nitrated fatty acids in membranes or lipoproteins remain unknown, probably affecting quantitation studies. Recent data suggested that nitrated fatty acids, upon partitioning or esterification to complex lipids, exist in a stabilized form that can be mobilized through esterases and phospholipases (Schopfer et al., 2005a). This means that detection and quantitation of nitrated lipids *in vivo* is complex, being influenced by the biological environment of target molecules. Acidic nitration during sample processing (i.e. lipid extraction and hydrolysis) can mediate artifactual generation of nitrated fatty acids due to the low pH and adventitious nitrite, leading to overestimated concentrations of nitrated fatty acids *in vivo*.

CONCLUDING REMARKS

The physicochemical properties of [•]NO and its derived reactive species determine the efficiency of the reactions that can take place in the lipid environment relative to the aqueous solution. The higher solubility of [•]NO in membranes than in water ($K_p \cong 3$) leads to an acceleration of the rate of [•]NO autoxidation in the membrane, while the low permeability and solubility of peroxy-nitrous acid in membranes is in part responsible for its low lipid oxidation yields. The fraction of peroxy-nitrous acid that penetrates the membrane will undergo homolysis as a major pathway of reaction and the derived radicals can then oxidize and nitrate protein tyrosines and fatty acids. Lipid oxidation products can further decompose to yield reactive aldehydes that can react with proteins and yield covalent lipid-protein adducts that will contribute to the nitrative damage, and are likely involved in the onset and/or development of atherosclerosis, sporadic Parkinson disease and other pathologies. However, the damage to lipid structures caused by RNS can be prevented by [•]NO itself. Since the diffusion in lipids is only ~6–10 times lower and the solubility is ~3 times higher than in water, [•]NO reacts with LOO[•] inhibiting oxidative damage at rates approaching those in solution. The antioxidant activity of [•]NO will be mainly defined by its rate of synthesis, whereas the simultaneous production of O₂^{•-} will divert [•]NO to a pro-oxidant activity by the formation of peroxy-nitrite.

Oxidation and nitration in lipid environments modify RNS-mediated cell signaling and injury processes. Under nitro oxidative stress conditions, the pathway of lipid nitration is up-regulated concomitantly with lipid oxidation and protein nitration. As a result, the nitration chemistry switches from signaling to damage, because lipid oxidation products as well

as nitrated proteins start to affect normal cellular functions and trigger processes such as mitochondrial cytochrome c release and apoptosis (Fig. 4). In this unfavorable biochemical scenario for cell and tissue homeostasis, the higher levels of nitrated lipids may serve as cyto- and tissue-protective agents, partially counteracting pro-inflammatory effects of oxidant exposure (Fig. 4). The final protective versus toxic effect of lipid and protein nitration processes during inflammation seems to depend on a delicate balance in cells, the mediators of which are just starting to be identified. Future research should identify which are the key molecules involved in both routes, how they are formed, what signaling pathways are used and what are the threshold levels that determine anti- or pro-inflammatory responses.

ACKNOWLEDGMENTS

This work was supported by grants from Wellcome Trust to H.R.; Programa de Desarrollo Tecnológico, Dinacyt, Uruguay to H.R. and to A.D.; FOGARTY-NIH to H.R. and to A.D.; Agencia Nacional de Investigación e Innovación (ANII)-Fondo Clemente Estable (Uruguay) to A.T. (FCE2007_516), S.B. (FCE2007_362) and H.B. (FCE2007_485); Howard Hughes Medical Institute and International Centre of Genetic Engineering and Biotechnology to R.R. We would like to thank Valeria Valez for helping in artwork.

REFERENCES

- Abraham, N.G., Kappas, A., 2005. Heme oxygenase and the cardiovascular-renal system. *Free Radic. Biol. Med.* 39, 1–25.
- Alderton, W.K., Cooper, C.E., Knowles, R.G., 2001. Nitric oxide synthases: structure, function and inhibition. *Biochem. J.* 357, 593–615.
- Alexander, R.L., Bates, D.J., Wright, M.W., King, S.B., Morrow, C.S., 2006. Modulation of nitrated lipid signaling by Multidrug Resistance Protein 1 (MRP1): Glutathione conjugation and MRP1-mediated efflux inhibit nitrooleic acid-induced, PPARgamma-dependent transcription activation. *Biochemistry* 45, 7889–7896.
- Alvarez, B., Ferrer-Sueta, G., Freeman, B.A., Radi, R., 1999. Kinetics of peroxynitrite reaction with amino acids and human serum albumin. *J. Biol. Chem.* 274, 842–848.
- Amirmansour, C., Vallance, P., Bogle, R.G., 1999. Tyrosine nitration in blood vessels occurs with increasing nitric oxide concentration. *Br. J. Pharmacol.* 127, 788–794.
- Asatryan, L., Hamilton, R.T., Isas, J.M., Hwang, J., Kaye, R., Sevanian, A., 2005. LDL phospholipid hydrolysis produces modified electronegative particles with an unfolded apoB-100 protein. *J. Lipid Res.* 46, 115–122.
- Augusto, O., Gatti, R.M., Radi, R., 1994. Spin-trapping studies of peroxynitrite decomposition and of 3-morpholinopyridone N-ethylcarbamide autooxidation: direct evidence for metal-independent formation of free radical intermediates. *Arch. Biochem. Biophys.* 310, 118–125.
- Augusto, O., Bonini, M.G., Amanso, A.M., Linares, E., Santos, C.C., De Menezes, S.L., 2002. Nitrogen dioxide and carbonate radical anion: two emerging radicals in biology. *Free Radic. Biol. Med.* 32, 841–859.
- Awad, H.H., Stanbury, D.M., 1993. Autoxidation of NO in aqueous solution. *Int. J. Chem. Kinet.* 25, 375–381.
- Baker, L.M., Baker, P.R., Golin-Bisello, F., Schopfer, F.J., Fink, M., Woodcock, S.R., Branchaud, B.P., Radi, R., Freeman, B.A., 2007. Nitro-fatty acid reaction with glutathione and cysteine. Kinetic analysis of thiol alkylation by a Michael addition reaction. *J. Biol. Chem.* 282, 31085–31093.

- Baker, P.R., Lin, Y., Schopfer, F.J., Woodcock, S.R., Groeger, A.L., Batthyany, C., Sweeney, S., Long, M.H., Iles, K.E., Baker, L.M., Branchaud, B.P., Chen, Y.E., Freeman, B.A., 2005. Fatty acid transduction of nitric oxide signaling: multiple nitrated unsaturated fatty acid derivatives exist in human blood and urine and serve as endogenous peroxisome proliferator-activated receptor ligands. *J. Biol. Chem.* 280, 42464–42475.
- Baker, P.R., Schopfer, F.J., Sweeney, S., Freeman, B.A., 2004. Red cell membrane and plasma linoleic acid nitration products: synthesis, clinical identification, and quantitation. *Proc. Natl. Acad. Sci. U S A* 101, 11577–11582.
- Balazy, M., Iesaki, T., Park, J.L., Jiang, H., Kaminski, P.M., Wolin, M.S., 2001. Vicinal nitrohydroxyeicosatrienoic acids: vasodilator lipids formed by reaction of nitrogen dioxide with arachidonic acid. *J. Pharmacol. Exp. Ther.* 299, 611–619.
- Balazy, M., Poff, C.D., 2004. Biological nitration of arachidonic acid. *Curr. Vasc. Pharmacol.* 2, 81–93.
- Bartesaghi, S., Ferrer-Sueta, G., Peluffo, G., Valez, V., Zhang, H., Kalyanaraman, B., Radi, R., 2007. Protein tyrosine nitration in hydrophilic and hydrophobic environments. *Amino Acids* 32, 501–515.
- Bartesaghi, S., Valez, V., Trujillo, M., Peluffo, G., Romero, N., Zhang, H., Kalyanaraman, B., Radi, R., 2006. Mechanistic studies of peroxynitrite-mediated tyrosine nitration in membranes using the hydrophobic probe N-t-BOC-L-tyrosine tert-butyl ester. *Biochemistry* 45, 6813–6825.
- Batthyany, C., Schopfer, F.J., Baker, P.R., Duran, R., Baker, L.M., Huang, Y., Cervenansky, C., Branchaud, B.P., Freeman, B.A., 2006. Reversible post-translational modification of proteins by nitrated fatty acids *in vivo*. *J. Biol. Chem.* 281, 20450–20463.
- Beckman, J.S., Beckman, T.W., Chen, J., Marshall, P.A., Freeman, B.A., 1990. Apparent hydroxyl radical production by peroxynitrite: implications for endothelial injury from nitric oxide and superoxide. *Proc. Natl. Acad. Sci. U S A* 87, 1620–1624.
- Bilato, C., Crow, M.T., 1996. Atherosclerosis and the vascular biology of aging. *Aging (Milano)* 8, 221–234.
- Boren, J., Lee, I., Zhu, W., Arnold, K., Taylor, S., Innerarity, T.L., 1998. Identification of the low density lipoprotein receptor-binding site in apolipoprotein B100 and the modulation of its binding activity by the carboxyl terminus in familial defective Apo-B100. *J. Clin. Invest.* 101, 1084–1093.
- Botti, H., Batthyany, C., Trostchansky, A., Radi, R., Freeman, B.A., Rubbo, H., 2004a. Peroxynitrite-mediated alpha-tocopherol oxidation in low-density lipoprotein: a mechanistic approach. *Free Radic. Biol. Med.* 36, 152–162.
- Botti, H., Trostchansky, A., Batthyany, C., Rubbo, H., 2005. Reactivity of peroxynitrite and nitric oxide with LDL. *IUBMB Life* 57, 407–412.
- Botti, H., Trujillo, M., Batthyany, C., Rubbo, H., Ferrer-Sueta, G., Radi, R., 2004b. Homolytic pathways drive peroxynitrite-dependent Trolox C oxidation. *Chem. Res. Toxicol.* 17, 1377–1384.
- Boullier, A., Gillotte, K.L., Horkko, S., Green, S.R., Friedman, P., Dennis, E.A., Witztum, J.L., Steinberg, D., Quehenberger, O., 2000. The binding of oxidized low density lipoprotein to mouse CD36 is mediated in part by oxidized phospholipids that are associated with both the lipid and protein moieties of the lipoprotein. *J. Biol. Chem.* 275, 9163–9169.
- Branco, M.R., Marinho, H.S., Cyrne, L., Antunes, F., 2004. Decrease of H₂O₂ plasma membrane permeability during adaptation to H₂O₂ in *Saccharomyces cerevisiae*. *J. Biol. Chem.* 279, 6501–6506.

- Buerk, D. G. (2001). Can We Model Nitric Oxide Biotransport? A survey of mathematical models for a simple diatomic molecule with surprisingly complex biological activities. *3*, 109–143.
- Chen, X., Jaron, D., Barbee, K.A., Buerk, D.G., 2006. The influence of radial RBC distribution, blood velocity profiles, and glycocalyx on coupled NO/O₂ transport. *J. Appl. Physiol.* *100*.
- Cheung, J.L., Li, Y.Q., Boniface, J., Shi, Q., Davidovits, P., Worsnop, D.R., Jayne, J.T., Kolb, C. E., 2000. Heterogeneous interactions of NO₂ with aqueous surfaces. *J. Phys. Chem. A* *104*, 2655–2662.
- Coles, B., Bloodsworth, A., Clark, S.R., Lewis, M.J., Cross, A.R., Freeman, B.A., O'Donnell, V.B., 2002. Nitrooleate inhibits superoxide generation, degranulation, and integrin expression by human neutrophils: novel antiinflammatory properties of nitric oxide-derived reactive species in vascular cells. *Circ. Res.* *91*, 375–381.
- Culbertson, S.M., Antunes, F., Havrilla, C.M., Milne, G.L., Porter, N.A., 2002. Determination of the alpha-tocopherol inhibition rate constant for peroxidation in low-density lipoprotein. *Chem. Res. Toxicol.* *15*, 870–876.
- Czapski, G., Goldstein, S., 1995. The reaction of NO• with O₂^{•-} and HO₂^{•-}: A pulse radiolysis study *Free Radic. Biol. Med.* *19*, 505–510.
- Damasceno, N.R., Sevanian, A., Apolinario, E., Oliveira, J.M., Fernandes, I., Abdalla, D.S., 2006. Detection of electronegative low density lipoprotein (LDL-) in plasma and atherosclerotic lesions by monoclonal antibody-based immunoassays. *Clin. Biochem.* *39*, 28–38.
- Davidson, W.S., Jonas, A., Clayton, D.F., George, J.M., 1998. Stabilization of alpha-synuclein secondary structure upon binding to synthetic membranes. *J. Biol. Chem.* *273*, 9443–9449.
- De Keulenaer, G.W., Chappell, D.C., Ishizaka, N., Nerem, R.M., Alexander, R.W., Griendling, K. K., 1998. Oscillatory and steady laminar shear stress differentially affect human endothelial redox state: role of a superoxide-producing NADH oxidase. *Circ. Res.* *82*, 1094–1101.
- Dedon, P.C., Tannenbaum, S.R., 2004. Reactive nitrogen species in the chemical biology of inflammation. *Arch. Biochem. Biophys.* *423*, 12–22.
- Denicola, A., Batthyany, C., Lissi, E., Freeman, B.A., Rubbo, H., Radi, R., 2002. Diffusion of nitric oxide into low density lipoprotein. *J. Biol. Chem.* *277*, 932–936.
- Denicola, A., Souza, J.M., Radi, R., 1998. Diffusion of peroxynitrite across erythrocyte membranes. *Proc. Natl. Acad. Sci. U S A* *95*, 3566–3571.
- Denicola, A., Souza, J.M., Radi, R., Lissi, E., 1996. Nitric oxide diffusion in membranes determined by fluorescence quenching. *Arch. Biochem. Biophys.* *328*, 208–212.
- Diamond, J.M., Katz, Y., 1974. Interpretation of nonelectrolyte partition coefficients between dimyristoyl lecithin and water. *J. Membr. Biol.* *17*, 121–154.
- Dobrovolskaia, M.A., Vogel, S.N., 2002. Toll receptors, CD14, and macrophage activation and deactivation by LPS. *Microbes. Infect.* *4*, 903–914.
- Espey, M.G., Thomas, D.D., Miranda, K.M., Wink, D.A., 2002. Focusing of nitric oxide mediated nitrosation and oxidative nitrosylation as a consequence of reaction with superoxide. *Proc. Natl. Acad. Sci. U.S.A.* *99*, 11127–11132.
- Esterbauer, H., Gebicki, J., Puhl, H., Jurgens, G., 1992. The role of lipid peroxidation and antioxidants in oxidative modification of LDL. *Free Radic. Biol. Med.* *13*, 341–390.
- Estevez, A.G., Crow, J.P., Sampson, J.B., Reiter, C., Zhuang, Y., Richardson, G.J., Tarpey, M. M., Barbeito, L., Beckman, J.S., 1999. Induction of nitric oxide-dependent apoptosis in motor neurons by zinc-deficient superoxide dismutase. *Science* *286*, 2498–2500.

- Feelisch, M., Schonafinger, K., Noack, E., 1992. Thiol-mediated generation of nitric oxide accounts for the vasodilator action of furoxans. *Biochem. Pharmacol.* 44, 1149–1157.
- Ferreira, A.M., Ferrari, M.I., Trostchansky, A., Batthyany, C., Souza, J.M., Alvarez, M.N., Lopez, G.V., Baker, P.R., Schopfer, F.J., O'Donnell, V., Freeman, B.A., Rubbo, H., 2009. Macrophage activation induces formation of the anti-inflammatory lipid cholesteryl-nitrolinoleate. *Biochem. J.* 417, 223–234.
- Fischkoff, S., Vanderkooi, J.M., 1975. Oxygen diffusion in biological and artificial membranes determined by the fluorochrome pyrene. *J. Gen. Physiol.* 65, 663–676.
- Ford, P.C., Wink, D.A., Stanbury, D.M., 1993. Autoxidation kinetics of aqueous nitric oxide. *FEBS Lett.* 326, 1–3.
- Freeman, B.A., Baker, P.R., Schopfer, F.J., Woodcock, S.R., Napolitano, A., d'Ischia, M., 2008. Nitro-fatty acid formation and signaling. *J. Biol. Chem.* 283, 15515–15519.
- Fruebis, J., Parthasarathy, S., Steinberg, D., 1992. Evidence for a concerted reaction between lipid hydroperoxides and polypeptides. *Proc. Natl. Acad. Sci. U S A* 89, 10588–10592.
- Goldstein, S., Czapski, G., 1995. Kinetics of nitric oxide autoxidation in aqueous solution in the absence and presence of various reductants. The nature of the oxidizing intermediates. *J. Am. Chem. Soc.* 117, 12078–12084.
- Goldstein, S., Czapski, G., 1996. Mechanism of the nitrosation of thiols and amines by oxygenated no solutions: the nature of the nitrosating intermediates. *J. Am. Chem. Soc.* 118, 3419–3425.
- Goldstein, S.J., Lind, J., Merenyi, G., 2004. Reaction of organic peroxy radicals with $\bullet\text{NO}_2$ and $\bullet\text{NO}$ in aqueous solution: intermediacy of organic peroxyxynitrate and peroxyxynitrite species. *J. Phys. Chem. A* 108, 1719–1725.
- Goodwin, D.C., Gunther, M.R., Hsi, L.C., Crews, B.C., Eling, T.E., Mason, R.P., Marnett, L.J., 1998. Nitric oxide trapping of tyrosyl radicals generated during prostaglandin endoperoxide synthase turnover. Detection of the radical derivative of tyrosine 385. *J. Biol. Chem.* 273, 8903–8909.
- Gorczynski, M.J., Huang, J., Lee, H., King, S.B., 2007. Evaluation of nitroalkenes as nitric oxide donors. *Bioorg. Med. Chem. Lett.* 17, 2013–2017.
- Guy, R.A., Maguire, G.F., Crandall, I., Connelly, P.W., Kain, K.C., 2001. Characterization of peroxyxynitrite-oxidized low density lipoprotein binding to human CD36. *Atherosclerosis* 155, 19–28.
- Hamilton, R.T., Asatryan, L., Nilsen, J.T., Isas, J.M., Gallaher, T.K., Sawamura, T., Hsiai, T.K., 2008. LDL protein nitration: implication for LDL protein unfolding. *Arch. Biochem. Biophys.* 479, 1–14.
- Hara, M.R., Agrawal, N., Kim, S.F., Cascio, M.B., Fujimuro, M., Ozeki, Y., Takahashi, M., Cheah, J.H., Tankou, S.K., Hester, L.D., Ferris, C.D., Hayward, S.D., Snyder, S.H., Sawa, A., 2005. S-nitrosylated GAPDH initiates apoptotic cell death by nuclear translocation following Siah1 binding. *Nat. Cell Biol.* 7, 665–674.
- Hazen, S.L., Zhang, R., Shen, Z., Wu, W., Podrez, E.A., MacPherson, J.C., Schmitt, D., Mitra, S.N., Mukhopadhyay, C., Chen, Y.R., Cohen, P.A., Hoff, H.F., Abu-Soud, H.M., 1999. Formation of nitric oxide-derived oxidants by myeloperoxidase in monocytes: pathways for monocyte-mediated protein nitration and lipid peroxidation *in vivo*. *Circ. Res.* 85, 950–958.
- Heitz, S., Lampka, R., Weidauer, D., Hese, A., 1991. Measurements of electric dipole moments on NO_2 . *J. Chem. Phys.* 94, 2532–2535.

- Herold, S., Exner, M., Nauser, T., 2001. Kinetic and mechanistic studies of the NO*-mediated oxidation of oxymyoglobin and oxyhemoglobin. *Biochemistry* 40, 3385–3395.
- Hogg, N., 2002. The biochemistry and physiology of S-nitrosothiols. *Annu. Rev. Pharmacol. Toxicol.* 42, 585–600.
- Horkko, S., Bird, D.A., Miller, E., Itabe, H., Leitinger, N., Subbanagounder, G., Berliner, J.A., Friedman, P., Dennis, E.A., Curtiss, L.K., Palinski, W., Witztum, J.L., 1999. Monoclonal autoantibodies specific for oxidized phospholipids or oxidized phospholipid-protein adducts inhibit macrophage uptake of oxidized low-density lipoproteins. *J. Clin. Invest.* 103, 117–128.
- Hristova, K., White, S.H., 1998. Determination of the hydrocarbon core structure of fluid dioleoylphosphocholine (DOPC) bilayers by x-ray diffraction using specific bromination of the double-bonds: effect of hydration. *Biophys. J.* 74, 2419–2433.
- Hsiai, T.K., Hwang, J., Barr, M.L., Correa, A., Hamilton, R., Alavi, M., Rouhanizadeh, M., Cadenas, E., Hazen, S.L., 2007. Hemodynamics influences vascular peroxynitrite formation: implication for low-density lipoprotein apo-B-100 nitration. *Free Radic. Biol. Med.* 42, 519–529.
- Huie, R.E., 1994. The reaction kinetics of NO₂. *Toxicology* 89, 193–216.
- Hutchinson, F., 1957. The distance that a radical formed by ionizing radiation can diffuse in a yeast cell. *Radiat. Res.* 7, 473–483.
- Ischiropoulos, H., 2003. Oxidative modifications of alpha-synuclein. *Ann. N. Y. Acad. Sci.* 991, 93–100.
- Itabe, H., Suzuki, K., Tsukamoto, Y., Komatsu, R., Ueda, M., Mori, M., Higashi, Y., Takano, T., 2000. Lysosomal accumulation of oxidized phosphatidylcholine-apolipoprotein B complex in macrophages: intracellular fate of oxidized low density lipoprotein. *Biochim. Biophys. Acta* 1487, 233–245.
- Itakura, K., Oya-Ito, T., Osawa, T., Yamada, S., Toyokuni, S., Shibata, N., Kobayashi, M., Uchida, K., 2000. Detection of lipofuscin-like fluorophore in oxidized human low-density lipoprotein. 4-hydroxy-2-nonenal as a potential source of fluorescent chromophore. *FEBS Lett.* 473, 249–253.
- Jain, K., Siddam, A., Marathi, A., Roy, U., Falck, J.R., Balazy, M., 2008. The mechanism of oleic acid nitration by *NO(2). *Free Radic Biol Med.* 45, 269–283.
- Ji, Y., Neverova, I., Van Eyk, J.E., Bennet, B.M., 2006. Nitration of tyrosine 92 mediates the activation of rat microsomal glutathione-S-transferase by peroxynitrite. *J. Biol. Chem.* 281, 1986–1991.
- Jo, E., McLaurin, J., Yip, C.M., St George-Hyslop, P., Fraser, P.E., 2000. Alpha-Synuclein membrane interactions and lipid specificity. *J. Biol. Chem.* 275, 34328–34334.
- Jourd'heuil, D., Jourd'heuil, F.L., Feelisch, M., 2003. Oxidation and nitrosation of thiols at low micromolar exposure to nitric oxide. Evidence for a free radical mechanism. *J. Biol. Chem.* 278, 15720–15726.
- Kaisho, T., Akira, S., 2006. Toll-like receptor function and signaling. *J. Allergy Clin. Immunol.* 117, 979–987; quiz 988.
- Kato, Y., Osawa, T., 1998. Detection of oxidized phospholipid-protein adducts using anti-15-hydroperoxyicosatetraenoic acid-modified protein antibody: contribution of esterified fatty acid-protein adduct to oxidative modification of LDL. *Arch. Biochem. Biophys.* 351, 106–114.
- Kenar, J.A., Havrilla, C.M., Porter, N.A., Guyton, J.R., Brown, S.A., Klemp, K.F., Selinger, E., 1996. Identification and quantification of regioisomeric cholesteryl linoleate

- hydroperoxides in oxidized human low density lipoprotein and high density lipoprotein. *Chem. Res. Toxicol.* 9, 737–744.
- Khairutdinov, R.F., Coddington, J.W., Hurst, J.K., 2000. Permeation of phospholipid membranes by peroxy nitrite. *Biochemistry* 39, 14238–14249.
- Kim, J.G., Sabbagh, F., Santanam, N., Wilcox, J.N., Medford, R.M., Parthasarathy, S., 1997. Generation of a polyclonal antibody against lipid peroxide-modified proteins. *Free Radic. Biol. Med.* 23, 251–259.
- Kusumi, A., Hyde, J.S., 1982. Spin-label saturation-transfer electron spin resonance detection of transient association of rhodopsin in reconstituted membranes. *Biochemistry* 21, 5978–5983.
- Leeuwenburgh, C., Hardy, M.M., Hazen, S.L., Wagner, P., Oh-ishi, S., Steinbrecher, U.P., Heinecke, J.W., 1997a. Reactive nitrogen intermediates promote low density lipoprotein oxidation in human atherosclerotic intima. *J. Biol. Chem.* 272, 1433–1436.
- Leeuwenburgh, C., Rasmussen, J.E., Hsu, F.F., Mueller, D.M., Pennathur, S., Heinecke, J.W., 1997b. Mass spectrometric quantification of markers for protein oxidation by tyrosyl radical, copper, and hydroxyl radical in low density lipoprotein isolated from human atherosclerotic plaques. *J. Biol. Chem.* 272, 3520–3526.
- Li, Y., Zhang, J., Schopfer, F.J., Martynowski, D., Garcia-Barrio, M.T., Kovach, A., Suino-Powell, K., Baker, P.R., Freeman, B.A., Chen, Y.E., Xu, H.E., 2008. Molecular recognition of nitrated fatty acids by PPAR gamma. *Nat. Struct. Mol. Biol.* 15, 865–867.
- Liao, J.C., T, W.H., Vaughn, M.W., Huang, K.T., Kuo, L., 1999. Intravascular flow decreases erythrocyte consumption of nitric oxide. *Proc. Natl. Acad. Sci. U S A* 96, 8757–8761.
- Lieb, W.R., Stein, W.D., 1986. Simple diffusion across the membrane bilayer. In: Stein, W.D. (Ed.), *Transport and Diffusion Across Cell Membranes*. Academic Press, Orlando, FL, pp. 69–112.
- Lim, D.G., Sweeney, S., Bloodsworth, A., White, C.R., Chumley, P.H., Krishna, N.R., Schopfer, F., O'Donnell, V.B., Eiserich, J.P., Freeman, B.A., 2002. Nitrolinoleate, a nitric oxide-derived mediator of cell function: synthesis, characterization, and vasomotor activity. *Proc. Natl. Acad. Sci. U S A*, 99, 15941–15946.
- Lima, E.S., Bonini, M.G., Augusto, O., Barbeiro, H.V., Souza, H.P., Abdalla, D.S., 2005. Nitrated lipids decompose to nitric oxide and lipid radicals and cause vasorelaxation. *Free Radic. Biol. Med.* 39, 532–539.
- Lima, E.S., Di Mascio, P., Abdalla, D.S., 2003. Cholesteryl nitrolinoleate, a nitrated lipid present in human blood plasma and lipoproteins. *J. Lipid Res.* 44, 1660–1666.
- Lima, E.S., Di Mascio, P., Rubbo, H., Abdalla, D.S., 2002. Characterization of linoleic acid nitration in human blood plasma by mass spectrometry. *Biochemistry* 41, 10717–10722.
- Liu, X., Miller, M.J., Joshi, M.S., Sadowska-Krowicka, H., Clark, D.A., Lancaster, Jr., J.R., 1998a. Diffusion-limited reaction of free nitric oxide with erythrocytes. *J. Biol. Chem.* 273, 18709–18713.
- Liu, X., Miller, M.J., Joshi, M.S., Thomas, D.D., Lancaster, Jr., J.R., 1998b. Accelerated reaction of nitric oxide with O₂ within the hydrophobic interior of biological membranes. *Proc. Natl. Acad. Sci. U S A* 95, 2175–2179.
- Liu, X., Samouilov, A., Lancaster, Jr., J.R., Zweier, J.L., 2002. Nitric oxide uptake by erythrocytes is primarily limited by extracellular diffusion not membrane resistance. *J. Biol. Chem.* 277, 26194–26199.

- Liu, X., Yan, Q., Baskerville, K.L., Zweier, J.L., 2007. Estimation of nitric oxide concentration in blood for different rates of generation. Evidence that intravascular nitric oxide levels are too low to exert physiological effects. *J. Biol. Chem.* 282, 8831–8836.
- Lopez, G.V., Batthyany, C., Blanco, F., Botti, H., Trostchansky, A., Migliaro, E., Radi, R., Gonzalez, M., Cerecetto, H., Rubbo, H., 2005. Design, synthesis, and biological characterization of potential antiatherogenic nitric oxide releasing tocopherol analogs. *Bioorg. Med. Chem.* 13, 5787–5796.
- Malinski, T., Taha, Z., Grunfeld, S., Patton, S., Kapturczak, M., Tombouljan, P., 1993. Diffusion of nitric oxide in the aorta wall monitored in situ by porphyrinic microsensors. *Biochem. Biophys. Res. Commun.* 193, 1076–1082.
- Mallozzi, C., Di Stasi, A.M., Minetti, M., 1997. Peroxynitrite modulates tyrosine-dependent signal transduction pathway of human erythrocyte band 3. *FASEB J.* 11, 1281–1290.
- Marla, S.S., Lee, J., Groves, J.T., 1997. Peroxynitrite rapidly permeates phospholipid membranes. *Proc. Natl. Acad. Sci. U S A* 94, 14243–14248.
- Marx, N., 2002. PPARgamma and vascular inflammation: adding another piece to the puzzle. *Circ. Res.* 91, 373–374.
- Marx, N., Duez, H., Fruchart, J.C., Staels, B., 2004. Peroxisome proliferator-activated receptors and atherogenesis: regulators of gene expression in vascular cells. *Circ. Res.* 94, 1168–1178.
- Marx, N., Kehrle, B., Kohlhammer, K., Grub, M., Koenig, W., Hombach, V., Libby, P., Plutzky, J., 2002. PPAR activators as antiinflammatory mediators in human T lymphocytes: implications for atherosclerosis and transplantation-associated arteriosclerosis. *Circ. Res.* 90, 703–710.
- Medana, C., Ermondi, G., Fruttero, R., Di Stilo, A., Ferretti, C., Gasco, A., 1994. Furoxans as nitric oxide donors. 4-Phenyl-3-furoxan carbonitrile: thiol-mediated nitric oxide release and biological evaluation. *J. Med. Chem.* 37, 4412–4416.
- Mendiara, S.N., Perissinotti, L.J., 2003. Dissociation equilibrium of dinitrogen tetroxide in organic solvents: An electron paramagnetic resonance measurement. *Appl. Magn. Reson.* 25, 323–346.
- Merenyi, G., Lind, J., Goldstein, S., Czapski, G., 1999. Mechanism and thermochemistry of peroxynitrite decomposition in water. *J. Phys. Chem. A* 103, 5685–5691.
- Miersch, S., Espey, M.G., Chaube, R., Akarca, A., Tweten, R., Ananvoranich, S., Mutus, B., 2008. Plasma membrane cholesterol content affects nitric oxide diffusion dynamics and signaling. *J. Biol. Chem.* 283, 18513–18521.
- Möller, M., Botti, H., Batthyany, C., Rubbo, H., Radi, R., Denicola, A., 2005. Direct measurement of nitric oxide and oxygen partitioning into liposomes and low density lipoprotein. *J. Biol. Chem.* 280, 8850–8854.
- Möller, M.N., Lancaster, Jr., J.R., Denicola, A., 2008. The interaction of reactive oxygen and nitrogen species with membranes. In: Matalon, S. (Ed.), *Free Radical Effects on Membranes*, Vol. 61. Academic Press Inc, pp. 23–43.
- Möller, M.N., Li, Q., Lancaster, Jr., J.R., Denicola, A., 2007a. Acceleration of nitric oxide autoxidation and nitrosation by membranes. *IUBMB Life* 59, 243–248.
- Möller, M.N., Li, Q., Vitturi, D.A., Robinson, J.M., Lancaster, Jr., J.R., Denicola, A., 2007b. Membrane “lens” effect: focusing the formation of reactive nitrogen oxides from the *NO/O₂ reaction. *Chem. Res. Toxicol.* 20, 709–714.
- Morrell, C.N., Matsushita, K., Chiles, K., Scharpf, R.B., Yamakuchi, M., Mason, R.J., Bergmeier, W., Mankowski, J.L., Baldwin, 3rd, W.M., Faraday, N., Lowenstein, C.J., 2005.

- Regulation of platelet granule exocytosis by S-nitrosylation. *Proc. Natl. Acad. Sci. U S A* 102, 3782–3787.
- Murray, J., Taylor, S.W., Zhang, B., Ghosh, S.S., Capaldi, R.A., 2003. Oxidative damage to mitochondrial complex I due to peroxynitrite: identification of reactive tyrosines by mass spectrometry. *J. Biol. Chem.* 278, 37223–37230.
- Napolitano, A., Camera, E., Picardo, M., d'Ischia, M., 2000. Acid-promoted reactions of ethyl linoleate with nitrite ions: formation and structural characterization of isomeric nitroalkene, nitrohydroxy, and novel 3-nitro-1,5-hexadiene and 1,5-dinitro-1, 3-pentadiene products. *J. Org. Chem.* 65, 4853–4860.
- Napolitano, A., Panzella, L., Savarese, M., Sacchi, R., Giudicianni, I., Paolillo, L., d'Ischia, M., 2004. Acid-induced structural modifications of unsaturated fatty acids and phenolic olive oil constituents by nitrite ions: a chemical assessment. *Chem. Res. Toxicol.* 17, 1329–1337.
- Nauser, T., Koppenol, W.H., 2002. The rate constant of the reaction of superoxide with nitrogen monoxide: approaching the diffusion limit. *J. Phys. Chem. A* 106, 4084–4086.
- Nottingham, W.C., Sutter, J.R., 1986. Kinetics of the oxidation of nitric oxide by chlorine and oxygen in nonaqueous media. *Int. J. Chem. Kinet.* 18, 1289–1302.
- O'Donnell, V.B., Eiserich, J.P., Chumley, P.H., Jablonsky, M.J., Krishna, N.R., Kirk, M., Barnes, S., Darley-Usmar, V.M., Freeman, B.A., 1999a. Nitration of unsaturated fatty acids by nitric oxide-derived reactive nitrogen species peroxynitrite, nitrous acid, nitrogen dioxide, and nitronium ion. *Chem. Res. Toxicol.* 12, 83–92.
- O'Donnell, V.B., Freeman, B.A., 2001. Interactions between nitric oxide and lipid oxidation pathways: implications for vascular disease. *Circ. Res.* 88, 12–21.
- O'Donnell, V.B., Taylor, K.B., Parthasarathy, S., Kuhn, H., Koesling, D., Friebe, A., Bloodsworth, A., Darley-Usmar, V.M., Freeman, B.A., 1999b. 15-Lipoxygenase catalytically consumes nitric oxide and impairs activation of guanylate cyclase. *J. Biol. Chem.* 274, 20083–20091.
- Orlova, E.V., Sherman, M.B., Chiu, W., Mowri, H., Smith, L.C., Gotto, Jr., A.M., 1999. Three-dimensional structure of low density lipoproteins by electron cryomicroscopy. *Proc. Natl. Acad. Sci. U S A* 96, 8420–8425.
- Padmaja, S., Huie, R.E., 1993. The reaction of nitric oxide with organic peroxy radicals. *Biochem. Biophys. Res. Commun.* 195, 539–544.
- Pannala, A.S., Mani, A.R., Spencer, J.P., Skinner, V., Bruckdorfer, K.R., Moore, K.P., Rice-Evans, C.A., 2003. The effect of dietary nitrate on salivary, plasma, and urinary nitrate metabolism in humans. *Free Radic. Biol. Med.* 34, 576–584.
- Parinandi, N.L., Sharma, A., Eubank, T.D., Kaufman, B.F., Kutala, V.K., Marsh, C.B., Ignarro, L.J., Kuppusamy, P., 2007. Nitroaspirin (NCX-4016), an NO donor, is antiangiogenic through induction of loss of redox-dependent viability and cytoskeletal reorganization in endothelial cells. *Antioxid. Redox Signal.* 9, 1837–1849.
- Peluffo, G., Radi, R., 2007. Biochemistry of protein tyrosine nitration in cardiovascular pathology. *Cardiovasc. Res.* 75, 291–302.
- Perrin, R.J., Woods, W.S., Clayton, D.F., George, J.M., 2000. Interaction of human alpha-Synuclein and Parkinson's disease variants with phospholipids. Structural analysis using site-directed mutagenesis. *J. Biol. Chem.* 275, 34393–34398.
- Podrez, E.A., Schmitt, D., Hoff, H.F., Hazen, S.L., 1999. Myeloperoxidase-generated reactive nitrogen species convert LDL into an atherogenic form *in vitro*. *J. Clin. Invest.* 103, 1547–1560.

- Potter, D.D., Sobey, C.G., Tompkins, P.K., Rossen, J.D., Heistad, D.D., 1998. Evidence that macrophages in atherosclerotic lesions contain angiotensin II. *Circulation* 98, 800–807.
- Radi, R., 1996. Kinetic analysis of reactivity of peroxynitrite with biomolecules. *Methods Enzymol.* 269, 354–366.
- Radi, R., 2004. Nitric oxide, oxidants, and protein tyrosine nitration. *Proc. Natl. Acad. Sci. U S A* 101, 4003–4008.
- Radi, R., Beckman, J.S., Bush, K.M., Freeman, B.A., 1991a. Peroxynitrite-induced membrane lipid peroxidation: the cytotoxic potential of superoxide and nitric oxide. *Arch. Biochem. Biophys.* 288, 481–487.
- Radi, R., Beckman, J.S., Bush, K.M., Freeman, B.A., 1991b. Peroxynitrite oxidation of sulfhydryls. The cytotoxic potential of superoxide and nitric oxide. *J. Biol. Chem.* 266, 4244–4250.
- Radi, R., Denicola, A., Alvarez, B., Ferrer, G., Rubbo, H., 2000. The Biological chemistry of peroxynitrite. In: Ignarro, L.J. (Ed.), *Nitric Oxide Biology and Pathobiology*. Academic Press, San Diego, pp. 57–82.
- Requena, J.R., Fu, M.X., Ahmed, M.U., Jenkins, A.J., Lyons, T.J., Baynes, J.W., Thorpe, S.R., 1997. Quantification of malondialdehyde and 4-hydroxynonenal adducts to lysine residues in native and oxidized human low-density lipoprotein. *Biochem. J.* 322, 317–325.
- Romero, N., Denicola, A., Souza, J.M., Radi, R., 1999. Diffusion of peroxynitrite in the presence of carbon dioxide. *Arch. Biochem. Biophys.* 368, 23–30.
- Romero, N., Peluffo, G., Bartsaghi, S., Zhang, H., Joseph, J., Kalyanaraman, B., Radi, R., 2007. Incorporation of the hydrophobic probe N-t-BOC-L-tyrosine tert-butyl ester to red blood cell membranes to study peroxynitrite-dependent reactions. *Chem. Res. Toxicol.* 20, 1638–1648.
- Rubbo, H., Batthyány, C., Freeman, B.A., Radi, R., Denicola, A., 1998. Nitric oxide diffusion across low density lipoprotein and inhibition of lipid oxidation-dependent chemiluminescence. *Nitric Oxide* 2, 117.
- Rubbo, H., Botti, H., Batthyany, C., Trostchansky, A., Denicola, A., Radi, R., 2002a. Antioxidant and diffusion properties of nitric oxide in low-density lipoprotein. *Methods Enzymol.* 359, 200–209.
- Rubbo, H., O'Donnell, V., 2005. Nitric oxide, peroxynitrite and lipoxygenase in atherogenesis: mechanistic insights. *Toxicology* 208, 305–317.
- Rubbo, H., Parthasarathy, S., Barnes, S., Kirk, M., Kalyanaraman, B., Freeman, B.A., 1995. Nitric oxide inhibition of lipoxygenase-dependent liposome and low-density lipoprotein oxidation: termination of radical chain propagation reactions and formation of nitrogen-containing oxidized lipid derivatives. *Arch. Biochem. Biophys.* 324, 15–25.
- Rubbo, H., Radi, R., 2001. Antioxidant properties of nitric oxide. In: Cadenas, E.a.P.L. (Ed.), *Handbook of Antioxidants*, vol. 32. Marcel Dekker Inc, New York, pp. 689–706.
- Rubbo, H., Radi, R., 2008. Protein and lipid nitration: role in redox signaling and injury. *Biochim. Biophys. Acta* 1780, 1318–1324.
- Rubbo, H., Radi, R., Anselmi, D., Kirk, M., Barnes, S., Butler, J., Eiserich, J.P., Freeman, B.A., 2000. Nitric oxide reaction with lipid peroxyl radicals spares alpha-tocopherol during lipid peroxidation. Greater oxidant protection from the pair nitric oxide/alpha-tocopherol than alpha-tocopherol/ascorbate. *J. Biol. Chem.* 275, 10812–10818.
- Rubbo, H., Radi, R., Trujillo, M., Telleri, R., Kalyanaraman, B., Barnes, S., Kirk, M., Freeman, B.A., 1994. Nitric oxide regulation of superoxide and peroxynitrite-dependent lipid peroxidation. Formation of novel nitrogen-containing oxidized lipid derivatives. *J. Biol. Chem.* 269, 26066–26075.

- Rubbo, H., Trostchansky, A., Botti, H., Batthyany, C., 2002b. Interactions of nitric oxide and peroxynitrite with low-density lipoprotein. *Biol. Chem.* 383, 547–552.
- Sackmann, E., 1995. Biological membranes: architecture and function. In: Lipowsky, R., Sackmann, E. (Eds.) *Structure and Dynamics of Membranes*, vol. 1A. Elsevier Science B.V, Amsterdam, pp. 1–62.
- Salvemini, D., Seibert, K., Masferrer, J.L., Settle, S.L., Currie, M.G., Needleman, P., 1995. Nitric oxide activates the cyclooxygenase pathway in inflammation. *Am. J. Ther.* 2, 616–619.
- Schartl, M., Bocksch, W., Koschyk, D.H., Voelker, W., Karsch, K.R., Kreuzer, J., Hausmann, D., Beckmann, S., Gross, M., 2001. Use of intravascular ultrasound to compare effects of different strategies of lipid-lowering therapy on plaque volume and composition in patients with coronary artery disease. *Circulation* 104, 387–392.
- Schonhoff, C.M., Matsuoka, M., Tummala, H., Johnson, M.A., Estevez, A.G., Wu, R., Kamaid, A., Ricart, K.C., Hashimoto, Y., Gaston, B., Macdonald, T.L., Xu, Z., Mannick, J.B., 2006. S-nitrosothiol depletion in amyotrophic lateral sclerosis. *Proc. Natl. Acad. Sci. U S A* 103, 2404–2409.
- Schopfer, F., Batthyany, C., Baker, P.R., Bonacci, G., Cole, M.P., Rudolph, V., Groeger, A.L., Rudolph, T.K., Nadtochiy, S.M., Brookes, P.S., Freeman, B.A., 2009. Detection and quantification of protein adduction by electrophilic fatty acids: mitochondrial generation of fatty acid nitroalkene derivatives. *Free Radic. Biol. Med.* 46, 1250–1259.
- Schopfer, F.J., Baker, P.R., Giles, G., Chumley, P., Batthyany, C., Crawford, J., Patel, R.P., Hogg, N., Branchaud, B.P., Lancaster, Jr. J.R., Freeman, B.A., 2005a. Fatty acid transduction of nitric oxide signaling. Nitrolinoleic acid is a hydrophobically stabilized nitric oxide donor. *J. Biol. Chem.* 280, 19289–19297.
- Schopfer, F.J., Lin, Y., Baker, P.R., Cui, T., Garcia-Barrio, M., Zhang, J., Chen, K., Chen, Y.E., Freeman, B.A., 2005b. Nitrolinoleic acid: an endogenous peroxisome proliferator-activated receptor gamma ligand. *Proc. Natl. Acad. Sci. U S A* 102, 2340–2345.
- Seccia, M., Perugini, C., Bellomo, G., 1997. The formation of some antigenic epitopes in oxidized human low-density lipoprotein is inhibited by nitric oxide. *Biochem. Biophys. Res. Commun.* 232, 613–617.
- Segrest, J.P., Jones, M.K., De Loof, H., Brouillette, C.G., Venkatachalapathi, Y.V., Anantharamaiah, G.M., 1992. The amphipathic helix in the exchangeable apolipoproteins: a review of secondary structure and function. *J. Lipid Res.* 33, 141–166.
- Shao, B., Bergt, C., Fu, X., Green, P., Voss, J.C., Oda, M.N., Oram, J.F., Heinecke, J.W., 2005. Tyrosine 192 in apolipoprotein A-I is the major site of nitration and chlorination by myeloperoxidase, but only chlorination markedly impairs ABCA1-dependent cholesterol transport. *J. Biol. Chem.* 280, 5983–5993.
- Shaw, A.W., Vosper, A.J., 1977. Solubility of nitric oxide in aqueous and nonaqueous solvents. *J. Chem. Soc. Faraday Trans.* 8, 1239–1244.
- Souza, J.M., Peluffo, G., Radi, R., 2008. Protein tyrosine nitration- functional alteration or just a biomarker?. *Free Radic. Biol. Med.* 45, 357–366.
- Stanbury, D.M., 1989. Reduction potentials involving inorganic free radicals in aqueous solution. *Adv. Inorg. Chem.* 33, 69–138.
- Steinbrecher, U.P., 1987. Oxidation of human low density lipoprotein results in derivatization of lysine residues of apolipoprotein B by lipid peroxide decomposition products. *J. Biol. Chem.* 262, 3603–3608.

- Steinbrecher, U.P., Loughheed, M., Kwan, W.C., Dirks, M., 1989. Recognition of oxidized low density lipoprotein by the scavenger receptor of macrophages results from derivatization of apolipoprotein B by products of fatty acid peroxidation. *J. Biol. Chem.* 264, 15216–15223.
- Steinbrecher, U.P., Witztum, J.L., Parthasarathy, S., Steinberg, D., 1987. Decrease in reactive amino groups during oxidation or endothelial cell modification of LDL. Correlation with changes in receptor-mediated catabolism. *Arteriosclerosis* 7, 135–143.
- Subczynski, W.K., Lomnicka, M., Hyde, J.S., 1996. Permeability of nitric oxide through lipid bilayer membranes. *Free Radic. Res.* 24, 343–349.
- Szabo, C., Ischiropoulos, H., Radi, R., 2007. Peroxynitrite: biochemistry, pathophysiology and development of therapeutics. *Nat. Rev. Drug Discov.* 6, 662–680.
- Tayeh, M.A., Scicli, A.G., 1998. Angiotensin II and bradykinin regulate the expression of P-selectin on the surface of endothelial cells in culture. *Proc. Assoc. Am. Physicians* 110, 412–421.
- Thoma-Uszynski, S., Stenger, S., Takeuchi, O., Ochoa, M.T., Engele, M., Sieling, P.A., Barnes, P.F., Rollinghoff, M., Bolcskei, P.L., Wagner, M., Akira, S., Norgard, M.V., Belisle, J.T., Godowski, P.J., Bloom, B.R., Modlin, R.L., 2001. Induction of direct antimicrobial activity through mammalian toll-like receptors. *Science* 291, 1544–1547.
- Trostchansky, A., Batthyany, C., Botti, H., Radi, R., Denicola, A., Rubbo, H., 2001. Formation of lipid-protein adducts in low-density lipoprotein by fluxes of peroxynitrite and its inhibition by nitric oxide. *Arch. Biochem. Biophys.* 395, 225–232.
- Trostchansky, A., Lind, S., Hodara, R., Oe, T., Blair, I.A., Ischiropoulos, H., Rubbo, H., Souza, J.M., 2006. Interaction with phospholipids modulates alpha-synuclein nitration and lipid-protein adduct formation. *Biochem. J.* 393, 343–349.
- Trostchansky, A., O'Donnell, V.B., Goodwin, D.C., Landino, L.M., Marnett, L.J., Radi, R., Rubbo, H., 2007a. Interactions between nitric oxide and peroxynitrite during prostaglandin endoperoxide H synthase-1 catalysis: a free radical mechanism of inactivation. *Free Radic. Biol. Med.* 42, 1029–1038.
- Trostchansky, A., Rubbo, H., 2008. Nitrated fatty acids: mechanisms of formation, chemical characterization, and biological properties. *Free Radic. Biol. Med.* 44, 1887–1896.
- Trostchansky, A., Souza, J.M., Ferreira, A., Ferrari, M., Blanco, F., Trujillo, M., Castro, D., Cerecetto, H., Baker, P.R., O'Donnell, V.B., Rubbo, H., 2007b. Synthesis, isomer characterization, and anti-inflammatory properties of nitroarachidonate. *Biochemistry* 46, 4645–4653.
- Tsai, L., Szweda, P.A., Vinogradova, O., Szweda, L.I., 1998. Structural characterization and immunochemical detection of a fluorophore derived from 4-hydroxy-2-nonenal and lysine. *Proc. Natl. Acad. Sci. U S A* 95, 7975–7980.
- Uchida, K., 2000. Role of reactive aldehyde in cardiovascular diseases. *Free Radic. Biol. Med.* 28, 1685–1696.
- Viner, R.I., Ferrington, D.A., Williams, T.D., Bigelow, D.J., Schoneich, C., 1999. Protein modification during biological aging: selective tyrosine nitration of the SERCA2a isoform fo sarcoplasmic reticulum Ca²⁺ + -ATPase in skeletal muscle. *Biochem. J.* 340, 657–669.
- Wallace, J.L., Ignarro, L.J., Fiorucci, S., 2002. Potential cardioprotective actions of no-releasing aspirin. *Nat. Rev. Drug Discov.* 1, 375–382.
- Wang, P.G., Xian, M., Tang, X., Wu, X., Wen, Z., Cai, T., Janczuk, A.J., 2002. Nitric oxide donors: chemical activities and biological applications. *Chem. Rev.* 102, 1091–1134.

- Weinreb, P.H., Zhen, W., Poon, A.W., Conway, K.A., Lansbury, Jr., P.T., 1996. NACP, a protein implicated in Alzheimer's disease and learning, is natively unfolded. *Biochemistry* 35, 13709–13715.
- Werling, D., Hope, J.C., Howard, C.J., Jungi, T.W., 2004. Differential production of cytokines, reactive oxygen and nitrogen by bovine macrophages and dendritic cells stimulated with Toll-like receptor agonists. *Immunology* 111, 41–52.
- Wever, R.M., Luscher, T.F., Cosentino, F., Rabelink, T.J., 1998. Atherosclerosis and the two faces of endothelial nitric oxide synthase. *Circulation* 97, 108–112.
- Wiener, M.C., White, S.H., 1992. Structure of a fluid dioleoylphosphatidylcholine bilayer determined by joint refinement of x-ray and neutron diffraction data. II. Distribution and packing of terminal methyl groups. *Biophys. J.* 61, 428–433.
- Wright, M.M., Schopfer, F.J., Baker, P.R., Vidyasagar, V., Powell, P., Chumley, P., Iles, K.E., Freeman, B.A., Agarwal, A., 2006. Fatty acid transduction of nitric oxide signaling: Nitrolinoleic acid potently activates endothelial heme oxygenase 1 expression. *Proc. Natl. Acad. Sci. U S A* 103, 4299–4304.
- Xu, S., Ying, J., Jiang, B., Guo, W., Adachi, T., Sharov, V., Lazar, H., Menzoian, J., Knyushko, T.V., Bigelow, D.J., Schoneich, C., Cohen, R.A., 2006. Detection of sequence-specific tyrosine nitration of manganese SOD and SERCA in cardiovascular disease and aging. *Am. J. Physiol. Heart Circ. Physiol.* 290, 2220–2227.
- Yao, D., Gu, Z., Nakamura, T., Shi, Z.Q., Ma, Y., Gaston, B., Palmer, L.A., Rockenstein, E.M., Zhang, Z., Masliah, E., Uehara, T., Lipton, S.A., 2004. Nitrosative stress linked to sporadic Parkinson's disease: S-nitrosylation of parkin regulates its E3 ubiquitin ligase activity. *Proc. Natl. Acad. Sci. U S A* 101, 10810–10814.
- Zacharia, I.G., Deen, W.M., 2005. Diffusivity and solubility of nitric oxide in water and saline. *Ann. Biomed. Eng.* 33, 21–222.
- Zhang, H., Bhargava, K., Keszler, A., Feix, J., Hogg, N., Joseph, J., Kalyanaraman, B., 2003. Transmembrane nitration of hydrophobic tyrosyl peptides. Localization, characterization, mechanism of nitration, and biological implications. *J. Biol. Chem.* 278, 8969–8978.
- Zhang, H., Joseph, J., Feix, J., Hogg, N., Kalyanaraman, B., 2001. Nitration and oxidation of a hydrophobic tyrosine probe by peroxynitrite in membranes: comparison with nitration and oxidation of tyrosine by peroxynitrite in aqueous solution. *Biochemistry* 40, 7675–7686.
- Zhang, H., Xu, Y., Joseph, J., Kalyanaraman, B., 2008. Influence of intramolecular electron transfer mechanism in biological nitration, nitrosation, and oxidation of redox-sensitive amino acids. *Methods Enzymol.* 440, 65–94.
- Zheng, L., Settle, M., Brubaker, G., Schmitt, D., Hazen, S.L., Smith, J.D., Kinter, M., 2005. Localization of nitration and chlorination sites on apolipoprotein A-I catalyzed by myeloperoxidase in human atheroma and associated oxidative impairment in ABCA1-dependent cholesterol efflux from macrophages. *J. Biol. Chem.* 280, 38–47.
- Ziegler, T., Bouzourene, K., Harrison, V.J., Brunner, H.R., Hayoz, D., 1998. Influence of oscillatory and unidirectional flow environments on the expression of endothelin and nitric oxide synthase in cultured endothelial cells. *Arterioscler. Thromb. Vasc. Biol.* 18, 686–692.
- Zwolinski, B.J., Eyring, H., Reese, C.E., 1949. Diffusion and membrane permeability. *J. Phys. Colloid Chem.* 53, 1426–1453.

TYROSINE NITRATION, DIMERIZATION, AND HYDROXYLATION BY PEROXYNITRITE IN MEMBRANES AS STUDIED BY THE HYDROPHOBIC PROBE *N-T-BOC-L-TYROSINE TERT-BUTYL ESTER*

Silvina Bartesaghi,^{*,†} Gonzalo Peluffo,^{*} Hao Zhang,[‡] Joy Joseph,[‡]
Balaraman Kalyanaraman,[‡] and Rafael Radi^{*}

Contents

1. Introduction	218
2. Methods	220
2.1. Synthesis of BTBE and its oxidation products	220
2.2. Preparation of BTBE-containing liposomes and peroxyxynitrite addition	221
2.3. Sample preparation	221
2.4. HPLC analysis	222
2.5. Spectrophotometric analysis	222
2.6. Mass spectrometry analysis of 3-hydroxy-BTBE	223
2.7. Electron spin resonance (ESR) measurements	223
3. Results	223
3.1. Electron spin resonance spin trapping of BTBE phenoxy radical	223
3.2. HPLC and spectroscopic analysis of BTBE, 3-nitro-BTBE, and 3,3'-di-BTBE	225
3.3. Peroxyxynitrite-mediated BTBE hydroxylation in DLPC liposomes	225
3.4. Mass spectrometry characterization of 3-hydroxy-BTBE	227

* Department of Biochemistry and Center for Free Radical and Biomedical Research, Facultad de Medicina Universidad de la República, Montevideo, Uruguay

† Department of Histology and Embryology, Facultad de Medicina, Universidad de la República, Montevideo, Uruguay

‡ Department of Biophysics and Free Radical Research Center, Medical College of Wisconsin, Milwaukee, Wisconsin

3.5. Enhancers and inhibitors of peroxynitrite-mediated tyrosine oxidation in membranes	228
3.6. Effect of pH on nitration, dimerization, and hydroxylation yields	231
4. Discussion	232
Acknowledgments	234
References	234

Abstract

Protein tyrosine oxidation mechanisms in hydrophobic biocompartments (i.e., biomembranes, lipoproteins) leading to nitrated, dimerized, and hydroxylated products are just starting to be appreciated. This chapter reports on the use of the hydrophobic tyrosine analog *N*-*t*-BOC-L-tyrosine *tert*-butyl ester (BTBE) incorporated to phosphatidyl choline liposomes to study peroxynitrite-dependent tyrosine oxidation processes in model biomembranes. The probe proved to be valuable in defining the role of biologically relevant variables in the oxidation process, including the action of hydrophilic and hydrophobic peroxynitrite and peroxynitrite-derived free radical scavengers, transition metal catalysts, carbon dioxide, molecular oxygen, pH, and fatty acid unsaturation degree. Moreover, detection of the BTBE phenoxyl radical and relative product distribution yields of 3-nitro-, 3,3'-di-, and 3-hydroxy-BTBE in the membrane fully accommodate with a free radical mechanism of tyrosine oxidation, with physical chemical and biochemical determinants that in several respects differ of those participating in aqueous environments. The methods presented herein can be extended to explore the reaction mechanisms of tyrosine oxidation by other biologically relevant oxidants and in other hydrophobic biocompartments.

1. INTRODUCTION

Protein tyrosine nitration has been associated with several pathologies (Beckman *et al.*, 1994), such as inflammation, cardiovascular disease, neurodegeneration, and diabetic complications, and has been revealed as a biomarker of oxidative stress *in vivo* and a predictor of disease progression and severity (Shishehbor *et al.*, 2003; Zhang *et al.*, 2001b; Zheng *et al.*, 2005).

The nitration of protein tyrosine residues constitutes the substitution of hydrogen by a nitro group ($-\text{NO}_2$; +45 Da) in the three position of the phenolic ring and represents a posttranslational modification produced by nitric oxide ($\cdot\text{NO}$)-derived oxidants, such as peroxynitrite (ONOOH , ONOO^-),¹ and nitrogen dioxide radical ($\cdot\text{NO}_2$).

¹ IUPAC-recommended names for peroxynitrite anion (ONOO^-) and peroxynitrous acid (ONOOH , $\text{pK}_a=6.8$) are oxoperoxynitrate (1-) and hydrogen oxoperoxynitrate, respectively. The term peroxynitrite is used to refer to the sum of ONOO^- and ONOOH .

Early work showed that nitration could result in dramatic changes in protein structure and function (Sokolovsky *et al.*, 1966), resulting in either a gain or a loss of function (Radi, 2004); however, it was not until the early nineties (Beckman *et al.*, 1990; Ischiropoulos *et al.*, 1992) when the biological significance of protein tyrosine nitration was really appreciated, after recognizing the formation of strong oxidizing and nitrating intermediates during the biological oxidation of $\cdot\text{NO}$ (Beckman *et al.*, 1990; Koppenol *et al.*, 1992; Radi *et al.*, 1991a,b). Since then, protein tyrosine nitration has been well established to occur both *in vivo* and *in vitro* (Ischiropoulos, 1998; Radi, 2004).

Tyrosine nitration takes place biologically by a variety of routes, all of them based in free radical chemistry. The oxidation of tyrosine² by different oxidants (such as hydroxyl radical ($\cdot\text{OH}$), carbonate radical ($\text{CO}_3^{\cdot-}$), $\cdot\text{NO}_2$, and oxo-metal complexes) yields tyrosyl radical ($\cdot\text{Tyr}$), which reacts with nitrogen dioxide ($\cdot\text{NO}_2$) or another tyrosyl radical to yield 3-nitrotyrosine (3- NO_2 -Tyr) and di-tyrosine (3,3'-di-Tyr), respectively. Alternatively, 3-nitrotyrosine can be formed secondary to the reaction of $\cdot\text{NO}$ with tyrosyl radical to yield the transient 3-nitrosotyrosine, which must be further oxidized by two consecutive one-electron steps with the intermediate formation of an iminoxyl radical (Radi, 2004; Sturgeon *et al.*, 2001); in conjunction with these radicals processes, the addition of $\cdot\text{OH}$ to the tyrosyl radical leads to the formation of a hydroxylated derivative, 3,4-dihydroxyphenylalanine (DOPA) (Barteseghi *et al.*, 2007; Radi, 2004; Santos *et al.*, 2000).

It has become evident that nitration of protein tyrosine can occur in both hydrophilic or hydrophobic biocompartments (e.g., in proteins associated to biomembranes and lipoproteins; reviewed in Barteseghi *et al.*, 2007) and that various factors controlling the nitration pathways may differ in both compartments. For instance, in the hydrophobic phase, several factors can promote tyrosine nitration, whereas others may inhibit this process. Enhanced nitration can be due to different factors, such as a higher concentration of $\cdot\text{NO}_2/\cdot\text{NO}$ in this phase, membrane-associated transition metal centers (e.g., heme), or the exclusion of antioxidants such as glutathione, which have a relevant role in aqueous phases. However, the high concentration of unsaturated fatty acids in membranes, which may outcompete for the radical species and therefore inhibit tyrosine nitration, as well as the lack of permeability of some of the oxidants to the hydrophobic compartment [e.g., $\text{CO}_3^{\cdot-}$ (Barteseghi *et al.*, 2006), compound I myeloperoxidase (Zhang *et al.*, 2003)] may lead to lower nitration yields relative to the aqueous phase.

Peroxynitrite does not react directly with tyrosine (Alvarez *et al.*, 1999), but peroxynitrite-derived radicals (e.g., $\cdot\text{OH}$, $\text{CO}_3^{\cdot-}$, NO_2) do. Because the peroxynitrite-derived radicals are short-lived, the nitration of tyrosine in membranes by ONOOH can occur mainly by two mechanisms: peroxynitrite

² The term oxidation refers to the sum of nitration, dimerization, and hydroxylation processes.

can decompose in the aqueous phase and its derived radicals diffuse into the hydrophobic phase or peroxyxynitrite can enter the hydrophobic compartment and the homolysis takes place in the interior of the membrane or lipoprotein. Radical species have a specific diffusion behavior towards the membrane and a different probability of formation in its interior. For instance, $\bullet\text{NO}_2$ can both readily permeate toward the membrane and be formed in its interior; however, $\bullet\text{OH}$ has a very short life and its diffusion is minimal (three to four molecular diameters), in which case its action would depend exclusively on ONOOH homolysis inside the hydrophobic compartment. We have previously described the formation of 3-hydroxy-BTBE (BTBE-OH) in model membranes that must be because of a site-specific homolysis in the bilayer (Bartesaghi *et al.*, 2006). In turn, $\text{CO}_3^{\bullet-}$ should not be either formed (by the reaction of ONOO⁻ with CO_2) in the membrane or permeate to it, as anions will be excluded from the hydrophobic phase.

The formation of 3-nitrotyrosine and other oxidation products in the membrane will depend on the distribution of radical intermediates, including the concentration of $\bullet\text{NO}_2$ and the competing pathway involving the recombination of two tyrosyl radicals to yield 3,3'-di-tyrosine; in hydrophobic environments, there are diffusional restrictions for the lateral movement of tyrosine residues that would not be present in aqueous phases. In this context, work has been directed to define mechanisms and product yields of tyrosine oxidation in hydrophobic compartments. Two main types of probes have been developed to study tyrosine nitration in membranes: hydrophobic tyrosine analogs such as *N*-*t*-BOC-L-tyrosine *tert*-butyl ester (BTBE) (Zhang *et al.*, 2001a) and tyrosine-containing transmembrane peptides (Zhang *et al.*, 2003). A description of BTBE and the methods for the detection of its nitration and dimerization products have been reported elsewhere in this series (Zhang *et al.*, 2005).

This chapter focuses on the utilization of BTBE incorporated to phosphatidyl choline (PC) liposomes to study the mechanisms of peroxyxynitrite-dependent tyrosine oxidation in model biomembranes. Variables that affect tyrosine oxidation yields can be tested, including the effect of transition metal catalysts, carbon dioxide, molecular oxygen, pH, hydrophilic and hydrophobic antioxidants, and fatty acid composition of the membrane and peroxyxynitrite-derived free radical scavengers (Bartesaghi *et al.*, 2006).

2. METHODS

2.1. Synthesis of BTBE and its oxidation products

The synthesis of BTBE and the standards 3-nitro-BTBE and 3,3'-di-BTBE has been described previously (Zhang *et al.*, 2005). 3-Hydroxy-BTBE is generated by a hydroxylation reaction mediated by a Fenton system (Bartesaghi *et al.*,

2006). The Fenton reagent is prepared by diluting 10 mM ferrous ammonium sulfate in 2.5 M sulfuric acid. The reaction is started by adding 0.3 mM H_2O_2 and 0.3 mM Fe^{II} to BTBE (0.3 mM)-containing liposomes.

2.2. Preparation of BTBE-containing liposomes and peroxynitrite addition

BTBE incorporation to liposomes is carried out as described previously (Bartesaghi *et al.*, 2006; Zhang *et al.*, 2001a). Briefly, a methanolic solution of BTBE (0.35 mM) is added to 35 mM PC lipids dissolved in chloroform. The mixture is then dried under a stream of nitrogen gas. Multilamellar liposomes are formed by thoroughly mixing the dried lipid with 100 mM potassium phosphate buffer, pH 7.4, plus 0.1 mM DTPA. Under these conditions, the BTBE incorporation degree is >98%.

Phosphatidyl choline liposomes of variable fatty acid composition can be prepared containing saturated 1,2-dimyristoyl-*sn*-glycero-3-phosphocholine (DMPC), 1,2-dilauroyl-*sn*-glycero-3-phosphocholine (DLPC), or unsaturated (egg PC, soybean PC) fatty acids. In addition, the unsaturation degree can be modulated by working with mixtures of DLPC and 1-palmitoyl-2-linoleoyl-*sn*-glycero-3-phosphocholine. It is important to note that experiments with liposomes must be performed in each case above the transition phase temperature (i.e., 23, -1, -3, and <0 °C for DMPC, DLPC, egg PC, and soybean PC, respectively).

Peroxynitrite synthesis is performed in a quenched-flow reactor from sodium nitrite (NaNO_2) and H_2O_2 under acidic conditions as described previously (Radi *et al.*, 1991b). The H_2O_2 remaining from the synthesis is eliminated by treating the stock solution with manganese dioxide. The peroxynitrite concentration is determined spectrophotometrically at 302 nm ($\epsilon = 1670 \text{ M}^{-1} \text{ cm}^{-1}$). The nitrite concentration in preparations is typically lower than 30%. Nitrite levels must be strictly controlled and are critical for obtaining reproducible data.

Peroxynitrite is added either as a single bolus or as multiple successive boluses under vigorous vortexing or by infusion with a motor-driven syringe under continuous stirring (Trostchansky *et al.*, 2001). In some control experiments, peroxynitrite is allowed to decompose to nitrate and nitrite in 100 mM phosphate buffer, pH 7.4, for 2 min before use, i.e., “reverse order addition” of peroxynitrite (RA).

2.3. Sample preparation

A 200- μl reaction mixture containing liposomes is mixed with 200 μl methanol and vortexed for 1 min to dissolve liposomes. The resulting solution is mixed with 400 μl chloroform and 80 μl 5 M NaCl and is vortexed for 2 min.

The final solution is centrifuged at 5000 rpm for 10 min, and the aqueous phase (supernatant) is removed. The chloroform layer is dried under a stream of nitrogen and kept at -20°C until use (Bartesaghi *et al.*, 2006; Zhang *et al.*, 2001a). Recovery efficiencies for all compounds are $>95\%$ (Zhang *et al.*, 2001a). Immediately before HPLC analysis, samples are resuspended in $100\ \mu\text{l}$ 85% methanol:15% 15 mM KPi, pH 3, sonicated for 10 min, and centrifuged before injection.

Because chloroform is used during sample preparation, and because of the affinity of lipids and BTBE for the hydrophobic components of plastic tubes, experiments should be performed preferentially in glass tubes.

2.4. HPLC analysis

BTBE, 3-nitro-BTBE, and 3,3'-di-BTBE are separated on a Gilson HPLC system equipped with UV-VIS and fluorescence detectors by reversed-phase HPLC using a Partisil ODS-3 10- μm column (250 mm length, 4.6 mm i.d.).

Mobile phase A consists of 15 mM phosphate potassium buffer, pH 3, and mobile phase B consists of methanol. Chromatographic conditions are as follows: flow, 1 ml/min; 75% mobile phase B for 25 min, followed by a linear increase to 100% mobile phase B for 10 min, which is essential for column reconstitution and elution of higher oxidation states of BTBE polymerization products and phospholipids. UV-VIS settings are 280 nm, $\epsilon = 1200\ \text{M}^{-1}\ \text{cm}^{-1}$ for BTBE and 360 nm, $\epsilon = 1500\ \text{M}^{-1}\ \text{cm}^{-1}$ for 3-nitro-BTBE. 3,3'-di-BTBE is detected fluorimetrically at $\lambda_{\text{ex}}=294\ \text{nm}$ and $\lambda_{\text{em}}=401\ \text{nm}$. Authentic 3-nitro-BTBE and 3,3'-di-BTBE are used as standards.

For the detection of 3-hydroxy-BTBE (i.e., 3,4-dihydroxy-*N-t*-BOC-L-phenylalanine *tert* butyl ester), the HPLC protocol is modified slightly to seek for more hydrophilic compounds derived from peroxyxynitrite-treated BTBE-containing liposomes. Mobile phase A consists of water, and the gradient is started at 50% methanol to 100% for 35 min.

2.5. Spectrophotometric analysis

In saturated fatty acid-containing PC liposomes (i.e., DLPC and DMPC), 3-nitro-BTBE can be quantitated by direct UV-VIS measurement. Briefly, liposomes are solubilized with 1.2% deoxycholate (Bartesaghi *et al.*, 2006; Buege and Aust, 1978), followed by alkalization to pH 10 with 5 M NaOH, and 3-nitro-BTBE is measured at 424 nm at pH 10, corresponding to the phenolate anion absorbance ($\epsilon = 4000\ \text{M}^{-1}\ \text{cm}^{-1}$).

Direct spectrophotometric measurement of 3-nitro-BTBE after deoxycholate solubilization turn out to be practical and reproducible for saturated fatty acid-containing liposomes and less time-consuming than the HPLC experiments. However, this method should not be applied to unsaturated fatty acid-containing liposomes, as peroxyxynitrite leads to the formation of

other absorbing species in the same region of the spectrum, such as nitrated and peroxidized lipids (Radi *et al.*, 1991b; Schopfer *et al.*, 2005).

2.6. Mass spectrometry analysis of 3-hydroxy-BTBE

3-Hydroxy-BTBE is analyzed using an Applied Biosystems QTRAP, triple quadrupole-linear ion trap (LIT) mass spectrometer equipped with a turbo ion spray ionization source (ESI). The mass spectrometer is operated in a positive mode, and the ESI settings are optimized as follows: ion spray voltage, 2500 V; temperature, 375 °C; declustering potential, 50 V; entrance potential, 10 V; nebulizer gas, 40 psi; heater gas, 25 psi. Samples collected from the HPLC are diluted in acidified methanol (0.1% formic acid) and infused continuously (10 μ M/min) at an estimated concentration of 10 nM. The molecular ion is identified at m/z 352.2. Fragmentation analysis of hydroxy-BTBE is conducted using the LIT in the enhanced product ion mode of the instrument. Fragmentation experiments of the molecular ion at 352.2 are conducted at different collision-assisted dissociation energies identifying fragments from the parent ion.

2.7. Electron spin resonance (ESR) measurements

Electron spin resonance spin-trapping experiments are performed to detect the one-electron oxidation product of BTBE (i.e., BTBE phenoxyl radical). DLPC liposomes are incubated with 20 mM 2-methyl-nitroso propane (MNP) and peroxynitrite for 1 min. The liposomes are diluted with water, spun down to remove MNP, and resuspended in phosphate buffer. Samples are subsequently transferred to a 100- μ l capillary tube for ESR measurements. ESR spectra are recorded at room temperature on a Bruker EMX spectrometer operating at 9.8 GHz. Typical spectrometer parameters are as follow: scan range, 100 G; field set, 3510 G; time constant, 0.64 ms; scan time, 20 s; modulation amplitude, 5.0 G; modulation frequency, 100 kHz; receiver gain, 2×10^5 ; microwave power, 20 mW. The obtained signals are the result of 200 scans.

3. RESULTS

3.1. Electron spin resonance spin trapping of BTBE phenoxyl radical

Electron spin resonance spin trapping was used to detect the BTBE phenoxyl radical formed during peroxynitrite-mediated BTBE oxidation with the spin trap MNP as described previously (Bartesaghi *et al.*, 2006). BTBE-containing liposomes treated with ONOO⁻ result in an anisotropic three line signal, suggesting the formation of a partially immobilized phenoxyl radical in the

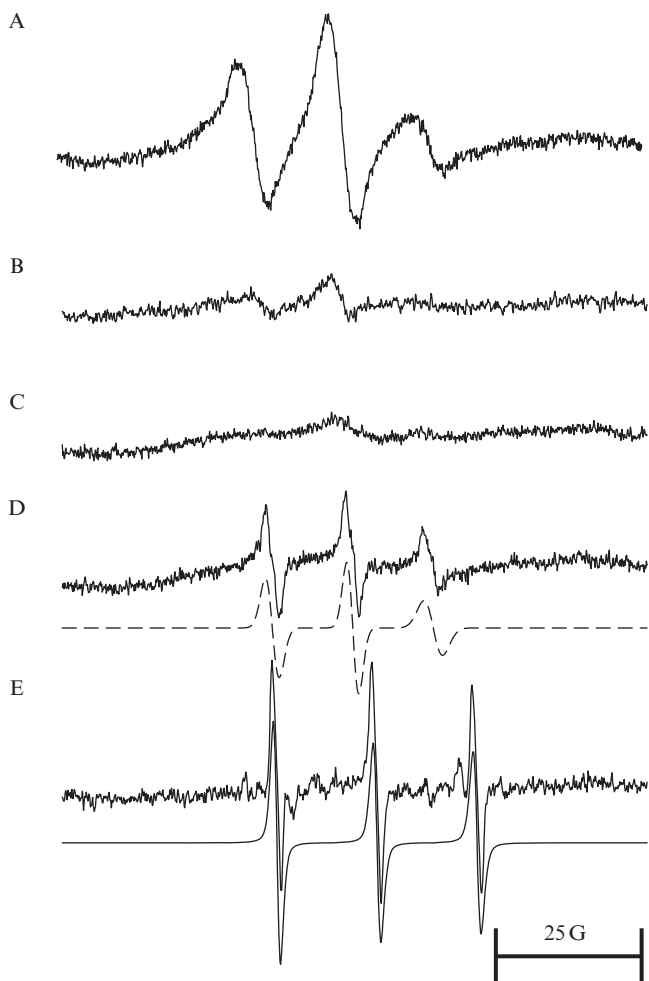


Figure 12.1 ESR spin-trapping measurements. Reaction mixtures consisting of BTBE (2.25 mM) incorporated into 45 mM DLPC liposomes in a phosphate buffer (100 mM, pH 7.4) containing DTPA (0.1 mM) were treated with a 20 mM 2-methyl-2-nitrosopropane (MNP) spin trap and mixed rapidly with 5 mM peroxyntirite. Samples were subsequently transferred to a 100- μ l capillary tube for ESR measurements. (A) BTBE-containing liposomes plus peroxyntirite. (B) BTBE-containing liposomes plus decomposed peroxyntirite (RA). (C) Liposomes plus peroxyntirite plus MNP. (D) Sample A was centrifuged and BTBE-containing liposomes were redissolved in ethanol $a_N = 13.8$ G. (E) Product of MNP photolysis, $a_N = 17.1$ G.

interior of the membrane (Fig. 12.1A). No ESR spectrum was obtained when liposomes were treated with decomposed peroxyntirite (Fig. 12.1B) or in the absence of BTBE (Fig. 12.1C). When peroxyntirite-treated BTBE-containing liposomes were dissolved in ethanol, a clear three line signal was

obtained (Fig. 12.1D). Despite the low signal-to-noise ratio, we can estimate a hyperfine constant of 13.8 G, which is consistent with the one-electron oxidation of BTBE by peroxynitrite-derived radicals (Mossoba *et al.*, 1982).³

MNP photolysis may occur during the experiments and leads to the formation of a three line signal corresponding to the di-*tert*-butyl nitroxide radical, which has a different a_N value, as shown in Fig. 12.1E.

3.2. HPLC and spectroscopic analysis of BTBE, 3-nitro-BTBE, and 3,3'-di-BTBE

BTBE oxidation products were quantitated by UV-VIS and/or fluorimetric measurements after either (a) reverse-phase-HPLC separation of organic extraction material or (b) deoxycholate solubilization. Figure 12.2A shows a typical HPLC chromatogram obtained from peroxynitrite-treated samples, and the elution of BTBE and its oxidation products 3-nitro-BTBE and 3,3'-di-BTBE is shown at 7, 9, and 19 min, respectively.

Alternatively, spectral analysis of 3-nitro-BTBE after liposome solubilization with 1.2% deoxycholate allowed carrying out direct measurements at the peak absorbance of 424 nm at pH 10 (Fig. 12.2B). In DLPC liposomes at pH 7.4, peroxynitrite (0–2 mM) caused a dose-dependent increase in BTBE nitration yields, with similar results obtained for both methods (Fig. 12.1C). While the 3% yield obtained for 3-nitro-BTBE with respect to added peroxynitrite compares well for that obtained for free tyrosine (6–10%), values for the corresponding dimer 3,3'-di-BTBE are considerably lower (0.11 and 0.02% for egg PC and DLPC, respectively) because of the lateral restriction of BTBE within the bilayer (Bartesaghi *et al.*, 2006). The direct spectroscopic measurement of 3-nitro-BTBE should be applied for saturated fatty acid-containing liposomes only, as mentioned in the description of the method.

3.3. Peroxynitrite-mediated BTBE hydroxylation in DLPC liposomes

In order to explore if the ONOOH-derived $\cdot\text{OH}$ in lipophilic environments could form the hydroxylated derivative of BTBE, chromatographic conditions were changed, as this product is less hydrophobic than the parent compound and therefore elutes at shorter times in our HPLC system. As a positive control for reactions of the $\cdot\text{OH}$ radical, BTBE-containing liposomes were incubated with a Fenton system. Indeed a peak eluting at 11 min was identified both in the Fenton and in the peroxynitrite addition experiments, collected, and characterized by mass spectrometry.

³ MNP adducts with free or peptide-bound tyrosyl radicals were reported to have a_N values of 16.5 (Mossoba *et al.*, 1982) and 15.6 G (Zhang *et al.*, 2003), respectively.

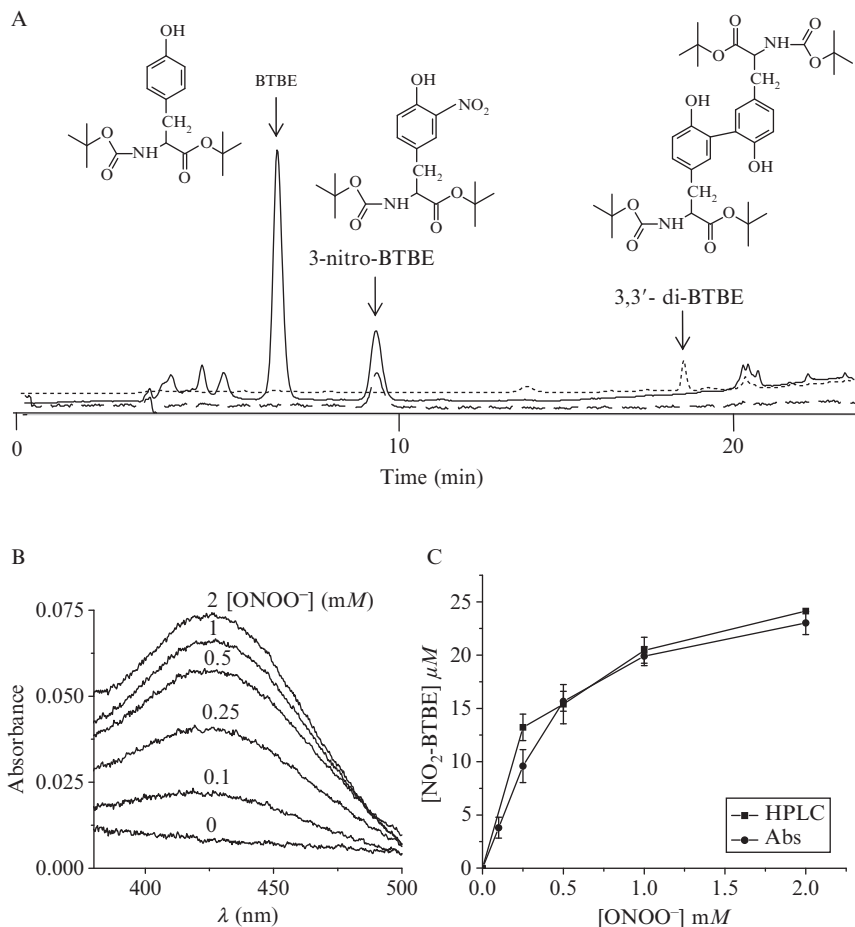


Figure 12.2 Analysis of 3-nitro-BTBE and 3,3'-di-BTBE after peroxynitrite addition. BTBE (0.3 mM) in DLPC liposomes (30 mM) was exposed to peroxynitrite in phosphate buffer (100 mM), pH 7.4, plus 0.1 mM DTPA. (A) After an organic extraction, products were separated by RP-HPLC as described in the text. The HPLC chromatogram shows the elution of BTBE, 3-nitro-BTBE, and 3,3'-di-BTBE after treatment with peroxynitrite (1 mM); structures have been drawn above the peaks. UV-VIS detection was done for BTBE and 3-nitro-BTBE at 280 nm (solid line) and 360 nm (dashed line). 3,3'-Di-BTBE was measured fluorimetrically at 294- and 401-nm excitation and emission wavelengths, respectively (dotted line). (B) Peroxynitrite-treated, BTBE-containing liposomes were solubilized with 1.2% deoxycholate, the pH was adjusted to 10 with NaOH, and UV-VIS spectra of 3-nitro-BTBE were recorded at different peroxynitrite concentrations. (C) Quantitation of 3-nitro-BTBE as a function of peroxynitrite concentration after HPLC separation (■) or deoxycholate solubilization (●). Reproduced from [Bartesaghi *et al.* \(2006\)](#).

3-Hydroxy-BTBE yields were extremely low, which is consistent with the fact that the competition reaction of $\cdot\text{OH}$ with the saturated fatty acids [60 mM lauric acid, $k = 6.4 \times 10^8 \text{ M}^{-1} \text{ s}^{-1}$ ([Barber, 1978](#))] will predominate over the $\cdot\text{OH}$ oxidation reaction with 0.3 mM BTBE.

3.4. Mass spectrometry characterization of 3-hydroxy-BTBE

An aliquot (100 μl) of the peak eluting at 11 min was diluted in 80% methanol 0.1 % formic acid and infused continuously to the mass spectrometer. [Figure 12.3](#) shows the enhanced resolution mass spectrum of the collected peak after the Fenton reagent and peroxyntirite addition to BTBE-containing liposomes where an ion of m/z 353.2 was identified in both experimental settings. A turbo electrospray ionization source was used,

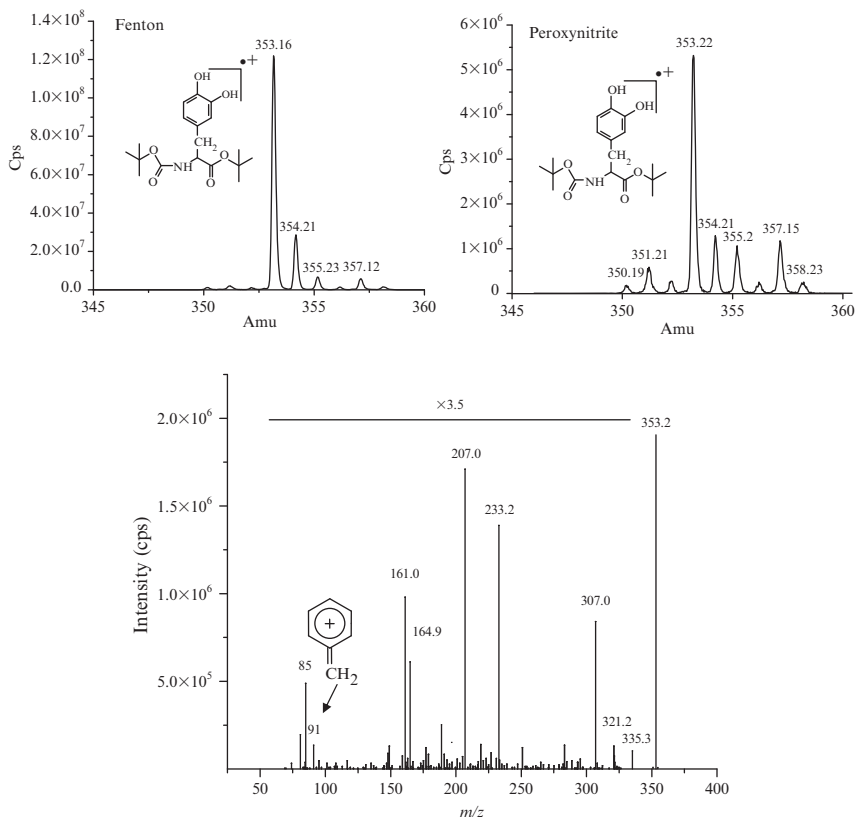


Figure 12.3 Mass spectrometry characterization of hydroxy-BTBE. BTBE (0.3 mM) in DLPC liposomes (30 mM) was exposed to FeSO_4 (0.3 mM) + H_2O_2 (0.3 mM) or peroxyntirite in phosphate buffer (20 mM), pH 6, supplemented with 0.4 mM DTPA and injected to HPLC. A peak eluting with a retention time of 11 min was collected and resuspended in 80% methanol plus 0.1% formic acid prior to injection into the mass spectrometer. (Top) Enhanced resolution mass scan of the peak eluting at 11 min shows an ion with an m/z of 353.2, which corresponds to the cation radical of hydroxy-BTBE for the Fenton (left) and peroxyntirite (right) reactions. (Bottom) MS/MS fragmentation pattern of the m/z 353.2 ion showing the typical fragment ion of m/z 91 (arrow) arising from phenolic cation radicals. Reproduced with modifications from [Bartesaghi et al. \(2006\)](#).

which produces mild ionization of molecules after vaporization of the liquid phase, minimizing in-source fragmentation. As opposed to atmospheric pressure chemical ionization (APCI) sources, ESI ionization typically produces protonation (positive mode under acidic conditions) of Bronsted–Lowry acids such as an amino group (e.g., $-\text{NH}_3^+$) giving rise to $(\text{M} + \text{H}^+)$ ions. The calculated monoisotopic molecular mass of BTBE is 337.2, whereas that of hydroxy-BTBE is 353.2. Mass spectrometry analysis of both compounds gives rise in our experimental settings to the molecular ion with a m/z of 337 and 353, respectively. This is indicative of formation of the cation radical ion of these molecules, most probably due to in-source electrochemistry as described previously for ESI ionization. To further confirm this observation, we conducted mass analysis of tyrosine and *N*-acetyl tyrosine, as both are phenolic compounds as BTBE; in the former molecule, protonation of the amino group is blocked by the acetyl moiety. We detected the well-characterized $[\text{M} + \text{H}^+]$ ion of tyrosine (m/z 182.2) but in agreement to what was observed for BTBE, the ion corresponding to *N*-acetyl tyrosine was M^+ with a m/z of 223.1. Furthermore, analysis of the peak corresponding to 3-hydroxy-BTBE carried out without acidification of the sample and in aprotic solvent (100% acetonitrile) to avoid the gas-phase proton transfer reaction still gave rise to the m/z 353.2 species, strongly suggesting formation of the cation radical ion (not shown). The fragmentation pattern observed after Fenton and peroxyxynitrite addition experiments were identical (Fig. 12.3).

3.5. Enhancers and inhibitors of peroxyxynitrite-mediated tyrosine oxidation in membranes

In order to study the mechanism of peroxyxynitrite-mediated tyrosine oxidation in hydrophobic environments, we studied the effect of different molecules known to react with peroxyxynitrite or its derived radicals and that can up- or downmodulate product formation. Tested scavengers may include polar compounds that will mainly react in the aqueous phase or hydrophobic, which may undergo reactions either in the lipophilic phase or in the aqueous/lipid interphase.

For instance, BTBE nitration and dimerization were inhibited by glutathione, lipoic acid (Trujillo *et al.*, 2005), pHPA, tyrosine, dimethyl sulfoxide, mannitol, desferrioxamine (Bartesaghi *et al.*, 2004), and uric acid in extents that are compatible with their different reactivities with peroxyxynitrite (e.g., GSH and lipoic acid) and peroxyxynitrite-derived radicals⁴ (Fig. 12.4). It is important to note that the presence of nitrite (NO_2^-) either remaining from

⁴ Specific rate constants of scavengers and metal centers with peroxyxynitrite, $\cdot\text{NO}_2$, $\cdot\text{OH}$, and $\text{CO}_3^{\cdot-}$, as well as reactant concentrations, critically influence tyrosine-oxidation yields. Exhaustive kinetic analyses of these processes have been performed elsewhere (Bartesaghi *et al.*, 2004, 2006; Trujillo *et al.*, 2005).

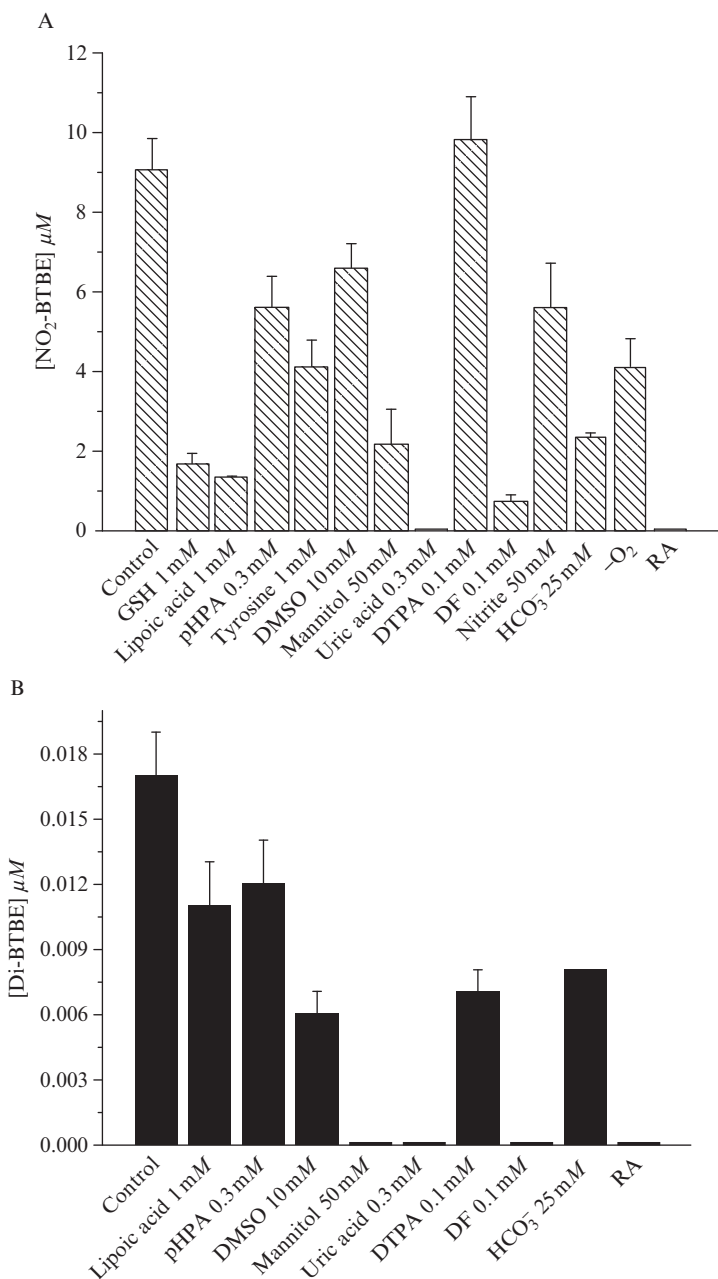


Figure 12.4 Effect of scavengers, carbon dioxide, and oxygen on BTBE nitration and dimerization. BTBE (0.3 mM) in DLPC liposomes (30 mM) was exposed to peroxy-nitrite (0.5 mM) in the presence of different compounds and concentrations, and 3-nitro-BTBE (A) and 3,3'-di-BTBE (B) were analyzed by RP-HPLC. The condition under low oxygen tensions (-O₂) was obtained by saturation of the samples under an argon atmosphere previous to peroxy-nitrite addition.

peroxynitrite synthesis or added may affect product distribution and yields due to its fast reaction with $\cdot\text{OH}$ to yield $\cdot\text{NO}_2$ ($k = 6 \times 10^9 \text{ M}^{-1} \text{ s}^{-1}$).

It is well known that some transition metal complexes enhance peroxynitrite-mediated tyrosine nitration of phenolic compounds in aqueous media via a catalytic redox cycle mechanism (Beckman *et al.*, 1992; Radi, 2004). The effect of different transition metal complexes on BTBE nitration and dimerization in either saturated (DLPC) or unsaturated (egg PC) BTBE-containing liposomes can be studied. In DLPC liposomes, nitration yields were enhanced in the presence of hemin, Fe-EDTA, and the metal porphyrins Mn (III) *meso*-tetrakis (4-carboxylatophenyl) porphyrin (Mn-tccp) and Fe (III) *meso*-tetrakis (4-carboxylatophenyl) porphyrin (Fe-tccp), while ferrioxamine had no effect. In egg PC liposomes, hemin clearly enhanced BTBE nitration fivefold, whereas Fe-EDTA, Mn-tccp and Fe-tccp did not (Fig. 12.5). It is clear that transition metal complexes act as nitration catalysts in simple saturated fatty acid-containing systems. Indeed, in DLPC liposomes, BTBE nitration is enhanced by hemin and Mn-tccp in a dose-dependent manner (Bartesaghi *et al.*, 2006). The effect of transition metal catalysts may be different in more complex systems, such as unsaturated fatty acid-containing liposomes where lipid peroxidation may play a

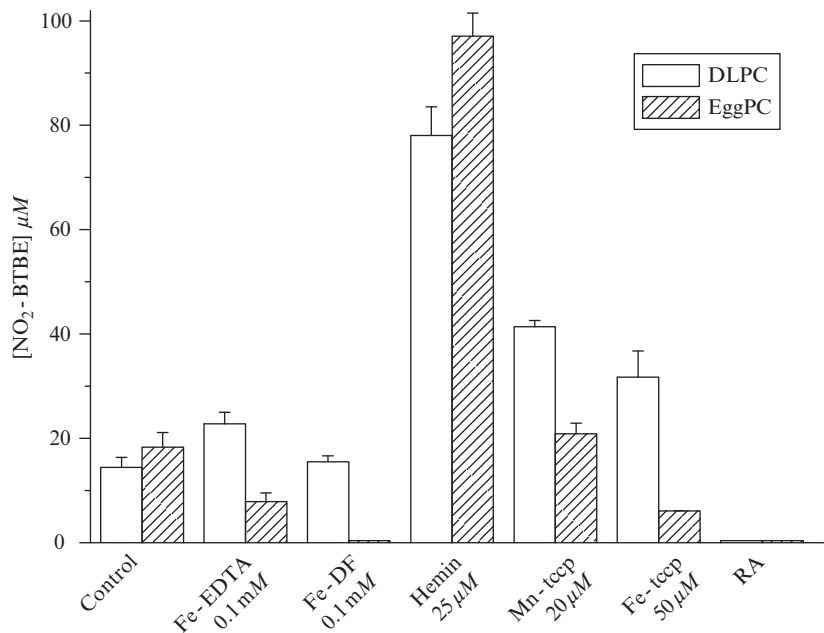


Figure 12.5 Effect of transition metal complexes on BTBE nitration. BTBE (0.3 mM) in DLPC and egg PC liposomes (30 mM) were incubated with the indicated concentration of different transition metal complexes and treated with peroxynitrite (0.5 mM). NO₂-BTBE yields were analyzed by R-P-HPLC. RA, reverse addition of peroxynitrite.

relevant role in the nitration process (Bartesaghi *et al.*, 2007). Importantly, oxygen depletion known to inhibit lipoperoxidation chain reactions was also strongly inhibitory of BTBE nitration (Fig. 12.4A).

3.6. Effect of pH on nitration, dimerization, and hydroxylation yields

The effect of pH on tyrosine oxidation has been established previously with nitration, dimerization, and hydroxylation yields as a function of pH having distinctive profiles (Beckman *et al.*, 1992; Santos *et al.*, 2000; van der Vliet *et al.*, 1995). The pH profiles are dictated by different reactions, some of which largely depend on the ionization state of the phenolic -OH group of tyrosine. Indeed, the deprotonated form of the tyrosine ring (i.e., phenolate) is the molecular species that reacts readily with $\cdot\text{NO}_2$. The effect of pH on BTBE oxidation aids in determining to what extent its incorporation to hydrophobic environments affects the dependency observed for tyrosine and therefore the reaction mechanism. Changes in pH will alter proton concentration in the aqueous phase and may affect the chemistry of BTBE in the bilayer directly or indirectly. 3-Nitro-BTBE formation as a function of pH resulted in a bell-shaped curve with a maximum yield at pH 7.5 (Fig. 12.6), similar to what is observed for nitro-tyrosine. 3,3'-Di-BTBE formation was very low at pH <8, but increased significantly towards

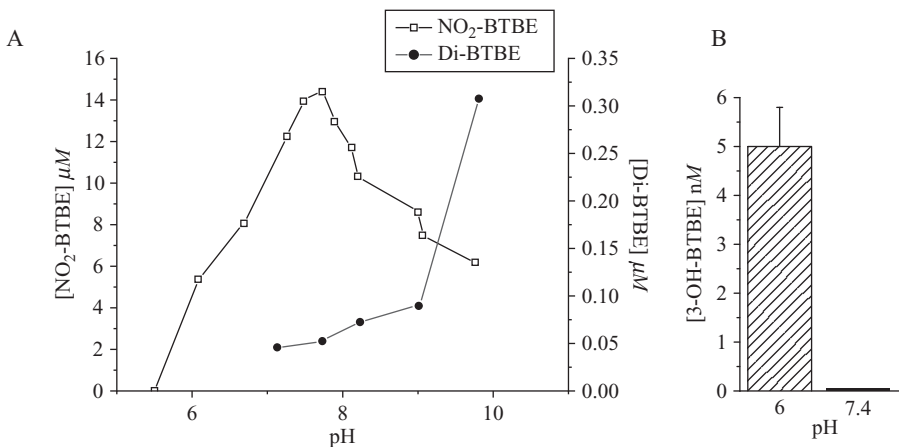


Figure 12.6 BTBE oxidation as a function of pH. BTBE-containing DLPC liposomes were prepared after lipid resuspension in phosphate buffer (100 mM) plus 0.1 mM DTPA at different pH values. Then BTBE (0.3 mM) was treated with peroxynitrite (0.5 mM) at each pH. (A) 3-NO₂-BTBE and 3,3'-di-BTBE were analyzed after organic extraction by RP-HPLC. (B) The 3-hydroxy-BTBE concentration at two pH values, estimated by using (3,4-dihydroxy-phenylalanine) DOPA as a standard. Reproduced with modifications from Bartesaghi *et al.* (2006).

alkaline pH. In addition, 3-hydroxy-BTBE was detected at pH 6 but not at pH 7.4.

The pH dependency of the three BTBE oxidation products can be fully rationalized kinetically by free radical-dependent mechanisms and has been reported elsewhere (Bartesaghi *et al.*, 2006). These data are also in agreement with BTBE being partially immersed in the bilayer with the $-OH$ being exposed towards the aqueous phase and therefore capable of ionization; thus, kinetic data are in agreement with structural information indicating that BTBE is located all through the bilayer with the highest concentration near the glycerol backbone of the phospholipids (Zhang *et al.*, 2001a).

4. DISCUSSION

BTBE incorporated to PC liposomes has been revealed to be a useful probe to study tyrosine oxidation processes in membranes (Fig. 12.7), particularly peroxynitrite-mediated nitration, dimerization, and hydroxylation; these oxidation processes require the intermediacy of BTBE phenoxyl radicals as evidenced by ESR spin-trapping studies.

In hydrophobic environments, tyrosine nitration is the predominant pathway, partly because of the physical chemical properties of nitrogen dioxide, that is, it partitions and diffuses favorably in hydrophobic environments and reacts with tyrosyl radicals close to diffusion-controlled rates. In contrast, tyrosine dimerization is hindered because of the limited lateral diffusion of tyrosyl radicals within the lipid bilayer structure, expected to occur at least 100 times slower than in the aqueous phase (Bartesaghi *et al.*, 2006). Small amounts of the hydroxylated tyrosine analog derivative were found, supporting the homolysis of ONOOH in the interior or the immediate proximity of the liposomal membrane. The role of hydrophilic and hydrophobic compounds that either enhance or inhibit tyrosine nitration processes in the membrane can be studied in detail through the use of membrane-containing BTBE. Additionally, the incidence of membrane fatty acid unsaturation and the role of lipid peroxidation processes in tyrosine oxidation product yields and distribution are just starting to be appreciated. While kinetic data on the reactions of $\cdot NO_2$, $CO_3^{\cdot -}$, and $\cdot OH$ radicals with BTBE or, in general, membrane-associated tyrosine residues are still lacking, the use of known rate constants with tyrosine in computer-assisted simulation studies recapitulates experimental data and fully supports a free radical mechanism of BTBE oxidation by peroxynitrite in biomembranes (Bartesaghi *et al.*, 2006). The use of BTBE can help to understand distinctive factors that affect tyrosine oxidation in hydrophobic environments, which clearly differ in several respects to those existing in aqueous phases. Importantly, BTBE incorporation and oxidation in red blood cell

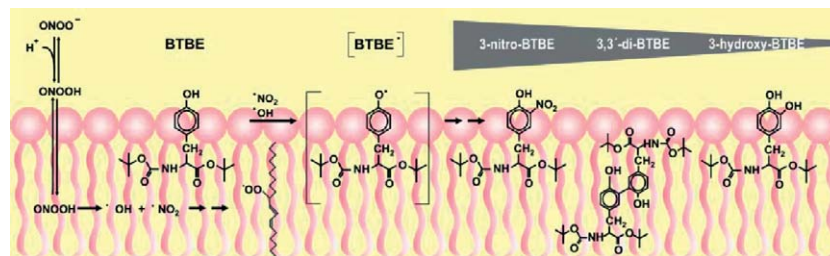


Figure 12.7 Tyrosine oxidation products in membranes induced by peroxynitrite. The structure of the hydrophobic probe BTBE, which undergoes one-electron oxidation to the corresponding BTBE phenoxyl radical either by peroxynitrite-derived radicals ($\cdot OH$, $\cdot NO_2$) or by membrane-derived lipid peroxy radicals ($ROO\cdot$), is shown. The transient BTBE phenoxyl radical either reacts at diffusion-controlled rates with $\cdot NO_2$ to yield 3-nitro-BTBE or recombines with another phenoxyl radical to yield 3,3'-di-BTBE; nitration yields are significantly larger than dimerization yields. The figure also indicates the formation of small amounts of the 3-hydroxy-BTBE from the addition reaction with hydroxyl radical and supports the diffusion and homolysis of ONOOH within the lipid bilayer.

membranes have been just reported (Romero *et al.*, 2007), opening the use of BTBE as a probe to study free radical-dependent processes in hydrophobic biocompartments. While tyrosine-containing transmembrane peptides (Zhang *et al.*, 2003) reflect the biochemical behavior of a membrane-associated protein more closely, the relative ease of BTBE synthesis, incorporation to model and biological membranes, extraction, and quantitation of reaction products offers a unique possibility to study oxidation mechanisms mediated by peroxynitrite and other reactive oxygen and nitrogen species and their modulation by biomolecules, xenobiotics, and drugs, as well as carbon dioxide and molecular oxygen.

ACKNOWLEDGMENTS

We thank Valeria Valez for her contribution to the artwork. This work was supported by grants from the Howard Hughes Medical Institute and the International Centre of Genetic Engineering and Biotechnology to R.R. and the National Institutes of Health to B.K. and R.R. (2 R01H1063119-05). A donation for research support from Laboratorios Gramón-Bagó Uruguay to R.R. and G.P. through Universidad de la República is gratefully acknowledged. S.B. is supported by a fellowship from Programa de Desarrollo de Ciencias Básicas (PEDECIBA-Química), Universidad de la República, Uruguay. R.R. is a Howard Hughes International Research Scholar.

REFERENCES

- Alvarez, B., Ferrer-Sueta, G., Freeman, B. A., and Radi, R. (1999). Kinetics of peroxynitrite reaction with amino acids and human serum albumin. *J. Biol. Chem.* **274**, 842–848.
- Barber, D. J. W., and Thomas, J. K. (1978). Reactions of radicals with lecithin bilayers. *Radiat. Res.* **74**, 51–65.
- Bartesaghi, S., Ferrer-Sueta, G., Peluffo, G., Valez, V., Zhang, H., Kalyanaraman, B., and Radi, R. (2007). Protein tyrosine nitration in hydrophilic and hydrophobic environments. *Amino. Acids.* **32**, 501–515.
- Bartesaghi, S., Trujillo, M., Denicola, A., Folkes, L., Wardman, P., and Radi, R. (2004). Reactions of desferrioxamine with peroxynitrite-derived carbonate and nitrogen dioxide radicals. *Free. Radic. Biol. Med.* **36**, 471–483.
- Bartesaghi, S., Valez, V., Trujillo, M., Peluffo, G., Romero, N., Zhang, H., Kalyanaraman, B., and Radi, R. (2006). Mechanistic studies of peroxynitrite-mediated tyrosine nitration in membranes using the hydrophobic probe N-t-BOC-L-tyrosine tert-butyl ester. *Biochemistry* **45**, 6813–6825.
- Beckman, J. S., Beckman, T. W., Chen, J., Marshall, P. A., and Freeman, B. A. (1990). Apparent hydroxyl radical production by peroxynitrite: Implications for endothelial injury from nitric oxide and superoxide. *Proc. Natl. Acad. Sci. USA* **87**, 1620–1624.
- Beckman, J. S., Ischiroopoulos, H., Zhu, L., van der Woerd, M., Smith, C., Chen, J., Harrison, J., Martin, J. C., and Tsai, M. (1992). Kinetics of superoxide dismutase- and iron-catalyzed nitration of phenolics by peroxynitrite. *Arch. Biochem. Biophys.* **298**, 438–445.
- Beckman, J. S., Zu Ye, Y., Anderson, P. G., Chen, J., Accavitti, M. A., Tarpey, M. M., and White, C. R. (1994). Extensive nitration of protein tyrosines in human atherosclerosis detected by immunohistochemistry. *Biol. Chem. Hoppe-Seyler.* **375**, 81–88.
- Buege, J. A., and Aust, S. D. (1978). Microsomal lipid peroxidation. *Methods Enzymol.* **52**, 302–310.

- Ischiropoulos, H. (1998). Biological tyrosine nitration: A pathophysiological function of nitric oxide and reactive oxygen species. *Arch. Biochem. Biophys.* **356**, 1–11.
- Ischiropoulos, H., Zhu, L., Chen, J., Tsai, M., Martin, J. C., Smith, C. D., and Beckman, J. S. (1992). Peroxynitrite-mediated tyrosine nitration catalyzed by superoxide dismutase. *Arch. Biochem. Biophys.* **298**, 431–437.
- Koppenol, W. H., Moreno, J. J., Pryor, W. A., Ischiropoulos, H., and Beckman, J. S. (1992). Peroxynitrite, a cloaked oxidant formed by nitric oxide and superoxide. *Chem. Res. Toxicol.* **5**, 834–842.
- Mossoba, M., Makino, K., and Riesz, P. (1982). Photoionization of aromatic amino acids in aqueous solutions: A spin-trapping and electron spin resonance study. *J. Phys. Chem.* **86**, 3478–3483.
- Radi, R. (2004). Nitric oxide, oxidants, and protein tyrosine nitration. *Proc. Natl. Acad. Sci. USA* **101**, 4003–4008.
- Radi, R., Beckman, J. S., Bush, K. M., and Freeman, B. A. (1991a). Peroxynitrite oxidation of sulfhydryls: The cytotoxic potential of superoxide and nitric oxide. *J. Biol. Chem.* **266**, 4244–4250.
- Radi, R., Beckman, J. S., Bush, K. M., and Freeman, B. A. (1991b). Peroxynitrite-induced membrane lipid peroxidation: The cytotoxic potential of superoxide and nitric oxide. *Arch. Biochem. Biophys.* **288**, 481–487.
- Romero, N., Peluffo, G., Bartesaghi, S., Zhang, H., Joseph, J., Kalyanaraman, B., and Radi, R. (2007). Incorporation of the hydrophobic probe N-t-BOC-L-tyrosine tert-butyl ester (BTBE) to red blood cell membranes to study peroxynitrite-dependent reactions. *Chem. Res. Toxicol.* **20**, 1638–1648.
- Santos, C. X., Bonini, M. G., and Augusto, O. (2000). Role of the carbonate radical anion in tyrosine nitration and hydroxylation by peroxynitrite. *Arch. Biochem. Biophys.* **377**, 146–152.
- Schopfer, F. J., Baker, P. R., Giles, G., Chumley, P., Batthyany, C., Crawford, J., Patel, R. P., Hogg, N., Branchaud, B. P., Lancaster, J. R., and Freeman, B. A. (2005). Fatty acid transduction of nitric oxide signaling: Nitrolinoleic acid is a hydrophobically stabilized nitric oxide donor. *J. Biol. Chem.* **280**, 19289–19297.
- Shishehbor, M. H., Aviles, R. J., Brennan, M. L., Fu, X., Goormastic, M., Pearce, G. L., Gokce, N., Keaney, J. F., Penn, M. S., Sprecher, D. L., Vita, J. A., and Hazen, S. L. (2003). Association of nitrotyrosine levels with cardiovascular disease and modulation by statin therapy. *JAMA* **289**, 1675–1680.
- Sokolovsky, M., Riordan, J. F., and Vallee, B. L. (1966). Tetranitromethane: A reagent for the nitration of tyrosyl residues in proteins. *Biochemistry* **5**, 3582–3589.
- Sturgeon, B. E., Glover, R. E., Chen, Y. R., Burka, L. T., and Mason, R. P. (2001). Tyrosine iminoxyl radical formation from tyrosyl radical/nitric oxide and nitrosotyrosine. *J. Biol. Chem.* **276**, 45516–45521.
- Trostchansky, A., Batthyany, C., Botti, H., Radi, R., Denicola, A., and Rubbo, H. (2001). Formation of lipid-protein adducts in low-density lipoprotein by fluxes of peroxynitrite and its inhibition by nitric oxide. *Arch. Biochem. Biophys.* **395**, 225–232.
- Trujillo, M., Folkes, L., Bartesaghi, S., Kalyanaraman, B., Wardman, P., and Radi, R. (2005). Peroxynitrite-derived carbonate and nitrogen dioxide radicals readily react with lipoic and dihydrolipoic acid. *Free Radic. Biol. Med.* **39**, 279–288.
- van der Vliet, A., Eiserich, J. P., O'Neill, C. A., Halliwell, B., and Cross, C. E. (1995). Tyrosine modification by reactive nitrogen species: A closer look. *Arch. Biochem. Biophys.* **319**, 341–349.
- Zhang, H., Bhargava, K., Keszler, A., Feix, J., Hogg, N., Joseph, J., and Kalyanaraman, B. (2003). Transmembrane nitration of hydrophobic tyrosyl peptides: Localization, characterization, mechanism of nitration, and biological implications. *J. Biol. Chem.* **278**, 8969–8978.

- Zhang, H., Joseph, J., Feix, J., Hogg, N., and Kalyanaraman, B. (2001a). Nitration and oxidation of a hydrophobic tyrosine probe by peroxynitrite in membranes: Comparison with nitration and oxidation of tyrosine by peroxynitrite in aqueous solution. *Biochemistry* **40**, 7675–7686.
- Zhang, H., Joseph, J., and Kalyanaraman, B. (2005). Hydrophobic tyrosyl probes for monitoring nitration reactions in membranes. *Methods Enzymol.* **396**, 182–204.
- Zhang, R., Brennan, M. L., Fu, X., Aviles, R. J., Pearce, G. L., Penn, M. S., Topol, E. J., Sprecher, D. L., and Hazen, S. L. (2001b). Association between myeloperoxidase levels and risk of coronary artery disease. *JAMA* **286**, 2136–2142.
- Zheng, L., Settle, M., Brubaker, G., Schmitt, D., Hazen, S. L., Smith, J. D., and Kinter, M. (2005). Localization of nitration and chlorination sites on apolipoprotein A-I catalyzed by myeloperoxidase in human atheroma and associated oxidative impairment in ABCA1-dependent cholesterol efflux from macrophages. *J. Biol. Chem.* **280**, 38–47.

Protein tyrosine nitration in hydrophilic and hydrophobic environments

Review Article

S. Bartesaghi¹, G. Ferrer-Sueta^{1,2}, G. Peluffo¹, V. Valez¹, H. Zhang³, B. Kalyanaraman³, and R. Radi¹

¹ Departamento de Bioquímica and Center for Free Radical and Biomedical Research, Facultad de Medicina, Universidad de la República, Montevideo, Uruguay

² Departamento de Físicoquímica Biológica, Facultad de Ciencias, Universidad de la República, Montevideo, Uruguay

³ Biophysics Research Institute and Free Radical Research Center, Medical College of Wisconsin, Milwaukee, Wisconsin, U.S.A.

Received May 28, 2006

Accepted June 20, 2006

Published online November 2, 2006; © Springer-Verlag 2006

Summary. In this review we address current concepts on the biological occurrence, levels and consequences of protein tyrosine nitration in biological systems. We focused on mechanistic aspects, emphasizing on the free radical mechanisms of protein 3-nitrotyrosine formation and critically analyzed the restrictions for obtaining large tyrosine nitration yields *in vivo*, mainly due to the presence of strong reducing systems (e.g. glutathione) that can potently inhibit at different levels the nitration process. Evidence is provided to show that the existence of metal-catalyzed processes, the assistance of nitric oxide-dependent nitration steps and the facilitation by hydrophobic environments, provide individually and/or in combination, feasible scenarios for nitration in complex biological milieux. Recent studies using hydrophobic tyrosine analogs and tyrosine-containing peptides have revealed that factors controlling nitration in hydrophobic environments such as biomembranes and lipoproteins can differ to those in aqueous compartments. In particular, exclusion of key soluble reductants from the lipid phase will more easily allow nitration and lipid-derived radicals are suggested as important mediators of the one-electron oxidation of tyrosine to tyrosyl radical in proteins associated to hydrophobic environments. Development and testing of hydrophilic and hydrophobic probes that can compete with endogenous constituents for the nitrating intermediates provide tools to unravel nitration mechanisms *in vitro* and *in vivo*; additionally, they could also serve to play cellular and tissue protective functions against the toxic effects of protein tyrosine nitration.

Keywords: Tyrosine nitration – Peroxynitrite – Nitrogen dioxide – Hemeperoxidases – Free radicals – Hydrophobic environments

Tyrosine nitration: definition, levels and biological significance

The nitration of protein tyrosine residues constitutes the substitution of hydrogen by a nitro group ($-\text{NO}_2$; +45 Da) in the 3-position of the phenolic ring and represents a post-translational modification produced by

nitric oxide (NO)-derived oxidants such as peroxynitrite¹ (ONOO^- ; ONOOH) and nitrogen dioxide radical (NO_2). Early protein chemistry work (Sokolovsky et al., 1966) indicated that nitration by agents such as tetranitromethane could result in dramatic changes in protein structure and function; however, it was not until early in the nineties (Beckman et al., 1990; Ischiropoulos et al., 1992) when the potential biological significance of protein tyrosine nitration was appreciated after recognizing the formation of strong oxidizing and nitrating intermediates during the biological oxidation of NO (Beckman et al., 1990; Koppenol et al., 1992; Radi et al., 1991a, b). Since then, protein tyrosine nitration by a number of biologically-relevant nitrating intermediates has been steadily established to occur both *in vitro* and *in vivo* (Ischiropoulos, 2003; Radi, 2004).

Protein tyrosine nitration is, in general terms, a low yield process and while substantial progress has been made in detecting nitrated proteins in biological samples by immunochemical methods (i.e. using antibodies against protein 3-nitrotyrosine) (Radi et al., 2001; Ye et al., 1996) and in identifying individual nitrated proteins by proteomic-based strategies (Turko et al., 2003), precise quantitative determination of 3-nitrotyrosine levels in fluids and tissues represents a real challenge as it requires, develop-

¹IUPAC recommended names for peroxynitrite anion (ONOO^-) and peroxynitrous acid (ONOOH) ($\text{pK}_a = 6.8$) are oxoperoxonitrate (1^-) and hydrogen oxoperoxonitrate, respectively. The term peroxynitrite is used to refer to the sum of ONOO^- and ONOOH .

ment of analytical methodologies that must both be highly specific and sensitive and avoid potential artifactual nitration which can easily occur during sample processing².

Indeed, reported levels of protein 3-nitrotyrosine in stressed tissues is in the range of 10–100 pmol/mg, corresponding to about 1–5 nitrated residues over 10,000 tyrosines (100–500 $\mu\text{mol/mol}$) (Radi, 2004; Zheng et al., 2005). The extent of tyrosine modification by nitration is comparable to that of other oxidative modifications including chlorination, bromination and hydroxylation to 3-chloro, 3-bromo and 3-hydroxy-tyrosine, respectively, modifications that may coexist with tyrosine nitration at variable ratios, depending on the dominant nitration mechanism (*vide infra*).

The increase of the basal levels of 3-nitrotyrosine found under normal conditions is established to serve as a footprint of nitro-oxidative damage in vivo both in animal models and human diseases; moreover, it has been also revealed as a strong biomarker and predictor of disease progression and severity in conditions such as acute and chronic inflammatory processes, cardiovascular disease, neurodegeneration and diabetic complications, among others (Ceriello, 2002; Radi, 2004; Shishebor et al., 2003; Zhang

et al., 2001; Zheng et al., 2005). In addition, protein tyrosine nitration could contribute to alterations (loss or gain) of protein function in vivo; in this regard, however, few examples of a correlation between the extents of protein nitration and inactivation in vivo have been substantiated because for a significant loss-of-function, a large proportion of nitrated protein molecules are required. Moreover, many times, protein tyrosine nitration occurs concomitantly with other oxidative modifications which may also influence protein function and therefore a cause-consequence relationship is in many cases not possible to demonstrate. A remarkable and well-documented example is constituted by the in vivo nitration and inactivation of MnSOD (MacMillan-Crow et al., 1996; Quijano et al., 2005; Radi, 2004), a critical mitochondrial antioxidant enzyme, that becomes modified in animal and human inflammatory disease conditions. MnSOD nitration occurs site-specifically in Tyr-34 located at 5 Å of the active site, with the manganese atom playing a key role on the nitration process (Beckman et al., 1992; Quijano et al., 2001; Quint et al., 2006; Yamakura et al., 1998). Other reported proteins to which extents of nitration might cause significant decrease in activity in vivo in cell and animal disease models are actin (in sickle cell disease) (Aslan et al., 2003), prostacyclin synthase (in vascular dysfunction) (Zou and Ullrich, 1996; Zou et al., 1997), tyrosine hydroxylase (in Parkinson's disease) (Giasson et al., 2002; Ischiropoulos and Beckman, 2003), and prostaglandin endoperoxide synthase-2 (PHS-2) (in vascular inflammation) (Schildknecht et al., 2006). Alternatively, and as a more novel concept, tyrosine nitration may promote a gain-of-function, in which case modification of only a small protein fraction may trigger a substantive signal from a previously weak or non-existent function; this appears to be the case of cytochrome c (i.e. peroxidase activity) (Batthyany et al., 2005; Cassina et al., 2000), protein kinase C ϵ (i.e. translocation and interaction with RACK2) (Balafanova et al., 2002) and glutathione S-transferase (i.e. enzyme activation) (Ji et al., 2006). Similarly, small amounts of a nitrated protein can serve in nucleation steps in the process of making protein fibers (e.g. fibrinogen and pro-coagulant activity) (Vadseth et al., 2004) or protein aggregates (e.g. α -synuclein and Lewy bodies) (Giasson et al., 2000; Hodara et al., 2004). Thus, considering the low yield of tyrosine nitration for most proteins, evaluation of new activities or interactions by nitrated proteins becomes a relevant matter in the context of alterations of cell homeostasis by nitro-oxidative stress.

In addition to functional changes, protein nitration may cause other biological effects: a) nitrated proteins may

² Techniques that are based on anti-protein 3-nitrotyrosine antibody (e.g. ELISA) should be considered semi-quantitative. At present, the gold standard analytical technique for the quantitation of 3-nitrotyrosine is either GC or LC coupled to MS/MS; recently, much improvement has been accomplished using LC/MS/MS due to the innovation on mild ionization sources such as electrospray ionization (ESI). The basal level of free 3-nitrotyrosine in human plasma is 1.5 ± 1.0 nM. Thus, analytical approaches to measure free 3-nitrotyrosine must have a limit of quantification (LOQ) below 0.5 nM. Care should be taken in sample preparation and processing since some of these techniques require derivatization reactions that can lead to artifactual acid-catalyzed nitration (for extensive reviews see (Duncan, 2003; Tsikas and Caidahl, 2005)). In this regard, isotope dilution methods using uniformly labeled tyrosine and 3-nitrotyrosine (e.g. ¹³C-tyrosine) represent major advances for quantitation purposes (see for example Gaut et al., 2002; Nicholls et al., 2005). The source of free 3-nitrotyrosine is not fully established but it should mainly arise from the turnover of nitrated proteins as free 3-nitrotyrosine can not be incorporated in the de novo synthesis of proteins. Quantitation of protein-3-nitrotyrosine involves total hydrolysis of sample proteins to release 3-nitrotyrosine. Acid or alkaline hydrolysis and enzymatic digestion of proteins is commonly used. In spite of the facts that protein acid hydrolysis is a tedious process and meticulous controls should be taken to cope with artifactual nitration, it still represents the most accepted approach (for further considerations on the hydrolysis methods, see (Fountoulakis and Lahm, 1998)). The reported basal concentration for human plasma protein 3-nitrotyrosine is in the range of 0.4–1.6 over 1×10^6 (3-nitro-Tyr/Tyr). However, more important discrepancies in values are found in the literature for protein-3-nitrotyrosine than for free 3-nitrotyrosine mainly because of the protein hydrolysis step required to perform this measurement (Tsikas and Caidahl, 2005). Other analytical techniques such as HPLC with electrochemical, fluorescence or even UV-Vis detection have been successfully applied for in vitro well-controlled biochemical experimental setups (Radi et al., 2001).

become auto-antigens and trigger immunological responses (Herzog et al., 2005; Radi, 2004; Whiteman et al., 2006); b) since nitrated tyrosines are incapable to undergo phosphorylation in the phenolic –OH (Kong et al., 1996; Tien et al., 1999), tyrosine kinase-dependent signal transduction could be affected, and c) nitrated proteins may be more readily targeted for protein degradation. The presence of repair systems for tyrosine nitrated proteins (e.g. the existence of “denitrase activity”) has been proposed (Irie et al., 2003; Kamisaki et al., 1998) but these pathways remain to be established.

Site- and protein-specificity in tyrosine nitration processes

Tyrosine in a protein constitutes in average 3–4 mol% of the amino acids and therefore proteins typically contain several tyrosine residues. However, peptide mapping studies have shown that within a protein typically one or two tyrosine residues become preferentially nitrated; the determinants of which are not fully established but depend on three main factors: a) protein structure, b) nitration mechanism, and c) environment where the protein is located. Regarding protein structure, the available information indicates that factors that favor nitration are the presence of an acidic amino acid close to tyrosine (Ischiropoulos, 2003; Souza et al., 1999), the localization of a tyrosine residue on a loop structure (Ischiropoulos, 2003; Souza et al., 1999; Sacksteder et al., 2006) and the nearby presence of transition metal centers and binding sites for hemeperoxidases (Shao et al., 2005). In particular, some transition metal centers site-specifically enhance peroxynitrite-dependent nitration (Quijano et al., 2001; Schmidt et al., 2003) and interactions of the positively charged myeloperoxidase with negatively charged clusters of a target protein can also focus protein nitration (Shao et al., 2005). The presence of amino acids such as cysteine, methionine and tryptophan that compete for the proximal nitrating species (e.g. $\cdot\text{NO}_2$), might be inhibitory for tyrosine nitration, although this view has been recently challenged (Sacksteder et al., 2006); moreover, cysteine can also promote electron transfer through the protein backbone and reduce a tyrosyl radical to tyrosine with the consequent formation of a cysteinyl radical and the inhibition of nitration (Zhang et al., 2005; Sacksteder et al., 2006). The influence of the nitration mechanism and the protein environment (polar or nonpolar) on the selectivity of the nitration site is discussed elsewhere in the review and new data is rapidly emerging (Sacksteder et al., 2006; Heijnen et al., 2006).

Proteomic based approaches involving peptide mapping and sequencing are revealing that some proteins are preferentially nitrated *in vivo*, and that within those proteins one or at most a few tyrosine residues are nitrated (see for example Kanski et al., 2005; Zheng et al., 2005) Thus, there is an ongoing interest in the identification of nitrated proteins in disease states and since nitrating intermediates react in the close proximity of their site of formation, intra- or extracellular distribution of nitrated proteins also provide information regarding the compartments on which nitration events predominantly take place (Heijnen et al., 2006). For example, the significant nitration of mitochondrial proteins observed in a variety of disease states, strongly suggests the contribution of mitochondria in the formation of $\cdot\text{NO}$ -derived oxidants in conditions associated to mitochondrial dysfunction and signaling of apoptosis (Quijano et al., 2005; Sacksteder et al., 2006), where some nitrated proteins, in addition, can play a key contributory role.

Structural and functional studies with pure and well-characterized (i.e. with identified nitration site(s)) mononitrated species are required to unambiguously and precisely define the potential biological effects of tyrosine nitration in specific proteins; isolation and characterization of mono-, di- and polynitrated species can be accomplished by chromatographic separation and peptide mapping of fractions derived from the *in vitro* treatment of native protein with nitrating agents (e.g. peroxynitrite), which will initially yield a mixture containing a variety of modified species plus the remaining native protein (Batthyany et al., 2005); among this mixture, a percentage will be one or more mononitrated species, which in turn may be the species preferentially formed *in vivo*. Importantly, depending on the protein under study, the nitration system and the experimental conditions, is possible that *in vitro* nitration does not completely match the nitration sites identified *in vivo*, an aspect that warrants evaluation in each specific case.

The free radical mechanism of tyrosine nitration

There is now agreement on that tyrosine nitration can occur biologically by a variety of routes (e.g. peroxynitrite- or hemeperoxidase-dependent) but that are all based in free radical chemistry. Indeed, 3-nitrotyrosine as evidenced *in vitro* and most probably *in vivo* is the product of at least two consecutive reactions. Peroxynitrite-mediated nitration is well studied and will serve as a starting point. Subsequently we will broaden the view to consider alternative precursors for the mechanism of nitration. In

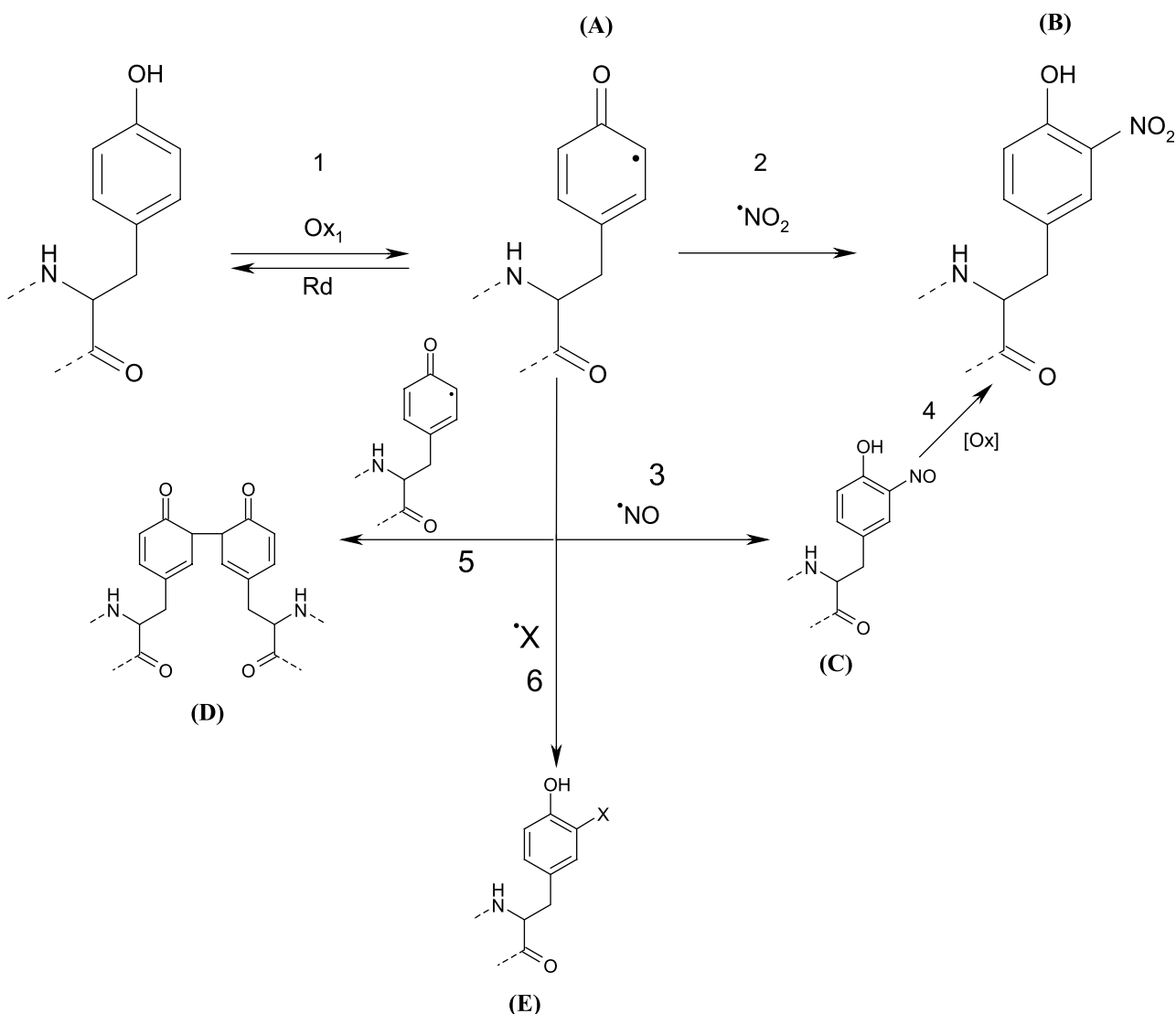


Fig. 1. Reactions leading to nitration or away from it. Reaction 1 is a one-electron oxidation that yields the intermediate tyrosine phenoxyl radical (A) this reaction reverts to tyrosine in the presence of numerous reductants. If (A) adds a nitrogen dioxide radical (reaction 2) the main product (B) is 3-nitrotyrosine. In reaction 3, the radical added to tyrosyl radical is nitric oxide and the new intermediate (C) is 3-nitrosotyrosine, which in turn can be oxidized by two one-electron steps (reaction 4) to yield (D). Intermediate (A) can dimerize (reaction 5) to yield 3,3'-dityrosine (D) or can add radicals other than [•]NO₂ in reaction 6, for instance, if X = [•]OH, then (E) is 3,4-dihydroxy-phenylalanine (DOPA). Reaction 3 constitutes a particular case of reaction 6. The sequence of reactions 1, 3 and 4 has been observed in systems containing tyrosine, H₂O₂ and a hemeperoxidase, see Sturgeon et al. (2001). Reactions and products shown in gray represent those diverting the (A) from nitration pathways

a chemical system consisting in tyrosine, peroxyntirite (added as bolus) and an inert buffer at neutral pH (such as 50 mM phosphate), tyrosine is first oxidized by either of the radicals arising from homolysis of ONOOH ([•]OH or [•]NO₂ radicals (Radi et al., 2001)) (see Fig. 1) yielding the tyrosine phenoxyl radical (A) which in turn couples with [•]NO₂ to produce 3-nitrotyrosine (B). Briefly, an oxidation step (Fig. 1, reaction 1) followed by an addition step (Fig. 1, reaction 2).

The identity of the first oxidant (Ox₁) is not critical and one-electron oxidants can produce A. In the original

example, [•]OH does it very fast ($1.3 \times 10^{10} \text{ M}^{-1} \text{ s}^{-1}$) but in a low yield (5%, which can be increased by the base-catalyzed dehydration of the main product) (Solar et al., 1984), whereas [•]NO₂ is much slower ($3.2 \times 10^5 \text{ M}^{-1} \text{ s}^{-1}$, pH 7.5) (Prutz et al., 1985). This example is of limited biological relevance (as ONOOH homolysis is a minor route of peroxyntirite decay in vivo (Radi et al., 2001)) but serves as a starting point to understand the reaction mechanism and its details. The next step in complexity involves the addition of a nitration promoter. Carbon dioxide, for instance, reacts with ONOO⁻ before homolysis

Table 1. Promoters of peroxynitrite-mediated tyrosine nitration: yields in in vitro systems for bolus addition

Promoter	Ox ₁	Ox ₁ yield (%)	k for reaction 1 (M ⁻¹ s ⁻¹)	NO ₂ -Y yield (%)	Ref
H ⁺	[•] OH	33	1.3 × 10 ¹⁰	6–10	Beckman et al. (1992)
CO ₂	CO ₃ ^{•-}	35	3.0 × 10 ⁷	35	Denicola et al. (1996)
MPO	compound II	100	1.6 × 10 ⁴		Marquez and Dunford (1995)
MnTM-2-PyP	O = Mn ^{IV} TM-2-PyP	100	4.9 × 10 ³	30	Ferrer-Sueta et al. (2003)
a	[•] NO ₂		3.2 × 10 ⁵		

^a [•]NO₂ can perform as Ox₁ and is produced during the reaction of peroxynitrite with all the promoters listed

to produce carbonate radical (CO₃^{•-}), which will be Ox₁ in this case (Radi et al., 2001). CO₃^{•-} excels in oxidizing tyrosine (3 × 10⁷ M⁻¹ s⁻¹) with quantitative yield. Another possible promoter would be myeloperoxidase (MPO), that is oxidized by peroxynitrite to yield compound II, which in turn reacts with tyrosine with a rate constant of 1.57 × 10⁴ M⁻¹ s⁻¹ (Marquez and Dunford, 1995). Finally, low molecular weight transition metal complexes such as MnPorphyrins, would yield a high oxidation state oxo-metal complex (e.g. O = Mn^{IV}) that can act as Ox₁ in Fig. 1, reaction 1 (in the case of MnTM-2-PyP with a rate constant of 4.9 × 10³ M⁻¹ s⁻¹ (Ferrer-Sueta et al., 1999)).

There is an apparent lack of correlation between the rate constant of reaction 1 and the maximum nitration yield achieved (see Table 1), even in relatively simple systems like those mentioned. One factor influencing the yield of nitration is the yield of formation of Ox₁ when ONOO⁻ is the precursor. Other important factors would be the relative stability of Ox₁ (Ferrer-Sueta et al., 2003) and its possible involvement in oxidation reactions not yielding 3-nitrotyrosine.

Reaction 2 is evidently much less ambiguous; the only possibility is [•]NO₂ reacting with the TyrO[•] formed in reaction 1. Nitrogen dioxide can be formed in the same reaction that produces Ox₁, as is the case of all the promoters of Table 1 reacting with ONOO⁻. It can also be formed independently, for instance, by oxidation of nitrite. In regard to this, some years ago a series of works disputed the prevalence of ONOO⁻ as being the only ultimate causative agent of tyrosine nitration in vivo (van der Vliet et al., 1997). The main alternative proposed the combined presence of H₂O₂ as the oxidant taking an electron each from nitrite and tyrosine in a reaction catalyzed by MPO (and potentially several other hemeperoxidases). In fact, this MPO-mediated tyrosine nitration also fits well in our general scheme, namely, the reaction of H₂O₂ with MPO produces compound I which can oxidize nitrite and tyrosine by one electron each yielding the TyrO[•] and [•]NO₂ necessary for reaction 2. In this case either compound I

or compound II can act as Ox₁. The rate constants indicate that nitrite is oxidized faster than tyrosine by compound I and the reverse is true for compound II (Burner et al., 2000; Marquez and Dunford, 1995).

An alternative mechanism to the addition of [•]NO₂ for the second step in nitration is the reaction with nitric oxide (Fig. 1, reaction 3) which can readily react with TyrO[•] radicals. Initially, reaction 3 was studied to understand the effect of [•]NO on catalytically-active TyrO[•] radicals (Eiserich et al., 1995) but then it was discovered that the nitroso intermediate (C) was further oxidized to form an iminoxyl radical and finally the nitro compound (Gunther et al., 1997; Sanakis et al., 1997). This reaction was initially identified in tyrosine residues of prostaglandin H synthase-2 (PHS-2) and photosystem II, but later on it was shown to take place with free tyrosine in solution in the presence of hydrogen peroxide, a peroxidase and [•]NO (Sturgeon et al., 2001). This alternate route to 3-nitrotyrosine has not been studied in detail as reactions 1 and 2, partly because of the elusive nature of intermediate (C), but offers an interesting bypass to the need of [•]NO₂ to reach the nitrated product (Chen et al., 2004).

In addition to the nitration of tyrosine, side reactions can divert TyrO[•] from adding to [•]NO₂ and result in the formation of secondary products. The most studied of these reactions is the dimerization to yield 3,3'-dityrosine (Product D, reaction 5). No other reactants are needed for this reaction, in fact even under strict stoichiometric conditions relating Ox₁ and [•]NO₂ concentrations, 3,3'-dityrosine is a readily observable product of the reaction and its proportion to the overall oxidation depends mainly on the relative concentrations of Tyr, TyrO[•] and [•]NO₂ during the reaction. Also the freedom of movement can govern the probability of the encounter of two TyrO[•] radicals, thus this reaction would be more important with free tyrosine in non-viscous solutions (*vide infra*). Excess radicals other than [•]NO₂ (X, Fig. 1, reaction 5) can convert TyrO[•] to a 3-substituted tyrosine derivative (E). For instance, during Fenton oxidation of tyrosine derivatives, excess

$\cdot\text{OH}$ leads to the formation of 3-hydroxylated derivatives (Bartesaghi et al., 2006). The colocalization of 3-hydroxytyrosine and 3-nitrotyrosine was once considered to be a useful tool to discriminate between peroxynitrite and other nitrating species (Santos et al., 2000), but it was later on discovered that 3-hydroxytyrosine formation can also be inferred from the observed tyrosine semiquinone radical in the reaction of cytochrome c with excess hydrogen peroxide (Chen et al., 2004). On the other hand, the concomitant presence of 3-chloro or 3-bromotyrosine with 3-nitrotyrosine, is indicative of the participation of MPO and eosinophil peroxidase (EPO), respectively in the nitration process (Brennan et al., 2002; Radi, 2004).

Tyrosine nitration in soluble proteins and proteins associated to hydrophobic phases

The hydrophathy of tyrosine (relative preference for aqueous and nonpolar environments) is in a midway value respect to highly hydrophilic (e.g. arginine, aspartate) and hydrophobic (e.g. phenylalanine, tryptophan) amino acids. The relatively hydrophilicity and hydrophobicity of tyrosine measured as free energy values derived from the partition coefficients in vapor/water and water/cyclohexane, respectively, are of -8.5 kcal/mol and -2.3 kcal/mol (considering a zero value for glycine), which can be compared, for example, to -22.31 and $+3.0$ kcal/mol for arginine and -3.15 and -2.5 kcal/mol for phenylalanine (Creighton, 1992). The free energy of transfer from water to nonpolar solvents of the side chain of tyrosine is close to zero kcal/mol, but reported values vary from slightly negative (ethanol and dioxane) to slightly positive (in cyclohexane), depending on the organic solvent used for the measurement. For comparative purposes, in the case of the more hydrophobic tryptophan and phenylalanine, the value is ~ -1.5 to 2 kcal/mol regardless of the organic solvent used.

The $-\text{OH}$ group in tyrosine tends to interact with water while the aromatic ring with other non-polar groups. Thus, it is difficult to *a priori* classify tyrosine as simply solvent-exposed or buried amino acid; in average only 15% of the residues are at least 95% buried and therefore inaccessible to the solvent (Creighton, 1992). In the case of mammalian cytochrome c, for example, which is highly soluble in aqueous environments³ and contains four highly

conserved tyrosine residues, two tyrosines are close to the protein surface (Tyr97; Tyr74), while one is in an intermediate position (Tyr67) and one protected from the solvent (Tyr48). Cytochrome c nitration by peroxynitrite-derived radicals ($\cdot\text{OH}$, $\text{CO}_3^{\cdot-}$ and $\cdot\text{NO}_2$) results in the preferential formation of mono-nitrated species in either Tyr97 or Tyr74 (the most solvent-exposed); importantly, di-nitrated species involve either 3-nitro-Tyr97 or 3-nitro-Tyr74 plus 3-nitro-Tyr67 since nitration of the first tyrosine residue (Tyr97 or 74) promotes a conformational change in cytochrome c which results in a easier accessibility for peroxides to the 6th coordination position of the heme-Fe (Batthyany et al., 2005), which would promote the direct reaction of peroxynitrite with the Fe^{III} and the site-specific nitration of the adjacent Tyr67. Interestingly, cytochrome c association to cardiolipin, the major phospholipid of the inner mitochondrial membrane, also promotes conformational changes in cytochrome c (Kagan et al., 2005) which may favor nitration of Tyr67, assuring that nonpolar environments can differentially modulate nitration sites and yields in proteins.

Most of the mechanistic studies of tyrosine nitration for free tyrosine or tyrosine analogs (e.g. p-hydroxyphenyl acetic acid), tyrosine-containing peptides or proteins have been performed in aqueous solution (Beckman et al., 1992; Cassina et al., 2000; Kong et al., 1996; Quijano et al., 2001; Radi, 2004; Tien et al., 1999). However, in many cases, tyrosine nitration can occur in vitro and in vivo in proteins associated to non-polar or hydrophobic compartments as indicated by early work in lipoproteins (Beckman et al., 1994) and biomembranes (Velsor et al., 2003). Indeed, the first in vivo report detecting nitrated protein in a human disease conditions, was performed in an atherosclerotic human coronary artery, where a significant portion of the nitrated protein, as detected by immunohistochemistry, was associated to the lipid-rich material of the atheroma plaque. Later studies involving isolation of lipoproteins and analytical detection of 3-nitrotyrosine revealed that both Apo A (Shao et al., 2005) and to a lesser extent Apo B (Hazen et al., 1999) are nitrated in vitro and in vivo and that apolipoprotein nitration increases in cardiovascular patients, correlating well with the severity of the disease and effectiveness of the treatment (Zhang et al., 2001; Zheng et al., 2004, 2005). In biomembranes, protein tyrosine nitration in specific proteins has been revealed at the plasma (e.g. erythrocyte membrane band 3 (Mallozzi et al., 1997), mitochondrial (e.g. complex I of the inner membrane) (Murray et al., 2003), sarcoplasmic reticulum (e.g. Ca^{2+} -ATPase, SERCA) (Viner et al., 1999; Xu et al., 2006) and microsomal (e.g. glutathione-S-transferase) membranes

³ Cytochrome c is a mitochondrial protein that interacts with the external leaflet of the inner mitochondrial membrane shuttling electrons from cytochrome b to cytochrome a; at least two different populations of cytochrome c exist at any time, one membrane-bound (through both electrostatic and hydrophobic interactions) and one soluble in the intermembrane space.

(Ji et al., 2006). In proteins associated to hydrophobic structures, nitration could occur in tyrosines located in hydrophobic domains but also in solvent-exposed tyrosines. Although with the structural data available sometimes is difficult to assign the position of a tyrosine within a protein because not in all cases the native three-dimensional structure is available, in some this information exists or can be inferred. For example, in case of erythrocyte membrane band 3, tyrosine nitration occurs in the cytosolic, solvent exposed, domain but not in the transmembrane domain (Mallozzi et al., 1997). In the case of SERCA, Tyr294 and 295, located on a transmembrane domain are nitrated, both in vitro and in vivo (Viner et al., 1999; Xu et al., 2006); indeed, the specific nitration of SERCA at tyrosines 294, 295, has been just reported in arteries and skeletal muscle during vascular degeneration and aging in both animals and human patients (Xu et al., 2006). For microsomal glutathione S-transferase, Tyr92 close to the active site and on a transmembrane domain becomes nitrated; nitration may be catalyzed by the heme center and would be responsible for the gain-of-function reported (Ji et al., 2006). Finally, in ApoA the relatively hydrophilic Tyr-192 results nitrated but becomes resistant to myeloperoxidase-dependent nitration once located more hydrophobically secondary to association to HDL (Shao et al., 2005).

Probes for studying tyrosine nitration in hydrophilic and hydrophobic environments

Most mechanistic studies of tyrosine nitration have been performed in aqueous environments. L-Tyrosine has low solubility in water (0.045 g/100 ml at 25 °C) (Dawson et al., 1986) and therefore its final concentration in buffers at physiological pH and temperature can rarely go above 2.0 mM. Thus, when higher concentrations are required for mechanistic studies, hydrophilic analogs such as p-hydroxyphenyl acetic acid (pHPA) have been extensively used (Beckman et al., 1992; Mani et al., 2003; Moore and Mani, 2002; Quijano et al., 2001). In addition, the first report on the formation of peroxyxynitrite by human cells was performed by following the nitration of pHPA added extracellularly to activated iNOS-containing rat alveolar macrophages, which evolved to 3-nitro-pHPA. Alternative probes have been represented by tyrosine-containing peptides (Eiserich et al., 1999; Kong et al., 1996; Zhang et al., 2003) and mutated forms of CuZn-SOD containing a tyrosine residue adjacent to the copper center that becomes prone to nitration (Macfadyen et al., 1999).

On the other hand, factors that influence tyrosine nitration in hydrophobic environments are just starting to

be defined (Bartesaghi et al., 2006; Trujillo et al., 2005; Zhang et al., 2001, 2003). To this aim, there has been a recent appreciation of the need to develop hydrophobic probes which should be a) incorporated and retained into a lipid phase, b) stable before and after nitration, and c) separated from the lipid phase components for quantitation purposes. In this regard, two types of hydrophobic probes have been recently generated and tested. On the first place, different hydrophobic tyrosine analogs have been evaluated, in particular tyrosine esters in liposomes. Of all the potential compounds studied, *N*-*t*-BOC L-tyrosine *tert* butyl ester (BTBE) resulted to be a valuable hydrophobic tyrosyl probe for investigating nitration and other oxidation reactions (i.e. dimerization, hydroxylation) in membranes. Indeed, BTBE was incorporated in high yields (>98%) into the lipid phase of phosphatidylcholine (PC) liposomes and turned to be an extremely stable compound being resistant to hydrolysis for at least 40 h. Spin-label data indicated that the highest concentration of BTBE was present near the glycerol backbone (Zhang et al., 2001) and kinetic data supported that the phenolic hydroxyl group was located towards the lipid-water interphase where it could dissociate with an apparent pK_a ~10 (Bartesaghi et al., 2006), in agreement with the structural properties of tyrosine (Fig. 2). The *tert*-butyl moieties of BTBE serve to “anchor” it in the lipid bilayer and to minimize its diffusion back to the aqueous phase. Other tested compounds such as tyrosine methyl and ethyl esters were not suitable since they underwent slow hydrolysis to form tyrosine, except for the case of tyrosine butyl ester which was resistant to hydrolysis but its level of incorporation into liposomes was only 53% of the initial amount added. Exposure of multi- and unilamellar liposomes to nitrating systems caused the formation of both 3-nitro-BTBE and 3,3'-di-BTBE, with the yield of the nitro-derivative much higher than that of the corresponding dimer (Bartesaghi et al., 2006; Zhang et al., 2001). More recently, we have also detected the transient formation of the corresponding BTBE-derived phenoxyl radical by spin trapping EPR, the one-electron oxidation product of BTBE, as well as small amounts of a hydroxylated derivative of BTBE, assigned as 3-hydroxy-BTBE, as determined by HPLC separation, fluorimetric detection and electrospray ionization mass spectrometry (ESI-MS/MS) analysis of parent and daughter ions of products arising from treatment of BTBE-containing PC liposomes with peroxyxynitrite (Bartesaghi et al., 2006).

Secondly, membrane spanning peptides containing 23 amino acids with a single tyrosine residue at position 4, 8 or 12 have been synthesized and incorporated success-

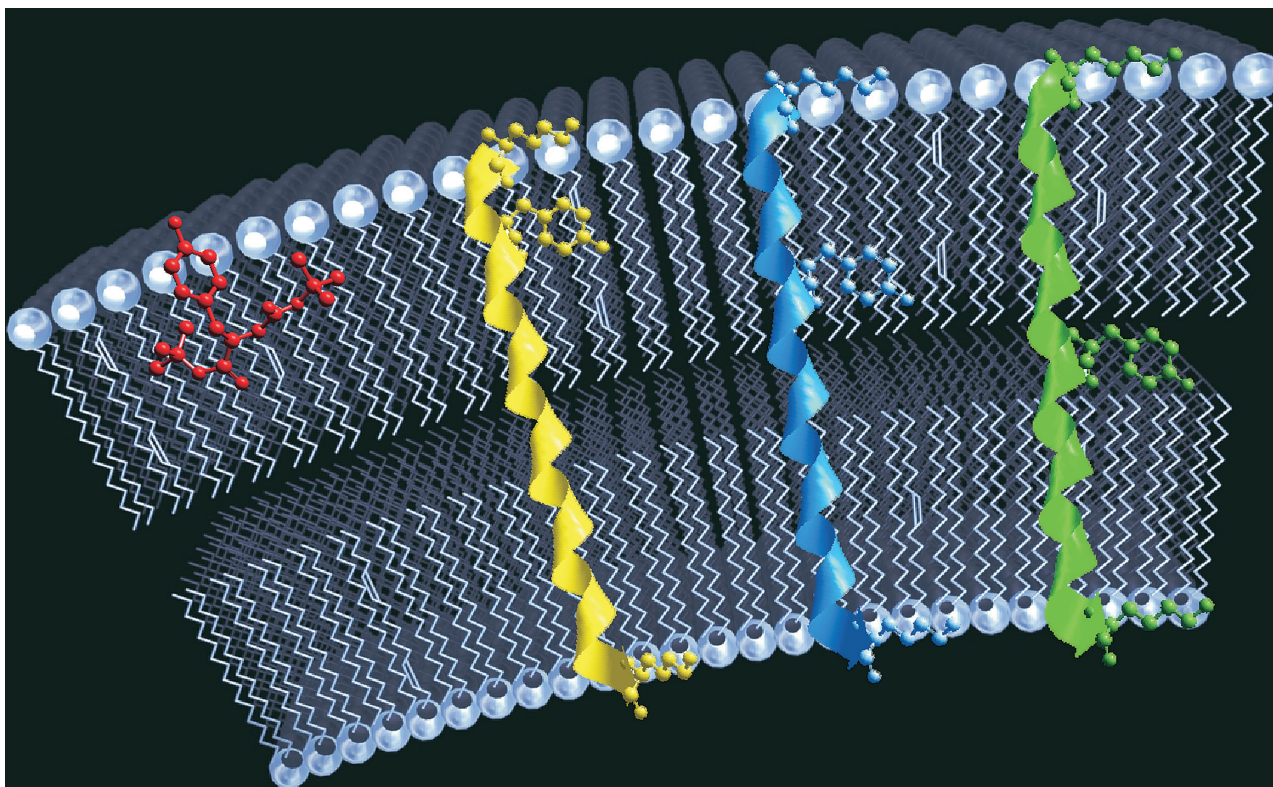


Fig. 2. Tyrosine analog, BTBE, and tyrosine-containing transmembrane peptides as hydrophobic probes to study tyrosine nitration in biomembranes. From left to right, the structure of BTBE (in red) and of transmembrane peptides are shown. BTBE is anchored to the bilayer by the hydrophobic *tert*-butyl moieties; while the aromatic ring is immersed in the bilayer, the phenolic –OH group emerges at the lipid-water interphase. The 23-amino acid transmembrane peptides (in yellow, blue and green) contain tyrosines at position 4-, 8- and 12, respectively which are located in the hydrophobic region of the bilayer; the side chains of the N- and C-terminal lysines are shown and, being highly hydrophilic, interact with the phospholipid polar head groups and water

fully to PC liposomes to study tyrosine nitration in biomembranes (Zhang et al., 2003) (Fig. 2). Indeed, these transmembrane peptides are formed by two hydrophilic and charged residues (e.g. K; Lys) both at the N- and C-terminus, and a hydrophobic sequence (repeats of AL; Ala-Leu) in the peptide central region containing the tyrosine residue at different positions. Prototypical peptides have the following general structure (in this example tyrosine is located in position 4 from the N-terminus):

Y-4 Ac-NH-KKAYALALALALALALALAKK
-CONH₂ 2350 Da

These peptides, designed as hydrophobic probes, resemble more closely the structure of a protein transmembrane domain of a protein and allow to study the influence of the intramembrane location of tyrosine and the role of neighboring amino acids on nitration yields. For instance, we have observed that peroxynitrite-dependent tyrosine nitration is favored for tyrosines located deeper in the membrane (e.g. Tyr12) while myeloperoxidase/hydrogen peroxide/nitrite-dependent nitration is favored in the tyrosine

closer to the membrane surface (e.g. Tyr4). The explanation for this different distribution is still not clear, but may be due to the fact that peroxynitrite can undergo homolysis inside the membrane to $\cdot\text{OH}$ and $\cdot\text{NO}_2$, while myeloperoxidase-derived oxidants will be only formed outside the liposome and will have to diffuse to reach a tyrosine residue, thus minimizing nitration of more distant tyrosines (e.g. Tyr12). In the case of peroxynitrite, in spite that ONOOH homolysis could occur throughout the membrane, tyrosyl radical formation from $\cdot\text{OH}$ requires the initial tyrosine-hydroxyl radical adduct to be dehydrated. The transient formation of peptide-derived tyrosyl radical has been detected by spin trapping-EPR, confirming that tyrosine nitration in transmembrane peptides, as in the case of BTBE, is a free radical-dependent mechanism. In the case of the transmembrane peptides, no dimer product from peroxynitrite-dependent oxidations was observed, and tyrosine hydroxylation has not been explored yet.

The data obtained with transmembrane peptides may be more easily extrapolable to biological systems as compared to BTBE that is an isolated amino acid in-

incorporated into a membrane. However, some advantages for BTBE also exist. Its synthesis is less costly and tedious, which allows to have larger quantities of the probe to perform a large number of experiments testing different variables that include alternative nitration systems and influence of pH, scavengers, catalysts and membrane composition on nitration yields (Bartasaghi et al., 2006). Also, incorporation of the transmembrane peptides to preformed hydrophobic structures such as lipoproteins is expected to be, at least, very difficult. On the other hand, we have successfully incorporated BTBE to erythrocyte membranes and lipoproteins (unpubl. data). BTBE and transmembrane peptides can both provide useful information and represent complementary probes to study physicochemical and biochemical factors that control tyrosine nitration and other oxidation processes in biologically-relevant hydrophobic environments.

The gathered data utilizing the available hydrophobic tyrosyl probes (Fig. 2), (Bartasaghi et al., 2006; Zhang et al., 2001, 2003) indicate that many assumptions valid for the aqueous phase are not readily applicable or not applicable at all in lipid phases due to the different polarity of the environment which will influence protein conformation, limit acid-base chemistry, cause spatial restrictions and diffusional constraints of both reactants and target molecules, and result in an unique distribution of free radical scavengers and nitration catalysts, among other factors.

Nitration, dimerization and hydroxylation in membranes

Tyrosine nitration processes usually occur concomitantly with other oxidative modifications, namely dimerization (to 3,3'-dityrosine) and hydroxylation (to 3-hydroxytyrosine) due to the nature of the nitration process and the chemical properties of the reactive species (e.g. $\cdot\text{OH}$, $\cdot\text{NO}_2$) (Fig. 1, reactions 5 and 6). In analogy to tyrosine in solution, BTBE nitration in PC liposomes occurs through free radical mechanisms and a pH-dependent distribution of the different oxidation products have been established⁴. Typically, at physiological pH nitration yields are higher than that of dimerization and hydroxylation. The relative

yields of tyrosine dimerization are diminished in biomembranes⁵, which can be fully explained by the diffusional constraints. Indeed, the kinetic competition between tyrosine nitration and dimerization in biomembranes will largely favor the first process due to a) the facile diffusion of $\cdot\text{NO}_2$ in hydrophobic environments which achieves efficient trapping of tyrosyl radicals and b) the low probability of reaction between two tyrosyl radicals within the organized structure of membranes, where lateral diffusion is at least two orders of magnitude slower relative to the aqueous phase (Vanderkooi and Callis, 1974). The D of molecules such as $\cdot\text{NO}$ (and $\cdot\text{NO}_2$) is also lowered once in liposomes, but to a much less extent (e.g. $D_{\text{NO}} = 4500$ vs $310 \mu\text{m}^2 \text{s}^{-1}$ for buffer and egg PC liposomes, respectively (Moller et al., 2005), since they do not follow the Stokes-Einstein law, i.e. their diffusion is not inversely related to the viscosity of the solvent (Moller et al., 2005). As $\cdot\text{NO}$ and $\cdot\text{NO}_2$ concentrate 4–5 fold in hydrophobic environments (Liu et al., 1998; Moller et al., 2005), the apparent D value ($D' = 1500 \mu\text{m}^2 \text{s}^{-1}$) (Denicola et al., 1996) results to be very close to that of the aqueous phase ($4500 \mu\text{m}^2 \text{s}^{-1}$) (Moller et al., 2005). On the other hand, the dimerization reaction constant between two BTBE-derived phenoxyl radicals has been estimated $\sim 10^6 \text{M}^{-1} \text{s}^{-1}$, 100 times less than that of tyrosyl radicals in aqueous solution ($k = 2.25 \times 10^8 \text{M}^{-1} \text{s}^{-1}$). Indeed, while the diffusion coefficient (D) value of amino acids such as tyrosine in the aqueous phase is in the order of $800\text{--}1000 \mu\text{m}^2 \text{s}^{-1}$ (Lide, 1990), the estimated D for BTBE in PC liposomes can be safely assumed as $\sim 5 \mu\text{m}^2 \text{s}^{-1}$ as extrapolated from data obtained with the hydrophobic fluorescence aromatic probe pyrene (Vanderkooi and Callis, 1974), implying a 100–200 fold decrease in tyrosyl radical diffusion in the membrane. Intermolecular tyrosine dimerization will be even less likely in integral peptides and proteins as D values become $>10^3\text{--}10^4$ times smaller than in solution (Sackmann et al., 1973; Vanderkooi and Callis, 1974) and on line the lack of tyrosine dimerization in peroxynitrite-treated transmembrane peptides (Zhang et al., 2003).

The presence of CO_2 limits peroxynitrite-dependent tyrosine oxidation (nitration, dimerization and hydroxylation) in hydrophobic phases because formation and decay of ONOOCO_2^- will occur exclusively in the aqueous phase, and the resulting negatively charged carbonate radical ($\text{CO}_3^{\cdot-}$; $\text{pK}_a < 0$) (Czapski, 1999) is incapable to permeate

⁴ The yields of 3-nitrotyrosine, 3,3'-dityrosine and 3,4-di-hydroxy-phenylalanine vary rather differently as a function of pH. Indeed, 3-nitrotyrosine yields are bell-shaped with a maximum around pH 7.4 (Ischiropoulos et al., 1992); on the other hand, 3,3'-dityrosine yields are minimal at low pH (van der Vliet et al., 1995) and increase towards alkaline pH and 3,4-di-hydroxy-phenylalanine yields are high at acidic pH and become null at $\text{pH} > 7.4$ (Santos et al., 2000).

⁵ For example, for 250 μM peroxynitrite and pH 7.4, the ratio for $[\text{3-nitro-BTBE}]/[\text{3,3'-di-BTBE}]$ and $[\text{3-nitro-tyrosine}]/[\text{3,3'-di-tyrosine}]$ is ~ 200 and 70, respectively (Bartasaghi et al., 2006; Zhang et al., 2001).

lipid bilayers (Bartesaghi et al., 2006; Khairutdinov et al., 2000) to promote the one-electron oxidation of tyrosine. The limited diffusion of anionic radical anions on membranes has been also well established for other species such as $\text{Br}_2^{\cdot-}$ and $\text{Cl}_2^{\cdot-}$ (Barber and Thomas, 1978).

In regard to tyrosine hydroxylation in hydrophobic phases concomitant to the process on nitration, it has been reported the hydroxylation of BTBE by peroxyntirite in PC liposomes; $\cdot\text{OH}$, formed from ONOOH in the aqueous phase is capable to penetrate PC vesicles and react with aromatic probe molecules incorporated in the membrane interior as long as it is formed in the immediacy of the bilayer and as previously shown in water radiolysis studies for pyrene hydroxylation (Barber and Thomas, 1978); importantly, $\cdot\text{OH}$ could be also formed inside the liposomes as ONOOH permeates the lipid bilayer (Denicola et al., 1998; Marla et al., 1997) and undergo homolysis of ONOOH in aprotic solvents (Zhang et al., 2001). Studies of tyrosine hydroxylation in peptides containing residues at different depths in the membrane will assist in defining the relevance of ONOOH homolysis in the aqueous vs lipid phase, as $\cdot\text{OH}$ diffusing from the bulk solution will mainly react with residues located near the liposome surface. On the other hand, during heme-dependent nitration, hydroxylation would be expected only at tyrosines located near the membrane surface in the case of soluble hemeperoxidases but could potentially occur in tyrosines located deep in the membrane both in the case of hemin that readily intercalates and undergoes redox chemistry in the phospholipid bilayer (Bartesaghi et al., 2006) and of integral membrane hemeperoxidases.

Mechanistic considerations for protein tyrosine nitration in vivo: limitations and alternatives

Although in controlled-biochemical systems, the free radical mechanisms of tyrosine nitration are now well established, we are confronted with a more complex problem in vivo where 1) oxidants are formed as a flux (instead of the usual chemical experiments using bolus additions) and 2) antioxidant and radical repair mechanisms largely limit nitration reactions.

Tyrosine nitration initiated by a flux of the precursors of peroxyntirite ($\cdot\text{NO}$ and $\text{O}_2^{\cdot-}$) in the presence of CO_2 has been studied by gamma radiolysis (Goldstein et al., 2000). The results of this study suggest that an optimum yield is achieved whenever the fluxes are equal and declines when either reactant is in excess, and this is explained by the excess precursor radicals ($\cdot\text{NO}$ and $\text{O}_2^{\cdot-}$) reacting with the nitration intermediates ($\text{CO}_3^{\cdot-}$, $\cdot\text{NO}_2$ and TyrO^{\cdot}) and di-

verting them from the nitration pathway. More recently, our group (Quijano et al., 2005) has shown, through numerical simulation of the reaction kinetics, that the maximum yield related to a 1:1 stoichiometric ratio is most probably unimportant in vivo. Provided that alternative consumption routes exist for $\cdot\text{NO}$ (diffusion to other compartments where it is consumed) and $\text{O}_2^{\cdot-}$ (SOD-catalyzed dismutation) the yield of peroxyntirite (and concomitantly of nitration) is only limited by the availability of the precursor radicals, irrespective of the ratio of their transient concentrations. In any case 3-nitrotyrosine is a very minor end product of the reaction of $\cdot\text{NO}$ with $\text{O}_2^{\cdot-}$; with relatively high fluxes ($>1 \mu\text{M}/\text{min}$) of the radicals only about one in 10^9 $\cdot\text{NO}$ molecules ends up in 3-nitrotyrosine in a system with $10 \mu\text{M}$ SOD and a cell membrane permeable to $\cdot\text{NO}$ but not to $\text{O}_2^{\cdot-}$.

The next and fundamental obstacle to nitration in vivo is the inclusion of reductants; as an example, 10mM glutathione (GSH) in the aforementioned simulation (Quijano et al., 2005) reduces the expected nitration yield by more than nine orders of magnitude. GSH can act in the system shown in Fig. 1 by intercepting a number of reactants and intermediaries. Besides reacting directly with ONOOH, GSH can react with TyrO^{\cdot} in the reverse of reaction 1, a reaction that has a relatively low rate constant (*ca.* $10^5 \text{M}^{-1} \text{s}^{-1}$) but becomes significant in view of the elevated GSH concentration. Additionally, GSH is an excellent scavenger of $\cdot\text{NO}_2$ ($2 \times 10^7 \text{M}^{-1} \text{s}^{-1}$). Thus, the formation of 3-nitrotyrosine tends to be inhibited in cellular systems with plenty of antioxidant compounds prone to intercept any oxidant functioning as Ox_1 , capable of pushing reaction 1 to the left, and proficient in scavenging any significant amount of $\cdot\text{NO}_2$ formed, and therefore it is difficult to imagine 3-nitrotyrosine being formed at all under these conditions. Nevertheless 3-nitrotyrosine has been shown to be formed in vivo beyond doubt and to correlate well with the increased tissue levels of $\cdot\text{NO}$. We will provide three possible explanations to account for presence of 3-nitrotyrosine in vivo.

Site-specific nitration

The cases of MnSOD (Quijano et al., 2001), cytochrome P450_{CAM} (Daiber et al., 2000) and prostaglandin H synthase-2 (Gunther et al., 1997) are often cited examples where the nitration of a specific tyrosine occurs via catalysis by an adjacent metal center of the enzyme. In site-specific nitration reaction intermediates may not be readily accessible to reductants and competitors and therefore nitration could not be abolished as easily. However, per-

oxynitrite-mediated MnSOD nitration is prevented by reductants and scavengers as shown in (Quijano et al., 2001) much in the same way as non-catalyzed nitration. Data on cytochrome P450_{CAM} are less clear cut as the authors have not shown the effect of reductants and competitors on the nitration yield, nevertheless the catalysis of phenol nitration and oxidation (Daiber et al., 2000) performed by this enzyme suggests that nitration intermediates are susceptible to interception by external scavengers. Other redox active metalloenzymes promote nitration, for example Cu/Zn-SOD (Crow et al., 1997) and the aforementioned hemeperoxidases, by stabilizing strong oxidants but in no case it seems that this site-specific nitration effectively isolates the protein self-catalyzed nitration from outside reductants. There is still one possibility by which metalloenzymes⁶ in vitro can promote site-specific nitration in vivo; this involves the selective formation of a protein TyrO[•] in a site not easily accessible for being repaired. As [•]NO₂ seems to be scavengeable in all cases studied so far, nitration should be explained by an alternative mechanism, such as the one involving [•]NO.

Additional mechanisms

Both PHS (Goodwin et al., 1998; Sturgeon et al., 2001) and cytochrome c (Chen et al., 2004) are nitrated via 3-nitrosotyrosine and 3-iminoxyl tyrosine radical intermediates. This alternative mechanism may be common in proteins capable of stabilizing a TyrO[•] followed by the addition of [•]NO and subsequent two steps of one-electron oxidation (most likely mediated by the protein oxo-metal centers) to yield 3-nitrotyrosine (Fig. 1, reaction 3) and bypasses the need of [•]NO₂ which is efficiently scavenged by GSH. The conjunction of a site-specific formation (catalyzed by a metal center), of a TyrO[•] protected from interaction with external reductants and a nitration pathway not involving [•]NO₂ (for instance, reactions 1, 3 and 4) appears as a kinetically sound candidate for rationalizing protein nitration in cellular milieu where reductants are abundant.

Compartmentalization

Nitration in hydrophobic environments such as membranes could be enhanced by a number of factors. First and foremost the great majority of antioxidants are ex-

cluded from the hydrophobic interior of a membrane, this includes low molecular weight reductants such as glutathione, ascorbate and urate, and also enzymatic antioxidants such as peroxiredoxins any one of which could abolish tyrosine nitration in aqueous solution. The reductants present in lipidic environments, such as tocopherols and carotenes, are much less efficient in scavenging [•]NO₂ and TyrO[•] than their water-soluble counterparts. Some oxidants capable of performing as Ox₁ precursors, (for instance [•]OH and [•]NO₂ from ONOOH homolysis) can freely diffuse in and out of membranes, others such as the polar and charged CO₃^{•-} and MPO compounds I and II can be excluded by partition. Additional oxidants can be formed locally as intermediates in lipid peroxidation chain reactions, of these, alkoxyl and alkylperoxyl radicals are strong oxidants ($E^{\circ} = +1.76$ V and $+1.02$ V, respectively (Jonsson, 1996; Merenyi et al., 2002)) that could contingently act as Ox₁. This provides an additional advantage because the original strong oxidants are not really scavenged by lipids (which are in large abundance in the membranes or lipoproteins and react fast with [•]OH ($k = \sim 10^9$ M⁻¹ s⁻¹ for PUFA) (Barber and Thomas, 1978)) and would outcompete protein tyrosine for the initial oxidants but transformed to species potentially performing as Ox₁ and even enhanced through the propagation phase of lipid peroxidation.

Thus, in spite of the chemical restrictions for obtaining tyrosine nitration in vivo, the combination of site-specificity, assistance of alternative mechanisms and favored nitration in hydrophobic compartments, can add up to provide feasible mechanisms of nitration in complex biological milieux. Indeed, recent studies using high-resolution immuno-electron microscopy have established that the sub-cellular distribution of tyrosine-nitrated proteins in different cells includes a substantial amount associated to the endoplasmic reticulum and mitochondrial membranes, consistent with an effect of the membrane environment in the facilitation of nitration (Heijnen et al., 2006).

Conclusions and perspectives

Tyrosine nitration has been revealed as a relevant post-translational modification linked to nitro-oxidative stress conditions and pathophysiology. Usually, the level of nitrated proteins in tissues and fluids correlate well with the severity of the disease and can be considered a useful biomarker and footprint of oxidative reactions mediated by [•]NO-derived oxidants. A number of biochemical precursor pathways of tyrosine nitration exist in vivo but current evidence supports free radical mechanisms with

⁶We should make a caution note here to make clear that various metal centers in proteins actually protect from peroxynitrite-mediated nitration by avoiding the oxidants to reach the tyrosine or diminishing the actual yield of oxidation. One example is the oxyhemoglobin-catalyzed isomerization of peroxynitrite to nitrate (Romero et al., 2003).

the transient formation of tyrosine-derived phenoxyl radicals. Nitration *in vivo* is limited by the presence of strong reductants such as glutathione, but metal-catalyzed site-specific nitration, transient formation and oxidation of 3-nitrosotyrosine and protein association to hydrophobic environments, among other factors, can partially circumvent antioxidant processes. While immunochemical-based methods have unambiguously revealed the presence of nitrated protein in a wide variety of disease states, analytical and proteomic-based methodologies are laboriously assisting on defining the levels of protein-3-nitrosotyrosine and the preferential nitrated proteins (and within those proteins which tyrosine residues), while functional studies are revealing the cases under which tyrosine nitration triggers changes in biological function. Recent studies utilizing hydrophobic probes, including the tyrosine analog ester BTBE (Bartesaghi et al., 2006; Zhang et al., 2001) or tyrosine-containing transmembrane peptides (Zhang et al., 2001) have focused in defining nitration mechanisms in tyrosines located in liposomal membranes and revealing particular characteristics on nitration processes that sometimes are markedly different to those previously shown to occur in aqueous phases. These studies should be expanded to other biologically-relevant hydrophobic phases, in particular, biomembranes and lipoproteins. Hydrophobic and hydrophilic tyrosine probes can be also potentially utilized to follow nitration processes *in vivo*. Moreover, in conditions under which nitration processes play a contributory role to cell dysfunction and tissue injury, tyrosine analogs and/or tyrosine-containing peptides may serve as nitration targets and spare critical tyrosines in proteins, therefore potentially serving protective roles. Finally, nitration processes are not exclusive to proteins and can also occur in other biomolecules such as DNA bases (Niles et al., 2006; Sawa and Ohshima, 2006; Sawa et al., 2006) and lipids (Baker et al., 2004; Schopfer et al., 2005). In the latter case, a relationship between protein and lipid nitration in biomembranes and lipoproteins should be explored in detail in future studies as both polyunsaturated fatty acids and tyrosine residues will compete for the same nitrating intermediates. Importantly, lipid peroxidation processes are being revealed as a key contributory factor to promote protein tyrosine nitration in hydrophobic environments (Bartesaghi et al., 2006).

Acknowledgements

This work was supported by grants from the Howard Hughes Medical Institute to RR and National Institutes of Health to BK and RR (2

R01HL063119-05). A donation for research support from Laboratorios Gramón-Bagó de Uruguay through Universidad de la República is gratefully acknowledged. SB was partially supported by a fellowship from the PhD Program of Facultad de Química, Universidad de la República, Uruguay.

References

- Aslan M, Ryan TM, Townes TM, Coward L, Kirk MC, Barnes S, Alexander CB, Rosenfeld SS, Freeman BA (2003) Nitric oxide-dependent generation of reactive species in sickle cell disease. Actin tyrosine induces defective cytoskeletal polymerization. *J Biol Chem* 278: 4194–4204
- Baker PR, Schopfer FJ, Sweeney S, Freeman BA (2004) Red cell membrane and plasma linoleic acid nitration products: synthesis, clinical identification, and quantitation. *Proc Natl Acad Sci USA* 101: 11577–11582
- Balafanova Z, Bolli R, Zhang J, Zheng Y, Pass JM, Bhatnagar A, Tang XL, Wang O, Cardwell E, Ping P (2002) Nitric oxide (NO) induces nitration of protein kinase Cepsilon (PKCepsilon), facilitating PKCepsilon translocation via enhanced PKCepsilon-RACK2 interactions: a novel mechanism of no-triggered activation of PKCepsilon. *J Biol Chem* 277: 15021–15027
- Barber DJW, Thomas JK (1978) Reactions of radicals with lecithin bilayers. *Radiation Res* 74: 51–65
- Bartesaghi S, Valez V, Trujillo M, Peluffo G, Romero N, Zhang H, Kalyanaraman B, Radi R (2006) Mechanistic studies of peroxynitrite-mediated tyrosine nitration in membranes using the hydrophobic probe *N-t*-BOC-L-tyrosine *tert*-butyl ester. *Biochemistry* 45: 6813–6825
- Batthyany C, Souza JM, Duran R, Cassina A, Cervenansky C, Radi R (2005) Time course and site(s) of cytochrome c tyrosine nitration by peroxynitrite. *Biochemistry* 44: 8038–8046
- Beckman JS, Beckman TW, Chen J, Marshall PA, Freeman BA (1990) Apparent hydroxyl radical production by peroxynitrite: implications for endothelial injury from nitric oxide and superoxide. *Proc Natl Acad Sci USA* 87: 1620–1624
- Beckman JS, Ischiropoulos H, Zhu L, van der Woerd M, Smith C, Chen J, Harrison J, Martin JC, Tsai M (1992) Kinetics of superoxide dismutase- and iron-catalyzed nitration of phenolics by peroxynitrite. *Arch Biochem Biophys* 298: 438–445
- Beckman JS, Zu Ye Y, Anderson PG, Chen J, Accavitti MA, Tarpey MM, White CR (1994) Extensive nitration of protein tyrosines in human atherosclerosis detected by immunohistochemistry. *Biol Chem Hoppe-Seyler* 375: 81–88
- Brennan ML, Wu W, Fu X, Shen Z, Song W, Frost H, Vadseth C, Narine L, Lenkiewicz E, Borchers MT, Lusic AJ, Lee JJ, Lee NA, Abu-Soud HM, Ischiropoulos H, Hazen SL (2002) A tale of two controversies: defining both the role of peroxidases in nitrotyrosine formation *in vivo* using eosinophil peroxidase and myeloperoxidase-deficient mice, and the nature of peroxidase-generated reactive nitrogen species. *J Biol Chem* 277: 17415–17427
- Burner U, Furtmuller PG, Kettle AJ, Koppenol WH, Obinger C (2000) Mechanism of reaction of myeloperoxidase with nitrite. *J Biol Chem* 275: 20597–20601
- Cassina AM, Hodara R, Souza JM, Thomson L, Castro L, Ischiropoulos H, Freeman BA, Radi R (2000) Cytochrome c nitration by peroxynitrite. *J Biol Chem* 275: 21409–21415
- Ceriello A (2002) Nitrotyrosine: new findings as a marker of postprandial oxidative stress. *Int J Clin Pract [Suppl]*: 51–58
- Chen YR, Chen CL, Chen W, Zweier JL, Augusto O, Radi R, Mason RP (2004) Formation of protein tyrosine ortho-semiquinone radical and nitrotyrosine from cytochrome c-derived tyrosyl radical. *J Biol Chem* 279: 18054–18062
- Creighton TE (1992) Proteins: structures and molecular properties, 2nd ed. Freeman WH & Company

- Crow JP, Ye YZ, Strong M, Kirk M, Barnes S, Beckman JS (1997) Superoxide dismutase catalyzes nitration of tyrosines by peroxynitrite in the rod and head domains of neurofilament-L. *J Neurochem* 69: 1945–1953
- Czapski G (1999) Acidity of the carbonate radical. *J Phys Chem A* 103: 3447–3450
- Daiber A, Schoneich C, Schmidt P, Jung C, Ullrich V (2000) Auto-catalytic nitration of P450CAM by peroxynitrite. *J Inorg Biochem* 81: 213–220
- Dawson RMC, Elliot DC, Elliot WH, Jones KM (1986) Data for biochemical research, Oxford University Press, New York, p 30
- Denicola A, Freeman BA, Trujillo M, Radi R (1996) Peroxynitrite reaction with carbon dioxide/bicarbonate: kinetics and influence on peroxynitrite-mediated oxidations. *Arch Biochem Biophys* 333: 49–58
- Denicola A, Souza JM, Radi R (1998) Diffusion of peroxynitrite across erythrocyte membranes. *Proc Natl Acad Sci USA* 95: 3566–3571
- Denicola A, Souza JM, Radi R, Lissi E (1996) Nitric oxide diffusion in membranes determined by fluorescence quenching. *Arch Biochem Biophys* 328: 208–212
- Duncan MW (2003) A review of approaches to the analysis of 3-nitrotyrosine. *Amino Acids* 25: 351–361
- Eiserich JP, Butler J, van der Vliet A, Cross CE, Halliwell B (1995) Nitric oxide rapidly scavenges tyrosine and tryptophan radicals. *Biochem J* 310: 745–749
- Eiserich JP, Estevez AG, Bamberg TV, Ye YZ, Chumley PH, Beckman JS, Freeman BA (1999) Microtubule dysfunction by posttranslational nitrotyrosination of alpha-tubulin: a nitric oxide-dependent mechanism of cellular injury. *Proc Natl Acad Sci USA* 96: 6365–6370
- Ferrer-Sueta G, Batinic-Haberle I, Spasojevic I, Fridovich I, Radi R (1999) Catalytic scavenging of peroxynitrite by isomeric Mn(III) N-methylpyridylporphyrins in the presence of reductants. *Chem Res Toxicol* 12: 442–449
- Ferrer-Sueta G, Vitturi D, Batinic-Haberle I, Fridovich I, Goldstein S, Czapski G, Radi R (2003) Reactions of manganese porphyrins with peroxynitrite and carbonate radical anion. *J Biol Chem* 278: 27432–27438
- Fountoulakis M, Lahm HW (1998) Hydrolysis and amino acid composition of proteins. *J Chromatogr A* 826: 109–134
- Gaut JP, Byun J, Tran HD, Heinecke JW (2002) Artifact-free quantification of free 3-chlorotyrosine, 3-bromotyrosine, and 3-nitrotyrosine in human plasma by electron capture-negative chemical ionization gas chromatography mass spectrometry and liquid chromatography-electrospray ionization tandem mass spectrometry. *Anal Biochem* 300: 252–259
- Giasson BI, Duda JE, Murray IV, Chen Q, Souza JM, Hurtig HI, Ischiropoulos H, Trojanowski JQ, Lee VM (2000) Oxidative damage linked to neurodegeneration by selective alpha-synuclein nitration in synucleinopathy lesions. *Science* 290: 985–989
- Giasson BI, Ischiropoulos H, Lee VM, Trojanowski JQ (2002) The relationship between oxidative/nitrative stress and pathological inclusions in Alzheimer's and Parkinson's diseases. *Free Radic Biol Med* 32: 1264–1275
- Goldstein S, Czapski G, Lind J, Merenyi G (2000) Tyrosine nitration by simultaneous generation of (\cdot)NO and O(-2) under physiological conditions. How the radicals do the job. *J Biol Chem* 275: 3031–3036
- Goodwin DC, Gunther MR, Hsi LC, Crews BC, Eling TE, Mason RP, Marnett LJ (1998) Nitric oxide trapping of tyrosyl radicals generated during prostaglandin endoperoxide synthase turnover. Detection of the radical derivative of tyrosine 385. *J Biol Chem* 273: 8903–8909
- Gunther MR, Hsi LC, Curtis JF, Gierse JK, Marnett LJ, Eling TE, Mason RP (1997) Nitric oxide trapping of the tyrosyl radical of prostaglandin H synthase-2 leads to tyrosine iminoxyl radical and nitrotyrosine formation. *J Biol Chem* 272: 17086–17090
- Hazen SL, Zhang R, Shen Z, Wu W, Podrez EA, MacPherson JC, Schmitt D, Mitra SN, Mukhopadhyay C, Chen YR, Cohen PA, Hoff HF, Abu-Soud HM (1999) Formation of nitric oxide-derived oxidants by myeloperoxidase in monocytes: pathways for monocyte-mediated protein nitration and lipid peroxidation in vivo. *Circ Res* 85: 950–958
- Heijnen HF, van Donselaar E, Slot JW, Fries DM, Blachard-Fillion B, Hodara R, Lightfoot R, Polydoro M, Spielberg D, Thomson L, Regan EA, Crapo J, Ischiropoulos H (2006) Subcellular localization of tyrosine-nitrated proteins is dictated by reactive oxygen species generating enzymes and by proximity to nitric oxide synthase. *Free Radic Biol Med* 40: 1903–1913
- Herzog J, Maekawa Y, Cirrito TP, Illian BS, Unanue ER (2005) Activated antigen-presenting cells select and present chemically modified peptides recognized by unique CD4 T cells. *Proc Natl Acad Sci USA* 102: 7928–7933
- Hodara R, Norris EH, Giasson BI, Mishizen-Eberz AJ, Lynch DR, Lee VM, Ischiropoulos H (2004) Functional consequences of alpha-synuclein tyrosine nitration: diminished binding to lipid vesicles and increased fibril formation. *J Biol Chem* 279: 47746–47753
- Irie Y, Saeki M, Kamisaki Y, Martin E, Murad F (2003) Histone H1.2 is a substrate for denitrase, an activity that reduces nitrotyrosine immunoreactivity in proteins. *Proc Natl Acad Sci USA* 100: 5634–5639
- Ischiropoulos H (2003) Biological selectivity and functional aspects of protein tyrosine nitration. *Biochem Biophys Res Commun* 305: 776–783
- Ischiropoulos H, Beckman JS (2003) Oxidative stress and nitration in neurodegeneration: cause, effect, or association? *J Clin Invest* 111: 163–169
- Ischiropoulos H, Zhu L, Chen J, Tsai M, Martin JC, Smith CD, Beckman JS (1992) Peroxynitrite-mediated tyrosine nitration catalyzed by superoxide dismutase. *Arch Biochem Biophys* 298: 431–437
- Ji Y, Neverova I, Van Eyk JE, Bennet BM (2006) Nitration of tyrosine 92 mediates the activation of rat microsomal glutathione-S-transferase by peroxynitrite. *J Biol Chem* 281: 1986–1991
- Jonsson M (1996) Thermochemical properties of peroxides and peroxy radicals. *J Phys Chem* 100: 6814–6818
- Kagan VE, Tyurin VA, Jiang J, Tyurina YY, Ritov VB, Amoscato AA, Osipov AN, Belikova NA, Kapralov AA, Kini V, Vlasova II, Zhao Q, Zou M, Di P, Svistunenko DA, Kurnikov IV, Borisenko GG (2005) Cytochrome c acts as a cardiolipin oxygenase required for release of proapoptotic factors. *Nat Chem Biol* 1: 223–232
- Kamisaki Y, Wada K, Bian K, Balabanli B, Davis K, Martin E, Behbod F, Lee YC, Murad F (1998) An activity in rat tissues that modifies nitrotyrosine-containing proteins. *Proc Natl Acad Sci USA* 95: 11584–11589
- Kanski J, Behring A, Pelling J, Schoneich C (2005) Proteomic identification of 3-nitrotyrosine-containing rat cardiac proteins: effects of biological aging. *Am J Physiol Heart Circ Physiol* 288: H371–H381
- Khairutdinov RF, Coddington JW, Hurst JK (2000) Permeation of phospholipid membranes by peroxynitrite. *Biochemistry* 39: 14238–14249
- Kong SK, Yim MB, Stadtman ER, Chock PB (1996) Peroxynitrite disables the tyrosine phosphorylation regulatory mechanism: Lymphocyte-specific tyrosine kinase fails to phosphorylate nitrated cdc2(6–20)NH₂ peptide. *Proc Natl Acad Sci USA* 93: 3377–3382
- Koppenol WH, Moreno JJ, Pryor WA, Ischiropoulos H, Beckman JS (1992) Peroxynitrite, a cloaked oxidant formed by nitric oxide and superoxide. *Chem Res Toxicol* 5: 834–842
- Lide DR (1990) Handbook of chemistry and physics, 71st ed. CRC Press, (section 6, p 151), Boca Raton
- Liu X, Miller MJ, Joshi MS, Thomas DD, Lancaster JR Jr (1998) Accelerated reaction of nitric oxide with O₂ within the hydrophobic interior of biological membranes. *Proc Natl Acad Sci USA* 95: 2175–2179
- Macfadyen AJ, Reiter C, Zhuang Y, Beckman JS (1999) A novel superoxide dismutase-based trap for peroxynitrite used to detect entry of peroxynitrite into erythrocyte ghosts. *Chem Res Toxicol* 12: 223–229
- MacMillan-Crow LA, Crow JP, Kerby JD, Beckman JS, Thompson JA (1996) Nitration and inactivation of manganese superoxide dismutase in chronic rejection of human renal allografts. *Proc Natl Acad Sci USA* 93: 11853–11858

- Mallozzi C, Di Stasi AM, Minetti M (1997) Peroxynitrite modulates tyrosine-dependent signal transduction pathway of human erythrocyte band 3. *Faseb J* 11: 1281–1290
- Mani AR, Pannala AS, Orie NN, Ollosson R, Harry D, Rice-Evans CA, Moore KP (2003) Nitration of endogenous para-hydroxyphenylacetic acid and the metabolism of nitrotyrosine. *Biochem J* 374: 521–527
- Marla SS, Lee J, Groves JT (1997) Peroxynitrite rapidly permeates phospholipid membranes. *Proc Natl Acad Sci USA* 94: 14243–14248
- Marquez LA, Dunford HB (1995) Kinetics of oxidation of tyrosine and dityrosine by myeloperoxidase compounds I and II. Implications for lipoprotein peroxidation studies. *J Biol Chem* 270: 30434–30440
- Merenyi G, Lind J, Goldstein S (2002) Thermochemical properties of alfa-hydroxy-alkoxyl radicals in aqueous solution. *J Phys Chem A* 106: 11127–11129
- Moller M, Botti H, Batthyany C, Rubbo H, Radi R, Denicola A (2005) Direct measurement of nitric oxide and oxygen partitioning into liposomes and low density lipoprotein. *J Biol Chem* 280: 8850–8854
- Moore KP, Mani AR (2002) Measurement of protein nitration and S-nitrosothiol formation in biology and medicine. *Methods Enzymol* 359: 256–268
- Murray J, Taylor SW, Zhang B, Ghosh SS, Capaldi RA (2003) Oxidative damage to mitochondrial complex I due to peroxynitrite: identification of reactive tyrosines by mass spectrometry. *J Biol Chem* 278: 37223–37230
- Nicholls SJ, Shen Z, Fu X, Levison BS, Hazen SL (2005) Quantification of 3-nitrotyrosine levels using a benchtop ion trap mass spectrometry method. *Methods Enzymol* 396: 245–266
- Niles JC, Wishnok JS, Tannenbaum SR (2006) Peroxynitrite-induced oxidation and nitration products of guanine and 8-oxoguanine: structures and mechanisms of product formation. *Nitric Oxide* 14: 109–121
- Prutz WA, Monig H, Butler J, Land EJ (1985) Reactions of nitrogen dioxide in aqueous model systems: oxidation of tyrosine units in peptides and proteins. *Arch Biochem Biophys* 243: 125–134
- Quijano C, Cassina AM, Castro L, Rodríguez M, Radi R (2005) Peroxynitrite: a mediator of nitric oxide-dependent mitochondrial dysfunction in pathology. In: Lamas S, Cadenas E (eds) *Nitric oxide, cell signaling, and gene expression*. Marcel Dekker Inc., New York, pp 99–143
- Quijano C, Hernandez-Saavedra D, Castro L, McCord JM, Freeman BA, Radi R (2001) Reaction of peroxynitrite with Mn-superoxide dismutase. Role of the metal center in decomposition kinetics and nitration. *J Biol Chem* 276: 11631–11638
- Quijano C, Romero N, Radi R (2005) Tyrosine nitration by superoxide and nitric oxide fluxes in biological systems: modeling the impact of superoxide dismutase and nitric oxide diffusion. *Free Radic Biol Med* 39: 728–741
- Quint P, Reutzel R, Mikulski R, McKenna R, Silverman DN (2006) Crystal structure of nitrated human manganese superoxide dismutase: mechanism of inactivation. *Free Radic Biol Med* 40: 453–458
- Radi R (2004) Nitric oxide, oxidants, and protein tyrosine nitration. *Proc Natl Acad Sci USA* 101: 4003–4008
- Radi R, Beckman JS, Bush KM, Freeman BA (1991) Peroxynitrite oxidation of sulfhydryls. The cytotoxic potential of superoxide and nitric oxide. *J Biol Chem* 266: 4244–4250
- Radi R, Beckman JS, Bush KM, Freeman BA (1991) Peroxynitrite-induced membrane lipid peroxidation: the cytotoxic potential of superoxide and nitric oxide. *Arch Biochem Biophys* 288: 481–487
- Radi R, Peluffo G, Alvarez MN, Naviliat M, Cayota A (2001) Unraveling peroxynitrite formation in biological systems. *Free Radic Biol Med* 30: 463–488
- Romero N, Radi R, Linares E, Augusto O, Detweiler CD, Mason RP, Denicola A (2003) Reaction of human hemoglobin with peroxynitrite. Isomerization to nitrate and secondary formation of protein radicals. *J Biol Chem* 278: 44049–44057
- Sackmann E, Trauble H, Galla H, Overath P (1973) Lateral diffusion, protein mobility and phase transitions in *Escherichia coli* membranes. A spin label study. *Biochemistry* 12: 5360–5369
- Sacksteder CA, Qian WJ, Knyushko TV, Wang H, Chin MH, Lacan G, Melega WP, Camp DG, Smith RD, Smith DJ, Squier TC, Bigelow DJ (2006) Endogenously nitrated proteins in mouse brain: links to neurodegenerative disease. *Biochemistry* 45: 8009–8022
- Sanakis Y, Goussias C, Mason RP, Petrouleas V (1997) NO interacts with the tyrosine radical Y(D) of photosystem II to form an iminoxyl radical. *Biochemistry* 36: 1411–1417
- Santos CX, Bonini MG, Augusto O (2000) Role of the carbonate radical anion in tyrosine nitration and hydroxylation by peroxynitrite. *Arch Biochem Biophys* 377: 146–152
- Sawa T, Ohshima H (2006) Nitrative DNA damage in inflammation and its possible role in carcinogenesis. *Nitric Oxide* 14: 91–100
- Sawa T, Tatemichi M, Akaike T, Barbin A, Ohshima H (2006) Analysis of urinary 8-nitroguanine, a marker of nitrative nucleic acid damage, by high-performance liquid chromatography-electrochemical detection coupled with immunoaffinity purification: association with cigarette smoking. *Free Radic Biol Med* 40: 711–720
- Schildknecht S, Heinz K, Daiber A, Hamacher J, Kavakli C, Ullrich V, Bachschmid M (2006) Autocatalytic tyrosine nitration of prostaglandin endoperoxide synthase-2 in LPS-stimulated RAW 264.7 macrophages. *Biochem Biophys Res Commun* 340: 318–325
- Schmidt P, Youhnovski N, Daiber A, Balan A, Arsic M, Bachschmid M, Przybylski M, Ullrich V (2003) Specific nitration at tyrosine 430 revealed by high resolution mass spectrometry as basis for redox regulation of bovine prostacyclin synthase. *J Biol Chem* 278: 12813–12819
- Schopfer FJ, Baker PR, Giles G, Chumley P, Batthyany C, Crawford J, Patel RP, Hogg N, Branchaud BP, Lancaster JR, Jr, Freeman BA (2005) Fatty acid transduction of nitric oxide signaling. Nitrolinoleic acid is a hydrophobically stabilized nitric oxide donor. *J Biol Chem* 280: 19289–19297
- Shao B, Bergt C, Fu X, Green P, Voss JC, Oda MN, Oram JF, Heinecke JW (2005) Tyrosine 192 in apolipoprotein A-I is the major site of nitration and chlorination by myeloperoxidase, but only chlorination markedly impairs ABCA1-dependent cholesterol transport. *J Biol Chem* 280: 5983–5993
- Shishehbor MH, Aviles RJ, Brennan ML, Fu X, Goormastic M, Pearce GL, Gokce N, Keaney JF Jr, Penn MS, Sprecher DL, Vita JA, Hazen SL (2003) Association of nitrotyrosine levels with cardiovascular disease and modulation by statin therapy. *Am Meol Assoc* 289: 1675–1680
- Sokolovsky M, Riordan JF, Vallee BL (1966) Tetranitromethane. A reagent for the nitration of tyrosyl residues in proteins. *Biochemistry* 5: 3582–3589
- Solar S, Solar W, Getoff N (1984) Reactivity of OH with tyrosine in aqueous solution studied by pulse radiolysis. *J Phys Chem* 88: 2091–2095
- Souza JM, Daikhin E, Yudkoff M, Raman CS, Ischiropoulos H (1999) Factors determining the selectivity of protein tyrosine nitration. *Arch Biochem Biophys* 371: 169–178
- Sturgeon BE, Glover RE, Chen YR, Burka LT, Mason RP (2001) Tyrosine iminoxyl radical formation from tyrosyl radical/nitric oxide and nitrosotyrosine. *J Biol Chem* 276: 45516–45521
- Tien M, Berlett BS, Levine RL, Chock PB, Stadtman ER (1999) Peroxynitrite-mediated modification of proteins at physiological carbon dioxide concentration: pH dependence of carbonyl formation, tyrosine nitration, and methionine oxidation. *Proc Natl Acad Sci USA* 96: 7809–7814
- Trujillo M, Folkes L, Bartesaghi S, Kalyanaraman B, Wardman P, Radi R (2005) Peroxynitrite-derived carbonate and nitrogen dioxide radicals readily react with lipoic and dihydrolipoic acid. *Free Radic Biol Med* 39: 279–288
- Tsikakos D, Caidahl K (2005) Recent methodological advances in the mass spectrometric analysis of free and protein-associated 3-nitrotyrosine in human plasma. *J Chromatogr B Anal Technol Biomed Life Sci* 814: 1–9

- Turko IV, Li L, Aulak KS, Stuehr DJ, Chang JY, Murad F (2003) Protein tyrosine nitration in the mitochondria from diabetic mouse heart. Implications to dysfunctional mitochondria in diabetes. *J Biol Chem* 278: 33972–33977
- Vadseth C, Souza JM, Thomson L, Seagraves A, Nagaswami C, Scheiner T, Torbet J, Vilaire G, Bennett JS, Murciano JC, Muzykantov V, Penn MS, Hazen SL, Weisel JW, Ischiropoulos H (2004) Pro-thrombotic state induced by post-translational modification of fibrinogen by reactive nitrogen species. *J Biol Chem* 279: 8820–8826
- van der Vliet A, Eiserich JP, Halliwell B, Cross CE (1997) Formation of reactive nitrogen species during peroxidase-catalyzed oxidation of nitrite. A potential additional mechanism of nitric oxide-dependent toxicity. *J Biol Chem* 272: 7617–7625
- van der Vliet A, Eiserich JP, O'Neill CA, Halliwell B, Cross CE (1995) Tyrosine modification by reactive nitrogen species: a closer look. *Arch Biochem Biophys* 319: 341–349
- Vanderkooi JM, Callis JB (1974) Pyrene. A probe of lateral diffusion in the hydrophobic region of membranes. *Biochemistry* 13: 4000–4006
- Velsor LW, Ballinger CA, Patel J, Postlethwait EM (2003) Influence of epithelial lining fluid lipids on NO₂-induced membrane oxidation and nitration. *Free Radic Biol Med* 34: 720–733
- Viner RI, Ferrington DA, Williams TD, Bigelow DJ, Schoneich C (1999) Protein modification during biological aging: selective tyrosine nitration of the SERCA2a isoform of the sarcoplasmic reticulum Ca²⁺-ATPase in skeletal muscle. *Biochem J* 340: 657–669
- Whiteman M, Spencer JPE, Zhu YZ, Armstrong JS, Schantz JT (2006) Peroxynitrite-modified collagen-II induces p38/ERK and NF-κB-dependent synthesis of prostaglandin E2 and nitric oxide in chondrogenically differentiated mesenchymal progenitor cells. *Osteo Arthritis Cartilage* 14: 460–470
- Xu S, Ying J, Jiang B, Guo W, Adachi T, Sharov V, Lazar H, Menzoian J, Knyushko TV, Bigelow DJ, Schoneich C, Cohen RA (2006) Detection of sequence-specific tyrosine nitration of manganese SOD and SERCA in cardiovascular disease and aging. *AJP-Heart* 290: 2220–2227
- Yamakura F, Taka H, Fujimura T, Murayama K (1998) Inactivation of human manganese-superoxide dismutase by peroxynitrite is caused by exclusive nitration of tyrosine 34 to 3-nitrotyrosine. *J Biol Chem* 273: 14085–14089
- Ye YZ, Strong M, Huang ZQ, Beckman JS (1996) Antibodies that recognize nitrotyrosine. *Methods Enzymol* 269: 201–209
- Zhang H, Bhargava K, Keszler A, Feix J, Hogg N, Joseph J, Kalyanaraman B (2003) Transmembrane nitration of hydrophobic tyrosyl peptides. Localization, characterization, mechanism of nitration, and biological implications. *J Biol Chem* 278: 8969–8978
- Zhang H, Joseph J, Feix J, Hogg N, Kalyanaraman B (2001) Nitration and oxidation of a hydrophobic tyrosine probe by peroxynitrite in membranes: comparison with nitration and oxidation of tyrosine by peroxynitrite in aqueous solution. *Biochemistry* 40: 7675–7686
- Zhang H, Xu Y, Joseph J, Kalyanaraman B (2005) Intramolecular electron transfer between tyrosyl radical and cysteine residue inhibits tyrosine nitration and induces thyl radical formation in model peptides with MPO, H₂O₂ and NO₂⁻: EPR spin trapping studies. *J Biol Chem* 280: 40684–40698
- Zhang R, Brennan ML, Fu X, Aviles RJ, Pearce GL, Penn MS, Topol EJ, Sprecher DL, Hazen SL (2001) Association between myeloperoxidase levels and risk of coronary artery disease. *Am Meol Assoc* 286: 2136–2142
- Zheng L, Nukuna B, Brennan ML, Sun M, Goormastic M, Settle M, Schmitt D, Fu X, Thomson L, Fox PL, Ischiropoulos H, Smith JD, Kinter M, Hazen SL (2004) Apolipoprotein A-I is a selective target for myeloperoxidase-catalyzed oxidation and functional impairment in subjects with cardiovascular disease. *J Clin Invest* 114: 529–541
- Zheng L, Settle M, Brubaker G, Schmitt D, Hazen SL, Smith JD, Kinter M (2005) Localization of nitration and chlorination sites on apolipoprotein A-I catalyzed by myeloperoxidase in human atheroma and associated oxidative impairment in ABCA1-dependent cholesterol efflux from macrophages. *J Biol Chem* 280: 38–47
- Zou M, Martin C, Ullrich V (1997) Tyrosine nitration as a mechanism of selective inactivation of prostacyclin synthase by peroxynitrite. *Biol Chem* 378: 707–713
- Zou MH, Ullrich V (1996) Peroxynitrite formed by simultaneous generation of nitric oxide and superoxide selectively inhibits bovine aortic prostacyclin synthase. *FEBS Lett* 382: 101–104

Authors' address: Rafael Radi, Departamento de Bioquímica, Facultad de Medicina, Avda. General Flores 2125, 11800 Montevideo, Uruguay, Fax: +598-2-9249563, E-mail: rradi@fmed.edu.uy

Mechanistic Studies of Peroxynitrite-Mediated Tyrosine Nitration in Membranes Using the Hydrophobic Probe *N*-*t*-BOC-*L*-tyrosine *tert*-Butyl Ester[†]

Silvina Bartesaghi,[‡] Valeria Valez,[‡] Madia Trujillo,[‡] Gonzalo Peluffo,[‡] Natalia Romero,[‡] Hao Zhang,[§] Balaraman Kalyanaraman,[§] and Rafael Radi^{*,‡}

Departamento de Bioquímica and Center for Free Radical and Biomedical Research, Facultad de Medicina, Universidad de la República, Montevideo 11800, Uruguay, and Biophysics Research Institute and Free Radical Research Center, Medical College of Wisconsin, Milwaukee, Wisconsin 53226

Received February 21, 2006; Revised Manuscript Received March 28, 2006

ABSTRACT: Most of the mechanistic studies of tyrosine nitration have been performed in aqueous solution. However, many protein tyrosine residues shown to be nitrated *in vitro* and *in vivo* are associated to nonpolar compartments. In this work, we have used the stable hydrophobic tyrosine analogue *N*-*t*-BOC-*L*-tyrosine *tert*-butyl ester (BTBE) incorporated into phosphatidylcholine (PC) liposomes to study physicochemical and biochemical factors that control peroxynitrite-dependent tyrosine nitration in phospholipid bilayers. Peroxynitrite leads to maximum 3-nitro-BTBE yields (3%) at pH 7.4. In addition, small amounts of 3,3'-di-BTBE were formed at pH 7.4 (0.02%) which increased over alkaline pH; at pH 6, a hydroxylated derivative of BTBE was identified by HPLC-MS analysis. BTBE nitration yields were similar in dilauroyl- and dimyristoyl-PC and were also significant in the polyunsaturated fatty acid-containing egg PC. •OH and •NO₂ scavengers inhibited BTBE nitration. In contrast to tyrosine in the aqueous phase, the presence of CO₂ decreased BTBE nitration, indicating that CO₃^{•-} cannot permeate to the compartment where BTBE is located. On the other hand, micromolar concentrations of hemin and Mn-tccp strongly enhanced BTBE nitration. Electron spin resonance (ESR) detection of the BTBE phenoxyl radical and kinetic modeling of the pH profiles of BTBE nitration and dimerization were in full agreement with a free radical mechanism of oxidation initiated by ONOOH homolysis in the immediacy of or even inside the bilayer and with a diffusion coefficient of BTBE phenoxyl radical 100 times less than for the aqueous phase tyrosyl radical. BTBE was successfully applied as a hydrophobic probe to study nitration mechanisms and will serve to study factors controlling protein and lipid nitration in biomembranes and lipoproteins.

Peroxynitrite¹ is a powerful oxidant formed *in vivo* by the diffusion-controlled reaction between nitric oxide (•NO) and superoxide radicals (O₂^{•-}), and it serves as a pathogenic mediator in a variety of disease states (1–4). Peroxynitrite can undergo a proton-catalyzed homolysis (5, 6) to nitrogen dioxide (•NO₂) and hydroxyl (•OH) radicals in ~30% yields, with a first-order rate constant of ~1 s⁻¹ at pH 7.4 and 37 °C (5, 7, 8). However, in biological systems, the reactivity of peroxynitrite is dictated mainly by direct reactions with different biological targets including thiols (6), transition metal-containing centers, and carbon dioxide (CO₂). Importantly, peroxynitrite-mediated one-electron oxidation of heme

iron-containing centers ($k = 10^4$ – 10^7 M⁻¹ s⁻¹ at pH 7.4 and 37 °C) leads to the formation of potent secondary oxidants such as oxo-iron (O=Fe⁴⁺) complexes and •NO₂, while the reaction with CO₂ ($k = 4.6 \times 10^4$ M⁻¹ s⁻¹ at pH 7.4 and 37 °C) yields the transient nitrosoperoxocarbonate adduct (ONOCO₂⁻) (4, 9) which is homolyzed to the carbonate radical (CO₃^{•-}) and •NO₂ in 33% yields (8, 10, 11). Thus, O=Fe⁴⁺, CO₃^{•-}, and •NO₂ ($E^\circ_{\text{O=Fe}^{4+}/\text{Fe}^{3+}} = 1.4$ – 1.8 V, $E^\circ_{\text{CO}_3^{\bullet-}/\text{CO}_3^{2-}} = 1.78$ V, and $E^\circ_{\text{•NO}_2/\text{NO}_2^-} = 0.99$ V), respectively, can be proximal reactive species in several peroxynitrite-mediated oxidations (12–14), including protein tyrosine nitration to 3-nitrotyrosine (1, 15).

Protein tyrosine nitration *in vivo* not only serves as a footprint to unravel the formation and reactions of •NO-derived oxidants but in some cases contributes to alterations (loss or gain) of protein function, affects tyrosine kinase-dependent signal transduction cascades, and triggers immunological responses (1, 16). There is an ongoing interest in the identification of nitrated proteins in disease states, in the mapping of nitrated tyrosine residues within a protein, and in defining the biologically relevant mechanisms of nitration (1, 17–19). It is now generally agreed that tyrosine nitration occurs by more than one mechanism (e.g., peroxy-nitrite or hemoperoxidase dependent) but which involves, in all cases, the action of reactive intermediates and/or radical

[†] This work was supported by grants from the Howard Hughes Medical Institute to R.R. and the National Institutes of Health to B.K. and R.R. (2 R01HL063119–05). A donation for research support from Laboratorios Gramón-Bagó through Universidad de la República is gratefully acknowledged. S.B. was partially supported by a fellowship from the Ph.D. Program of Facultad de Química, Universidad de la República, Uruguay.

* To whom correspondence should be addressed. Telephone: 598-2-9249561. Fax: 598-2-9249563. E-mail: rradi@fmed.edu.uy.

[‡] Universidad de la República.

[§] Medical College of Wisconsin.

¹ IUPAC recommended names for peroxynitrite anion (ONOO⁻) and peroxynitrous acid (ONOOH) (pK_a = 6.8) are oxoperoxonitrate(1-) and hydrogen oxoperoxonitrate, respectively. The term peroxynitrite is used to refer to the sum of ONOO⁻ and ONOOH.

species (1). In the case of peroxyxynitrite, $\text{CO}_3^{\bullet-}$ and oxo-metal complexes (1, 17, 20) initially attack the tyrosine phenol moiety to form the tyrosyl (phenoxy) radical which can react with either $\bullet\text{NO}_2$ to form 3-nitrotyrosine or another phenoxy radical to form 3,3'-dityrosine. Another tyrosine product arising during peroxyxynitrite-dependent reactions is 3,4-dihydroxyphenylalanine (DOPA),² formed by reaction with $\bullet\text{OH}$ which preferentially adds to the tyrosine ring instead of performing one-electron abstraction or by reaction with oxo-metal complexes. The yields of 3-nitrotyrosine, 3,3'-dityrosine, and 3,4-dihydroxyphenylalanine vary rather differently as a function of pH, with the largest tyrosine-derived product being 3-nitrotyrosine at physiological pH. Indeed, 3-nitrotyrosine yields are bell-shaped with a maximum around pH 7.4 (21); on the other hand, 3,3'-dityrosine yields are minimal at low pH and increase significantly under alkaline conditions (15), and 3,4-dihydroxyphenylalanine yields are high at acidic pH and decrease with the pH increase (22). So far, and although the pH dependency for peroxyxynitrite-dependent reactions has been rationalized for a series of biotargets (6, 8, 11), no kinetic mechanism has been offered to explain these pH dependencies of the yields obtained for the three different tyrosine-derived products. In phosphate buffer, pH 7.4, yields with respect to peroxyxynitrite are about 6–8% for nitration, 0.24% for dimerization, and 0% for hydroxylation; nitration yields could increase up to 14–16% in the presence of CO_2 and to even higher values in the presence of transition metal complexes (21, 23, 24).

Most of the mechanistic studies of tyrosine nitration have been performed in aqueous solution. However, many tyrosine residues shown to be nitrated *in vitro* and *in vivo* are associated to nonpolar compartments such as biomembranes [e.g., erythrocyte membrane band 3 (25), red cell membrane proteins (26), complex I of the mitochondrial inner membrane (27), sarcoplasmic reticulum Ca^{2+} -ATPase (28), and microsomal glutathione *S*-transferase (29)] and within the structure of lipoproteins [e.g., Apo A and Apo B (30)]. In many of these cases (27–29) nitration occurs in tyrosines located in transmembrane domains, while in other cases nitration is directed to solvent-exposed tyrosines (25) or is decreased after tyrosine association to hydrophobic domains (30). Therefore, there is a need to develop and validate hydrophobic probes to study and rationalize nitration processes in hydrophobic environments. In this regard, *N-t*-BOC-L-tyrosine *tert*-butyl ester (BTBE) is a stable tyrosine analogue that has been efficiently incorporated (>98%) into the lipid phase of phosphatidylcholine (PC) liposomes with the highest concentration near the glycerol backbone (31). Peroxyxynitrite addition to both multi- and unilamellar liposomes caused formation of both 3-nitro-BTBE and 3,3'-di-

BTBE, with the yield of the nitro derivative much higher than that of the corresponding dimer.

Peroxyxynitrite can diffuse through and interact with biomembranes (32, 33) and lipoproteins (34, 35) and promote oxidation and nitration reactions in protein and lipid targets (1, 25, 36, 37). However, mechanistic insights on peroxyxynitrite-mediated tyrosine nitration in hydrophobic compartments are lacking; some of the assumptions valid for the aqueous phase may not be valid due to the different polarity of the environment and to spatial restrictions and diffusional constraints of both reactants and target molecules, among several other factors. Moreover, the relevance of tyrosine dimerization and, the previously unexplored, hydroxylation in the lipid phase remains to be specifically assessed.³ Thus, in this work we have used the hydrophobic tyrosine analogue BTBE incorporated into different types of PC liposomes as a probe to study physicochemical and biochemical factors that control peroxyxynitrite-dependent tyrosine nitration in membrane model systems.

MATERIALS AND METHODS

Chemicals. Diethylenetriaminepentaacetic acid (dtpa), ethylenediaminetetraacetic acid (edta), manganese dioxide, sodium bicarbonate, potassium phosphate, L-tyrosine, desferrioxamine mesylate, α -lipoic acid, *p*-hydroxyphenylacetic acid (pHPA), uric acid, mannitol, hemin, deoxycholic acid, 3-nitrotyrosine, 2-methyl-2-nitrosopropane (MNP), and *N*-acetyltyrosine were purchased from Sigma. *N-t*-BOC-L-tyrosine *tert*-butyl ester (BTBE), 3-nitro-*N-t*-BOC-L-tyrosine *tert*-butyl ester (3-nitro-BTBE), and 3,3'-di-*N-t*-BOC-L-tyrosine *tert*-butyl ester (3,3'-di-BTBE) (see structures in Figure 1) were prepared and handled as previously (31). Stock BTBE solutions (1 M) were prepared in methanol immediately before use. 3,3'-Dityrosine was kindly provided by Dr. Stanley Hazen (Cleveland Clinic Foundation). 1,2-Dimyristoyl-*sn*-glycero-3-phosphocholine (DMPC), 1,2-dilauroyl-*sn*-glycero-3-phosphocholine (DLPC), and egg and soybean phosphatidylcholine were from Avanti Polar Lipids. Mn-tccp [manganese(III) *meso*-tetrakis(4-carboxylatophenyl)porphyrin] and Fe-tcpp [iron(III) *meso*-tetrakis(4-carboxylatophenyl)porphyrin] were from Calbiochem. Hydrogen peroxide (H_2O_2) was from Fluka. Organic solvents for synthesis of standards and chromatography were from Baker. All other compounds were of reagent grade.

Stock hemin solution was freshly prepared in 0.1 N NaOH and kept in the dark at 4 °C until use. The ferric iron-edta and ferric iron-desferrioxamine (ferrioxamine) complexes were prepared by mixing equal volumes of edta and desferrioxamine with ferric chloride, respectively, in a concentration ratio of 1.1:1. Mn-tccp and Fe-tcpp stock solutions were 1.21 and 1.10 mM, respectively, and were diluted in 0.1 N NaOH. Fenton chemistry was performed by preparing a stock solution of 10 mM FeSO_4 in 2.5 mM H_2SO_4 which was then added to BTBE-containing liposomes in the presence of hydrogen peroxide (H_2O_2) to a final Fe^{2+} : H_2O_2 ratio of 1. All solutions were prepared with highly pure deionized nanopure water to minimize trace metal contamination.

² Abbreviations: BOC, *tert*-butyl pyrocarbonate; BTBE, *N-t*-BOC-L-tyrosine *tert*-butyl ester; DMPC, 1,2-dimyristoyl-*sn*-glycero-3-phosphocholine; DLPC, 1,2-dilauroyl-*sn*-glycero-3-phosphocholine; dtpa, diethylenetriaminepentaacetic acid; edta, ethylenediaminetetraacetic acid; ONOO \bullet , peroxyxynitrite; Mn-tccp, manganese(III) *meso*-tetrakis(4-carboxylatophenyl)porphyrin; Fe-tcpp, iron(III) *meso*-tetrakis(4-carboxylatophenyl)porphyrin; PC, phosphatidylcholine; HPLC, high-performance liquid chromatography; MNP, 2-methyl-2-nitrosopropane; DF, desferrioxamine; Fe-DF, ferrioxamine; LA, lipoic acid; pHPA, *p*-hydroxyphenylacetic acid; DMSO, dimethyl sulfoxide; UA, uric acid; GSH, glutathione; ESR, electron spin resonance; LIT, linear ion trap; DOPA, 3,4 dihydroxyphenylalanine; RA, reverse addition.

³ Throughout this paper, we will refer as BTBE oxidation to the sum of nitration, dimerization, and hydroxylation on the BTBE moiety.

Peroxynitrite Synthesis and Addition. Peroxynitrite was synthesized in a quenched-flow reactor from sodium nitrite (NaNO_2) and H_2O_2 under acidic conditions as described previously (36). The H_2O_2 remaining from the synthesis was eliminated by treating the stock solutions of peroxynitrite with granular manganese dioxide, and the alkaline peroxynitrite stock solution was kept at -20°C until use. Peroxynitrite concentrations were determined spectrophotometrically at 302 nm ($\epsilon = 1670 \text{ M}^{-1} \text{ cm}^{-1}$). The nitrite concentration in the preparations was typically lower than 30% with respect to peroxynitrite. Control of nitrite levels proved to be critical for obtaining reproducible data (see Results). In some control experiments, peroxynitrite was allowed to decompose to nitrate and nitrite in 100 mM phosphate buffer, pH 7.4, before use, i.e., “reverse order addition” of peroxynitrite (RA).

BTBE Incorporation into Phosphatidylcholine Liposomes. BTBE incorporation into liposomes was carried out as in ref 31 with minor modifications. Briefly, a methanolic solution of BTBE (0.35 mM) was added to 35 mM PC lipids dissolved in chloroform. Under these conditions more than 98% BTBE was incorporated (31). The mixture was then dried under a stream of nitrogen gas. Multilamellar liposomes were formed by thoroughly mixing the dried lipid with 100 mM potassium phosphate buffer, pH 7.4, plus 0.1 mM dtpa. Liposomes (0.3 mM BTBE) were exposed to peroxynitrite under different conditions throughout the work. BTBE and BTBE-derived products (e.g., 3-nitro-BTBE and 3,3'-di-BTBE) were extracted with chloroform, methanol, and 5 M NaCl as reported previously [1:2:4:0.4, sample:methanol:chloroform:NaCl (v/v) with recovery efficiencies for all compounds >95% (31)]. Samples were then dried and stored at -20°C . Immediately before HPLC separation, samples were resuspended in 100 μL of a mixture containing 85% methanol and 15% KPi (15 mM), pH 3. Experiments with liposomes were performed at 37°C for DMPC and at 25°C for DLPC, egg PC, and soybean PC, in all cases above the transition phase temperatures (i.e., 23, -1 , -3 , and $<0^\circ\text{C}$, respectively).

HPLC Analysis. BTBE, 3-nitro-BTBE, and 3,3'-di-BTBE were separated on a Gilson HPLC system equipped with UV-vis and fluorescence detectors by reverse-phase HPLC using a Partisil ODS-3 10 μm column (250 mm length, 4.6 mm i.d.). Mobile phase A consisted in 15 mM phosphate buffer, pH 3, and mobile phase B consisted in methanol. Chromatographic conditions were as follows: flow, 1 mL/min; 75% mobile phase B for 25 min, followed by a linear increase to 100% mobile phase B for 10 min. UV-vis settings were for BTBE (280 nm, $\epsilon = 1200 \text{ M}^{-1} \text{ cm}^{-1}$) and for 3-nitro-BTBE (360 nm, $\epsilon = 1500 \text{ M}^{-1} \text{ cm}^{-1}$). 3,3'-Di-BTBE was detected fluorometrically at λ_{ex} 294 nm and λ_{em} 401 nm. Authentic 3-nitro-BTBE and 3,3'-di-BTBE were used as standards.

For the detection of 3-hydroxy-BTBE (i.e., 3,4-dihydroxy-*N-t*-BOC-L-phenylalanine *tert*-butyl ester), the HPLC protocol was slightly modified. Mobile phase A consisted of water, and the gradient was started at 50% methanol to 100% for 35 min. UV-vis detection was at 280 nm while fluorometric detection was performed at λ_{ex} 280 nm and λ_{em} 306 nm.

Artifactual BTBE nitration during the chromatographic separation procedure due to nitrite-dependent nitration at

acidic pH was ruled out by appropriate controls using predecomposed peroxynitrite.

Spectrophotometric Analysis. In some experiments using the saturated fatty acid-containing PC (DLPC, DMPC), 3-nitro-BTBE was quantitated by direct UV-vis measurement. Briefly, liposomes were solubilized with 1.2% deoxycholate (38) followed by alkalization to pH 10 with 5 M NaOH, and 3-nitro-BTBE was measured at 424 nm at pH 10 ($\epsilon = 4000 \text{ M}^{-1} \text{ cm}^{-1}$). Similarly, 3-nitrotyrosine was measured by absorbance measurements at 430 nm at pH 10 ($\epsilon = 4100 \text{ M}^{-1} \text{ cm}^{-1}$).

Mass Spectrometry Analysis of Hydroxy-BTBE. Hydroxy-BTBE was analyzed using an Applied Biosystems QTRAP, triple quadrupole-linear ion trap (LIT) mass spectrometer equipped with a turbo ion spray ionization source (ESI). The mass spectrometer was operated in positive mode, and the ESI settings were optimized as follows: ion spray voltage 2500 V, temperature 375°C ; declustering potential 50 V, entrance potential 10 V, nebulizer gas 40 psi; heater gas 25 psi. The samples collected from the HPLC were diluted in acidified methanol (0.1% formic acid) and continuously infused (10 $\mu\text{L min}^{-1}$) at an estimated concentration of 10 nM. We identified the molecular ion at m/z 353.2. Fragmentation analysis of hydroxy-BTBE was conducted utilizing the LIT in the enhanced product ion mode of the instrument. Fragmentation experiments of the molecular ion at 353.2 were conducted at different collision-assisted dissociation energies identifying fragments from the parent ion.

ESR Measurements. ESR spectra were recorded at room temperature on a Bruker EMX spectrometer operating at 9.8 GHz. Typical spectrometer parameters were as follows: scan range, 100 G; field set, 3510 G; time constant, 0.64 ms; scan time, 20 s; modulation amplitude, 5.0 G; modulation frequency, 100 kHz; receiver gain, 2×10^5 ; microwave power, 20 mW. Samples were subsequently transferred to a 100 μL capillary tube for ESR measurements.

General Experimental Conditions. Experiments were typically carried out in the presence of BTBE (0.3 mM) in PC liposomes (30 mM) in 100 mM potassium phosphate plus 0.1 mM dtpa, pH 7.4 and 25°C unless otherwise stated. When the effect of pH on BTBE oxidation yields was studied, potassium phosphate was also used throughout the pH range to avoid confounding reactivities with other buffer system components. The reported final pH after addition of the alkaline peroxynitrite solution was systematically measured and never increased more than 0.2 units.

Estimation of Peroxynitrite Diffusion Distances in the Liposome Suspensions. Estimation of peroxynitrite diffusion distances was made assuming multilamellar liposomes (20 mg/mL) of a mean external diameter of 1000 nm and five-concentric lamellae (39). According to previous data (40, 41) a vesicle concentration can be estimated around 0.20 nM corresponding to 3.65×10^{11} vesicles/mL or 190 μL of liposomes/mL of suspension.

On the basis of a previous model developed in our laboratory (13) the average diffusion distance (Δx) of aqueous phase-added peroxynitrite before reaching a liposome vesicle can be calculated as

$$\Delta x = r \sqrt{\frac{3}{4} \left(\sqrt[3]{\frac{4n\pi}{3}} \right)^2 - 1} \quad (1)$$

where n represents the ratio between the total suspension volume and the total liposome volume and r represents the liposome radius. Solution of this equation yields an Δx value of 1.1 μm . The percentage of added peroxyntirite that could effectively reach a vesicle is determined from the equation:

$$\ln \frac{[\text{ONOO}^-]_x}{[\text{ONOO}^-]_0} = \frac{-\ln 2(\Delta x^2)}{2D_{\text{ONOO}^-}t_{1/2}} \quad (2)$$

where $t_{1/2}$ represents the half-life of peroxyntirite in the extracellular medium and D_{ONOO^-} the diffusion coefficient of peroxyntirite, considered to be similar to that of NO_3^- , 1500 $\mu\text{m}^2 \text{s}^{-1}$ (32, 42).

Computer-Assisted Simulations. Computer-assisted simulations were performed using the GEPASI program (43).

Data Analysis. All experiments reported herein were reproduced a minimum of three times. Results are expressed as mean values with the corresponding standard deviations. Graphics and data analysis were performed using Origin 6.1.

RESULTS

HPLC and Spectroscopic Analysis of BTBE, 3-Nitro-BTBE, and 3,3'-Di-BTBE. To study biochemical and physicochemical factors that control tyrosine nitration in hydrophobic environments, BTBE was incorporated into PC liposomes which then were treated with peroxyntirite. BTBE-derived products were quantitated by UV-vis and/or fluorometric measurements after either (a) reverse phase-HPLC separation of organic extraction material or (b) deoxycholate solubilization. Figure 1A shows a typical HPLC chromatogram obtained from peroxyntirite-treated samples, where BTBE, 3-nitro-BTBE, and 3,3'-di-BTBE eluted at 7, 9, and 19 min, respectively. Alternatively, spectral analysis of 3-nitro-BTBE after liposome solubilization with 1.2% deoxycholate allowed to carry out direct measurements at the peak absorbance of 424 nm at pH 10 (Figure 1B). In DLPC liposomes and pH 7.4 (Figure 1C), peroxyntirite (0–2 mM) caused a dose-dependent increase in BTBE nitration with yields of $\sim 3\%$ (e.g., 15 μM 3-nitro-BTBE at 500 μM peroxyntirite), with similar results obtained with both methods. Importantly, while the direct spectrophotometric measurement of 3-nitro-BTBE after deoxycholate solubilization turned to be practical and reproducible for saturated fatty acid-containing liposomes (e.g., DMPC and DLPC), it should not be reliably applied to unsaturated fatty acid-containing liposomes (e.g., egg and soybean PC) since peroxyntirite leads to the formation of other absorbing species in the same spectral region such as nitrated and oxidized lipids (36, 44).

Peroxyntirite-Mediated BTBE Hydroxylation in DLPC Liposomes. While in previous work (31) the formation on 3-nitro- and 3,3'-di-BTBE was detected upon treatment with peroxyntirite and the myeloperoxidase/nitrite/hydrogen peroxide systems, formation of hydroxylated derivatives of BTBE was not explored. The hydrophobic analogue of 3,4-dihydroxyphenylalanine named herein as 3-hydroxy-BTBE, should be a more polar compound than BTBE, and therefore chromatographic conditions were adjusted to search for compounds eluting at earlier times than BTBE. Initial experiments with peroxyntirite were performed at pH 6.0 as BTBE hydroxylation arising from ONOOH homolysis would

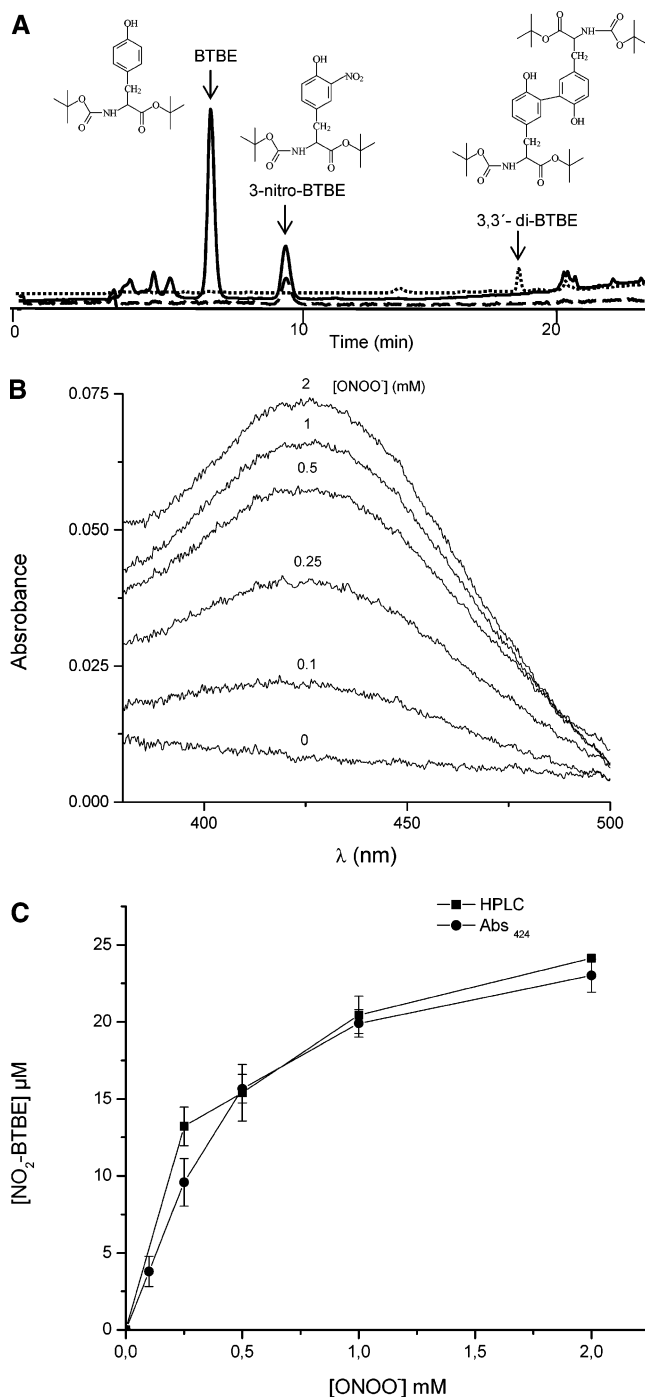


FIGURE 1: Analysis of 3-nitro- and 3,3'-di-BTBE after peroxyntirite addition. BTBE (0.3 mM) in DLPC liposomes (30 mM) was exposed to peroxyntirite in phosphate buffer (100 mM), pH 7.4, plus 0.1 mM dtpa. (A) After an organic extraction, products were separated by RP-HPLC as described under Materials and Methods. The HPLC chromatogram shows the elution of BTBE, 3-nitro-BTBE, and 3,3'-di-BTBE after treatment with ONOO^- (1 mM); the structures have been drawn above the peaks. UV-vis detection was done for BTBE and 3-nitro-BTBE at 280 nm (solid line) and 360 nm (dashed line). 3,3'-Di-BTBE was measured fluorometrically at 294 and 401 nm excitation and emission wavelengths, respectively (dotted line). (B) Peroxyntirite-treated BTBE-containing liposomes were solubilized with 1.2% deoxycholate, the pH was adjusted to 10 with NaOH, and UV-vis spectra of 3-nitro-BTBE were recorded at different peroxyntirite concentrations. (C) Quantitation of 3-nitro-BTBE as a function of peroxyntirite concentration after HPLC separation (■) or deoxycholate solubilization (●).

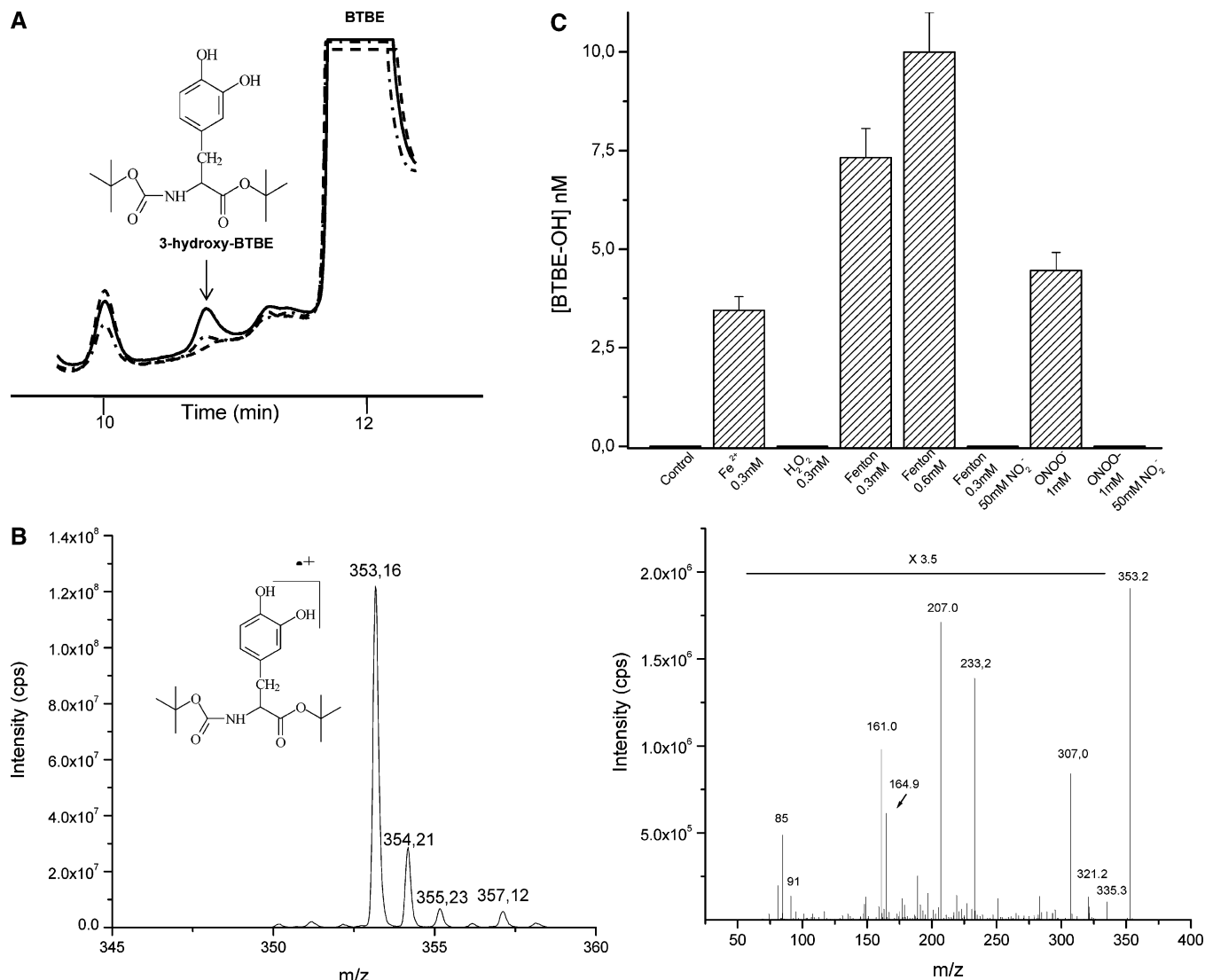


FIGURE 2: HPLC and MS characterization of 3-hydroxy-BTBE. BTBE (0.3 mM) in DLPC liposomes (30 mM) (dashed line) was exposed to FeSO₄ (0.3 mM) + H₂O₂ (0.3 mM) (solid line) or peroxynitrite (1 mM) (dot-dashed line) in phosphate buffer (20 mM), pH 6, plus 0.4 mM dtpa. (A) After an organic extraction products were separated by RP-HPLC, and a product eluting immediately before BTBE (12 min) only present in the Fenton and peroxynitrite conditions was obtained as described under Materials and Methods. (B) ES-MS characterization of the peak eluting at 11 min. Left panel: Enhanced resolution mass scan showing the molecular ion at 353.2 and its isotopic distribution. The proposed structure of the compound has been drawn and corresponds to 3-hydroxy-BTBE. Right panel: MS-MS scan (using the LIT) of the ion at *m/z* 353.2 showing the fragmentation pattern of 3-hydroxy-BTBE. (C) Quantitation of 3-hydroxy-BTBE formation by a Fenton system or peroxynitrite and the effect of nitrite. The reactions were carried out at pH 6, and conditions are indicated in the graph. 3-Hydroxy-BTBE values were estimated assuming a similar fluorescence quantum yield to that of 3,4-dihydroxyphenylalanine.

be favored under acidic conditions, and additionally, as a positive control of hydroxylation, we used a Fenton system. In both the Fenton and peroxynitrite addition experiments a new peak eluting at 11 min was detected (Figure 2A), which was collected and characterized by MS spectrometry (Figure 2B). Indeed, the molecular mass detected for the peak was *m/z* 353.2. Although ES-MS in the positive mode usually produces protonated ions (M + H⁺) which would yield a principal ion for hydroxy-BTBE of *m/z* 354.2, we detected the molecular ion as happens with *N*-acetyltyrosine (data not shown) and α -tocopherol (45, 46). The absence of a protonatable group and the readily oxidizable phenolic moiety in BTBE favors this type of ionization. The ion *m/z* 353.2 corresponds to the molecular radical cation of a hydroxylated derivative of BTBE that we assign as 3-hydroxy-BTBE by analogy with the preferential hydroxylation site of tyrosine and phenolic compounds in general (22, 47).

Importantly, the fragmentation pattern of the parent ion at *m/z* 353.2 was identical for samples obtained from the Fenton or peroxynitrite addition to liposomes preloaded with BTBE. Among the fragments, one with a *m/z* of 335.3 could correspond to the loss of a water molecule from the parent ion. Assuming the fluorescence quantum yield of 3-hydroxy-BTBE to be similar to that of 3,4-dihydroxyphenylalanine, it can be calculated that approximately 5 nM product was formed from 1 mM peroxynitrite at pH 6.0, indicating a low-yield process. No hydroxylated derivative was measured when reactions were conducted at pH 7.4. Figure 2C shows a comparative quantitation of the hydroxylated BTBE derivative formed under different conditions. Hydroxylation in the presence of ferrous iron is due to its fast oxidation to yield O₂^{•-}/H₂O₂ under aerobic conditions, thus secondarily generating a Fenton reagent; however, H₂O₂ alone was unable to hydroxylate BTBE, compatible with the need of an iron-

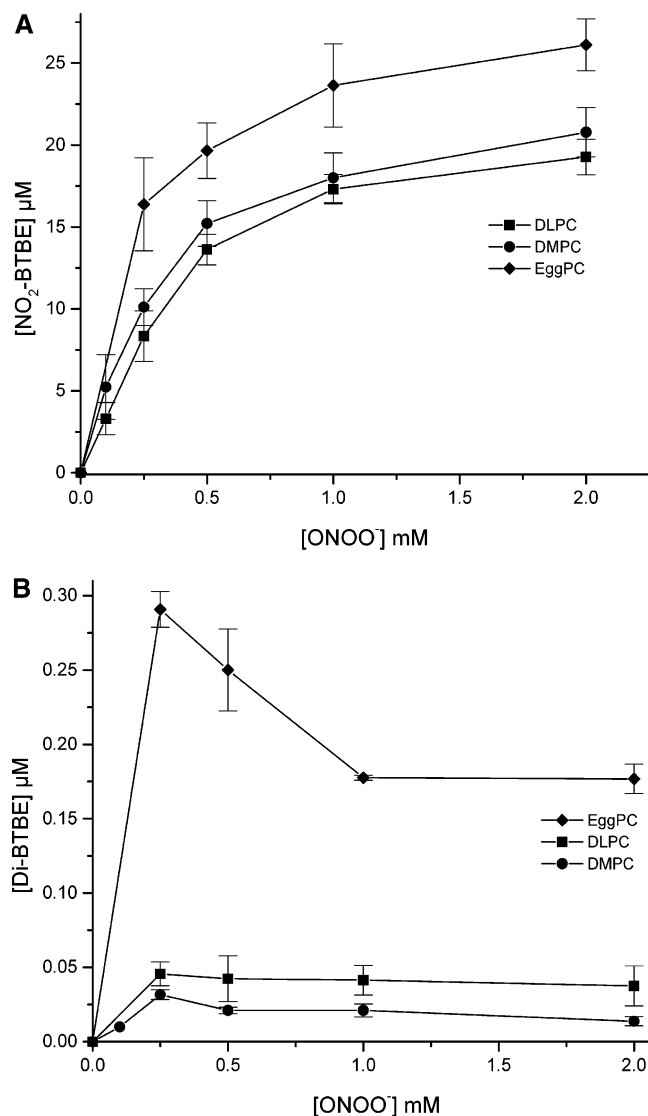


FIGURE 3: Peroxynitrite-mediated BTBE nitration and dimerization in PC liposomes with different degrees of fatty acid unsaturation. BTBE (0.3 mM) in DLPC (■), DMPC (●), and egg PC (◆) liposomes (30 mM) was treated with different concentrations of peroxynitrite in phosphate buffer (100 mM), pH 7.4, plus 0.1 mM dtpa; incubation temperatures were 21 °C for all liposomes except for DMPC, which was incubated at 37 °C. (A) 3-Nitro-BTBE and (B) 3,3'-di-BTBE were measured after RP-HPLC separation. For DLPC and DMPC direct spectrophometric measurements after 1.2% deoxycholate solubilization were also performed, yielding similar results.

catalyzed reaction to yield $\cdot\text{OH}$. While Fenton systems promoted hydroxylation with yields which were dependent on concentration of reagents (i.e., 0.3 and 0.6 mM), the presence of nitrite (NO_2^-) which readily reacts with $\cdot\text{OH}$ to yield $\cdot\text{NO}_2$ ($k = 6 \times 10^9 \text{ M}^{-1} \text{ s}^{-1}$) was fully inhibitory. Peroxynitrite (1 mM) also caused BTBE hydroxylation, with somewhat less efficiency than the Fenton system, and, again, the presence of NO_2^- was completely inhibitory.

While in Figures 1 and 2 the formation of the three BTBE oxidation products by peroxynitrite, i.e., 3-nitro-BTBE, 3,3'-di-BTBE, and 3-hydroxy-BTBE, was established, ESR studies using the spin trap MNP revealed the transient formation of the BTBE phenoxyl radical (Supporting Information, Figure 1S).

Peroxynitrite-Mediated BTBE Oxidation in Saturated and Unsaturated Fatty Acid-Containing Liposomes. Peroxynitrite-

Table 1: Effect of Different Scavengers on BTBE Nitration and Dimerization^a

condition ^b	NO ₂ -BTBE (μM)	di-BTBE (μM)
ONOO ⁻ (0.5 mM)	9.06 ± 0.78	0.017 ± 0.002
+GSH (0.1 mM)	5.1 ± 1.0	ND
+GSH (1.0 mM)	1.65 ± 0.26	ND
+LA (0.1 mM)	1.32 ± 0.01	0.011 ± 0.002
+pHPA (0.3 mM)	5.60 ± 0.77	0.012 ± 0.002
+tyrosine (1 mM)	4.10 ± 0.66	ND
+DMSO (10 mM)	6.59 ± 0.60	0.006 ± 0.001
+mannitol (50 mM)	2.15 ± 0.87	0
+uric acid (0.3 mM)	0	0
+DTPA (0.1 mM)	9.8 ± 1.1	0.007 ± 0.001
+DF (0.1 mM)	0.71 ± 0.15	0
+nitrite (50 mM)	5.6 ± 1.1	ND
+HCO ₃ ⁻ (25 mM)	2.32 ± 0	0.008 ± 0
reverse addition of ONOO ⁻	0	0

^a BTBE (0.3 mM) in DLPC liposomes (30 mM) was exposed to peroxynitrite (0.5 mM) in the presence of the different indicated compounds and concentrations, and 3-nitro-BTBE and 3,3'-di-BTBE were analyzed after RP-HPLC. In the cases where only 3-nitro-BTBE values are provided, direct measurements were made after deoxycholate solubilization. Reverse addition of peroxynitrite represents a control condition with predecomposed peroxynitrite in buffer. ND: not determined. ^b The individual rate constants of the tested scavengers with peroxynitrite, $\cdot\text{OH}$ and $\cdot\text{NO}_2$, are indicated in Supporting Information (Table 2S).

derived $\cdot\text{OH}$ and $\cdot\text{NO}_2$ readily react with unsaturated fatty acids (36, 37); therefore, we investigated the extents of BTBE nitration and dimerization in PC liposomes of different fatty acid composition. Peroxynitrite (0–2 mM) caused a dose-dependent increase in BTBE nitration and oxidation products in DLPC, DMPC, and egg PC liposomes with preincorporated BTBE (Figure 3A). BTBE nitration yields were similar in DLPC and DMPC liposomes while, surprisingly, nitration yields were slightly higher in egg PC liposomes despite the substantial percentage of polyunsaturated fatty acids (~24%) present in this phospholipid (39). On the other hand, BTBE nitration was low (~4.8 μM 3-nitro-BTBE for 500 μM peroxynitrite) in soybean PC that contains the highest level of polyunsaturated fatty acids (57%) (data not shown). In any event, 3-nitro-BTBE was formed after peroxynitrite addition to all four classes of PC liposomes.

In addition, peroxynitrite caused oxidation of BTBE to yield the corresponding dimer, 3,3'-di-BTBE, being the maximal yields at 250 μM peroxynitrite and higher for egg PC than for DLPC (~0.11% and 0.02%, respectively; Figure 3B). The dose-response profile of BTBE dimerization was similar to that of tyrosine, which presented higher maximal yields (~0.24%) at 200 μM peroxynitrite (31). In all cases, BTBE nitration yields were significantly higher than those of dimerization at pH 7.4, providing support to the concept that nitration is by far the predominant oxidative modification of tyrosine in membranes challenged with peroxynitrite at physiologically relevant pH (31).

Inhibition of Peroxynitrite-Mediated BTBE Oxidation by Scavengers and Carbon Dioxide. To explore the nitration mechanism by peroxynitrite of the membrane-associated hydrophobic tyrosine analogue, we studied the effect of selected scavengers that react with known rate constants with peroxynitrite and/or its derived radicals, namely, $\cdot\text{OH}$ and $\cdot\text{NO}_2$ (Table 1). While most of the tested scavengers are polar and will mainly react in the aqueous phase, lipoic acid has a hydrophobic character and could undergo reactions in the

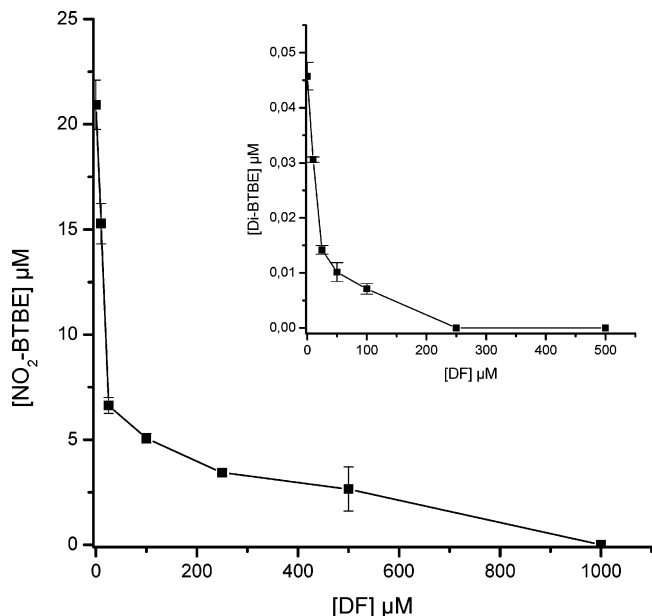


FIGURE 4: Desferrioxamine inhibition of BTBE nitration. BTBE (0.3 mM) in DLPC liposomes (30 mM) was exposed to different concentrations of desferrioxamine (0–1 mM) and treated with peroxynitrite (0.5 mM). 3-Nitro-BTBE was quantitated by UV–vis measurement after RP-HPLC separation of organic extraction products of liposome suspensions. Inset: 3,3′-Di-BTBE was measured fluorometrically after RP-HPLC.

lipid phase or in the aqueous/lipid interphase (48). BTBE nitration and dimerization were inhibited by glutathione, lipoic acid, pHPA, tyrosine, DMSO, mannitol, and uric acid in extents that are compatible with their different reactivities with peroxynitrite and peroxynitrite-derived radicals (see Supporting Information, Tables 1S and 2S). The metal chelator dtpa did not affect BTBE nitration (Table 1), but desferrioxamine was capable to potently and dose-dependently inhibit 3-nitro-BTBE and 3,3′-di-BTBE formation (Figure 4) in extents that are consistent with its reactions with •OH and •NO₂ (49) (Supporting Information, Figure 4S). Notably, the presence of NO₂[−] was also inhibitory of nitration, underscoring the role of •OH radicals in the formation of 3-nitro-BTBE, despite a larger formation of •NO₂ in this condition.

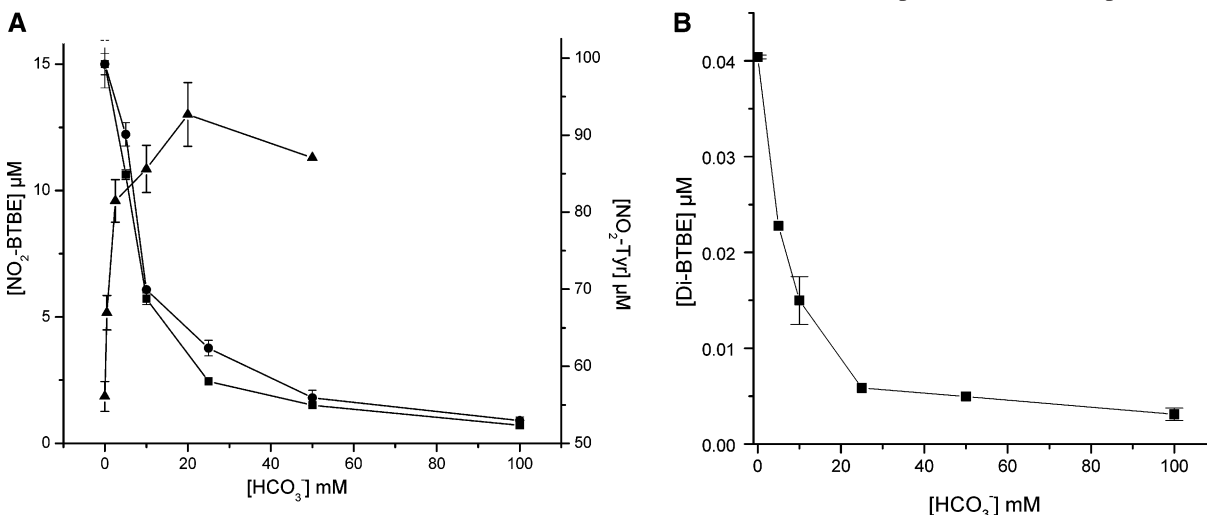


FIGURE 5: Bicarbonate modulation of BTBE and tyrosine nitration. BTBE (0.3 mM) in DLPC liposomes (30 mM) was treated with peroxynitrite (0.5 mM) at different concentrations of bicarbonate (0–100 mM) in phosphate buffer (100 mM). (A) BTBE nitration and (B) dimerization products were analyzed by UV–vis after either RP-HPLC (■) or 1.2% deoxycholate solubilization of liposomes (●). (A) 3-Nitrotyrosine (▲) was measured directly by spectrophotometry.

Table 2: Effect of Transition Metal Complexes on BTBE Nitration^a

condition	NO ₂ -BTBE (µM)	
	DLPC	egg PC
ONOO [−] (0.5 mM)	14.1 ± 1.9	18.0 ± 2.8
+Fe-EDTA (0.1 mM)	22.5 ± 2.2	7.5 ± 1.7
+Fe-DF (0.1 mM)	15.2 ± 1.1	ND
+hemin (25 µM)	78.0 ± 5.5	97.1 ± 4.4
+Mn-tccp (20 µM)	41.2 ± 1.2	20.6 ± 2.0
+Fe-tccp (50 µM)	31.5 ± 5.0	5.71 ± 0.05
reverse addition of ONOO [−]	0	0

^a BTBE (0.3 mM) in DLPC and egg PC liposomes (30 mM) were incubated with the indicated transition metal complexes and concentrations and treated with peroxynitrite (0.5 mM). Samples were analyzed for 3-nitro-BTBE content after RP-HPLC.

Importantly, while bicarbonate/carbon dioxide typically increase tyrosine nitration in aqueous phase (1, 11, 50) due to a more efficient formation of tyrosyl radical promoted by CO₃^{•−} (1), the presence of bicarbonate (25 mM) decreased the nitration of liposome-incorporated BTBE (Table 1). Moreover, bicarbonate inhibited BTBE nitration and dimerization (Figure 5, left and right panels) in a dose-dependent manner.

Transition Metal Complexes Catalyze Peroxynitrite-Dependent BTBE Nitration. Some transition metal complexes enhance peroxynitrite-mediated nitration of phenolic compounds in aqueous environments via a catalytic redox cycle mechanism (1, 23). We studied the effect of different transition metal complexes on peroxynitrite-dependent BTBE nitration and dimerization in saturated (DLPC) and unsaturated (egg PC) liposomes. In DLPC liposomes nitration yields were enhanced in the presence of hemin, Fe-edta, and the metal porphyrins Mn-tccp and Fe-tccp, while ferrioxamine had no stimulatory effect. In egg PC liposomes, hemin and Mn-tccp enhanced BTBE nitration, while Fe-edta and Fe-tccp did not (Table 2). It is clear that, in the more simple system containing saturated phospholipids (DLPC), redox-active metal complexes served as nitration catalysts. Indeed, in DPLC liposomes hemin and Mn-tccp enhanced peroxynitrite-dependent BTBE nitration (Figure 6) and dimerization (not shown) in a dose-dependent manner. In particular, hemin

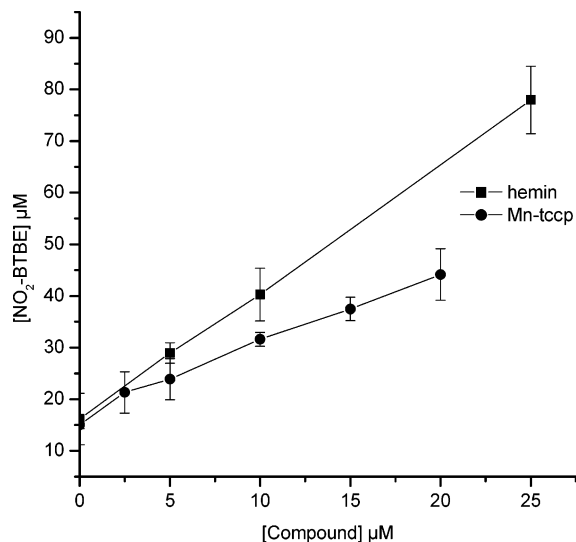


FIGURE 6: Hemin and Mn-tccp catalysis of BTBE nitration. BTBE (0.3 mM) in DLPC liposomes (30 mM) was treated with peroxy-nitrite (0.5 mM) in the presence of different concentrations of hemin (■) or Mn-tccp (●) at pH 7.4, and samples were analyzed for 3-nitro-BTBE content after RP-HPLC.

was a potent catalyzer, causing an ~5-fold increase in nitration yields (15% at pH 7.4) at 25 μM.

Effect of pH on BTBE Nitration, Dimerization, and Hydroxylation Yields. The effect of pH on BTBE nitration and dimerization was studied to determine to what extent its incorporation into a hydrophobic environment affects the dependency observed for tyrosine. Changes in pH will alter the proton concentration in the aqueous phase and may indirectly influence the chemistry of BTBE occurring in the liposomes. Formation of 3-nitro-BTBE as a function of pH resulted in a bell-shaped curve with a maximum yield at pH 7.5 (Figure 7A) and comparable to that of 3-nitrotyrosine; 3,3'-di-BTBE formation was very low at pH <8 but significantly increased toward alkaline pH (Figure 7B). As indicated previously, 3-hydroxy-BTBE was detected at pH 6 (Figure 2C) but not at pH 7.4. The pH profiles of tyrosine and BTBE nitration, dimerization, and hydroxylation were fully reproduced in silico by computer-assisted simulations considering a free radical mechanism of peroxy-nitrite-mediated tyrosine oxidations (1, 8, 11) and a relatively slow dimerization rate constant for the BTBE-phenoxy radicals (see Supporting Information, Table 1S and Figures 2S and 3S).

On the other hand, the pH profiles of BTBE nitration presented a completely different behavior in the presence of hemin and Mn-tccp, which resulted in a continuous increase of 3-nitro-BTBE toward alkaline pH (Figure 8), reaching nitration yields of 17% and 20%, respectively, at pH 9.

DISCUSSION

In this work we have used the hydrophobic tyrosine analogue BTBE to establish mechanisms of peroxy-nitrite-mediated tyrosine nitration in membranes and explore factors that control the extents of nitration as well as other oxidative modifications, i.e., tyrosine dimerization and tyrosine hydroxylation. Herein, we confirmed that peroxy-nitrite was able to induce the formation of 3-nitro-BTBE and 3,3'-di-BTBE in DLPC liposomes (Figure 1) and, importantly, a hydroxylated derivative of BTBE, assigned as 3-hydroxy-BTBE, was

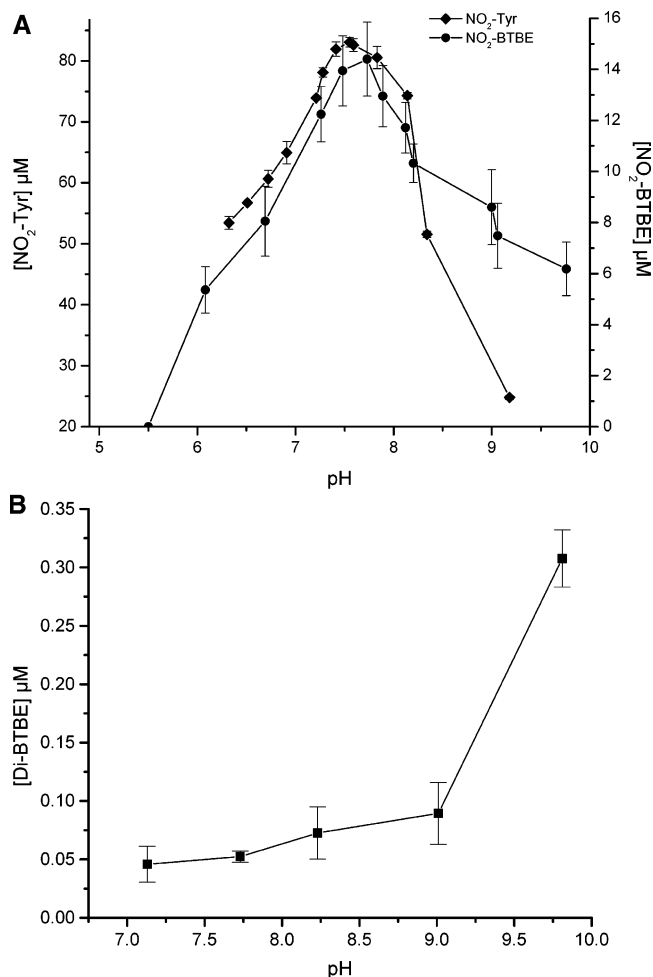


FIGURE 7: BTBE and tyrosine oxidation as a function of pH. DLPC liposomes containing BTBE were prepared after lipid resuspension in phosphate buffer (100 mM) plus 0.1 mM dtpa at different pHs. Then, BTBE (0.3 mM) or tyrosine (0.3 mM) was treated with peroxy-nitrite (0.5 mM) under different pHs. (A) 3-Nitro-BTBE (●) and (B) 3,3'-di-BTBE (■) were analyzed after organic extraction by RP-HPLC, while in (A) 3-nitrotyrosine (◆) was measured directly by spectrophotometry.

for the first time detected (Figure 2). At pH 7.4, nitration was the predominant process with 3% yield with respect to peroxy-nitrite in DLPC liposomes (versus 6–8% for free tyrosine) as compared to dimerization (0.02% yield) and hydroxylation (0% yield). In addition to being formed in saturated fatty acid-containing liposomes (DLPC and DMPC), 3-nitro-BTBE was also present in egg (Figure 3) and soybean PC (data not shown), containing substantial amounts of polyunsaturated fatty acids which are readily oxidizable by peroxy-nitrite-derived species (36, 37). Moreover, despite being modest, dimerization yields were even higher in egg PC than in DLPC liposomes (Figure 3B), which suggests that secondary processes such as lipid peroxidation may participate in BTBE oxidation reactions when polyunsaturated fatty acids are present (see below).

Tyrosine in aqueous solution does not react directly with peroxy-nitrite (51), and thus formation of 3-nitrotyrosine depends on reactions of peroxy-nitrite-derived radicals (*OH, *NO₂, CO₃*-) (1). In the case of BTBE nitration, the data also support a free radical mechanism initiated by the homolysis of ONOOH either in close proximity or inside the membrane. First, BTBE hydroxylation (Figure 2) is

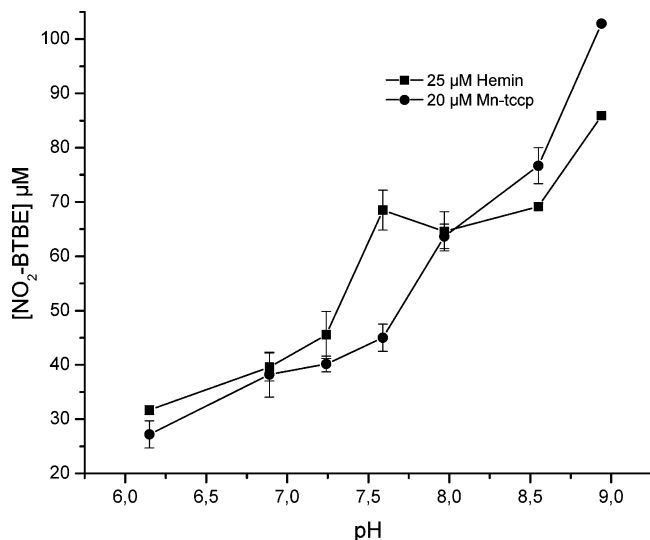


FIGURE 8: Effect of pH on metal complex-catalyzed BTBE nitration. DLPC liposomes containing BTBE were prepared as in Figure 7 and exposed to peroxynitrite (0.5 mM) in the presence of hemin (25 μM) and Mn-tccp (20 μM) at different pHs.

explained by addition of $\cdot\text{OH}$ to BTBE in the immediacy of the site of homolysis as $\cdot\text{OH}$ reacts with target molecules within a few molecular diameters of its site of formation; $\cdot\text{OH}$, formed from ONOOH in the aqueous phase, is able to penetrate PC vesicles and react with aromatic probe molecules incorporated in the membrane interior as previously shown in water radiolysis studies (52); importantly, $\cdot\text{OH}$ could be also formed inside the liposomes as ONOOH permeates the lipid bilayer (32, 33), and we have previously established the homolysis of ONOOH in aprotic solvents (31). Second, inhibitions in nitration and dimerization (Table 1 and Supporting Information) could be explained, in good part, on the basis of simple competition kinetics with free radical scavengers.⁴ Third, the detection of the BTBE-derived phenoxyl radical and the pH profile of nitration was fully consistent with a free radical mechanism of reaction leading to the observed BTBE oxidative modifications.

Importantly, to our knowledge this is the first report where the processes of tyrosine (and tyrosine analogue) nitration, dimerization, and hydroxylation from the proton-catalyzed homolysis of peroxynitrite as a function of pH are rationalized with a kinetic model involving free radical reactions⁵ (Figure 7 and Supporting Information). Both, the pH profiles and yields of oxidation obtained *in silico* agree well with the experimental *in vitro* data for tyrosine and BTBE. In the case of BTBE, the actual rate constants of its reactions with the primary radicals (i.e., $\cdot\text{OH}$, $\cdot\text{NO}_2$) are not known and were assumed to be the same as for tyrosine; however, for the dimerization reaction (i.e., combination of two BTBE-derived phenoxyl radicals to form 3,3'-di-BTBE), the rate constant value was lowered 100-fold ($k = 2.25 \times 10^6 \text{ M}^{-1} \text{ s}^{-1}$) with

respect to the corresponding one of tyrosyl radicals ($k = 2.25 \times 10^8 \text{ M}^{-1} \text{ s}^{-1}$) due to the restricted lateral motion of molecules in the organized membrane bilayer, which results in a low yield of dimerization with respect to nitration (Figures 3 and 7 and Supporting Information). Indeed, while the diffusion coefficient (D) value of amino acids such as tyrosine in the aqueous phase is in the order of $800\text{--}1000 \mu\text{m}^2 \text{ s}^{-1}$ (42), the estimated D for BTBE in PC liposomes can be safely assumed as $\sim 5 \mu\text{m}^2 \text{ s}^{-1}$ as extrapolated from data obtained with the hydrophobic fluorescence aromatic probe pyrene (53), inferring a 100–200-fold decrease in tyrosyl radical diffusion in the membrane. Intermolecular tyrosine dimerization will be even less likely in integral peptides and proteins as D values become $>10^3\text{--}10^4$ times smaller than in solution (53, 54) and in line with recent data reporting a lack of tyrosine dimerization in peroxynitrite-treated transmembrane peptides (55). On the other hand, $\cdot\text{NO}$ and $\cdot\text{NO}_2$ concentrate 4–5-fold in hydrophobic environments, and the apparent D value ($D'_{\text{NO}} = 1500 \mu\text{m}^2 \text{ s}^{-1}$) is very close to that of the aqueous phase of $4500 \mu\text{m}^2 \text{ s}^{-1}$ (56). The kinetic model proposed herein also predicts that the phenolic hydroxyl group of liposome-incorporated BTBE plays a role, as in the case of tyrosine, in the pH dependency ($\text{p}K_a \sim 10$) and that there is no need to invoke other dissociable moieties present in PC such as the phosphate and choline moieties of the polar headgroup. Thus, the kinetic data support that liposomal BTBE accommodates its hydroxyl group toward the lipid/water interphase, in agreement with the structural data (31) indicating that the highest concentration of BTBE is present near the glycerol backbone of the phospholipid.

In contrast to what is observed with tyrosine (Figure 5), the presence of bicarbonate decreased BTBE nitration (and dimerization, Figure 5). In heterogeneous systems the presence of bicarbonate may limit the oxidant actions of peroxynitrite (11, 13, 50) by mechanisms that involve the fast reaction of ONOO⁻ with CO₂ in the aqueous phase. At 25 mM bicarbonate at pH 7.4 (1.3 mM CO₂) and 25 °C, the half-life of peroxynitrite is reduced from 2.7 s to 24 ms (13, 50), corresponding to an average diffusion distance in homogeneous solution of $\sim 8.5 \mu\text{m}$. However, as indicated in Materials and Methods and from eq 1, under the vesicle concentration of our experiments (i.e., 3.65×10^{11} vesicles/mL), the average peroxynitrite diffusion distance to a liposome (Δx) is only 1.1 μm . Thus, according to eq 2 in the presence of 1.3 mM CO₂ less than 2% of added peroxynitrite will react with CO₂ before finding a liposome vesicle. Even at the highest CO₂ concentrations tested (5.4 mM CO₂ in equilibrium with 100 mM HCO₃⁻, Figure 5) less than 5% of peroxynitrite diffusion will be inhibited by external CO₂. Thus, added peroxynitrite had access to the vesicles in the suspension under all of the experimental conditions, and the inhibition of BTBE oxidations by CO₂ cannot be a consequence of diffusion limitations due to shortening of peroxynitrite lifetime as previously (13, 50) but is due to a more subtle reason. Peroxynitrous acid, but not peroxynitrite anion, permeates the liposomal membrane (32, 33, 41); however, ONOOH acid does not react directly with either PC or BTBE, and therefore its consumption inside the membrane will depend only on homolysis to $\cdot\text{OH}$ and $\cdot\text{NO}_2$, which will be rate-limiting and relatively slow; in this scenario, a quasi-equilibrium will be established between

⁴ For instance, the data on desferrioxamine (Figure 4 and Supporting Information) provide mechanistic support to a previous report showing inhibition of red cell membrane protein tyrosine nitration by desferrioxamine during exposure to $\cdot\text{NO}_2$ gas (26).

⁵ In one previous paper (11), kinetic modeling of tyrosine nitration as a function of pH was performed in the presence of CO₂. Under this condition (+CO₂), the reaction has a pH dependency substantially different from the H⁺- or metal-catalyzed nitration reported herein and elsewhere (15, 23) with larger values of nitration at acidic pH.

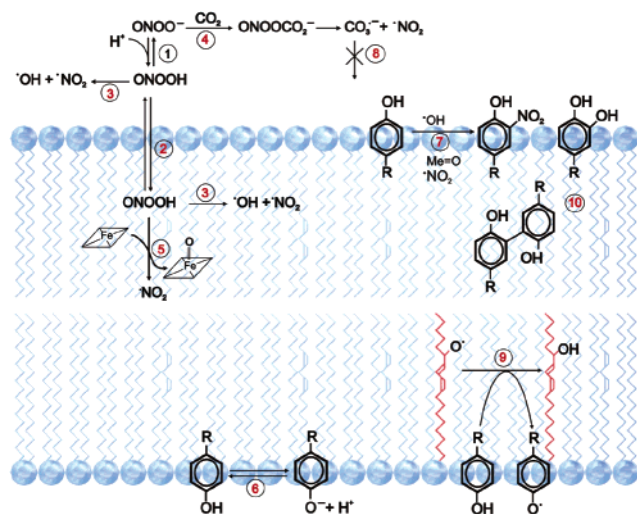
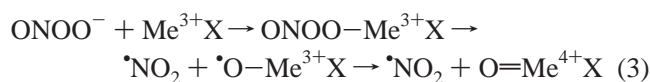


FIGURE 9: Proposed mechanism of nitration of the hydrophobic tyrosine analogue BTBE in phosphatidylcholine bilayers. Peroxynitrite anion (ONOO^-) added in the aqueous phase is in equilibrium (pK_a = 6.8) with peroxynitrous acid (ONOOH) (1), and ONOOH can readily permeate the phospholipid bilayer (2); ONOOH can undergo homolysis in either the aqueous or lipid phases (3), and ONOO^- can react with CO_2 only in the aqueous phase (4) to yield a transient adduct followed by formation of $\text{CO}_3^{\bullet-}$ and $\bullet\text{NO}_2$. In the lipid phase, ONOO^- could react directly with hemin to yield the $\text{O}=\text{Fe}^{4+}$ metal complex and $\bullet\text{NO}_2$ (5). BTBE is incorporated into the bilayer, accommodating its phenolic hydroxyl group toward the lipid-water interphase (6) and can undergo a one-electron oxidation to the BTBE phenoxyl radical by either $\bullet\text{OH}$ or the oxo-metal complex (Fe or Mn) followed by reaction with $\bullet\text{NO}_2$ (7). $\text{CO}_3^{\bullet-}$ formed in the aqueous phase does not permeate into the hydrophobic compartment where BTBE is located (8). In the presence of polyunsaturated fatty acids, the primary radicals will preferentially initiate lipid peroxidation, and we propose that lipid alkoxyl (9) and peroxy radicals are responsible of a significant fraction of BTBE one-electron oxidation. In addition to 3-nitro-BTBE, the formation (in lower yields) of 3,3'-di-BTBE and 3-hydroxy-BTBE is indicated (10).

peroxynitrite in the aqueous and lipid phases (41) (Figure 9). In the presence of CO_2 , only the fraction of peroxynitrite anion present in the aqueous phase will readily react to yield ONOOCO_2^- and the resulting $\text{CO}_3^{\bullet-}$ and $\bullet\text{NO}_2$ radicals. The negatively charged $\text{CO}_3^{\bullet-}$ (pK_a < 0) (57) is incapable of permeating the lipid bilayer (41) to promote the one-electron oxidation of BTBE as has been also well established in studies of the reaction of PC membranes with other radical anions such as $\text{Br}_2^{\bullet-}$ and $\text{Cl}_2^{\bullet-}$ (52). As the “extraliposomal” peroxynitrite is being consumed, there will be a backward diffusion of ONOOH to the bulk solution and after deprotonation will further react with CO_2 , with an overall effect of a decrease on BTBE oxidation yields. Globally, the data support that bicarbonate will facilitate nitration of water-exposed tyrosine residues while it will inhibit nitration of tyrosine residues buried in transmembrane domains or associated to lipoprotein environments.

An interesting observation of this work was that transition metal complexes were capable of significantly enhancing peroxynitrite-dependent BTBE nitration (Table 2 and Figure 6). In particular, hemin and Mn-tccp were strong catalyzers. Hemin is extremely hazardous when it is released from its natural anchor, the globin moiety, as observed in a variety of pathophysiological conditions and aged red blood cells (58). Being a hydrophobic molecule, hemin has a high affinity for cell membranes, intercalating into the phospho-

lipid bilayer, and can participate in oxidation and nitration reactions (17, 59). In turn, Mn-tccp (also known as Mn-tbap) and other Mn porphyrins have been extensively used as SOD mimics and peroxynitrite reductases. While peroxynitrite-mediated Mn-tccp-catalyzed nitration was reported for tyrosine, the presence of water-soluble reductants such as glutathione, ascorbate, and uric acid inhibits the process due to their fast reaction with the $\text{O}=\text{Mn}^{4+}$ species formed by peroxynitrite (see eq 3); however, these reductants will not penetrate to membranes, and therefore the prooxidant actions in hydrophobic environments of $\text{O}=\text{Mn}^{4+}$ -tccp and also $\text{O}=\text{Fe}^{4+}$ -hemin can be more pronounced (35) and may explain part of their toxicity. For both hemin and Mn-tccp, nitration yields are greatly enhanced (Figure 6), indicating that the metal complexes were in close proximity to BTBE and support a reaction chemistry under which the transition metal (Me^{3+}X ; eq 3) serves as a Lewis acid facilitating the formation of a transient complex with peroxynitrite ($\text{ONOO}-\text{Me}^{3+}\text{X}$); in this complex the O–O bond is weakened and undergoes homolysis to $\bullet\text{NO}_2$ plus a high oxidation state oxo-metal intermediate (I) that efficiently promotes the one-electron oxidation of BTBE to its corresponding phenoxyl radical (BTBE*):



This mechanism (eqs 3–5) is further supported by the pH dependency of the nitration yields in the presence of transition metal complexes (Figure 8), which is completely different than in their absence (Figure 6) and totally consistent with the higher stability of oxo-metal complexes at alkaline pH (60), which increase their oxidation efficiency to BTBE and consistent with previous data (17, 59).

Nitration and dimerization of the hydrophobic tyrosine analogue were observed both in the absence (Figure 3) and in the presence (Figure 6) of transition metal complexes in both saturated (DLPC and DMPC) and polyunsaturated fatty acid-containing liposomes (egg and soybean PC). Polyunsaturated fatty acids are good targets of strong oxidants such as $\bullet\text{OH}$ and oxo-metal complexes. Moreover, in both egg and soybean PC liposomes (30 mM) the concentration of polyunsaturated fatty acids (7.3 and 17 mM, respectively) (39) is much higher than that of BTBE (0.3 mM) and would out compete for the reaction with peroxynitrite-derived radicals known to lead to lipid peroxidation (36) and nitration (37). Thus, considering simple competition kinetics a profound inhibition in BTBE oxidations in egg and soybean PC liposomes would be expected, unless BTBE oxidation is associated to the lipid oxidation process; i.e., lipid-derived radicals promoting one-electron oxidation of BTBE to the corresponding BTBE (phenoxyl) radical ($E^{\circ'} = +0.88 \text{ V}$) (61). This is possible with a highly oxidizing intermediate such as alkoxyl radical ($E^{\circ'} = +1.76 \text{ V}$) (62) and maybe also with the less reactive peroxy radical ($E^{\circ'} = +1.02 \text{ V}$) (63). Once formed, the BTBE phenoxyl radical would react with $\bullet\text{NO}_2$ ($k > 10^9 \text{ M}^{-1} \text{ s}^{-1}$) or with another BTBE phenoxyl radical (this latter indicated by the significant increase on

dimerization yields in egg PC liposomes; Figure 3B). $\cdot\text{NO}_2$ could also be consumed by lipid radicals to yield nitro lipids as the reaction is also close to diffusion-controlled; thus, the influence of BTBE (or tyrosine-containing peptides and proteins) on the extents of lipid nitration arises as a relevant issue for future studies.⁶ The role of lipid peroxidation in BTBE oxidation is supported by a significant decrease on nitration and dimerization (~50%) by incubation of reaction mixtures under low oxygen tension (unpublished data).

BTBE is relatively easy to synthesize, is stable, and can be readily utilized as a probe to perform a wide range of studies on tyrosine nitration in hydrophobic environments. BTBE incorporated into liposomes represents a model system to study a variety of factors that may control nitration processes in biomembranes, including the role of aqueous and lipid-soluble free radical scavengers and catalyzers. In this regard, in addition to the method that involves separation of BTBE-derived products with the more demanding HPLC-based techniques (Figure 1A), the protocol presented herein using deoxycholate solubilization of saturated fatty acid-containing liposomes followed by direct spectrophotometric determination of 3-nitro-BTBE (Figure 1B) proved to be simple and reproducible (Figures 1C and 5). On the other hand, we have successfully incorporated BTBE to both red blood cell membranes and lipoproteins (unpublished data), which opens the possibility of its use as a tracer molecule to follow nitration processes in more complex biochemical/biological systems. As an option to BTBE, tyrosine-containing transmembrane peptides have also been synthesized and incorporated into liposomes (55). While the structure and reaction chemistry in these peptides can more closely reflect that of membrane proteins (55, 64) in comparison to BTBE, their synthesis is a more complex endeavor; moreover, they are unlikely to be incorporated into biological membranes or lipoproteins. Thus, BTBE and tyrosine-containing transmembrane peptides constitute complementary probes. For example, studies of tyrosine hydroxylation in peptides containing residues at different depths in the membrane will assist in defining the relevance of ONOOH homolysis in the aqueous vs lipid phase, as $\cdot\text{OH}$ diffusing from the bulk solution will mainly react with residues located near the liposome surface (52).

In summary, BTBE was a useful probe to define peroxy-nitrite-dependent mechanisms of biomembrane nitration and provided new information regarding factors, such as CO_2 and hemin, that will down- or upmodulate, respectively, nitration and other oxidation processes in hydrophobic environments. In addition, due to the minimal diffusion of $\cdot\text{OH}$, the detection of 3-hydroxy-BTBE supports the "site-specific" homolysis of ONOOH to $\cdot\text{OH}$ and $\cdot\text{NO}_2$ in the immediacy or even inside the phospholipid bilayer and consistent with the previously reported larger yields of tyrosine-containing transmembrane peptide nitration for tyrosine residues located deeper in the bilayer (55). Further studies utilizing BTBE incorporated into liposomes, cell membranes, and lipoproteins will serve to further unravel

factors that control peroxy-nitrite-dependent as well as independent (i.e., via hemin and metalloproteins) protein and lipid nitration.

ACKNOWLEDGMENT

We thank Joy Joseph (Medical College of Wisconsin) for the synthesis of BTBE, 3-nitro-BTBE, and 3,3'-di-BTBE and Virginia Lopez (Universidad de la República) for helpful discussion on mass spectrometry analysis of 3-hydroxy-BTBE.

SUPPORTING INFORMATION AVAILABLE

ESR-spin trapping data and kinetic simulations that support a free radical mechanism of BTBE oxidation by peroxy-nitrite. This material is available free of charge via the Internet at <http://pubs.acs.org>.

REFERENCES

- Radi, R. (2004) Nitric oxide, oxidants, and protein tyrosine nitration, *Proc. Natl. Acad. Sci. U.S.A.* 101, 4003–4008.
- Estevez, A. G., Crow, J. P., Sampson, J. B., Reiter, C., Zhuang, Y., Richardson, G. J., Tarpey, M. M., Barbeito, L., and Beckman, J. S. (1999) Induction of nitric oxide-dependent apoptosis in motor neurons by zinc-deficient superoxide dismutase, *Science* 286, 2498–2500.
- Ischiropoulos, H. (2003) Oxidative modifications of alpha-synuclein, *Ann. N.Y. Acad. Sci.* 991, 93–100.
- Radi, R., Peluffo, G., Alvarez, M. N., Naviliat, M., and Cayota, A. (2001) Unraveling peroxy-nitrite formation in biological systems, *Free Radical Biol. Med.* 30, 463–88.
- Beckman, J. S., Beckman, T. W., Chen, J., Marshall, P. A., and Freeman, B. A. (1990) Apparent hydroxyl radical production by peroxy-nitrite: implications for endothelial injury from nitric oxide and superoxide, *Proc. Natl. Acad. Sci. U.S.A.* 87, 1620–1624.
- Radi, R., Beckman, J. S., Bush, K. M., and Freeman, B. A. (1991) Peroxy-nitrite oxidation of sulfhydryls. The cytotoxic potential of superoxide and nitric oxide, *J. Biol. Chem.* 266, 4244–4250.
- Augusto, O., Gatti, R. M., and Radi, R. (1994) Spin-trapping studies of peroxy-nitrite decomposition and of 3-morpholinolysidoneimine *N*-ethylcarbamide autooxidation: direct evidence for metal-independent formation of free radical intermediates, *Arch. Biochem. Biophys.* 310, 118–125.
- Goldstein, S., Czapski, G., Lind, J., and Merenyi, G. (2000) Tyrosine nitration by simultaneous generation of (\cdot)NO and O⁻(2) under physiological conditions. How the radicals do the job, *J. Biol. Chem.* 275, 3031–3036.
- Lymar, S. V., and Hurst, J. K. (1995) Rapid reaction between peroxy-nitrite ion and carbon dioxide: implications for biological activity, *J. Am. Chem. Soc.* 117, 8867–8868.
- Bonini, M. G., Radi, R., Ferrer-Sueta, G., Ferreira, A. M., and Augusto, O. (1999) Direct EPR detection of the carbonate radical anion produced from peroxy-nitrite and carbon dioxide, *J. Biol. Chem.* 274, 10802–10806.
- Lymar, S. V., Jiang, Q., and Hurst, J. K. (1996) Mechanism of carbon dioxide-catalyzed oxidation of tyrosine by peroxy-nitrite, *Biochemistry* 35, 7855–7861.
- Lymar, S. V., Schwarz, H. A., and Czapski, G. (2000) Medium effects on reactions of the carbonate radicals with thiocyanate, iodide and ferrocyanide ions., *Radiat. Phys. Chem.* 59, 387–392.
- Romero, N., Denicola, A., Souza, J. M., and Radi, R. (1999) Diffusion of peroxy-nitrite in the presence of carbon dioxide, *Arch. Biochem. Biophys.* 368, 23–30.
- Stanbury, D. M. (1989) Reduction potentials involving inorganic free radicals in aqueous solutions., *Adv. Inorg. Chem.* 33, 69–138.
- van der Vliet, A., Eiserich, J. P., O'Neill, C. A., Halliwell, B., and Cross, C. E. (1995) Tyrosine modification by reactive nitrogen species: a closer look, *Arch. Biochem. Biophys.* 319, 341–349.

⁶ $\cdot\text{NO}_2$ is a one-electron oxidant and could potentially oxidize BTBE (Supporting Information, Table 1S) or polyunsaturated fatty acids ($k = 10^5 \text{ M}^{-1} \text{ s}^{-1}$); however, these rate constant values are relatively low, and in our system $\cdot\text{NO}_2$ will preferentially react with BTBE- or lipid-derived radical species.

16. Herzog, J., Maekawa, Y., Cirrito, T. P., Illian, B. S., and Unanue, E. R. (2005) Activated antigen-presenting cells select and present chemically modified peptides recognized by unique CD4 T cells, *Proc. Natl. Acad. Sci. U.S.A.* *102*, 7928–7933.
17. Bian, K., Gao, Z., Weisbrodt, N., and Murad, F. (2003) The nature of heme/iron-induced protein tyrosine nitration, *Proc. Natl. Acad. Sci. U.S.A.* *100*, 5712–5717.
18. Batthyany, C., Souza, J. M., Duran, R., Cassina, A., Cervenansky, C., and Radi, R. (2005) Time course and site(s) of cytochrome *c* tyrosine nitration by peroxynitrite, *Biochemistry* *44*, 8038–8046.
19. Zhang, R., Brennan, M. L., Shen, Z., MacPherson, J. C., Schmitt, D., Molenda, C. E., and Hazen, S. L. (2002) Myeloperoxidase functions as a major enzymatic catalyst for initiation of lipid peroxidation at sites of inflammation, *J. Biol. Chem.* *277*, 46116–46122.
20. Ferrer-Sueta, G., Vitturi, D., Batinic-Haberle, I., Fridovich, I., Goldstein, S., Czapski, G., and Radi, R. (2003) Reactions of manganese porphyrins with peroxynitrite and carbonate radical anion, *J. Biol. Chem.* *278*, 27432–27438.
21. Ischiropoulos, H., Zhu, L., Chen, J., Tsai, M., Martin, J. C., Smith, C. D., and Beckman, J. S. (1992) Peroxynitrite-mediated tyrosine nitration catalyzed by superoxide dismutase, *Arch. Biochem. Biophys.* *298*, 431–437.
22. Santos, C. X., Bonini, M. G., and Augusto, O. (2000) Role of the carbonate radical anion in tyrosine nitration and hydroxylation by peroxynitrite, *Arch. Biochem. Biophys.* *377*, 146–152.
23. Beckman, J. S., Ischiropoulos, H., Zhu, L., van der Woerd, M., Smith, C., Chen, J., Harrison, J., Martin, J. C., and Tsai, M. (1992) Kinetics of superoxide dismutase- and iron-catalyzed nitration of phenolics by peroxynitrite, *Arch. Biochem. Biophys.* *298*, 438–445.
24. Daiber, A., Bachschmid, M., Beckman, J. S., Munzel, T., and Ullrich, V. (2004) The impact of metal catalysis on protein tyrosine nitration by peroxynitrite, *Biochem. Biophys. Res. Commun.* *317*, 873–881.
25. Mallozzi, C., Di Stasi, A. M., and Minetti, M. (1997) Peroxynitrite modulates tyrosine-dependent signal transduction pathway of human erythrocyte band 3, *FASEB J.* *11*, 1281–1290.
26. Velsor, L. W., Ballinger, C. A., Patel, J., and Postlethwait, E. M. (2003) Influence of epithelial lining fluid lipids on NO₂-induced membrane oxidation and nitration, *Free Radical Biol. Med.* *34*, 720–733.
27. Murray, J., Taylor, S. W., Zhang, B., Ghosh, S. S., and Capaldi, R. A. (2003) Oxidative damage to mitochondrial complex I due to peroxynitrite: identification of reactive tyrosines by mass spectrometry, *J. Biol. Chem.* *278*, 37223–37230.
28. Viner, R. I., Ferrington, D. A., Williams, T. D., Bigelow, D. J., and Schoneich, C. (1999) Protein modification during biological aging: selective tyrosine nitration of the SERCA2a isoform of the sarcoplasmic reticulum Ca²⁺-ATPase in skeletal muscle, *Biochem. J.* *340*, 657–669.
29. Ji, Y., Neverova, I., Van Eyk, J. E., and Bennet, B. M. (2006) Nitration of tyrosine 92 mediates the activation of rat microsomal glutathione-S-transferase by peroxynitrite, *J. Biol. Chem.* *281*, 1986–1991.
30. Shao, B., Bergt, C., Fu, X., Green, P., Voss, J. C., Oda, M. N., Oram, J. F., and Heinecke, J. W. (2005) Tyrosine 192 in apolipoprotein A-I is the major site of nitration and chlorination by myeloperoxidase, but only chlorination markedly impairs ABCA1-dependent cholesterol transport, *J. Biol. Chem.* *280*, 5983–5993.
31. Zhang, H., Joseph, J., Feix, J., Hogg, N., and Kalyanaram, B. (2001) Nitration and oxidation of a hydrophobic tyrosine probe by peroxynitrite in membranes: comparison with nitration and oxidation of tyrosine by peroxynitrite in aqueous solution, *Biochemistry* *40*, 7675–7686.
32. Denicola, A., Souza, J. M., and Radi, R. (1998) Diffusion of peroxynitrite across erythrocyte membranes, *Proc. Natl. Acad. Sci. U.S.A.* *95*, 3566–3571.
33. Marla, S. S., Lee, J., and Groves, J. T. (1997) Peroxynitrite rapidly permeates phospholipid membranes, *Proc. Natl. Acad. Sci. U.S.A.* *94*, 14243–14248.
34. Goss, S. P., Singh, R. J., Hogg, N., and Kalyanaram, B. (1999) Reactions of *NO, *NO₂ and peroxynitrite in membranes: physiological implications, *Free Radical Res.* *31*, 597–606.
35. Trostchansky, A., Ferrer-Sueta, G., Batthyany, C., Botti, H., Batinic-Haberle, I., Radi, R., and Rubbo, H. (2003) Peroxynitrite flux-mediated LDL oxidation is inhibited by manganese porphyrins in the presence of uric acid, *Free Radical Biol. Med.* *35*, 1293–300.
36. Radi, R., Beckman, J. S., Bush, K. M., and Freeman, B. A. (1991) Peroxynitrite-induced membrane lipid peroxidation: the cytotoxic potential of superoxide and nitric oxide, *Arch. Biochem. Biophys.* *288*, 481–487.
37. Rubbo, H., Radi, R., Trujillo, M., Telleri, R., Kalyanaram, B., Barnes, S., Kirk, M., and Freeman, B. A. (1994) Nitric oxide regulation of superoxide and peroxynitrite-dependent lipid peroxidation. Formation of novel nitrogen-containing oxidized lipid derivatives, *J. Biol. Chem.* *269*, 26066–26075.
38. Buege, J. A., and Aust, S. D. (1978) Microsomal lipid peroxidation, *Methods Enzymol.* *52*, 302–310.
39. New, R. R. C. (1989) *Liposomes: a Practical Approach*, IRL Press at Oxford University Press, New York.
40. Huang, C., and Mason, J. T. (1978) Geometric packing constraints in egg phosphatidylcholine vesicles, *Proc. Natl. Acad. Sci. U.S.A.* *75*, 308–310.
41. Khairutdinov, R. F., Coddington, J. W., and Hurst, J. K. (2000) Permeation of phospholipid membranes by peroxynitrite, *Biochemistry* *39*, 14238–14249.
42. Lide, D. R. (1990) *Handbook of Chemistry and Physics*, 71st ed., CRC Press, Boca Raton, FL.
43. Mendes, P. (1997) Biochemistry by numbers: simulation of biochemical pathways with Gepasi 3, *Trends Biochem. Sci.* *22*, 361–363.
44. Schopfer, F. J., Baker, P. R., Giles, G., Chumley, P., Batthyany, C., Crawford, J., Patel, R. P., Hogg, N., Branchaud, B. P., Lancaster, J. R., Jr., and Freeman, B. A. (2005) Fatty acid transduction of nitric oxide signaling. Nitrooleic acid is a hydrophobically stabilized nitric oxide donor, *J. Biol. Chem.* *280*, 19289–19297.
45. Lauridsen, C., Leonard, S. W., Griffin, D. A., Liebler, D. C., McClure, T. D., and Traber, M. G. (2001) Quantitative analysis by liquid chromatography-tandem mass spectrometry of deuterium-labeled and unlabeled vitamin E in biological samples, *Anal. Biochem.* *289*, 89–95.
46. Mottier, P., Gremaud, E., Guy, P. A., and Turesky, R. (2002) Comparison of gas chromatography-mass spectrometry and liquid chromatography-tandem mass spectrometry methods to quantify alpha-tocopherol and alpha-tocopherolquinone levels in human plasma, *Anal. Biochem.* *301*, 128–135.
47. Solar, S., Solar, W., and Getoff, N. (1984) Reactivity of OH with tyrosine in aqueous solution studied by pulse radiolysis, *J. Phys. Chem.* *88*, 2091–2095.
48. Trujillo, M., Folkes, L., Bartasaghi, S., Kalyanaram, B., Wardman, P., and Radi, R. (2005) Peroxynitrite-derived carbonate and nitrogen dioxide radicals readily react with lipoid and dihydroliipoic acid, *Free Radical Biol. Med.* *39*, 279–288.
49. Bartasaghi, S., Trujillo, M., Denicola, A., Folkes, L., Wardman, P., and Radi, R. (2004) Reactions of desferrioxamine with peroxynitrite-derived carbonate and nitrogen dioxide radicals, *Free Radical Biol. Med.* *36*, 471–483.
50. Denicola, A., Freeman, B. A., Trujillo, M., and Radi, R. (1996) Peroxynitrite reaction with carbon dioxide/bicarbonate: kinetics and influence on peroxynitrite-mediated oxidations, *Arch. Biochem. Biophys.* *333*, 49–58.
51. Alvarez, B., Ferrer-Sueta, G., Freeman, B. A., and Radi, R. (1999) Kinetics of peroxynitrite reaction with amino acids and human serum albumin, *J. Biol. Chem.* *274*, 842–848.
52. Barber, D. J. W., and Thomas, J. K. (1978) Reactions of radicals with lecithin bilayers, *Radiat. Res.* *74*, 51–65.
53. Vanderkooi, J. M., and Callis, J. B. (1974) Pyrene. A probe of lateral diffusion in the hydrophobic region of membranes, *Biochemistry* *13*, 4000–4006.
54. Sackmann, E., Trauble, H., Galla, H., and Overath, P. (1973) Lateral diffusion, protein mobility and phase transitions in *Escherichia coli* membranes. A spin label study, *Biochemistry* *12*, 5360–5369.
55. Zhang, H., Bhargava, K., Keszler, A., Feix, J., Hogg, N., Joseph, J., and Kalyanaram, B. (2003) Transmembrane nitration of hydrophobic tyrosyl peptides. Localization, characterization, mechanism of nitration, and biological implications, *J. Biol. Chem.* *278*, 8969–8978.
56. Moller, M., Botti, H., Batthyany, C., Rubbo, H., Radi, R., and Denicola, A. (2005) Direct measurement of nitric oxide and oxygen partitioning into liposomes and low-density lipoprotein, *J. Biol. Chem.* *280*, 8850–8854.

57. Czapski, G. (1999) Acidity of the carbonate radical, *J. Phys. Chem. A* 103, 3447–3450.
58. Sullivan, S. G., Baysal, E., and Stern, A. (1992) Inhibition of hemin-induced hemolysis by desferrioxamine: binding of hemin to red cell membranes and the effects of alteration of membrane sulfhydryl groups, *Biochim. Biophys. Acta* 1104, 38–44.
59. Thomas, D. D., Espey, M. G., Vitek, M. P., Miranda, K. M., and Wink, D. A. (2002) Protein nitration is mediated by heme and free metals through Fenton-type chemistry: an alternative to the NO/O₂⁻ reaction, *Proc. Natl. Acad. Sci. U.S.A.* 99, 12691–12696.
60. Ferrer-Sueta, G., Batinic-Haberle, I., Spasojevic, I., Fridovich, I., and Radi, R. (1999) Catalytic scavenging of peroxynitrite by isomeric Mn(III) *N*-methylpyridylporphyrins in the presence of reductants, *Chem. Res. Toxicol.* 12, 442–449.
61. Stubbe, J., and van der Donk, W. A. (1998) Protein radicals in enzyme catalysis, *Chem. Rev.* 98, 705–762.
62. Merenyi, G., Lind, J., and Goldstein, S. (2002) Thermochemical properties of alpha-hydroxy-alkoxyl radicals in aqueous solution, *J. Phys. Chem. A* 106, 11127–11129.
63. Jonsson, M. (1996) Thermochemical properties of peroxides and peroxy radicals, *J. Phys. Chem.* 100, 6814–6818.
64. Zhang, H., Xu, Y., Joseph, J., and Kalyanaraman, B. (2005) Intramolecular electron transfer between tyrosyl radical and cysteine residue inhibits tyrosine nitration and induces thiyl radical formation in model peptides with MPO, H₂O₂ and NO₂⁻: EPR spin trapping studies, *J. Biol. Chem.* 280, 40684–40698.

BI060363X

11. Anexos

Abreviatura	Nombre del compuesto
-------------	----------------------

Moléculas Relevantes

$\alpha\text{-TO}\cdot$	Radical α -tocoferoxilo
$\alpha\text{-TOH}$	alfa-tocoferol
$\gamma\text{-TOH}$	gamma-tocoferol
CO_2	Anhídrido carbónico
$\text{CO}_3\cdot^-$	Radical carbonato
H_2O_2	Peróxido de Hidrógeno
HCO_3^-	Bicarbonato
HCO_4^-	Peroximonocarbonato
HOCl	Acido hipocloroso
$\text{L}\cdot$	Radical alquilo
$\text{LO}\cdot$	Radical alcoxilo
$\text{LOO}\cdot$	Radical peroxilo
LOOH	Hidroperóxido lipídico
LOONO	Nitro lípido
N_2O_3	Trióxido de dinitrógeno
N_2O_4	Tetraóxido de dinitrógeno
$\text{NO}\cdot$	Oxido nítrico sintasa
$\cdot\text{NO}_2$	Radical dióxido de nitrógeno
NO_2Cl	Cloruro de nitrilo
$\text{O}_2\cdot^-$	Radical superóxido
O_2	Oxígeno
$\cdot\text{OH}$	Radical hidroxilo
ONOO^-	peroxinitrito anión

ONOOH Acido peroxinitroso

Proteínas

APO-A Apolipoproteína A
APO-B Apolipoproteína B
EPO Eosinófilo Peroxidasa
GPX Glutación Peroxidasa
HRP Peroxidasa de rábano
LDL Lipoproteína de baja densidad
MPO Mieloperoxidasa
NOS Oxido nítrico sintasa
PHS-2 prostaglandina endoperóxido sintasa-2
PRX Peroxiredoxinas
SERCA Ca²⁺-retículo-sarcoplásmico ATPasa
SOD Superóxido dismutasa

Sondas hidrofóbicas

3,3'-di-BTBE 3,3 'di-N-*t*-BOC *tert* butil ester L-tirosina
3-NO₂-BTBE 3-nitro-N-*t*-BOC *tert* butil ester L-tirosina
3-OH-BTBE 3-hidroxi-BTBE
BPBE N-*t*-BOC *tert* butil ester fenialalanina
BTBE N-*t*-BOC *tert* butil ester L-tirosina

Y4 Péptido transmembrana Y4
Y8 Péptido transmembrana Y8
Y12 Péptido transmembrana Y12

•Tyr	Radical tirosilo
3,3'-di-Tyr	3,3'-di-tirosina
3-NT	3-nitrotirosina
ABAP	2,2'-Azobis (2-amidinopropano) hidrocloreuro
ALS	Esclerosis Lateral Amiotrófica
BHT	Butilhidroxitolueno
BOC	Butoxipirocarbonato
DF	Desferrioxamina
DCM	Diclorometano
DHLA	Acido dihidrolipoico
DIC	di-isopropilcarbodi-imida
DMSO	Dimetilsulfóxido
DNA	Acido desoxirribonucleico
DTPA	Acido dietilentriaminopentacético
EDTA	Acido etilendiaminotetracético
EPR	Resonancia Paramagnética Electrónica
ESI	Fuente de ionización de iones turbo spray
Fe-tcpp	porfirina de Fe (III) meso-tetrakis (4-carboxilatofenilo)
Fmoc	n-(9-fluororenil) metoxicarbonilo
FOX	Xylenol Orange ferroso
GSH	Glutación
HOBt	1-hidroxibenzotriazol
LA	Acido lipoico
LIT	Triple cuadrupolo lineal
MBHA	p-amida metilbenzilhidrilamina

MDA	Malondialdehído
MNP	2-metil-3-nitrosopropano
Mn-tcpp	porfirina de Mn (III) meso-tetrakis (4-carboxilatofenilo)
NMP	<i>N</i> -metil piperidina
PC	Fosfatidilcolina
<i>p</i> HPA	Acido <i>para</i> -hidroxifenilacético
PUFA	Acidos grasos polinsaturados
RNS	Especies Reactivas del Nitrógeno
ROS	Especies Reactivas del Oxígeno
RP-HPLC	Cromatografía Líquida de Alta Resolución- Fase Reversa
TBA	Acido Tiobarbitúrico
TFA	Acido Trifluoracético
TIS	Tri-isopropilsilano
TNM	Tetranitrometano

Lípidos

DMPC	1,2-dimiristoil- <i>sn</i> -glicero-3-fosfocolina
DLPC	1,2-dilauril- <i>sn</i> -glicero-3-fosfocolina
EYPC	Fosfatidilcolina de yema de huevo
PLPC	1-palmitoil-2-linoleil- <i>sn</i> -glicero-3-fosfocolina
SBPC	Fosfatidilcolina de soja

12. Agradecimientos

- ✓ A Rafa, querido maestro y amigo. Gracias por enseñarme a trabajar con rigurosidad, aplicando el método científico, a ser estricta y ordenada en el pensamiento y a encarar sin miedo y con confianza los nuevos desafíos. Por encontrar siempre la parte positiva de cada resultado y por tu orientación crítica y estricta, pero siempre acertada. Por ser una persona que ha sabido sacar adelante un grupo de referencia mundial pese a todas las dificultades que existen en Uruguay, y por las miles de horas de tu vida que dedicaste para que esta y otras tesis salieran adelante. Por acompañarme incondicionalmente a lo largo de todo este tiempo, en las buenas y en las malas. Por haber impulsado la generación del CEINBIO, y generado este espacio nuevo de Laboratorio donde es un placer trabajar cada día. Es un orgullo pertenecer a este Grupo de Investigación, y espero con mi trabajo y dedicación, haber contribuido en parte a esa tarea imposible que empezaste hace 20 años. Muchas gracias, este trabajo no hubiera sido lo que es, sino fuera por vos.

- ✓ A Madia, baluarte fundamental de este laboratorio que me ha acompañado en todas las etapas de mi formación, enseñándome con dedicación y trabajando intensamente en los aspectos más complicados de ésta tesis, siempre dispuesta a darme una mano. Gracias por estar ahí, y por tener a mano cada una de las constantes cinéticas que necesité!

- ✓ A mi querido amigo Gonza, por tener siempre la palabra justa, por haberme enseñado tanto de HPLC y arreglarme el equipo cada vez que hizo falta. Por las horas que dedicó un mes de enero a los experimentos de masa y por haber estado ahí desde siempre. Gracias Pelu por todo.

- ✓ A Vicky, compinche de todas las horas además de una secretaria perfecta. Por hacer que este laboratorio funcione y estar siempre dispuesta a ayudarme a mí y a todos en lo que haga falta. Gracias amiga por acompañarme con alegría y locura durante mis ratos libres en el Laboratorio.

- ✓ A Vale por el trabajo intenso que compartimos en la primera etapa de esta tesis, por las otras cosas que aprendimos juntas y por haber dedicado tiempo y esmero a generar el "artwork" del laboratorio.

- ✓ A Lolo, por sus ganas de aprender, y trabajar. Por todo lo que compartimos y aprendimos en esta última etapa de la tesis, por todo lo que me enseñaste y las miles de horas que le dedicaste a trabajar mano a mano conmigo en los

experimentos. Por poner a punto el Ensayo de FOX, los métodos de HPLC para los péptidos y las medidas de MDA; y por tu calidez y disposición para ayudarme en la etapa final de este trabajo. Gracias Lolo sos un grande.

- ✓ A Adri, por las miles de cosas que hace por el Grupo y el Laboratorio.
- ✓ A Ana Denicola, por ser quien me trajo a Facultad de Medicina y me acompañó en las primeras etapas. Gracias por tu cariño a lo largo de todos estos años.
- ✓ A Gerardo por su aporte siempre fundamental en las discusiones del grupo y por haberme enseñado a trabajar con peroxinitrito.
- ✓ A Carlitos, por enseñarme a trabajar con el HPLC, y por los experimentos con LDL, en la época que estaba prohibida la entrada en el tercer piso.
- ✓ A la banda joven del Centro; Martincho, Pablito, Vale, Lolo, Veros y a toda la nueva generación por haber traído alegría y aire fresco al Laboratorio.
- ✓ A todo el resto del grupo, a todos, porque cada resultado compartido en las reuniones de los viernes fue sometido a la opinión y crítica de todos y porque el aporte de ideas y soluciones, permitieron que el trabajo siguiera avanzando.
- ✓ A Seba, por su apoyo permanente en todo.
- ✓ A Balaraman Kalyanaraman, por su aporte fundamental en este trabajo y por recibirme en Wisconsin durante mis estadías para la síntesis de péptidos. También a Chris, Joy, Jimmy, Jane y Sandy que estuvieron a disposición durante esos días, e hicieron que todo fuera más fácil.
- ✓ A mis queridos amigos del MCW, Mica, Marcos y Ana D por haberme acompañado durante mis pasantías allá y haberme recibido como si me conocieran de toda la vida.
- ✓ A los otros amigos llegados desde afuera, Susana, Miguel A, Rodrigo, Barbarita, Katia y Bea por las horas que compartimos dentro y fuera del Laboratorio, y porque también trajeron un aire nuevo siempre enriquecedor. A Su, especialmente, por su apoyo y cercanía durante la preparación de esta

tesis, por haberme recibido en Portugal con inmensa hospitalidad, y por haber venido especialmente a la defensa de esta tesis.

- ✓ A Huguis, Alfonso, Dieguito y Nicolás, porque gracias a ellos tenemos el Laboratorio impecable cada día y por su disposición para ayudarnos frente a cualquier inconveniente. Por los almuerzos en el lavadero y a Alfon, especialmente, por ayudarme a concretar "nuestro" museo.
- ✓ A Darío Estrín, Marcelo Martí y Ariel Petruk de la Facultad de Ciencias Exactas, Universidad de Bs. As., por los estudios de dinámica molecular realizados en los péptidos.
- ✓ A Christian Stadler, por los estudios *in vivo* que está realizando.
- ✓ A la Facultad de Medicina, por brindarnos este espacio físico para trabajar y darnos el marco académico para desarrollar esta carrera.
- ✓ A PEDECIBA QUIMICA, por darnos el marco para realizar los estudios de Doctorado, por el apoyo que me otorgó para realizar las Pasantías en Wisconsin y por la beca de Doctorado.
- ✓ A mi madre y mis hermanos, a mis sobrinos, y a mis gorditas queridas, por todo lo demás, pero sobre todo, por las miles de horas que les quité durante los últimos años.

